Late Holocene diatom community responses to climate variability along the southern Cape coastal plain, South Africa

Kelly Kirsten

Thesis Presented for the Degree of

DOCTOR OF PHILOSOPHY

in the Department of Environmental and Geographical Science

UNIVERSITY OF CAPE TOWN

February 2014

ABSTRACT

In recent decades an emphasis on understanding the long-term variability of ecosystems and their responses to environmental changes has been undertaken. This has mainly been achieved through the identification and analysis of fossil material in lake sediments. In the South Africa, the relative paucity of available sites and the semi-arid nature of the region have led to incomplete or discontinuous palaeoclimatic records. However, lakes along the southern Cape coastal plain have shown promise.

With this in mind palaeo-records from neighbouring rainfall regimes were used to evaluate the spatial and temporal patterns of climatic fluctuations during the late Holocene. Diatom analysis was conducted on sediment cores retrieved from coastal lakes at two localities, namely the Wilderness Lake Complex, near Knysna, as a representative of the year-round rainfall zone, and Princessvlei on the Cape Flats, as a representative of the winter rainfall zone of the southern African coastal zone. Additionally, oxygen isotopic analysis was performed on the silicate frustules from Princessvlei. On the basis of this evidence, it can be stated with some confidence that salinity is the driving mechanism governing the state of the Wilderness lake systems, which in turn is a response to sea level changes and climatic fluctuations, in particular moisture availability. Alternatively, the Princessvlei system is governed by changes in nutrients and water turbidity, which have been shown to be proxies for moisture availability and wind. This makes moisture availability a primary controlling factor over the environment along the southern coastal plain, with shifts between wet and dry periods occurring rapidly. Notable shifts in precipitation coincide with global climatic phenomena, including the Medieval Climate Anomaly (~1200 – 700 cal yrs BP) and the Little Ice Age (~700 – 125 cal yrs BP). Marine transgressions during the late Holocene are also recorded in the diatom assemblage particularly in the Wilderness region, as is the system's recovery during the subsequent regressions. However, anthropogenic forcings during the last few centuries have resulted in considerable modifications in the natural functioning of all systems, altering flow dynamics and nutrient influx. The outcome of this study shows that diatom analysis is a powerful tool in the reconstruction of past environments under conditions wherein other typical palaeoenvironmental proxies may be less adequately represented.

Keywords

Diatoms, late Holocene, southern Cape coastal plain, palaeoclimate, sea level changes

ACKNOWLEDGEMENTS

This project would not have been possible without the assistance, belief and motivation of my supervisor Professor Mike Meadows. Thanks are also extended to the copious number of people who were bombarded with emails relating to diatom analysis and statistics (special mention to fellow diatomist, Liandra Bertolli) as well as to the conservationists at the SANParks Sedgefield office and Cape Nature (Princessvlei). This degree has afforded many opportunities, particularly through various laboratory visits to Friedrich Schiller University of Jena and Forschungszentrum Jülich which were wonderful and interesting experiences.

The Institute of Geography at FSU-Jena provided various additional data to compliment this research, including grain size analysis and seismic profiles for the Wilderness Lakes. In particular, I'd like to thank Dr. Torsten Haberzettl, Bastian Reinwarth, Sarah Franz, Thomas Kasper and Siegfried Clausnitzer as well as acknowledging their insightful discussions during the interpretation stages. I'm grateful to Dr. Andreas Lücke for hosting me at the Forschungszentrum Jülich where the isotopic analysis was conducted. The moral support and encouragement recieved from friends, family and departmental colleagues is something I will always be grateful for, especially to my eternally present office mate, Lynne Quick and my father who has supported me for all these years.

The generous funding received from the Deutscher Akademischer Austauschdienst (DAAD), National Research Foundation (NRF), the University of Cape Town's Postgraduate Funding Office and the Bundesministerium für Bildung und Forschung (BMBF) (the Wilderness sites form part of a bilateral - South African/German - project between the University of Cape Town and Friedrich Schiller University of Jena) greatly assisted in the successful conclusion of this project. The financial assistance of the National Research Foundation (NRF) towards this research is hereby acknowledged. Opinions expressed and conclusions arrived at, are those of the author and are not necessarily to be attributed to the NRF.

TABLE OF CONTENTS

LIST OF FIGURES

LIST OF TABLES

Chapter 1. INTRODUCTION

The present ecological state of any landscape is a response to the current environmental conditions affecting it, both natural and anthropogenic (Huntley, 1996). However, the latter two processes are variable both through time and space. It stands to reason then that the ecological state of a landscape is dynamic in nature and will respond to variability in the range of driving mechanisms it is subjected to. These responses may be of interest to a variety of disciplines, especially where conservation and management efforts are being employed to maintain and/or improve the current state of a system. Transformations in a system, whether due to a natural process or anthropogenic forcing may pre-date monitored information, hence alternative methods are needed to understand the natural variability that a system experiences. This can be achieved through the analysis of stratigraphical records from numerous representative sites (Denys and de Wolf, 1999; Fritz et al., 1999). When attempting to reconstruct past environments from stratigraphical records certain fundamental principles are applied, the most well-known being the uniformitarian approach, which implies that fossil organisms have the same biological and environmental requirements as their modern day counterparts (Lawrence, 1971). Thus, by transferring an organism's modern ecological situation to its fossilised occurrences within the palaeo-record, one can create a snapshot of the environment at the time of deposition and with it resolve external environmental factors relating to climate and distribution. The paleorecord may manifest itself in various forms, although lake sediments have shown particular promise in this regard. Changes within a lake related to environmental drivers can be rapid and normally are translated to the biological community; in this way, the examination of fossil assemblages provides key insights into changes in the environment and their related causes.

Palaeolimnology in itself is a diverse and multi-proxy discipline which attempts to "…*establish baseline values for* [a] *lake ecosystem, quantifying and evaluating directional changes in lake status, and evaluating why change has occurred*" (Battarbee, 1999, Pp 151). The discipline is primarily based on the analysis of fossil material preserved in the sediments within a lake insofar as the fossil assemblage is an archive of changing environmental and climatic conditions. The fossil deposits are intricately linked to the climate within the region as climate directly influences the hydrological budget of the lake, which has implications for the ecological and sedimentological characteristics of the system (Fritz et al., 1999).

Therefore, the stratigraphic sequence in lacustrine sediments can offer a valuable source of evidence for the reconstruction of high temporal resolution environmental dynamics (Anderson, 1995). Thus, by determining the evolution of a lake system through time and space one can indirectly resolve the changes in the underlying mechanisms driving the system (Wolin and Duthie, 1999), as well as establish a baseline that facilitates the monitoring of environmental transformations in the future (Anderson, 1995). These facts make palaeolimnologically based reconstructions powerful tools in establishing natural changes in climate variability and in providing a context against which anthropogenic forcings can be measured (Fritz et al., 1999).

Multiple spheres of interest within palaeoecology contribute a greater overall snapshot of the environment at any given point in time, these spheres include but are not limited to, hydrology, limnology and vegetation dynamics relative to the proxies incorporated into the analysis (Huntley, 1996). Coupled with these advancements is the development of more robust chronologies, which can provide direct correlations between sites and ultimately create a regional perspective (Huntley, 1996). Additionally, with the development of the discipline from a largely qualitative science through the descriptive reconstruction of past environments, to a considerably more quantitative science mainly due to advancements in statistical techniques has allowed for cross-validation of sites and proxies (Birks, 1996). By incorporating a palaeoecological approach it is possible to provide an additional dimension against which the nature and scale of human influences can be measured while, at the same time, offering an improved understanding of modern environmental systems (Cooper, 1999; Fritz et al., 1999).

1.1. THE SIGNIFICANCE OF PALAEOENVIRONMENTAL RESEARCH IN SOUTH AFRICA

Palaeolimnological studies throughout South Africa are rather limited due to the relative paucity of suitable sites and the discontinuous accumulation of lake sediments over time (Scott and Lee-Thorp, 2004). This trend is primarily due to the poor development of wetlands associated with dry, seasonal climates, which are prevalent across the region (Chase et al., 2010). However, sites along the south coast of South Africa have shown considerable potential for analysis. Research conducted in the 1950s by ARH Martin indicated fossil rich deposits at Groenvlei, a closed basin lake near Knysna (Martin, 1956, 1959, 1962, 1968). Peat deposits near Norga revealed a dynamic climatic state during the Holocene epoch (Scholtz, 1986). In addition, sand deposits in the form of dunes and lunettes have revealed the dominance of prevailing winds during certain periods of the Holocene along the southern Cape coastal

plain (Fig. 1.1) (Carr et al., 2010, 2006a, 2006b; Jerardino, 1995). These records and many more have provided some details of long-term environmental and climatic changes experienced in the region, however, most of them are either discontinuous in nature or have been sampled at a low temporal resolution or both. Additionally, the south coast has some of the most important archaeological sites in the country, these include Die Kelders (e.g. Grine et al., 1991; Avery, 1997), Pinnacle Point (e.g. Marean et al., 2000; Bar-Matthews et al., 2010), Klasies River (e.g. Deacon and Geleijnse, 1988; Thackeray, 1988), Blombos Cave (e.g. Henshilwood et al., 2001; Duller et al., 2006) and Nelson's Bay Cave (Deacon, 1978) to name a few (Fig. 1.1). The relevance of these sites to early human behaviour and habitation has been relatively well established, although the environment in which these prehistoric humans lived is still comparatively poorly resolved (Rector and Verrelli, 2010). The above mentioned factors alone provide the support for the necessity of palaeoenvironmental research, which can not only shed light on the natural variability of climatic systems but also provide evidence of the environment in which modern *Homo sapiens sapiens* evolved.

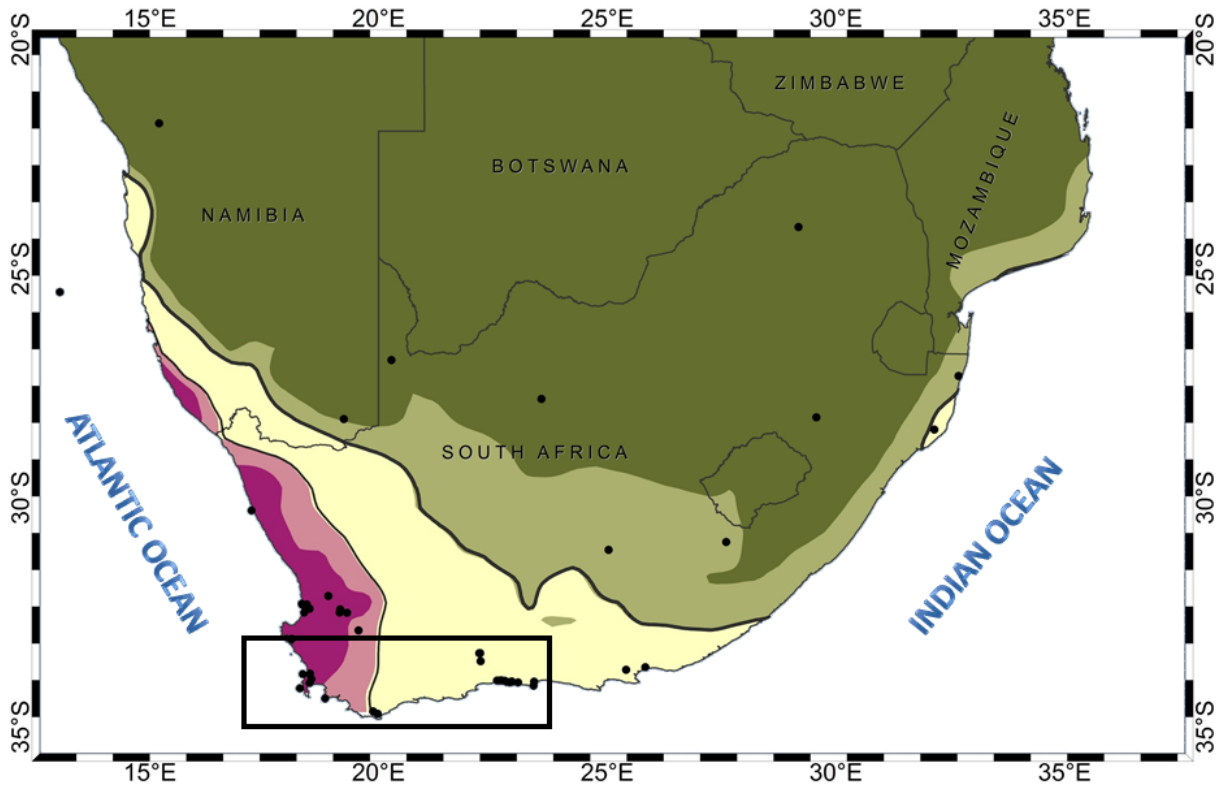

Figure 1.1: Selected southern African palaeosites across the three rainfall regimes, from west – east: winter rainfall zone (WRZ), year-round rainfall zone (YRZ) and summer rainfall zone (SRZ) also indicating the southern coast of South Africa (source: see Appendix One)

In the quest to provide a more complete picture of the changes experienced in the different regions, the past two decades has witnessed an increase in long term palaeoenvironmental studies in a number of different disciplines. This has provided a more reliable assessment of the nature and scale of the natural variability of the Earth's climate system in the broader sense, as well as the extent of human impacts on the present and future climate. Even with these advancements there are still huge gaps in our knowledge of environmental change in the late Quaternary, as well as indications of inconsistencies between different regions across the country due to diverse climatic regimes. These shortcomings warrant further investigation at greater temporal resolution. With this in mind, lakes between the towns of George and Knysna along the south coast and a lake in near Cape Town are seen as representatives of two of the three climate regimes that characterize the southern coast of South Africa, namely the year-round rainfall zone (YRZ) and the winter-rainfall zone (WRZ) (Fig. 1.1) and should provide a regional scope to the study. Additionally, these lakes are ideally situated to provide an understanding of the environment within which modern humans lived and developed in recent millennia.

1.2. RESEARCH QUESTIONS:

This project addresses the following main research objectives:

i. *What approaches are available in palaeoecology for reconstructing past communities and past environments in semi-arid regions such as the southern Cape coast of South Africa? With particular reference to which biological indicators can be used to best represent the conditions of present and past ecosystems?*
    a. *Hence, what is the potential of diatoms as sensitive indicators of past environments and climates in South Africa?*
ii. *How can palaeolimnological multi-proxy studies of lake sediments be used to determine environmental changes during the late Holocene?*
iii. *What are the defining drivers responsible for regional environmental changes across the southern Cape coastal plain during the late Holocene?*
iv. *How have these drivers changed in space and time and what are the underlying mechanisms responsible for the variability*
v. *How do local palaeo-records link up to regional and global climatic aspects, in both a spatial and temporal manner?*

1.3. AIMS AND OBJECTIVES:

This project aims to develop, against a suitably accurate chronology, an understanding of changes in the sedimentary sequence in lakes along the south and south-western coast in relation to evolution of the associated biological communities. Diatom analysis is used to determine environmental factors responsible for any observed changes. This analysis is expected to offer insight into the history of suitable coastal lakes during the Holocene, with particular reference to alterations in the physicochemical parameters of the water body.

Therefore, the main objectives of this study are:

- *Obtain sediments from selected lake sites representing YRZ and WRZ climate zones?*
- *Create a robust age model for these sediments using radiocarbon analysis*
- *Reconstruct water quality indices through quantitative and qualitative approaches, using preserved diatom fossil assemblages*
- *Relate the changes in the diatom assemblages to climatic and environmental changes*
- *Ascertain any lateral shifts in marine influences and their effects on the coastal environment*
- *Cross-examine the sites to provide a regional climate and environmental reconstruction of the late Holocene*
- *Determine the evolution of each area based on theorised environmental changes already suggested in other studies with the hope of substantiating their findings and providing a foundation for the development of the southern coast of South Africa*

The ecologically based indicator approach provides indirect evidence of changes within each respective lake catchment in addition to providing comparative insights between sites, as well as with previously published work to expand and reinforce regional palaeoenvironmental reconstructions. Recent advances in palaeolimnology that have moved it from a primarily qualitative descriptive subject with basic depictions to a quantitative analytical science provide insights into the rates of change and to natural background conditions of limnic systems (Birks, 1998). In this study, diatom fossils are used to determine which environmental factors are responsible for any recorded changes. This analysis is expected to offer insight into the development of each of the lakes during the late Holocene. The intention is to create a high temporal resolution study to present as much information as possible on patterns of climatic variability in an extremely significant environmental area.

1.4. THESIS STRUCTURE:

- The intention of the above introduction is to present a framework on which this project is based; in essence, this establishes the fundamental principles required and the need for palaeo-based studies particularly in South Africa.
- A review of the literature available for the study sites is presented in ***Chapter Two***, outlining the contemporary setting and geological development of the physical environment in the region, based on climate, relief and ecology.
- ***Chapter Three*** investigates the importance of lakes and the broad application of diatoms as proxies to environmental change.
- ***Chapter Four*** describes the methods employed in the study and their relevance to the current study. The chapter concentrates on the coring methods undertaken to retrieve the sediments from the individual sites and the preparation of subsamples to isolate the diatom fossils from the bulk sediment, as well as the statistical approached to be undertaken.
- A more detailed account of the Wilderness Region is provided in ***Chapter Five***, including a full description of statistical analysis of each diatom assemblage from the respective site, which form the basis for the interpretation of trends and observed changes are presented in ***Chapter Six***.
- The Cape Flats site, Princessvlei, is introduced and discussed in full in ***Chapter Seven***, where the development of the system is assessed over the last 2600 years and the drivers responsible are examined.
- ***Chapter Eight*** discusses the main trends and changes in underlying mechanisms evident at the two locations with respect to regional and global dynamics.
- ***Chapter Nine*** offers concluding remarks on the project as a whole and how it has addressed the research objectives and aims, as well as exploring future trends and management options for the investigated sites.

Chapter 2. THE ENVIRONMENT OF THE SOUTHERN CAPE COASTAL PLAIN

2.1. CONTEMPORARY ENVIRONMENTAL SETTING

The complex interplay of climate, geology and topography has given rise to a highly diverse vegetation matrix along the southern coastal plain of South Africa set against the Cape Fold Mountains (Fig. 2.1) (Raal and Burns, 1996). The Cape Fold Mountains are generally composed of folded quartzites and quartzitic sandstones of the Cape Supergroup, in particular the Table Mountain Sandstone, the Bokkeveld and Witteberg Groups (Mucina and Rutherford, 2006; Cowling et al., 2009). Although only of moderate elevation, reaching altitudes of 1000 – 2000m above mean sea level (AMSL), the relief is relatively steep (Cowling et al., 2009). Deeply-incised valleys are characteristic of the Cape Fold Belt, which are the product of river rejuvenation during sea level fluctuations (Mucina and Rutherford, 2006). At lower elevations and towards the coast, the base geology is predominantly of Precambrian Malmesbury Shale and Bokkeveld Groups with intrusions of the Cape Granite Suite (Mucina and Rutherford, 2006; Cowling et al., 2009). Soils derived from the Malmesbury and Bokkeveld Shale Groups range from fertile to moderately fertile with predominantly fine sand and silty textures (Mucina and Rutherford, 2006; Cowling et al., 2009). On the other hand, relatively acidic, sandy soils are commonly formed from the erosion of the sandstone and quartzite based geology (Mucina and Rutherford, 2006). Weathered Pleistocene and Holocene aeolianite dune sands occur along the west and south coast providing a buffering capacity in the form of exchangeable calcium cations with dark alluvium, rich in organic matter, located in larger river valley bottoms (Martin, 1960b; Allanson and Whitfield, 1983; Mucina and Rutherford, 2006; Cowling et al., 2009).

According to Kruger (2004a) the Cape Floristic Region (CFR) is confined to the winter and year round rainfall zones where mean annual rainfall ranges from 210mm to greater than 3000mm and where extreme temperature minima are rare, i.e. <2°C. The CFR covers 90 000km^2 and is subdivided into a western and an eastern unit, as well as a lowland and a mountain subregion (Cowling et al., 2009) (Fig. 2.1). The entire region hosts approximately 9000 vascular plants of which nearly 70% are endemic, consisting of five endemic families and 160 endemic genera (Cowling et al., 2009). Diversification appears to be centred on fire and drought-adapted lineages, with Cowling et al. (2009) arguing that the driving mechanisms for the high degree of endemism are related to the combination of cooling and

drying during the late Cenozoic and possibly based on the geomorphic evolution of the landscape. The western and eastern units broadly follow the parallel ridges of the Cape Fold Mountain range, which trends from the north to the south along the Atlantic coastline and west to east along the Indian Ocean coastline, with the former experiencing extensive deformation, folding and thrust faults and the latter showing large, gentle folding (Mucina and Rutherford, 2006; Cowling et al., 2009). The western CFR spans from Cape Agulhas to the northern extent of the Cape Fold Mountains and receives predominantly winter rainfall (Cowling et al., 1999). The eastern section receives rains almost all year round from three sources; namely frontal depressions, anticyclone ridging highs and cut-off lows (Cowling et al., 1999).

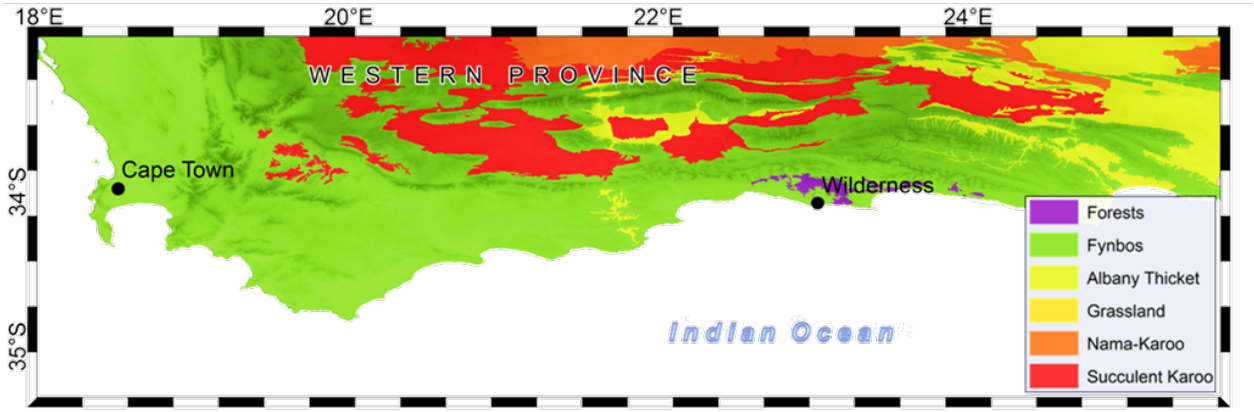

Figure 2.1: The major biomes of the southern Cape coastal plain of South Africa bounded to the north by the Cape Fold Mountains (Source: Appendix One)

The fynbos biome consists of many Mediterranean-type plant species and is considered a biological hotspot with approximately 5600 endemic plant species (Cowling, 1992; Myers et al., 2000). A diverse array of fynbos vegetation units occur along the south coast, although their continued expansion is limited by mesophytic forest elements and Albany thicket to the east and by succulent Karoo and Nama-Karoo to the north (Fig. 2.1) (Martin, 1968; Schalke, 1973; Mucina and Rutherford, 2006). The forest element at the eastern extent of the CFR is the largest and most southerly complex in southern Africa (Geldenhuys, 1993). While relic patches occur along the south coast they are confined to sheltered, moist mountain ravines and gorges (Schalke, 1973; Baxter, 1989). The Southern Afrotemperate Forest extends from Mossel Bay in the west to Humansdorp in the east and spans from an altitude of 800m on the Outeniqua and Langkloof Mountains to the coastal plain (Martin, 1968; Mucina and Rutherford, 2006). The forest complex is dominated by *Podocarpus* and *Olea* species with a well-developed understorey and several endemics interspersed by stands of mesic mountain fynbos, limestone fynbos

and coastal fynbos (Schalke, 1973; Raal and Burns, 1996; Mucina and Rutherford, 2006). Rain forest elements occur in river gorges (Martin, 1968). Unlike elements of the Cape Floristic Region, the Southern Afrotemperate Forest is classified as "Least Threatened" with many sections falling within national parks (Mucina and Rutherford, 2006).

Permanent and temporary wetlands and waterbodies occasionally occur along the coastal plain, creating aquatic micro-ecosystems. The dynamic nature of these systems is dependent on the seasonality of rainfall, resulting in highly variable aquatic plant communities through space and time (Adams and Bate, 1994). Mostly dominated by *Phragmites australis* and *Typha capensis*, the aquatic plant community is usually highly adaptive to fluctuations in salinity originating through high precipitation to evapotranspiration ratios or marine water intrusions (Adams and Bate, 1994).

2.2. OCEANIC CIRCULATION

The South African coastline is primarily bounded by two ocean currents, one originating from the equator, while the other originates from the polar region. The southern coastal plain therefore experiences the effects of the cold Benguela, eastern boundary current running along the west coast and the warm Agulhas, western boundary current, which flows along the eastern and southern coastline (Fig. 2.2) (Scott and Lee-Thorp, 2004). Both currents play significant roles in the global ocean circulation and distribution of heat to and from the equator. These ocean currents also play an important role on moisture availability to the continent (Scott and Lee-Thorp, 2004).

2.2.1. Agulhas System

The Agulhas system can be divided into three components, *viz.* the current itself, the intermediary area between the current and the present day coastline - termed the Agulhas Bank - and the leakage of Agulhas waters into the south Atlantic. The Agulhas current (AC) transports large volumes of warm, salty water southward at transport speeds of up to 70Sv (one Sverdrup (Sv) is equal to 10^6 cubic meters per second) at mean current velocities of 1 – 1.5ms^{-1} (Rouault et al., 2009). The western boundary current forms part of the wind-driven, anticyclonic Southern Indian Ocean Subtropical Gyre, of which the most southerly extent is demarcated by the subtropical front (STF) (Fig. 2.2) (Barlow et al., 2010; Beal et al., 2011). The fast moving current provides tropical and subtropical waters originating from the South Equatorial Current (SEC) and the East Madagascar Current (EMC) to the polar region (Lutjeharms et al., 2001; Backeberg et al., 2012). The AC flows parallel to the continental shelf which remains quite narrow along the east coast; before the current moves offshore as the shelf begins to broaden from 27°E to

extend nearly 250km from the present day coastline adjacent to Cape Agulhas (Schumann et al., 1995). It is near this position that the current retroflects back into the south-western Indian Ocean forming the Agulhas Return current (ARC) (Rouault, 2011). The position at which the current retroflects is dependent on the location of the subtropical front, which in turn is dependent on the expansion or contraction of the circumpolar vortex (Caley et al., 2011). An additional dimension of the current is the shedding of warm saline water from the Indian Ocean into the Atlantic Ocean (Fig. 2.2) (Beal et al., 2011; Caley et al., 2011). Recent research by Beal et al. (2011) and Caley et al. (2011) suggests that leakage into the Atlantic significantly feeds into the surface arm of the Atlantic Meridional Overturning Circulation (AMOC) influencing its strength and stability. Lutjeharms et al. (2001) also add that ring propogation affects sea surface temperatures in regions that influence rainfall over South Africa. Ring shedding is governed by the Indian Ocean Dipole and El Niño–Southern Oscillation (ENSO) events (Beal et al., 2011). During periods where a northward migration of the STF occurs, the current retroflects further east leading to a diminished or even a complete shutdown of leakage into the Atlantic, as well as altering the circulation of the subtropical gyre, the converse is also true (Caley et al., 2011; Backeberg et al., 2012) .

Seasonal to millennial-scale variability in the current is still relatively unknown, although the current is primarily driven by high latitude climate mechanisms and wind stress curl between the westerlies and the easterlies (Beal et al., 2011; Caley et al., 2011). Backeberg et al. (2012) have shown that the southern arm of the Agulhas current has become more variable in the last two decades as easterly winds have intensified, causing an increase in eddies from the Mozambique Channel and the SEC. These eddies result in a shift in energy contained within the current, providing an increase in water transportation and a more turbulent AC (Backeberg et al., 2012). In contrast, the strength of the AC diminishes relative to the weakening of the wind patterns (Caley et al., 2011). Hence, the position and strength of either of the latter wind systems directly influences the flow dynamics of the system (Backeberg et al., 2012).

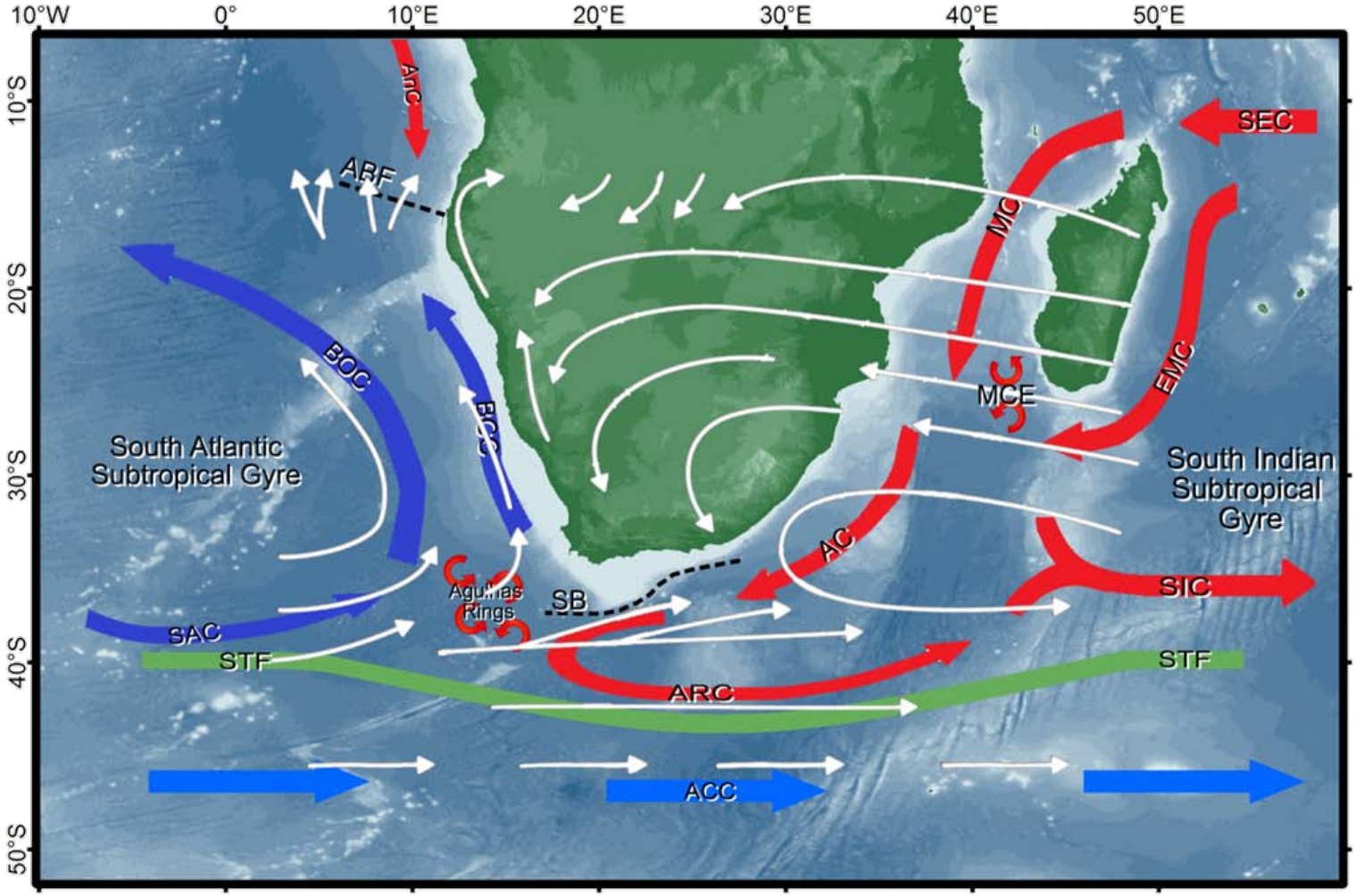

Figure 2.2: Generalised schematic of major atmospheric (white) and oceanic circulation (warm currents = red, cold currents = blue) across southern Africa. AnC = Angola Current, SEC = South Equatorial Current, MC = Mozambique Current, MCE = Mozambique Current Eddies, EMC = East Madagascar Current, AC = Agulhas Current, ARC = Agulhas Return Current, SIC = South Indian Ocean Current, STF = Subtropical Front, ACC = Antarctic Circumpolar Current, SAC = South Atlantic Current, BOC = Benguela Ocean Current, BCC = Benguela Coastal Current, SB = southern boundary, ABF = Angola-Benguela Front (Source: see Appendix One)

2.2.2. Benguela System

The Benguela system, on the other hand, is an eastern boundary current of the South Atlantic Gyre (Romero et al., 2002). It is bordered to the north by the Angola-Benguela Front (ABF), which separates the Benguela system from the Angola current, while the Agulhas retroflection at Cape Agulhas provides a southerly boundary for the Benguela current (Fig. 2.2) (Lutjeharms et al., 2001). However, the southerly boundary is not fixed, and it has been suggested that at times incursions of cold ocean water can reach as far east as Knysna (Schalke, 1973). Essentially, the Benguela Upwelling System (BUS) can be defined as the wind-driven vertical upward movement of nutrient-rich, cold Antarctic deep waters to the surface along the west coast (Schalke, 1973; Schumann et al., 1982; Romero et al., 2002). Furthermore, the system is subdivided into the southern Benguela region and the northern Benguela region based on the location of the Luderitz upwelling cell (Romero et al., 2002). The northern region experiences a year-round upwelling regime, whereas the southern region is more seasonal (Farmer et al., 2005).

Both currents are driven by mesoscale and submesoscale wind processes and play a pivotal role in the global thermohaline circulation (Rouault et al., 2009; Beal et al., 2011). Rouault (2011) has shown that in the last three decades both currents have warmed by up to 1.5°C as well as but to a lesser degree, coastal cooling occurring from Cape Agulhas to the Namibian border due to the intensification of atmospheric circulation at relevant latitudes. This trend has knock on effects for both ocean and atmospheric circulation, primarily through the increase in transportation of warm, salty waters into the Atlantic influencing the AMOC and North Atlantic Deep Water formation (Biastoch et al., 2009).

2.3. CONTEMPORARY CLIMATE DYNAMICS

The climate across South Africa is the result of the dynamic interplay between atmospheric and oceanic circulation. Their interaction has given rise to three rainfall regimes, namely the winter rainfall zone (WRZ), the summer rainfall zone (SRZ) and a transitional zone between the latter two, which receives rainfall throughout the year and termed the year-round rainfall zone (YRZ) (Tyson, 1999; Scott and Lee-Thorp, 2004). The generally accepted demarcation of the zones is related to the percentage allocation of rainfall that a region receives during a given period. The south-western tip of Africa receives more than 66% of its rainfall during the austral winter months defining the boundary between the WRZ and the YRZ (Meadows and Baxter, 1999 as cited by Carr et al. 2006a). The WRZ boundary is the theoretical limit for the influences of tropical and subtropical atmospheric related climatic disturbances (Carr et al. 2006b).

Presently, the most easterly position of the WRZ boundary is located at the most southerly tip of the continent where the Agulhas Current and the Benguela current meet (Carr et al., 2006b). The rest of the country falls within the SRZ with the exception of a small region localised predominantly along the south coast, which experiences climatic anomalies associated from both the WRZ and the SRZ climate processes (Tyson, 1999).

2.3.1. Ocean-to-Atmosphere Feedbacks

In general, climate in southern Africa is an expression of two competing systems, the westerly winds and their associated oceanic feedbacks and easterly winds and their accompanying oceanic influences (Fig. 2.2) (Chase and Meadows, 2007). The prevailing climate patterns are therefore a direct consequence of the interaction of these circulation features (Nicholson, 2000). The position and impact of these competing wind patterns on the subcontinent is relative to the placement of a discontinuous high pressure belt located at approximately 30°S (Kruger, 2002; Kruger, 2004a). The belt consists of the South Atlantic High Pressure cell (SAHP) and the South Indian High Pressure cell (SIHP) positioned on either side of the continent and experiences a N-S seasonal displacement of four to six degrees (Schalke, 1973; Kruger, 2002).

During the austral summer, the South Atlantic high pressure cell draws close to the west coast of southern Africa providing an influx of dry air from the southwest, while the eastward movement of South Indian high pressure cell serves as a source of humid air from the east and southeast (Kruger, 2004a). As these high pressure cells converge the humid air is uplifted over the dry air, creating a moisture boundary and causing widespread rainfall over the interior (Kruger, 2004a). Easterly winds develop along the south coast as the South Atlantic Anticyclone ridges eastwards, promoting upwelling on the Agulhas Bank (Schumann et al., 1982). The south coast is not known as a major upwelling region but does experience short-lived events driven by easterly winds, which are more prevalent during summer and autumn (Cohen and Tyson, 1995; Barlow et al., 2010). Upwelling of cold South Indian Central Water is isolated to the capes along the south coast and thereafter propagates westward into the bays (Schumann et al., 1982; Cohen and Tyson, 1995; Schumann et al., 1995). The onset of upwelling can proceed rather rapidly as waters pass from the narrow shelf edge to the wider shelf increasing bottom stress on the current and leading to a drop in water temperatures of up to 8°C within hours (Cohen and Tyson, 1995; Schumann et al., 1995; Lutjeharms et al., 2001; Barlow et al., 2010).

The poleward displacement of the anticyclones assists in the southward expansion of the tropical easterly winds, which are fuelled by increased sea surface temperatures in the Indian Ocean and solar insolation (Backeberg et al., 2012). A significant moisture potential related to high evaporation over the Agulhas Current is an artefact of the character of the western boundary current which experiences high land-sea flux (Beal et al., 2011). The advection of this moisture potential from the southeast towards the coast is a considerable source of summer rainfall (Carr et al. 2006b). Additionally, the southern Benguela experiences major upwelling during the austral spring and summer months, when prevailing tropical easterlies promote alongshore winds (Romero et al., 2002, 2003). The duration and intensity of upwelling, as well as the displacement of the upwelled water offshore, is relative to the latitudinal position and strength of the tropical easterly wind system (Romero et al., 2003). During these events sea surface temperatures (SST) can drop by up to 5°C, while during the winter months SST remain low due to low insolation and stormy weather (Schumann et al., 1982; Romero et al., 2002). The Benguela Upwelling System (BUS) has a profound effect on the adjacent coastal region, which experiences widespread aridity and seasonal diurnal fog which can extend 20-30km inland (Schalke, 1973; Scott and Lee-Thorp, 2004).

The winter migration of the high pressure cells westward and equatorward allows for weather systems generated over the Southern Ocean to infiltrate the South African coast (Lutjeharms et al., 2001; Kruger, 2004a). During this period the westerly winds expand to 35°S at sea level (Schalke, 1973). This migration allows for the penetration of rain-bearing frontal systems embedded in the circumpolar westerlies to reach southern Africa (Schumann et al., 1995; Cowling et al., 1999; Nicholson, 2000). The cold fronts bring overcast conditions to the south-western parts of the subcontinent, providing the region with its primary source of precipitation (Kruger, 2004a). The dominance of westerly winds during the austral winter maintains turnover of surface waters on the Agulhas Bank, creating a thoroughly mixed and homogeneous water column extending 10 to 20m in depth, which overlies cooler, deeper waters leading to a drop in water temperatures (Schumann et al., 1995; Barlow et al., 2010). Advection of warm surface plumes towards the south coast also takes place when south-easterly winds prevail during this time (Cohen and Tyson, 1995; Schumann et al., 1995). Conversely, in summer a thermocline develops creating a boundary between warm surface waters and cool deeper waters (Schumann et al., 1982). A surface frontal zone results when the thermocline breaks the surface providing cooler water to the landward side of the zone (Schumann et al., 1982); coupled by frequent onshore winds which bring in warm and salty water to the Agulhas Bank area (Lutjeharms et al., 2001).

Variability in the position and strength of the high pressure belt, as well as in the westerly winds, are the main underlying mechanisms in interannual SST change on the Agulhas Bank (Cohen and Tyson, 1995). Hence, annual water temperature on the Agulhas Bank generally ranges from 14°C in winter to 20°C in summer but can drop to 10°C during upwelling events (Cohen and Tyson, 1995). These wind systems have resulted in the high wave energy producing wave-dominant estuaries along the southern coast (Bateman et al., 2011), promoting primary productivity, which is greater during cooler water period, particularly in autumn and winter with peaks occurring in summer during upwelling events (Schumann et al., 1982; Barlow et al., 2010).

The lateral shift of the high pressure cells along a west to east transect influences atmospheric circulation and wind patterns on a synoptic scale (Kruger, 2004a, 2004b). Along the south-western to southern coast the shift of the systems results in winds from the south-to-south-east in summer and the north-to-north-west in winter (Schalke, 1973). Strong winds are frequent particularly along the coast, with the windiest conditions most prevalent during the months from October to January and calm winds occurring during May (Schalke, 1973; Kruger, 2002). However, land and sea breezes can dominate on a local scale at coastal sites (Kruger, 2002).

2.3.2. Long-term Climate Variability

Long-term climate variability stems from the teleconnectivity between the mid-latitudes to the latitudinal shifts of high latitude climate processes. In relation to the SRZ, Cohen and Tyson (1995) propose two extreme alternative climatic states, namely an extended cool, dry condition and an extended warm, wet condition, although transitional phases between these two extremes can occur (Fig. 2.3). The extended cool, dry period relates to the expansion of the circumpolar vortex, leading to the enhanced influence of the westerlies over South Africa while weakening and forcing the high pressure cells further northward (Cohen and Tyson, 1995). This would result in an increase in frontal systems to the south-western coast of southern Africa coupled by a decline in summer rainfall (Cohen and Tyson, 1995). As both ocean current systems are influenced by the anticyclones, the displacement of the weakened HP cells would cause a weaker flow of the Agulhas current, while increasing warm water surface plumes toward the south coast, hence raising sea surface temperatures on the Agulhas Bank (Cohen and Tyson, 1995). Additionally, a decline in upwelling in the Benguela current in response to the decrease in intensity of the easterlies occurs (Cohen and Tyson, 1995).

On the other hand, during extended warm, wet periods the circumpolar vortex contracts southwards, displacing the westerlies with it and minimising coastal contact of frontal depressions (Cohen and Tyson, 1995). With weakened westerlies, the anticyclones over the South Atlantic and South Indian strengthen, enhancing in the influence of the easterlies (Cohen and Tyson, 1995). The prolonged dominance of the easterly winds provides a constant supply of tropical, humid air leading to an increase in summer rainfall (Cohen and Tyson, 1995). The intensification of the easterlies supports increased water transport through the Agulhas system and amplifies upwelling events in both the Benguela and the Agulhas currents, leading to lower sea surface temperatures along the South African coast (Cohen and Tyson, 1995).

The conceptual model hypothesised by Cohen and Tyson (1995) and outlined above was used by the authors as a means to explain global climate changes experienced in southern Africa, such as the Little Ice Age and the Medieval Climate Anomaly. However, Tyson (1999, p. 194) identifies several other controlling factors that play a significant role in atmospheric circulation and consequently climate. These are as follows: a) the latitudinal displacement and/or intensification of the high pressure belt, which affects the distribution and amount of precipitation a region receives, as well as the wind patterns over the subcontinent, primarily through the deflection of rain-bearing mid-latitude cyclones, from the coast; b) the "longitudinal displacement of major cloud bands" is linked to the development of tropical-temperate troughs (TTT) between the equator and the mid-latitudes leading to wet conditions along the band; c) a change in the **"**planetary-waves configuration" can shift zones of convergence and divergence longitudinally across the subcontinent resulting in shifts in precipitation patterns. Essentially, Tyson (1999) outlined the fact that changes in sea surface temperatures, moisture source areas, transport patterns and land-to-atmosphere feedbacks are factors leading to changes in the prevailing patterns in climate (Nicholson, 2000; Rouault, 2011). These factors are prevalent at a range of time scales from seasonal, short-term and long-term temporal scales.

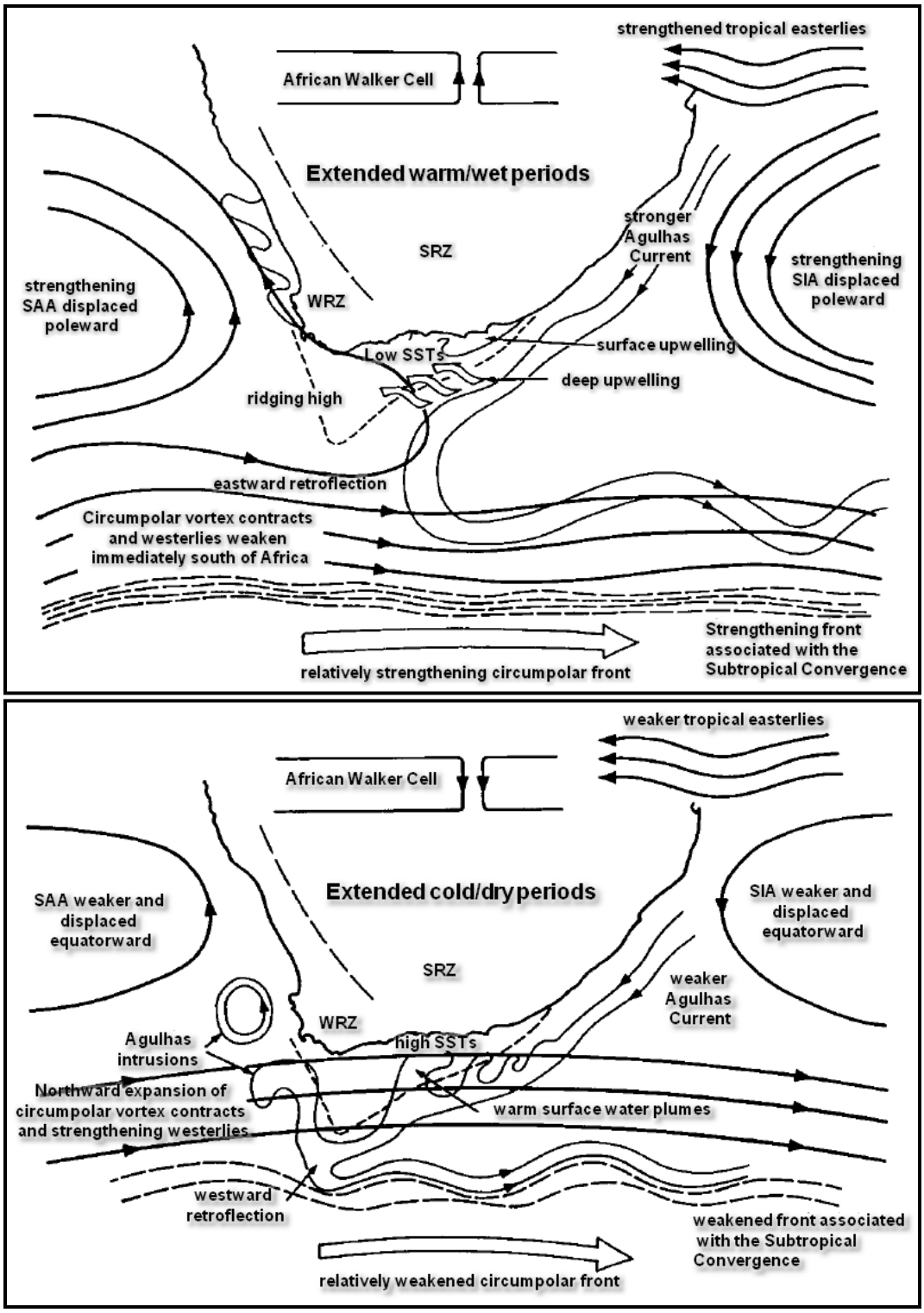

Figure 2.3: A conceptual model of the response of oceanic circulation and coastal sea surface temperatures (SST) to atmospheric circulation anomalies responsible for extended wet spells (A) and extended dry spells (B) in South Africa (after Cohen and Tyson, 1995).

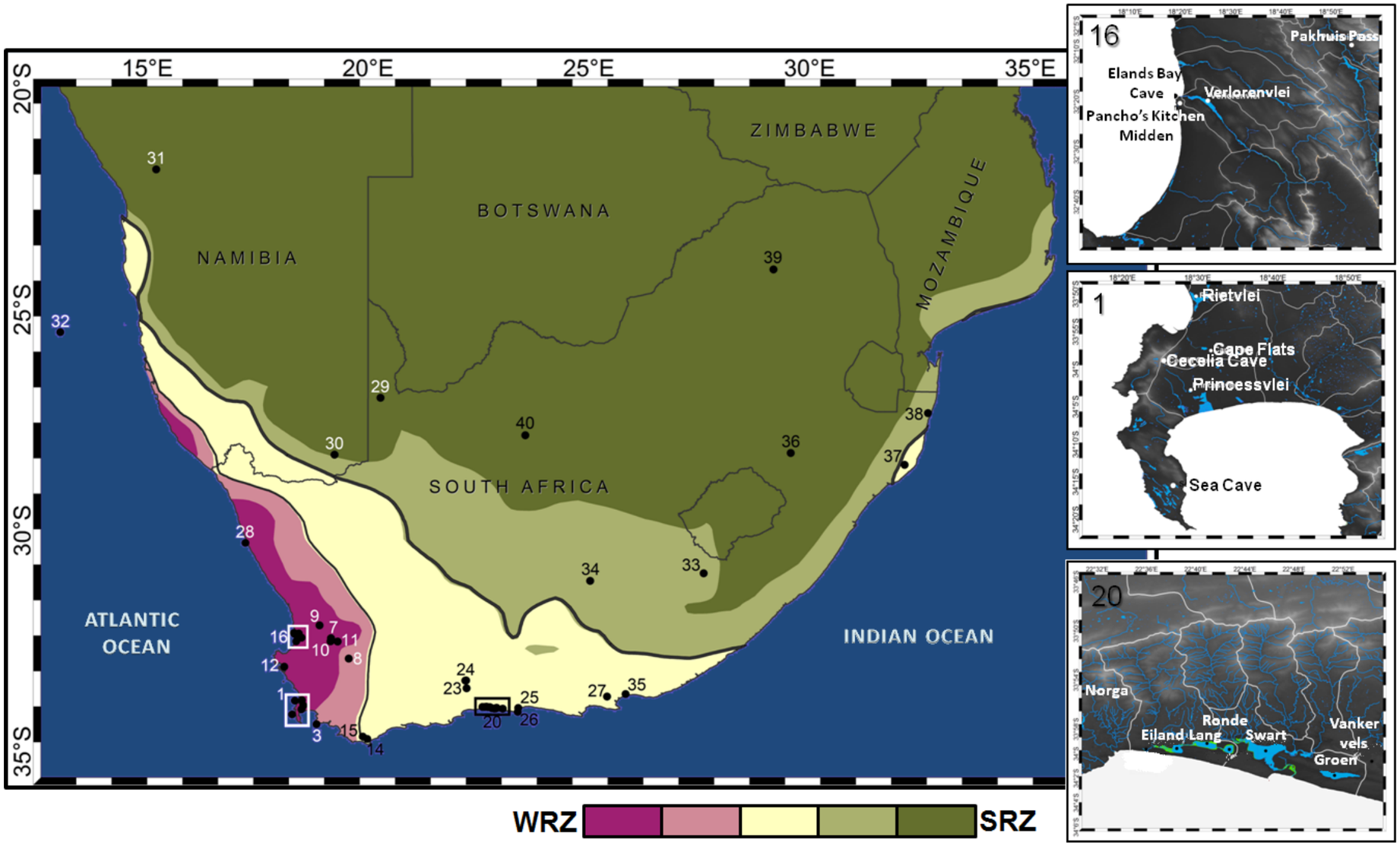

1. Cape Flats (inset)	7. Driehoek	14. Soetendalsvlei	20. Wilderness Lakes (inset)	25. Keurbooms Estuary/strand	30. Austerlitz	36. Braamhoek
Cecilia Cave	8. Katbakkies Pass	15. Voelvlei	Swartvlei Complex	26. Nelson Bay Cave	31. Klein Spitzkoppe	37. Lake Eteza
Princessvlei	9. Pakhuis Pass	16. Verlorenvlei (inset)	Vankervelsvlei	27. Uitenhage Aquifer	32. ODP 1084B	38. Lake Sibaya
Rietvlei	10. Sneeuberg	Pancho's Kitchen	Norga	28. Spoeg River Cave	33. Barkly East District	39. Cold Air Cave
Sea Cave	11. Tuitjes Kraal	Langdam	23. Boomplaas Cave	29. Kalahari salt pans	34. Blydefontein Basin	40. Wonderwerk Cave
3. Hangklip	12. Langebaan Lagoon	Elands Bay Cave	24. Cango Cave		35. Algoa Dunefields	

Figure 2.4: Distribution of palaeo-sites across southern Africa discussed in text with respect to rainfall regimes, the demarcation of the rainfall zones are based on the percentage rainfall received over the course of the year. Winter rainfall = shades of pink, Year-round rainfall = yellow, Summer rainfall zone = shades of green (sources: see Appendix One).

2.4. LATE HOLOCENE PALAEOENVIRONMENT

The palaeoenvironmental record for South Africa is both temporally and spatially fragmented (Fig. 2.4). In particular, the late Holocene has only been described in general terms, with a poor characterization of microscale fluctuations in climate the poor temporal resolution of most records, as well as a poorly resolved chronology at sites. In contrast, global research has shown that the Holocene has been anything but stable with four notable periods of rapid climate change occurring, namely 9 – 8ka[1], 6 – 5ka, 3.5 – 2.5ka and the last 600 years (Mayewski et al., 2004). Additionally, some evidence exists for discreet climatic events, such as those occurring between 4.2 – 3.8ka and between 1.2 – 1.0ka (Mayewski et al., 2004). The postulated mechanisms responsible for the aforementioned events are manifold - from solar variability to bipolar cooling and/or regional glacier advances (Mayewski et al., 2004). Although the South African record is sparse and intermittent, some evidence is available to support the occurrence of rapid climate change events that are coincident with global trends. The following section reviews the palaeoenvironment during the late Holocene. With respect to this review, the late Holocene is regarded as the last 4000 years; hypothesised mechanisms, as well as the effects of climatic anomalies in each respective rainfall zone are presented. The information presented below is summarised in tabular form in Appendix 3.

2.4.1. Palaeoclimate

Winter Rainfall Zone (WRZ)

The relative scarcity of high resolution records from the winter rainfall region has given rise to many generalised and sweeping statements about the climate during the Holocene and in particular the late Holocene. For instance, analysis of the terrigenous fraction of sediments recovered from the marine core, MD96-2094 on the Walvis Ridge characterised the entire Holocene epoch as a period of low trade wind intensity coupled with low winter rainfall (Stuut et al., 2002, 2004). Pollen sequences from lake sediments from Sneeuberg and Driehoek in the Cederberg Mountains suggested relatively little vegetation change throughout the Holocene (Meadows and Sugden, 1993; Meadows and Baxter, 1999), whereas charcoal analysis at Elands Bay Cave indicated a general dominance of xeric shrub over the last 4000 years (Cartwright and Parkington, 1997; Cowling et al., 1999).

A few records do exist that provide greater detail about climate variability during the late Holocene (e.g. Cohen et al., 1992; Miller et al., 1993; Miller et al., 1995; Jerardino, 1997; Scott and Woodborne, 2007).

[1] Unless otherwise stated all ages mentioned are calibrated (cal years BP before 1950)

Most records from the winter rainfall region suggested a generally cooler and wetter period spanning from 4000 – 2000 cal yrs BP. Peat accumulation and humic soil development was initiated or renewed from 5000 – 3500 cal yrs BP in most regions across the country, suggesting a consistent supply of rainfall over the region and a relatively moist phase (Meadows, 1988; Hassan, 1997). The proposed wetter and cooler period was corroborated by Baxter (1989), who analysed cave sediments at Cecilia Cave on Table Mountain and found an abundance of Ericaceae, Restionaceae and Iridaceae - typical Fynbos indicators - and minimal Poaceae pollen, interpreting this as a sign of increased moisture between 4000 and 2000 cal yrs BP (Fig. 2.4, inset 1). Research conducted along the west coast of South Africa at such sites as Langdam, Elands Bay Cave and Spring Cave has identified periods of increased aeolian activity and sand movement during the late Holocene, particularly between 4000 and 3000 cal yrs BP, with large scale sand deposition concluding by ~2300 cal yrs BP (Fig. 2.4, inset 16) (Miller et al., 1995, 1993; Jerardino, 1997; Chase, 2005). Dune building at Table Bay and St Helena Bay mimicked the development witnessed in the Elands Bay area, with the initial phase of aeolian deposition occurring between 3800 and 2800 cal yrs BP (Miller et al., 1993). Miller et al. (1995) attributed the enhanced sand movement to sea level fluctuations and coastal sediment instability. However, Schalke (1973) suggested that increased aeolian activity between 5800 – 1580 cal yrs BP at Hangklip further to the south was an indicator for drier conditions.

Fossil pollen preserved in a hyrax midden from Pakhuis Pass in the Cederberg Mountains showed an increase in succulents and a decline in arboreal pollen, coupled with an enrichment in stable carbon isotopes, between 5000 and 2000 cal yrs BP, which implied cooler conditions with peaks in moisture availability at 2800 and 2000 cal yrs BP (Scott and Woodborne, 2007), where moisture availability refers to an increase in precipitation or a surplus in the moisture budget. An additional hyrax midden record from the nearby Katbakkies Pass showed high Asteraceae with a decline in Cyperaceae and peaks in Podocarpaceae from 3500 to 1600 cal yrs BP, followed by an increase in Cyperaceae until 600 cal yrs BP (Meadows et al., 2010). Hence, the Katbakkies Pass sequence suggested marginally wetter conditions between 2400 and 1300 cal yrs BP, however the overarching trend of the Katbakkies record is a shift to xeric conditions after 3600 cal yrs BP with fluctuating moisture availability (Meadows et al., 2010). A hyrax midden from De Rif, also in the Cederberg Mountains, used a multiproxy approach to interpret climatic fluctuations during the Holocene including pollen, stable isotope and charcoal analysis (Valsecchi et al., 2013). This study argued for generally dry conditions for most of the late Holocene, with brief periods of increased humidity at ~4600, 3200 and 2200 cal yrs BP (Valsecchi et al., 2013). Pollen deposits at Princessvlei, a small coastal lake on the Cape Flats, limited this wet episode to 3400 –

2600 cal yrs BP, which coincided with a higher sea level until 2500 cal yrs BP as interpreted by the increase in occurrence of *Morella* (Neumann et al., 2011). On either side of this 800 year moist period are two relatively dry episodes, which occurred at 4200 – 3500 cal yrs BP and 2500 – 1900 cal yrs BP (Neumann et al., 2011). During the latter dry period, an increase in *Crassula* pollen was observed in the record; the genus *Crassula* contains many succulent species that favour dry environments (Neumann et al., 2011). Additionally, evidence from the Klaarfontein spring deposits, near Verlorenvlei, substantiated a drier climate between 6000 and 3500 cal yrs BP as poor pollen preservation was interpreted as an indicator for the cessation of spring flow during this time (Fig. 2.4, inset 16) (Meadows and Baxter, 1999). Substantial fossil pollen preservation at the spring from 3500 to 2000 cal yrs BP suggested possibly wetter conditions promoting afromontane and scrub elements in sheltered ravines (Meadows and Baxter, 1999).

Baxter (1989) further reported minor oscillations in Ericaceae and Fabaceae, with a continued dominance of Asteraceae, at Cecelia Cave from 2000 to 400 cal yrs BP. However, the Cecelia Cave deposits were highly discontinuous, providing only a fragmented understanding of the climatic trends for the entire expanse of the record. From 2000 to 1500 cal yrs BP, the Klaarfontein record proposed a drier climate at the site promoting saline conditions and possibly a marine transgression (Meadows and Baxter, 2001). Relative stability in heterogeneous vegetation composition prevailed at Elands Bay Cave from 1400 – 320 cal yrs BP, dominated by xeric thicket/Asteraceous shrubland community complex (Cowling et al., 1999). The Pakhuis Pass $\delta^{13}C$ signal progressively declined from 2000 to 1200 cal yrs BP coupled with an increase in the representation of fynbos taxa, until a short-lived dry interval occurred between 1300 and 1100 cal yrs BP (Scott and Woodborne, 2007). Furthermore, a brief episode of dune formation along the False Bay coast at 1680±100 yrs BP suggested a dominance of south–south-easterly winds, which is a prerequisite for dune building in the area (Roberts et al., 2009). Winds from the southerly quadrant are fuelled by the ridging of the anticyclones as they draw toward the South African coast particularly during the summer months, which may validate the arid spell in the Klaarfontein record. Although xeric conditions prevailed at Hangklip until ±1580 cal yrs BP, Schalke (1973) suggested alternating humid–dry phases subsequently, continuing until present. However, an increase in indicator species for damp environments such as *Carpacoce*, Cyperaceae and Ericaceae, is observed at Princessvlei from 1900 to 1000 cal yrs BP, after which a hiatus in sedimentation obstructs climatic interpretation until the record resumed at 350 cal yrs ago (Neumann et al., 2011). A high-resolution diatom record from Verlorenvlei showed an intricate link between dilute, planktonic species and river runoff, which tied into the advancement and retreat of the westerly belt (Fig. 2.5) (Stager et al., 2012).

Thereby, Stager et al. (2012) identified an initial wet phase from 1400 to 1200 cal yrs BP, implying a slight increase in the precipitation-evaporation index, after which rainfall declined until 960 cal yrs BP (Stager et al., 2012).

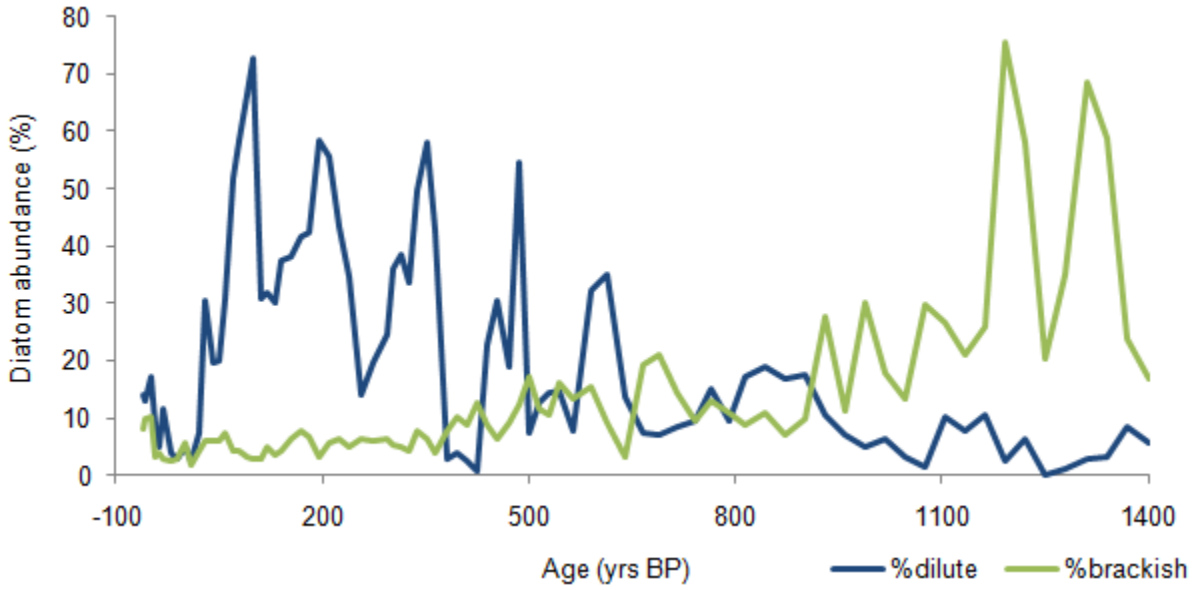

Figure 2.5: A 1400 year record of diatom abundance at Verlorenvlei (data source: Stager et al., 2012)

Scott and Woodborne (2007) maintained that a moist climate prevailed at Pakhuis Pass between 1000 and 400 cal yrs BP, which overlaps and correlates with the Verlorenvlei diatom record for the later stages, which proposed generally wetter conditions for at least the last 700 years as westerly winds advanced equatorward (Stager et al., 2012). This period corresponded to the global cooling event termed the Little Ice Age (LIA). Tyson and Lindesay (1992) reviewed available records for southern Africa and determined that the expression of the LIA across the subcontinent was in response to the expansion of the circumpolar vortex and the increased occurrence of frontal depressions, as well as weakened easterly flow. Although a generally cooler climate prevailed throughout the LIA, conditions were far from stable and uniform (Tyson and Lindesay, 1992). The LIA is commonly divided into two phases, the first occurring from ca. 700 – 500 cal yrs BP and the second from 325 – 125 cal yrs BP separated by a sudden warmer interval from ca. 500 to 325 cal yrs BP (Tyson and Lindesay, 1992). Both cooler phases of the LIA correspond to periods of reduced solar activity, namely the Spörer minimum and the Maunder minimum (Stuiver, 1980; Eddy, 1983). The Spörer minimum lasted for 110 years from 550 – 440 cal yrs BP and may be the result of reduced sunspot activity (Eddy, 1976; Jiang and Xu, 1986). In contrast, the Maunder minimum lasted for 70 years from 305 – 235 cal yrs BP when the sun's radiative output was

reduced and advances in local glaciers were observed globally (Eddy, 1976; Mayewski et al., 2004). Analysis of tree rings of *Widdringtonia cedarbergensis* from Die Bos in the Cederberg region identified a quasi-18 year oscillation in the 370 year record and showcased the transition from the warm phase into the second cooling phase (Dunwiddie and LaMarche, 1980). Below-normal growth was shown between 370 to 330 cal yrs BP, but above-normal growth occurred from 330 – 230 cal yrs BP (Dunwiddie and LaMarche, 1980; Tyson, 1991). An abundance of Poaceae in the pollen spectra from Verlorenvlei between 300 and 200 cal yrs BP provided some substance to a warmer and possibly drier spell mid-LIA in the WRZ (Meadows et al., 1996). A high evaporation index coupled with increased marine influences may have assisted in hypersaline conditions at the vlei during this time (Meadows et al., 1996). However, through an analysis of a series of cores taken from the length of Verlorenvlei, Meadows et al. (1996) determined a progressive retreat of saline conditions from c. 300 cal yrs BP, before the vlei reverted to freshwater conditions with emergent reeds colonising the banks. The climatic influences imprinted in the surface deposits from Verlorenvlei show a growing anthropogenic influence with farming pursuits being the most prevalent, through overgrazing and pastoralism (Meadows et al., 1996). Stager et al. (2012) supported the Meadows et al. (1996) interpretation showing that peaks in dilute diatom taxa, a proxy for increased precipitation are centred at ~600, 530, 470, 330, 200, 90 and 20 cal yrs BP in the Verlorenvlei record.

The winter rainfall zone has experienced some major fluctuations in moisture availability and temperature during the late Holocene, linked primarily to the strength of the westerlies in the polar region but also to external forcings such as solar variability. However, very little is still known about the timing of events and the influence of changing climatic forcings in a highly sensitive and biologically diverse area.

Year-round Rainfall Zone (YRZ)

Scholtz (1986) postulated that the commencement of year-round rainfall along the south coast occurred from about 4000 cal yrs BP with the initiation of peat formation at Norga, near George. This surplus of moisture assisted in forest spread near Norga between 4000 and 2600 cal yrs BP (Figure 2.4, inset 20) (Scholtz, 1986). Although the region receives rainfall throughout the year, a tendency towards a more winter rainfall seasonality between 5000 and 2000 cal yrs BP is suggested from the Cango Cave speleothem record, which showed a gradual increase from -8.05‰ $\delta^{13}C$ at 5000 cal yrs BP to a maximum of -4.68‰ $\delta^{13}C$ at ~2000 cal yrs BP (Talma and Vogel, 1992; Jerardino, 1995). The Cango Cave $\delta^{18}O$ stalagmite sequence recorded a generally warmer episode from 4500 to 3400 cal yrs BP as temperatures

fluctuated by about 1°C (Talma and Vogel, 1992). Thereafter, a sharp decline in average temperature occurred within two hundred years from ~3550 cal yrs BP to 3350 cal yrs BP (Talma and Vogel, 1992). Temperatures remained relatively low between 3350 and 2500 cal yrs BP before steadily increasing and peaking by 2100 cal yrs BP (Fig. 2.6) (Talma and Vogel, 1992).

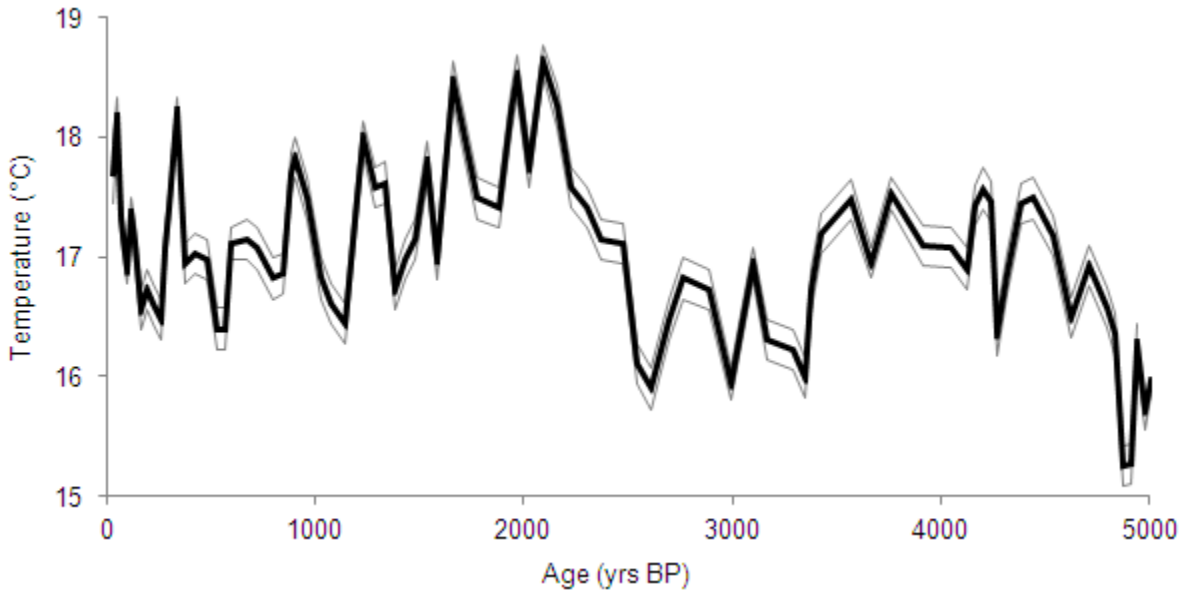

Figure 2.6: late Holocene temperature curve with standard deviation derived from the Cango Cave $\delta^{18}O$ stalagmite sequence (Source: Talma and Vogel, 1992, Pg 208)

Concurrently, extensive aeolian deposition and dune instability in the Wilderness region and at Cape Agulhas occurred from 3700 – 2400 cal yrs BP and 2800 – 2500 cal yrs BP, respectively (Martin, 1968; Carr et al., 2006a; 2006b; Bateman et al., 2011). Westerly winds are the primary mechanism in dune building along the south coast (Bateman et al., 2011). The proposal by Bateman et al. (2011) of enhanced westerly winds between 3700 and 2400 cal yrs BP supports the dominance of a winter rainfall seasonality along the south coast, as hypothesised by Talma and Vogel (1992). In contrast, Carr et al. (2006a, 2006b) suggested that the predominance of westerly winds responsible for lunette accretion between 2800 and 2500 cal yrs BP at Cape Agulhas implied a drier climate. This interpretation correlates with the Norga peat sequence where a decline in forest taxa is evident from 2600 to 1400 cal yrs BP, which was attributed to the dominance of dry, winter winds leading to a cooler but drier environment (Scholtz, 1986). In contrast, Deacon (1995) interpreted the $\delta^{13}C$ record from Cango Caves as a transition from winter rainfall seasonality prior to 3000 cal yrs BP to a summer rainfall seasonality between 3000 and 2000 cal yrs BP. Deacon (1995) reasoned that the increase in $\delta^{13}C$ was due to the advance of C4 grasses in response to higher summer temperature; this trend is reiterated by Scott and Lee-Thorp

(2004). Deacon (1995) attributed the shift in rainfall seasonality in the Cango Valley to the strengthening of the anticyclones, which promoted summer precipitation (Deacon, 1995). Directly to the south of the Cango Valley lies the Wilderness Embayment, where an array of analyses was conducted by ARH Martin in the 1950s (Table 2.1). Martin (1968) speculated that it was the extensive sand movement that restricted forest spread between 7000 and 2000 cal yrs BP, as a high percentage of Chenopodiaceae and Restionaceae in the pollen sequence from Groenvlei indicated a high water table (Table 2.1). A decline in sand movement from 2500 cal yrs BP promoted the development of dune heath, leading to a stabilisation in dune activity, before an increase in scrub species occurred in the region at 2000 cal yrs BP (Martin, 1968). The inner lunette at Voelvlei, near Cape Agulhas, suffered from the effects of water erosion at 2000 cal yrs BP as water levels in the vlei rose rapidly; thereafter the region experienced a relatively dry climate (Carr et al., 2006a). This widespread but relatively brief climatic event centred on ~2000 cal yrs BP occurs in several other records other than those mentioned previously, including Lee-Thorp et al. (2001), Scott et al. (2005), Scott and Woodborne (2007), as well as Talma and Vogel (1992) who reported an abrupt decline in temperature by 1°C at ~2050 cal yrs BP (Fig. 2.6).

Table 2.1: Environmental evolution and accompanying climatic influences for the Wilderness region by Martin (1959, 1962, 1968) based on sediment cores extracted from Groenvlei

Years BP	Depth (cm)	Pollen Zones	Vegetation	Diatom Zones	Lake Evolution	Climate	
	25	C3	Clearance of Forest	P2	Peat Formation	Drier (?)	
			Regression (?)				
1000		C2	Forest Spread	F2 (25 - 294)	Freshwater calcareous lake	More effective moisture, conducive to forest spread	
1905 ± 60							
2000		C1	Scrub spread				
	300					*Alternative 1*	*Alternative 2*
			Dune heath	L2 (294 - 350)	Lagoon stage II less saline (Campylodiscus clypeus/Tropidoneis)		
3000							
	350		Unstable Dunes		Lagoon Stage I (Tropidoneis/Navicula yarrensis)	Probably rather dry, or hotter; not conducive to forest spread	Climate possibly wetter; vegetation cover restricted by sand movement
4000				L1 (350 - 395)			
		B3	Forest restricted				
5000	400				Marine Stage II temperate diatoms		
			(Increased Chenopodiaceae and Restionaceae in valleys and flats	M2 (395 - 440)			
6000					Marine stage I warmwater diatoms		
	450			M1 (440 - 524)			

From 2000 cal yrs BP until 500 cal yrs BP, sand movement in the Groenvlei catchment declined sufficiently to allow for the immigration and spread of wet and dry forest types, particularly *Podocarpus* (Table 2.1) (Martin, 1968). However, aeolian activity persisted to the west of Groenvlei with OSL ages of 1.87±0.27, 1.66±0.09 and 1.39±0.09 ka indicated possible intermittent dune movement on the Sedgefield Ridge between 1900 and 1300 cal yrs BP (Bateman et al., 2011). Temperatures, based on the Cango speleothem, continued to fluctuate by 1-2°C between 2000 and 1000 cal yrs BP (Fig. 2.6) (Talma and Vogel, 1992). At Norga, palynological evidence implied warmer and more mesic conditions from 1400 cal yrs BP to present as current climatic conditions were established (Fig. 2.4, inset 20) (Scholtz, 1986). Lunette deposition at Cape Agulhas coincides with a warming peak in the Cango Cave record at ~1250 cal yrs BP, suggesting a brief warm and dry spell (Fig. 2.6) (Talma and Vogel, 1992; Carr et al.,

2006a). Alluvial sediments on the south coast plain alluded to a wetter climate with constant flooding events between c. 1215 and 875 cal yrs BP, with an initial cooler phase between c. 1200 and 1100 cal yrs BP (Damm and Hagedorn, 2010). Persistently cooler temperatures are witnessed at Cango Caves from 850 – 150 cal yrs BP, only providing a brief respite to warmer conditions from 450 to 325 cal yrs BP (Talma and Vogel, 1992). Lunette accretion at Voëlvlei and Buffeljacht pan recommenced at 700 and 450 cal yrs BP as does dune building to the east of the Swartvlei estuary with OSL ages at 0.54±0.06 and 0.50±0.07 ka (Carr et al., 2006b; Bateman et al., 2011). The combination of these two factors implied a drier and possibly cooler climate with increased westerly wind, a pattern also observed in the Stager et al. (2012) record. The last 200 years along the south coast plain appeared to be relatively warm and arid after the culmination of the LIA and subjected to increased anthropogenic influences (Talma and Vogel, 1992; Damm and Hagedorn 2010).

The extent of the year-round rainfall zone is likely to be relatively fluid in space and time in response to the competing climatic forcings in the winter rainfall zone and the summer rainfall zone. Intermittent preservation at sites in the region suggests that summer and winter rainfall seasonality has fluctuated during the late Holocene. The combination of atmospheric disturbances has lead to both major and minor environmental changes as the region responds to this dynamic interplay, however, as in the western half of South Africa, long continuous records are still relatively scarce and a complete understanding of the regions development is still lacking.

Summer Rainfall Zone (SRZ)

Late Holocene climate throughout the summer rainfall region appears to be spatially heterogeneous across the country. According to Lewis (2011) the southern Drakensberg region was moist enough for human occupation from 6300 cal yrs BP to present. An abundance of mangrove and swamp elements from the Lake Eteza pollen record suggested increased precipitation leading to a rise in the groundwater table from 6500 – 3600 cal yrs BP (Fig. 2.4) (Neumann et al., 2010). A speleothem record from Cold Air Cave showed higher humate mobilisation and increased organic matter between 4300 and 3200 cal yrs BP, suggesting a period of variable warmth and moisture availability, which supported a dense vegetation mass in the surrounding area (Lee-Thorp et al., 2001). The remainder of the record shows lower humate mobilisation and decreased organic matter indicating an increase in tropical grasses with a notable peak in C4 grasses occurring at 2100 cal yrs BP (Lee-Thorp et al., 2001). The decline in organic matter coincided with a generally cooler and more arid phase between 3200 and 2100 cal yrs BP, with peaks in aridity and cooler conditions centred at 3100 and 2600 cal yrs BP as $\delta^{18}O$ reach minimum values

(Fig. 2.7) (Holmgren et al., 1999; Lee-Thorp et al., 2001). Along the east coast, pollen analysis on peat sediments from Mfabeni suggested a cooler, drier phase from 3000 - ~2500 cal yrs BP (Finch and Hill, 2008).

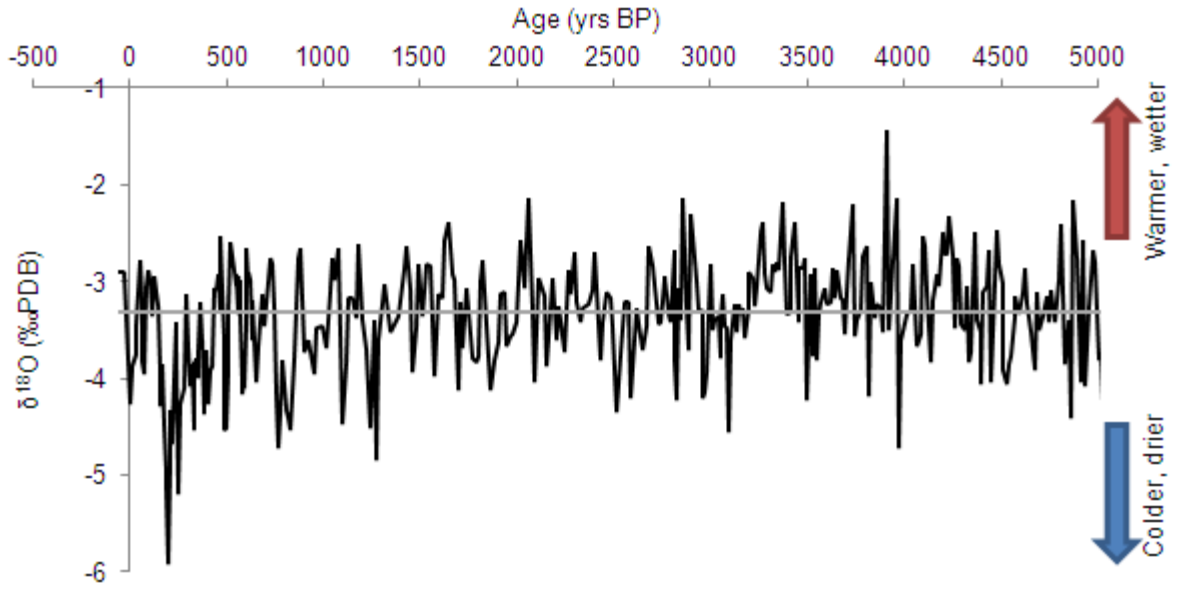

Figure 2.7: late Holocene $\delta^{18}O$ stalagmite sequence from Cold Air Cave; horizontal line indicates the average for the entire 6300 yr record (Source: Lee-Thorp et al., 2001, Pg 4908)

According to the analysis of 13 archaeological sites from the Northern Cape and Free State, Klein (1979) proposed a relatively moist phase between 4600 and 1100 cal yrs BP. However, most other records from the summer rainfall region indicate an arid period for most of the late Holocene. Hyrax midden records from Klein Spitzkoppe and Austerlitz indicated a progressive trend towards aridification from 4800 cal yrs BP; the authors argued that this may be related to variations in solar activity and a reduction in Benguela upwelling (Chase et al., 2009; Chase et al., 2010). In an exception to this general aridity a brief period of increased humidity between 4200 and 3500 cal yrs BP at Klein Spitzkoppe is documented (Chase et al., 2009). To the east of the Austerlitz site, isotope and pollen records from a speleothem record at Wonderwerk Cave showed continued deposition over the last 4000 years. The combination of layered carbonate, $\delta^{18}O$ and $\delta^{13}C$ at Wonderwerk Cave showed alternating episodes of wet and dry phases, with the initial generally dry phase occurring between 4000 and 3000 cal yrs BP, after which a decline in both $\delta^{18}O$ and $\delta^{13}C$ suggested an increase in moisture availability until 1300 cal yrs BP (Brook et al., 2010). Alternating phases of wet-dry conditions also occurred in the Eastern Cape Drakensberg region, as shown by episodic sedimentary movement during the late Holocene (Lewis, 2005). Semi-arid conditions prevailed in the Glenmore area from 7000 – 3200 cal yrs BP, before increased precipitation

occurred from 3200 – 2500 cal yrs BP, as witnessed by increasing geomorphic activity in the region, thereafter declining until 2000 cal yrs BP (Lewis, 2005). Extensive gully erosion at Tiffendell between 2800 – 2700 cal yrs BP may support increased rainfall during this short-lived event producing a rise in surface runoff in the Eastern Cape Drakensberg region (Lewis, 2008). The dominance of *Euryops* in the charcoal record from Barkly East, near Lesotho, suggests generally dry conditions from ~7200 – 1800 cal yrs BP (Lewis, 2008). To the west of Barkly East, lies the Blydefontein wetland; pollen analysis from a combination of cave and swamp deposits showed a relatively cool and dry climate from 4100 – 3100 cal yrs BP (Scott et al., 2005). Further towards the east along the Kwa-Zulu Natal coast, a 6500 year pollen record from Lake Eteza revealed a period of increased precipitation from 6500 to 3600 cal yrs BP, before experiencing a prolonged dry environment dominated by grasses until 2000 cal yrs BP (Neumann et al., 2010). Outer lunette activity in the Kalahari culminated at 2000 cal yrs BP after approximately 400 years of activity (Lawson and Thomas, 2002).

Most records agreed that the climate of the last 2000 years in the summer rainfall region was generally wetter, punctuated by brief drier conditions. Pollen analysis from Lake Eteza, Blydefontein Basin, Braamhoek wetland and Barkly East indicated a subhumid, moist environment over most of the previous two millennia (Scott et al., 2005; Lewis, 2008; Neumann et al., 2010; Norström et al., 2009). Increases in forest-, swamp-, riverine-, and mangrove-forest elements became more pronounced at Lake Eteza indicating that more moist coastal forest elements in the region began at 2000 cal yrs BP prior to a switch to savanna conditions at 800 cal yrs BP (Neumann et al., 2010). Inland from Lake Eteza, the Braamhoek wetland showed a shift from a predominantly dry climate to subhumid conditions at 2500 cal yrs BP, before a substantial increase in forest elements and extensive grass cover occurred at 1500 cal yrs BP (Norström et al., 2009). Finne et al. (2010) further showed that the wetland experienced an increase in siliceous microfossil preservation after 2000 cal yrs BP, implying enhanced local moisture. Generally, subhumid conditions prevailed at Blydefontien between 2000 and 600 yrs BP, only switching to a drier climate for a brief time between 1300 and 1100 cal yrs BP (Scott et al., 2005). The dominance of grass taxa in the Blydefontien pollen record further suggested that summer precipitation was more prevalent than winter during this period (Scott et al., 2005). A predominantly warmer, wetter spell was established between 1950 to 1650 cal yrs BP as viewed from the $\delta^{18}O$ sequence from Cold Air Cave before a series of cooler and drier conditions prevailed until approximately 1100 cal yrs BP (Holmgren et al., 1999). By coupling the $\delta^{18}O$ sequence with the $\delta^{13}C$ sequence the drier, cooler climate was shown to commence at 1400 cal yrs BP and continued until the culmination of the Little Ice Age, approximately 250 years ago, as witnessed through the decline in C4 grasses (Fig. 2.7) (Lee-Thorp et al., 2001).

However, Huffman (1996) showed that the Shashi Limpopo basin supported an extensive human population, providing a booming sorghum trade for the surrounding communities between 1050 – 650 cal yrs BP. The sorghum crop requires 350mm a^{-1} during its growing season, substantiating the claims of a wetter climate in the region (Huffman, 1996). After this the settlement was abandoned as agricultural pursuits could not be supported, and widespread drought set in (Huffman, 1996).

A wetter period was also recorded in the Klein Spitzkoppe hyrax midden from 1150 to 750 cal yrs BP, which the authors suggested was an expression of the Medieval Climate Anomaly (MCA) (Chase et al., 2009). The timing of the MCA is frequently placed between 1200 yrs ago to 700 yrs ago; however the global expression of this event is debatable (Hughes and Diaz, 1994; Broecker, 2001). Tyson and Lindsey (1992) present the MCA across the summer rainfall region as a period of enhanced easterly flow inducing tropical disturbances across the subcontinent, providing warmer conditions, which peak at 1000 and 900 yrs ago. At the beginning of the LIA, a retreat in forest and swamp elements along the east coast was recorded at Lake Eteza and Lake Sibaya, conveying a combination of a drier climate, but this period also witnessed the introduction of farming and herding activities into the region during the past 700 years (Huffman, 1996; Neumann et al., 2008, 2010). The $\delta^{18}O$ values from Cold Air Cave became more enriched by nearly 2‰ from -4.7 to -2.9‰ in just ~150 years between 770 to 615 cal yrs BP, corresponding to the transition from the MCA to LIA (Fig. 2.7) (Holmgren et al., 1999). A brief, intermittent warming phase from 450 – 375 cal yrs BP is observed in the Cold Air Cave speleothem $\delta^{18}O$ record, before temperatures declined to their lowest values as the second phase of the LIA set in (Holmgren et al., 1999). The period defined as the LIA appears to coincide with weakened tropical easterly flow leading to drier conditions in the SRZ, as moisture transport from the tropics was limited (Tyson and Lindesay, 1992). Drier and cooler climes are also evident across the interior, such as shown at Blydefontein, where Asteraceae gradually amasses in the pollen records from 300 to 100 cal yrs BP (Scott et al., 2005). Borehole temperature records from several locations between Upington and Polokwane registered a temperature peak at 350 cal yrs BP before declining to reach a minimum at ca. 150 cal yrs BP; with ground surface temperature increased by 1°C along this transect from about 175 cal yrs ago to present (Jones et al., 1999).

2.4.2. Palaeo-Oceanic Influences

Sea-level fluctuations and their effect on climate and coastal water bodies can be determined through the analysis of fossil remains at coastal sites. A variety of mechanisms have been ascribed to sea level changes, including isostatic adjustment, ice volume changes, local tectonic movement and/or thermal expansion (Compton, 2001). Several studies have attempted to reconstruct changes in sea level along the South African coast as demonstrated in Figure 2.8. Most studies agree that the late Holocene experienced several marine transgressions, however the magnitude and timing is still debated.

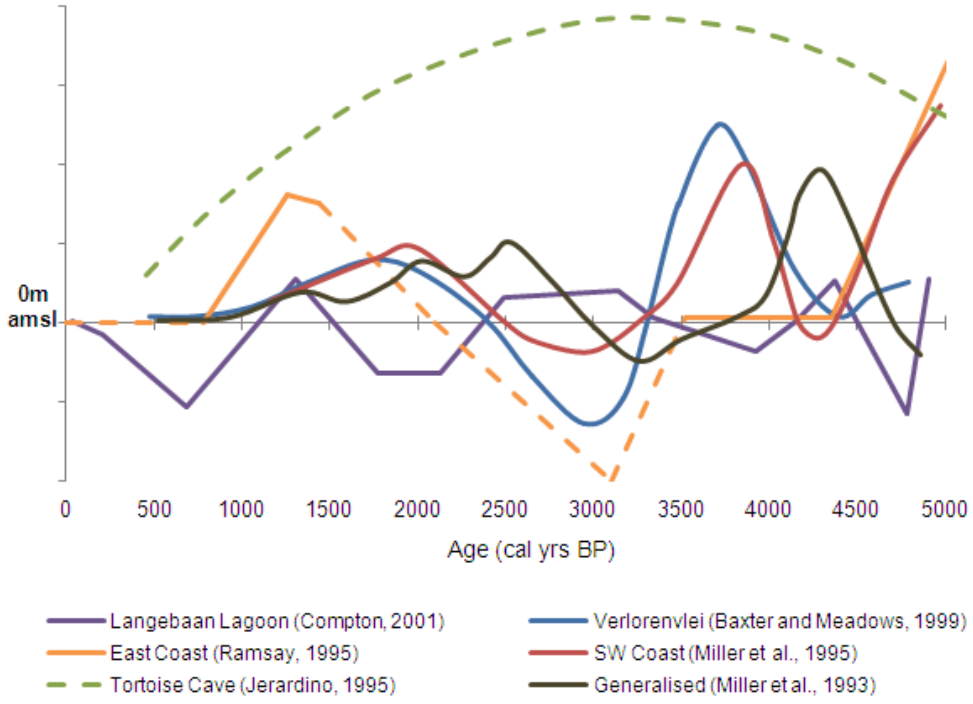

Figure 2.8: Reconstructed sea level curves (in meters AMSL and BMSL) for the last 5000 years from sites along the South African coast as discussed in the text

Along the west coast, Compton (2001) analysed sediments from Langebaan Lagoon and proposed a marine highstand between 6000 to 4000 cal yrs BP, consistent with the culmination of the Flandrian transgression at 3800 cal yrs BP, which Grindley et al. (1988) estimated peaked at ±2m above mean sea level (AMSL) (Fig. 2.8). The timing of this initial late Holocene transgression appears to have occurred at some point between 4400 and 3800 cal yrs BP. Changes in mollusc midden composition and shell size at the Pancho's Kitchen Midden, near Elands Bay agree with Grindley et al. (1988), placing the ±2m AMSL highstand at 4000 – 3800 cal yrs BP (Jerardino, 1997). Miller et al. (1995) also identified a marine transgression when investigating low-lying coastal platforms along the southwestern Cape coast, with

an initiation at ~4200 cal yrs BP, peaking at ±2m AMSL at ~3800 cal yrs BP before dropping to present level by ~3250 cal yrs BP. This initial late Holocene transgression is also evident in the Verlorenvlei deposits; however Baxter and Meadows (1999) place this transgression at ~4000 cal yrs BP, peaking at ±3m AMSL but also reaching present level at ~3250 cal yrs BP. The effects of the transgression reached 15km inland from the vlei mouth (Baxter and Meadows, 1999), and continued influencing sediment dynamics until 1500 cal yrs BP (Miller et al., 1995).

Along the south coast, elevated shell layers at Keurbooms Estuary and Fishwater Flats indicate higher sea levels than present between 5140 and 4000 cal yrs BP in the range of 0.6 – 1.5m AMSL, considerably lower than proposed highstands along the west coast (Reddering, 1988; Marker and Miller, 1995); however Bateman et al. (2011) suggested a highstand in the range of 2 – 3m in the Wilderness region, as determined through dune activity and sediment recycling. Coastal lakes show constant marine derived sedimentation from at least 7500 to 2000 cal yrs BP before freshwater and eutrophic conditions were reached and maintained (Martin, 1959; Gordon et al., 2012). Groenvlei, a coastal lake near Knysna has become progressively less saline since the mid-Holocene (Table 2.1) (Martin, 1959). Marine conditions were evident from 6000 cal yrs BP, supporting a diverse marine diatom community before receding seas transformed the lake from a marine embayment into a brackish lagoon and finally into an isolated freshwater lake (Martin, 1959).

Holocene aged beachrock and planation depositional episodes along the east coast provided robust evidence of sea-level fluctuations which appear to occur loosely in tandem with west coast curves (Ramsay and Cooper, 2002). Rising sea levels at ca. 5000 cal yrs BP initiated the deposition of beachrock along the Kwa-Zulu Natal coast, peaking at ±3m AMSL at ~3900 cal yrs BP and again at ~3300 cal yrs BP before receding to ±2m below mean sea level (BMSL) between 3100 and 2900 cal yrs BP (Ramsay, 1995). Sea levels recovered steadily from this regression, rising to ±1.5m AMSL by 1400 cal yrs BP before reaching present levels (Fig. 2.8) (Ramsay, 1995). Present level or below mean sea level estimations are proposed for most sites along the west coast from ~1500 cal yrs BP until present, with only minor fluctuations in the range of 0.5 – 1.0m AMSL recorded at selected sites. Compton (2001) identified a minor transgression of a magnitude of 0.7m at 1400 cal yrs BP, before leading to a 1m regression at 800 cal yrs BP, at the same time warmer sea surface temperatures were experienced along the west coast (Jerardino, 1997). The late Holocene marine transgression has been attributed to the combination of isostatic emergence and thermal expansion of sea water (Miller et al., 1995; Ramsay and Cooper, 2002). The later regressions appear to coincide with global cooling phases (Ramsay and Cooper, 2002).

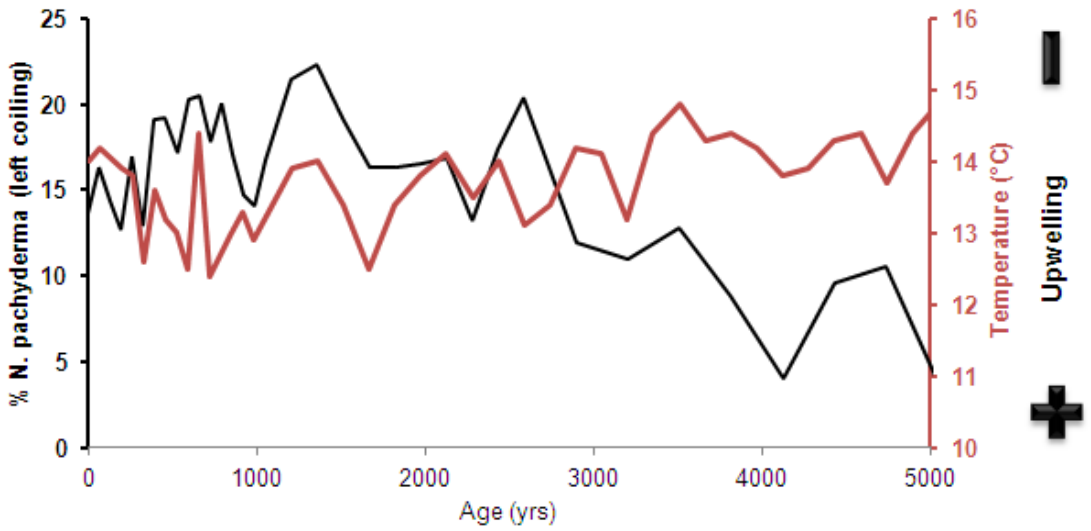

Figure 2.9: Presence of N. pachyderma *and temperature fluctuations in the Luderitz cell of the Benguela Upwelling System over the last 5000 years (source: Farmer et al., 2005)*

Isotopic analysis on the mollusc, *Patella tabularis* from archaeological deposits from Nelson Bay Cave also suggests relatively lower summer maximum sea surface temperature in the Agulhas Current between 4000 – 2000 cal yrs BP (Cohen and Tyson, 1995), while the Agulhas Bank experienced cooler surface waters between 3500 and 2500 cal yrs BP (Cohen and Tyson, 1995). Mollusc shells retrieved from middens along the west coast showed a drop in sea surface temperatures in the Benguela Upwelling System (BUS) occurred between ~4000 and 2000 cal yrs BP, with a possible decline of 1 – 2°C at ca. 3190 cal yrs BP (Cohen et al., 1992; Jerardino, 1997). The combination of Mg/Ca values from the foraminifera *Neogloboquadrina pachyderma* (% NPS) and the growth of *Globigerina bulloides* from the Ocean Drilling Project Core 1084B were used as a proxy to determine the upwelling history of the Benguela system. It was determined that, after a prolonged period of warmer sea surface temperatures from 5800 to 3400 cal yrs BP, cooler sea surface temperatures (SST) and increased upwelling in the BUS are evident between 3400 and 300 cal yrs BP (Fig. 2.9) (Farmer et al., 2005). Increased upwelling would have provided nutrients to the coastal shelf sustaining primary productivity of the marine ecosystem. Hence, human inhabitants along the west coast and as far north as Spoeg River Cave were able to exploit marine resources until at least 1300 cal yrs BP before conditions became too adverse and settlements were abandoned (Jerardino, 1997; Webley, 2007). Cooler SST are experienced for most of the first phase of the LIA, up to 500 cal yrs BP but a definitive decline to the magnitude of 1 – 2°C occurs at 500 cal yrs BP (Cohen et al., 1992; Cohen and Tyson, 1995; Jerardino, 1997).

2.5. CONCLUSIONS

The southwestern to southern Cape coast of South Africa is aligned along a west to east axis along a gradient of predominantly winter rainfall to a more transitional year-round rainfall seasonality, respectively. As demonstrated, the rainfall zones shift through time, migrating in response to changes in atmospheric and oceanic circulation. While the ocean plays a pivotal role in defining the southern African environment at a range of spatial and temporal scales, the relative instability and the dynamic nature of the climate with the landscape over the millennia has given rise to a highly diverse and ecologically significant region.

Climatic fluctuations and defined events during the late Holocene across South Africa appear to loosely correspond with the global rapid climatic change (RCC) events as identified by Mayewski et al. (2004). A widespread cooler phase, probably extending from 4000 to 2000 cal yrs BP, but more likely constrained to 3500 to 2500 cal yrs BP, is apparent across the country. Following this, alternating warm-cool periods define the remaining 2000 years with clear expressions of the Medieval Climate Anomaly, particularly in the summer rainfall zone, and the Little Ice Age. One of the localised RCC events pointed out by Mayewski et al. (2004) is clearly manifested in coastal site records, which is the 4.2 – 3.8ka event, which correlates to a widely accepted marine transgression. Where high resolution records are available from sites across the three rainfall zones, two definitive yet brief events stand out. Firstly, a distinct event at ~2100 – 2000 cal yrs BP and secondly, the two centuries spanning from ~1300 – 1100 cal yrs BP. The mechanisms behind these events have been alluded to in this chapter; however the need for more information in the form of multi-proxy studies is required to determine the extent and effects of these events across South Africa.

Chapter 3. PROXIES and DEPOSITIONAL ENVIRONMENTS

Diatoms are generally cosmopolitan in distribution and are found in a range of habitats where water is at least occasionally available (Cooper et al., 2010; Smol and Stoermer, 2010). Habitats include the open ocean, estuaries and shallow coastal environments (see Fritz et al., 2010; Trobajo and Sullivan, 2010) to lakes and rivers (see Bennion et al., 2010; Reavie and Edlund, 2010; Wolin and Stone, 2010) subaerial habitats, as well as including soils and bryophytes (see Gaiser and Ruhland, 2010; Johansen, 2010). This broad spectrum of environments provides a context for a mostly well-defined ecological niche specificity (Denys and de Wolf, 1999; Gaiser and Ruhland, 2010; Hall and Smol, 2010). Through sheer abundance and diversity diatoms are often the dominant component of the microalgal assemblage (Sullivan, 1999; Julius and Theriot, 2010). Diatoms are microscopic, unicellular algae belonging to the phylum Heterokontophyta (Smol and Stoermer, 2010), in which three subdivisions occur, namely i) Coscinodiscophyceae, commonly referred to as the centrales or centrics, ii) Fragilariophyceae, and iii) Bacillariophyceae commonly referred to as the pennates or pennales. The latter two groups are differentiated by either the absence or presence of a raphe, respectively (Julius and Theriot, 2010). The classification of centrics from pennales is based on the formation of the valve, that is either radially symmetric around a point in centrics or along a plane for pennales (Julius and Theriot, 2010). Diatoms are most easily recognised by their opaline silica (SiO_2) frustule, composed of two valves, the P-valve and the R-valve, and several girdle bands (Hall and Smol, 2010; Julius and Theriot, 2010). Further taxonomic identification to species level is primarily based on the size, shape and sculpturing of the cell wall (Smol and Stoermer, 2010).

Several environmental parameters are required for a diatom-based microalgae community to thrive, including the availability of light, carbon, silica, and several biolimiting nutrients, the most important of which are iron, nitrogen and phosphorus (Finkel et al., 2009; Jordan and Stickley, 2010). The community as a whole responds to changes in pH, turbidity, water temperature and nutrient concentrations, with the composition being a reflection of hydrology and habitat availability (Reid and Ogden, 2009; Jordan and Stickley, 2010; Julius and Theriot, 2010). Essentially, community composition generally relates to the chemical, physical and biological variables present in the habitat (Fritz et al., 1999).

Diatoms are extremely powerful and sensitive biological indicators and have been utilised in numerous studies, especially in assessing human-induced influences on a system and evaluating whether steps should be taken to restore the system to its original state (Hall and Smol, 2010; Julius and Theriot, 2010). Diatoms are sensitive to biotic and abiotic ecological processes, therefore the analysis of the assemblage composition and knowledge of the relevant autecological characteristics of the taxa present aids in inferring environmental conditions (Denys and de Wolf, 1999; Julius and Theriot, 2010). Their rapid growth rate and immigration rates ensure early colonization within a habitat after a disturbance making them an ideal indicator of environmental change over varying time scales (Cooper et al., 2010; Hall and Smol, 2010).

Diatom fossil deposits are often well preserved in the sedimentary record (Stoermer and Smol, 1999), and may reflect hundreds to thousands of years of sediment accumulation (Cooper, 1999; Julius and Theriot, 2010). This trait combined with their microhabitat preferences makes them ideal candidates for environmental and climatic reconstructions (Fritz et al., 2010; Gaiser and Ruhland, 2010). The unique morphology of the frustules allows for the identification of fossils to species level through which their autecological information can be acquired (Spaulding et al., 2010). Both spatial and temporal patterns of environmental change can be discerned through the analysis of fossil deposits, limited only by the preservation potential of the depositional environment (Fritz et al., 2010).

3.1. DEPOSITIONAL ENVIRONMENTS

Sedimentary records can provide a unique insight into past environmental changes. These records can be retrieved from a number of sources, but wetlands and lakes have usually shown more promise than other depositional environments. The stability of lake sediments and their general resistance to erosion by such physical processes as tidal currents, wind-induced waves and bioturbation (Sullivan, 1999) allows for the use of palaeolimnology as a tool in identifying probable causes of change in environmental conditions, either by reconstructing the history of individual sites or by the comparison between sites (Battarbee, 1999). The primary value of palaeolimnologically based reconstructions of past hydrology and climate is to "…establish natural patterns of climate variability at a variety of spatial and temporal scales" (Fritz et al., 1999, p. 45). Lakes are the expression of the relationship between the catchment's inputs and outputs (Fig. 3.1) (Wolin and Stone, 2010). Hydrological inputs include precipitation, stream flow, surface runoff and groundwater inflow (Fritz et al., 1999), whereas outputs

involve evaporation, stream outflow, groundwater recharge and in some cases deep seepage (Wolin and Stone, 2010). This interplay will have direct effects on water chemistry and lake levels (Fritz et al., 2010).

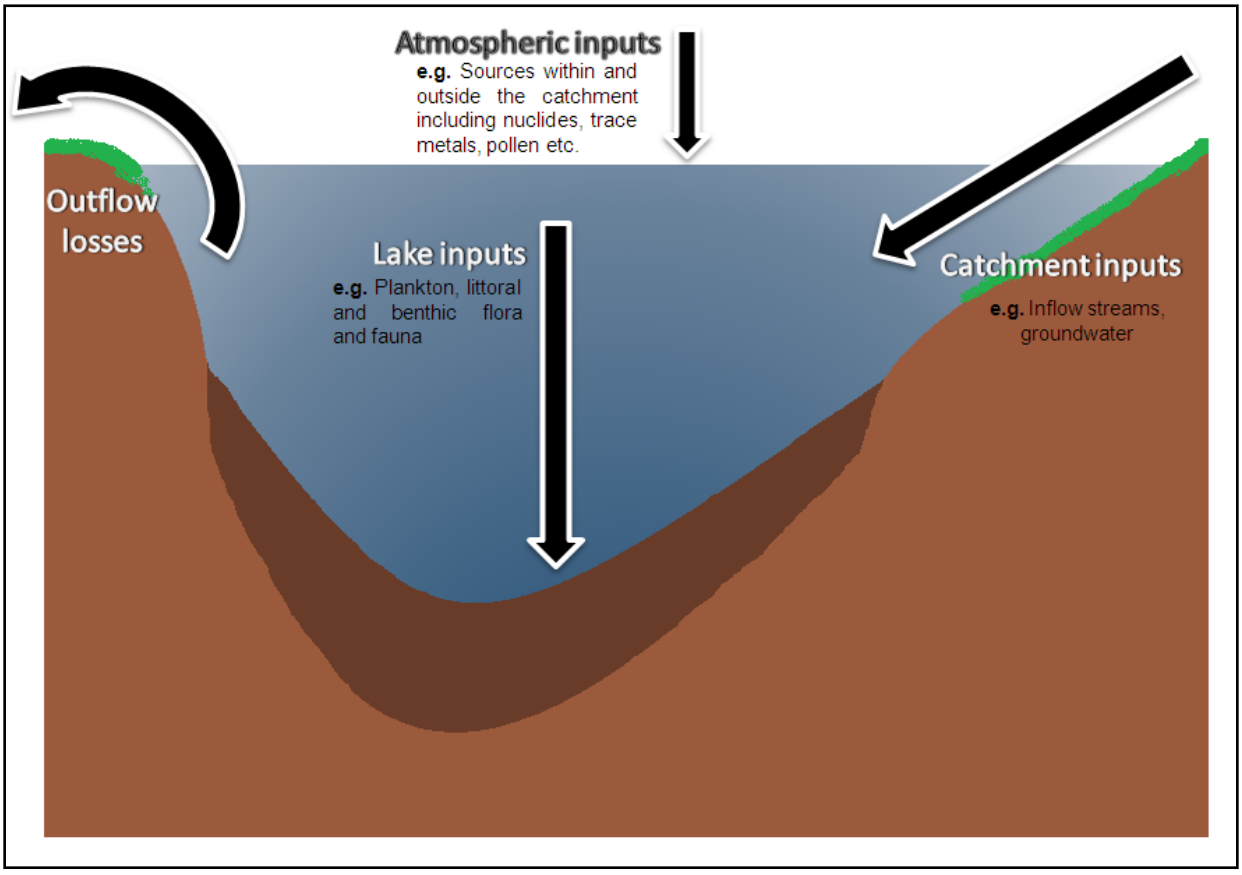

Figure 3.1: Simplified cross section of a lake showing source materials into and out of the system (adapted from: Battarbee, 1999)

3.2. LAKES AND DIATOMS

The strength of the climatic signal preserved in the sedimentary sequence is dependent on the type of lake, with closed basin lakes having the strongest response to changes in precipitation minus evaporation (Wolin and Duthie, 1999). Lakes that are ideal as indicators of water level changes are dependent on their basin morphology allowing for littoral zone expansion or contraction (Gaiser and Ruhland, 2010). The fluctuation of water levels in an open basin would need to be sufficiently large to be reflected in the fossil record (Fritz et al., 2010). A lake subjected to periodically lower water levels may have a well-established littoral wetland (Gaiser and Ruhland, 2010), which will record both episodes of drying and flooding in the microfossil assemblages (Weilhoefer et al., 2008). During drier episodes, peat accumulation may increase due to a decrease in wave action (Finkelstein and Davis, 2006). Water depth

and therefore light penetration, nutrients and substrate availability play an important role in determining life form structure in the diatom community composition (Bennion et al., 2010). The structure and size of the diatom community is controlled by a variety of biotic and abiotic influences.

Diatom life form refers to the changes in abundance of planktonic and benthic diatoms (Battarbee, 1986). Planktonic diatoms are those which are free floating, living in the open lake water, whereas benthic diatom communities are those which are non-planktonic or littoral forms, which live attached to various substrates (Wolin and Duthie, 1999). Tycoplanktonic forms are usually associated with the benthic or the near-shore community but can be easily transported into the plankton (Wolin and Duthie, 1999). It is worthy to note that there are some inconsistencies between reference material denoting life form allocation (Wolin and Stone, 2010).

The planktonic community usually dominates in open water or when turbidity hinders benthic growth (Wolin and Stone, 2010). The relative abundance and fluctuation in dominance of the plankton is typically linked to changes in water depth, where deeper water should reflect a greater percentage of planktonic species (Wolin and Stone, 2010). These trends can also be attributed to temperature, as Baars (1979) has shown that a reduction in the plankton was observed when temperatures dropped below 12°C and other studies have shown that high levels of nutrients and stagnant water promote plankton blooms (Reavie and Edlund, 2010). A large proportion of the plankton community can be representative of allochthonous material, that is material derived from elsewhere, particularly in coastal areas where tides influence sediment influx (Vos and De Wolf, 1993).

Benthic taxa are more diverse than planktonic ones, as most species adapt to specific substrates (Julius and Theriot, 2010). The periphyton consists of species that live on the bottom of the lake floor within the limits of the photic zone (Hall and Smol, 2010), but other adaptations include attachment to rocks/stones (epilithic diatoms), sand (epipsammic diatoms), fine sediments in the littoral zone (epipelic diatoms), plants (epiphytic diatoms) and mosses (epibryophytic) where they are either permanently attached or are motile and actively migrate (Vos and De Wolf, 1993; Hall and Smol, 2010). The varying composition of these diatoms is based on the availability of the substrata in the photic zone and flow dynamics in the lake (Julius and Theriot, 2010). Typically, benthic taxa thrive in clear, shallow water (Bennion et al., 2010); due to a wider availability of habitat (Wolin and Stone, 2010) and high oxygen concentrations during low water levels (Bradshaw et al., 2005), although this relationship is a function of basin morphology (Vadeboncoeur et al., 2008). In comparison to the plankton, benthic communities are deposited *in situ* (Horton and Sawai, 2010; Reavie and Edlund, 2010).

Dominance or shift to any one of the distinct benthic communities can be suggestive of modifications within the catchment or changes in the hydrological regime (Reavie and Edlund, 2010). For example, fluctuations in epiphytic taxa can indirectly indicate the expansion or retraction of submerged macrophytes (Wolin, 1996). Submerged macrophytes are an important constituent of the lake ecosystem, contributing to nutrient cycling, productivity, soil formation, and stabilization of the nearshore environment (Jacobs and Noten, 1980; Thoms et al., 1999; Cooper et al., 2010). Therefore, a shift toward epiphytic diatoms may convey a greater distribution in submerged macrophytes in a low energy environment (Vos and De Wolf, 1993; Reavie and Edlund, 2010). The epipelic component is frequently observed in tandem with the epiphytes and suggests that colonization by the submerged vegetation has not been concluded (Bao et al., 2007).

Aerophilic diatoms are a form of benthic diatoms that are able to survive in subaerial habitats where their diversity and species richness is moisture content dependent (Van de Vijver and Beyens, 1997; Spaulding et al., 2010). Areas that are subject to periodic drying include wet to semi-wet soils and mosses (Spaulding et al., 2010). Numerous categories have been established based on the degree of desiccation these species are able to tolerate and the habitat that they occupy. Typically, aerophilic diatoms fall into either the 'xerotic' type or the 'hydrotic' type; the former are able to survive dry periodically moistened habitats with the latter occupying permanently wet mosses (Van de Vijver and Beyens, 1997). Johansen (2010) elaborates further by categorising the algae based on specific substrata and moisture sources; for instance the category 'terrestrial algae' is subdivided into three classes namely 'aeroterrestrial', algae, surviving on moisture directly from the atmosphere; 'euterrestrial', diatoms, occurring on periodically dry soils and 'hydroterrestrial', which are diatoms living on continually wet soils. The occurrence of aerophilic species in the fossil records have been interpreted in numerous ways; the most common is that the dominance of aerophilic species is representative of shallow waters and possibly drought events (Gell et al., 2007; Gaiser and Ruhland, 2010). However, peaks in both aerophilic species and sedimentation rates may be a reflection of flooding events, resulting in increased erosion and surface runoff (van der Putten et al., 2008). Although adapted to drier habitats, long periods of desiccation and changes in pH are limiting factors to the distribution of aerophilic species (Johansen, 2010).

Inferences related to changes in the composition of life forms have been undertaken, most notably determination of changes in water levels over time. Changes in the ratio between planktonic and benthic taxa (P:B) or centrics and pennates (C:P) have been used to infer lake level fluctuations (Punning

and Puusepp, 2007; Cooper et al., 2010; Wolin and Stone, 2010). In theory, during low lake levels an increase in benthic forms is observed as shallow water habitats increase, whereas during high lake levels planktonic species increase due to the increase of the aphotic zone limiting benthic forms (Punning and Puusepp, 2007). This trend is most easily observed at the marginal lake sediments, where the transition from one life form to the other is more apparent (Wolin and Stone, 2010). Punning and Puusepp (2007) showed that in water depths less than 3.5m, the species richness and periphytic community is highest, with 60-80% of the total community composition occurring between 0.8 and 3.5m. For water depths greater than 4m, the plankton community represented 80% of the total (Punning and Puusepp, 2007). Strong vertical zonation can also be observed on intertidal mud flats and saltmarsh environments, with diatom distribution reflecting elevation (Zong and Horton, 1999; Horton et al., 2006). However, these ratios are only accurate if the underlying mechanism for changes in lake levels is the availability of moisture. This is not always the case and other factors such as nutrients, sedimentation, water clarity, sea level changes and wind can play a role (Punning and Puusepp, 2007; Gaiser and Ruhland, 2010).

Changes in water chemistry, nutrients and lake salinity can be an indirect measure of climate variability, as lake water generally becomes more concentrated when regional climates become drier and lakes change to closed basin (Anderson, 1995). Scheffer et al. (1993) discuss the theory of alternative stable states of shallow lakes, where lakes can alternate between two equilibria based on nutrient availability. During periods of high concentrations lakes are turbid and are typically dominated by planktonic species, which may cause a drop in water transparency creating a turbid state and preventing macrophyte growth (Scheffer et al., 1993). Conversely, during periods of low nutrient availability a clear water state may occur with a well-established photic zone, which would promote the growth of submerged macrophytes and benthic communities, creating a positive feedback mechanism (Scheffer et al., 1993). A transition from one state to the other may need a profound reduction or enhancement in nutrients, although Scheffer et al. (1993) noted that the transition is not limited to changes in nutrients and may be affected by other external factors.

3.3. LAKE CHARACTERISTICS

Variations in the precipitation to evaporation ratio (P/E) have consequences for the concentration or dilution of dissolved salts (Gasse et al., 1995; Haynes et al., 2007), particularly in closed basin lakes, and may lead to shifts in the ionic composition and concentration (Fritz et al., 2010). However, lakes that shift between open and closed hydrology may exhibit large fluctuations in salinity as they respond to the

changes, which are not necessarily related to climatic forcing but is one of the main drivers (Fritz et al., 1999). Salinity can also vary in relation to the inflow of source waters where changes in landscape dynamics alter freshwater and marine water influx (Snoeijs, 1999). Lakes and the rivers that feed them each have distinct biological communities (Reid and Ogden, 2009). A greater influx of freshwater into a system through flooding events will cause dilution of the lake chemistry, flush out the biota and increase turbidity (Weilhoefer et al., 2008). The duration, degree and frequency of flooding events will affect the magnitude of the response of the system (Weilhoefer et al., 2008). The greater the degree and frequency of the flood the more the system will reflect riverine attributes, such as conductivity and total nitrogen (Weilhoefer et al., 2008). High intensity floods may disturb the sediment profile and/or lead to scouring of the lake floor creating discontinuities in the palaeorecord (Gaiser and Ruhland, 2010).

Salinity may also be affected by proximity to the ocean. Lakes connected to the ocean may be linked to the intertidal zone of the coast through a transitional zone (Cooper et al., 2010). The variability and physical gradients of salinity, sediments and water currents, among other factors, all characterize an estuary and promote system productivity and diversity (Jacobs and Noten, 1980; Cooper et al., 2010). Marine sediments and species may be transported into the estuary and possibly beyond into the connecting lake through tidal action or storm intensity (Cooper et al., 2010). In environments such as these, salinity will be directly influenced by the interplay of both marine and freshwater components, eventually resulting in proportionate shifts in the biological community. Ultimately, a lake's response is related to both the lake and the catchment morphometry, local hydrology and the position of the lake within the landscape (Anderson, 1995).

Salinity, and by proxy conductivity, has demonstrated to be a dominant physical parameters shaping an aquatic community across the transition from fresh to brackish to marine (Fritz et al., 2010; Horton and Sawai, 2010; Snoeijs and Weckström, 2010). Snoeijs and Weckström (2010, pp. 287) define salinity based on the haline system for lakes as "the total concentration of ionic components in g per kg water, [where] generally accepted approximate limits are: freshwater <0.5 ppt, oligohaline 0.5–5 ppt, mesohaline 5–18 ppt, polyhaline 18–30 ppt, euhaline 30–40 ppt, hyperhaline >40 ppt." This system is the one most commonly utilised for lakes and waterbodies that experience at least partial marine influences. Hence, salinity is the reflection of the interaction of source waters and inputs (Fritz et al., 2010). Over time changes in salinity of a lake may be the product of varying influences of fresh water or alternatively, marine water, but vegetation clearance and other human activities can play a role (Bennion et al., 2010). The degree of freshwater taxa in the sedimentary record can indicate the

periodicity of freshwater inputs into the system or the influence of wind on the ecosystem (Abrantes et al., 2007).

In transitional zones between marine and freshwater, such as those occurring in estuaries or coastal lakes, salinity can be one of the most important parameters in species distribution (Saunders et al., 2007). Biota will respond to the extent of tidal waters mixing with freshwater inputs and, depending on the temporal resolution, can also reflect the seasonal changes in the P/E ratio (Saunders et al., 2007). The mixing of source waters will produce a gradient across the estuary or lake (Saunders et al., 2007), creating a vertical zonation from the tidal flat to the high marsh vegetation zone (Horton and Sawai, 2010); where a high marsh environment has a low frequency of marine influences and the tidal flats experiences the frequency and variability of ocean tides (Zong and Horton, 1999). The distribution of the biological community will then be a function of species salt tolerances and elevation, with many species living at the limit of their tolerance (Horton et al., 2006; Snoeijs and Weckström, 2010). Species living in these environments must be able to cope with a regularly evolving environment (Snoeijs and Weckström, 2010).

Through the understanding of species distribution across these transitional zones, an attempt at identifying past sea level changes is possible. In general, sea level transgressions relate to the contraction of global ice sheets, thermal expansion of oceanic waters and extreme events, such as storm surges and tsunamis (Engelhart et al., 2009; Horton and Sawai, 2010). The vast literature available on diatom ecological classifications makes them ideal indicators of such events (Horton and Sawai, 2010). Four factors determine the distribution of marine taxa; namely light, temperature, salinity and water movement (Jacobs and Noten, 1980), these factors can give insight into the dynamics of ocean currents. For example, in coastal regions where upwelling is prevalent, cold water species will dominant (Abrantes et al., 2007). However, if the assemblage has a concurrence of cold water and warm water species then evidence of mixing of water masses can be identified (de Vries and Schrader, 1981). The changes in the balance between the assemblages can indicate variability of mixing through time (Abrantes et al., 2007). In this respect, diatom species variability from coastal sediments can provide great insight into the mechanisms driving salinity in a system (Fritz et al., 2010).

The pH of a lake is a reflection of the availability of cations in the catchment and the quality of the groundwater influx (Wolin and Stone, 2010). If the soil in the catchment has low concentrations of base cations then waters will tend toward being acidic in nature, likewise during periods of peat development pH decreases (Battarbee et al., 2010; Wolin and Stone, 2010). However, increases in erosion through

such activities as vegetation clearance may promote the transport of base cations and lead to an increase in pH (Thoms et al., 1999); this clearance may either be natural or human induced. A close relationship exists between pH and temperature, where outside of external influences increases in temperature can lead to an increase in pH (Battarbee et al., 2010). Preservation of diatom fossils is directly linked to pH and temperature; dissolution of silica-based frustules occurs at increased temperature and pH (Bennion et al., 2010). pH appears to have a strong influence in diatom distribution (Battarbee et al., 2010), by affecting the solubility of CO_2 and the availability of key trace elements and nutrients (Chen and Durbin, 1994). This distribution is related to a species' ability to survive across the acid to alkaline thresholds, to this end species fit into one of five categories based on the Hustedt's Classification (see below) (Battarbee et al., 2010, pp. 99).

Alkalibiontic	: occurring at pH values > 7
Alkaliphilous	: occurring at pH ~ 7 with widest distribution at pH > 7
Indifferent/Circumneutral	: equal occurrences on each side of pH 7
Acidophilous	: occurring at pH ~ 7 with widest distribution at pH < 7
Acidobiontic	: occurring at pH values <7, with the optimum distribution at pH = 5.5

The supply rates and concentration of various nutrients can play a pivotal part in the diatom community structure and diversity; phosphorus, for example, is known to be one of the most commonly limiting factors in productivity in freshwater systems (Hall and Smol, 2010). Hall and Smol (2010, p. 124) state that "…each taxon has an optimum and a tolerance for nutrients"; therefore knowledge of a species' range may assist in the reconstruction of an environment, especially where nutrient availability has played a central role in community development and change. Most species fall within one of four broad categories, in order of increasing nutrient requirements, *viz.* oligotrophic, mesotrophic, eutrophic and hypertrophic. The composition of nutrients and the supply thereof is determined by the watershed characteristics and by the amount of precipitation, respectively (Underwood and Kromkamp, 1999). During periods when nutrients are limited, such as phases of submerged macrophyte expansion where the uptake of nutrients are enhanced or when precipitation increases (Finkelstein and Davis, 2006; Gell et al., 2007), planktonic populations are suppressed (Wolin, 1996).

Diatoms are commonly used in studies of eutrophication of lakes (Hall and Smol, 2010). Eutrophication occurs when an aquatic system undergoes enrichment in inorganic plant nutrients, usually phosphorus

and/or nitrogen either naturally or through human influences (Hall and Smol, 2010). Natural eutrophication can occur for instance, when an area experiences high incidence of fires, during soil development or increased tree die off (Wolin, 1996); eutrophication is however related mostly to anthropogenic forcing through farming activities or sewage disposal (Hall and Smol, 2010). Increased nutrient supplies initially result in a surge in primary productivity in the biological community (Hall and Smol, 2010), but adversely affect species diversity and richness in the long term (Trobajo and Sullivan, 2010). At an ecosystem level, eutrophication can lead to the expansion of the reed belt in the littoral zone to the expense of open water lake conditions (Bao et al., 2007).

Anthropogenic activities can alter or obscure the climatic signal present in the sedimentary record (Wolin and Duthie, 1999). Over the past few centuries human impacts on the natural environment have accelerated (Hall and Smol, 2010). Landscape modification through activities, such as the removal of the natural vegetation either through deforestation or for agricultural purposes, has led to increases in nutrient and particulate loading into rivers and lakes (Reavie and Edlund, 2010); coupled also by decreases in evapotranspiration, increased surface runoff leading to soil erosion and deposition and rapid water level changes (Bradshaw et al., 2005; Wolin and Stone, 2010). A long term perspective on the magnitude of these activities cannot always be gauged, as historical data can be limited in many regions of the world (Bradshaw et al., 2005). Changes in the watershed and in the hydrologic budget due to natural or anthropogenic forcings will directly affect the ecosystem, possibly leading to regime shifts (Snoeijs and Weckström, 2010); all of which will be recorded in the sedimentary record (Fritz et al., 1999). By determining the anthropogenic signal from the natural, a clear indication of human versus natural modifications can possibly be determined (Wolin and Duthie, 1999). The microfossil record preserved in the sediments is used to identify early changes in the biological record, as the extent of these changes can be used to reconstruct changes in water quality; in particular diatom analysis is now sufficiently well established to allow for quantitative reconstructions (Battarbee, 1999).

3.4. LIMITATIONS:

Diatom analysis has certain limitations and assumptions that need to be considered. The importance of determining the ontogeny of the fossil assemblage has to be stressed; transported material within the assemblage may represent species that never lived together in either space or time (Bradbury, 1999). Parautochthonous assemblages may also arise when different habitats occur close to each other, as is the case in some coastal situations (Denys and de Wolf, 1999). For this reason guidelines have been set

out to limit the distortion of misplaced fossils when attempting a reconstruction; these include the consideration of life form, where sessile or benthic species are less likely to be transported than planktonic or tycoplanktonic species, the abundance or commonness of a species, valve preservation or the ecological compatibility within the assemblage and the consistency to the known palaeoecological trends for the region (Denys and de Wolf, 1999). However, small amounts of displaced species may provide valuable insight into environmental conditions during the time interval, for instance the occurrence of marine species in non-marine deposits that occur in close proximity to the sea may provide evidence of increased marine activity (Denys and de Wolf, 1999). Mixing and transport of frustules before burial may cause distortion or inaccurate shifts in the diatom assemblage resulting in an imprecise environmental reconstruction (Fritz et al., 1999). The selective removal of certain taxa from the record may occur either through dissolution, that being the dissolving of the frustule into its constituent elements, or diagenesis, where the frustule dissolves into its constituent elements and the subsequent recombination of the elements (Fritz et al., 1999). The diatom assemblage composition can be affected by the physical processes within the water body, some of these processes are the changing velocity of the water currents, the intensity and frequency of upwelling events, the resuspension and erosion of particles; and biological processes, such as bioturbation (Snoeijs, 1999). Additionally, conservative estimates put the total number of diatoms species at around 200 000, of which only 12% has been taxonomically classified and ecologically described, as well as species constantly being re-categorised and/or placed in newly established genera (Cooper et al., 2010; Julius and Theriot, 2010).

3.5. CONCLUSIONS

As indicated throughout this chapter, diatoms can provide an excellent repository of information on past environmental changes beyond historical records. Although limitations to the proxy have been outlined, they do not outweigh the value of diatom analysis as a palaeoenvironmental tool. Classification schemes based on species optimum requirements and range tolerances aid in identifying periods of significance, ultimately assisting in inferring environmental and climatic changes. In essence, studies into fossil remains contribute to the reconstruction of the past environment and, with additional quantitative assessment and assemblage statistics, further valuable insights are possible (Cooper, 1999; Denys and de Wolf, 1999).

Chapter 4. METHODS

In order to achieve the aims of the project, suitable methods were employed to ascertain the changing nature of the lakes and the mechanisms responsible; this chapter provides a discussion of these key methods.

4.1. SEDIMENT SAMPLING:

Seismic profiling was employed to characterise the lake stratigraphy and identify priority sites for coring. A parametric sediment echo-sounder was used, as it is ideal for shallow lake environments from depths of one meter to 400 meters (Wunderlich and Muller, 2003; Vasudevan et al., 2007). The system works on the basis of transmitting two primary frequencies at high sound pressure through the water column (Lowag and van den Heuvel, 2000). The higher frequency is able to resolve water depth, while the secondary lower frequency is able to penetrate the bottom sediment layers (Lowag and van den Heuvel, 2000). A non-linear or parametric echo-sounder has the advantage over its linear counterpart in that it provides high resolution detail of the sediment profile while improving the signal-noise ratio (Lowag and van den Heuvel, 2000). In this study the parametric echo-sounder, SES-96 light developed by Innomar Technologie (GmbH) was utilised with primary frequencies of 95 and 105 kHz (Lowag and van den Heuvel, 2000; Clausnitzer, 2011). The transducer is compact enough to be mounted to the side of a boat with accompanying equipment. Eleven transects covering a total of 75km were conducted across Swartvlei, Eilandvlei and Rondevlei to determine basin morphology, water depth, sediment layering and accumulation hotspots (Clausnitzer, 2011). Clausnitzer (2011) provides a detailed account of the hydroacoustic profiles for the coastal lakes in the Wilderness Region and identifies depositional focal points within the lakes.

Sediment cores were extracted from several localities within the Wilderness Lakes system using a vibracorer and a modified gravity corer during two field campaigns in 2010 and 2011. The vibracorer is an effective instrument to extract deep, continuous wetland or lacustrine sediment sequences for investigation. Modifications on the vibracorer by Smith (1984, as cited in Baxter, 1997) and Baxter (1997) on the initial design by Lanesky et al. (1979, as cited in Baxter, 1997) allowed for the greater accessibility to a variety of depositional terrains including fluvial, lacustrine and estuarine environments

(Fig. 4.1) (Baxter, 1997). The only requirement for its effective use is that the sediments are unconsolidated and water saturated (Baxter, 1997).

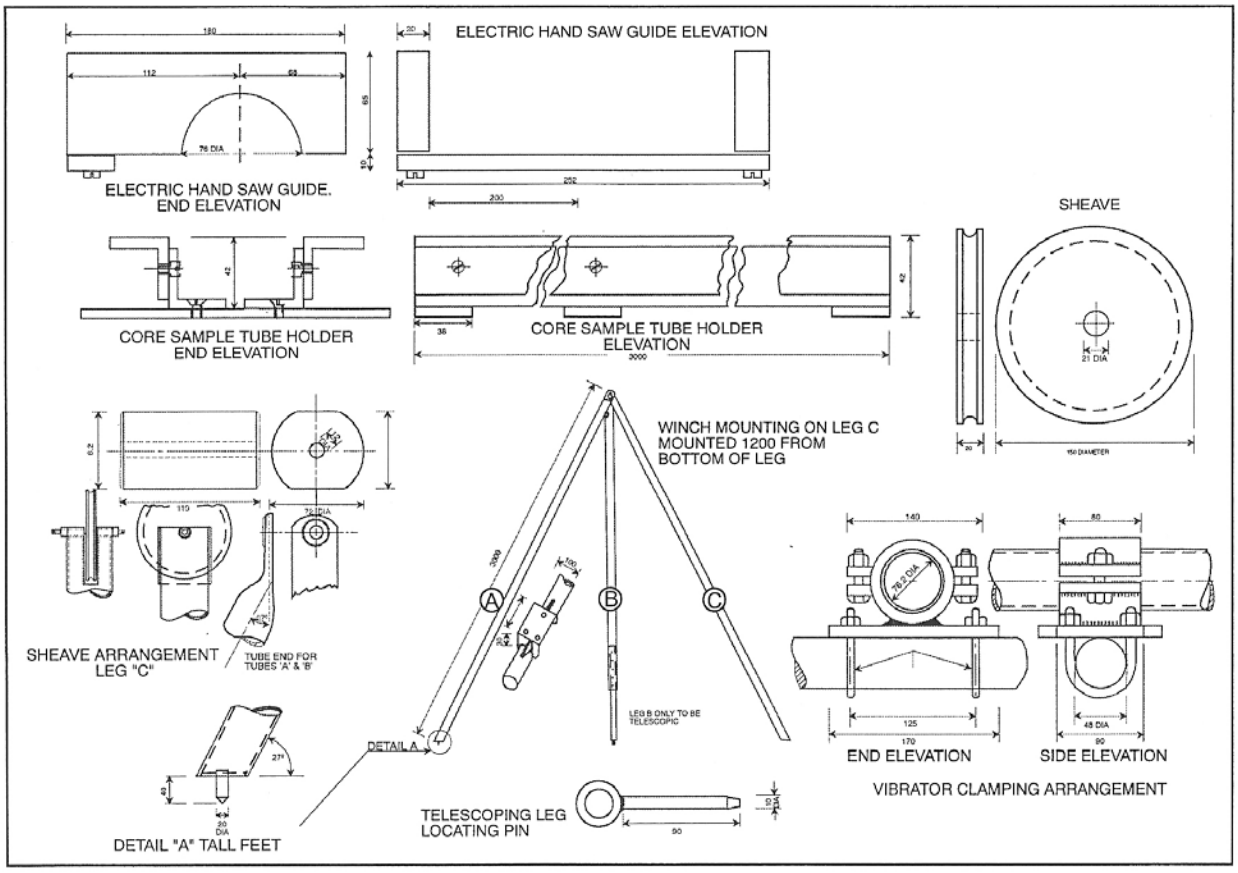

Figure 4.1: The vibracorer and associated equipment as adapted by Baxter 1997

The vibracorer works on the basis of continuous source, high frequency vibrations, which create a low amplitude standard wave throughout the core (Baxter, 1997). A portable generator supplies power to the vibracorer, for this study the University of Cape Town's vibracorer was powered by a 144cm^3, 3.7kW Yanmar GE 50 motor (Baxter, 1997). The core tubing used in this study was standard thin-walled aluminium 'irrigation' tubing, which is available in 6 m lengths, with a diameter of 7.8cm (Baxter, 1997).

The gravity corer works on the principle of the application of kinetic energy created during free-fall of the corer as it passes through the water column. The modified gravity corer used in this study consists of a steel tube to which four steel fins are attached at 90° angle to each other (Meischner and Rumohr, 1974). A flexible plastic tube is secured to the steel barrel, extending beyond the steel tube (Fig. 4.2) (Meischner and Rumohr, 1974). A thin-walled plastic tube provides reduces sediment disturbance during extraction of the core from the sediment by minimising friction. A rope of required length is

connected to opposing fins allowing for the corer to be suspended in the water column and retrieved post sediment collection (Meischner and Rumohr, 1974). The rope also acts as an indicator for sediment penetration, remaining rigid while moving downward and slacking after hitting the water-sediment interface (Meischner and Rumohr, 1974). Initially, the corer is gradually lowered through the water column before being allowed to free-fall the remaining ten or so meters. Once the plastic tubing has fully penetrated the accumulated sediment, the equipment is raised to the water surface and capped to prevent loss of sediment (Meischner and Rumohr, 1974). Additional weights can be added to the steel tube to improve passage through the water column and increase energy.

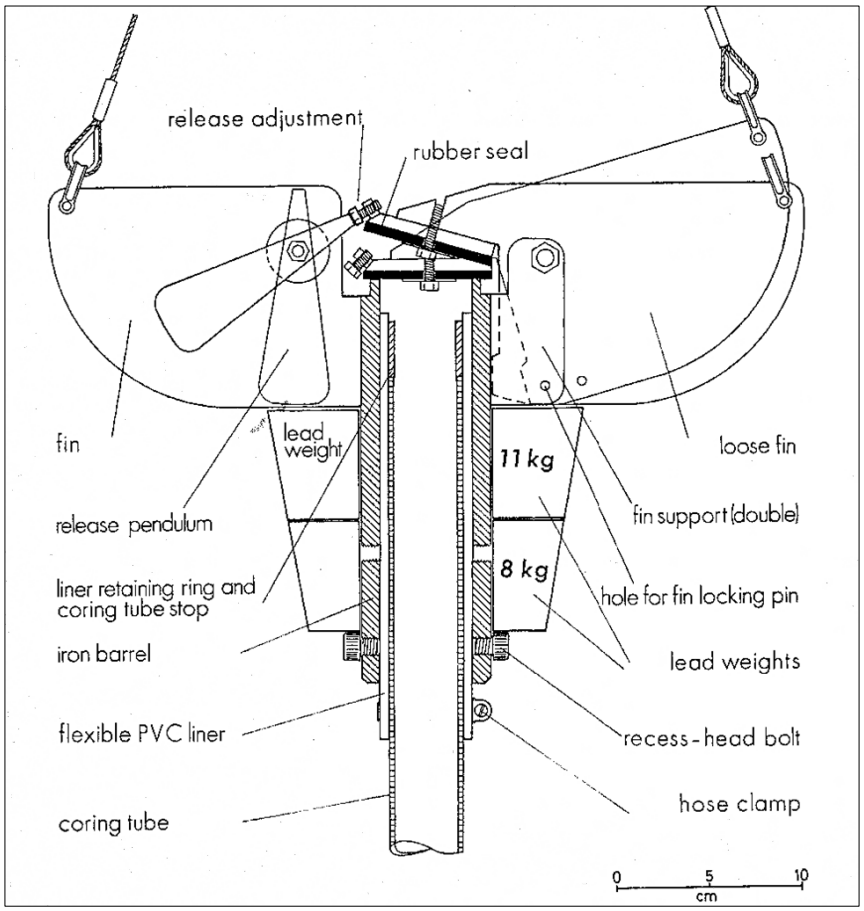

Figure 4.2: Schematic of a gravity corer (source: Meischner and Rumohr, 1974)

Following the retrieval of each core, they were sealed, labelled and transported back to the laboratory. Afterwards each core was split lengthwise for stratigraphical description based on texture, colour and organic content. All cores were described based on grain-size distribution, munsell colour notation and organic content and where available radiograph images. The Troels-Smith scheme for stratigraphic notation was used to indicate changes in lithology (Troels-Smith, 1955).

4.1.1. The Wilderness Cores

Suitable sites were located in the lake based on seismic profiling, which identified areas in the lake that had thick depositional units. The vibracorer was used to obtain two cores from Eilandvlei (EV11.1 and EV11.2) and an additional three cores were retrieved using the gravity corer, i.e. two from Swartvlei (SV10.1 and SV10.2) and one from Eilandvlei (EV10.1). SV10.2 was an exact duplicate of SV10.1 in order to provide additional material for analysis and may be regarded as identical to SV10.1. Of the cores taken from the Wilderness Lakes region, three were used in this study, namely EV11.1, EV10.1 and SV10.1 (Fig. 4.6). SV10.1 and EV10.1 were transported to the Institute of Physical Geography at the Friedrich-Schriller University Jena, Germany, where additional analyses could be conducted including grain size, magnetic susceptibility and inductively coupled plasma optical emission spectrometry (ICP-OES); the results of these analyses form part of two Master's projects coordinated by the Institute in Jena.

EV10.1 (33°59'35.04"S; 22°38'24.84"E) is located at a distance of approximately 590m, on a 130° bearing from the jetty along the eastern shore of the lake, ~215m, at a 180° bearing from the most western tip of the island, and ~590m from the present day outlet. The inlet is situated ~600m to the NNE of EV10.1. Evidence from the seismic profile indicates that the water depth at the site is approximately five meters, with at least two meters of sediment accumulation (Fig. 4.3). EV11.1 (33°59'23.10"S; 22°38'17.60"E) is located at a distance of approximately 280m, on a 90° bearing from the jetty, ~230m at a 310° bearing from the most western point of the island, and ~820m from the present day outlet. The inlet is situated ~670m to the east of the EV11.1. Evidence from the seismic profile indicates that the water depth at the site is between five and six meters (Fig. 4.4). The lateral distance between the two EV cores is approximately 150m (Fig. 4.6). The gravity core retrieved 66.5cm of sediment, whereas EV11.1 retrieved 155cm of sediment. EV10.1 was sampled at 1 – 4cm intervals, generating 25 samples whereas EV11.1 was sampled at 2cm intervals generating 72 samples.

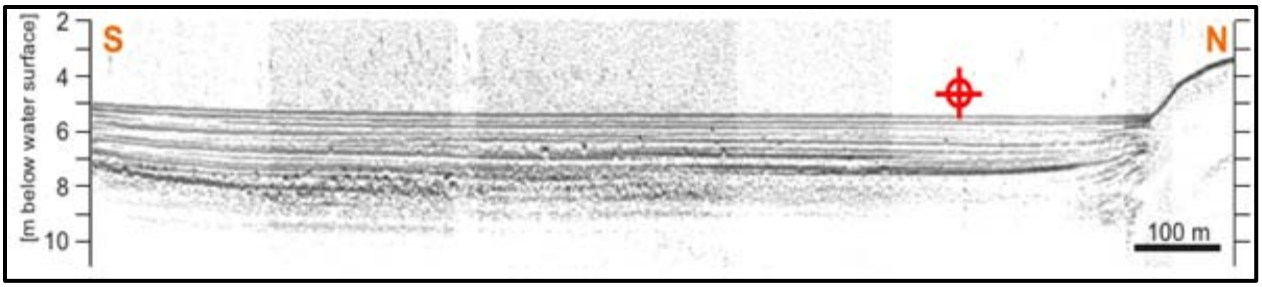

Figure 4.3: Seismic profile from Eilandvlei showing the location of EV10.1 coring site (Courtesy Kasper, 2013)

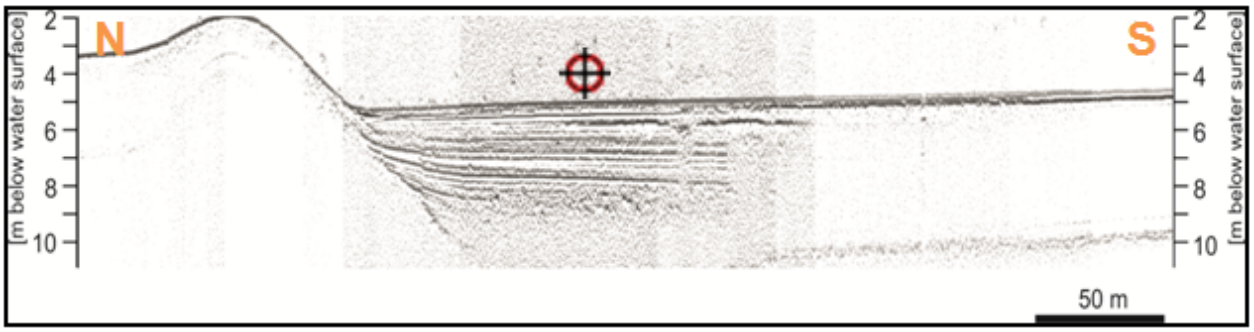

Figure 4.4: Seismic profile from Eilandvlei showing the location of EV11.1 coring site (Courtesy Kasper, 2013)

SV10.1 (33°59'33.42"S; 22°45'26.76"E) core site is located approximately 1600m on a true bearing of 45° from the Pine Lake Marina jetty, and about 400m from the northern shore, and around 1900m from the present day outlet to the Swartvlei estuary (Fig. 4.6). The lake basin morphology shows a series of sub-basins possibly separated by sand barriers. It is from the western sub-basin that the SV10.1 core was obtained. Evidence from the seismic profile indicates that the water depth at the site is between 10 and 11m, with approximately five meters of sediment accumulation (Fig. 4.5). The gravity core retrieved 96.5cm with minimal compaction of the sediment. SV10.1 was sampled at 1 – 4cm intervals, generating 38 samples

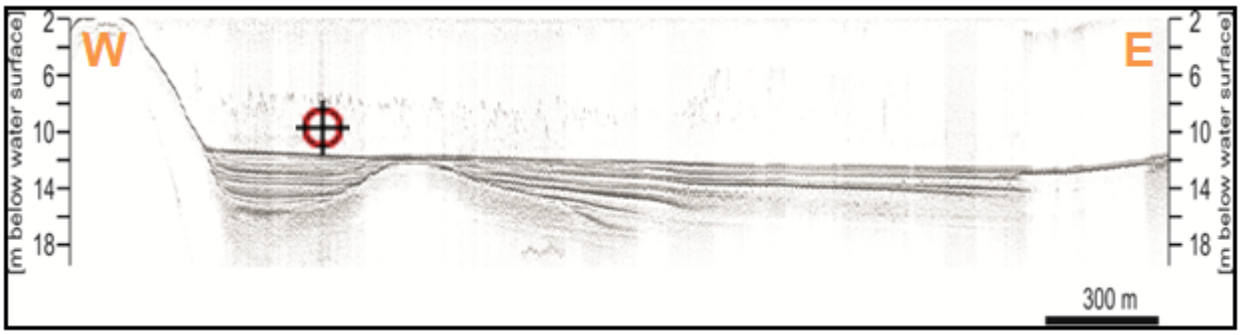

Figure 4.5: Seismic profile from Swartvlei showing the location of SV10.1 coring site (Courtesy Kasper, 2013)

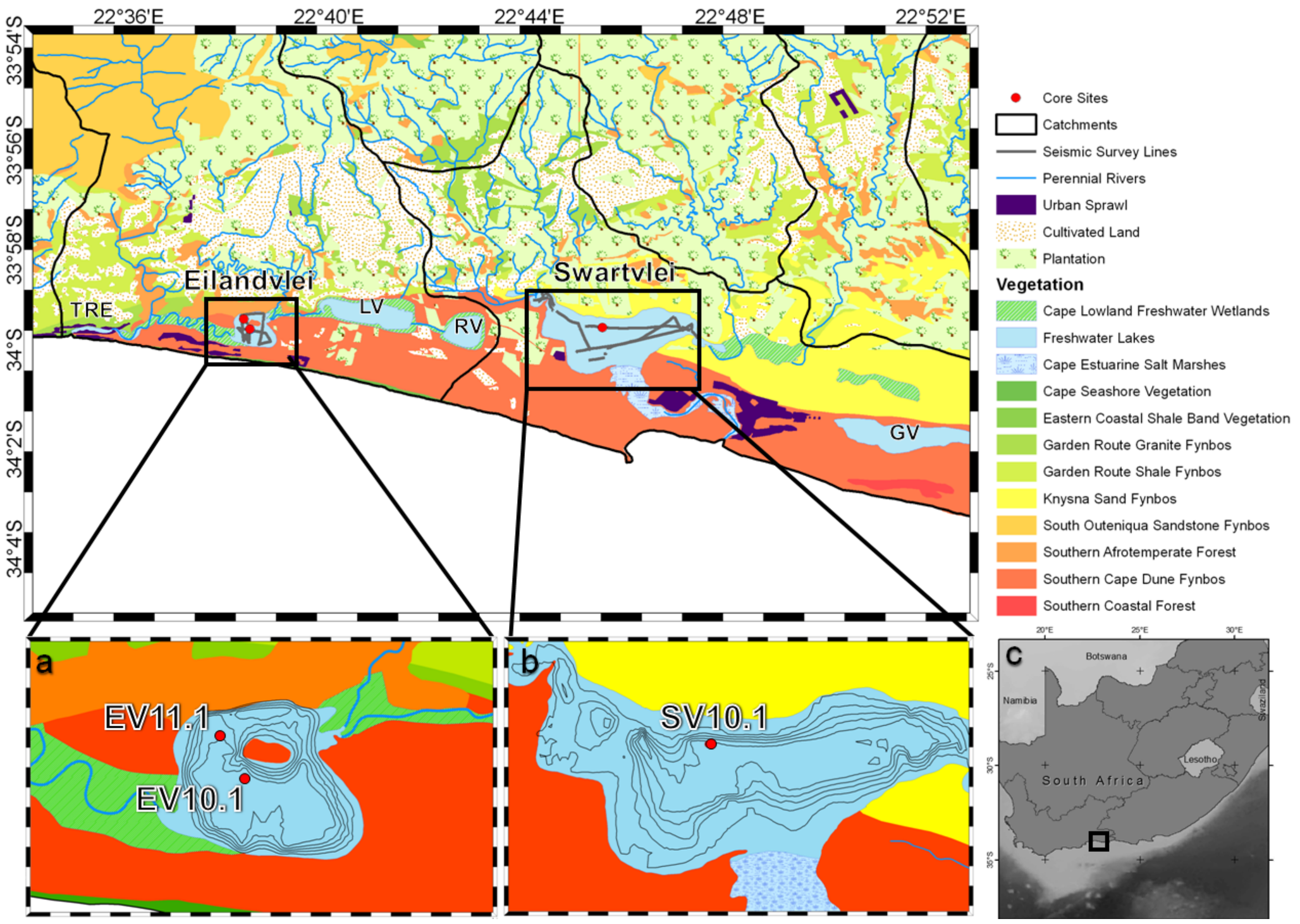

Figure 4.6: Bathymetry of Eilandvlei (1m intervals, inset a) in the Wilderness Lake complex and Swartvlei (2m intervals, inset b) indicating the three core localities incorporated into this study in relation to the south coast of South Africa (inset c) (sources: Appendix One)

4.1.2. The Princessvlei Core

Four cores were obtained from Princessvlei (PV11.1, PV11.2, PV11.3 and PV11.4) at several localities within the lake and around the lake margin. PV11.3 was incorporated into the study as the core chronologically correlated to EV11.1. The PV11.3 site (34°02'44.91"S; 18°28'59.59"E) is situated on the periphery of the northern shore about 250m, on a 80° bearing to the modern day inlet and ~490m at a 160° bearing to the present outlet (Fig. 4.7). The vibracorer retrieved a 210.5cm core. However, the top few centimetres of the core had to be excluded from analysis due to post core-retrieval disturbance. Due to this disturbance and because of the absence of fossils in basal sediments, only 170cm was actually subsampled for diatom analysis, generating 67 samples at approximately two to three centimetre intervals.

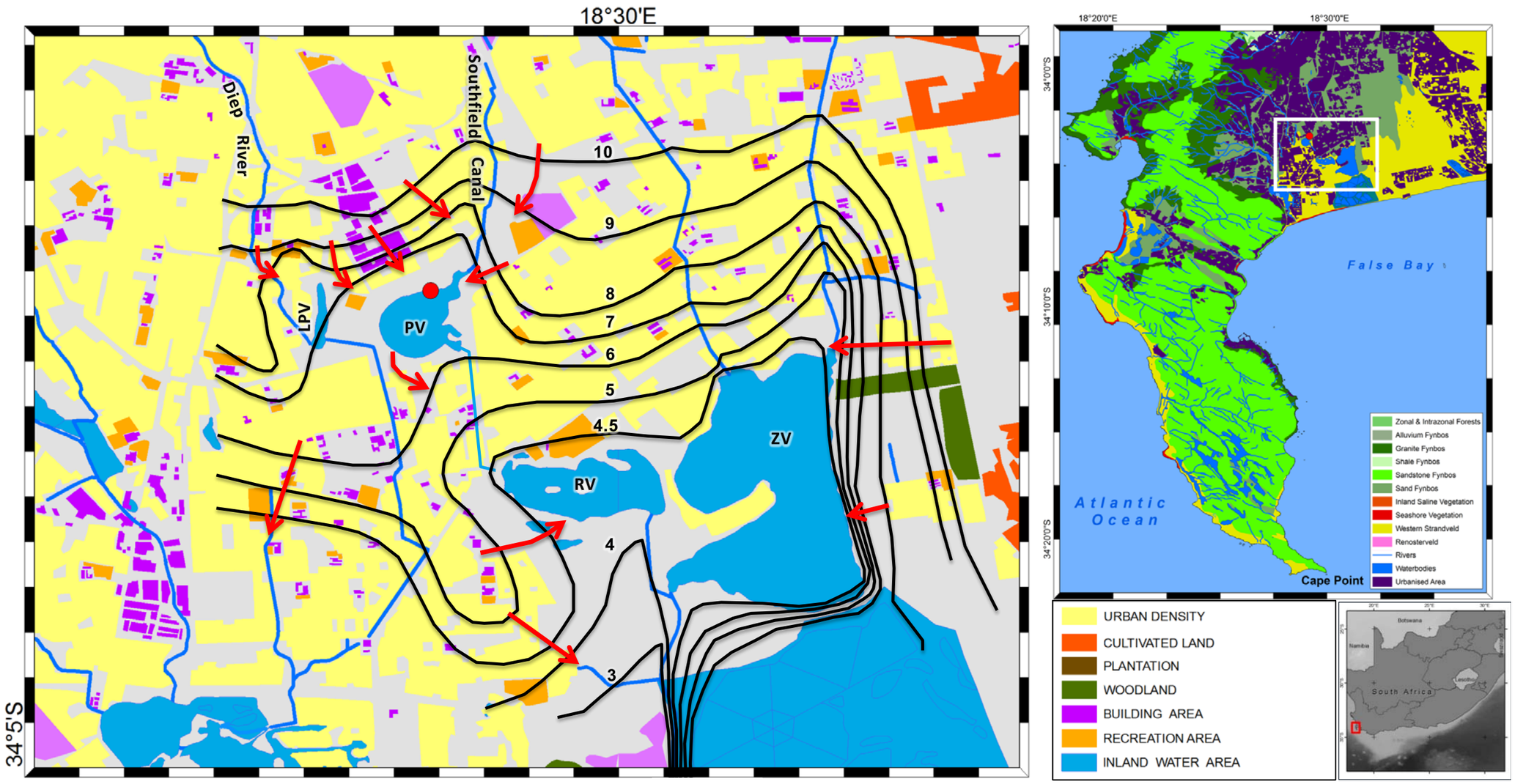

Figure 4.7: The Cape Flats lakes situated on the Cape Peninsula (inset) showing PV11.3 core locality (red dot) at Princessvlei as well as groundwater contour lines and direction (source: Appendix One)

4.2. CHRONOLOGY

Several radiocarbon samples were submitted from both cores to determine the sedimentation history. Samples suitable for radiocarbon analysis were submitted to Beta Analytic Inc., Miami, USA. The radiocarbon method is based on the rate of decay of the radioactive or unstable carbon isotope 14 (^{14}C) in organic material (Walker, 2005). The rate of radioactive decay of the unstable isotope is constant; therefore by measuring the amount of ^{14}C remaining in a sample of fossil material and comparing to modern ^{14}C material, an age can be determined (Walker, 2005). The half-life of the radioactive isotope is ~5730 years, giving an upper dateable age limit of approximately 45 000 years (Walker, 2005). The returned radiocarbon ages were analysed using the package clam v2.2 (Blaauw, 2010) in the open-source statistical software program **R** with the SHCal13 calibration dataset for Southern Hemisphere terrestrial samples (Hogg et al., 2013). The SHCal13 calibration dataset takes into account the temporal offset between the hemispheres (Hogg et al., 2013). The calibration curve is based on a combined set of dendrochronologically-dated records from sites in the Southern Hemisphere and can be confidently applied to ^{14}C measurements from 12.7 cal kyr BP to pre-bomb ages (Hogg et al., 2013; Reimer et al., 2013). Post-bomb samples are represented by the percentage carbon within the sample and can be calibrated using the Wellington $^{14}CO_2$ (carbon dioxide) dataset hosted by the ^{14}CHRONO Centre, Queens University Belfast website[2] (Manning and Melhuish 1994). The temporal scale is directly proportionate to the accumulation rate of the sediments, which are highly variable through space and time (Hall and Smol, 1999). It is important to note that accumulation rates are difficult to estimate accurately (Hall and Smol, 1999). Radiocarbon ages were analysed using the package clam v2.2 in the open-source statistical software package R (Blaauw, 2010) with the SHCal13 calibration dataset for Southern Hemisphere terrestrial samples (Hogg et al., 2013). Probabilities are ranked to a 95% confidence interval, i.e. 2σ (sigma). Post bomb ages were calibrated using the atmospheric $^{14}CO_2$ measurements from Wellington (Manning and Melhuish, 1994).

Most sites incorporated in this study have at least intermittent oceanic exchanges with the possibility of a marine carbon component being highly likely. A marine carbon reservoir correction has been determined for the southwestern Cape of South Africa, which showed a weighted mean ΔR of 146 ± 85 ^{14}C years based on eight known pre-bomb shells from both marine and terrestrial habitats (Dewar et al., 2012). This correction should be applied to mixed terrestrial and marine ^{14}C ages taken from west coast sites; however a south coast calibration correction has never been ascertained. Reinwarth et al. (2013)

[2] http://calib.qub.ac.uk/CALIBomb/frameset.html).

note that samples submitted for radiocarbon analysis from Eilandvlei returned post-modern carbon indicating a reservoir effect of less than 60 years, and therefore a correction for a possible marine reservoir effect was not applied. The Swartvlei system is slightly more complicated with variable exchanges of terrestrial and marine source components being deposited into the system over the course of the last 1400 years. For this study, a chronology was developed without employing a correction for the reservoir effect although it is acknowledged that this may be a factor.

4.3. SEDIMENT ANALYSES

Particle size analysis assists in determining the sorting and size distribution of individual particles within a soil sample thereby establishing sedimentation processes and changes in source material (Menounos, 1997; Gee and Or, 2002). One method to determine size distribution is through the diffraction of a laser beam by the particles within an aqueous solution, which this study utilised (Eshel et al., 2004). The outcome of this is the percentage of the total mass of the sample by set size fractions, which can then be converted relative to standardised international particle size classification (Gee and Or, 2002; Eshel et al., 2004).

Particle size analysis was conducted in conjunction with subsampling for diatom analysis. Samples were sent to the Physical Geography laboratories at the Friedrich-Schiller University for processing using the Beckmann Coulter Laser Diffraction Particle Size Analyzer (LS 13320). The LS13320 is able to measure a range of individual particles from a diameter of 0.045µm to 2000µm (Eshel et al., 2004). Samples were run multiple times, and an average per size classification was taken and presented in a cumulative particle size curve. The results from the sediment analysis, which was used as supplementary information for this project, forms the basis of the Reinwarth (2012), Franz (2012) and Georgiou (2011) investigations on Eilandvlei, Swartvlei and Princessvlei, respectively. For this study the International Soil Science Society (ISSS) Classification of soil particles was used as specified in Table 4.1.

Table 4.1: Particle size classification following the ISSS distribution

	Particle Diameter (µm)
Clay	< 2
Silt	2 - 20
Fine Sand	20 - 200
Medium Sand	200 - 500
Coarse Sand	500 - 2000

4.4. DIATOM ANALYSIS:

Upon inspection it was shown that diatoms occur throughout the cores. In general, a sub-sample with the thickness of 0.5cm was extracted from the core at 2 – 3 cm intervals, as the larger the stratigraphic sample thickness, the more time will be averaged in the prepared sample material and the more difficult it will be to relate the fossil assemblages to modern diatom communities and populations (Bradbury, 1999). However, the sampling was ultimately dependent on changes in lithology and sedimentation rates. Extraneous materials required removal so as to concentrate the diatom sample; this included salts, organic matter and minerogenic matter. The main objective in chemically treating the samples extracted from the individual cores was to obtain satisfactory microscope slides for analysis. For this to succeed a systematic procedure was followed to ensure effective extraction of the fossils; these steps are outlined in Appendix One (as adapted from Battarbee, 1986) and displayed in Figure 4.8 below:

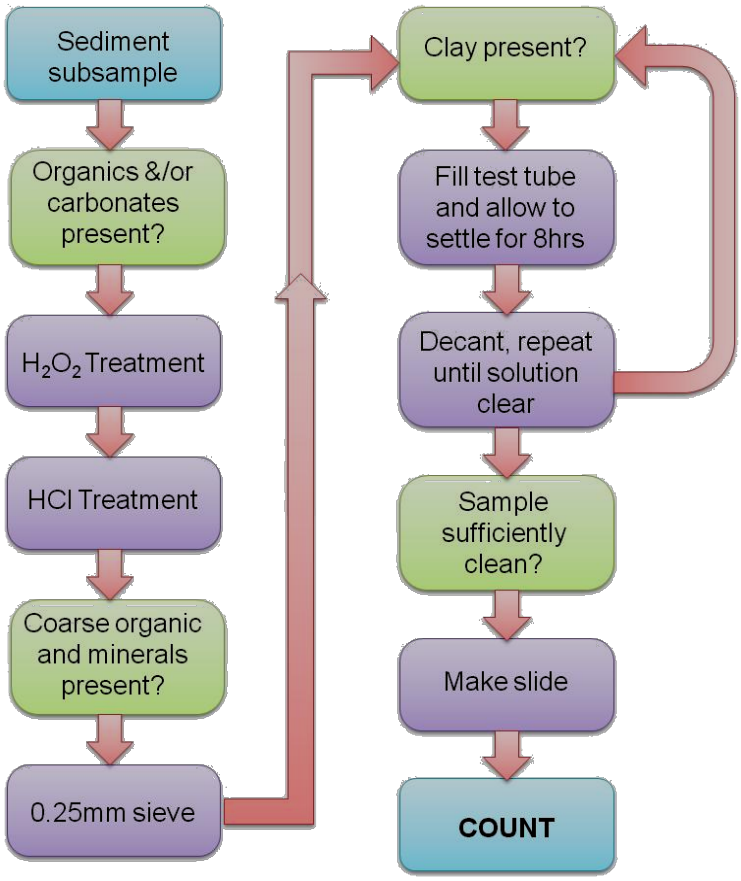

Figure 4.8: Summary of laboratory preparation of lake sediments for diatom analysis (adapted from: Battarbee, 1986, p. 531)

After mounting the slide, diatoms were counted under a light microscope at a magnification of up to X1000 (Lowe and Walker, 1984). To improve precision and significance a count of approximately 500 diatom valves was undertaken. A larger count is necessary if ecologically important taxa are obscured by mass occurrences of more common taxa (Battarbee, 1986). Fragments were also included in the count; but to avoid double counting, only fragments that include the valve centre or a single characteristic feature of the valve were included. Identification of diatom species was based on type collections, keys and photographs in diatom manuals and catalogues, for example Schoeman and Archibald (1976), Bate et al. (2004), Kelly et al. (2005) and Taylor et al. (2007) (Lowe and Walker, 1984). Once identified the diatom assemblage was analysed and displayed using the TILIA and TILIAGRAPH computer package programme (Grimm, 1997). Qualitative and quantitative statistical methods were incorporated to describe trends within the data and to identify underlying mechanisms shaping the sequence and are discussed later in this chapter.

4.5. ISOTOPIC ANALYSIS

Isotopic analysis was conducted on the diatom frustules from the PV11.3 core as a comparative analysis to oxygen isotopic analysis based on carbonate fossils. The aim is to determine the validity of the analysis to South African deposits and compare the results to local records from other coastal regions. The analysis is based on the measurement of the oxygen molecules that comprise the silicate molecule of the frustules. According to Leng and Swann (2010) the frustules are composed of an inner layer and an outer layer, namely a tetrahedrally bonded silica (–Si–O–Si) layer and a hydrous (–Si–OH) layer (Fig. 4.9), respectively. During silicification, oxygen molecules are incorporated into the inner –Si–O–Si layer, while "...the oxygen in the –Si–OH layer is able to freely exchange with any water the diatom comes into contact with" (Leng and Swann, 2010, p. 576). Exchanges occur continuously between the outer layer and the surrounding water; hence during sample preparation the outer –Si-OH layer is either fully removed or taken into account post analysis (Swann and Leng, 2009). Therefore, the $\delta^{18}O_{diatom}$ isotopic composition is the reflection of the ambient water temperature, as well as the isotopic composition of the surrounding water (Swann and Leng, 2009; Leng and Swann, 2010). The analysis assumes that, post depositionally; isotopic exchange between the inner and outer layers of the frustule ceases (Leng and Swann, 2010).

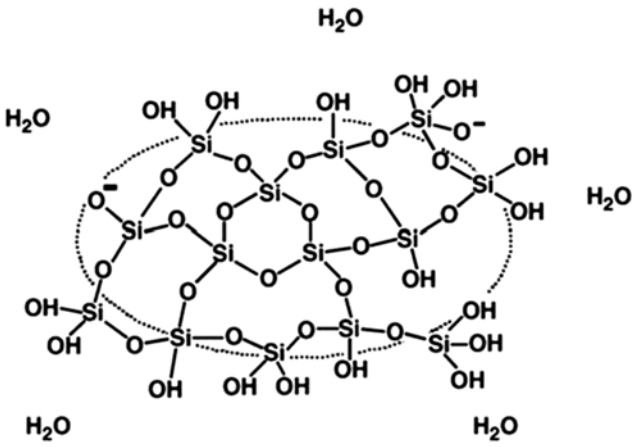

Figure 4.9: Generalised molecular structure of amorphous silica of the diatom frustule (source: Leng and Swann, 2010)

Three techniques have been developed to determine the isotopic composition of the frustules, for a full review see Leng and Swann (2010). For this study inductive high temperature carbon reduction (iHTR) was utilised, which fully removes the outer hydrous layer (Swann and Leng, 2009). The technique superheats a sample of pure diatom frustules, which was placed within a graphite rod, to two preset temperatures under vacuum (see Appendix One) (Swann and Leng, 2009). To remove organic impurities within the frustule casing as well as the hydrous layer, the sample was heated to 850-1050°C before being further heated to 1550°C, which liberates the oxygen from the Si-O-Si bonds converting it to carbon monoxide ($SiO_2 + 3C \rightarrow SiC + 2CO$). The carbon monoxide is then passed through to the mass spectrometer for analysis (Swann and Leng, 2009).

Table 4.2: Princessvlei samples and depths (cm) taken for isotope analysis

Sample	Depth (cm)
PV3.1	19-20
PV3.2	39-40
PV3.3	53-54
PV3.4	72-73
PV3.5	85-86
PV3.6	99-100
PV3.7	114-115
PV3.8	134-135
PV3.9	154-155
PV3.10	170-171

Ten samples were obtained from the PV11.3 core at 15-20cm intervals due to time constraints imposed by the laboratory visit to Forschungszentrum Jülich, Germany (Table 4.2). Initially the samples were chemically treated with 30% hydrogen peroxide (H_2O_2) and 5-10% hydrochloric acid (HCl) to remove organic matter and carbonates, respectively. Between each chemical treatment the solution was washed at least three times. Following this, the residue was diluted with 1000ml of distilled water and allowed to settle overnight to remove clays, with excess supernatant liquid removed through vacuum pump the following morning. The resultant supernant was then passed through a series of sieves to separate large diatoms and silt particulates (>60µm) from mostly diatom and some clay (10 - 60µm) and fine particulates and broken frustules (<10µm). If sufficient sample was rendered in the larger fractions, then each fraction was analysed separately, otherwise upon visual inspection to validate the purity of the larger fraction the samples 10-60µm and >60µm were once again combined. Finally, each sample was subjected to differential settling through sodium polytungstate separation and washed thrice before being freeze-dried overnight (Appendix One, Fig. 11.2). Approximately 600-800mg was required for each run, hence where sufficient sample was recovered, multiple runs were undertaken. Two laboratory standards where run between each PV11.3 sample to correct for drift in the instrument. Leng and Barker (2006) provide a detailed account of the general laboratory protocol for preparation of sediment samples for oxygen isotopic analysis using diatom fossil frustules.

4.6. STATISTICAL ANALYSES

TILIA and TILIAGRAPH present stratigraphic data against either a primary y-axis of depth or age with an option of a secondary y-axis (Grimm, 1997). The x-axis represents the variable, which is typically species (Grimm, 1997). Data can be displayed as a line graph or bar graph with an option to use point symbology for rare taxa (Grimm, 1997). If the autecology of the species is known ecological groups can be shown as well. Autecological classification creates groups within the fossil assemblage which share the same physiological requirements and tolerances. Additionally, TILIA can perform stratigraphically constrained cluster analysis by incremental sum of squares (CONISS) creating a dendrogram which can be appended to the end of the graph (Grimm, 1987, 1997). This assists in identifying zones within the data by creating clusters within which adjacent samples are considered for merging (Grimm, 1987). Ultimately, stratigraphically constrained cluster analysis reveals relationships within and between zones (Grimm, 1987).

Leventer et al. (2010) recognized that changes in species abundance and diversity can be a measure of biological productivity, which in itself is closely linked to the hydrological regime (Abrantes et al., 2007; Weilhoefer et al., 2008). The relationship between species diversity and productivity has generally been found to be unimodal with both negative and positive correlations (Huston, 1979; Mittelbach et al., 2001). Therefore, two biological indices, namely species richness and species diversity, were incorporated to assess the community diversity and productivity within and between the sites through time. The indices provide a numerical documentation of population extinctions and explosions relative to changes in the environment (Gotelli and Colwell, 2001). Species richness (*S*) is a measure of the relative prosperity of a given community (Peet, 1974). In essence, the index calculates the number of species per site/sample and provides a basic comparison of each community (Gotelli and Colwell, 2001). The index is limited, however, as it only reports on the turnover of species numbers and not on the evenness of the community structure (Grubb, 1977). By including a species diversity index, such as the Shannon diversity index (H'), it is possible to provide an additional dimension to the assessment of community structure (Spellerberg and Fedor, 2003). The Shannon index (also known as Shannon's diversity index, the Shannon-Wiener index and the Shannon-Weaver index) is defined as heterogeneous through the act of combining two aspects, namely richness and evenness into its calculation (Magurran, 2004). According to Peet (1974), p. 304), the Shannon formula (shown below) is a 'type one' heterogeneity index, implying that it is "…sensitive to changes in the importance of rare species in the sample".

$$H' = -\sum_{i=1}^{S}[(p_i)\ln(p_i)]$$

where p_i is the relative abundance of each group of organisms. The formula usually returns a value between 1.5 and 4, reflecting changes in species richness and/or species evenness. The value can then be raised to the power, $e^{H'}$; which assists in interpreting the species abundance distribution by indicating the "number of species that would have been found in the sample had all species been equally common" (Magurran, 2004, p. 108). The combination of both indices should provide a quantitative measure of the dynamics of the biological community through time and provide a comparison between sites during overlapping periods. When incorporating biological indices as a measure of productivity it is important to have an understanding of community dynamics as increases in diversity may not be related to the productivity of the system.

Additionally, cluster analysis and principal component analysis (PCA) were included to determine similarity/dissimilarity and underlying driving mechanisms between samples and sites. Cluster analysis partitions data in discrete subgroups relative to some measure of similarity or distance. The Bray–Curtis dissimilarity coefficient was utilised as it has shown "to be one of the most robust and ecologically interpretable measures for species abundance data [by performing] pairwise comparisons between all sample pairs" (Qian et al., 2003, p. 91). Ward's Algorithm was used in this analysis as it identifies relationships between the variables formulating clusters to a significant degree but does poorly in recognizing outliers. The robustness of the algorithm was determined by calculating the cophenetic correlation. The output of the analysis was shown in one of two forms, either a cluster dendrogram or a cluster heat map. The data in a heat map are represented by a colour scaled matrix indicating the degree of similarity of corresponding samples (Wilkinson and Friendly, 2009). The data were ordered based on hierarchical clustering algorithms so that samples are placed near to similar samples (Wilkinson and Friendly 2009). The cluster dendrograms were appended to the y- and x-axes (Wilkinson and Friendly, 2009). A heat map differs from the simplified dendrogram in presentation only, creating a simple visual diagram that reveals the relationship of the samples in the data (Rajaram and Oono, 2010). On the other hand, principal component analysis (PCA) aids in establishing relationships between environmental parameters as well as identifying the most influential environmental factor. This is achieved by reducing a multivariate, inter-correlated data set into several uncorrelated principal components (Jolliffe, 2002; Abdi and Williams, 2005). The components condense the important information within the data set, so that the greatest variance is contained within the first component (Abdi and Williams, 2005). To facilitate the interpretation, the data can be rotated, which simplifies the principal components (Jolliffe, 2002). Both statistical analyses were performed using the package VEGAN v2.0-5 in the open-source statistical software program **R** (Oksanen et al., 2012).

Each individual assemblage was also used in diatom-based water quality indices, in particular the Indice de Polluosensibilité (Index Polluo-Specific sensitivity (IPS)). The IPS measures the sensitivity of the biological community to pollutants, which include organic loading, salinity and any anthropogenic toxins (Raunio and Soininen, 2007). Hence, the index would likely be a measure of the former two variables, namely organic loading and salinity, as most of the individual records utilised in this study experienced either minimal or no human occupation/influences. IPS ranges from a scale of 1 to 5, where 1 represents a very tolerant community and 5 corresponds to a very sensitive community (Raunio and Soininen, 2007). The index was calculated using the Omnidia 7^3 version 8.1 which included the South African Diatom Inventory (SADI 2010 V1) (Harding and Taylor, 2011). The inclusion of the index is as a possible

gauge of the natural development of the system versus the post-human impacted system. In addition to providing a long term assessment of the natural variaibility of the sites incorporated into this project, it may be beneficial in assessing and validating the current and future management practices at each site.

Transfer functions have been increasingly applied to diatom-based studies. In general, the method assigns each species an optimum and a tolerance for the given environmental variable, which ultimately assists in determining the desired variable for the study site with weighted average (Reavie et al., 2004). However, an extensive database is required for these types of reconstructions which incorporate the autecology of the species present in the assemblage. Currently, no such database exists in South Africa and, since endemic species occur within the assemblage any attempt to perform a reconstruction would be unbalanced. Therefore it was decided not to utilise the transfer function methodology in this study.

4.7. CONCLUSIONS

The understanding of the various methods incorporated and outlined above provides a framework on which changes in natural processes can be measured. The interpretation of these methods can aid in the understanding of any variations in the diatom community observed over time and lead to inferences on environmental changes.

Chapter 5. WILDERNESS REGION AND ITS PALAEO-DIATOM ASSEMBLAGES

The Wilderness region is located along the southern Cape coast of South Africa and experiences both rainfall originating from the polar westerlies and the sub-tropical easterlies. This chapter details important physical environmental elements of the Wilderness region, including geology, climate, hydrology, as well as human impacts, before going into the results from the current study.

5.1. REGIONAL SETTING

The Wilderness region can be characterized by three geomorphic elements, namely the Outeniqua Mountains, the coastal platform and the coastal embayment (Birch et al., 1978; Russell, 2013). The Outeniqua Mountains is a series of ridges composed of intensely folded Table Mountain Sandstone reaching elevations of up to 1600m AMSL (Birch et al., 1978; Geldenhuys, 1993). The mountain range acts as a barrier between the moist coastal zone and the more arid interior, and provides the coastal zone with acidic, leached soils that are typically nutrient-poor with low buffering capacity (Geldenhuys, 1993; Russell, 2013). The 200m AMSL coastal platform was once a sea floor during the Tertiary Period but has since experienced uplift and been subjected to sea attack, producing a palaeo-sea cliff that forms the landward boundary of the coastal embayment of the Wilderness (Martin, 1962, 1956; Birch et al., 1978; Illenberger, 1996).

The southern Cape coastline is exceedingly susceptible to high-energy wave action brought about by the strong Agulhas current (James and Harrison, 2008). Successive marine transgressions and regressions assisted erosional processes; this has resulted in deeply incised valleys, broadening and deepening of coastal rivers and the formation of undulating hills ranging in elevations of 180 –240m AMSL across the 5 – 10km platform (Allanson and Whitfield, 1983; Geldenhuys, 1993; Russell, 2013). The platform is underlain by igneous and metamorphic rocks of the pre-Cape granite and Kaaimans group, including phyllites, schists and shales in the west and Table Mountain Sandstone in the east (Fig. 5.1) (Martin, 1962; Dunajko and Bateman, 2010; Russell et al., 2012). Non-calcareous coversands of varying thickness cover much of the Tertiary platform but have been extensively dissected by rivers which are the primary controlling erosional process (Marker and Holmes, 2002; Dunajko and Bateman, 2010; Damm and Hagedorn, 2010; Bateman et al., 2011). Carr et al. (2010) attributed a minimum age of 1.7Ma to the

coversand deposits from a site to the north of the town of Knysna, with reworking of the sediments having occurred in the recent past (Marker and Holmes, 2002).

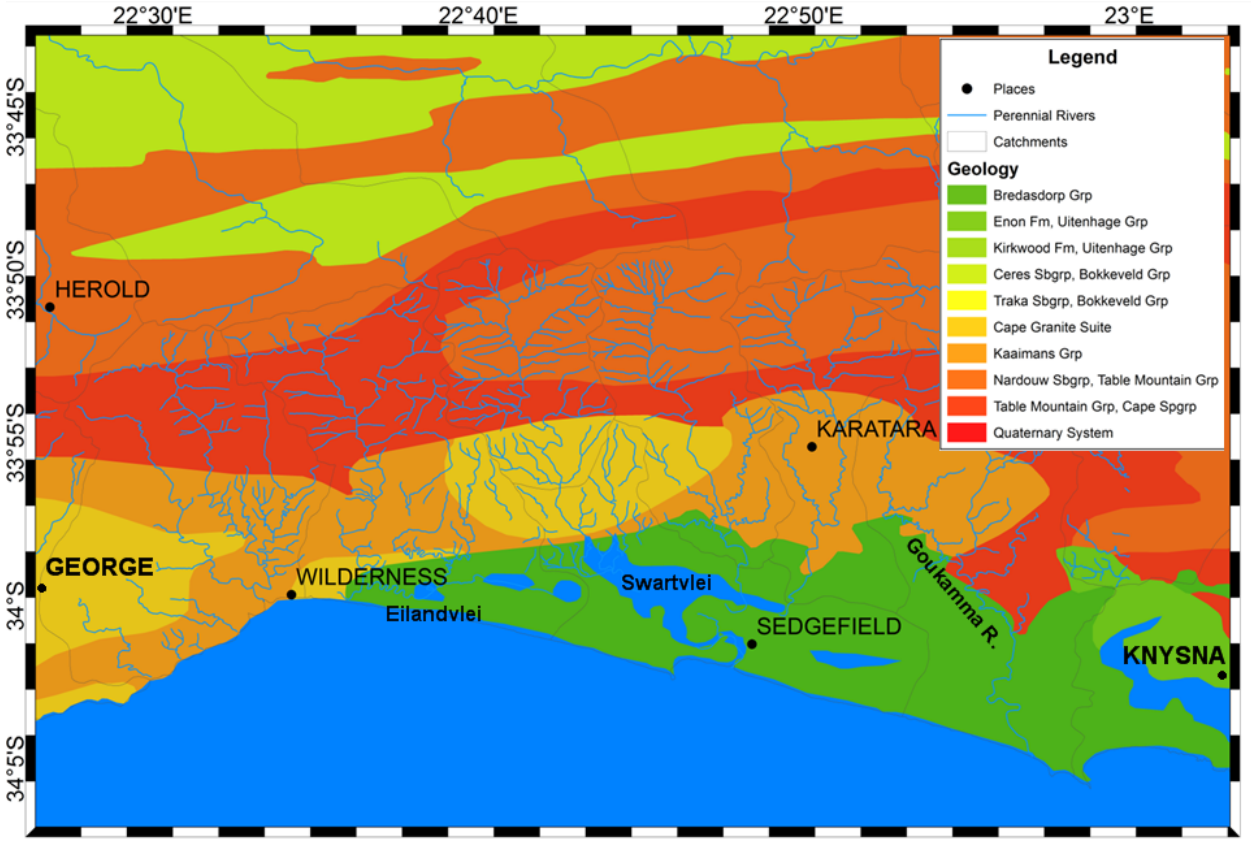

Figure 5.1: Geographical setting of the Wilderness Region showing underlying geology, rivers and water bodies (source: see Appendix One)

The low-relief coastal embayment is characterised by high-rise dune cordons dissected in several places by rivers and extensive back-barrier lake systems (Birch et al., 1978; Dunajko and Bateman, 2010; Bateman et al. 2011; Russell et al., 2012). Three dune cordons run near parallel to each other and converge to the east (Illenberger, 1996; Dunajko and Bateman, 2010). These have been identified as the landward barrier, the middle barrier and the seaward barrier (Bateman et al., 2011). Two further barrier dunes occur offshore (Birch et al., 1978). Each dune is generally composed of carbonate-rich aeolianite mantled by Holocene unconsolidated sand (Birch et al., 1978; Illenberger, 1996; Dunajko and Bateman, 2010). The barrier dunes formed during Quaternary interglacials when successive sea level transgressions and a dominant westerly wind component led to increased aeolian activity (Bateman et al., 2011). Each cordon developed at a point further west to the preceding cordon advancing eastwards along the shore with each new depositional phase (Birch et al., 1978). The landward cordon is the oldest

of the series reaching a maximum height of 280m AMSL and is composed of cemented coastal sands (Bateman et al., 2011). The middle barrier extends from Langvlei to the Goukamma River and reaches a maximum elevation of 210m AMSL (Bateman et al., 2011). Illenberger (1996) proposed that the seaward cordon developed as a barrier island behind which lakes and lagoons formed (Birch et al., 1978). The dune spans the area between the towns of Wilderness in the west and Brenton-on-Sea in the east (Bateman et al., 2011). Although more or less continuous, the dune is breached by the Goukamma, Swart and Touw Rivers resulting in erosion and re-working of sediment (Birch et al., 1978; Bateman et al., 2011). At the Goukamma River mouth, parabolic dunes merge into the seaward dune indicating recent sand movement (Illenberger, 1996). Stabilisation of these mobile coastal dunes has occurred since the AD 1940s through the introduction of alien (Australian) *Acacia* species to inhibit sand encroachment into the Goukamma River and maintain the present river course (Hellström, 1996; Illenberger, 1996). Stabilisation results when shelf sediments are immobilised, and dunes become vegetated (Birch et al., 1978; Dunajko and Bateman, 2010). Hence, the mobile dune field near the Goukamma River has developed a fully vegetated zone (Hellström, 1996). The most recent phase of dune building occurred since the mid-Holocene, when the sea level highstand and later stabilisation supplied the region with sufficient sediment, possibly resulting in the broadening of the seaward cordon (Martin, 1962; Birch et al., 1978; Dunajko and Bateman, 2010; Bateman et al., 2011). Butzer and Helgren (1972) suggest partial stabilisation of the dunes by ca. 4500 cal yrs BP, although Bateman et al. (2011) has shown that Holocene dune development continued between ~3.7 – 2.4ka and 1.7 – 0.6ka. The rivers and longshore drift supply the embayment with sands and finer materials, which has resulted in sandy to loamy-sandy soils with the floodplain veiled with dark, organic-rich alluvium (Illenberger, 1996; Russell et al., 2012).

5.1.1. Regional Climate

The Wilderness Embayment falls within the southern Cape forest-type climatic region as defined by Kruger (2004a). Climate is generally mild, with a mean daily temperature maximum of 19.8°C and mean daily temperature minimum of 13.0°C (Allanson and Whitfield, 1983; Kruger, 2004a). The region experiences bimodal year-round rainfall, ranging from 800mm to more than 1000mm per annum peaking during October (Kruger, 2004b). Sources of precipitation are variable with frontal depressions bringing winter rains, ridging anticyclones bringing spring rains and cut-off lows occurring during early autumn (Cowling et al., 1999). Wind speeds are typically low, flowing parallel to the coast thereby

originating in the westerly and easterly sectors (Kruger, 2004b). Offshore winds occur during the winter months peaking in July, with onshore winds prevalent during summer (Fig. 5.2) (Kruger, 2002).

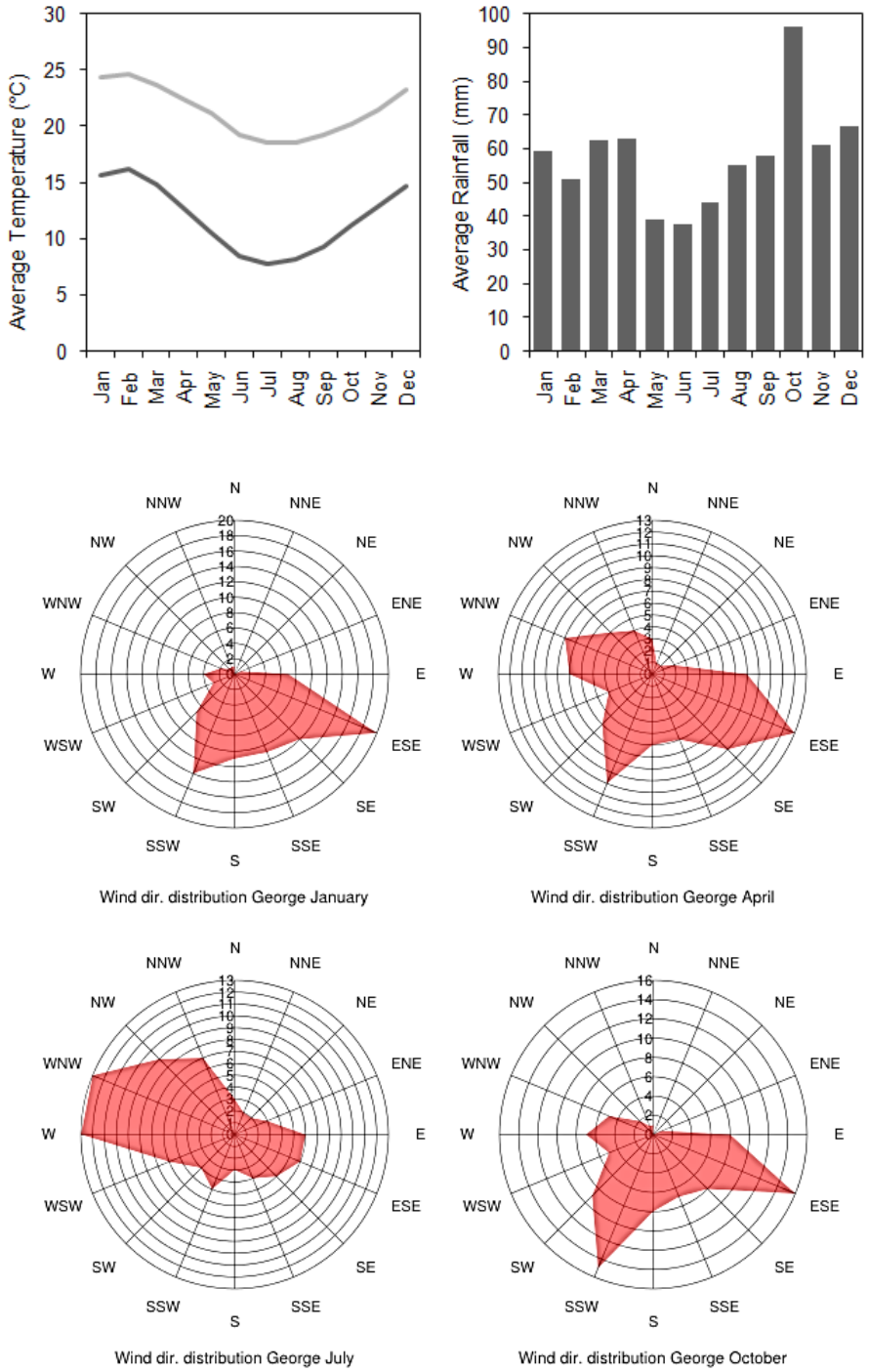

Figure 5.2: Temperature minimum and maximum and rainfall averages per month for the George weather station (Data source: http://cip.csag.uct.ac.za and http://www.windfinder.com)

5.1.2. Hydrology

The Wilderness embayment can be subdivided into two catchments, one comprising the Wilderness Lake complex and the other consisting of the Swartvlei complex. The Wilderness Lake complex is defined by the series of interconnected lakes, which in turn are connected to the Touws River estuary via the Serpentine channel. On the other hand, the Swartvlei complex incorporates Swartvlei Lake, Karatara Lake, Ruigtevlei and the Swartvlei estuary itself. The lakes of the Wilderness embayment owe their formation to the back-ponding of rivers into east-west oriented valleys between each dune (Fig. 5.3) (Hart, 1995; Martin, 1956; Russell, 2013). This led to a network of estuarine lagoons behind barrier islands prior to the current structure of the coastline post dune stabilisation (Illenberger, 1996). Sand movement during the Quaternary is responsible for infilling of the lake valleys and isolating the lagoons into distinct lakes (Hart, 1995; Illenberger, 1996). Martin (1956; 1962) assigns the origins of the lakes to three phases of submergence and emergence during the Pleistocene, with the present configuration taking shape about 7000 years ago (Allanson and Whitfield, 1983). Currently, the Wilderness and Swartvlei systems are the only marine-connected, warm-temperate coastal lakes along the South African coast; the complex forms part of the Wilderness National Park (Hart, 1995; Randall, 1995).

Included in the complexes are the rivers and their tributaries, which feed into the lakes. The rivers flow southward from the mountains delivering $570X10^{3}m^{3}a^{-1}$ of sediment, which is entrained by the lake basins or flows out into the ocean (Fig. 5.3) (Geldenhuys, 1993; Dunajko and Bateman, 2010). River inflow is an important source of nutrients, particularly during flood events; although rivers flowing through areas dominated by Table Mountain Sandstone deliver waters with low concentrations of dissolved solids (Allanson and Whitfield, 1983; Russell, 1999). The relatively porous nature of the underlying soils assists in groundwater flow, which closely conforms to the water table, particularly in summer (Martin, 1956, 1962). The predominantly calcareous nature of the surrounding environment, as well as the relatively constant supply of seawater, has produced rather alkaline systems (Fig. 5.3) (Martin, 1956; Russell, 1999). Notwithstanding, pH fluctuations in the lake complexes respond to four processes as outlined by Russell (1999) *viz*. the inflow of either poorly buffered water, e.g. waters originating from a fynbos dominated area or well buffered water, e.g. seawater influx; biological activity which removes CO_2 from the water column or through the periodic flushing of the system by freshwater (Fig. 5.3).

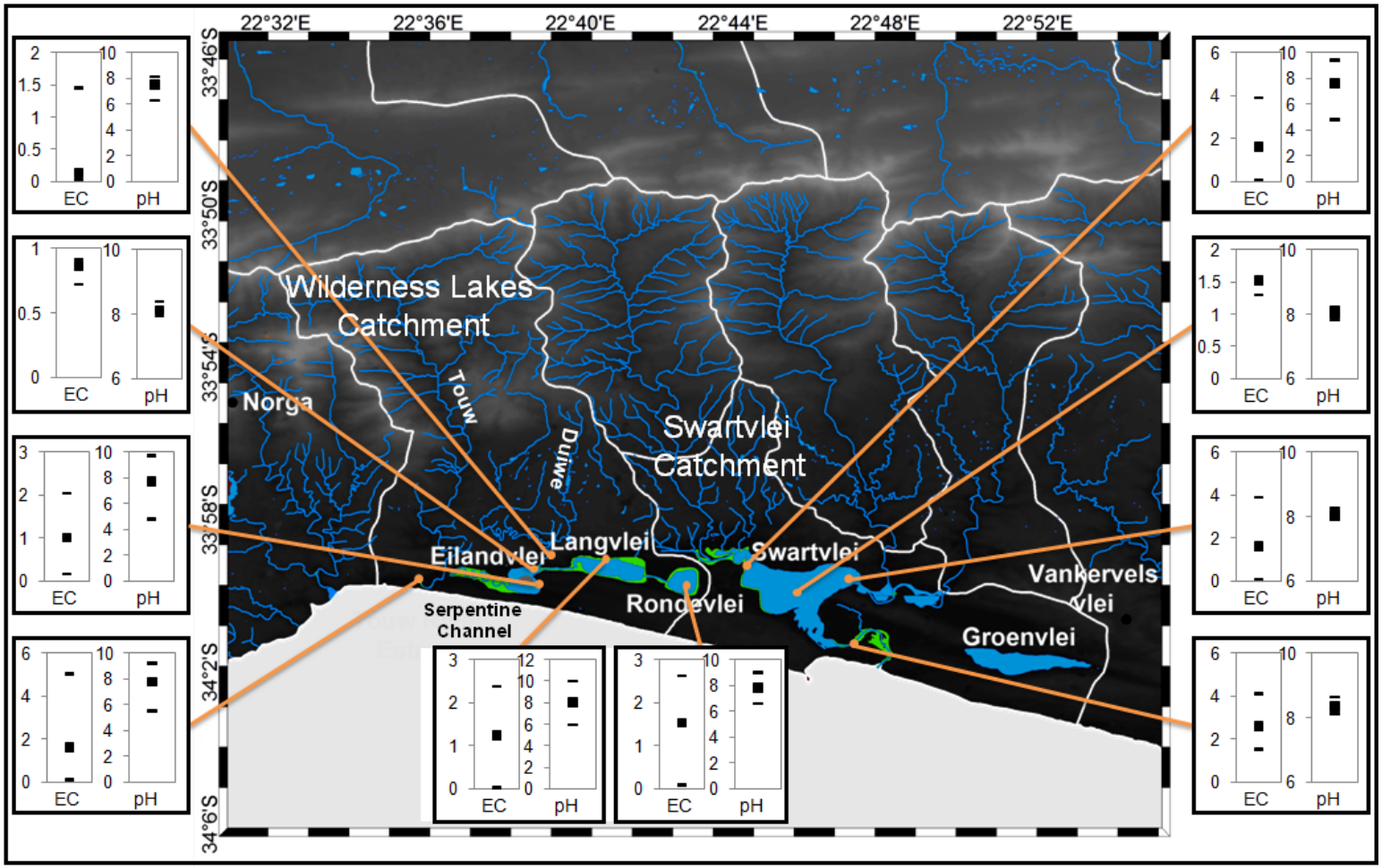

Figure 5.3: The lakes and rivers within the catchments (white lines) of the Wilderness Embayment against elevation, indicating the variability in electrical conductivity (in thousands mS) and pH of selected sites monitored by the Department of Water Affairs (source: see Appendix One)

Both complexes are connected to the ocean to a varying degree via their respective estuaries. Therefore, salinity in both systems is an expression of the mixing of marine waters from the Indian Ocean and freshwater from the rivers, rainfall and groundwater, as well as the relatively low P:E ratio (Martin, 1962, 1968; Adams and Bate, 1994). Tidal level can fluctuate between 1.96m and 0.31m during the transition from mean high water spring tide and mean low water spring tide, causing variations in salinity through the estuaries and ultimately the lakes (Randall, 1995). Generally high wave energy is experienced along the coast with a modal oceanic swell height of 2.1m creating a wave-dominant estuary (Bateman et al., 2011). Onshore winds assist in the propagation of seawater up the estuaries and into the lake systems (Martin, 1962). South-westerly waves dominate the coast particularly during spring and winter, turning south-easterly during summer and autumn (Russell, 2013). South-westerly wave conditions encourage littoral sand movement leading to mouth closure, a decrease in seawater penetration and an increase in freshwater retention in the estuaries and lakes, with the reverse occurring during open phases (Martin, 1962; James and Harrison, 2008; Russell, 2013). The water flow through the estuaries is insufficient to circumvent sand build-up (James and Harrison, 2008). The near continuous exchange of freshwater and seawater into the lake systems has resulted in a rather continuous supply of source waters, thus limiting lake level fluctuations (Randall, 1995).

Wilderness Lake Complex

Figure 5.4: Eilandvlei, looking eastward

The Wilderness Lake Complex consists of the lake Langvlei around which Eilandvlei (Fig. 5.4) and Rondevlei developed (Martin, 1962). The three lakes lie between dune ridges in an east-west valley and are connected via narrow channels (Martin, 1956). Rondevlei is the most eastern lake in the system and is the product of wind deflation during the Pleistocene and back-ponding of freshwater from Langvlei (Martin, 1962). Langvlei is a shallow, elongated lake with a surface area of 210ha and freshwater inflow from the Langvlei Spruit on its north-eastern shore (Adams and Bate, 1994; Hart, 1995; Russell, 1999). Eilandvlei situated to the west of Langvlei and is distinguished by an island of aeolianite near the centre

of the lake (Martin, 1962). The island is thought to have developed either through marine or river erosion separating it from the middle dune cordon (Martin, 1962). The northern shore shows signs of recent sea attack, while the formation of the dune ridge along the coast defined the southern shoreline and lake basin (Martin, 1962). Other than its narrow connection with Langvlei, Eilandvlei is also connected to the Touws River and, ultimately, the Touws Estuary/Wilderness Lagoon via the Serpentine channel (Martin, 1956; Adams and Bate, 1994; Russell, 1999). Hart (1995, p. 114) classifies Eilandvlei as shallow lake with a surface area of 143ha; experiencing "seasonal/intermittent ectogenic meromixis", implying vertical layering of water with the basal water layer being more dense and from an extraneous origin (Martin, 1962). Eilandvlei experiences weak marine exchanges particularly during periods where the Touws River mouth is open (Fig. 5.5) (Russell, 1999).

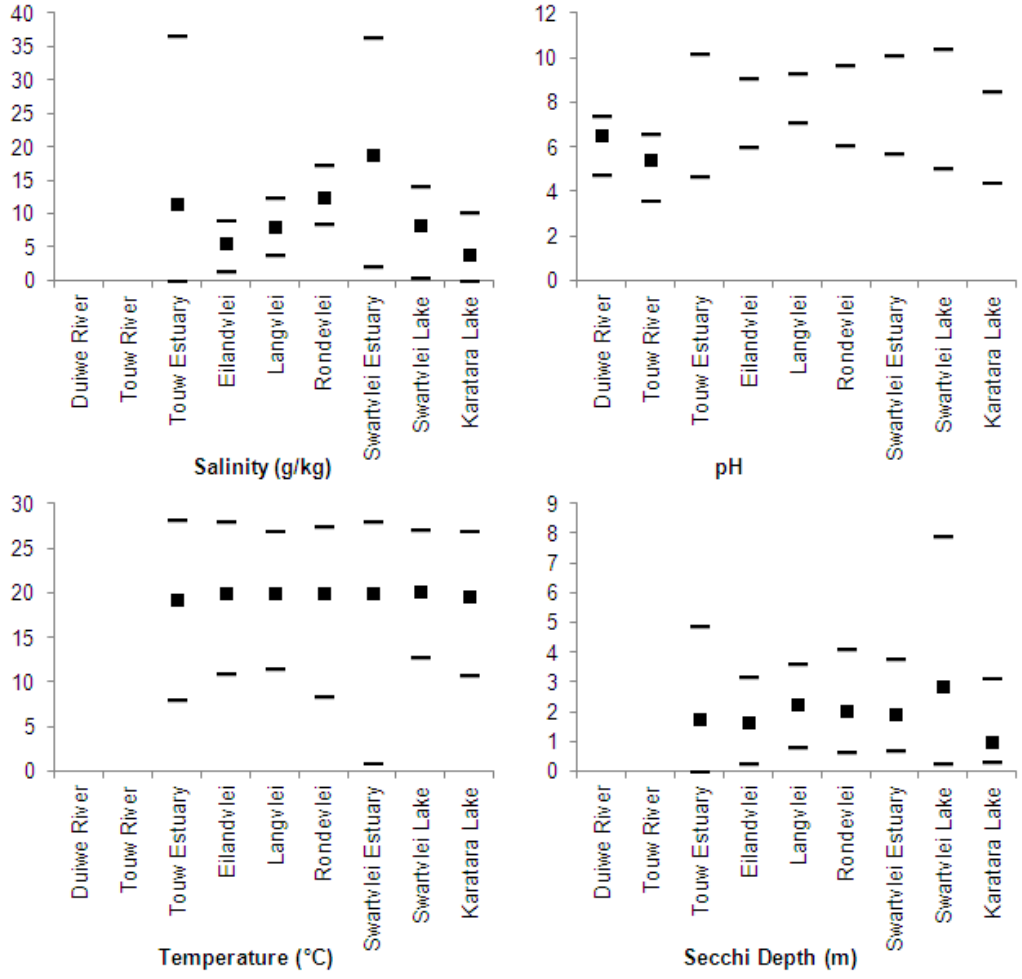

Figure 5.5: Water quality parameters in the Wilderness and Swartvlei lake systems between 1991 and 1997 indicating the extremes (dash) and the mean (square) values (data source: Russell, 1999, p. 60)

The Serpentine Channel meanders through a cultivated alluvium border and sand flat before converging with the Touws River three kilometres upstream of the mouth (Martin, 1956; James and Harrison, 2008). The channel represents the abandoned lower reaches of the Touw River, which may have previously run through Eilandvlei but shortened its course during the relatively recent past in response to sand movement (Martin, 1956, 1962). The Duiwe River is an additional source of freshwater inflow entering Eilandvlei along its north-eastern shore (Adams and Bate, 1994; Russell, 1999; Russell and Kraaij, 2008). With no riverine inputs and dependent on surface runoff, Rondevlei is the most saline of the three lakes, followed by Langvlei and then Eilandvlei (Fig. 5.3 and 5.5) (Allanson and Whitfield, 1983). This salinity gradient is related to the distance from freshwater inputs from the Touws River and reverse freshwater flow through the system (Martin, 1962; Randall, 1995; Russell, 1999). Additionally, a strong axial salinity gradient occurs along the length of the Touws Estuary, which acts as an intermediary between the lakes and sea (James and Harrison, 2008). The salinity gradient is more pronounced during phases where the river mouth is open; however, natural mouth closure frequently occurs to the extent that breaching of the sand bar is undertaken by the managing authorities to prevent flooding (James and Harrison, 2008).

Lake levels respond to the state of mouth closure and rainfall, where highstands often occur during periods of mouth closure and high rainfall, which negates evaporation losses (Russell and Kraaij, 2008). Although water clarity is generally high, surface runoff generated during heavy rains causes an increase in turbidity in all three lakes (James and Harrison, 2008). Sediment and nutrient loading have been altered by dune stabilisation efforts and agricultural pursuits in the catchment (Hart, 1995). The margins of the lakes and the banks of the interconnecting channels have a well-developed emergent and submerged aquatic plant community (Russell and Kraaij, 2008). The community is dominated by a mosaic of *Phragmites australis, Juncus kraussi* and *Scirpus scirpoideus* as well as stands of *Ruppia cirrhosa*, *Stuckenia pectinata* and species of Charophyta (Russell, 1999; Russell and Kraaij, 2008).

Approximately 1300ha of the Wilderness Lake Complex was designated a Ramsar site in 1991, which included the three lakes and the adjoining area spanning from Swartvlei to the convergence of the Serpentine Channel and the Touws River (Randall, 1995). The designation was based primarily on the significance of the region as a refuge and habitat for water birds (Randall, 1995). Although the site does not include the entire Touws River floodplain, the system has been identified as a wetland of conservation importance (Allanson and Whitfield, 1983; Russell et al., 2012).

Swartvlei Complex

Figure 5.6: Swartvlei from the pier at Pine Lake Marina Holiday Resort looking eastward

The Swartvlei system is composed of the Karatara Lake, Ruigtevlei, Swartvlei (Fig. 5.6) and the Swartvlei Estuary (Russell, 1999). As with most of the lakes along the embayment, Swartvlei can be described as a barrier lake formed through the drowning of the valley between the middle and seaward dune cordons and the subsequent build-up of sediment along its southern shore before overflowing into its estuary (Martin, 1962, 1956; Birch et al., 1978; Allanson, 2001). Swartvlei experiences meromixis during the summer months, but stratification disintegrates during winter months when high rainfall delivers an increased volume of freshwater coupled with mouth closure limiting seawater transport up the estuary (Hart, 1995). Sources of freshwater to the lakes are primarily through the perennial rivers, which drain the 402.2km^2 catchment; namely the Diep River, Klein Wolwe River, Hoëkraal River and Karatara River (Martin, 1962; Russell, 1999). Swartvlei is classified as a clear water lake, with light penetration to beyond 5m below the surface; however river inflow carrying substantial sediment loads can result in a decrease in water transparency (Fig. 5.5) (Martin, 1962; Hart, 1995; Russell, 1999). Evaporative losses can amount to nearly 20% of the annual freshwater input into the system (Russell et al., 2012; Russell, 2013). Periodic exchanges of marine water have resulted in increases in pH and salt concentrations (Fig. 5.3 and 5.5) (Martin, 1962; Hart, 1995; Russell, 1999). However, hypersalinity does not appear to be a factor for the system (Russell et al., 2012; Russell, 2013).

Allanson (2001, p. 377) described the Swartvlei Estuary as a “mature shallow sinuous system which is frequently closed during the winter months”. From end to end the estuary stretches 7.2km through sands flats and connects the lake to the sea (James and Harrison, 2008). The estuary, as well as the lake occurs below mean sea level, such that the average tidal amplitude of 0.6m has significant effects on the water chemistry and ecology of the system (Adams and Bate, 1994; Allanson, 2001). An axial salinity gradient is prevalent through the length of the estuary, varying between 8 and 35ppt (Fig. 5.7) (Adams and Bate, 1994; James and Harrison, 2008). Waters are generally warm and saline during the summer months or open phases, cooling and freshening during the winter months or closed phases (James and

Harrison, 2008). This trend is particularly evident between May and October when winter precipitation slowly raises water levels which gradually flow down the winding channel of the estuary (Allanson, 2001). With the onset of spring rains, when peak precipitation occurs, the mouth is breached, and tidal influence is once again instituted (Allanson, 2001). The regular breaching of the mouth acts as an important facilitator in nutrient flushing and re-establishing water transparency (Adams and Bate, 1994).

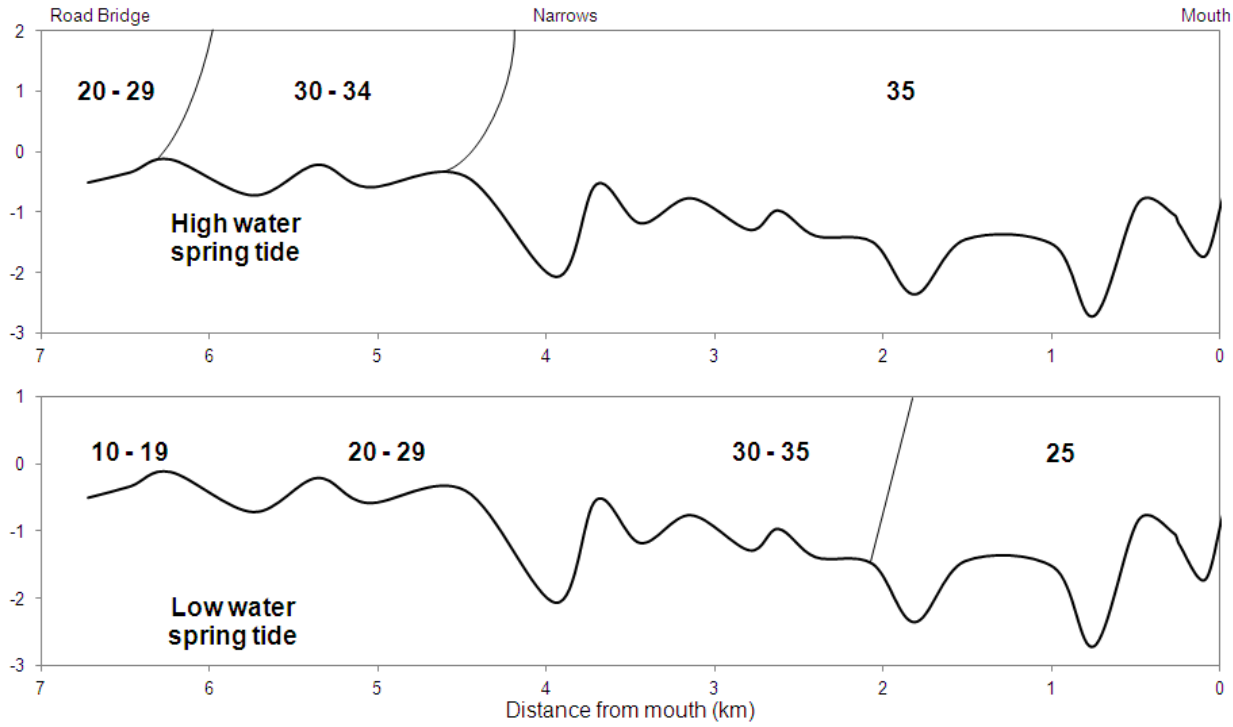

Figure 5.7: Salinity (ppt) profile along the length of the Swartvlei Estuary expressing the extremes of spring high (top) and spring low tide (bottom) against height above mean sea level (source: Allanson, 2001, p. 377)

A palaeochannel is believed to have at some stage connected Swartvlei to Groenvlei, a lake to the immediate east; however sand movement during the mid-to-late Holocene led to infilling of the channel and the isolation of Groenvlei from the Swartvlei catchment (Martin, 1959; Kirsten, 2008). Groenvlei is a closed basin lake with neither inlet nor outlet having developed through the drowning of an interdunal depression (Martin, 1959, 1968). Research conducted by ARH Martin in the 1950s demonstrated that Groenvlei showed signs of sea-level fluctuations, and that its history was mirrored by Ruigtevlei, a wetland in the neighbouring valley to the north (Martin, 1956, 1959, 1960a, 1960b, 1962, 1968). In contrast, Ruigtevlei has maintained its connection to Swartvlei, experiencing periodic influxes of freshwater overflow during flood events (Martin, 1962).

The submerged macrophyte community of the Swartvlei system is extensive, comprising 52.5% of the total aquatic plant community, the remaining 47.5% consists of 12% emergent macrophytes, 14% phytoplankton, 14% benthic macroalgae and 7% microphytes (Hart, 1995). The macrophyte community is similar to that which occurs in the neighbouring Wilderness system, with the inclusion of emergents *Typha latifola* and *Scirpus littoralis* and submerged *Chara* sp (Adams and Bate, 1994; Russell, 1999). *Zostera capensis* is widespread in both estuaries but in greater abundance in the Swartvlei estuary, particularly close to the mouth (Russell, 1999). Although spatially dominant, phytoplankton only contribute 6% to the productivity of the system, which is primarily governed by macrophytes (Adams and Bate, 1994). Diatoms are the prevailing phytoplankton in both systems (Russell et al., 2012; Russell, 2013;).

5.1.3. Vegetation

The Wilderness Embayment stretching from the Touw River Estuary to the western edge of the Knysna Lagoon is classified as the Eastern fynbos-renosterveld bioregion and consists of a mosaic of vegetation units from the fynbos and forest biomes including Garden Route granite fynbos, Garden Route shale fynbos, southern Cape dune fynbos, eastern Coastal shale band fynbos, south Outeniqua sandstone fynbos, Knysna sand fynbos, Cape seashore vegetation and Southern Afrotemperate forest (Mucina and Rutherford, 2006). Although a variety of fynbos-type vegetation units occur in the vicinity of the lakes, the forest component takes precedence especially in the wetter micro-climates such as the river gorges and seaward slopes of the Outeniqua Mountains (Martin, 1968). Patches of Cape Lowland freshwater wetlands and Cape estuarine salt marshes are isolated around the numerous water bodies found in the region (Mucina and Rutherford, 2006).

Table 5.1: Vegetation character and soil dynamics of the Wilderness flora (Mucina and Rutherford, 2006)

Vegetation Unit	Vegetation Character	Status	Soils
Cape Seashore vegetation	Grassy, herbaceous - dwarf-shrubby vegetation	Least threatened	Young, coastal sand derived from Strandveld formation
Eastern Coastal shale band fynbos	Shrublands including thicket, renosterveld and fynbos	Endangered	Clays derived from Shales of the Cedarberg Formation
Garden Route granite fynbos	Proteoid and graminoid fynbos, with ericaceous fynbos in seeps	Endangered	Deep, prismacutanic- and pedocutanic-dominated soils derived from Gape Granite Suite
Garden Route Shale fynbos	Proteoid and ericaceous fynbos, with graminoid fynbos	Endangered	Acidic, moist clay-loam, prismacutanic- and pedocutanic soils derived from Caimans and Ecca shales
Knysna sand fynbos	Dense, moderately tall, microphyllous shrubland	Endangered	Lamotte form derived from Deep, acidic Tertiary sands inland of coastal dunes forming regic sand
Southern Afrotemperate Forest	Tall, multilayered forest with well-developed understorey	Least threatened	Shallow to sandy humic derived from TMG sandstone and shales of the Cape Supergroup
Southern Cape dune fynbos	Fynbos heath dominated by sclerophyllous shrubs and restio undergrowth	Least threatened	Lamotte form derived from Stabilised calcareous or neutral dunes
South Outeniqua Sandstone fynbos	Mainly proteoid and restioid with extensive ericaceous fynbos	Vulnerable	Acidic lithosols derived from Ordovician sandstones of the TMG

5.1.4. Human Impact

Modern *Homo sapiens sapiens* has exploited resources in the region since at least 164ka (Marean, 2010). Caves in the surrounding mountains have provided an archive of *strandloper*[3] occupation, which loosely correlated with periods of surplus shellfish supplies on the coast (Kingston, 1900). Intermittent development occurred since the first cattle farmers entered the area from AD 1730 – 1750, before establishing a permanent settlement of Plettenberg Bay in AD 1787 (Butzer and Helgren, 1972). The forest stands provided opportunities for these early settlers with the population gradually increasing during the 1800s (Randall, 1995). The subsequent completion of a road in AD 1883, a railway line in AD 1928 and the coastal paved road in AD 1948 has made the region more accessible (Randall, 1995). Forestry and agricultural activities have converted nearly 50% of the land cover (Russell, 1999). Tourism and recreational pursuits has become an increasingly important contributor to the local economy (Allanson and Whitfield, 1983). Currently, most of the area of both lake complexes falls under the

[3] *Strandloper* is a cultural reference to Late Stone Age individuals who partook in a beach-combing lifestyle along the west and south coasts of South Africa (Tobias, PV. 1995. Physical anthropology and somatic origins of the Hottentots. *African Studies* 14(1). Pp. 1-15)

management of the South African National Parks (SANParks) while Groenvlei is administered by the Western Cape Nature Conservation Board, Cape Nature. SANParks monitors the status of both the Swart and Touw estuary mouths, breaching the sand bar when lake levels begin to rise and threaten residential properties (Russell, 1999). The interconnecting channels between the Wilderness lakes are periodically dredged to prevent infilling (Randall, 1995).

5.1.5. Summary

The Wilderness Embayment is situated between the Cape Fold Mountains to the north and the Indian Ocean to the south with its western and eastern boundary defined by the Touws River estuary and Buffels Bay, respectively (Butzer and Helgren, 1972; Bateman et al., 2011). The region is characterised by back-barrier lake systems, dune cordons and palaeo-sea cliffs. Hence, its geomorphic evolution is closely related to oceanic influences, particularly marine transgressions. The lake systems are transitional zones that reflect changes in the natural fluctuations of climate and the ocean and more recently anthropogenic forcings and should provide a detailed account of environmental variability (Allanson and Whitfield, 1983). It is under this assumption that several cores were retrieved from two of the coastal lakes and analysed for microfossil remains to determine hydrological fluctuations during the late Holocene.

5.2. RESULTS: EILANDVLEI

Two cores, EV11.1 and EV10.1, were extracted from Eilandvlei and have overlapping records for the last ~600 years. EV11.1 was 155cm and composed primarily of silty clay from 0 – 155cm of varying shades of brown, from 110 – 155cm mollusc shell fragments also occur (Fig. 5.8). EV11.1 was subsampled at a 2cm resolution from 11 – 153 cm generating 72 samples for analysis. EV10.1 was 66.5cm in length and composed of the same silty clay of varying shades of brown (Fig. 5.9). EV10.1 core was subsampled on average at a three centimetres resolution from 64 – 25cm and from 10 – 1cm; however between 25 and 10cm every second centimetre was included for analysis. This generated 25 samples from the EV10.1 core. The diatom species composition of the cores reflects high diversity and richness, particularly during the initial phase of deposition in the EV11.1 core, with later peaks coinciding with increased sand inputs (Fig. 5.8). Both cores show increases in richness and diversity near the surface, which may coincide with the introduction of human activities in the catchment (Fig. 5.8 and 5.9). Post core retrieval of the EV11.1 showed mixing of the top 10cm leading to poor stratigrapical preservation; hence this section was removed from the analysis. The surface disturbance in EV11.1, which was excluded from analyses, is covered by EV10.1. Cross examination of the trends in species diversity implies an exclusion of approximately the last 30 years in EV11.1.

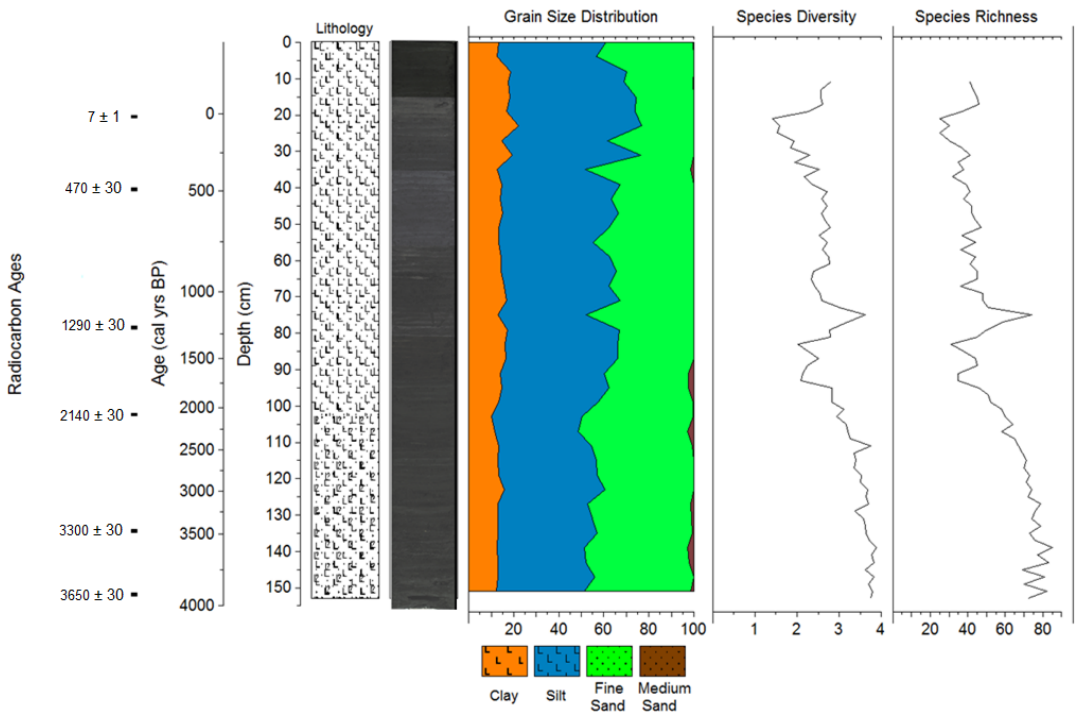

Figure 5.8: Eilandvlei (EV11.1) core description based on Troels-Smith notation, particle size distribution, diatom species diversity and richness against depth (cm)

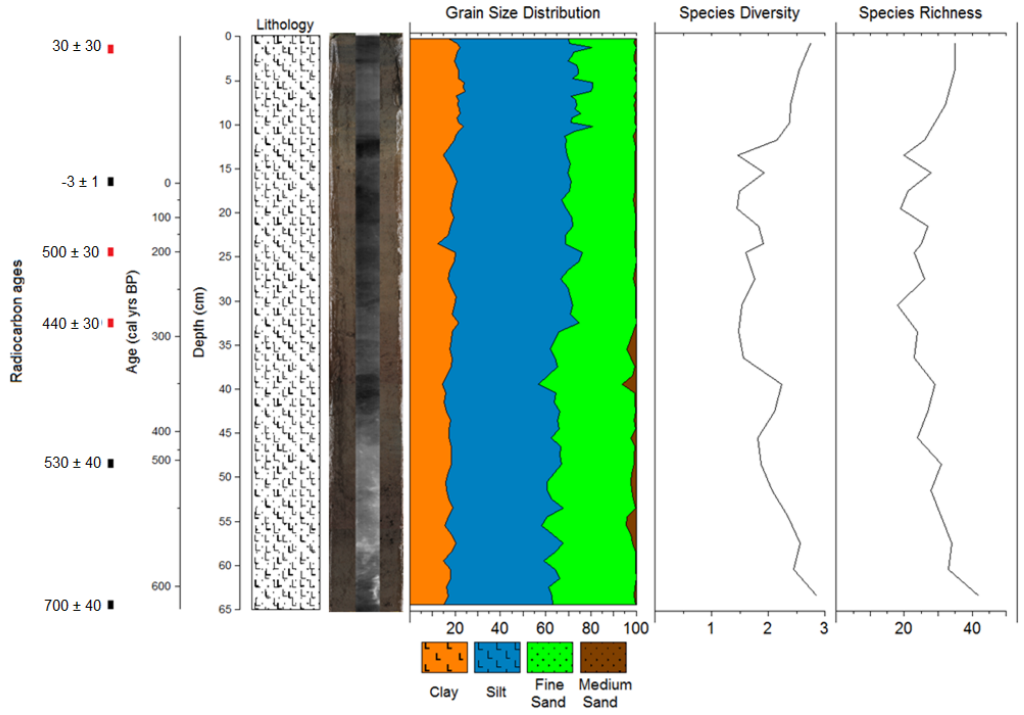

Figure 5.9: Eilandvlei (EV10.1) core description based on Troels-Smith notation, particle size distribution, diatom species diversity and richness against depth (cm)

5.2.1. Chronology:

Both cores show postbomb deposits. Age reversals in EV10.1 occur at 24.5cm and near the surface; both reversals have been classified as outliers and were not incorporated into the age-depth model. The reversal near the surface may be the result from the resuspension and the subsequent deposition of sediment during the dredging of the channels, which are periodically undertaken by the managing authorities SANParks (pers. comm. Ian Russell, 2011). It was assumed that the positioning of the EV10.1 made it more susceptible to the effect of lake level fluctuations, which may have re-mobilised older sediments and caused the reversal observed at 24.5cm. The chronology of EV10.1 was further tuned to the EV11.1 chronology to account for the age reversals experienced downcore based on evidence of known lower lake levels in Eilandvlei. This resulted in the exclusion of the radiocarbon age at 32.5cm, as well. This was achieved through the alignment of peaks in dominant species, particularly the aerophilic species, *Pinnularia borealis* var. 1 (see below). It is assumed that the EV10.1 record still represents a constant period of sediment accumulation. The average accumulation rate for the EV11.1 core is ~0.1cm/yr. However, sedimentation rates appear to be more in the range of 0.04±0.02 cm/yr for most of the record, with recent deposition accelerating to ~0.38cm/yr over the last 50 years (the top 20cm) (Fig. 5.10). The data in summarised in Table 5.2 and 5.3, including the extremes of the lower (yrmin) and upper (yrmax) calibrated range are reported when more than one range is produced.

Table 5.2: The radiocarbon ages of the Eilandvlei EV11.1 core calibrated to the SHCal13 curve indicating the upper and lower calibration range in units, BP with their median probability and corresponding depths

Sample label	Depth (cm)	C14 age	Cal BP	Error	yrmin	yrmax	probability
EV11.1-2	20		-7	1	-9	-6	95
EV11.1-3	40	470		30	341	351	2.8
					452	526	92.1
EV11.1-7	78	1290		30	1071	1193	61
					1197	1262	34
EV11.1-4	102	2140		30	1951	1960	1.8
					1970	1979	1.5
					1986	2147	91.6
EV11.1-6	134	3300		30	3389	3559	95
EV11.1-5	151	3650		30	3733	3742	0.8
					3774	3790	1.7
					3827	3986	90.9
					4048	4064	1.5

Table 5.3: The radiocarbon ages of the Eilandvlei EV10.1 cores calibrated to the SHCal13 curve indicating the upper and lower calibration range in units, BP with their median probability and corresponding depths, ages that have been excluded from analysis are indicated in red whereas ages incorporated in the age-depth model are indicated in black.

Sample label	Depth (cm)	C14 age	Cal BP	Error	yrmin	yrmax	probability
EILAND 0-1cm	**0**	**30**		**30**	**-5**	**-1**	**82.2**
					33	**56**	**8.4**
					123	**133**	**4.8**
EILAND 15-16cm	15.5		-7	1	-9	-6	100
EILAND 24-25cm	**24.5**	**490**		**30**	**470**	**536**	**100**
EILAND 32-33cm	**32.5**	**440**		**30**	**330**	**374**	**18.8**
					441	**512**	**76.6**
EILAND 48-49cm	48.5	530		40	490	555	100
EILAND 64-65cm	64.5	700		40	559	667	100

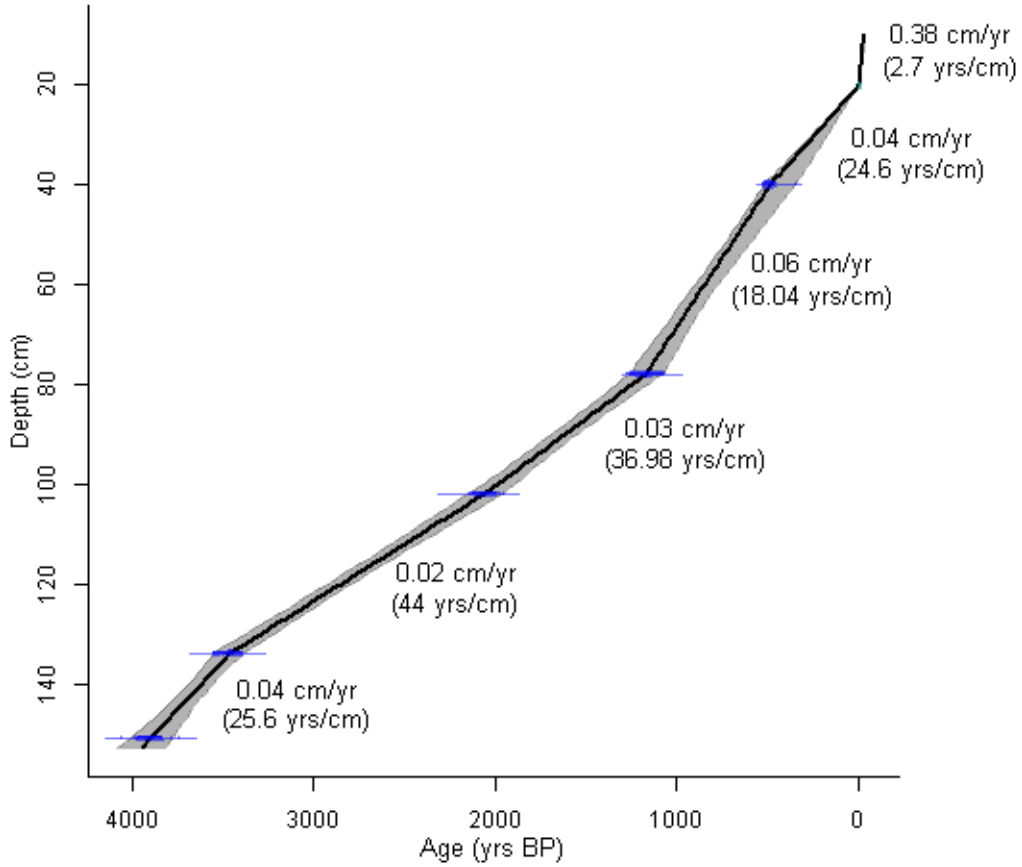

Figure 5.10: Age-depth model for Eilandvlei EV11.1 core calibrated to the SHCal13 curve indicating the upper and lower calibration range in units, BP with their median probability and corresponding depths

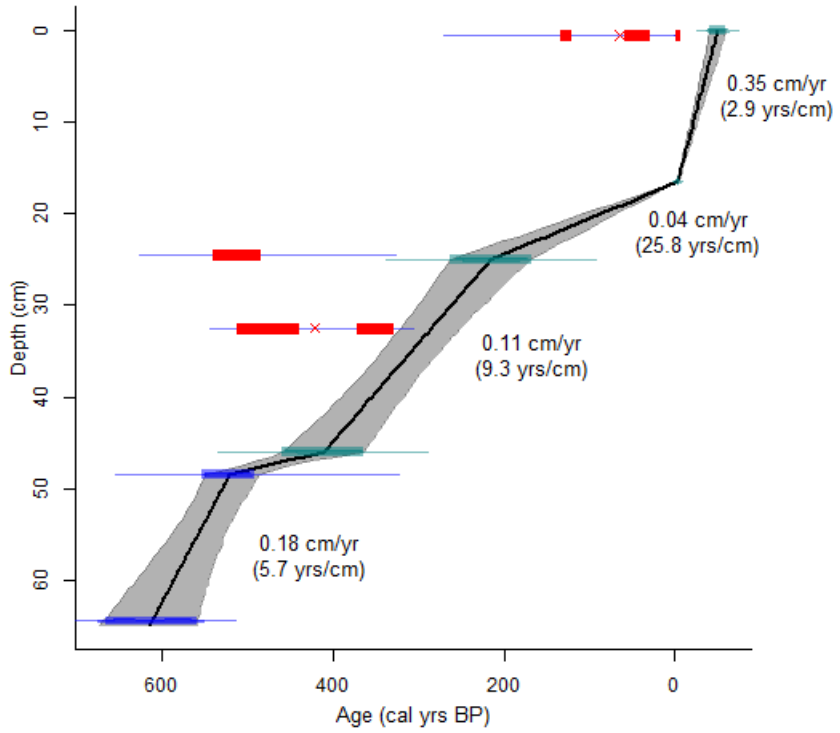

Figure 5.11: Age-depth model for Eilandvlei EV10.1 core calibrated to the SHCal13 curve indicating the upper and lower calibration range in units, cal yrs BP with their median probability and corresponding depths. Samples that have been excluded from analysis are indicated in red whereas samples incorporated in the age-depth model are indicated in blue while samples related to the alignment of the diatom species, Pinnularia borealis *var. 1 are shown in green .*

The diatom assemblage is mostly dominated by alkaliphilous, meso-eutrophic taxa. A complete list of each species autecological preference based on salinity, pH, life form and nutrients can be found in Appendix Two (Table 11.4, Pg. 249 and Table 11.2, Pg. 240). Generally, brackish species dominate, although phases of marine and fresh-brackish indicator dominance do occur. Based on CONISS (Grimm, 1987), the EV11.1 assemblage can be divided into five zones, *viz.* zone EV11.1a (approximately 4000 – ~2050 cal yrs BP; 154 – 103cm), which is further subdivided into zone EV11.1a.1 and zone EV11.1a.2 at ~3450 cal yrs BP (134 cm), zone EV11.1b (approximately 2050 – ~1200 cal yrs BP; 103 – 78 cm), zone EV11.1c (approximately 1200 – ~500 cal yrs BP; 78 – 40 cm), which is further subdivided into zone EV11.1c.1 and zone EV11.1c.2 at ~1050 cal yrs BP (60cm), zone EV11.1d (approximately 500 – 0 cal yrs BP; 40 – 20 cm) and zone EV11.1e (0 – -31 cal yrs BP; 20 – 11 cm) (Fig. 5.12). The EV10.1 core overlaps EV11.1 from zone EV10.1c.2 to zone e and is defined as the same zones relative to the core length and chronological expanse. For simplicity the zones in EV10.1 are labelled as follows: zone EV10.1c.2 (~600 –

520 cal yrs BP; 65.5 – 48 cm), zone EV10.1d (520 – 0 cal yrs BP; 48 – 19 cm) and zone EV10.1e (0 cal yrs BP – Present; 19 – 0 cm) (Fig. 5.13).

5.2.2. Assemblage Zonation

The assemblage of zone EV11.1a (approximately 4000 – ~3450 cal yrs BP) is primarily dominated by marine to marine-brackish species. However, the continual occurrences of brackish taxa, such as *Cyclotella caspia*, *Mastogloia smithii*, the indifferent species *Tabellaria fenestrata* and the diatom *Thalassirosira weissflogii* suggests mixing of water sources of various salinities (Taylor et al., 2007). Fluctuations in *Paralia sulcata* appear to characterise these early stages particularly at the transition from zone EV11.1a.1 to zone EV11.1a.2. *P. sulcata* typically occurs in cool (>3°C) (McQuoid and Nordberg, 2003), newly upwelled waters that have high primary productivity (McQuoid and Nordberg, 2003; Abrantes et al., 2007). *Amphora ovalis* is generally present throughout zone EV11.1a but shows greater abundance between 3425 and 3075 cal yrs BP, peaking at 3250 cal yrs BP and again at 2900 cal yrs BP. The species, along with *Cocconeis scutellum*, is classified as epipsammic and able to colonise sandy substrates (Harper, 1969; Horton et al., 2006). Epiphytic species, such as *Cocconeis costata*, a marine species, *C. scutellum* a brackish marine species, and, to a minor degree, *Cocconeis placentula*, a fresh-brackish species suggest a distinct salinity gradient across the lake with a more direct oceanic influence in the nearshore area and a defined submerged macrophyte region (Main and McIntire, 1974; Howard-Williams and Liptrot, 1980; Sawai et al., 2004; Taylor et al., 2007). It has been suggested that *C. scuttelum* should be classified as allochthonous, since following death the P-valve is easily transported (Sawai et al., 2004; Horton and Sawai, 2010). Nevertheless, both the R-valve and P-valve remains of this species occur in the fossil record and the occurrence is therefore viewed as autochthonous.

The wide range of marine species is indicative of a well-established *in situ* community. A decline in the abundance but not richness of marine species is observed during zone EV11.1a.2 (~3450 - ~2050 cal yrs BP, 134 – 103 cm), since the brackish-marine component persists until the termination of the stage. This trend is accompanied by a dramatic increase in the fresh-brackish, aerophilic species *Pinnularia borealis* var. 1 (Sawai et al., 2004; Johansen, 2010). The classification of *P. borealis* into the variant *Pinnularia borealis* var. 1 is based on both frustule morphologies occurring throughout the core. The fresh-brackish component is more distinct during zone EV11.1a.2 possibly due lower marine influence. The co-occurrence of *Pinnularia borealis* var. 1 and *Diploneis elliptica* points to an abundance of mosses along the shore, which may be subject to periodic drying (Sawai et al., 2004).

The next c. 850 years, from 2050 – ~1200 cal yrs BP (zone EV11.1 b), is predominately defined by brackish species. *Cyclotella caspia, Cyclotella distinguenda*, *Cocconeis engelbrechtii* and *Tabularia fasciculata* are abundant during this period but subdominant to *Melosira nummuloides*. The co-occurrence of *C. caspia* and *M. nummuloides* implies a dynamic environment with fairly regular mixing of source waters. *C. placentula* is more abundant during this stage than in the previous and coupled with *Cocconeis pediculus* and *M. nummuloides* indicate that macrophyte growth was not hindered in the transition from zone EV11.1a.2 to zone EV11.1b (Main and McIntire, 1974). Periodic influxes of marine water are evident in the minor peaks in *Coscinodiscus radiatus* and the occurrence of *Catenula adhaerens* (Schuette and Schrader, 1981; Sundbäck and Medlin, 1986). Near the termination of zone EV11.1 b and following into zone EV11.1 c.1 (81 – 69 cm, *ca*. 1275 – 1000 cal yrs BP), there is a rapid emergence of *Cyclotella choctawhatcheena* suggestive of greater concentrations of salts and increased turbidity (Gasse et al., 1995; Snoeijs and Weckström, 2010). Subsequently, a sudden and persistent abundance in *P. borealis* var. 1 and, to a greater degree, *C. radiatus* occurs from 79cm (*ca.* 1200 cal yrs BP) until the end of zone c.1 at 63cm (~900 cal yrs BP). *C. radiatus* commonly occurs along the coast of South Africa particularly in summer blooms (Romero et al., 2002), where populations can tolerate the elevated water temperatures of the upper water layers (Baars, 1979). Schuette and Schrader (1981) also characterised *Coscinodiscus* species as pioneers in newly upwelled water in the Benguela system on the west coast of South Africa. At 75cm (approximately 1120 cal yrs BP) a peak in the Shannon Index and in species richness with a recovery in marine diversity is observed. A drop in pH toward more neutral water is identified during this period as well as a decline in planktonic species, which may be related to the increase in *P. borealis* var. 1.

The upper half of zone EV11.1 c from 63 – 41 cm (900 – 500 cal yrs BP) is characterised by brackish, alkaliphilous and meso-eutrophic taxa. *M. nummuloides, C. caspia, C. distinguenda* and *C. engelbrechtii* are the main constituents of the biological community, a composition reminiscent of zone EV11.1b. *C. radiatus* is still present in the assemblage but diminished in distribution. The overlap with the EV10.1 occurs at ~600 cal yrs BP, with the same species composition prevalent. EV10.1 records a greater range of marine species other than *C. radiatus* including *P. sulcata, Petroneis humerosa and Delphineis minutissima* are in greater abundance during this period. The position of the cores may provide an explanation for this signal. EV10.1 is directly in line with the modern day outlet and, accordingly, is influenced by tidal backwash, whereas EV11.1 is slightly shielded by the island and hence is less influenced by marine deposition (Fig. 4.6). The inverse is also evident, the fresh-brackish species *C.*

placentula occurs in higher frequencies in EV11.1 than in EV10.1, as it is closer to the modern day freshwater inlet.

Zone EVd is almost entirely dominated by *M. nummuloides* and *C. radiatus*, and combined they form approximately 82% of the EV11.1 assemblage at 25cm (180 years ago). This period can be defined by low productivity in a brackish, eutrophic system. Minor peaks in *P. borealis* var. 1 in EV11.1 and more pronounced peaks in EV10.1 suggest lower lake levels and the expansion of wetland habitat. The end of this zone at 20cm (~ AD 1950) is characterised by almost 70% *M. nummuloides*, suggesting distinctly adverse conditions possibly related to or exacerbated by human activities in the catchment. In this respects, adverse conditions would generally be affiliated with conditions that do not favour biological activity and hinders the development of the diatom community. The last 50 years of the record represented by zone EVe sees a dramatic increase in brackish species similar to zone b. *M. nummuloides* and *C. radiatus* occur in trace amounts. Although *Chaetoceros* resting spores (CRS) occur throughout both cores, it is only during zone EVe that their distribution increases to just over 13% at ca. -30 cal yrs BP. CRS are indicators of shallow water mixing and high nutrient pulses resulting in algae blooms (Leventer et al., 2010).

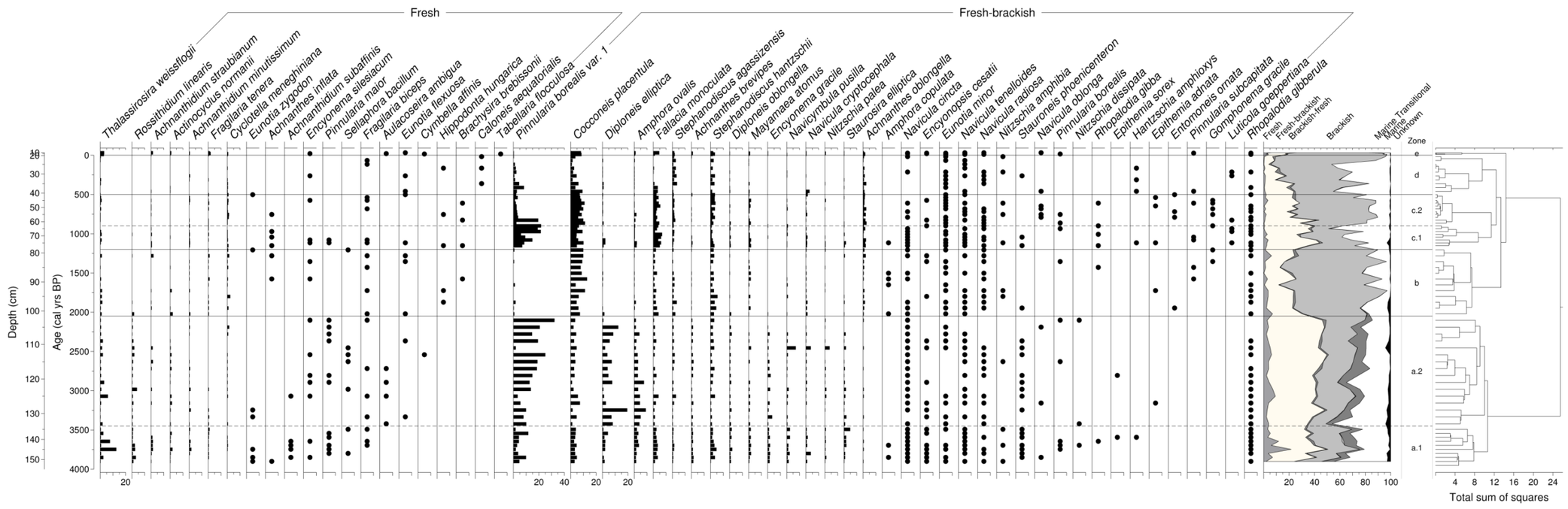

Figure 5.12.1: The Eilandvlei EV11.1 core stratigraphy and percentage diatom representation against depth (cm) and age (cal yrs BP), diatom species are grouped based on salinity preferences (% Fresh to % Fresh-brackish). Five zones were identified based on CONISS

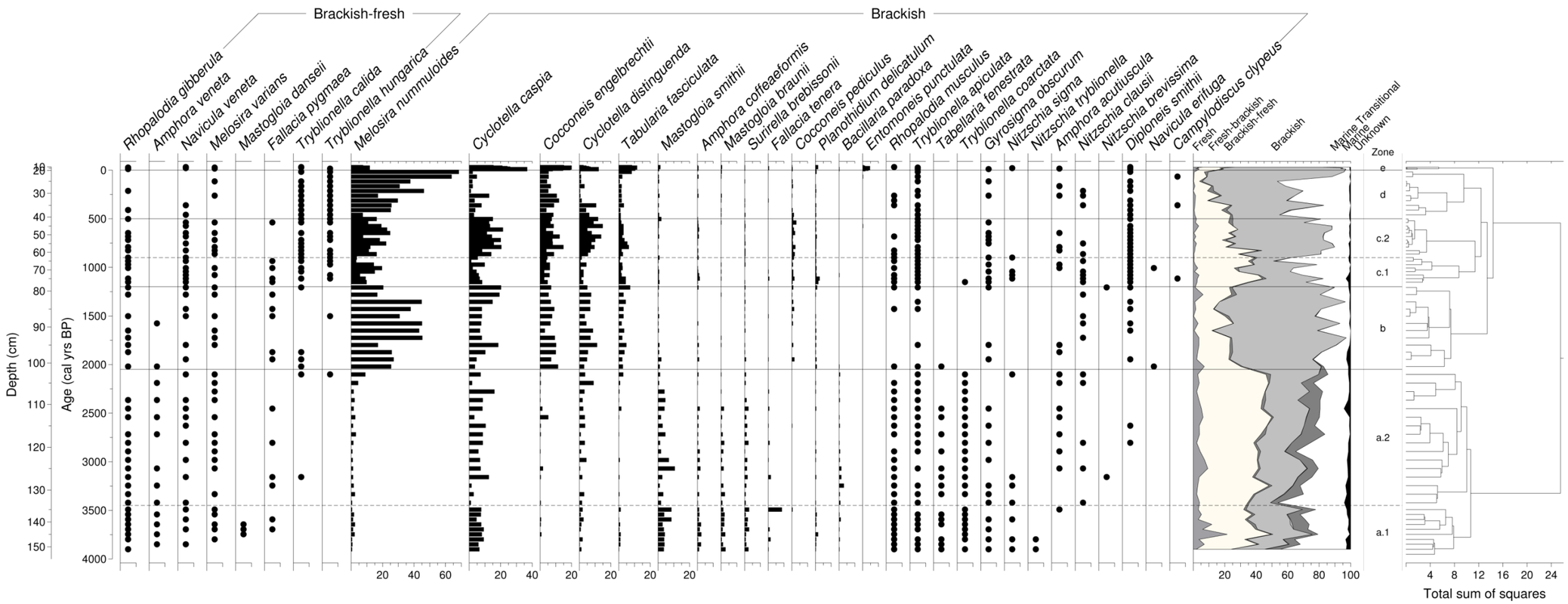

Figure 5.12.2: The Eilandvlei EV11.1 (cont.) core stratigraphy and percentage diatom representation against depth (cm) and age (cal yrs BP), diatom species are grouped based on salinity preferences (% Brackish-fresh to % Brackish). Five zones were identified based on CONISS

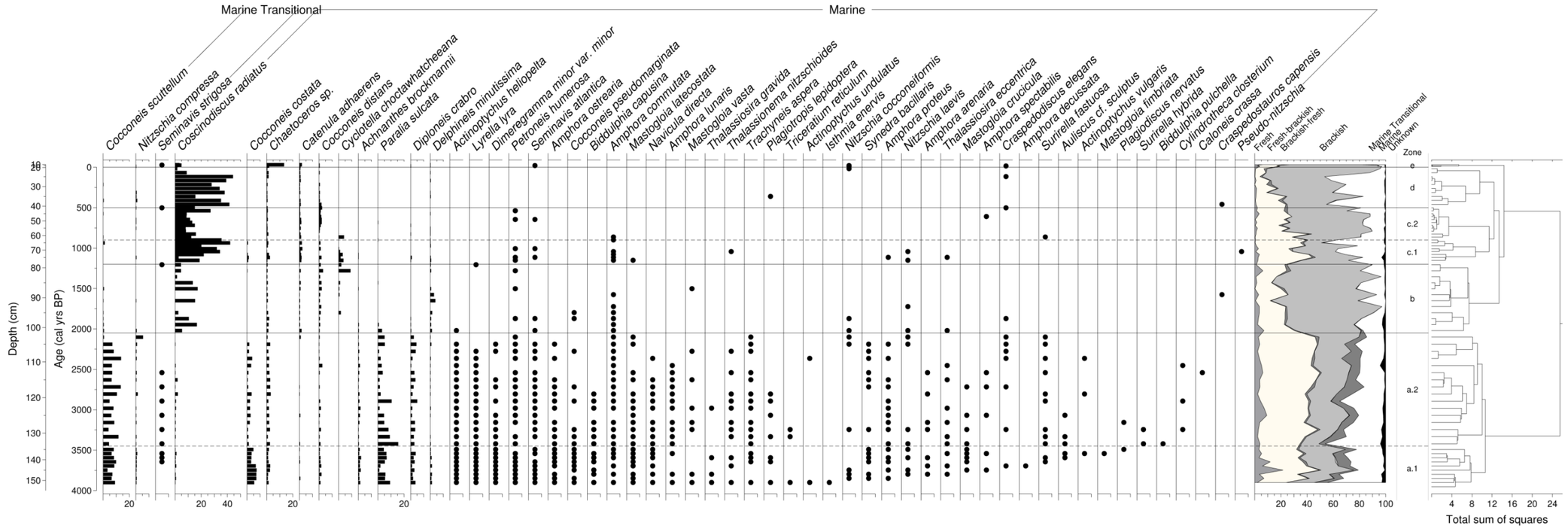

Figure 5.12.3: The Eilandvlei EV11.1 (cont.) core stratigraphy and percentage diatom representation against depth (cm) and age (cal yrs BP), diatom species are grouped based on salinity preferences (% Marine Transitional to % Marine species). Five zones were identified based on CONISS

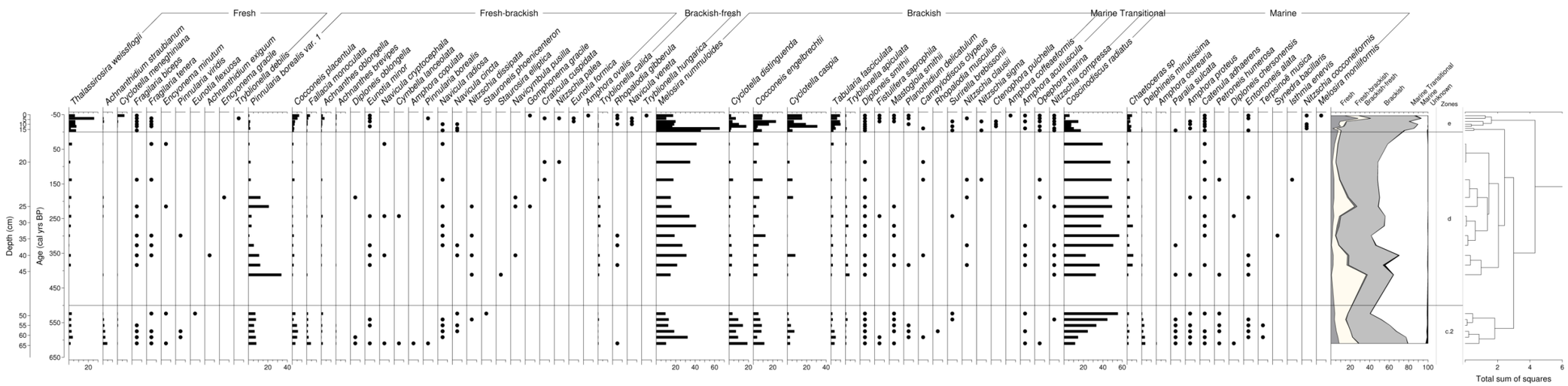

Figure 5.13: The Eilandvlei EV101.1 core stratigraphy and percentage diatom representation against depth (cm) and age (cal yrs BP), diatom species are grouped based on salinity preferences. Three zones were identified based on CONISS

5.2.3. Statistical Anaylsis

The degree of similarity between samples was tested using cluster analysis. A cophenetic correlation of 0.85 implies a robust model based on Ward's method. Three clusters were identified as observed in Fig. 5.14. Cluster one incorporates all samples from zone EV11.1a, confirming the distinctive character of this zone compared to the rest of the assemblage, primarily based on the enhanced diversity observed in the marine species. Cluster two grouped zone EV11.1e and most of zone EV11.1c.2 with the exception of 43cm and 59cm together, possibly based on the diversity observed in brackish species within the diatom assemblage at these levels, such as *Cocconeis engelbrechtii*, *Cyclotella caspia* and *Cyclotella distinguenda*. The final cluster incorporates zone EV11.1c.1, zone EV11.1d and most of zone EV11.1b, with the exception of 79cm, 81cm and 95cm which was grouped with samples in cluster two. Cluster three does not appear to conform to any one environmental parameter but may be an expression on the near monospecific diatom community evident in the assemblage during these periods. Zone EV11.1b and zone EV11.1d both show a high proportional community of epiphytic diatoms attributed mainly to the appearance of *Melosira nummuloides*, whereas zone EV11.1c.1 and zone EV11.1d show a strong marine component through the prevalence of *Coscinodiscus radiatus*.

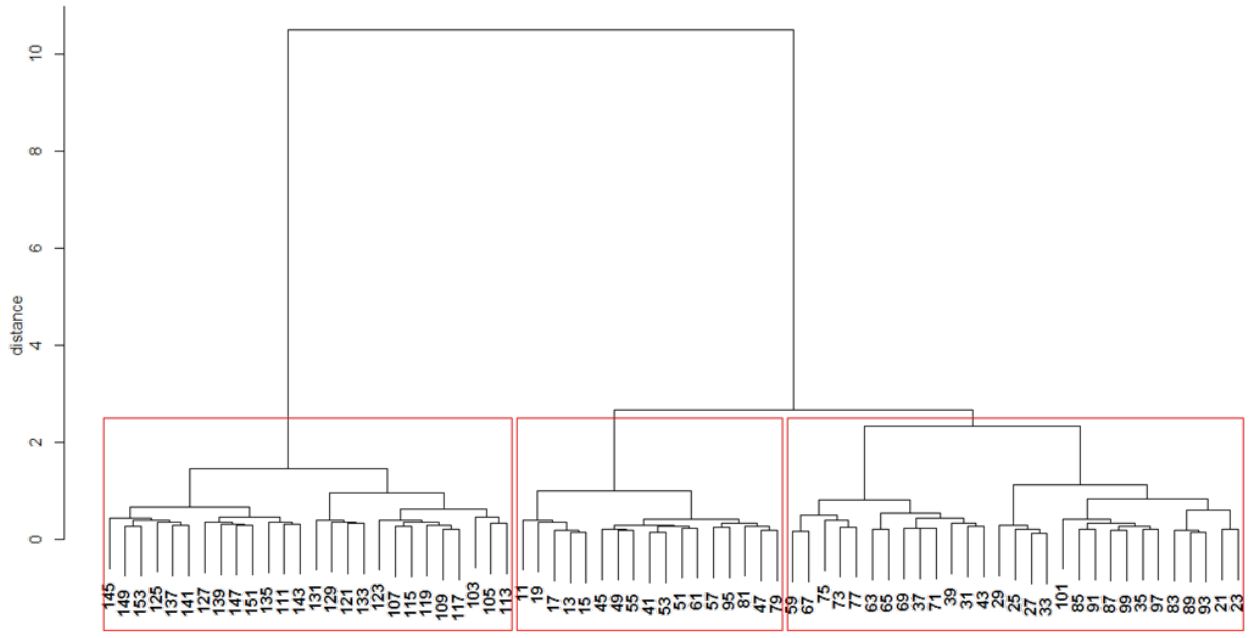

Figure 5.14: Cluster analysis on the Eilandvlei EV11.1 core using the Ward's method against a Bray-Curtis dissimilarity index, the analysis indicates three significant clusters

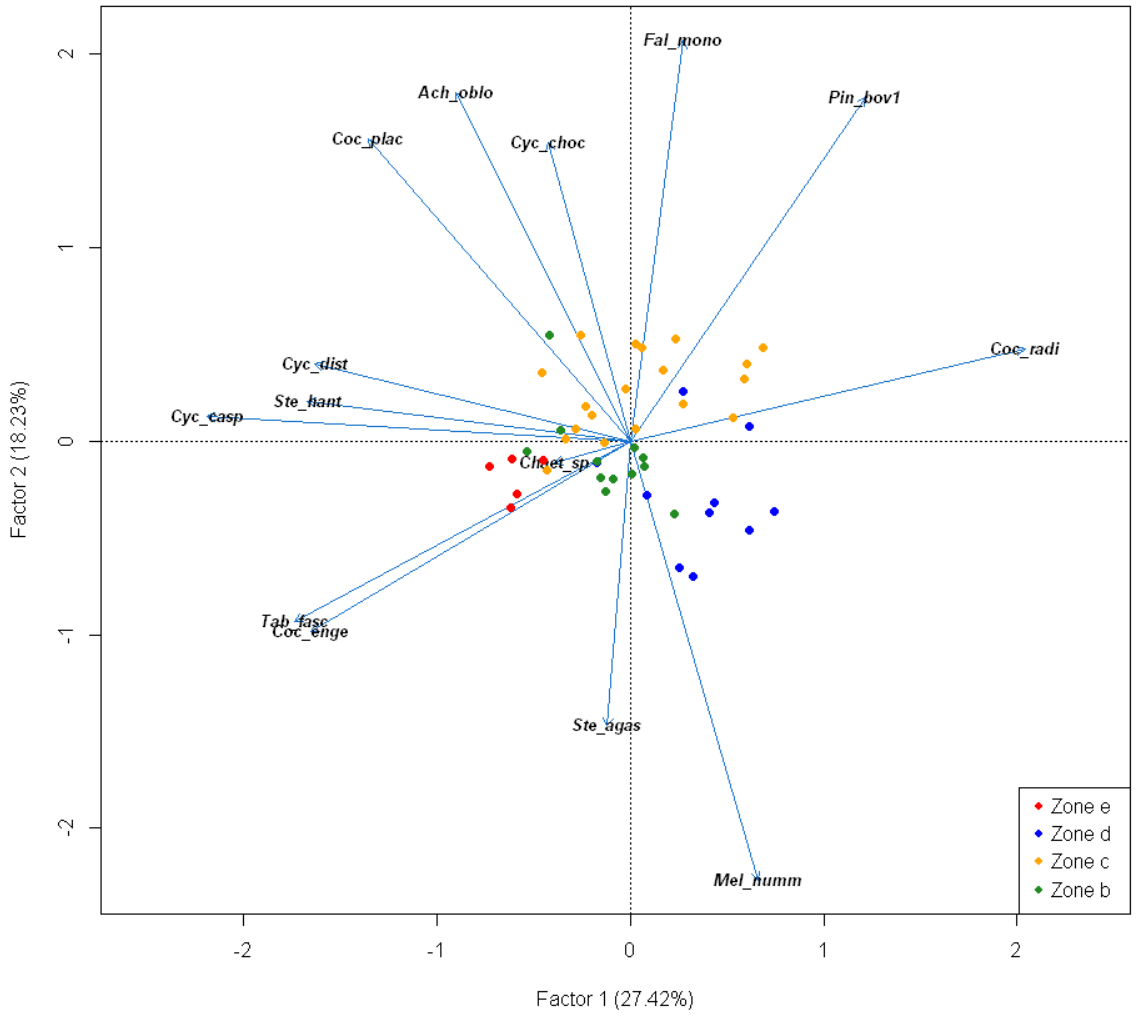

Figure 5.15: Principal component analysis representing the relationship between species and samples at the Eilandvlei EV11.1 site for the last 2000 years. Sample points are colour coded based on zones identified by CONISS in TILIA. Coc_plac = Cocconeis placentula*, Fal_mono* = Fallacia monoculata*, Pin_bov1*= Pinnularia borealis var 1*, Ste_hant* = Stephanodiscus hantzschii*, Coc_enge* = Cocconeis engelbrechtii*, Cyc_casp* = Cyclotella caspia*, Mel_numm* = Melosira nummuloides*, Tab_fasc* = Tabularia fasciculata*, Cyc_dist* = Cyclotella distinguenda*, Chaet_sp* = Chaetoceros *sp, Coc_radi* = Coscinodiscus radiatus*, Cyc_choc* = Cyclotella choctawhatcheeana*, Ach_oblo* = Achnanthes oblongella*, Ste_agas* = Stephanodiscus agassizensis

Principal component analysis (PCA) was conducted on the full EV11.1 record, although the marked dissimilarity of zone EV11.1a from the rest of the assemblage resulted in its exclusion from a follow-up PCA. In so doing, the mechanisms underlying the last 2000 years of the region's development may be discerned unaffected by the dominance of the marine phase represented in zone EV11.1a. The remaining 46 samples and 118 species were subject to the analysis, thereby identifying the key species influencing patterns within the dataset and determining other underlying aspects of the data. This resulted in the inclusion of 14 potential environmental indicator species in the PCA as shown in Fig. 5.15.

Two principal component axes were determined to be significant, contributing 45.65% to the overall explained variance. Component one, which explains 27.42% of the variance, has large positive loadings on *Coscinodiscus radiatus*. *Coscinodiscus radiatus* has a cosmopolitan distribution in warmer marine waters where water temperatures range from 5 – 30°C (Baars, 1979). Along the South African coast, *C. radiatus* is common in the near shore environments, particularly in the well mixed waters or as a pioneer species in newly upwelled water (Schuette and Schrader, 1981; Barron et al., 2004). Component one has large negative loadings on *Cyclotella caspia, Tabularia fasciculata, Cocconeis engelbrechtii, Cyclotella distans, Cocconeis placentula* and *Stephanodiscus hantzschii* all of which are typically classed as brackish to fresh-brackish and eutrophic (Fig. 5.16) (Harding and Wright, 1999). *Cyclotella caspia* has been observed during transitional periods particularly in an estuarine environment (Marshall and Alden, 1990). Component one appears to represent the productivity of the system as it transitions from an estuarine/brackish lake to marine dominated system during periods of reduced freshwater. Hence, during periods of increased precipitation, the diatom diversity of the lake increases, dominated by an estuarine or brackish-based diatom community along a salinity gradient (Fig. 5.12 and 5.13). On the other hand, during periods of reduced precipitation, marine elements dominate the system as productivity declines and aerophilic species thrive. The marine element may be an expression of two possible scenarios; 1) either a marine transgression occurred inundating the low elevated valley or 2) the event represents the effects of back-flow along the channel connecting Eilandvlei to the ocean more frequently exceeding freshwater inputs.

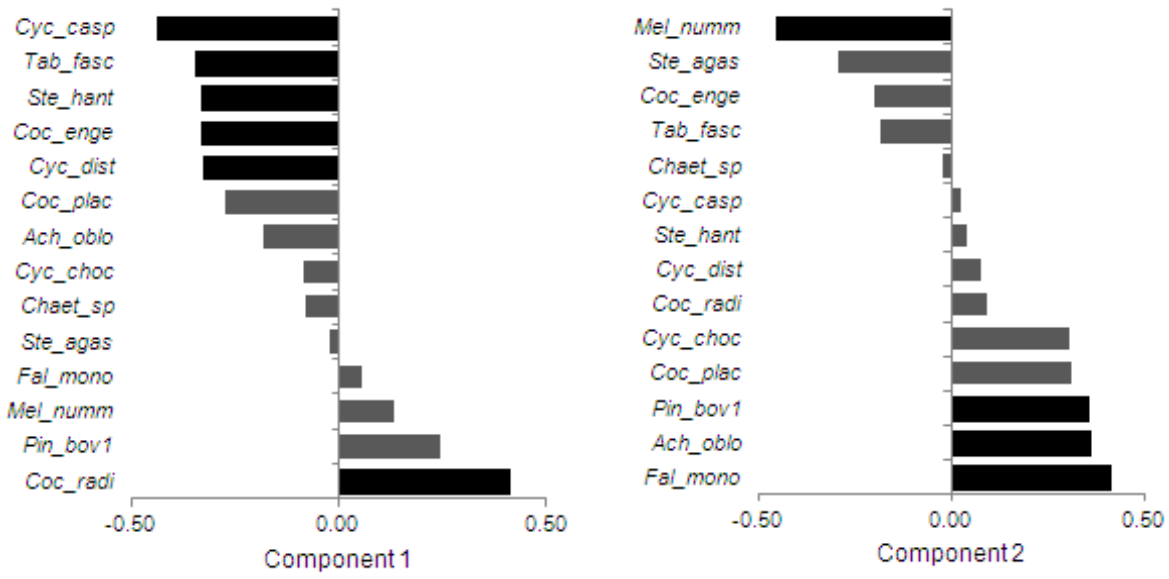

Figure 5.16: Factor loadings for principal components one and two for the Eilandvlei EV11.1 core.

Component two contributes 18.23% of the explained variance. Species with high positive loadings on the second component are *Achnanthes oblongella, Pinnularia borealis* var. 1 and *Fallacia monoculata*, and to a lesser degree *Cyclotella choctawhatcheeana* and *Cocconeis placentula* (Fig. 5.16). *Fallacia monoculata* can thrive in heavily polluted waters where concentration of nitrites and ammonia are high (Wojtal and Sobczyk, 2006; Bere and Tundisi, 2010). *Cyclotella choctawhatcheeana* is a eutrophic, planktonic species commonly found in sulfate-dominated, saline lakes particularly where the depth of the photic zone is diminished due to turbidity (Fritz et al. 2010; Snoeijs and Weckström, 2010; Wachnicka et al., 2011). Conversely, *Achnanthes oblongella* prefers nutrient-poor environments (Battegazzore et al., 2004). *A. oblongella* is typically found in the upper reaches of an estuary or in streams where flash flooding is a common occurrence (Hodgson et al., 1996; O'Driscoll et al., 2012); while *Pinnularia borealis* var. 1 is an aerophilic species preferring mosses and slightly brackish habitats (Sawai et al., 2004; Johansen, 2010; Spaulding et al., 2010). Species with high negative loadings on the second component are *Melosira nummuloides* and, to a lesser degree, *Stephanodiscus agassizensis* (Fig. 5.16). Both species thrive in light-limited, nutrient-rich environments (McLean et al., 1981; Rendall and Wilkinson, 1986; Findlay et al., 1998). However, where *S. agassizensis* favours warmer waters (Findlay et al., 1998), *M. nummuloides* is found in cooler waters in the range of -1.5 – 10°C (Baars, 1979). Furthermore, *M. nummuloides* can outcompete other species during periods of rapid salinity changes, low levels in oxygen saturation and/or organically polluted waters (McLean et al., 1981; Rendall and Wilkinson, 1986). It can be stated with some confidence that Eilandvlei remained relatively nutrient-rich

throughout its history, although the status of the system has fluctuated considerably and may be represented by component two (Fig. 5.17). The placement of *A. oblongella* with respect to *M. nummuloides* in the PCA is testament to this state (Fig. 5.15). During periods where biological activity is adversely affected, whether human-induced or natural, *M. nummuloides* thrives; natural conditions may be cooler periods, high water turbidity, or low solar irradiance.

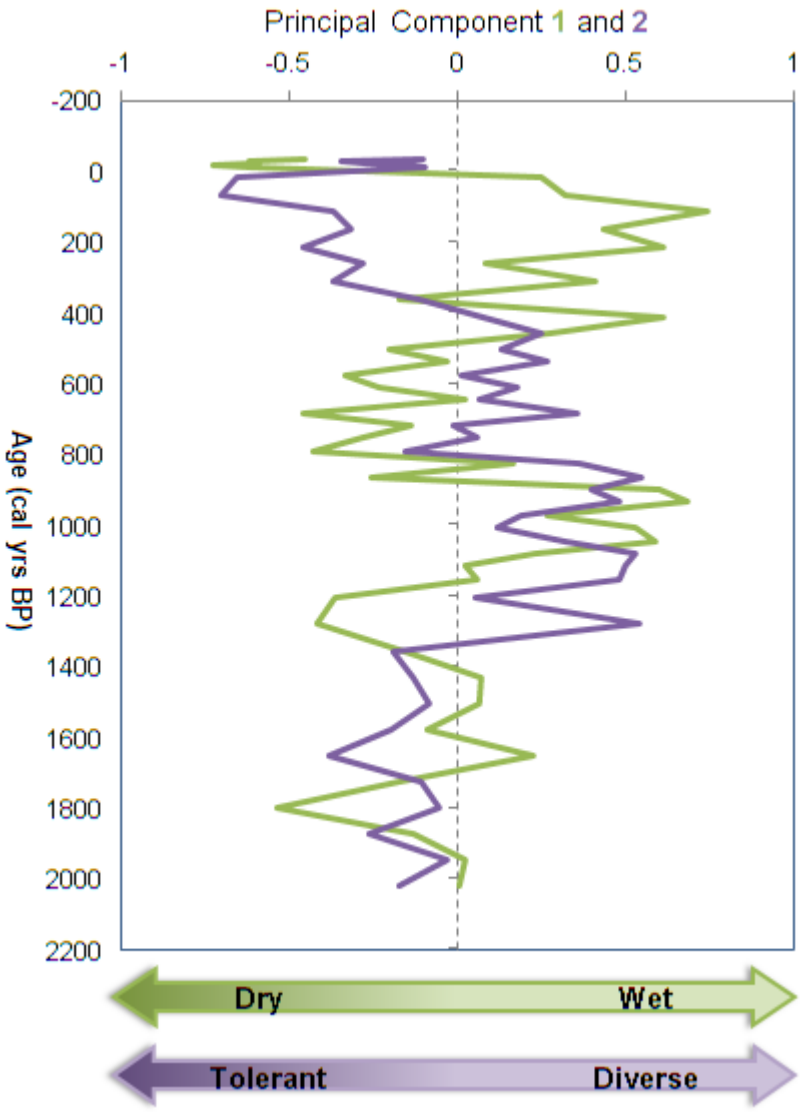

Figure 5.17: The first two statistically significant principal components generated for the Eilandvlei EV11.1 site representing the last 2000 years of the record

5.2.4. Indice de Polluosensibilité

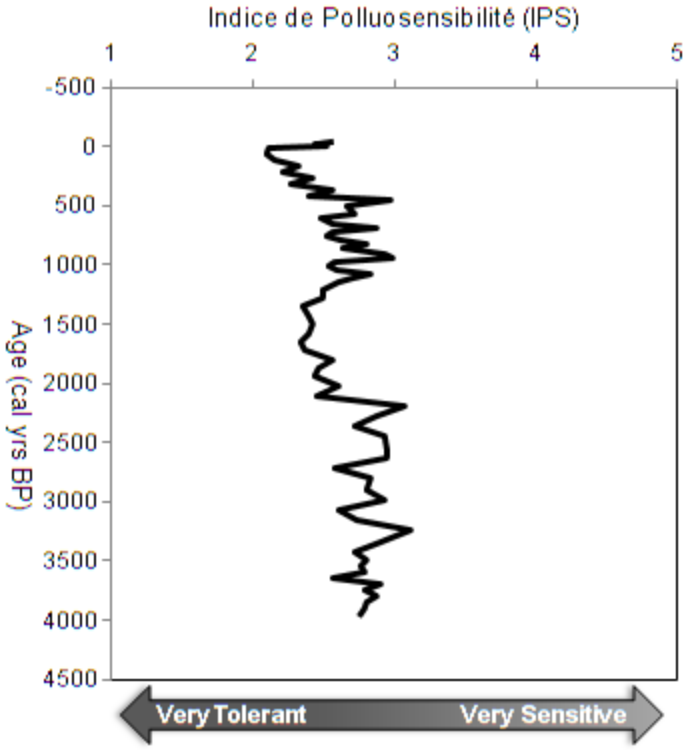

Figure 5.18: Pollution Sensitivity Index for the Eilandvlei EV11.1

The above outputs suggest that Eilandvlei has remained consistently nutrient-rich with a high variability in saline inputs throughout the late Holocene. The Indice de Polluosensibilité (IPS) further substantiates this interpretation. The IPS is a relevant measure of the effects of nutrient variability and salinity inputs for the Wilderness region as human occupation only occurred in the last 300 years. The IPS can therefore provide a assessment of pre- and post-anthropogenic forcings. The index calculation included more than 90% of the species for all measured levels of the EV11.1 core, the output of which is displayed in Fig. 5.18. In general terms the lake has fluctuated from moderate to high periods of nutrient content throughout the 4000 year record, which include saline inputs. A distinct shift to high nutrient loading occurred at ~2100 cal yrs BP, persisting until about 1500 cal yrs BP. Following this, a slight decline in nutrient loading is observed between 1100 to ~500 cal yr BP, before a shift in environmental conditions contributed toward a high nutrient state until AD 1950. A recovery in the system is observed in the remainder of the record, which may be due to conservation efforts. Although, there are periods of increased nutrient loading throughout the record, the system as a whole does not shift into an altered state and remains within the threshold of moderate-heavy nutrient loading.

5.3. RESULTS: SWARTVLEI:

SV10.1 was 96.5cm in length and composed of silty clay of varying shades of brown (Fig. 19). The 96.5cm core was subsampled at varying resolutions; from 90 – 40cm every four centimetres was analysed for diatom fossils, whereas every centimetre in the top 20cm was included for analysis. This generated 38 samples in all. Species diversity and richness remained relatively stable throughout the core, with the exception from 24 – 6cm where both indices rapidly fluctuate. The top six centimetres has an increase in species richness but a stabilisation in diversity. The radiograph image of the core indicates fine sediment layers possibly providing evidence of little to no disturbance to sediment deposition (Fig. 5.19). An incursion of fine and medium sands is observed at ~20cm before sediments tend towards finer particle sizes.

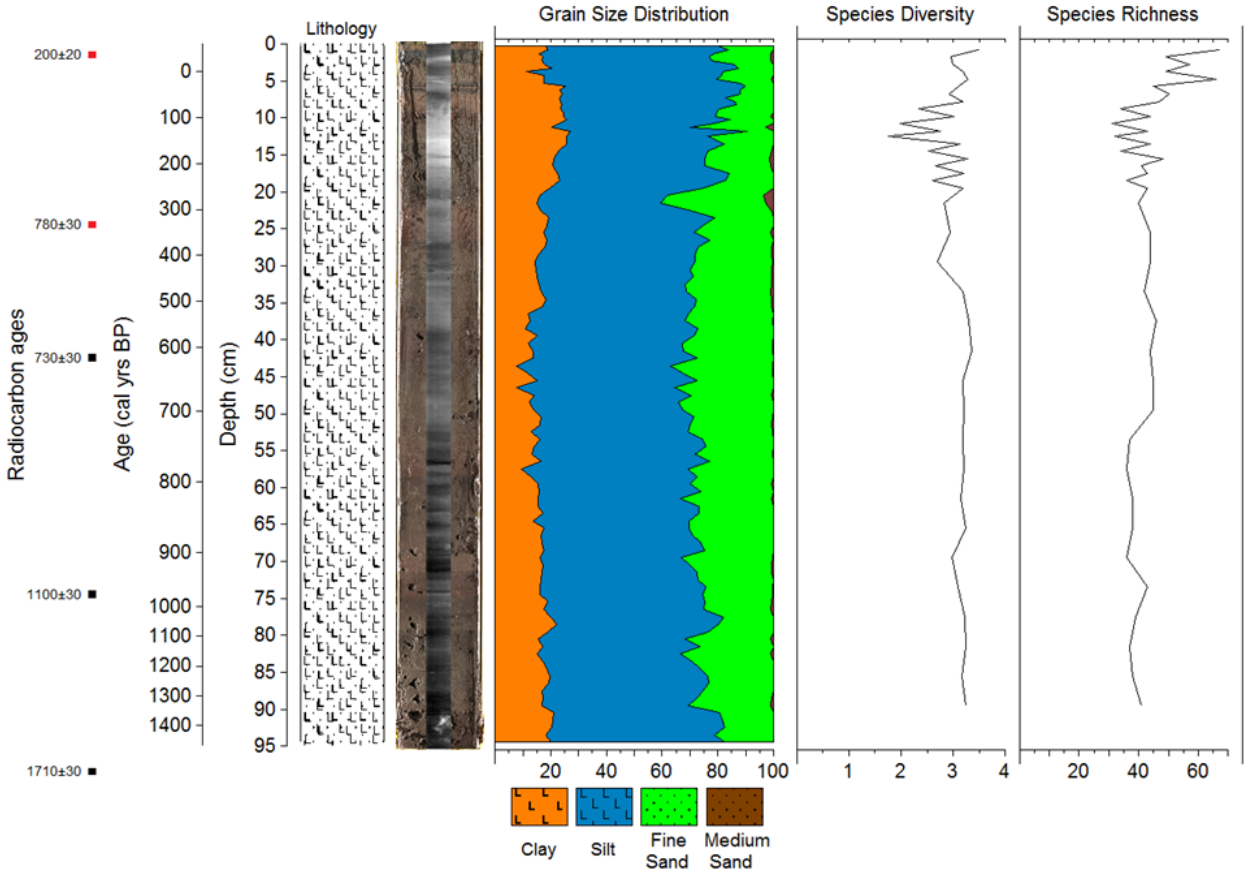

Figure 5.19: Swartvlei (SV10.1) core description based on Troels-Smith notation, particle size distribution, diatom species diversity and richness against depth (cm) (radiograph image courtesy: S. Franz)

5.3.1. Chronology:

Five samples were submitted for radiocarbon analysis revealing a record that spans the last 1400 years. The data are summarised in Table 5.4, including the extremes of the lower (yrmin) and upper (yrmax) calibrated range reported when more than one range is produced.

Table 5.4: The radiocarbon ages of the Swartvlei SV10.1 core calibrated to the SHCal13 curve indicating the upper and lower calibration range in units, BP with their median probability and corresponding depths, ages that have been excluded from analysis are indicated in red whereas ages incorporated in the age-depth model are indicated in black.

Sample label	Depth	C14 age	Error	yrmin	yrmax	probability
SWART 0-1cm	0.5	200	20	141	229	61.8
				251	289	23.3
SWART 24-25cm	24.5	780	30	650	728	93.2
SWART 42-43cm	42.5	730	30	564	601	38.4
				629	676	56.4
SWART 74-75cm	74.5	1100	30	920	1003	85.8
SWART 98-99cm	98.5	1710	30	1506	1628	78.9
				1418	1467	9.2

Of the five samples submitted for radiocarbon analysis two samples indicated age reversals in the sediment record. Similar to the EV10.1 core, age reversals occur at 24.5cm and again near the surface. These were labelled as outliers and were excluded from the age-depth model. The age reversal at 0.5cm may be due to agricultural activities or the deepening of the river channels by SANParks, leading to the remobilisation of older sediments in the catchment, which were deposited in surface sediments in Swartvlei. However, the possibility that the surface age represents some form of a marine reservoir effect can not be eliminated. The second reversal at 24.5cm, as with the EV10.1 core, may be as a result of the resuspension and deposition of older carbon material during periods affected by lake level fluctuations. The SV10.1 core is located in close proximity to the northern shore of the lake, possibly making the site susceptible to the lake-level variation. Evidence from the diatom assemblage shows a period of lower lake levels between the depths of 36cm and 20cm via the peak occurrence of the aerophilic species, *Pinnularia borealis* var. 1. Sedimentation rates for most of the SV10.1 core range from 0.1cm.yr^{-1} (10.51yr.cm^{-1}) from the base of the core to 43cm and then on average 0.06cm.yr^{-1} (16.1yr.cm^{-1}) from 43cm to the surface of the analysed record (Fig. 5.20). Accumulation rates suggest an approximately consistent supply in sediments to the lake throughout the retrieved record.

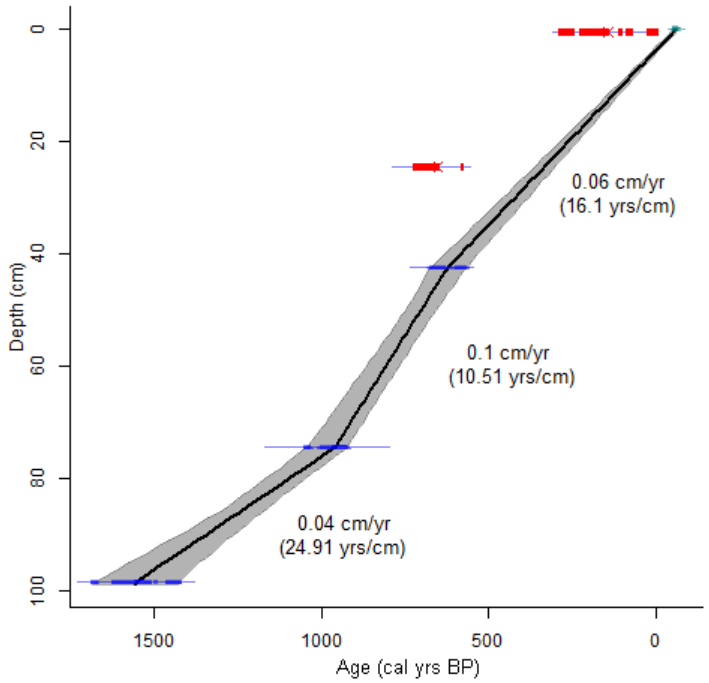

Figure 5.20: Age-depth model for Swartvlei SV10.1, indicating the two age reversals which were removed from the model. Sedimentation rates (cm.yr^{1}) are also shown.

5.3.2. Assemblage Zonation

The division of the Swartvlei assemblage is also based on CONISS analysis in Tilia (Grimm, 1987). Four zones are identified based on a split at five total sum of squares from the CONISS-based cluster analysis. As with the other sites the zones are alphabetically labelled oldest to youngest as follows: zone SV10.1a: 94 – 52 cm (1400 – 730 cal yrs BP); zone SV10.1b: 52 – 20 cm (730 – 250 cal yrs BP); zone SV10.1c: 20 – 6.5 cm (250 – 45 cal yrs BP) and zone SV10.1d: 6.5 – 0 cm (45 - -50 cal yrs BP) (Fig. 5.21).

Between ~1400 and ~730 cal yrs BP a mixed assemblage is prevalent. At the start of the zone *Pinnularia borealis var. 1* and several marine species, including *Catenula adhaerens, Diploneis chersonensis/crabro*, *Chaetoceros* sp. and *Paralia sulcata* are strongly represented between 1400 and 1000 cal yrs BP, before declining coincident with a steady increase in the brackish taxa *Cyclotella distingueda* and *Cocconeis engelbrechtii*, which peak between 74 and 65cm (~950 and ~860 cal yrs BP). This short lived brackish period gives way to a diverse range of marine species. *Craspedodiscus elegans* and *Pinnularia maior* return stronger than prior to the minor brackish intrusion and follow on into the corresponding zone, the former is a marine species and the latter is a freshwater, oligotrophic species (Fig. 5.21) (Kain and Schultze, 1886; Cremer and Wagner, 2003).

The marine component is still prominent during zone SV10.1b with *C. elegans* being succeeded by *Diploneis chersonensis/crabro*, while *P. sulcata* declines to minimal amounts. Although in minor quantities during zone SV10.1a, *Cocconeis placentula* doubles its mean abundance during zone SV10.1b. *Pinnularia maior* and *Cyclotella meneghiniana* persist until mid-zone SV10.1b, where they are replaced by *Pinnularia borealis* var. 1 from 32cm (~450 cal yrs BP) to ~20cm (~250 cal yrs BP) (Fig. 5.21). Concurrently, marine and brackish taxa decline with a minor recovery in the marine and marine-brackish species near the termination of the stage. *Nitzschia compressa* is a marine-brackish epiphyte, which occurs consistently throughout the core but increases to over 7% of the assemblage between ~38 - ~19 cm (~370 – 250 cal yrs BP) (Espinosa et al., 2003).

Zone SV10.1c is a highly variable stage with considerable marine and freshwater influences. *Coscinodiscus radiatus* alternates between high (maximum of 55% at 150 cal yrs BP) and low (minimum of 3.8% at 200 cal yrs BP) frequencies during this period and appears out of phase with peaks in *C. adhaerans, D. chersonensis/crabro* and *Amphora proteus.* Initially, peaks and troughs in *C. radiatus* are mirrored by brackish species, such as *M. nummuloides, C. distinguenda* and *C. engelbrechtii*. The previous high abundance of fresh-brackish species is not observed during this time with only minimal frequencies of *P. borealis* var. 1. Fresh water species are continually observed especially, *Thalassiosira weissflogii* and *Cyclotella meneghiniana*, both of which prefer high nutrient availability as well as fluctuations in salinity. Most of the freshwater species present during the last 100 years (top 6 cm) (zone SV10.1d) are mesotrophic to eutrophic in nature. Marine species become increasingly rare, initially comprising nearly 33% of the diatom community to just less than 14% of which 8.5% is *C. adhaerans* and *Chaetoceros* sp. Brackish species remain between 40 - 50% of the overall assemblage, peaking at 51% at about 30 ± 5 years ago before dropping to 35%. The originally saline habitat develops into a fresh-brackish/fresh system expressed by the variability in the fresh-brackish community.

In general, a pronounced marine influence occurs throughout the record but declines in the last 100 years. The transition from zone SV10.1a to zone SV10.1b is pivoted on an increase in benthic, alkaliphilic taxa and a moderate decline in marine species. Zone SV10.1b consists of two phases, before and after the increase of *Pinnularia borealis var. 1* at 450 cal yrs BP. A complete list of the autecological preferences of each species based on salinity, pH, life form and nutrients can be found in Appendix Two (Table 11.6, Pg. 279).

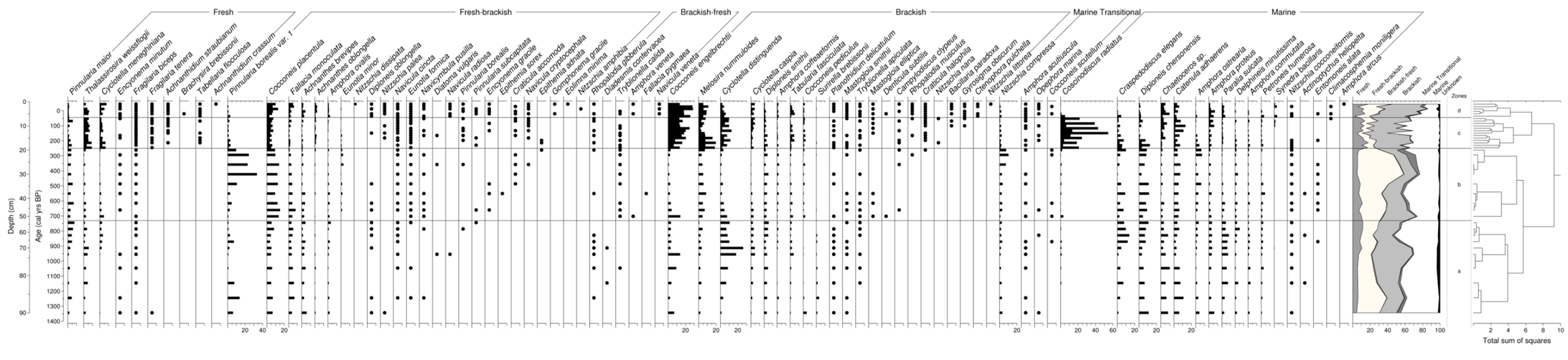

Figure 5.21: The Swartvlei SV10.1 core stratigraphy and percentage diatom representation against depth (cm) and age (cal yrs BP), diatom species are grouped based on salinity preferences. Four zones were identified based on CONISS

5.3.1. Statistical Analysis

The degree of similarity between samples throughout the core is shown in Fig. 5.22. The analysis shows the majority of samples within zone SV10.1a and zone SV10.1b from ~1400 – 260 cal yrs BP (90 – 20cm) share some similarity with each other, as well as with the diatom community assemblage present at 230 cal yrs BP (18cm) and 200 cal yrs BP (16cm). Species richness and diversity remains relatively high and constant (Fig. 5.19). The exception lies with samples from 420 – 300 cal yrs BP (30 – 22cm), which form an isolated cluster from the rest of the assemblage; this is a direct consequence of the strong dominance of the aerophilic species *Pinnularia borealis* var. 1, which peaks during this time. In general, zone SV10.1c (~250 – 50 cal yrs BP, 19 – 7cm) appears to be influenced primarily by fluctuations in salinity. Alternating samples between 19 and 7cm occur in neighbouring clusters and as, discussed previously, represent the cyclic rise and fall in *C. radiatus* versus brackish species. The remaining samples cover the last 100 years/the top 6cm and bear some similarity to the sample at 700 cal yrs BP (50cm), which is a transitional sample between the zones SV10.1a and SV10.1b; as well as 70 cal yrs BP (8cm), 100 cal yrs BP (10cm), 130 cal yrs BP (12cm), 165 cal yrs BP (14cm), all of which are strongly brackish in nature coupled with a large benthic component.

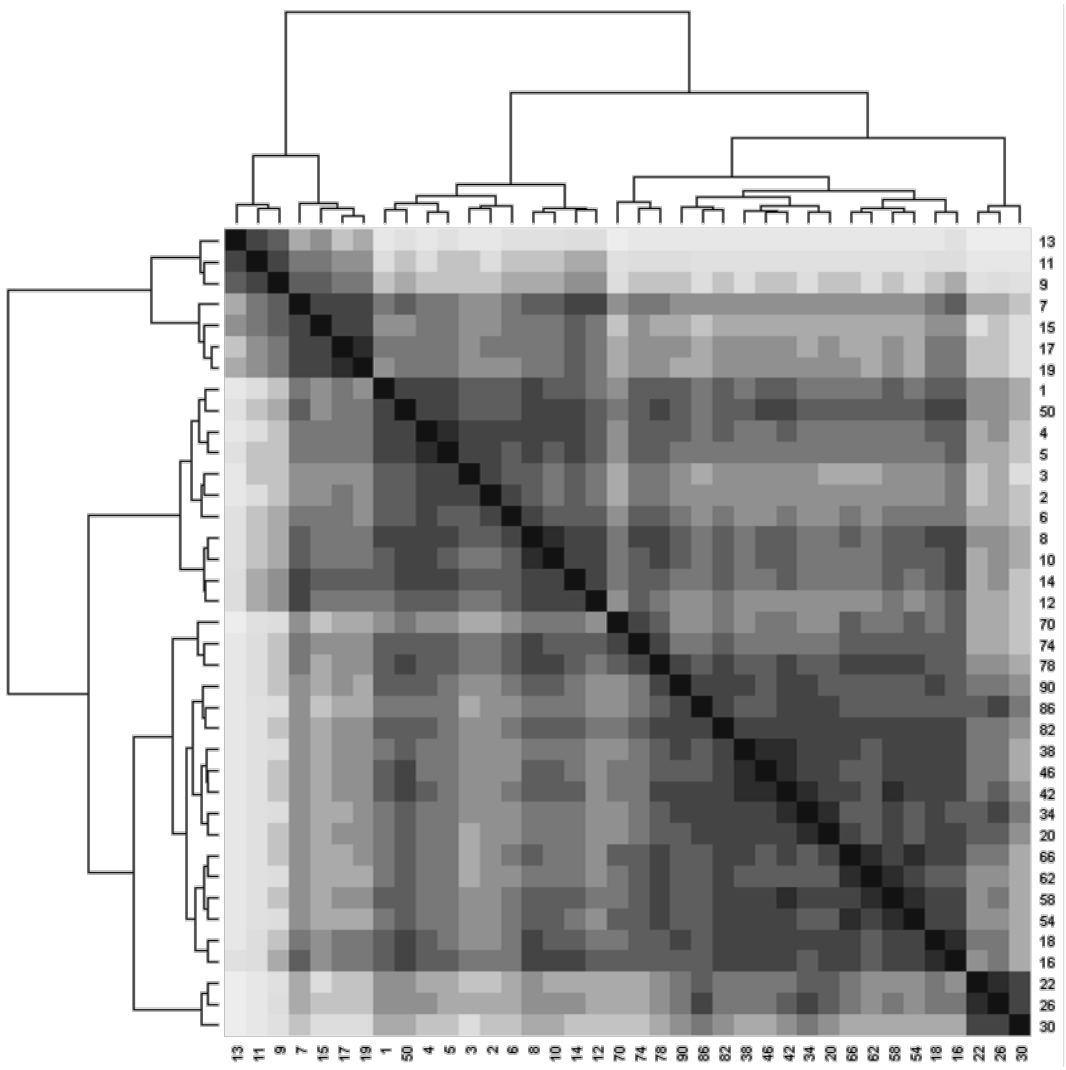

Figure 5.22: Heat map showing similarity/dissimilarity between samples of the Swartvlei SV10.1 site

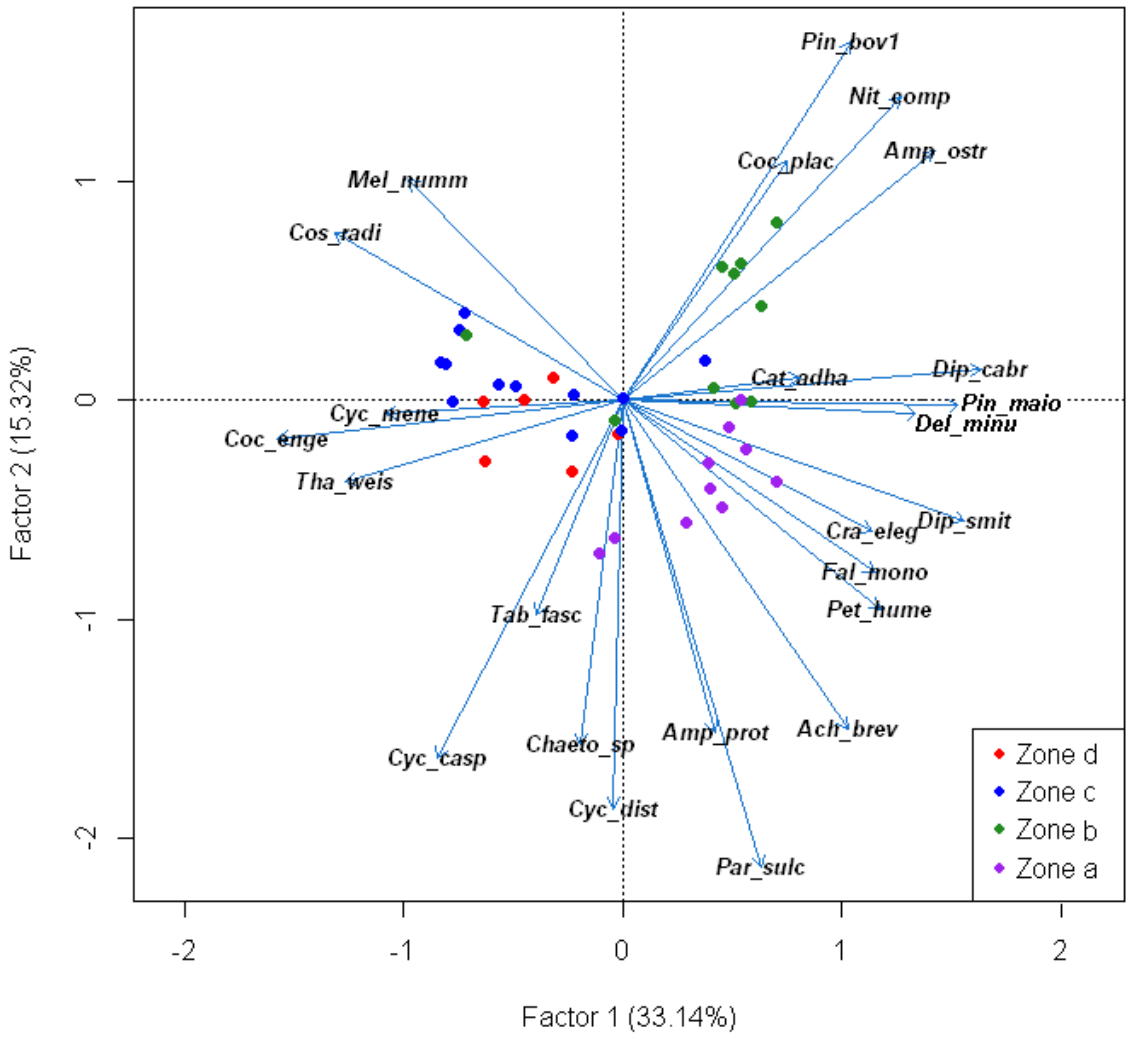

Figure 5.23: Principal component analysis representing the relationship between species and samples at the Swartvlei SV10.1 site. Sample points are colour coded based on zones identified by CONISS in TILIA. Ach_brev = Achnanthes brevipes*, Amp_ostr =* Amphora ostrearia*, Amp_prot =* Amphora proteus*, Cat_adha =* Catenula adhaerens*, Chaeto_sp =* Chaetoceras *sp, Coc_enge =* Cocconeis engelbrechtii*, Coc_plac =* Cocconeis placentula*, Cos_radi =* Coscinodiscus radiatus*, Cra_eleg =* Craspedodiscus elegans*, Cyc_casp =* Cyclotella caspia*, Cyc_dist =* Cyclotella distinguenda*, Cyc_mene =* Cyclotella meneghiniana*, Del_minu =* Delphineis minutissima*, Dip_cabr =* Diploneis crabro*, Dip_smit =* Diploneis smithii*, Fal_mono =* Fallacia monoculata*, Mel_numm =* Melosira nummuloides*, Nit_comp =* Nitzschia compressa*, Par_sulc =* Paralia sulcata*, Pet_hume =* Petroneis humerosa*, Pin_maio =* Pinnularia maior*, Pin_bov1 =* Pinnularia borealis var 1*, Tab_fasc =* Tabularia fasciculata*, Tha_weis =* Thalassiosira weissflogii

Initially, the full SV10.1 diatom species record was used in a PCA to resolve the key influential species determining environmental trends. From the original 100 species, 24 species were identified and incorporated into a follow-up PCA (Fig. 5.23). Two principal component axes were determined to be significant, contributing 48.46% to the overall explained variance. Component one, which explains 33.14% of the variance, has large positive loadings on *Diploneis crabro*/*chersonensis*, *Diploneis smithii*

and *Pinnularia maior* (Fig. 5.24). *Diploneis crabro/chersonensis* and *Diploneis smithii* are cosmopolitan marine species occurring in the near shore environment (Navarro, 1982). *D. smithii* extends into estuarine habitats occupying the littoral zone (Dawson, 2007; Hendrarto and Nitisuparjo, 2011); whereas *D. crabro/chersonensis* are found in the photic zone attached to submerged macrophyte (Niyomsilpchai et al., 2009). Conversely, *P. maior* is a freshwater, oligotrophic species favouring circumneutral to acidophilic waters (Whitmore, 1989; Zalat, 2000). Large negative loadings are concentrated on *Cocconeis engelbrechtii* and, to a lesser degree, *Coscinodiscus radiatus* (Fig. 5.24).

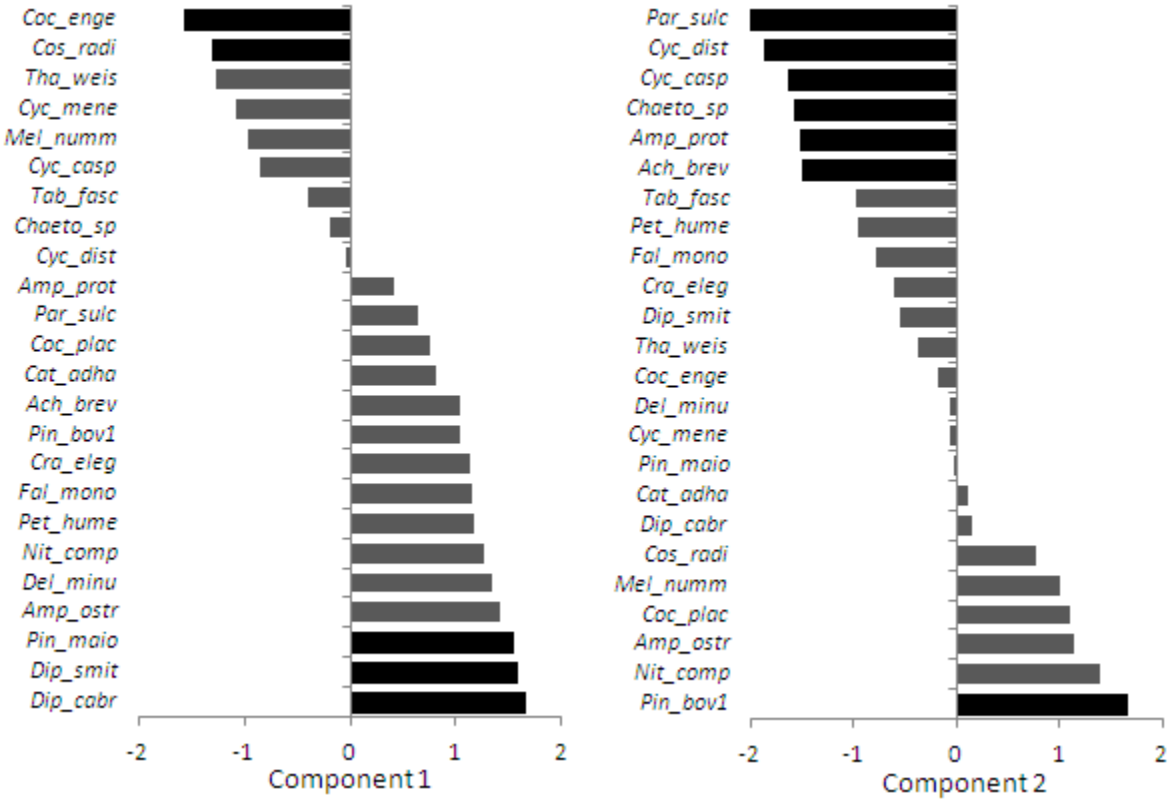

Figure 5.24: Factor loadings for principal components one and two for the Swartvlei SV10.1 core.

The first component therefore appears to be an indication of the status of the system relative to freshwater and marine water inputs (Fig. 5.25). During periods of increased freshwater inputs a distinct salinity gradient is formed along the length of the lake. Greater numbers of *Diploneis crabro/chersonensis* and *Diploneis smithii* at the coring site compared to *P. maior* and similar species can give an indication as to how much freshwater was feeding the system at any one point or how far up-valley marine waters penetrated. On the opposite end of the spectrum, the prevalence of *C. engelbrecthii* and *C. radiatus* may imply reduced precipitation whereby brackish to marine elements

dominate the system. As in the EV11.1 record, the marine element may be an expression of either the occurrence of a marine transgression inundating the low-lying valley or that reverse flow along the Swartvlei channel connecting to the ocean is greater than freshwater inputs. This correlates well with the EV11.1 first component interpretation, the only difference lies in the actual species composition making up the first PCA axis. However, this is easily explained in that the Swartvlei system has a more direct connection to the ocean, as well as a greater number of rivers and their tributaries draining into the coastal lake as compared to Eilandvlei.

Component two contributes 15.32% of the explained variance. *Pinnularia borealis* var. 1 is the species with the highest positive loading on the second component and, as discussed previously, its ecological requirements indicate fresh-brackish conditions in shallow waters. *Paralia sulcata, Cyclotella caspia, Cyclotella distinguenda, Chaetoceras* sp, *Achnanthes brevipes, Amphora proteus* have the highest negative loadings on the second component (Fig. 5.24). The ecology and distribution of *Paralia sulcata* and *Chaetoceras* sp indicates that they are essentially favoured in newly upwelled to well-mixed marine waters. *Achnanthes brevipes* appears to have a wide distribution in a range of water types, including marine and marsh environments, although it does appear to be restricted to oligotrophic conditions (Aleem, 1950; Sherrod, 2001), as is the case for *Amphora proteus* which also favours marine and unpolluted sites (Hassan et al., 2006; Petrov and Nevrova, 2007). Additionally, Aleem (1950) noted that low water temperatures and limited light penetration did not appear to affect the growth of *A. brevipes*. *C. caspia* and *C. distinguenda* are dominant in the SV10.1 core as they were in EV11.1; both favour brackish-marine environments and are typical occurrences in estuarine diatom communities (Marshall and Alden, 1990; Wachnicka et al., 2011).

The second component is defined by the prevalence of *P. borealis* var. 1, suggesting lower lakes levels with increased nutrient loadings possibly sourced through the die-back of the submerged macrophyte community (Fig. 5.25). Conversely, a well-established community and diverse array of species are observed on the negative loadings mostly defined by nutrient-poor conditions. Hence, the second component may be representative of a drier climate versus a wetter climate and possibly closely linked to the first component, as well as the response of the system to the changes in environment. It seems that components one and two may be interlinked. In general, it appears that, during drier conditions, brackish-marine elements are more evident than during wetter climates where brackish-fresh constituents are apparent.

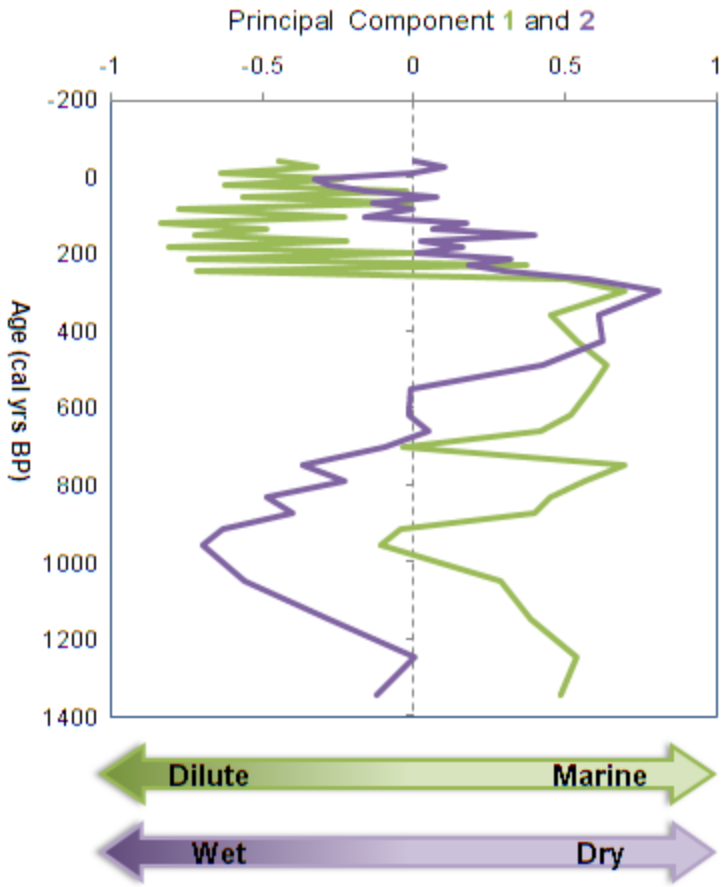

Figure 5.25: The first two statistically significant principal components generated for the Swartvlei SV10.1 site

5.3.2. Indice de Polluosensibilité

The Indice de Polluosensibilité (IPS) incorporated at least 90% of the species for all measured levels of the SV10.1 core. The output of which is displayed below (Fig. 5.26). Swartvlei appears to consistently receive moderate amounts of nutrients throughout the record with a slight shift toward less polluted conditions at ~750 cal yrs BP. However, a period of constant and rapid fluctuating nutrient loading is observed between 260 and 40 cal yrs BP before conditions stabilise.

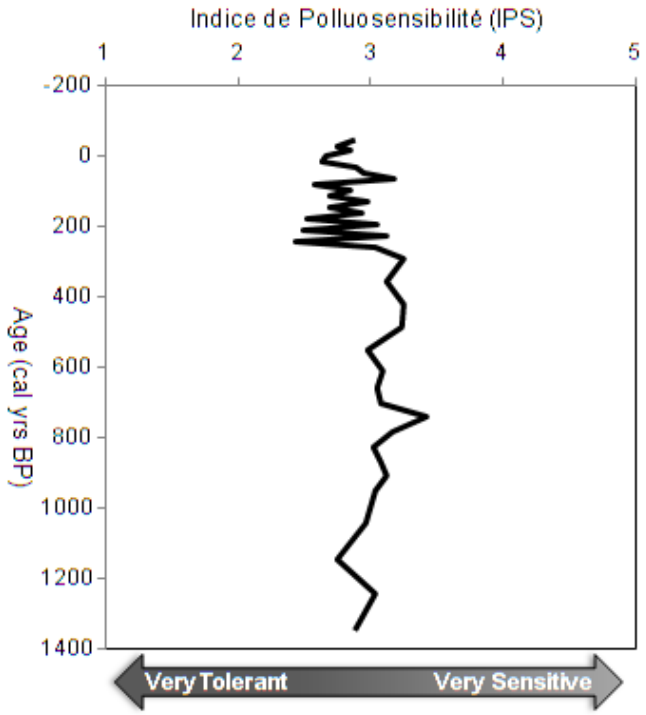

Figure 5.26: Pollution Sensitivity Index for the Swartvlei SV10.1 core

5.4. Conclusions:

Eilandvlei in the Touw River floodplain and Swartvlei in the neighbouring catchment should express the same climatic signals for portions of the record that overlap, i.e. the last 1400 years. The two Eilandvlei cores are indeed well correlated, with only minor discrepancies in the individual abundance of species, e.g. *Pinnularia borealis* var. 1 possibly related to the different positions of the cores within the lake. Of the 78 species present in EV10.1 and the 166 species present in EV11.1, 63 species occur in both cores. The greater number of species present in EV11.1 related to the extended record retrieved. SV10.1 has 100 species present throughout the core of which 73 also occur in EV11.1 and 60 in EV10.1. Related environmental conditions within the neighbouring lakes gave rise to similar diatom communities, with variability between assemblages possibly related to catchment influences (Fig. 5.26).

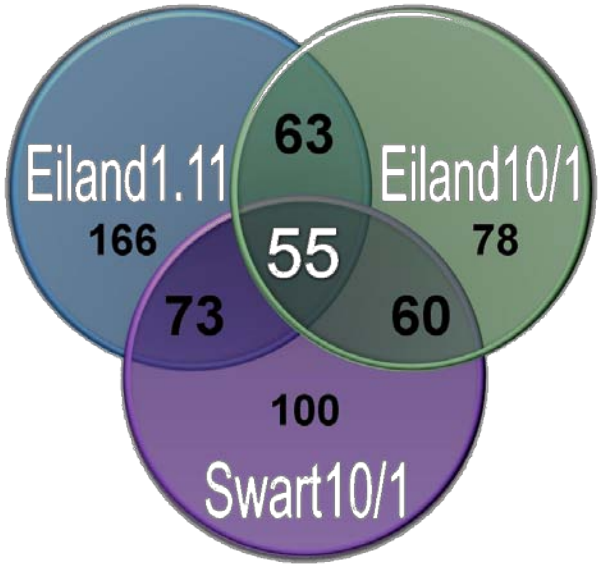

Figure 5.26: Summary of species numbers within and across the Wilderness cores, displaying overlapping species occurrences between sites

The CONISS zone classification between Eilandvlei and Swartvlei do not perfectly match up, but this may be due to differing sampling resolutions as well as differences in underlying mechanisms responsible for the nature of the respective lakes (Table 5.5). The difference between sampling resolution of SV10.1 and EV11.1/EV10.1 does make direct comparisons problematic; however both show a shift toward drier conditions at around 500 cal yrs BP. Climatic influences are secondary to salinity, which is the main driving mechanism in SV10.1 compared to the EV11.1 record where climate appears to be the primary underlying mechanism. Both lakes appear to be a repository for organic material from the catchment as well as *in situ* deposition, boasting a significant macrophyte community through most of the time span analysed.

Table 5.5: Zonation comparison between Eilandvlei and Swartvlei

Eiland		Swart	
zone EV11.1e	0 - -31	**zone SV10.1d**	45 - -50
zone EV11.1d	500 – 0	**zone SV10.1c**	250 – 45
zone EV11.1c.2	900 – 500	**zone SV10.1b**	730 – 250
zone EV11.1c.1	1200 – 900	**zone SV10.1a**	1400 – 730
zone EV11.1b	2050 – 1200		
zone EV11.1a.2	3450 – 2050		
zone EV11.1a.1	4000 – 3450		

Chapter 6. HYDROLOGICAL DEVELOPMENT OF THE WILDERNESS EMBAYMENT

The Wilderness Embayment features several back barrier lakes of Pleistocene origin, creating a transitional environment between the freshwater inputs from rivers and surface runoff and the marine influx from the seaward direction. The incorporation of three records from adjacent catchments can provide insights into a region that experiences multiple climatic influences but also offers the opportunity to remove catchment-based biases that may be affecting the biological community, thereby providing a clearer environmental signal. Fossil diatom evidence from the region revealed three phases of development in response to sea level fluctuations and sand movement; these phases are the marine embayment phase, the lagoonal phase and the coastal lake phase. Therefore, the following subsections have been structured based on these phases and include a tentative regional overview formed through the correlation of suitable sites. The paucity of high-resolution records in close proximity to the Wilderness area makes regional comparisons tenuous; hence sites further afield have been incorporated that have similar temporal resolutions. A more complete synthesis is undertaken in Chapter 8 to relate changes within the records to regional and global events. The following discussion interprets the trends imprinted in the changing community structure of the diatom assemblages with the aim of identifying key controlling mechanisms responsible for shifts in their composition.

6.1. MARINE EMBAYMENT PHASE (~4000 – 3450 cal yrs BP):

A late Holocene marine transgression in the order of ±2m AMSL has been recorded at several sites along the South African coast (see section **2.3.2**); generally peaking sometime between 4500 and 3500 cal yrs BP depending on the locality but all agreeing that modern sea level was achieved by about 3200 cal yrs BP. In general, the EV11.1 record supports the evidence of a higher sea level during this time but is unable to substantiate the ±2 ASML magnitude of the transgression. Evidence of direct marine influences in the lake is apparent until ~3750 cal yrs BP, implying a sea level rise of sufficient magnitude to penetrate the back-barrier lake, which presently lies at 4-5 m AMSL (Fig. 6.1). The maximum extent of the marine transgression appears to occur at around 3900 cal yrs BP for the known EV record. The underlying mechanisms responsible for the transgression have been attributed to isostatic emergence

and thermal expansion of sea water (Miller et al., 1995; Ramsay and Cooper, 2002). A warmer climate is evident as interpreted by the Cango Caves $\delta^{18}O$ record and is coupled with slightly drier conditions in the Wilderness region between ~4000 and ~3850 cal yrs BP. The reduction in moisture availability resulted in lower lake levels, which gave rise to the higher frequencies of the aerophilic species, *Pinnularia borealis* var. 1. The higher sea level and increased wave action along the coast may have led to erosion of the lake's southern shore line, recycling dune sands and inundating the Wilderness Valley forming a large marine embayment which possibly extended as far eastward along the valley as Rondevlei (Fig. 6.1).

Figure 6.1: Hypothetical generalised schematic representation for the Wilderness catchment based on zone EV11.1a.1, showing possible regions of marine inundation (blue polygon) and freshwater inputs (orange arrows)

A rise in freshwater supply, probably through precipitation between ~3750 cal yrs BP and 3650 cal yrs BP transformed the embayment to less saline conditions and initiated a flushing of the system, shifting it toward fresh-brackish conditions as the sea regressed. High river current velocities are prevalent at this time substantiating the possibility of flash flooding and increased storminess (Plenković-Moraj et al., 2008). Although considerably wetter from ~3750 and 3650 cal yrs BP, a brief respite in high moisture availability led to predominantly fresh-brackish to brackish conditions at 3700 cal yrs BP. This period coincides with the onset of westerly winds and dune building in the Wilderness region from 3700 cal yrs BP as reported by Bateman et al. (2011). Most records from the summer rainfall region suggest a warm and moist period from ~6500 to 3200 cal yrs BP before more arid conditions set in thereafter (e.g. Cold Air Cave (Lee-Thorp et al., 2001), Lake Eteza (Neumann et al., 2010)). It is noted that the

aforementioned SRZ sites are geographically distant from the Wilderness region, however, the relative scarcity of high resolution sites across South Africa makes these comparisons necessary and worthwhile. In addition, generally warmer conditions are reported at Cango Caves and Seweweekspoort between approximately 4500 and 3400 cal yrs BP, which suggests that atmospheric disturbances could be affecting the south coast, resulting in a greater variability in moisture availability (Talma and Vogel, 1992; Chase et al., 2013). Hence, the resultant influx of freshwater into the Wilderness lake systems may be the product of the combined influences of polar- and tropical-based climatic systems reaching the coast.

A short-lived dry episode from ~3650 to ~3550 cal yrs BP led to a steady decline in water levels before a recovery at ~3500 cal yrs BP. During this period many benthic species decline and are replaced by aerophilic taxa. The balance of evidence suggests that in response to drier conditions between ~3650 and 3550 cal yrs BP the system was unable to support the larger aquatic vegetation matrix, resulting in mass macrophyte mortality, which provided an injection of organic matter and nutrients into the system. In general, the period between 3750 – 3500 cal yrs BP appears to be climatically variable, where neither tropical- nor polar- rainfall influences dominate along the south coast. Climatic instability may be the definitive driver in moisture availability, and the data suggest that the diatom assemblage adapted by shifting to a community that is tolerant to fluctuations in salinity. The ultimate cause for the prevailing circumstances is probably related to the combination of sea level decline toward present levels and cooler conditions. As the sea retreats, marine and salt influences wane, however storm surges and high tides are able to penetrate the system periodically, creating a mixed diatom assemblage favourable to species that are able to withstand the variability in water quality. The previously dry climate may also have caused a concentration of salts and nutrients along the shore as dissolution within the water column would be limited; as water levels recovered these salts would have affected water quality and the diatom community.

6.2. LAGOON PHASE (~3450 – 2000 cal yrs BP):

The progression from zone EV11.1a.1 to EV11.1a.2 at ~3450 cal yrs BP hinges on a peak abundance of marine species, which steadily decline over the subsequent centuries to the termination of the zone. Peaks in *Paralia sulcata* at around 3425 and c.2900 cal yrs BP are interpreted as an indicator for upwelling events along the south coast. Upwelling is initiated when easterly winds originating from the South Atlantic Anticyclone (SAA) are maintained along the coast. Typically this occurs during the austral

summer months, when the anticyclones draw towards the continent and the westerly belt contracts toward the polar region. Additionally, both episodes are associated with a spike in marine species, possibly indicating a brief resurgence of marine influences in the wave-dominated estuary. Between these two distinct events, conditions appear to be relatively moist, with peak moisture availability occurring at ~3250 cal yrs BP. In comparison to the previous wet spell between ~3750 and 3650 cal yrs BP, which appears to be associated with a combination of polar- and tropical- climate influences resulting in intermittent high frequency precipitation, this later period suggests a more consistent freshwater supply, maintaining fresh-brackish conditions. Hence, a shallow open lake is prevalent during this time with an established littoral zone and submerged macrophyte community (Fig. 6.2) (McGlone et al., 1984).

Figure 6.2: Generalised schematic representation for the Wilderness catchment based on zone EV11.1a.2 (3450 – 2050 cal yrs BP), showing possible regions of marine inundation (blue polygon) and exchanges (red arrows) and freshwater inputs (orange arrows)

A cooler climate as reported at both Cango Caves and Cold Air Cave, particularly between around 3350 and 2500 cal yrs BP, may be linked to the prevalence of the westerly winds, suggesting that cold fronts are the primary and dominating source of moisture to the region (Talma and Vogel, 1992; Holmgren et al., 1999; Lee-Thorp et al., 2001; Bateman et al., 2011; Chase et al., 2013). Increases in fine sand sediments and the abundance of *Amphora ovalis* and *C. scuttellum* supplement the notion of extensive sand movement and deposition into the region during this period (Harper, 1969; Horton et al., 2006; see also Martin, 1968; Miller et al., 1993; Miller et al., 1995; Jerardino, 1997; Carr et al., 2006a; 2006b;

Bateman et al. 2011). A reduction in the influx of marine water provided salinity stability, which diminished the representation of species tolerant of fluctuating salinities. Hence, the likely mechanism responsible for the lake's condition during zone EV11.1a.2 is the retreating sea resulting in a waning marine and brackish element within the lake but also accompanied by a consistent freshwater supply shifting the system to more brackish-fresh conditions (Fig. 6.2) (Miller et al., 1995; Baxter and Meadows, 1999). There is an excursion within the largely moist phase at around 3075 – 2975 cal yrs BP, which resulted in an increase in turbidity as water levels and salinity fluctuated in response to the changing regime. This brief phase pre-dates the strengthening of the SAA and may be an expression of the alteration in climatic influences over the region.

Generally, conditions remain relatively wet as increased river flow flushes the system and deposits finer sediments from the catchment but the moisture diminishes as westerly winds strengthened between 3000 and 2275 cal yrs BP, coinciding with fine sand deposition (Carr et al. 2006a; 2006b; Bateman et al. 2011). Lower water levels from around 2975 cal yrs BP to at least c. 2100 cal yrs BP led to a steady decline in species richness and diversity as *Pinnularia borealis* var. 1 continually increased. This suggests generally lower moisture availability but with sufficient freshwater entering the system to maintain the fresh-brackish diatom community, coupled with poor penetration and circulation through the lake system. A more brackish to brackish-marine character is prevalent and at times alternating dominance between the two states is observed during this ~900 year period. The establishment of the littoral zone is maintained and progressively expands as water levels decline and stabilise to provide a variety of benthic habitats. Palaeo-records across the region suggest a drier period in the summer rainfall zone and possibly wetter conditions in the winter rainfall zone during this interval (Lee-Thorp et al. 2001; Scott and Woodborne 2007; Chase et al. 2009; Finne et al. 2010). Hence, from the body of evidence it appears that the year round rainfall zone, although influenced predominantly by the westerlies, remained relatively dry in accordance with Carr et al. (2006a; 2006b). Carr et al. (2006b) identified this dry episode through lunette accretion near Cape Agulhas from 2800 – 2500 cal yrs BP, which coincides with the EV11.1 diatom record.

Pollen analysis from Norga to the west of the Wilderness region shows optimal forest spread until ~2600 cal yrs BP before cooler and drier conditions resulted in a decline in forest stands, lasting until about 1400 cal yrs BP (Scholtz, 1986). The expansion of the westerlies at the expense of the high pressure belt would have weakened the Agulhas Current velocity, encouraging warm surface plumes on to the Agulhas Bank and a drop in sea levels (Jerardino, 1993; Cohen and Tyson, 1995). The decline in marine

species during the later stages of the zone confirms the decrease in marine influences, accompanied by dune development that constructed a significant and persistent barrier on the seaward side of the Wilderness Lakes, particularly at Eilandvlei (Bateman et al., 2011). The spread of dune heath between ~2400 and ~2100 cal yrs BP assisted in the stabilisation of the shoreline and probably settled the formation of the Serpentine Channel and Wilderness Estuary into its present configuration (Martin, 1956, 1962). The commencement of dune heath coincides with rising temperatures as recorded by the Cango Caves speleothem record (Talma and Vogel, 1992). The period from around 2375 until at least 2100 cal yrs BP was probably warmer and drier leading to the lowest lake levels observed throughout the entire record. However, the magnitude of lake level decline cannot be solely attributed to low freshwater inputs but must be coupled with the limitation of marine incursions into the lake basin, which eventually led to the near complete removal of the marine to brackish-marine component in the habitat by ~1950 cal yrs BP.

Freshwater inputs into the system were maintained until ~2200 cal yrs BP. A shallow open lake with an established littoral zone but with limited nutrient availability appears to be the prevalent state of the system during this time. This period also sees the demise of brackish-marine elements, which occur only in trace amounts later in the record with the proposition that marine influences retreated westward along the Serpentine Channel. The maintenance of the marine to brackish-marine element throughout zone EV11.1a suggests that an active estuary to lagoon habitat was sustained over the 2000 year period. This is in agreement with Martin (1968), who showed the development of Groenvlei from a marine lake to a lagoon occurred between 6000 and 2000 cal yrs BP (see also 2.3.1). Taxa characteristic of estuarine conditions maintain a steady proportion of the assemblage throughout zone EV11.1a. *Cyclotella caspia* and *Mastogloia smithii* provide the foundation of the biological community; as both species are able to tolerate the near constant flux in salinity (Marshall and Alden, 1990; Romundset et al., 2010). The later stages of this period appear to be predominantly dry with lower water levels but with adequate freshwater supply to sustain the lake ecosystem and enhance the vegetation growth in and around the lake.

6.2.1. 2200 – 2000 cal year BP

A regime shift occurred during this 200 year interval, correlating with the highest temperature recorded for the late Holocene from the Cango Caves record. A maximum average temperature at c. 2088 cal yrs BP is reported before dropping by nearly a degree some 60 years later (Talma and Vogel, 1992). The increase in temperature combined with the rise in *P. sulcata*, particularly between around 2200 – 2025

cal yrs BP, suggests a shift towards a more dominant anticyclonic circulation, which intensified and drew in toward the continent. The region remained dry with peak aridity occurring at c. 2100 cal yrs BP. The rise in aridity resulted in the contraction of the open water environment, possibly leading to the encroachment of a wetland-like system throughout the entire Wilderness lake complex driving the decline in species diversity and richness and enhanced habitat preference for the aerophilic species. Scott and Lee-Thorp (2004) suggests a rise of summer rainfall seasonality between 5000 and 2000 cal yrs BP, of which the discussed event may be the peak of its expression.

As average temperatures declined between c.2088 and c.2028 cal yrs BP (Talma and Vogel, 1992), an increase in moisture availability occurred. Epiphytic species, predominantly *M. nummuloides* and *C. placentula*, respond to the rise in lake levels as freshwater inundates the once partially emergent vegetation zone. It appears that this occurred rather rapidly, increasing sediment resuspension and erosion from the catchment and resulting in high water turbidity. The lakes in the Wilderness region have been known to experience vegetation encroachment within and along the periphery of the lakes (Russell and Kraaij, 2008); this transitional period from zone EV11.1a to zone EV11.1b appears to be the first sign of a long-term trend within the region. As discussed previously (see section **2.4**), a number of sites across South Africa record a short-lived shift in environmental conditions between 2100 and 2000 cal yrs BP. The winter rainfall region appears to be generally wetter (e.g. Baxter, 1989; Jerardino, 1995; Meadows and Baxter, 2001; Scott and Woodborne, 2007; Meadows et al., 2010), whereas the summer rainfall region appears to be generally drier (e.g. Scott et al., 2005; Finne et al., 2010; Neumann et al., 2010). The year-round rainfall region may be more variable than the uniform interpretations made in the aforementioned studies. High resolution records are limited for the YRZ, as is the case for most of South Africa, which makes it difficult to discern the dimensions of the event across the region. This period correlates to subzone C1 of the Groenvlei record (Martin, 1968), which also suggested a transitional phase promoting scrub spread, after which *Podocarpus* and local woodland taxa rapidly increases. Cconcurrent with these events Carr, et al. (2006a) reports extensive water erosion on the inner lunette on the Agulhas Plain as water levels rose rapidly. The EV11.1 record substantiates this summary as a peak in aridity shifts to considerably wetter conditions within a short period of time. Alternatively, evidence of Khoisan activities on the south coast plain is recorded from 2000 years BP and may be a factor in landscape dynamics (Damm and Hagedorn, 2010). The impacts of local herders and hunter gatherers have not been fully ascertained, although the broader regional scale of this ~2100 – 2000 cal yrs BP event is perhaps more likely driven by climate changes than human action (Talma and Vogel, 1992).

6.3. COASTAL LAKE PHASE (2000 cal yrs BP - present:

Post 2000 yrs cal BP, Eilandvlei remained predominantly brackish in nature with occasional influxes of freshwater. The dominance of epiphytic species remained, maintaining the longevity of the submerged macrophyte community in the development of the Wilderness Lakes (Adams and Bate, 1994). The expansion of the macrophyte community sustained the alkaline nature of the system, as well as recycled nutrients within the system. PCA identified *Stephanodiscus hantzschii* and *Stephanodiscus agassizensis* as the defining species between c. 2025 and 1700 cal yrs BP. Both species plus *M. nummuloides* can thrive in nutrient-enriched, light-limited environments, thereby affirming the increase in lake nutrients, which was possibly linked to the increase of sediment washed in from the catchment during the early stages of the zone (Rendall and Wilkinson, 1986; Findlay et al., 1998). The mineralogy of the record shifted towards a more silt and clay fraction during this zone, which progressively increased at the expense of fine and medium sands providing plausible evidence of a greater riverine/surface runoff influence over marine and/or aeolian inputs.

Presently, water transparency at Eilandvlei ranges from a few centimetres to just over three meters in the lake, which has a maximum depth of around six meters (Russell, 1999). Russell (2013) has shown that Eilandvlei experiences higher turbidity than either Langvlei or Rondevlei due to the silt-dominated inputs from the Duiwe River, which enter to the north-east of the lake. A decline in water transparency is also related to wind action, which is the fundamental cause of water column mixing, as well as to higher precipitation leading to greater surface runoff and river inputs (Russell, 2013). The effect of conditions experienced during this phase and until at least after ~1650 cal yrs BP hindered species richness and diversity. The proportional representation of fresh to fresh-brackish species can assist in tracking the freshwater/brackish water interface. Therefore, greater moisture availability during this zone can be constrained to two events at around ~2025 and at ~1275 cal yrs BP (Fig. 6.3). Freshwater inputs peaked at c. 2025 cal yrs BP and then remained stable until at least c. 1725 cal yrs BP. Furthermore, the occurrence of the freshwater diatom, *Achnanthidium minutissimum* provides evidence of flooding in the catchment at ~2025 cal yrs BP. Studies have shown that populations of *A. minutissimum* can maintain and thrive in and after flooding events, and it has been classified as an indicator species for natural disturbances (Weilhoefer et al., 2008; Mihaljević and Pfeiffer, 2012). Mostly, the environmental trends observed during this interval conform to many summer rainfall and some winter rainfall records indicating wetter conditions after 2000 cal yrs BP (Fig. 6.3) (e.g. Baxter,

1989; Holmgren et al., 1999; Scott and Woodborne, 2007; Lewis, 2008; Brook et al., 2010; Meadows et al., 2010).

Figure 6.3: Schematic representation of higher lake levels on the landscape in the Wilderness Valley showing possible sources of marine exchanges (red arrows) and freshwater inputs (orange arrows)

The great diversity in marine species present in earlier zones is replaced by minimal representation in the following stages, mainly through the representation of *Coscinodiscus radiatus*. *C. radiatus* is classified as a warm meso-eurytherm, tolerant of a water temperature in the range of 5 – 30°C (Baars, 1979). The species along with *Chaetoceros* sp. is common along the South African coast, particularly in well mixed near-shore waters (Schuette and Schrader, 1981; Romero et al., 2002; Barron et al., 2004). These species suggest that warm water plumes are periodically being reflected onto the Agulhas Bank and either enter Eilandvlei through the Serpentine Channel or through sea spray. Dunajko and Bateman (2010) showed that dune activity occurred on the seaward flank of the barrier crest until at least c. 1900 cal yrs BP; this may coincide with the spike in marine taxa as enhanced westerly winds responsible for dune development would assist in mixing and transporting warm waters onto the Agulhas Bank and into Eilandvlei (Cohen and Tyson, 1995; Horton et al., 2006). Penetration of marine waters may be hindered by the shifting sands, as well as distance travelled through the channel; presently Eilandvlei only experiences weak marine influence which is at this time directly related to the state of the Touw River mouth (Russell, 1999). The mouth remains open during high rainfall periods allowing reverse flow to occur in the estuary and channel and enter Eilandvlei from the south-west. The abundance of freshwater coupled with enhanced wind activity may have influenced the transport of the marine

species into the system. For the most part, the near absence of brackish-marine species throughout the zone indicated that marine influx was periodic as opposed to a permanent feature over prolonged periods of time and may partially eliminate a marine transgression of any great magnitude.

An extended period of exceptionally low productivity is observed from c. 1725 – 1350 cal yrs BP, when *M. nummuloides* and a selection of brackish species dominate the diatom community. Research has shown that *M. nummuloides* has an optimum temperature growth range of between -1.5 and ~10°C and a wide salinity preference (Baars, 1979; McLean et al., 1981; Rendall and Wilkinson, 1986). These ecological requirements allow the diatom to have a competitive edge when conditions deteriorate within a lake system. This combination suggests that sudden fluctuations in salinity may have led to a decline in species diversity (McLean et al., 1981; Rendall and Wilkinson, 1986). However, cooler water temperatures may be the primary factor limiting the diversity of the biological community during this period. Scholtz (1986) proposed cold, winter winds predominated between c. 2600 and 1400 cal yrs BP, which led to a decline in forest taxa as drier conditions prevailed. Additionally, OSL ages from the Sedgefield Ridge indicated dune activity between approximately 1750 and 1300 cal yrs BP (Bateman et al., 2011). The abundance of *M. nummuloides* and the evidence from Norga and the Wilderness dunes implies a cooler and/or windier climate showing some recovery near the culmination of the EV11.1b zone. The Cango Caves speleothem record showed fluctuating temperatures but a downward trend toward cooler temperatures between 1900 and 1400 cal yrs BP after peaking at 2100 cal yrs BP (Talma and Vogel, 1992), substantiating the trends evident in the diatom record between 1725 – 1350 cal yrs BP. The consistently low proportions of aerophilic species throughout zone EV11.1b, as well as the regular presence of fresh-brackish species, albeit at times diminished, suggests that while this period was possibly cooler and drier, freshwater inputs maintained open water conditions of varying salinities (Fig. 6.4).

Figure 6.4: Schematic representation of lower lake levels on the landscape in the Wilderness Valley showing possible sources of marine exchanges (red arrows) and freshwater inputs (orange arrows)

A recovery in species diversity and richness is observed after c. 1350 cal yrs BP, with many brackish species showing greater abundance and representation in the assemblage. The dramatic increase in *Cyclotella choctawhatcheeana* at around 1275 cal yrs BP was accompanied by a rise in proportional representation of fresh to fresh-brackish taxon. *C. choctawhatcheeana* occurs in the plankton of turbid coastal lakes or where nutrients are elevated and salinities are lower than that experienced in marine environments (Wachnicka et al., 2011). Wachnicka et al. (2011) further state that blooms of *C. choctawhatcheeana* at Biscayne Bay, Florida coincided with the wet season after flushing of evaporative nutrients entered the system. This appears to be the case at Eilandvlei, after a long-standing interval of relatively drier climate after c. 1725 cal yrs BP, a pulse of freshwater was introduced into the lake providing optimum conditions for the growth of *C. choctawhatcheeana*. It is possible that this pulse of freshwater increased turbidity and limited light penetration in the water column. A review of palynological evidence from the Wilderness region was interpreted as indicating more arid conditions until 1300 cal yrs BP, which appears to conform to the environmental development of the region encompassed in zone EV11.1b (Scholtz, 1986; Chase and Meadows, 2007).

The transition from zone EV11.1a to zone EV11.1b appears to have been sudden. Following what could be argued as the driest period of the EV11.1 record at ~2100 yrs (Fig. 6.3), conditions dramatically and rather rapidly altered to a wetter regime over what is likely to have been a matter of decades (Fig. 6.4). The shift resulted in greater water turbidity and nutrient enrichment, which persisted throughout the

zone. This wetter state was maintained, although in a slightly diminished capacity, until about 1700 cal yrs BP, before reverting to somewhat drier conditions (Fig. 6.3). Open water conditions persisted however, either the magnitude of the dry phase was not as great as to cause a decline in lake levels or the wet phase increased lake levels to a degree that evaporation and the intermittent freshwater inputs during the arid period did not hinder the planktonic community to a great degree.

6.3.1. Swart and Wilderness Catchment Dynamics

The two EV records, EV11.1 and EV10.1, overlap from 600 to -30 cal yrs BP and are discussed concurrently relative to their zones below. The Eilandvlei, EV11.1 record and the Swartvlei, SV10.1 record overlap from around 1350 cal yrs BP onwards and where possible are discussed simultaneously. The suppression of the marine signal after 2000 cal yrs BP in the EV11.1 record becomes more apparent when comparing it to the SV10.1 record. Swartvlei has a more direct connection to the open ocean via the 7.2km Swartvlei Channel winding through low elevation sand flats. A strong marine signal was evident throughout most of the record, particularly in reference to the proportional representation of *Catenula adhaerens, D. chersonensis/crabro, Chaetoceros* sp.*, Craspedodiscus elegans* and *P. sulcata*. These species generally occur on the inner shelf and are probably prevalent in the littoral zone of the Agulhas Bank.

Medieval Climate Anomaly (MCA)

For the most part zone EV11.1c, which commences at 1200 cal yrs BP, can be classified as an expression of a drier climate with limited moisture availability, with its timing overlapping with the global climatic event known as the Medieval Climate Anomaly (see pg. 32). The system still experienced flushing but to a lesser degree as the effects of a more persistent dry season became more prevalent. A lower lake level with a gradually expanding benthic habitat occurred from about 1150 to 1115 cal yrs BP before the intertidal shoreline became more aerially-exposed by about 1080 cal yrs BP (Fig. 6.4) (Taylor et al., 2007). Evidence suggested that coastal upwelling became more pronounced between c. 1150 and 750 cal yrs BP, implying an inclination toward tropical to sub-tropical climatic influences with a strengthening of the high pressure cells. Tyson and Lindesay (1992) proposed an increase in tropical easterly wind flow between c. 1100 and 700 cal yrs BP, evidenced by the higher average temperatures experienced in the Cango Valley, with which the SV10.1 record concurred.

A brief respite from the lower moisture availability occurred at some point after c. 1115 cal yrs BP, and climate remained relatively moist until about 1000 cal yrs BP (Fig, 6.3). Episodes of increased water turbidity probably related to inputs from the Duiwe River define this wet period (Russell, 2013). This

rapid shift between wet and dry conditions between c. 1200 and 1000 cal yrs BP is identified by Mayewski et al. (2004) as a period of rapid climatic change, which coincided with a reduction in North Atlantic Deep Water (NADW) flow and drier conditions in Chile. A regional expression of this rapid climate change event appears to be recorded in the EV11.1 sequence but also appeared in other local sites, including to the west on the Agulhas Plain, where Carr et al. (2006a; 2006b) also proposed drier conditions at ~1200 cal yrs BP and 1000 cal yrs BP which allowed for phases of lunette accretion. Greater aridity set in thereafter as aerophilic species came to dominate the assemblage until about 825 cal yrs BP. A drier phase was also evident in the SV record from ~1250 cal yrs BP, leading to a decline in lake levels but experiencing episodic occurrences of increased surface runoff and river inputs (Fig. 6.5). A gradual increase in the brackish component occurs between c. 1200 and 950 cal yrs BP before fresh to fresh-brackish conditions rise and continue until c. 615 cal yrs BP. This suggests that for much of the period between 1200 – 950 cal yrs BP a drier climate with moderate freshwater inputs prevailed.

Figure 6.5: Schematic representation of lower lake levels on the landscape in the Swartvlei Valley showing possible sources of marine exchanges (red arrows) and freshwater inputs (orange arrows)

The Agulhas Bank environment experienced mixing of its surface waters as witnessed through the constant appearance and relatively high proportional representation of *Chaetoceros* sp. until at least 750 cal yrs BP. Most South African coastal records suggest a marine transgression to the magnitude of 1.5m AMSL at about c. 1600 – 1400 cal yrs BP before reaching present levels by ~800 cal yrs BP (see

section 2.3.2, Fig. 2.8). This would be sufficient to inundate Swartvlei and account for the greater marine diversity and abundance evident during the zone (Fig. 6.6). The exact timing of the development of the Swartvlei channel into its present configuration cannot be ascertained, so it is possible that a shorter connection between the lake and the shoreline may have prevailed during the early stages of the zone. The overall representation of marine taxa during zone SV10.1a, coupled with the relative species richness, may imply minor fluctuations in sea level between 1400 and ~550 cal yrs BP before marine exchanges with the lake became tenuous and only species which are easily transported being present in the upper part of the zone.

Figure 6.6: Schematic representation of higher lake levels and increased marine exchanges on the landscape in the Swartvlei Valley showing possible sources of marine (red arrows) and freshwater inputs (orange arrows)

An influx of river inputs into Swartvlei between 950 and 900 cal yrs BP may have caused the mobilisation of salts deposited during the preceding arid phase thus providing a primarily brackish habitat. Greater evaporation potential may have assisted in the preservation of the brackish taxa beyond 900 cal yrs BP, as well as providing a niche for marine taxa that are able to extend into slightly less saline waters to exploit. During this period, lake levels rose dramatically in Swartvlei, peaking at ~915 cal yrs BP in response to the higher freshwater influx and possibly lower lake levels experienced during the preceding dry phase, after which lake levels continually declined until 300 cal yrs BP. A relative stasis in the proportional representation of fresh to brackish species from 875 and 615 cal yrs BP substantiates the shift toward relatively wetter but stable conditions.

In the adjacent catchment, Eilandvlei experiences a period of lake confinement with a limited interaction with marine waters from c. 870 to 575 cal yrs BP. The restriction of marine reverse flow to the Wilderness Lakes may be related to the status of the estuary mouth. The mouth remains open during periods of high precipitation which assists in breaching sand accumulated in the mouth region and is typically followed by a rise in salinity in the estuary (Russell, 2013). Conversely, during periods where the mouth is closed, salinity in the system can rise, which is probably related to restricted freshwater flow and greater evaporation (Russell, 2013). Hence, the dynamics at play during this ~300 year period may be related to prolonged mouth closure with minor breaching phases. A relatively stable environmental period is experienced across both catchments from c. 825 cal yrs BP, until c. 650 cal yrs BP, particularly with respect to moisture availability. Lake levels are also moderately high and stable. The relative environmental stasis provides an opportune period of recovery for the submerged macrophyte community, which suffered during the arid phases in the preceding subzone. The period may not have been extensively dry, but rather evaporation may have exceeded precipitation with the latter being more consistent than occurring as high frequency events.

An interesting pattern is observed in frequencies of *C. radiatus* and *P. borealis* var. 1 between approximately 1080 and 750 cal yrs BP in the EV11.1 record. After a brief break, the synchronicity of *C. radiatus* and *P. borealis* var. 1 resumes from c. 720 until c. 360 cal yrs BP. The mechanism governing this trend may be related to the greater inputs of reverse marine water flow into Eilandvlei overwhelming *in situ* conditions during periods when lake levels are lower and freshwater inputs were limited. The restriction in freshwater inflow from the catchment may have hindered biodiversity as well as limited habitat availability. Lower productivity and species richness in the lake during periods of environmental stress may make the marine species appear in greater relative abundance. The planktonic *C. radiatus* appears to be more easily transported than other marine species, and this may be the cause of its elevated frequencies during the last 2000 years. Compton (2001) suggested a minor marine regression at ~800 cal yrs BP on the west coast (see section **2.3.2**), the timing of which corresponds to the disconnect in the observed trend and possibly indicates the intricate link between the nature of the terrestrial and marine influences on coastal landscapes.

The timing of this phase loosely correlates to what is globally termed the “Medieval Climate Anomaly” (MCA) (Hughes and Diaz, 1994; Mann, 2007). Hughes and Diaz (1994) concluded that average summer temperatures during the MCA were higher than normal but the synchronous nature of this event has not been established. The summer rainfall zone appears to have experienced enhanced rainfall as per

the warmer and wetter conditions prevalent in the Transvaal region between 1100 and 700 cal yrs BP and wetter conditions occurring at Klein Spitzkoppe from 1150 to 750 cal yrs BP (Huffman, 1996; Chase et al., 2009). Notwithstanding, this environmental expression appears to generally concur with conditions in the Wilderness area from about 900 to 650 cal yrs BP, with an overall wet climate leading to a rise in water levels, but warmer temperatures probably enhanced evaporation to the favour of a brackish diatom community. Tyson and Lindsey (1992) proposed that during the MCA a dominance of tropical easterly winds were experienced. At this time, the easterlies were possibly accompanied by an intensification of the anticyclones, leading to a prevalence of easterly winds along the south coast. The prominence of the tropical easterlies would have provided a constant supply of humid air to the eastern half of the country and parts of the south coast and may be the contributing factor in the relative environmental stasis experienced during the MCA (Cohen and Tyson, 1995).

Little Ice Age (LIA)

Fluctuating freshwater inputs between 700 and 500 cal yrs BP at Swartvlei may be linked to increases in westerly wind influences and inadvertently precipitation as interpreted from the Verlorenvlei diatom record (Stager et al., 2012). This 200 year time interval also corresponds to the first phase of the Little Ice Age as defined by Tyson and Lindsey (1992), and hence may be described as being variable but generally wetter. The freshwater inputs from c. 700 cal yrs BP assisted with the development of the fresh-brackish community and the persistence of diatom species that are able to tolerate a wide salinity range. The connectivity between Swartvlei and the open ocean may have also been impacted by the reactivation of the Sedgefield Dune between 600 and ~430 cal yrs BP (Bateman et al., 2011), which could have limited tidal in-wash and initiated the formation of the current configuration of the Swartvlei Channel. The sand fraction of the sediment matrix increases from 700 to ~450 cal yrs BP and is generally maintained above 30% which coincides with dune development (Bateman et al., 2011). This may have impacted the two kilometre stretch separating the lake basin from the continental shelf environment. Up to this point, Swartvlei may have been more like a lagoon than a back-barrier coastal lake, but with the mobilisation of the sands the lake became increasingly isolated. During this isolation, between around 700 and 600 cal yrs BP, the development of the submerged macrophyte community in Swartvlei is once again instigated. Intrusions of marine water, particularly from around 660 cal yrs BP, were not sufficient to maintain the brackish element of the lake and led to the decline in their proportional abundance. Both EV records on the other hand, suggested that marine influences increased from c. 600 to 500 cal yrs BP. Greater marine diversity is evident through the ubiquitous occurrence of *C. radiatus* in

the EV cores, as well as *P. sulcata, Chaetoceras sp* and *Delphineis minutissima* in EV10.1 and *Cocconeis distans* and *Catenula adhaerens* in EV11.1. The latter three species are classified as epipsammic occurring in shallow marine waters and the tidal zone, their appearance accompanied by the coarser sediment is likely a direct response to the breaching of the estuary mouth, remobilisation of dune sands and enhanced interaction between the coast and the back-barrier lake system (Muylaert et al., 2002; McGee et al., 2008).

Conditions appear to become drier at Swartvlei, producing a decline in lake levels from ~500 to ~300 cal yrs BP (Fig. 6.5). Although, lake levels are generally maintained through the regular inputs from the rivers and oceanic exchanges, fluctuations are evident in the record. The lower lake levels coupled with shifting sands may have led to the lake becoming predominantly isolated, as well as temporarily closing the estuary mouth at ~425 cal yrs BP before the connection was re-established thereafter. The isolation of the lake would have resulted in a rise in salinity along the axial length of the estuary, providing a habitat for the brackish-marine and marine taxa. During periods of rare reconnection between lake and ocean an adjustment to the two contrasting environments was undertaken by the biological community with an initial influx of brackish-marine/marine elements inundating the lake ecosystem. Lower lake levels also prevail in Eilandvlei, particularly between 500 and ~325 cal yrs BP as a rise in proportional representation of *P. borealis* var. 1 occurs and then again between ~220 and 190 cal yrs BP (Fig. 6.4). A number of factors appear to be influencing the character of the Wilderness Lake Complex during this period, but primarily the main limitation is freshwater availability. However, the freshwater signal in the Eilandvlei records is not prominent at any stage in the record, fresh taxa only occur in trace quantities over the last 1000 years. Therefore, the presence/absence of freshwater taxa may not be an ideal indicator of wetter/drier conditions for the region. On the other hand, the fresh-brackish to brackish community during this zone may be a more reliable indicator of limited freshwater inputs, as the community would respond to the mixing regime of fresh and saline inputs. During zone EV11.1d a gradual decline of the fresh-brackish community is observed as the zone progressed, suggesting a diminished freshwater flow into the system. The mechanisms responsible for this shift could be the combination of reduced precipitation, as well as the westward migration of the Touw River, which would directly affect the flow of freshwater into Eilandvlei. The decline in freshwater inputs would limit nutrient inputs and progressively put strain on the biological community, resulting in a period of low productivity and a decline in species diversity and richness.

This phase of lower lake levels in both lake systems corresponds to the warmer event which separates the two phases of the LIA (see page 24). The warmer conditions would have enhanced evaporation and, accompanied by limited freshwater inputs would have assisted in the decline in lake levels. During this initial drier period, marine inputs appear to inundate the lake as *C. radiatus* increased in proportional representation. The second dry period between ~220 and 190 cal yrs BP loosely correlated with trends observed in the SV10.1 record. Of interest is the overlap of this period with below average tree-ring widths recorded in *Widdringtonia cedarbergensis* specimens from the Cederberg Mountains along the west coast of South Africa (Dunwiddie and LaMarche, 1980); the correlation of these two sites may suggest some spatially-constrained aridity across the winter and year-round rainfall regions.

Conditions during the intermittent interval between these two distinguished arid phases mentioned above, appears to be that of high water turbidity as lake levels respond to the minor fluctuations in water availability and the overall decline in freshwater inputs, particularly between 415 and 240 cal yrs BP. Peaks in a variety of planktonic species, as well as fresh-brackish taxa at ~260, ~160 and ~70 cal yrs BP substantiates the variability in lake levels in the EV11.1 record, coupled with a rise in *T. weissflogii* between 190 and 140 cal yrs BP in the EV10.1 record suggests a slight increase in freshwater inputs during this interval. Ultimately, a shift from an aerophilous-based community to a benthic-based community provides evidence of the transformation and inundation of the inter-tidal zone to a littoral zone by *ca.* 275 cal yrs BP in Swartvlei. This transformation can be broadly associated with the onset of the second phase of the LIA, which Tyson and Lindsey (1992) constrained to 325 – 125 cal yrs BP. Given a margin of error relative to the age-depth models employed by Tyson and Lindsey (1992) and the SV10.1 record, the minor discrepancy to the onset of this event can be explained.

Zone SV10.1b spans the period from ~250 to ~50 cal yrs BP and is typified by the alternating rise and fall of several species, particularly in the marine taxa. From c. 250 to 135 cal yrs BP, *C. radiatus* and *M. nummuloides* are generally in phase with each other, peaking at ~245, ~215, ~180 and ~150 cal yrs BP but only declining at ~230, ~200 and ~135 cal yrs BP. The in-phase periods where the two species are at minimal frequencies are accompanied by a rise in freshwater taxa. This association suggests that during periods of low precipitation and/or freshwater inputs, marine reverse flow dominates the Swartvlei system, but as freshwater inputs rise the net flow of the system is dominated by lake water outputs. Hence, the abundance of *C. radiatus* at the aforementioned times may be indicative of lower precipitation periods, whereas *M. nummuloides* is responding to the increase in turbidity as lake levels recede during the drier phase leading to the resuspension of shoreline sediments. The relatively

persistent freshwater component would be sufficient to maintain open mouth conditions of the estuary assisting in the transport and interaction of marine water between the waterbodies.

Introduction of Anthropogenic Forcing

The later stages of deposition at the Wilderness sites also correspond with the European colonisation and expansion. Initially, disturbances are minimal, however intensive modification of the landscape occurs from the late 19th Century as first a coastal road (AD 1883), then a railway (AD 1928) and finally a tar road (AD 1948) were constructed. These developments steadily impacted both the lake ecosystem and flow dynamics (Randall, 1995). From ~120 cal yrs BP until the early 21th century a dramatic rise in *M. nummuloides* in Eilandvlei corresponds with the arrival of European colonists and the resultant intensive landscape modification which defined their settlement. The construction of the railway and coastal road which run along the northern and southern shoreline of Eilandvlei, respectively would have mobilised sediments during construction and vegetation clearance. The in-wash of the sediments would have affected the water transparency, as well as increase sediment deposition; thus providing an optimal environment for the development of a *M. nummuloides* dominated community.

The most profound trend observed over the last 120 years is a distinct freshening of the systems. Only minor marine intrusions occur in Eilandvlei, supporting Russell's (2013) findings that the salt budget is only slightly impacted by tidal penetration from the estuary. It appears that marine reverse flow may be hindered by the establishment of permanent settlements and transport routes, encouraging the stabilisation of the landscape, as well as the rise in human activities in the catchment, such as dune stabilisation programmes and indigenous vegetation clearance making way for forestry and plantation activities. In the last 50 years, some recovery and modification of the system could be related to active conservation efforts within the catchment by government and SANParks authorities. Hence, the final stages in the Wilderness records is distinguished by the ebb and flow of the marine signal, with an overall relatively dry climate punctuated by short-lived wet spells before human activities obscure the natural environmental signal. Disentangling the anthropogenic forcing from natural climatic influences remains difficult.

6.4. CONCLUSIONS

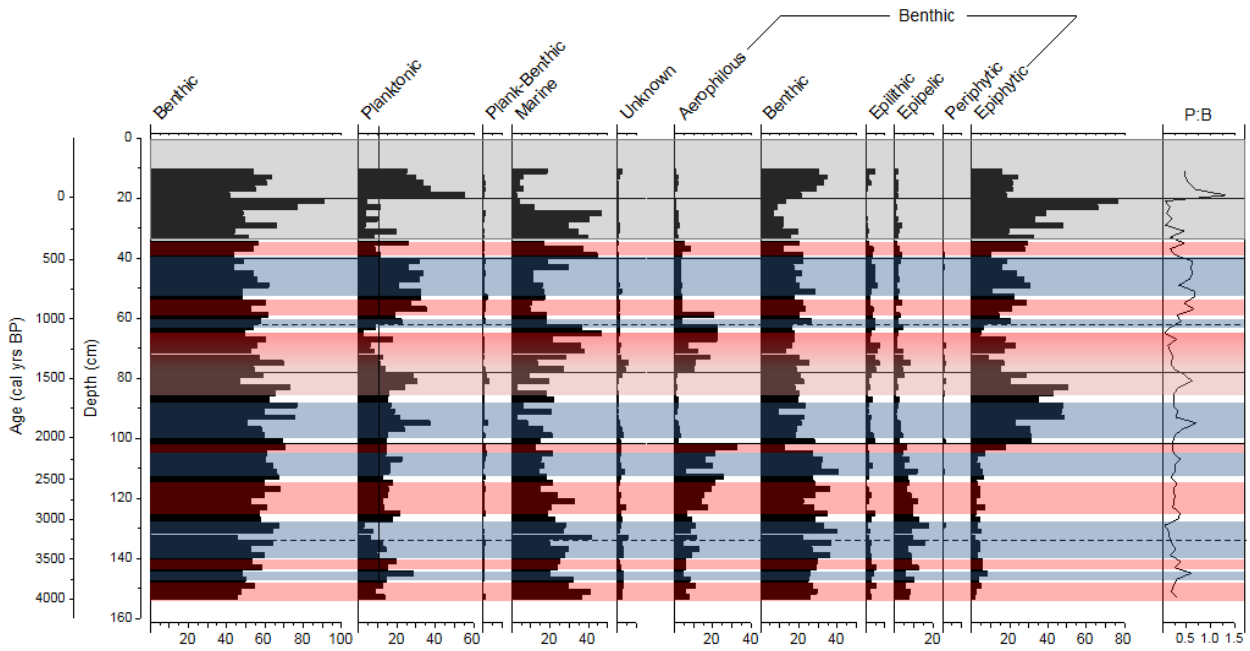

Figure 6.7: Summary of environmental conditions for the Wilderness region as based on the EV11.1 diatom community, proposed drier conditions are indicated by red shaded boxes whereas wetter conditions are indicated by blue shaded boxes and period of human occupation in a grey box

Climatically, the region experiences alternating wet-dry phases throughout the late Holocene, which appear to last for around 300 to 400 years (Fig. 6.7). Fluctuations in moisture availability are driven by changes in the predominance of tropical/subtropical forcings or polar forcings, as both systems can influence the climatic expression over the YRZ. During the interchange between the competing climatic systems where neither system dominates, the Wilderness region appears to consistently record a transitional phase, which ushers in the transformation of the climate. Furthermore, the proximity of the sites to the ocean provides insights into the variability of ocean-atmosphere dynamics, as well as sea level changes and its effects on the landscape and coastline. Initially, both lake systems are defined by their connection to the ocean, however as the coastline relative to dune activity develops, Eilandvlei becomes increasingly isolated from marine influences. On the other hand, the nature of Swartvlei would indicate that marine influences will always be a factor in defining the character and development of the lake. The Wilderness region has also been greatly impacted by anthropogenic forcings in the last two centuries, primarily altering river flow dynamics through modifications of the natural landscape. Some effects have been limited through management schemes implemented by conservation authorities, which presently has halted a complete regime shift within the lake systems.

The combination of the three records from the Wilderness region provides a detailed account of the hydrological and to a degree the underlying climatic conditions over periods of time covering the last 4000 years. For the most part all records agree on the temporal onset of or change in climatic conditions, however where they do differ, it is by a marginal degree. The differences between the temporal resolution along the length of a sequence and between records may be the main limitation when attempting to link records in a region. Notwithstanding, the evidence suggests changes that are comparable with other events recorded in the region and even globally.

Chapter 7. CAPE FLATS AND ITS ASSOCIATED LATE HOLOCENE PALAEOENVIRONMENT

7.1. REGIONAL SETTING

The Cape Flats (CF) region has been broadly described as a 400km^2 area of undulating sand with an average elevation of 30m (Schalke, 1973). The underlying geology is of Precambrian and Palaeozoic origin belonging to the Malmesbury formation and the Table Mountain Group with intrusions of granite batholiths (Schalke, 1973; Harris et al., 1999). Erosion of the Table Mountain Group since the Palaeozoic era separated the peninsula from the mainland, creating a low-lying topography between the Hottentots-Holland Mountains and the Cape Peninsula Mountains (Bickerton, 1982; Harris et al., 1999). The base geology of the Cape Flats is overlain by the Cenozoic Sandveld Group and the Springfontyn formation (Fig. 7.1) (Harris et al., 1999). Periodic deposition of Cenozoic sands and marine sediments is an artefact of the depositional environment and development history of the region (Schalke, 1973).

Sea level and isostasy played a defining role in the further development of the landscape. Higher sea levels submerged the Cape Flats region, isolating the Peninsula and creating a shallow channel between the two mountain ranges (Bickerton, 1982). Sand deposition in the channel resulted in the formation of a tombolo between the offshore Peninsula islands and the mainland (Bickerton, 1982). Subsequent uplift and marine regression produced a low-lying topography with numerous drowned depressions, resulting in many interconnected lakes, swamps and wetlands (Harrison, 1962). Continual sand movement during the Pleistocene and changes in drainage patterns led to infilling of some of these depressions and isolation of others (Harrison, 1962).

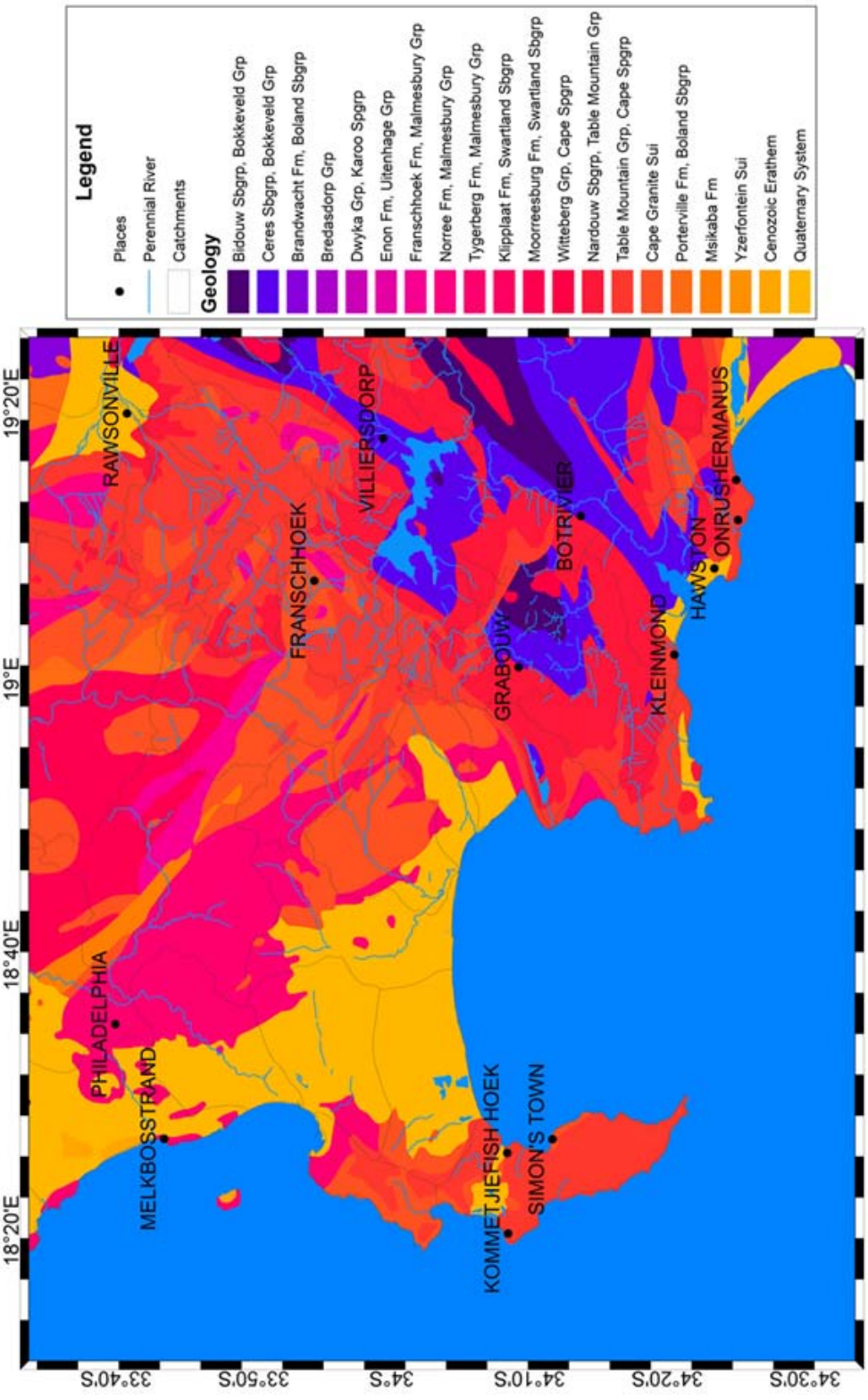

Figure 7.1: The geology of the Cape Flats (source: see Appendix One)

Unconsolidated sand dominates most of the area, originating from river and wind erosion and deposition, with increased transport during periods of summer aridity and anomalously high southerly wind velocities (Harris et al., 1999; Roberts et al., 2009). Offshore sand transportation via longshore drift returns nearly three quarters of the sediment to the land as dune deposits (Franceschini et al., 2003). The deposits move onshore as barchanoid dunes before transforming into parabolic dunes following partial vegetation (Roberts et al., 2009). Hence, a coastal dune system characterizes the southern extent of the CF, covering 243km^2 and extending 14.5km inland from False Bay (Franceschini et al., 2003; Roberts et al., 2009). The False Bay dune plume system is one of the most complex and largest along the west coast consisting primarily of Holocene sands of the Witzand formation (Roberts et al., 2009). The dunes have a southerly to south-easterly orientation mirroring the prevailing summer winds, which run parallel to the coast (Schalke, 1973; Roberts et al., 2009). The extension of the plume inland and thickness of accumulated sediments conform to maximum wind velocity and wind flow through the Cape Flats (Roberts et al., 2009). On average dunes reach between 10 to 35m above mean sea level (AMSL), with the highest dune reaching 65m AMSL, and range from cemented and fully vegetated to unconsolidated and partially vegetated (Bickerton, 1982; Harris et al., 1999; Roberts et al., 2009). During European colonisation the CF was cleared of vegetation to supply firewood to the settlement, this resulted in the reactivation of the dunes to the extent that encroachment on standing waterbodies occurred (Bickerton, 1982). In the late AD 1930s, stabilisation of the shifting dunes was initiated by introducing exotic plants, such as *Acacia saligna*, *Acacia cyclops*, marram grass and indigenous plants (Bickerton, 1982). Furthermore, sewage effluent was diverted into the dunes to promote growth of the introduced vegetation (Bickerton, 1982). However, the eastern and western flanks of the dunes remain active today (Roberts et al., 2009).

The occurrence of Cape Flats Sand fynbos on the western and northern shores of Princessvlei reflects the underlying deep, acidic soils. Sand-based soils of Tertiary to Recent origin sustain stands of Cape Flats Dune Strandveld (Mucina and Rutherford, 2006). Soils are either loamy-sandy or sandy ranging from fine to medium grained, with coarse grains occurring closer to the coastline (Bickerton, 1982; Neumann et al., 2011). The high carbonate content of the sands may explain the high pH of the soils and most of the water bodies (Neumann et al., 2011). However, in places the mobilisation of iron and decalcification of the superficial sands has led to the formation of podsols with pH ranging from 5.5 or less (Neumann et al., 2011). Peats with sandy clays of marine origin beneath have developed in many of the depressions beyond the western flank of the dune plume (Roberts et al., 2009).

7.1.1. Regional Climate

Kruger (2004a) identified the Cape Flats area as part of the South Western Fynbos-type climatic region. The area experiences a typical 'Mediterranean-type' climate, which appears to have developed during the late Tertiary and Quaternary (Linder et al., 1992). Precipitation generally occurs between May and August brought about by the westerly migration of mid-latitude cyclones (Neumann et al., 2011; Tadross et al., 2012). However, due to orographic influences precipitation is unevenly distributed across the region, with the Cape Flats receiving 580-980mm yr^{-1} and the Cape Peninsula receiving approximately 1200mm yr^{-1} (Kruger, 2004b; Neumann et al., 2011). The presence of the South Atlantic high pressure anticyclone during the summer months deflects the frontal systems southward maintaining a dry, warm and windy climate over the southwestern Cape (Fig. 7.2) (Cowling et al., 1999; Tadross et al., 2012). Temperatures are generally moderate throughout the year, reaching a maximum in February and a minimum in July (Fig. 7.2) (Kruger, 2004b; Neumann et al., 2011). The dominant wind components in summer are south to southeast, which create extensive cloud cover over mountain ranges of the Peninsula (Kruger, 2002, 2004b), whereas the prevailing winter winds are north to north-northwest (Fig. 7.2) (Harding, 1997; Kruger, 2002). Southerly component winds are established by September but become progressively north-westerly towards winter (Kruger, 2002). Coastal adiabatic processes further influence the prevailing winds and can result in onshore mist particularly during the autumn months (Harding, 1997; Tadross et al., 2012). Sea breezes only occur during the winter months between late afternoon and evening (Kruger, 2002). Winds appear to be a driving force of the landscape's expression; northerly wind components are responsible for carrying in frontal depressions resulting in rain, increasing surface runoff and inducing a rapid rise in water levels in the CF (Harrison, 1962; Neumann et al., 2011). South-easterly winds on the other hand contribute to evaporation and large scale sand movements as manifested through dune orientation (Harrison, 1962; Bickerton, 1982).

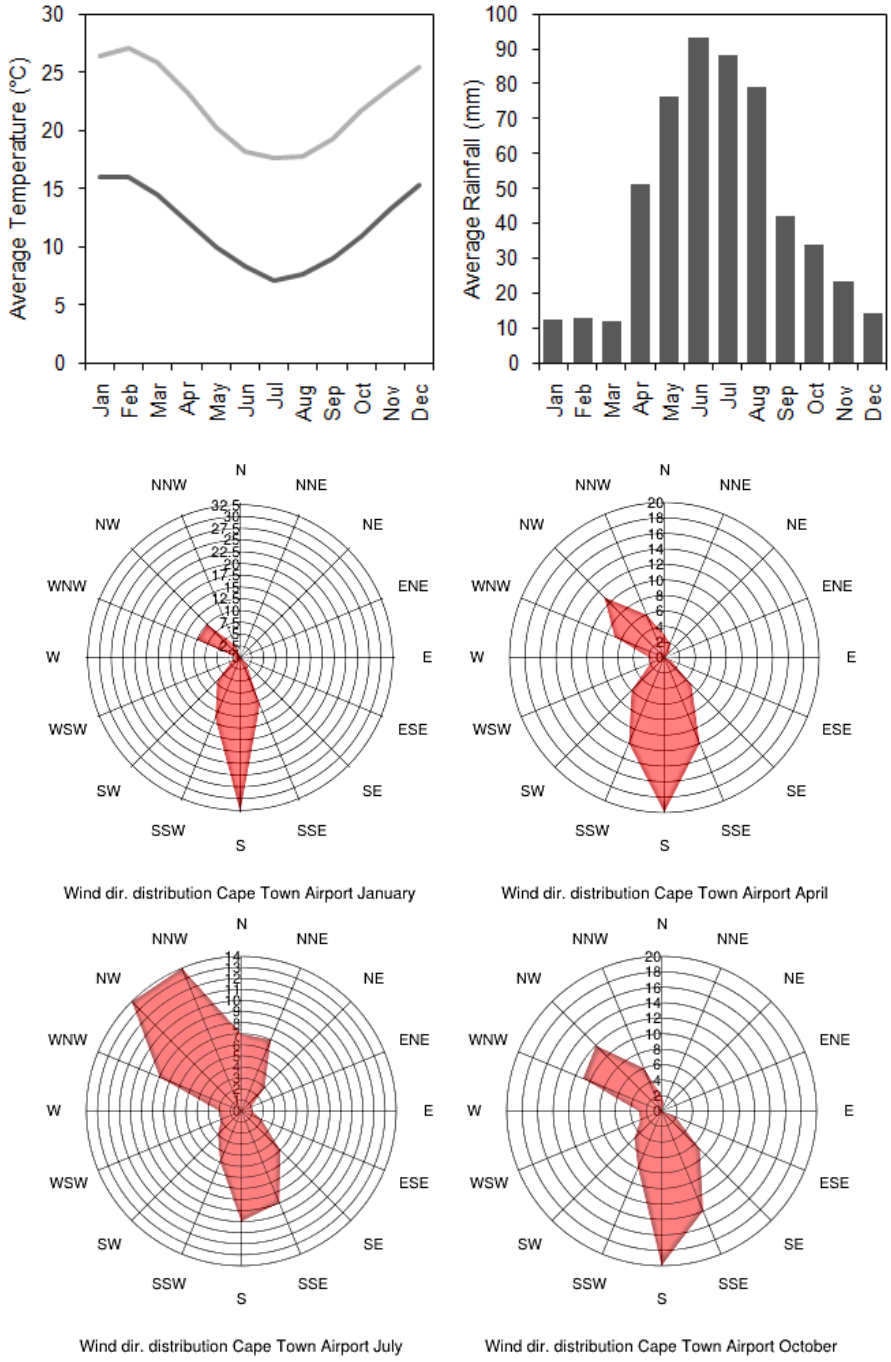

Figure 7.2: Temperature minimum and maximum and rainfall averages per month including wind strength and direction for selected months of the year at the Cape Town International Airport weather station (Data source: http://cip.csag.uct.ac.za; http://www.windfinder.com)

7.1.2. Hydrology

Freshwater sources into Princessvlei include precipitation, river runoff and the Cape Flats aquifer. The aquifer has an estimated storage capacity of approximately 53Mm^3/a, with mean annual precipitation contributing 30% to recharge (Parsons and Harding, 2002). Most of the vleis overlie the aquifer where groundwater is just a few centimetres below the surface, but during the drier summer months the water table can drop to several meters below the surface (see subsection 4.1.2, Fig. 4.7) (Harris et al., 1999; Neumann et al., 2011). Groundwater flow in this region of the Cape Flats is in a southerly direction (Bickerton, 1982; Parsons and Harding, 2002). In general, groundwater is fresh and nutrient poor but can be in excess of 750mS/m (Harris et al., 1999; Parsons and Harding, 2002; Brown and Magoba, 2009). During the summer months, where rainfall and river inflow is limited, groundwater can be the sole source of freshwater and combat evaporative losses at many of the water bodies (Parsons and Harding, 2002). Parsons and Harding (2002) showed that water levels in Zeekoevlei dropped by about 3mm/d during summer, although the evaporative index indicated an expected loss of 7mm/d; the 4mm/d difference was attributed to the buffering effect of groundwater flow.

Rivers arising from the surrounding mountain ranges feed into some of the vleis (Harrison, 1962), although most of these rivers and streams are ephemeral and are directly dependent on winter rainfall and surface runoff (Fig. 7.3) (Bickerton, 1982; Harris et al., 1999). The canalisation of the Big and Little Lotus Rivers, which flow into Zeekoevlei occurred in the 1950s as a preventative measure against flooding. During the winter months water flowing from the rivers into Zeekoevlei, can cause water level fluctuations in the order of 0.8m (Bickerton, 1982). Canals have also been built to drain residential areas as is the case with the Southfield Canal, which drains into Princessvlei (Bickerton, 1982; Harding, 1992). The high degree of canalisation and the degraded nature of the natural riparian vegetation along the rivers and wetlands have led to increased sediment loads reaching the vleis; this has resulted in periodic dredging to combat flooding (Bickerton, 1982).

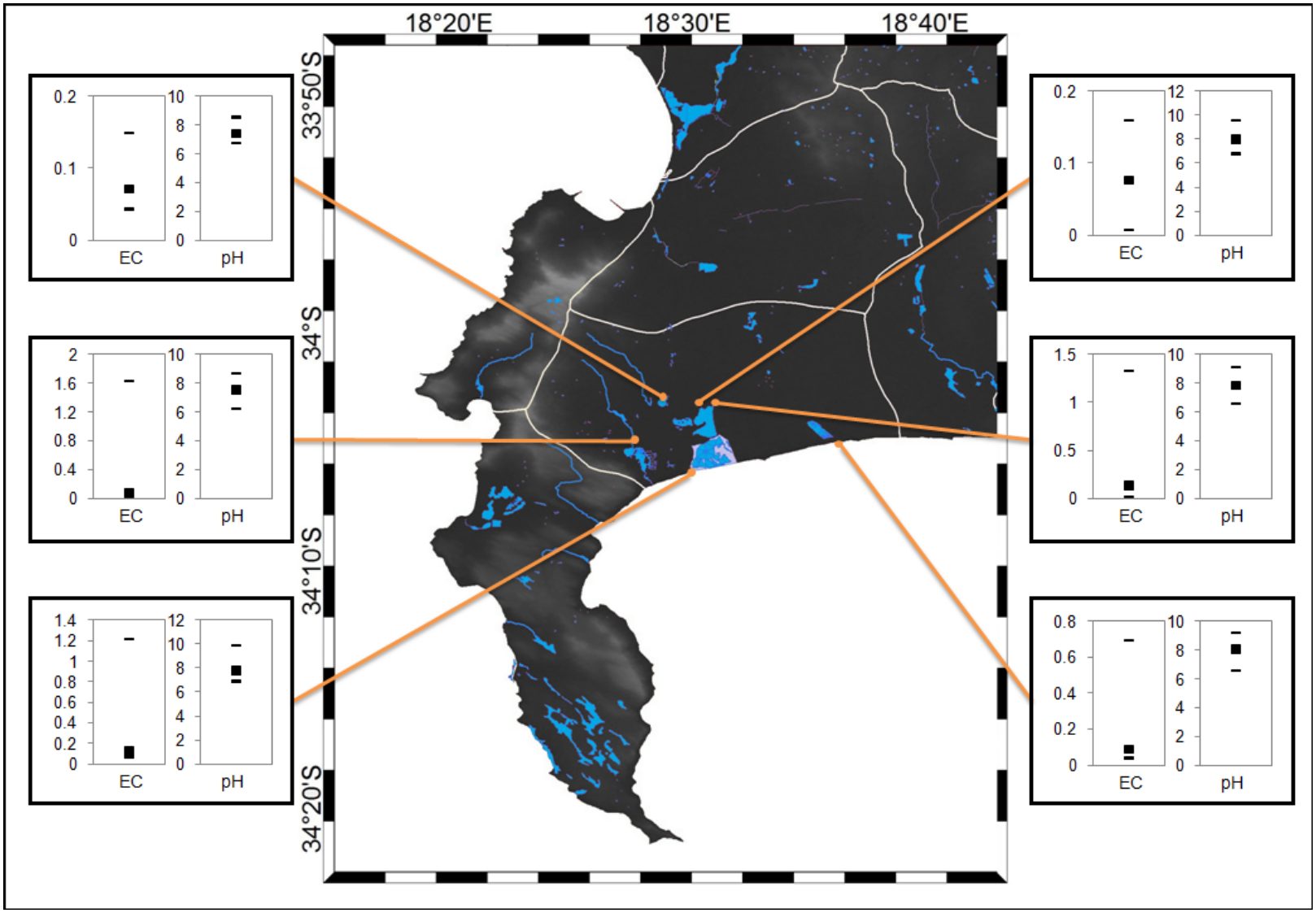

Figure 7.3: The lakes and rivers within the catchments (white lines) of the Cape Flats Region, indicating the variability in electrical conductivity (in thousands mS) and pH of selected sites monitored by the Department of Water Affairs (data source: see Appendix One)

Harrison (1962, pp 214) defines a vlei as a "marshy or swampy depression with or without open water". The main vleis on the Cape Flats are Zandvlei, Rondevlei, Princessvlei and Zeekoevlei (Fig. 4.7, 7.3 and 7.4) (Harding, 1992); with the latter three lying two kilometres apart on a NW – SE axis and connected either naturally or through canals. Harrison (1962) classifies lakes in the Western Cape as either having a high total alkalinity with pH consistently above 8.0, or acidic humic waters with pH below 6.0. The vleis on the Cape Flats coastal plain fall within the former category. The vleis are all relatively shallow with well-mixed water columns due to strong prevailing winds (Harding, 1997). All water bodies have been extensively impacted by human activities. The ecology of Princessvlei and Zeekoevlei is discussed in full below.

The largest lake on the Cape Flats is Zeekoevlei, which at its widest is ~2.5km with a surface area of 260ha (Harrison, 1962; Bickerton, 1982). Zeekoevlei is a relatively shallow, alkaline lake with a well-established submerged and emergent macrophyte community, including *Stuckenia pectinata*[4] and *Typha capensis* (Harrison, 1962; Das et al., 2008a). The vast expanse of submerged macrophytes has a commanding role in water clarity and pH. During periods of high macrophytic biomass water clarity increases, as does pH; Harrison (1962) also noted that pH showed diurnal fluctuations possibly related to photosynthetic activity. Mass mortality of macrophytes, in particular *Phragmites* stands, gave rise to a vast microalgae community in the 1950s which resulted in a dramatic increase in turbidity (Bickerton, 1982; Harrison, 1962). Algal blooms occur during winter months where surface runoff increases nutrient loads into the system (Das et al., 2008a). The basal lake sediments are generally fine muds and clays, which are also exposed along the shoreline however, occasional sand beaches and recent limestone exposures do occur (Harrison, 1962). Originally connected to the sea via a lagoon exiting from its southeastern corner, the natural outlet closed permanently in the 1940s, this led to flooding of the surrounding residential area particular during the development of Grassy Park in 1940s (Bickerton, 1982). A canal was built to negate the effects of periodic flooding and to re-establish the connection to the sea (Bickerton, 1982). The interconnecting area, which runs through the dunes in the south, is occupied by Cape Flats Sewage Works maturation ponds (Bickerton, 1982). The output of which is controlled by a weir on the canal (Harrison, 1962); however treated effluent seeps into Zeekoevlei from the sewage works resulting in increases in nutrient loads and algal blooms (Bickerton, 1982; Das et al., 2008b). Zeekoevlei is also connected to Rondevlei, a small lake to the west, which is in turn connected to

[4] Common synonym *Potamogeton pectinatus* (see Kaplan 2008. A taxonomic revision of *Stuckenia* (Potamogetonaceae) in Asia, with notes on the diversity and variation of the genus on a worldwide scale. *Folia Geobot*. 43:159‑234)

Princessvlei via a feeder canal under Prince George Drive (Harrison, 1962; Bickerton, 1982). Hence, the Zeekoe catchment encompasses 8334 hectares and consists of four drainage elements; namely Rondevlei and the overflow from Princessvlei, Zeekoevlei and the Big and Little Lotus Rivers, sewage effluent from the Cape Flats Sewage Works (CFSW) and seepage from the Cape Flats aquifer (Bickerton, 1982).

Figure 7.4: Contrasting environments of the Rondevlei Nature Reserve (L) and Princessvlei (R) (Courtesy of S. Clausnitzer 2010)

Princessvlei lies two kilometres to the northwest of Zeekoevlei in a shallow inter-dunal depression, covering a surface area of approximately 35ha and draining a catchment area of 800ha (Harrison, 1962; Neumann et al., 2011). Historically, Princessvlei was linked to Little Princessvlei, which lies ca. 0.5km to the west and ultimately to the Diep River catchment although Little Princessvlei is no longer in the same surface water catchment (Brown and Magoba, 2009). Princessvlei is a permanent, alkaline, freshwater coastal lake with a maximum water depth of 2.4m at an elevation of approximately 6m AMSL (Harding, 1992). Water levels fluctuate around a mean height of 6.43m AMSL to an overall magnitude of 0.78m between the wet and dry season (Harding, 1992). During low water levels sandy beaches are exposed along the shoreline, an artefact of the lake's origins (Harrison, 1962). Currently, inflow into Princessvlei is limited to engineered feeder canals and urban runoff (Harding, 1992; Hart, 1995; Brown and Magoba, 2009). The canal receives stormwater from the surrounding residential area, as well as sewage effluent (Harrison, 1962; Bickerton, 1982; Hart, 1995). An additional canal at the southern end serves as a drainage outlet and connects Princessvlei to Rondevlei via a flood control weir (Harrison, 1962; Neumann et al., 2011). The lake is eutrophic in nature with a high concentration of dissolved solids, mainly alkali chlorides (Harrison, 1962). Rainfall has a commanding role in aspects of the system's functioning where nutrient concentrations decline during the summer months but are re-introduced

during the winter months (Harrison, 1962; Harding, 1992). Water clarity is variable, increasing during winter months from approximately -0.2m to -1.5m, accompanied by declines in pH (from 10 – 7), conductivity (from 80 – 30mS/m) and phytoplankton biomass as rainfall induces flushing of the system (Fig. 7.3 and 7.5) (Harrison, 1962; Harding, 1992). In contrast to Zeekoevlei, Princessvlei has limited vegetation bordering its periphery; with expanses of *Paspalum vaginatum* dominating with stands of *Typha capensis* (Harrison, 1962; Harding, 1992). Algal blooms are common in the system sustained by the continual influx of nutrient rich waters (Hart, 1995). Harrison (1962) noted a marked abundance of *Micratinium* and *Microcystis* spp with trace occurrences of blue-green algae and filamentous algae of the genera *Stigeoclonium* and *Oedogonium*. Harding (1992) also recorded diatom species from the genera *Cyclotella*, *Nitzschia*, *Navicula* and *Melosira*. Annual hydraulic flushing during winter rains and flooding events control algae populations and acts as a significant control on system dynamics (Harding, 1992; Hart, 1995).

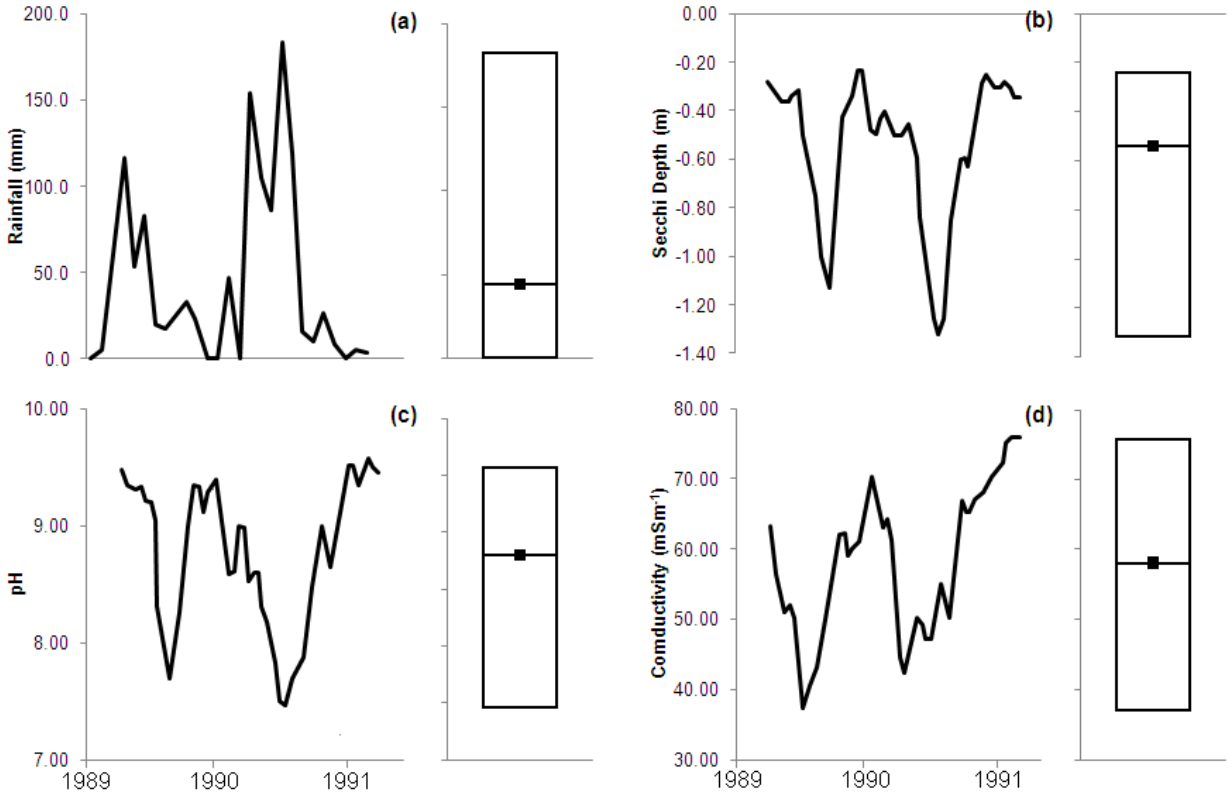

Figure 7.5: Fluctuations in water quality at Princessvlei in response to rainfall from 1989 – 1991, showing variables a) rainfall, b) water column visibility, c) pH and d) conductivity (Adapted from Harding, 1992)

7.1.3. Vegetation

According to Mucina and Rutherford (2006) the Cape Flats region consists of three bioregions, namely West Strandveld bioregion, Southwest Fynbos bioregion and West Coast Renosterveld bioregion. The region is therefore dominated by Cape Flats Sand Fynbos and Cape Flats Dune Strandveld vegetation units with isolated pockets of Cape Winelands Shale fynbos, Peninsula Granite fynbos, Southern Afrotemperate forest, Peninsula shale renosterveld, Cape lowland freshwater wetlands and Cape Seashore Vegetation (Table 7.1) (Mucina and Rutherford, 2006). Most of the aforementioned vegetation stands are threatened due to increasing pressures from urban sprawl (Anderson and O'Farrell, 2012; Holmes et al., 2012). Along the western and northern shores of Princessvlei, isolated stands of Cape Flats Dune Strandveld occur with Cape Flats Sand Fynbos occurring along the eastern shore; the latter are critically endangered and the former classified as endangered (Kotzé, 2011).

Table 7.1: Vegetation units, character and underlying soil dynamics of the Cape Flats flora (Mucina and Rutherford, 2006)

Vegetation Unit	Vegetation Character	Status	Soil
Cape Flats Sand Fynbos	Mainly proteoid and restioid elements with ericaceous and asteraceous fynbos occurring	Critically endangered	Acid, Tertiary, deep, grey regic sands usually white, often Lamotte form
Cape Flats Dune Strandveld	Tall, evergreen, hard-leaved shrubland with grasses and annual herbs	Endangered	Tertiary to Recent calcareous sand of marine origin with outcrops of Sandveld Group limestone
Cape Winelands Shale fynbos	Dense shrubland dominated by proteoid and closed-scrub fynbos	Endangered	Acidic, moist clay-loamy apedal and Glenrosa and Mispah forms derived from Malmesbury Shales
Peninsula Granite fynbos	Diverse type dominated by asteraceous and proteoid fynbos	Endangered	Deep loamy, sandy soils derived from Cape Peninsula Pluton of the Cape Granite Suite
Peninsula shale renosterveld	Tall, open shrubland and grassland, typically with renosterbos	Critically endangered	Clay soils derived from shale of the Tygerberg formation, Malmesbury Group
Southern Afrotemperate Forest	Tall, multilayered forest with well-developed understorey	Least threatened	Shallow to sandy humic derived from TMG sandstone and shales of the Cape Supergroup
Cape Seashore vegetation	Grassy, herbaceous - dwarf-shrubby vegetation	Least threatened	Young, coastal sand derived from Strandveld formation
Cape Lowland Freshwater Wetlands	*Phragmites australis* and *Thypha capensis* with flooded restiolands, sedgelands etc.		Fine sandy, silty and clayey soils over young Quaternary sediments

7.1.4. Land-use

As mentioned previously, the Cape Flats region has been significantly impacted by human activities, be it through the introduction of exotic vegetation to stabilise sand movement or clearance of indigenous vegetation for urban or agricultural pursuits (Anderson and O'Farrell, 2012). Exotic vegetation has invaded nearly 50% of the fynbos biome, outcompeting the natural vegetation and affecting groundwater levels and stream flow (Richardson and van Wilgen, 2004). Programmes have been implemented, such as Working for Water, an initiative of the Department of Water Affairs and Forestry, which aims to control the spread of or removal of alien species (Van Wilgen et al., 1998; Richardson and van Wilgen, 2004; Anderson and O'Farrell, 2012). Most of the area surrounding the vleis on the Cape Flats has either been converted for agricultural purposes as, is the case to the east of Zeekoevlei, or for either formal or informal residential housing, as well as for industrial purposes (Fig. 4.7) (Bickerton, 1982). Most of the vleis are recreational areas for water-based activities, with the exception of Rondevlei which was proclaimed a nature reserve and bird sanctuary in 1952 (Bickerton, 1982). The effects of these activities are varied and complex. The canalisation of many rivers, the hardening of formerly permeable surfaces and dense stands of alien vegetation have led to evolution of upper catchment dynamics and increased surface runoff at the expense of infiltration (Bickerton, 1982; Neumann et al., 2011). Recent interest in the land surrounding Princessvlei has been expressed for development pursuits by Insight Property Developers and has created tension in the surrounding communities due to the historical and cultural importance of the site (Kotzé, 2011). The company hopes to convert the eastern side of the wetland into a mall complex; however petitions have temporarily suspended ground-break (Kotzé, 2011). Although drastic modifications of the landscape only occurred post-European settlement, the region has experienced other human-based activities for at least the last 2000 years either as a base for stock herding or through the occupation of hunter-gatherers in many of the coastal caves in the surrounding mountain ranges (Marean, 1985; Neumann et al., 2011).

7.2. RESULTS: PRINCESSVLEI

PV11.3 core consists principally of fine sand with consistent occurrences throughout of medium sand. The base and top of the analysed core has a minor component of coarse sand. Finer particles, such as clays and silts, coincide with high organic content from the base of the core until 130cm (Fig. 7.6). Other than these principal organic units, other sediment of organic nature occurs discontinuously throughout. A fibrous rootmat occurs at the top of the core. The topmost sedimentary unit was excluded from analysis due to post core-retrieval disturbance. The species composition of the core reflects periods of high diversity and richness alternating with periods of low diversity and decreases in species richness (Fig. 7.6).

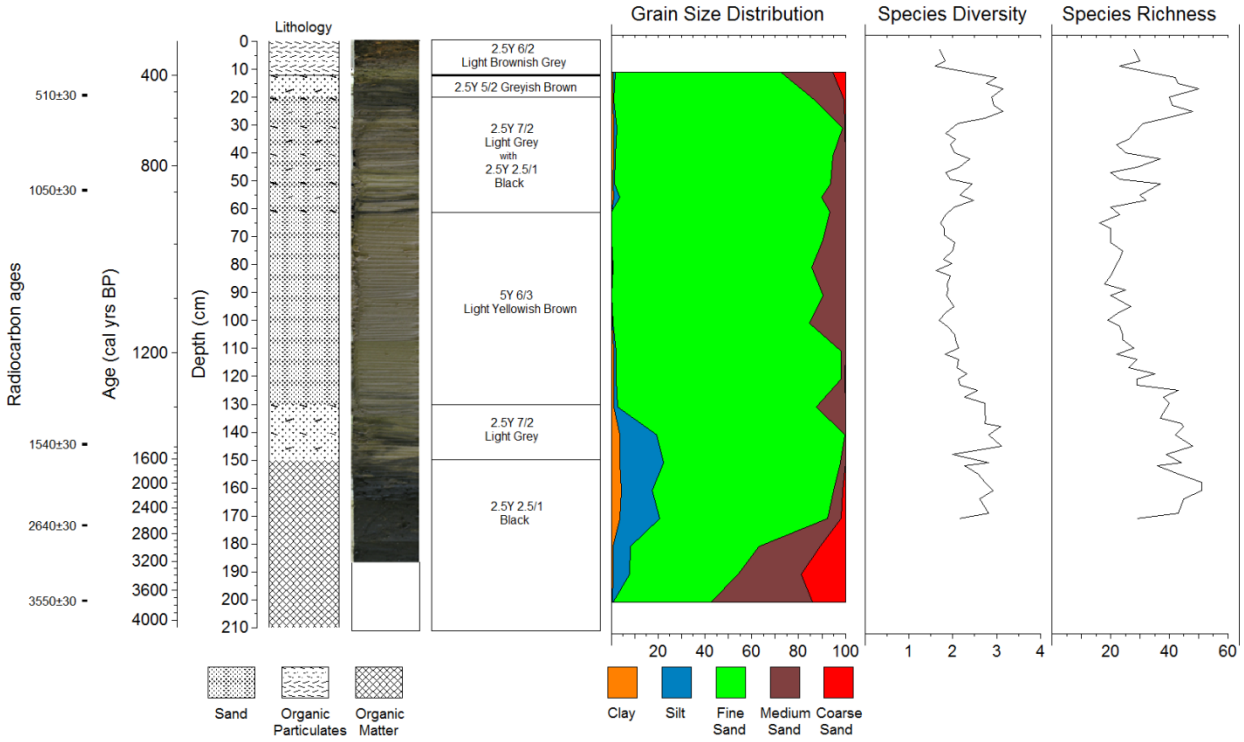

Figure 7.6: Princessvlei (PV11.3) core description based on Troels-Smith notation, munsell colour notation, particle size distribution, organic content, diatom species diversity and richness against depth (cm)

7.2.1. Chronology:

Five samples were submitted for radiocarbon analysis. In Table 7.2, the extremes of the lower (yrmin) and upper (yrmax) calibrated range are reported when more than one range is produced.

Table 7.2: The radiocarbon ages of the Princessvlei PV11.3 core calibrated to the SHCal13 curve indicating the upper and lower calibration range in units, BP with their median probability and corresponding depths

Sample label	Depth (cm)	C14 age	Cal BP	Error	yrmin	yrmax	probability
PV2011-3E	19.5	510		30	505	554	90.6
					610	621	4.2
PV2011-3F	53.5	1050		30	924	1004	84.2
					1031	1052	10.7
PV2011-3D	144.5	1540		30	1360	1361	0.5
					1366	1519	94.3
PV2011-3C	173.5	2640		30	2729	2791	93
					2829	2839	1.9
PV2011-3A	200.5	3550		30	3722	3799	27.4
					3813	3923	67
					3952	3956	0.6
Rootmat	7.5		300		As per Neumann et al. 2011		
Rootmat	0		200		As per Neumann et al. 2011		

The sedimentary sequence of the PV11.3 core corresponds well with the core examined in the study conducted by Neumann et al. (2011). Hence, a cross comparison was made to determine the age of the root mat, which occurs near the surface of the core. The timing of this depositional unit is based on chronological markers outlined by Neumann et al. (2011). The introduction of exotic species into the Cape is well documented and forms the basis for the estimated age-model developed by Neumann et al. (2011) for the root-mat. Although, the root mat in the Neumann et al. (2011) core was ~40cm long, it is believed that some compaction of the PV11.3 root-mat occurred during the coring exercise. The base of the unit is estimated to be around 320 years old; this would imply that the rate of accumulation of the most recent phase of deposition is ~0.07 $cm.yr^{-1}$ (Fig. 7.7). It is also possible to consider that the root-mat represents a continual phase of recent deposition. However, given that pollen analysis has not been conducted for the PV11.3 core, the chronology applied to the root-mat cannot be independently verified in this way.

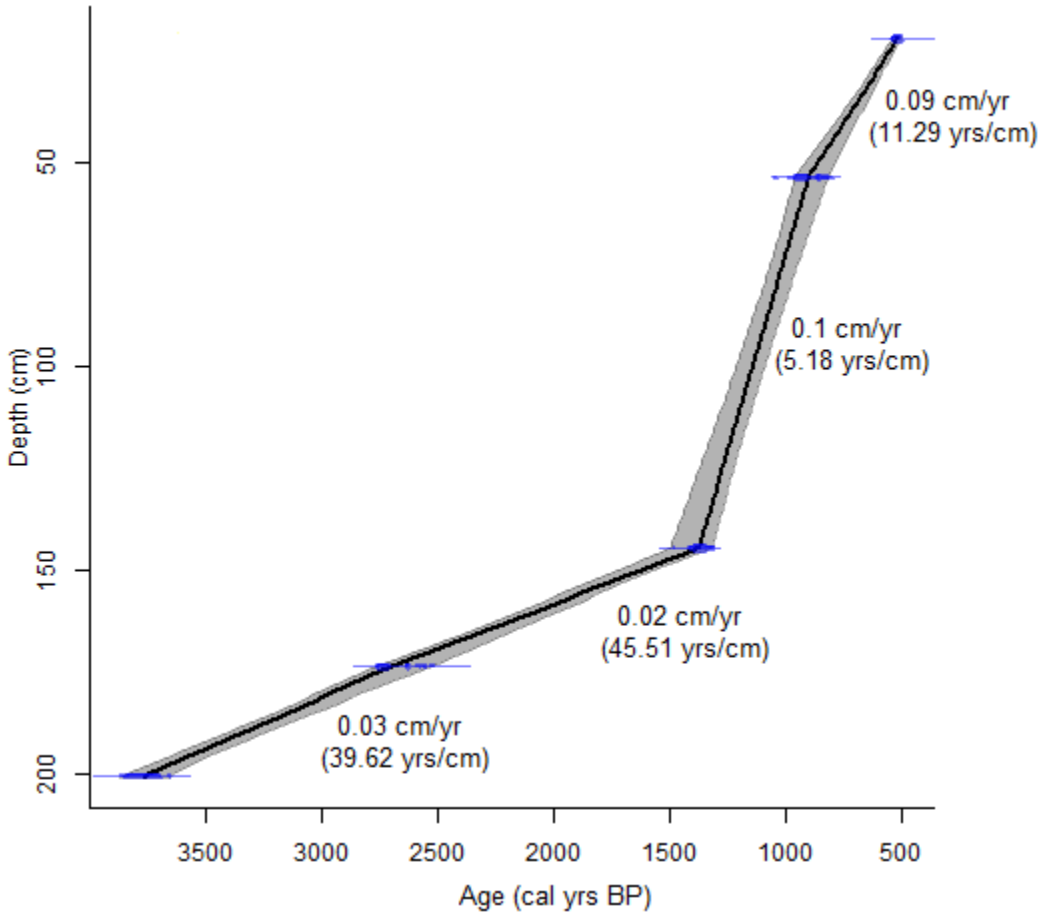

Figure 7.7: Age-depth model for the Princessvlei PV11.3 core calibrated to the SHCal13 curve indicating the upper and lower calibration range in units, BP with their median probability and corresponding depths

Slow sedimentation and possibly high salinities led to the dissolution of diatom frustules between 4000 and 2600 cal yrs BP. Despite the lack of preservation during this period and a short lived hiatus spanning c. 100 years at 10cm, the site contained a diatom rich record from ~2600 to 200 cal yrs BP. The assemblage can be divided into four zones, namely PV11.3a, PV11.3b, PV11.3c and PV11.3d based on constrained cluster analysis (CONISS) in the TILIA program (Fig. 7.8) (Grimm, 1987). A description of each zone with associated prominent diatom species occurrence is given below.

7.2.2. Assemblage Zonation

A complete list of each species autecological preference based on salinity, pH, life form and nutrients can be found in Appendix Two (Table 11.8, Pg. 291).

2600 – 1300 cal yrs BP [Zone PV11.3a]

Zone PV11.3a lasted c. 1300 years and is characterised by great diversity and species richness throughout the zone. It is subdivided into zone PV11.3a.1 (c. 2600 – 1400 cal years BP) and zone PV11.3a.2 (c. 1400 – 1300 cal yrs BP). At the start of zone PV11.3a.1 a strong eutrophic signal is observed coupled with a substantially brackish and alkaliphilic diatom community. *Melosira nummuloides* constitutes nearly 50% of the diatom assemblage (Fig. 7.8). *M. nummuloides* has the competitive edge over most other taxa as it is able to thrive during episodes of severe water deoxygenation, cooler water temperatures, low light penetration or fluctuations in salinity (McLean et al., 1981; Rendall and Wilkinson, 1986). As the stage develops, the dominance of *M. nummuloides* gives way to *A. ambigua* at ~1700 cal yrs BP. A diverse array of *Aulacoseira* species occurs, including *Aulacoseira ambigua, Aulacoseira granulata* and *Aulocoseira muzzanensis*, but diminishes in the following subdivision; these species are common in eutrophic lakes and rivers (Taylor et al., 2007). A constant representation of *Achnanthes subaffinis* and *Planothidium biporomum* prevails throughout both subdivisions, with *A. subaffinis* slightly increasing its distribution during the second sub-stage; both species are benthic and oligotrophic in nature. A strong indication of marine influence is observed during zone PV11.3a.2. The once dominant brackish, planktonic element is steadily replaced by fresh-brackish/benthic taxa. From the beginning of zone PV11.3a.2 and into zone PV11.3b a rise in the oligotrophic to mesotrophic group at the expense of the eutrophic to polytrophic group is witnessed.

~1300 – (920) – 610 cal yrs BP [Zone PV11.3b]

A strong oligotrophic to mesotrophic signal defines zone PV11.3b (Fig. 7.8). As in zone PV11.3a, zone PV11.3b is subdivided into two stages PV11.3b.1 and PV11.3b.2. Zone PV11.3b.1 extends from 1300 to ~920 cal yrs BP, with the follow up sub-stage PV11.3b.2 terminating at 620 cal yrs BP. The previously diverse community rapidly declines with a prevalent large benthic community. *Achnanthes subaffinis, Planothidium biporomum* and *Planothidium rostratum* constitute on average 72% of the assemblage but peak at 84% at ~1140 cal yrs BP. The marine influence, indicated primarily by the occurrence of *Cocconeis distans*, persists throughout PV11.3b.1, escalating toward the termination of the sub-stage to encompass ~16% of the total assemblage. *Planothidium* species are alkaliphilic and epilithic in nature, associated with fresh-brackish waters. *Achnanthes swazi,* an endemic to South Africa, *Achnanthidium*

minutissimum and *Pseudostaurosira brevistriata* consistently occurs during both sub-stages indicating clean, well oxygenated water. *Achnanthes oblongella* is also well represented during PV11.3b.1, a benthic species favouring electrolyte poor, fresh-brackish waters. Following low frequencies during PV11.3b.1, *M. nummuloides* re-emerges during PV11.3b.2.

~620 – 450 cal yrs BP [Zone PV11.3d]

Variations in the community structure from c. 620 – 445 cal yrs BP define zone PV11.3c. Most of the dominant benthic species of zone PV11.3b, such as *A. subaffinis, P. biporomum* and *P. rostratum*, disappear to be replaced by planktonic and epiphytic taxon. *Discotella stelligera* and *Cocconeis placentula*, having only occurred in trace amounts previously are the predominant taxa during this zone. *D. stelligera* is associated with the summer plankton of a deep, stable, stratified water column (Wolin and Stone, 2010), whereas *C. placentula* dominates on submerged macrophytes in the tidal flats and marsh fringe area (Horton et al., 2006). *Craspedostauros capensis*, a marine species recorded in modern samples from St. Helena Bay, also makes an appearance during this period (Giffen, 1973) (Fig. 7.8).

~320 – 240 cal yrs BP [Zone PV11.3d]

After a c. 125 year hiatus, the record continues at c. 320 cal yrs BP concluding at 240 cal yrs BP. The mechanisms behind the hiatus are poorly understood however, Neumann et al. (2011) reports the presence of a water layer in their core, which they suggest represents a suspension in sedimentation between ~1000-350 cal yrs BP (105-75 cm). The discrepancy between the lengths of the hiatus may be a reflection of the position of the core sites relative to each other. The assemblage is very strongly dominated by *Eolimna subminuscula*, an epilithic, polytrophic to hypertrophic diatom (Stancheva et al., 2007). A rather rapid shift at the end of the zone to the fresh, planktonic diatom *Aulacoseira ambigua* is reminiscent of earlier zones. Although diversity and species richness of the assemblage is similar to values observed during zone PV11.3b, taxa that prefer eutrophic to polytrophic systems and fresh-brackish to fresh waters thrive. Occurrences of brackish and marine species are not truly observed during this stage contrary to all previous zones.

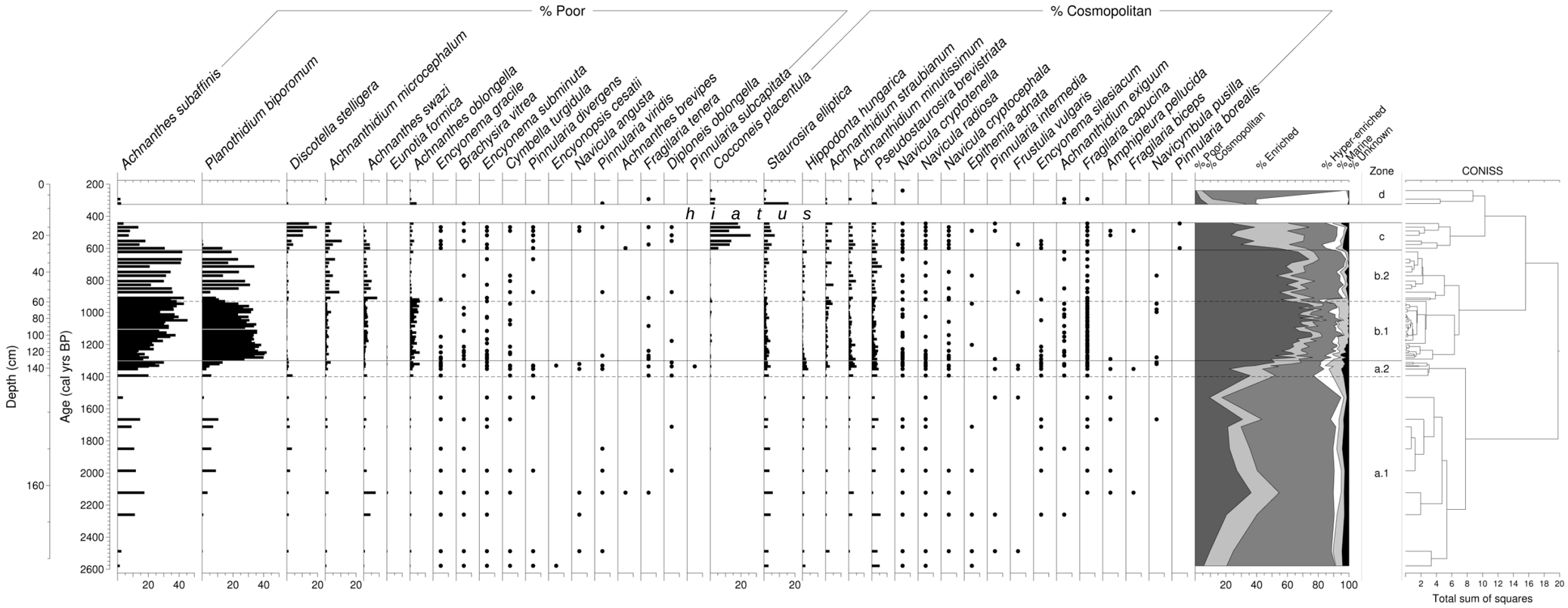

Figure 7.8.1: Princessvlei core stratigraphy and percentage diatom representation against depth (cm) and age (cal yrs BP), diatom species are grouped based on nutrient preferences. Four zones were identified based on CONISS

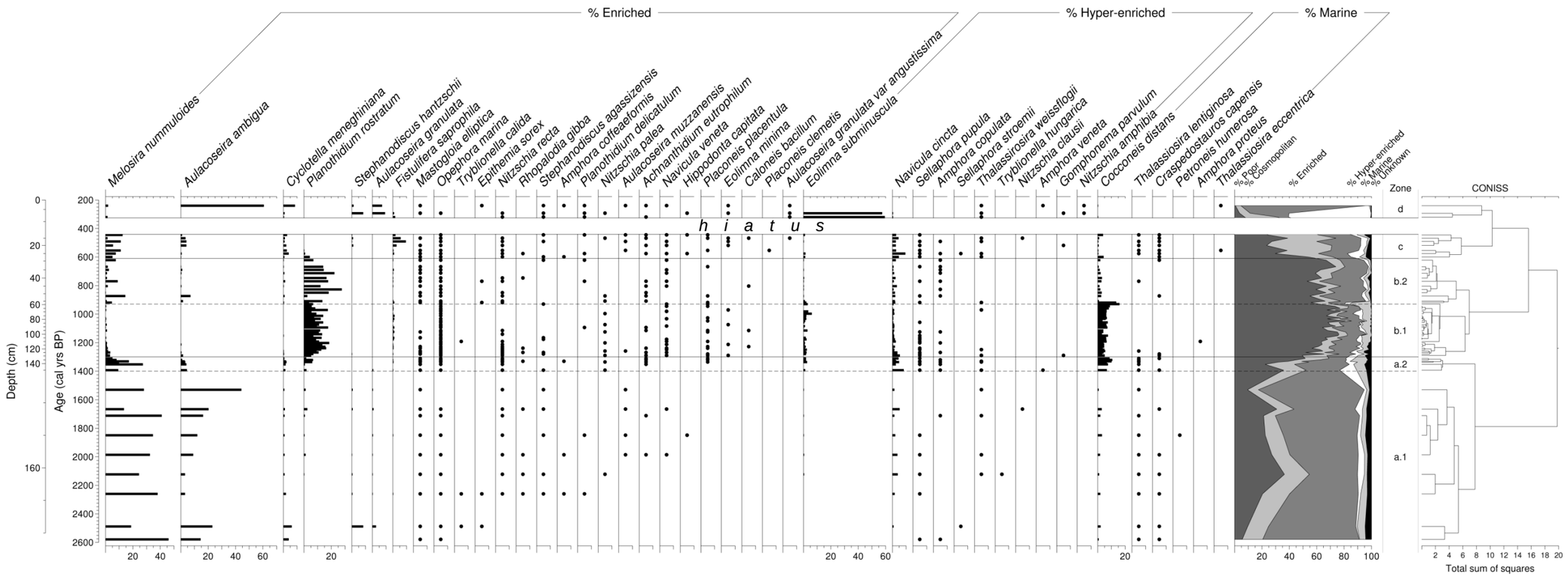

Figure 7.8.2: Princessvlei core stratigraphy and percentage diatom representation against depth (cm) and age (cal yrs BP), diatom species are grouped based on nutrient preferences. Four zones were identified based on CONISS

7.2.3. Statistical Analysis

The similarity between samples throughout the core is shown in Fig. 7.9. The analysis reveals that zone PV11.3a.1 from 148 – 171cm (~1400 – 2600 cal yrs BP) shares some similarity with the diatom community assemblage present at 3cm (240 cal yrs BP); this probably relates to the high occurrences of *Aulacoseira ambigua* and a strong eutrophic state during these periods. In general, zone PV11.3a.2 (1400 – 1300 cal yrs BP, 145 – 133cm) appears to be a reflection of a radical transition from one state to another and correlates to samples at the termination or initiation of subsequent zones; e.g. 59.5 – 57 and 51 cm (930 – 920 and 875 cal yrs BP), which is the transition from zone PV11.3b.1 to zone PV11.3b.2, and again at 27.5cm (600 cal yrs BP), which is the transition from zone PV11.3b.2 to zone PV11.3c. This trend is not evident in the transition from zone PV11.3c to zone PV11.3d and may be a reflection of the effect of the hiatus, which occurs between these zones. The full extent of zone PV11.3b (1300 – 620 cal yrs BP), with the exception of the samples discussed previously, can be interpreted as reflecting a shift from a eutrophic state to an oligo/mesotrophic state. The conversion between the two states is not smooth, and fluctuations in nutrient availability are observed. Zone PV11.3c (25 – 13cm; 580 – 445 cal yrs BP) shows major dissimilarity to all other zones. This zone has a diverse and rich assemblage, but the dominant taxa occur only in trace amounts during other periods, if at all. It may be that this stage was influenced by environmental variables that differ greatly to the other zones. The final stage, zone PV11.3d, shows great similarity between 320 and 290 cal yrs BP but differs considerably from the other zones. This may be a reflection of the predominant occurrence of *Eolimna subminuscula*, signifying hyper to polytrophic conditions.

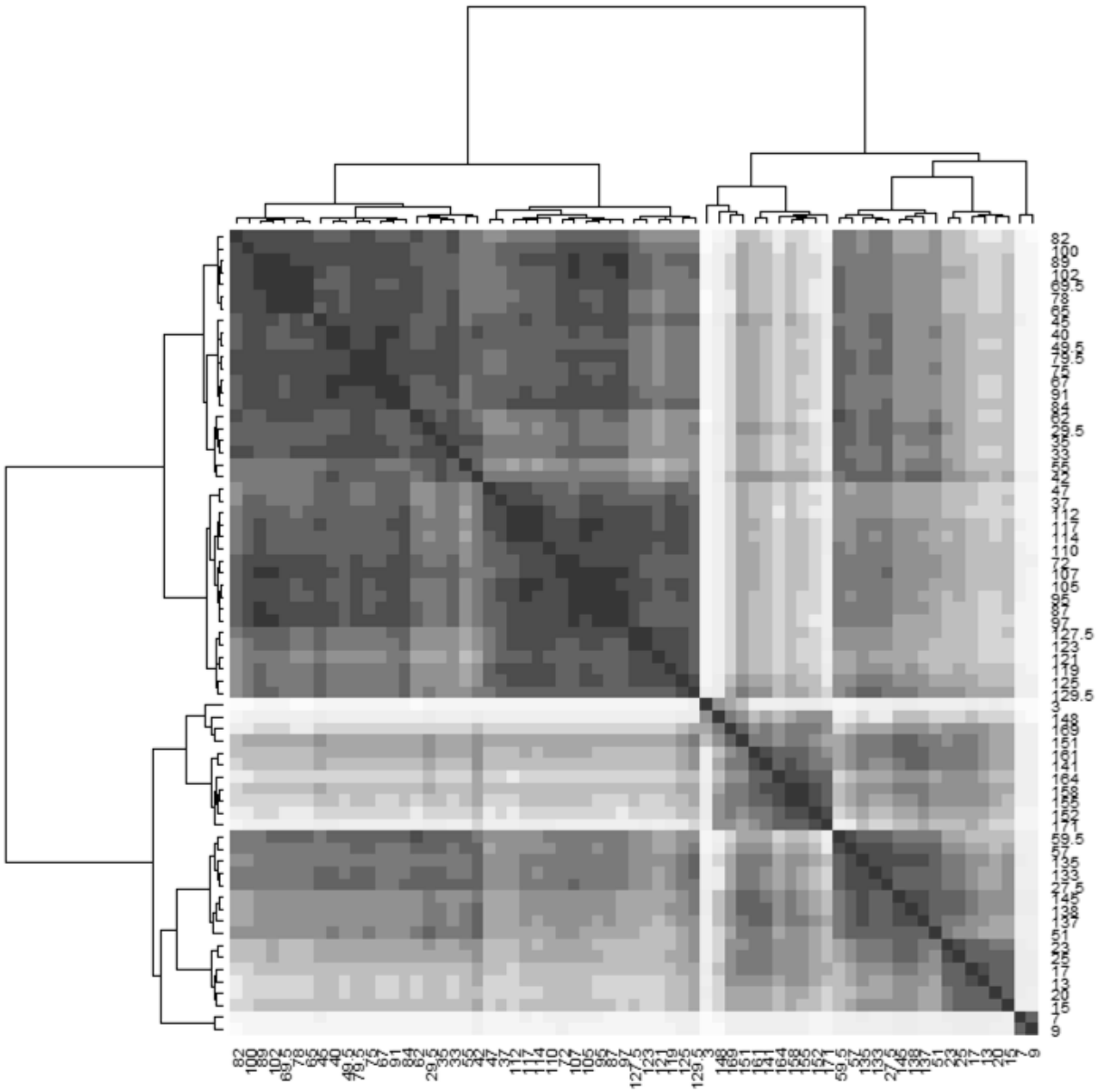

Figure 7.9: Heat map showing similarity/dissimilarity between samples of the Princessvlei PV11.3 site

Initially, the full PV11.3 diatom species record was used in a PCA to resolve the key influential species in determining environmental trends. From the original 94 species, 24 species where identified and incorporated into a follow up PCA (Fig. 7.10).

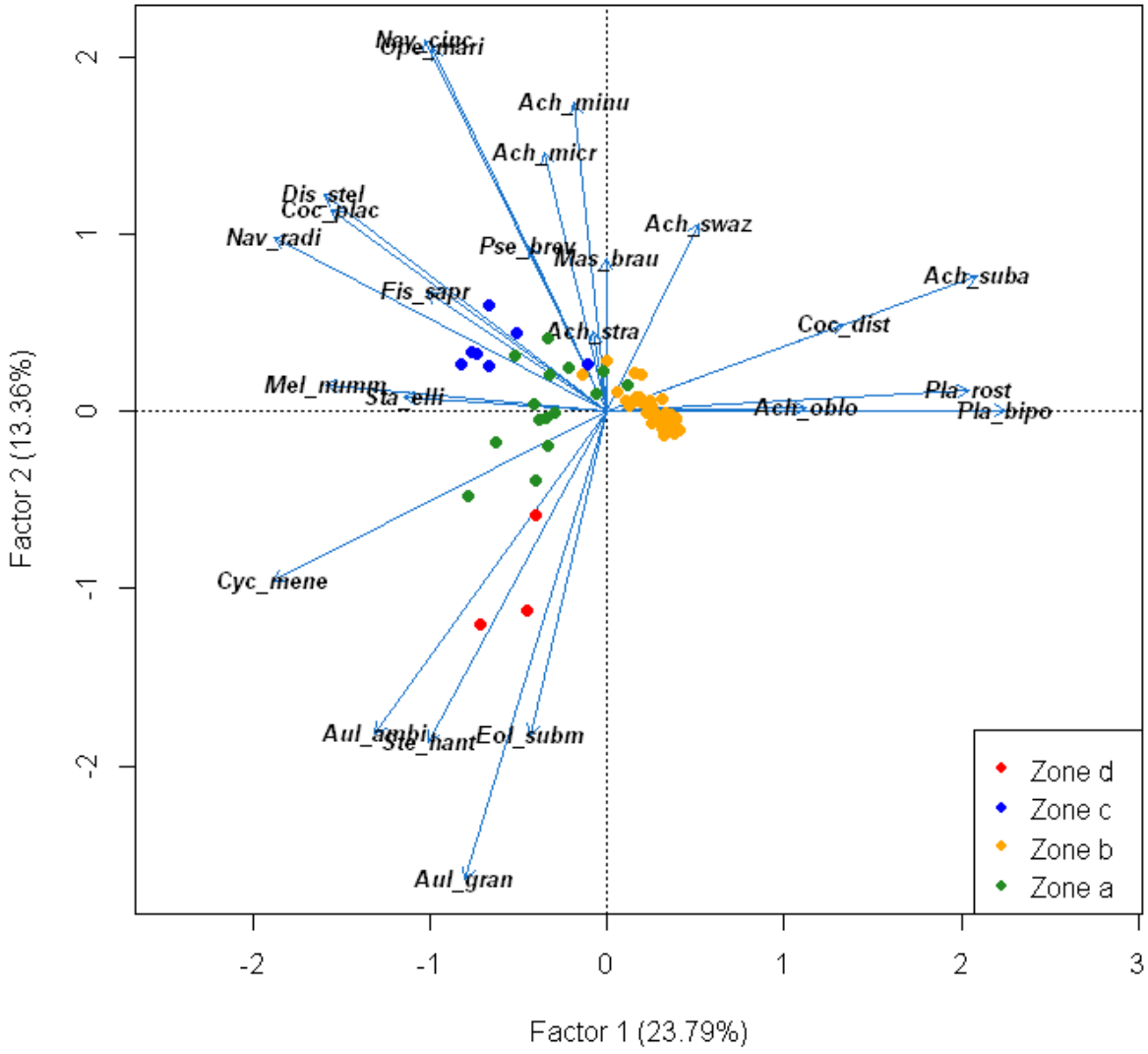

Figure 7.10: Principal component analysis representing the relationship between species and samples at the Princessvlei PV11.3 site, between factor one and factor two. Sample points are colour coded based on zones identified by CONISS in TILIA. Achnanthidium microcephalum = *Ach_micr,* Achnanthidium minutissimum = *Ach_minu,* Achnanthes oblongella = *Ach_oblo,* Achnanthidium straubianum = *Ach_stra,* Achnanthes subaffinis = *Ach_suba,* Achnanthes swazi = *Ach_swaz,* Aulacoseira ambigua = *Aul_ambi,* Aulacoseira granulata = *Aul_gran,* Cocconeis distans = *Coc_dist,* Cocconeis placentula = *Coc_plac,* Cyclotella meneghiniana = *Cyc_mene,* Discotella stelligera = *Dis_stel,* Eolimna subminuscula = *Eol_subm,* Fistulifera saprophila = *Fis_sapr,* Mastogloia braunii = *Mas_brau,* Melosira nummuloides = *Mel_numm,* Navicula cincta = *Nav_cinc,* Navicula radiosa = *Nav_radi,* Opephora marina = *Ope_mari,* Planothidium biporomum = *Pla_bipo,* Planothidium rostratum = *Pla_rost,* Pseudostaurosira brevistriata = *Pse_brev,* Staurosira elliptica = *Sta_elli,* Stephanodiscus hantzschii = *Ste_hant*

Three principal component axes were determined to be significant, contributing 48.57% to the overall explained variance. Component one, which explains 23.79% of the variance, has large positive loadings on *Planothidium biporomum, Achnanthes subaffinis* and *Planothidium rostratum*. All three species have a preference for clean, non-polluted waters (Fig. 7.10 and 7.11) (Kelly et al., 2005). Conversely, negative loadings are concentrated on *Cyclotella meneghiniana, Navicula radiosa, Discotella stelligera, Melosira nummuloides* and *Cocconeis placentula*, all of which show a preference toward nutrient enriched environments (Fig. 7.11). Therefore, it can be stated that the primary control on the diatom community and the first component of the PCA is related to be the availability of nutrients and the state of organic loading into the system (Fig. 7.12). The distribution of samples identified the contrast of zone PV11.3b to the rest of the assemblage. The environmental conditions are optimal for the dominance of the species *Planothidium biporomum* and *Planothidium rostratum* during zone PV11.3b, with *Achnanthes subaffinis*, *Cocconeis distans*, *Achnanthes oblongella* and *Achnanthes swazi* also playing a role in the distribution of the samples in Zone PV11.3b (Fig. 7.8).

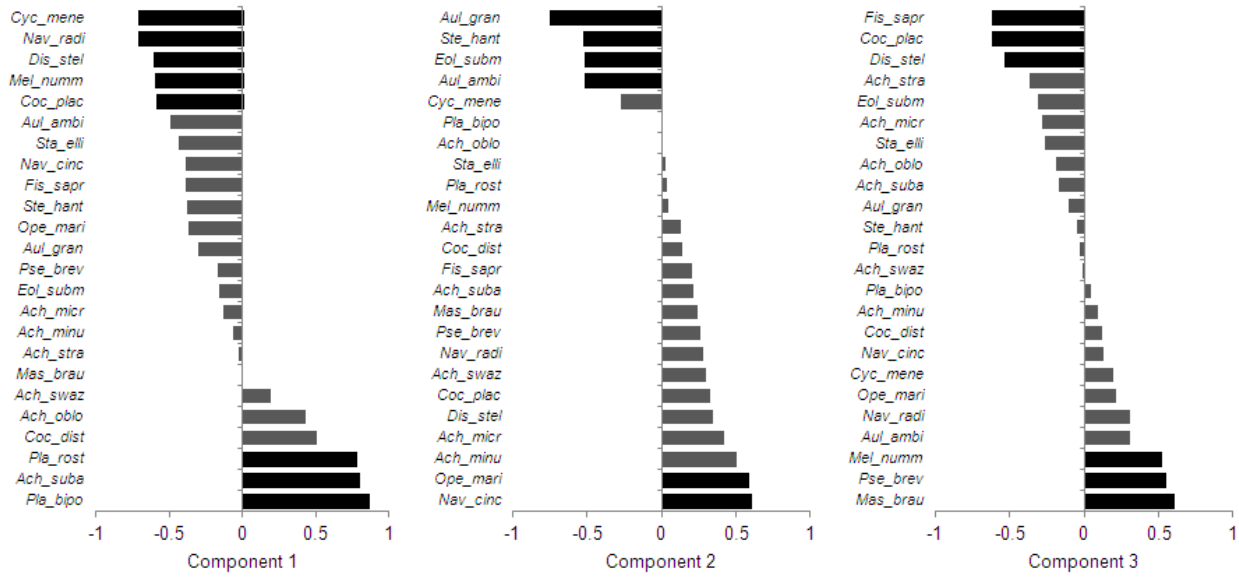

Figure 7.11: Factor loadings for principal components one, two and three for the Princessvlei PV11.3 core.

The second component represents 13.36% of the explained variance. Notable positive loadings are centred on *Navicula cincta* and *Opephora marina*, where both species appear on tidal flats or along the marsh fringe (Fig. 7.11) (Horton et al., 2006). Negative loadings, which define the second component, centre on *Aulacoseira granulata, Stephanodiscus hantzschii, Eolimna subminuscula* and *Aulacoseira ambigua* (Fig. 7.11). *A. granulata, A. ambigua* and *S. hantzschii* are all planktonic species, whereas *E. subminuscula* is a benthic species inhabiting the littoral zone (Gell et al., 2002). The second component

appears to define the alternating states between shallow water and deep water environments, which could be closely linked to component one but appears not to be a driving mechanisms defining zone PV11.3b (Fig. 7.12).

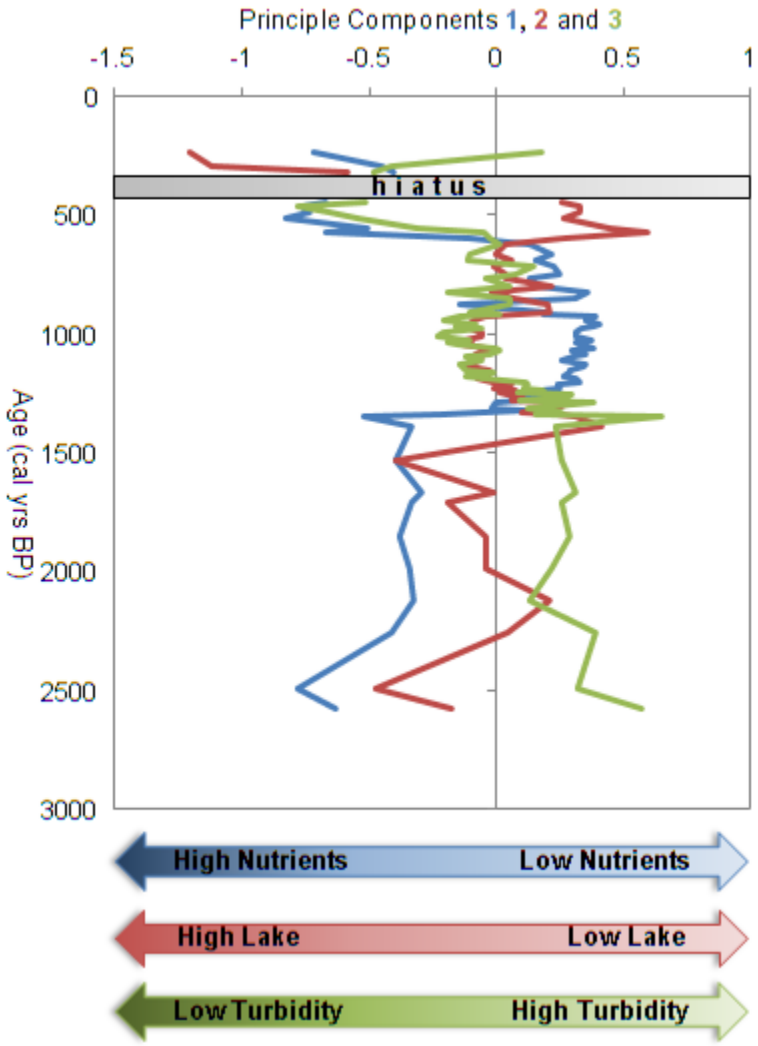

Figure 7.12: Factor 1, Factor 2 and Factor 3 values derived from PCA for Princessvlei

The third component identified by the PCA explains 11.42% of the variance. The third component is defined on the positive loadings by the prevalence of *Mastogloia braunii, Pseudostaurosira brevistriata* and *M. nummuloides* (Fig. 7.11). The negative loadings are primarily composed of *Fistulifera saprophila, Cocconeis placentula* and *Discotella stelligera*. *M. braunii* and *M. nummuloides* have been reported to thrive in light limited environments, whereas *D. stelligera* is dependent on high light penetration of the water column (Fig. 7.11) (Croome and Tyler, 1973; Underwood, 2002). The implication would be that the

third component is related to the turbidity of the system and the light penetration within the water column (Fig. 12).

As previously stated, all three components are at times co-dependent as shown in Fig. 7.12. Initially, high lake levels appear to be associated with high nutrient inputs and increased turbidity, but as lake levels decline, a period of low nutrients and clearer water transparency prevail. A further decline in lake levels occurs at the same time as a shift to low turbidity/solar outputs but a rise in nutrient loading between 30 cm (650 cal yrs BP) and 13 cm (445 cal yrs BP) (Fig. 7.12). The scenario outlined above is of course a highly generalised depiction, as the system may be far more complicated and may be governed by several environmental parameters beyond those already mentioned.

7.2.4. Indice de Polluosensibilité

The index calculation included more than 90% of the species for all measured levels of the PV11.3 core the output is displayed below. As the examined record corresponds to a period of no human influence, pollution in this instance relates to organic loading coupled with possible shifts in salinity. The index suggests an initial fluctuating period of moderate nutrient loading before an extended period of low lake inputs occurred between ~1300 and 600 cal yrs BP, punctuated by a short-lived episode of increased loading at 880 cal yrs BP (Fig. 7.13). From 600 until ~480 cal yrs BP, the system becomes progressively more nutrient rich. Post hiatus the lake's diatom assemblage indicates moderate to high nutrient influx, which may reflect the added influence of European settlement. The index also closely mimics the first component of the PCA (Fig. 7.12 and 7.13), suggesting a link between organic loading and nutrient availability.

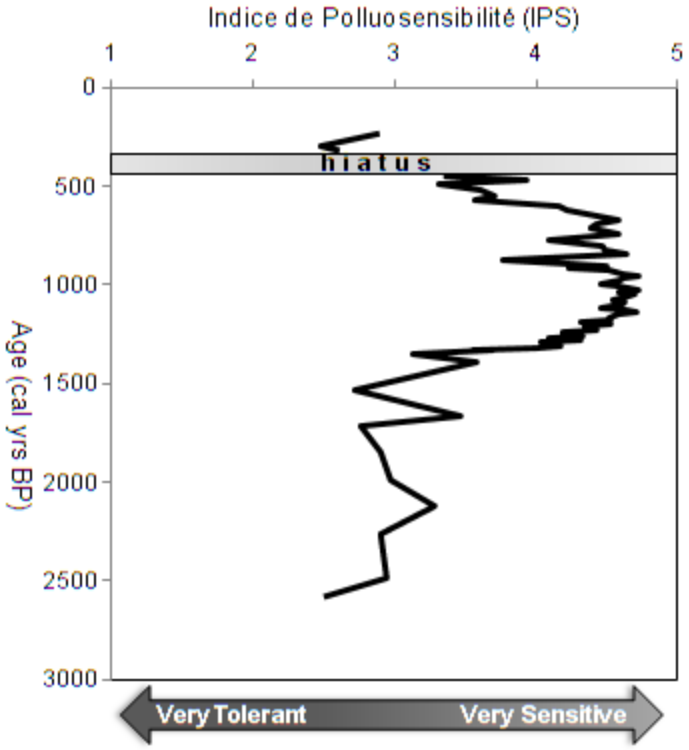

Figure 7.13: Pollution Sensitivity Index for the Princessvlei PV11.3 core

7.2.5. Isotopic Analysis

The isotopic composition of the water within the lake is related to changes in the inputs, e.g. precipitation, groundwater and outputs, e.g. evaporation (Leng and Swann, 2010). Generally, open-basin lakes reflect the isotopic composition of the precipitation received in the region (Leng and Barker, 2006). Insufficient material was rendered from samples PV3.4 – PV3.6, leading to a 300 year gap in the isotope record. Upon visual inspection to confirm that a high concentration of diatom frustules remained in the >60µm portion, the two fractions, namely >60µm and 10 – 60µm fraction were combined with the exception of PV3.10. The >60µm of sample PV3.10 proved to be rich in sponge spicules hence remained separate from the 10 – 60µm PV3.10 fraction. Where possible, repeat measurements of each sample were made as outlined in Table 7.3

Table 7.3: Summary of oxygen isotope data samples taken from the Princessvlei (PV11.3) core

Sample	Depth (cm)	Age (cal yrs BP)	Size Fraction (µm)	Repetitions	Raw	Error	Calibrated (‰ SMOW)
Modern Water Sample (May, 2012)						0.04	1.15
PV3.1	19-20	510	10-60	5	36.76	0.13	38.76
PV3.2	39-40	747	10-60	1	35.12		36.66
PV3.3	53-54	900	10-60	5	34.41	0.65	37.43
PV3.3	53-54	900	10-60	3	35.17	0.00	36.59
PV3.4	72-73			Insufficient material rendered			
PV3.5	85-86			Insufficient material rendered			
PV3.6	99-100			Insufficient material rendered			
PV3.7	114-115	1213	10-60	1	34.90		36.46
PV3.8	134-135	1321	10-60	5	34.63	0.25	36.66
PV3.9	154-155	1800	10-60	5	34.71	0.24	36.28
PV3.10	170-171	2530	10-60	5	35.61	0.44	37.31
PV3.10	170-171	2530	10-60	7	35.47	0.38	36.89
PV3.10	170-171	2530	> 60	1	36.65		38.64

The modern water sample shows some isotopic enrichment (pers. comms C. Harris). Samples remain within the minimum of 36.00‰ and the maximum of 39.00‰ along the length of the core. Initially showing some enriched values at ~2500 cal yrs BP, $\delta^{18}O_{diatom}$ remains between 36.28‰ and 36.66‰ from 1800 to 1200 cal yrs BP, before a break in the record renders no data for 300 years. Samples representative of 900 cal yrs BP show the greatest variability. The first PV3.3 sample run may have experienced instrumental drift; this led to running the laboratory standards again to assist in instrument

calibration, thereafter a second run of the PV3.3 sample was performed. A continued enrichment occurs from 900 cal yrs BP to the greatest enrichment at the final sample at ~500 cal yrs BP (Fig. 7.14). A 12 year study indicates a $\delta^{18}O$ range of -8.1 to +3.5‰ for modern rainwater in the Cape region (Harris et al., 2010). Samples taken from across the Cape Peninsula also suggest that enrichment in $\delta^{18}O$ occurs during intense rain events linked to cold fronts (Harris et al., 2010). Hence, enrichments in the record maybe related in part to increasing occurrences of cold fronts.

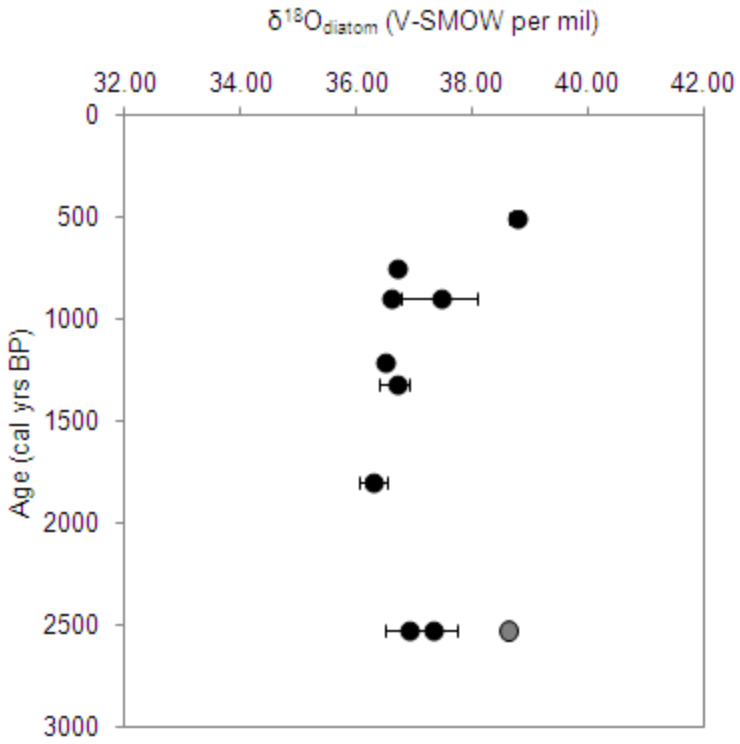

Figure 7.14: The $\delta^{18}O_{diatom}$ profile (black circles) against age for the Princessvlei (PV11.3) core, while the outlier, >60µm sample from PV3.10, is shown as a grey circle

7.2.6. Conclusions

Slow deposition during the early stages of the record provides a low temporal resolution for the environmental reconstruction between 2600 and 1400 cal yrs BP, during which time a eutrophic system dominates with a high organic loading. However, after a short-lived transitional period a shift to oligotrophic conditions lasts until at least ~600 cal yrs BP where benthic habitats prevail over open water, planktonic conditions. A possible modification in moisture availability enhances nutrient delivery into the system. After a brief hiatus, the record resumes at 320 cal yrs BP with a strong polytrophic signal coinciding with European settlement of the region. The primary controlling mechanism defining

the character of the system appears to be the delivery of nutrients, which in turn may be a proxy of moisture availability and ultimately precipitation as well as catchment dynamics.

7.3. A 2600 YEAR PALAEOENVIRONMENTAL RECORD FROM PRINCESSVLEI, CAPE FLATS:

Princessvlei and its surrounding wetlands primarily receive freshwater through precipitation during the winter months; this delivers nutrient rich surface runoff and river inputs to the lake systems of the Cape Flats. The principal source of precipitation across the region lies in frontal depressions embedded in the westerlies. On the other hand, the system is maintained during the dry months by nutrient-poor, groundwater. The palaeoenvironment of the Cape Flats region is discussed below with some inferences regarding the mechanisms driving the dynamics of the system.

7.3.1. 2600 – 1300 cal yrs BP

For two centuries between 2600 and 2400 cal yrs BP Princessvlei experienced high turbidity within a deep lake basin, which is exposed to high winds evidenced by the high concentrations of the *Aulacoseira* community. The high wind turbulence may be generated by an increase in intensity of the prevailing seasonal winds and the possible dominance of the westerly wind system, which carries rain-bearing systems to the coast. These frontal depressions provide the region with precipitation and in due course affect the water accumulation and water depth in the numerous lakes across the Cape Flats (Fig. 17.15 and 7.16). Slightly enriched $\delta^{18}O$ values at ~2500 cal yrs BP may be a result of a cooler climate, which promoted the expansion of the rain-bearing winter westerlies. Cooler water temperatures are also evident through the trace occurrence of *Sellaphora stroemii* at ~2500 cal yrs BP, which thrives in cold electrolyte rich environments (Taylor et al., 2007). Generally, conditions remained predominantly eutrophic, implying a constant supply in nutrients probably originating from surface runoff and precipitation which may bring in coarser grained material from the catchment.

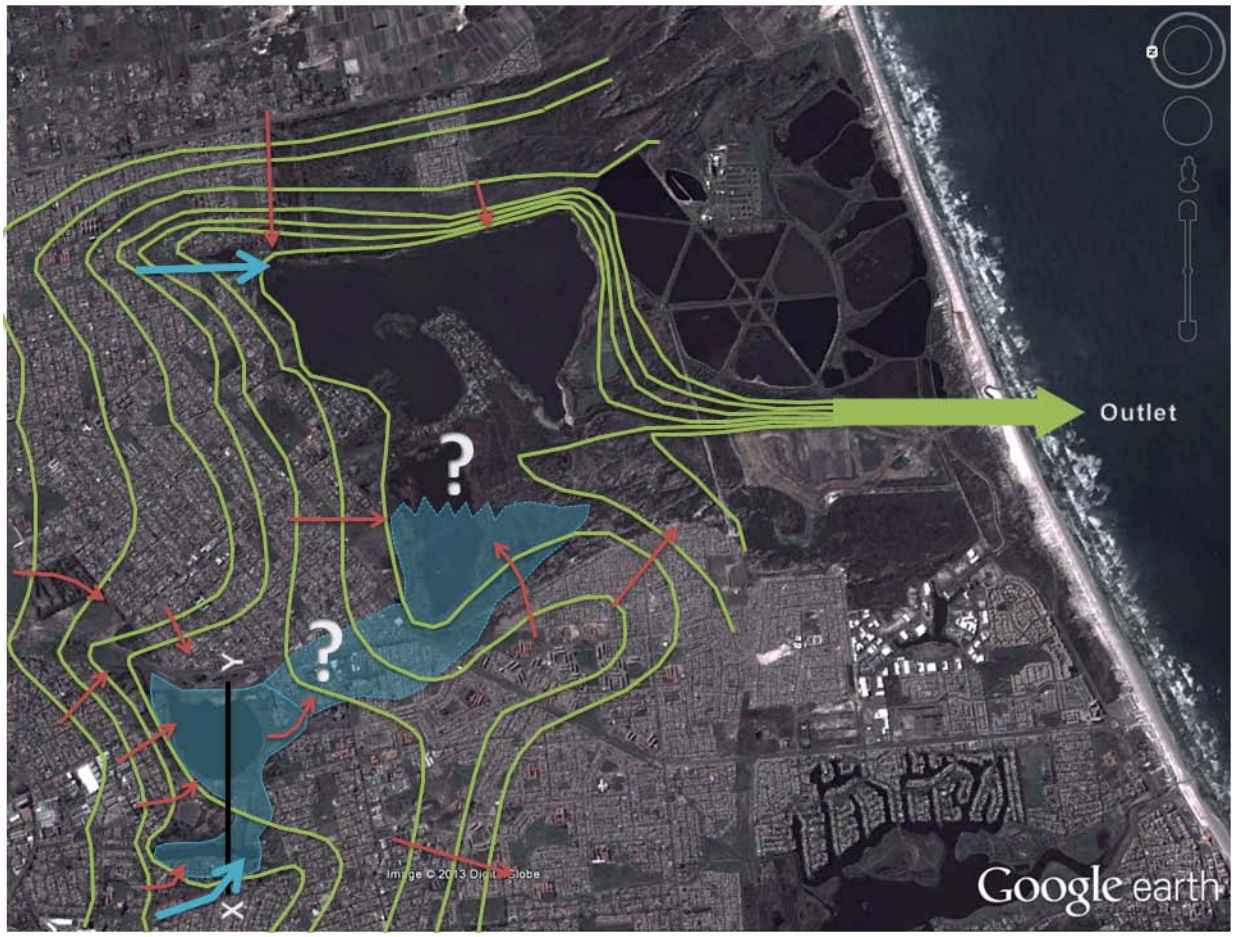

Figure 7.15: Schematic representation of wetter intervals prior to mass sand movement at Princessvlei, indicating freshwater inputs (blue arrows), generalised modern groundwater level contours (green lines) and groundwater flow directions (red arrows) (groundwater lines modified from Parsons and Harding, 2002)

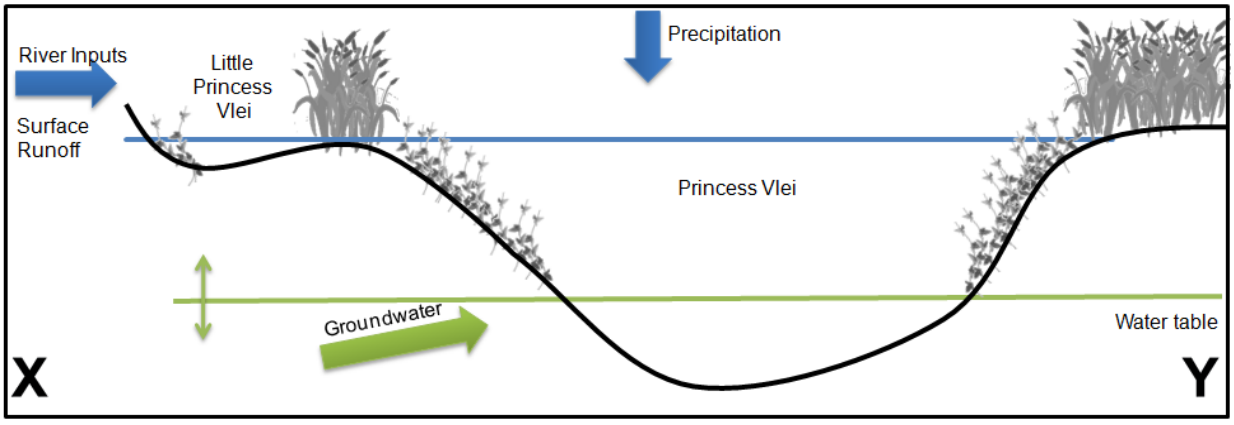

Figure 7.16: Proposed schematic representation of wetter intervals prior to mass sand movement at Princessvlei, indicating freshwater inputs (blue arrows), groundwater level (green lines) along the X – Y cross-section as depicted in Figure 7.15

A prominent macrophyte community most likely limited sediment distribution within the lake and provided the foundation of the high organic content observed during these early stages as well as stabilising the pH of the system. The submerged macrophyte community maintained itself throughout the zone, providing a habitat for *M. nummuloides* even as water levels declined and nutrients progressively diminished from c. 2400 to 2100 cal yrs BP. During this 300 year interval the mixing of the water column generated by the high wind exposure became progressively limited as wind strength and prominence decreases, as documented by the steady decline in *A. ambigua* but also through the increase in benthic and oligotrophic taxa such as *A. subaffinis* and *P. biporomum.* Oligotrophic conditions appear to dominate when nutrient-poor groundwater is the primary source of water into Princessvlei. Additionally, due to the course resolution of samples, this period may be an amalgamation of several seasonal cycles, showing the alternation between relatively wet conditions to considerably dry conditions, with the latter conditions being more prevalent than the former. The initial drier episode from 2400 – 2100 coincides with warmer conditions reported at Cango Caves and to a degree an arid phase suggested by the pollen sequence from the Neumann et al. (2011) core also from Princessvlei. The shift towards a drier climate gave rise to a predominantly benthic community, as lake levels respond to the decline in water supply and led to the development of the marsh fringe. The marsh fringe provided a habitat for several species including *Navicula cincta, Opephora marina* and *Pinnularia intermedia* suggesting a continuous expansion and contraction of the riparian vegetation throughout the zone (Horton et al., 2006; Long et al., 2010).

The first marsh expansion occurs just after a rise in the pioneer species, *Staurosira elliptica* and *Pseudostaurosira brevistriata* at 2250 cal yrs BP and remains until ~2000 cal yrs BP (Bao et al., 2007). Species from the *Fragilaria* genus are known to thrive during periods of environmental instability (Bao et al., 2007), in this case responding to the changes in water supply and may provide evidence of a shift in climatic forcings over the region. Regionally cooler and wetter conditions are reported at Cecilia Cave and Klaarfontein until 2000 cal yrs BP (Baxter, 1989; Meadows and Baxter, 2001), with a marginally wetter environment prevailing at Katbakkies Pass to the north of Princessvlei between 2400 and 1300 cal yrs BP (Meadows et al., 2010). The absence of the drier episodes at these sites may be related to the sampling resolution of the records taken by the authors, with Meadows et al. (2010, 791) noting that “sub-centennial environmental fluctuations may be obscured by the size of the subsamples”.

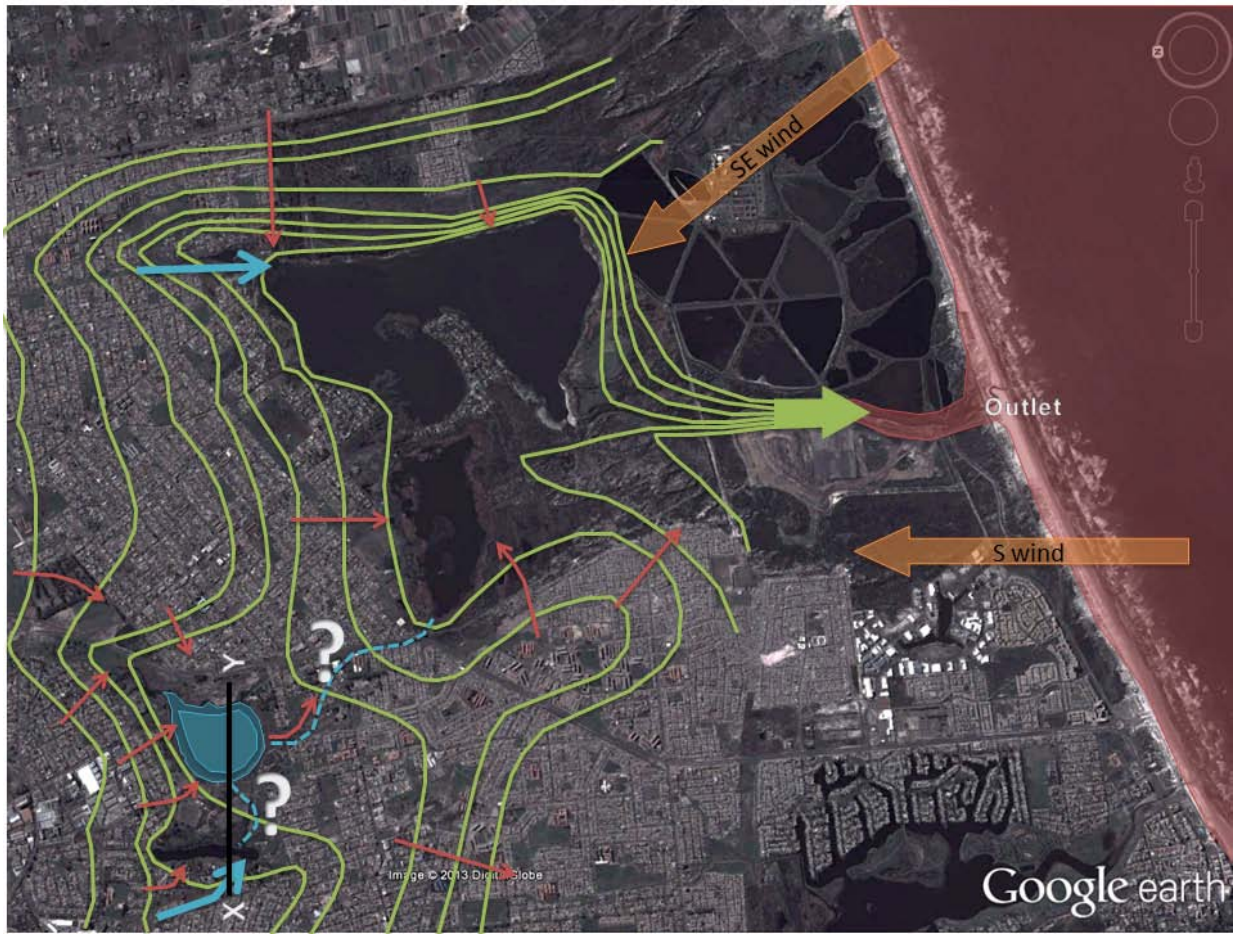

Figure 7.17: Schematic representation of drier intervals during and subsequent to mass sand movement at Princessvlei, indicating freshwater inputs (blue arrows), generalised modern groundwater level contours (green lines) and modern groundwater flow directions (red arrows) (modified from Parsons and Harding, 2002)

The expansion of the riparian vegetation was initiated by the decline in lake levels and the encroachment of emergent macrophytes along the periphery of the lake. Afterward a slight recovery in lake levels occurs from 1900 cal yrs BP and steady increases until 1530 cal yrs BP, only modestly interrupted by a minor second expansion of the marsh fringe at 1650 cal yrs BP. The second dry spell at ~1650 cal yrs BP corresponds with dune development in the False Bay area (Roberts et al., 2009). As discussed previously (see subsection 5.1.1), sand movement in the Cape Flats is a function of southerly to southeasterly winds originating through anticyclone atmospheric circulation patterns (Fig. 7.17). The combination of southeasterly winds and marsh development at Princessvlei would support the brief shift to a more arid climate before wetter conditions predominate. The oligotrophic element peaks at 1650 cal yrs BP simultaneously with the second pulse of marsh expansion, substantiating a dry episode during this time, before the greatest proportional representation of *A. ambigua* of zone PV11.3a occurs suggesting strong winds and increased nutrient loading into the lake leading to highly turbid waters. The

consistent increase in *A. ambigua* suggests a return in turbulent winds, providing nutrient enriched waters to the system. As before, the source of this water would primarily be through surface runoff, and hence the implication of increased precipitation originating from frontal depressions is the likely cause. The oligotrophic component represents the drier periods when groundwater maintains open water conditions. It appears that this wetter episode is relatively short-lived, as a notable shift in the diatom community occurs after ~1530 cal yrs BP.

The change in the diatom community after c. 1530 cal yrs BP is interpreted as a transitional phase, which ended at about 1300 cal yrs BP. Lake levels begin to fluctuate but are still sufficient to maintain the planktonic component until c. 1290 cal yrs BP with sporadic occurrences until c. 1215 cal yrs BP. The period appearred to remain relatively wet, but nutrient availability became increasingly limited, having indirect effects on the vegetation dynamics of the Princessvlei ecosystem. The marsh fringe and macrophyte community initially appears to thrive during this period, although as the nutrients that are required to sustain wetland vegetation became increasingly limited, vegetation growth is stunted and inevitably declines. The decrease in nutrients began to shape the system creating an opportunity for the oligotrophic taxa to provide the foundation of the biological community primarily through small, benthic species, such as *A. subaffinis* and *P. biporomum* (Taylor et al., 2007). Minor river influences occur, possibly through the linkage of Princessvlei to Little Princessvlei and the Diep River catchment. A natural seepage point of nutrient-poor groundwater along the northern shore of Princessvlei also provides a supplementary source of freshwater into the lake (Parsons and Harding, 2002). The combination of these source waters could be factor contributing to the dominance of the oligotrophic community.

During this transitional period, *M. nummuloides* takes advantage of the fluctuating environmental conditions before diminishing to minimal proportional representation by c. 1200 cal yrs BP, in so doing providing a point of reference where conditions became predominantly dry. The main trend observed during this period is the relative diversity in the biological community, with oligotrophic to polytrophic taxa accompanied by a decline in species that are tolerant of organic loading. Additionally, coarser material of similar character to beach sand begins to dominate the sediment matrix (pers. obs). Dune development and shifting sands may be the causal mechanism that initiated the transitional phase, followed by or driven by a shift to drier or windier conditions. The Cape Flats acts as a sand corridor between the False Bay supply zone and west coast deposition zone. South-easterly winds are required to activate sand movement along the False Bay coast and in so doing provide the marine element prevalent in the sequence (Roberts et al., 2009). The increased sediment supply promoted infilling of the

Princessvlei basin and may be a factor in the restriction of wetland vegetation; additionally, the high rate of sand deposition would have affected water depth and basin morphology.

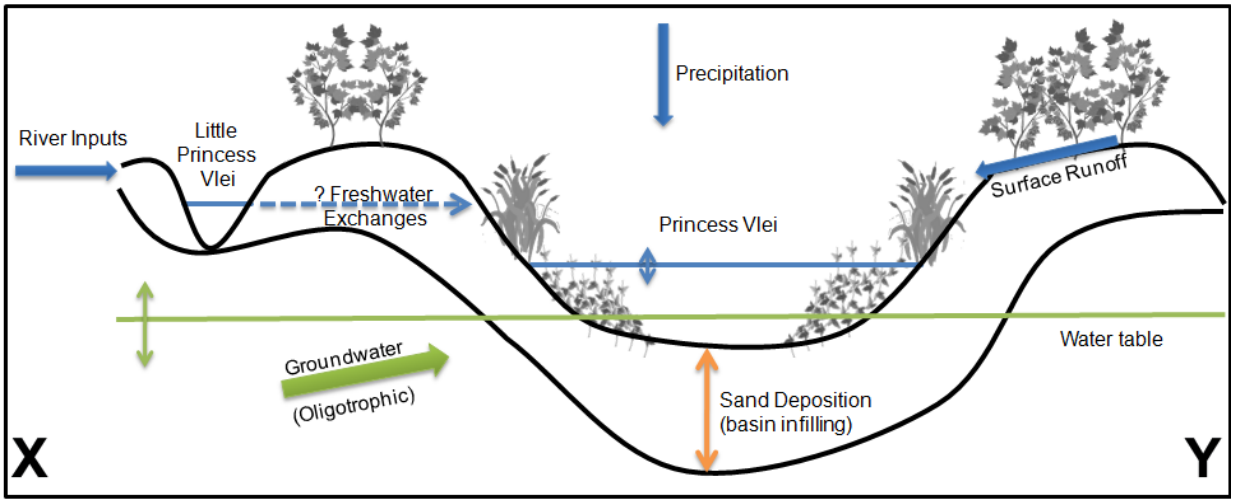

Figure 7.18: Proposed schematic representation of drier intervals during and subsequent to mass sand movement at Princessvlei, indicating freshwater inputs (blue arrows), groundwater level (green lines) along the X – Y cross-section as depicted in Figure 7.17

Aerial deposition of marine diatoms is limited in range and may be linked to wind strength and longevity. A consistent but fluctuating marine aspect is present throughout the sequence, with a prominent peak between c. 1350 and 1310 cal yrs BP; this may be the first sign of a greater influence from the South Atlantic Anticyclone (SAA) and its associated climatic phenomena, as well as one of the causes in the environmental instability. The predominance of south-easterly winds would indicate an inclination toward SAA circulation patterns with a southward displacement of the westerlies, which would minimise the penetration of precipitation-laden frontal depressions (Fig. 7.17). On the other hand, the preceding period from c. 1530 to at least c. 1200 cal yrs BP indicates sufficient precipitation to maintain open water conditions, suggesting a pattern of more prominent polar circulation patterns. Wetter conditions are also recorded in the diatom sequence from further up the west coast at Verlorenvlei, which showed greater moisture availability from c. 1340 to 1190 cal yrs BP (Stager et al., 2012). The two diatom records overlap reasonably well, with only minor discrepancies between the commencement and termination of events on the scale of a few decades, which can be attributed to variations in the age-depth models utilised. Isotopic values between c. 1800 and 1200 cal yrs BP remain relatively stable with only minor fluctuations, although samples depleted in $\delta^{18}O$ are recorded at ~1200 cal yrs BP. This conforms to a relatively warmer climate in comparison and reflects the stability represented by the diatom community composition during this period. The shift in species composition

from ~1350 cal yrs BP may have been initiated by a slow decline in freshwater but also by the changes in sediment supply.

7.3.2. Medieval Climate Anomaly (MCA)

Successive peaks in marine species between 1190 – 1150, 1095 – 1060 and 1030 – 920 cal yrs BP provide evidence of renewed intensity of south-easterly winds and ultimately a tendency toward a dominance of SAA atmospheric circulation, which initiated a period of progressive aridity. This period of increased SAA-activity corresponds with the Medieval Climate Anomaly. The decline in moisture availability reduced lake levels, which were already adjusting to the increase in sediment deposition. The tidal flats and benthic habitats became more pronounced during this period, showing enhanced expansion, which coincided with the peaks in the marine element substantiating the transformation to a drier period (Fig. 7.18). The region appears to experience more high intensity but less frequent rain events, with species indicative of flash flooding becoming more prevalent in the assemblage from c. 1200 until at least 920 cal yrs BP. These sudden events may be providing the system with nutrients upon which the eutrophic community is dependent. However, the infrequent nature of these events and the constant supply of nutrient-poor groundwater sourced through the Cape Flats Aquifer instigates a shift to an alternate state (see Scheffer et al., 1993).

Originally the lake system was eutrophic with deeper waters, but as moisture availability is reduced, the lake becomes primarily oligotrophic and shallow. Additionally, the lake basin experiences infilling due to sand deposition brought in by more dominant southly to southeasterly winds. The shallower nature of the lake promotes the turnover of the water column, which inhibits stratification and affects turbidity. This new state supports a biological community that thrives in well-aerated, standing water, with a pronounced intrusion of species adapted to more calcareous based water, probably supplied by the leaching of the surrounding sands. The noteworthy persistence of the *Fragilaria* complex throughout the record and particularly during this period substantiates the instability experienced and may be a reflection of the fluctuations in freshwater supply. The oligotrophic state persists until ca. 670 cal yrs BP, before increased instability initiates a slow reversion to a transitional state. Both the Verlorenvlei and Princessvlei records indicate a shift to a drier climate from 1200 cal yrs BP until ~950 cal yrs BP at Verlorenvlei and 920 cal yrs BP at Princessvlei, which Stager et al. (2012) attributed to a weakening in the austral westerlies. This is a plausible scenario for the PV11.3 record, as the site suggests intensification of anticyclonic flow, which may be responding to the displacement of the westerlies poleward. Alternatively, Neumann et al. (2011) maintains a relatively moist environment was prevalent

on the Cape Flats from 1900 – 1000 cal yrs BP; this setting only loosely correlates to PV11.3 record as well as with the Verlorenvlei reconstruction.

From ~920 cal yrs BP until ca. 650 cal yrs BP, periodic increases in brackish species coupled with distinct reductions in oligotrophic elements, particularly involving species that are intolerant of organic pollution, define the episode. The mechanism underlying this shift in the biological community is consistent with slightly greater moisture availability than was experienced during the previous dry period. Specifically, increases in moisture between ~915 - ~870 cal yrs BP provided a deeper water column in which planktonic species could thrive. The composition of the diatom community suggests that the depth in the water column achieved prior to the arid period was not reached during this period. Alternatively, sediment infilling during the previous phase may have created a much shallower basin mildly inhibiting a planktonic community. The interpreted increased precipitation and surface runoff provides the foundation for a more pronounced and sustained eutrophic assemblage. Although nutrients still remained generally low, the beginning of a submerged macrophyte community was initiated in response to the intermittent availability of nutrients and moisture from ~900 cal yrs BP. Oxygen isotopic data from the diatom frustules conform to a slightly cooler but still relatively warm climate between 900 and 700 cal yrs BP, which may be reflecting the increase in precipitation received from mid-latitude cyclones. This period seems to be defined by the gradual reintroduction of westerly-based phenomena, providing sporadic moisture availability across the region before a wetter climate dominates from 700 cal yrs BP onwards (Fig. 7.19 and 7.20) (Meadows and Baxter, 2001; Scott and Woodborne, 2007; Stager et al., 2012).

7.3.3. Little Ice Age (LIA)

A distinctive shift in the biological community occurs between c. 700 and 600 cal yrs BP, which coincides with the onset of the Little Ice Age. *P. brevistriata* with *S. elliptica* are species that are tolerant of the overall dynamic nature in the area since 910 cal yrs BP through their roles as a pioneer species; they may stabilise the benthic habitat for occupation by other diatom species. A transition from discontinuous to continuous stands of the submerged macrophyte community occurs at ~625 cal yrs BP, implying that the influx of nutrients into Princessvlei became more frequent and constant, probably through a more persistently wetter climate.The rise of the macrophyte community opened an additional habitat that epiphytic diatoms were able to occupy, particularly *Cocconeis placentula* (Troeger, 1978). The increase in representation of *C. placentula* and *Achnanthidium microcephalum* from c. 600 to 445 cal yrs BP attests to the continued environmental fluctuations experienced at the site; both species are able to

tolerate disturbances to their habitat in environments where water movements are at a medium to high velocity (Plenković-Moraj et al., 2008).

Figure 7.19: Schematic representation of wetter intervals subsequent to mass sand movement at Princessvlei, indicating freshwater inputs (blue arrows), generalised groundwater level contours (green lines) and groundwater flow directions (red arrows) (modified from Parsons and Harding, 2002)

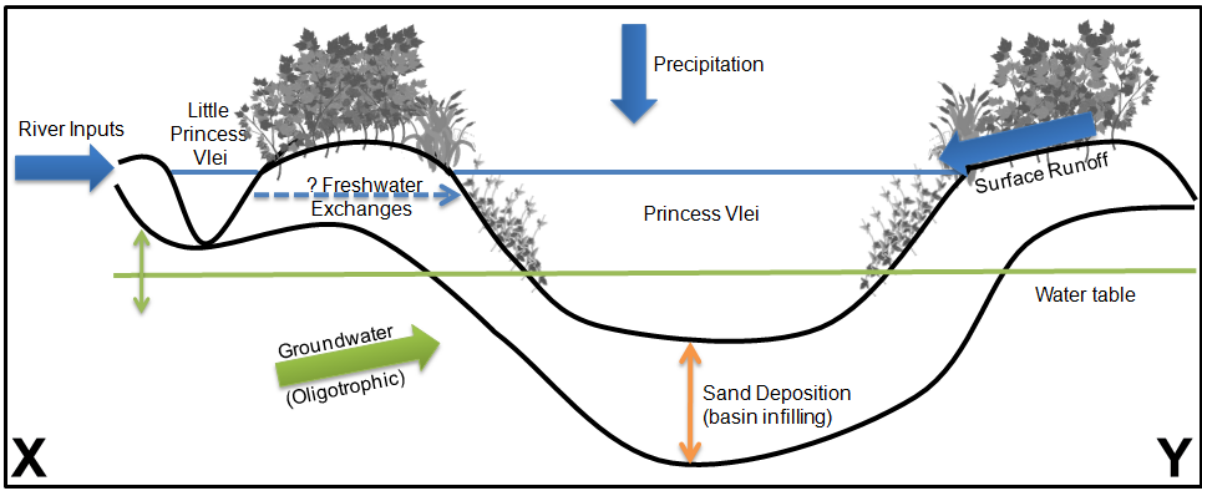

Figure 7.20: Proposed schematic representation of wetter intervals subsequent to mass sand movement at Princessvlei, indicating freshwater inputs (blue arrows), groundwater level (green lines) along the X – Y cross-section as depicted in Figure 7.19

A relative decline in summer wind disturbances led to the stabilisation and eventual stratification of the water column (Wolin, 1996; Wolin and Stoermer, 2005; Wolin and Stone, 2010). The $\delta^{18}O$ signal culminates at c. 510 cal yrs BP with the most enriched sample of the record, suggesting that with the wetter climate conditions were also far cooler than what was experienced throughout the PV11.3 record (Fig. 7.14). The biological community outlined above gives a clear indication of environmental conditions from around 600 – 445 cal yrs BP, *viz.* a generally wet, cool climate, which provided the lake with high volumes of water and possibly linked it via a wetland corridor to Rondevlei in the south, creating a low water resident time within the lake itself (Fig. 7.19 and 7.20). The Cape Flats is known to experience flooding during the winter months as the water table rises in response to increased precipitation; this scenario appears to define this period. Generally, summer months were dry and calm, wind velocities were low, suggesting weakened or removed SAA atmospheric circulation from the region. The diversity and richness of the biological community relative to nutrient requirements confirms the mixing of different water bodies, with water supply during the "dry period" being maintained through the raised watertable and seepage of groundwater, which sustained the oligotrophic community while the wet period brought in nutrient rich waters and promoted the eutrophic community.

This period correlates to the first phase of the LIA as elaborated by Lindsey and Tyson (1992) and as depicted by the Wilderness diatom records. Most sites in the winter rainfall zone lack continuous deposition during this time or have unreliable age models. However, evidence from both Verlorenvlei and Princessvlei indicate a period of increased precipitation, probably sourced through frontal

depressions embedded in the southern westerlies. The expansion of the westerly belt equatorward has been proposed by Stager et al. (2012) and is supported by the Princessvlei diatom record. Additionally, the onset of the hiatus in the PV11.3 record at c. 440 to ~300 cal yrs BP coincides with the intermittent warming interval between the two LIA phases. A decline in the percentage representation of dilute diatom species from Verlorenvlei between c. 440 and 370 cal yrs BP, coupled with slow growth rates in *W. cederbergensis* until c. 330 cal yrs BP, may be sufficient confirmation of a distinctly drier interval along the western coast of South Africa (Dunwiddie and LaMarche, 1980; Stager et al., 2012). The dry interval may account for the break in sedimentation at the PV11.3 core site.

Upon resumption of the record following the hiatus, the biological community appears to indicate high nutrient loading but within a shallow water environment. The near dominance of the assemblage by a small benthic species, coupled with a peak in *S. elliptica*, implies an emergence from a highly dynamic environment, which received little moisture. It also appears that groundwater or possibly river inputs had less influence on the system during this phase. A possible explanation for this may lie in the disconnection of Princessvlei from Little Princessvlei and, ultimately, cessation of river inputs via the Diep River (see Brown and Magoba, 2009). Additionally, the depth of the watertable with respect to the surface of the lake may have been affected by the rapid infilling of the lake during the late Holocene. Princessvlei is characterised as a shallow lake with an average maximum depth of 2.4m AMSL; according to Parsons and Harding (2002) groundwater currently lies on average between 6 to 7m below the surface. These factors taken together may indicate that the lake may have had more direct exchanges with groundwater in the past, which sustained the oligotrophic community; but rapid sediment deposition then raised terrain and infilling of the lake basin would have limited groundwater seepage into the lake itself.

The lack of groundwater penetration following the hiatus may also be associated with a drier climate experienced during the hiatus phase. Replenishment of the watertable would be directly related to aquifer recharge, as well as moisture availability; if either or both of the former are reduced the water table will recede. If indeed the period encompassing the hiatus saw little to no groundwater inputs, the nature of the lake would be related to the periodic inflow of surface runoff, which eventually evaporated leading to a concentration of nutrients. This scenario may have occurred during the hiatus, however, the causes behind the hiatus in the record are currently unknown. What can be noted is that the recorded environment within the rootmat deposits suggests that a gradual recovery in lake levels is observed. The progressive increase in moisture availability assisted in flushing the system and changing

the biological community to a predominantly eutrophic assemblage. It definitely appears that the root-mat represents a recovery phase after a period of adverse environmental conditions. According to Neumann et al. (2011) the development of the root mat occurred between ca. 300 and ~150 cal yrs BP and coincided with European occupation; the influence of human activities certainly cannot be disregarded. Although the development of the root-mat may not have been initiated by European colonisation, the environment recorded within the deposits may have been influenced by their activities. The chronology for this period is uncertain, however, and so attempts at aligning fluctuations in the diatom assemblage relative to known environmental changes or anthropogenic forcings have not been undertaken.

7.3.4. The Neumann et al. (2011) pollen record

It is interesting to note that the pollen and the diatom assemblages from Princessvlei only broadly concur with each other, with greater disparities occurring nearer the onset of the hiatus at 1000 cal yrs BP in the pollen record (Table 7.4). The hiatus seen in the Neumann et al. (2011) record from c.1000 – 350 cal yrs BP far exceeds the one evident in the current study, which is constrained from c.450 – 300 cal yrs BP, which may suggest external factors affecting the record post-deposition. The departure of the environmental signal in records from the same lake basin is an anomaly. In general, the pollen-based reconstruction indicates extended wet periods from 3400 – 2600 cal yrs BP and 1900 – 1000 cal yrs BP (averaging ~850 years in duration) and extended dry periods from 4150 – 3400 cal yrs BP and 2600 – 1900 cal yrs BP (averaging ~700 years in duration) (Table 7.4). These trends are primarily based on the percentage representation of key vegetation taxa, particularly *Crassula*, *Carpococe* and typical fynbos elements including Restionaceae, Asteraceae and Ericaceae. In contrast, the diatom-based reconstruction suggests somewhat shorter spells of relative moisture availability and relative aridity, as detailed in the previous sections and outlined in Table 7.4.

A notable inconsistency between the two proxies is the short lived dry spell occurring at c.1650 cal yrs BP. Since the sampling interval employed by Neumann et al. (2011) is 5cm, this may have obscured some of the shorter-term oscillations identified in the diatom record. Moreover, the diatom sequence may be far more sensitive to the environmental changes occurring in the Cape Flats area in comparison to the vegetation occupying the surrounding landscape and therefore are able to register the fluctuations in moisture availability to a greater degree (see Cowling 1983; Cowling and Holmes 1992; Linder et al. 1992). It is also interesting to note that as the ZB48 record approaches the hiatus at 1000 cal yrs BP (105cm), the PV11.3 record indicates a shift toward drier conditions starting at 1200 cal yrs

BP. As discussed previously, this episode (1200 – 940 cal yrs BP) was characterised by exposure to high wind energies from the south to south-easterly quadrant. The strong, dry winds may be partially responsible for the hiatus in causing deflation and mixing of deposited sediment. Adjusting the chronology to take this factor into account and providing for a linear interpolation between the radiocarbon ages at 166.25cm and 127.5cm would place the culmination of the ZB48 moist phase at ~1100 cal yrs BP. This expands the hiatus in the ZB48 core by ~100 years but aligns the interpretation of the two proxy records to a far greater degree.

Table 7.4: Comparison of the generalised reconstructions of environmental conditions at Princessvlei during the late Holocene based on the pollen and diatom proxy records

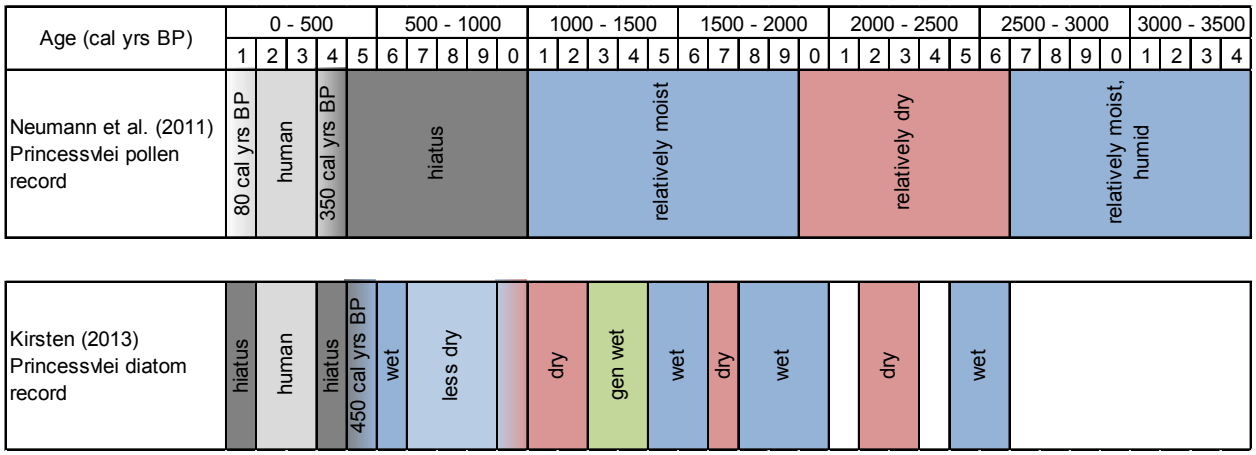

The culmination/initiation in shifts in climatic conditions are generally offset by 100-200 years, e.g. relatively moist conditions begin at 1900 cal yrs BP in the pollen record, whereas the diatom record suggests a wetter climate from 2000 cal yrs BP. The reason behind this trend may be related to the age-depth model proposed by Neumann et al. (2011), who employed a regression line through several AMS and two conventional radiocarbon ages. This technique may not hold as the reconstruction approaches the hiatus and sedimentation either slowed or ceased. Additionally, a regression line does not take into account the character of the sediments, where accumulation rates may differ depending on the core lithology. The PV11.3 core has shown that sand-dominated units accumulate far more rapidly than organic/peat units; this factor would alter the ZB48 core chronology significantly. Furthermore, the current study (PV11.3) identifies water exchanges that have occurred in the past (and indeed may still be occurring) between Little Princessvlei and Princessvlei, possibly at a subterranean level during drier periods. The position of the van Zinderen Bakker core of 1948 (ZB48) on the northwestern shore would mean it may be more susceptible to such water exchanges. This may affect the sedimentary record during periods of increased flow between the two water bodies, where flow velocity may disturb, mix or

remove sediments post-deposition. The numerous age reversals in the ZB48 core may provide evidence of this, but several other mechanisms may also be contributing factors, many of which have been addressed by the authors (see Neumann et al. 2011, p. 1141). Even with the chronology issues the environmental reconstruction based on the pollen record provides a broad overview of climatic conditions during the late Holocene.

From the review and direct comparison of the two palaeo-records it can be stated that, although discrepancies currently exist, the reconstructions are comparable. The chronology of the ZB48 core requires some attention as the method employed to construct the age-depth model is problematic. The acquisition of a new sediment core for pollen analysis is desirable.

7.3.5. Isotopic comparisons

The availability of isotopic records along the coast of South Africa is relatively limited. Research conducted by Cohen et al. (1992) and Jerardino (1997) provide some indication of water temperature variability during the late Holocene, although both are temporally discontinuous (Fig. 7.21). Both molluscan records employed isotopic analysis of the marine species, *Patella granatina*, making them directly comparable, while the PV11.3 used a bulk diatom sample from the predominantly freshwater lake. The $\delta^{18}O_{diatom}$ record shows a consistent enrichment per sample compared with the $\delta^{18}O_{molluscs}$ records. This enrichment may be related to the source waters, as well as increased evaporation potential in a lake system in comparison to the marine environment.

The records appear to be in broad agreement in that enriched $\delta^{18}O$ values occur between ~3200 and ~2500 cal yrs BP, implying a stepwise shift to cooler climes before peaking at ~2500 cal yrs BP. Following this, depleted $\delta^{18}O$ values prevail between around 2200 to 1000 cal yrs BP suggesting a relatively warm environment which may have been sustained through to ~800 cal yrs BP. However, greater variability in the oxygen isotope record may indicate some environmental instability between 1000 and 600 cal yrs BP (Fig. 7.21). This trend may be an expression of the intermittent reintroduction of westerly influences over South Africa before coming to dominate by 600 cal yrs BP. The remainder of the isotope record shows a transition toward enriched $\delta^{18}O$ values possibly signifying a return to a predominantly cooler climate.

The resolution of the records is rather poor since the mollusc records are dependent on midden accumulation by pre-historic communities while the diatom record was sampled at a coarse resolution to determine the potential of the proxy. The broad agreement of the three oxygen isotope records is

encouraging and points to the potential of utilising diatom rich records as a source of isotopic data in South Africa where carbonate fossils are absent.

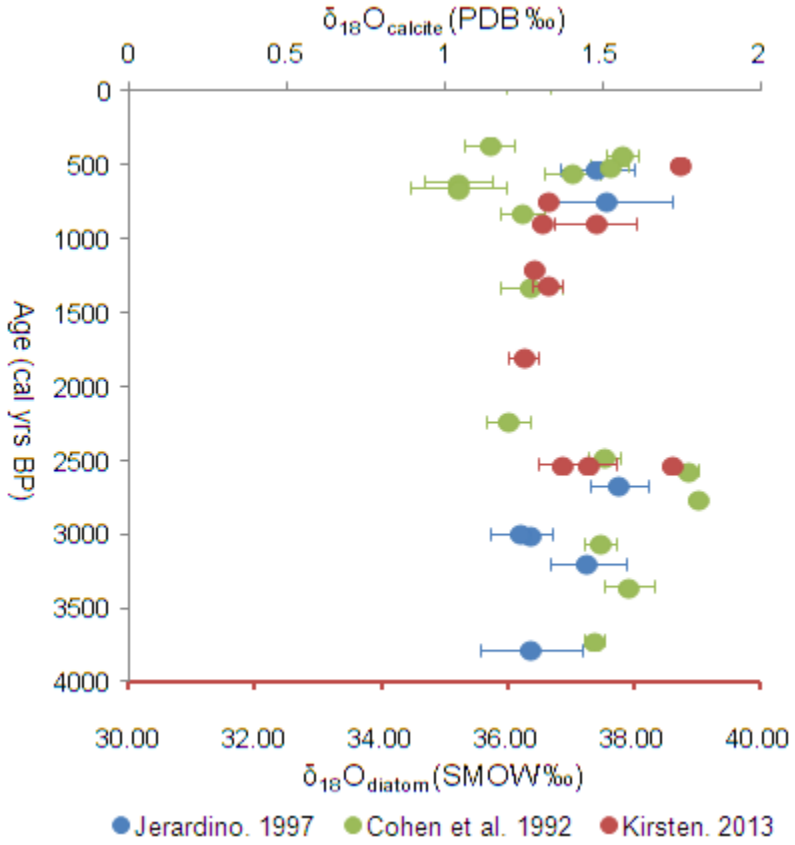

Figure 7.21: Oxygen isotope records from sites along the west and south coast of South Africa, namely Eland Bay Cave mollusc record (Jerardino, 1997), Nelson Bay Cave mollusc record (Cohen et al., 1992) and the current study.

7.3.6. Conclusion:

The Princessvlei diatom assemblage provides a unique record of the hydrological dynamics during the late Holocene, particularly during a period where most winter rainfall sites have experienced a hiatus in deposition due to arid conditions. The complex supply in water sources have enabled near continuous deposition to occur and provide insight into a region where sites are still relatively rare at a variety of temporal scales. While the PV11.3 record is interrupted by a hiatus, the hiatus appears to be temporally constrained to approximately 150 years. The record shows a clear interplay and exchange between the dominance of the westerly belt and the South Atlantic High Pressure cell. The system is highly responsive to nutrient loading, which appears to be, in general, a proxy for moisture availability, which in turn affects lake levels and water turbidity. At the initiation of the record, the influence of the westerlies is strong, creating a turbulent water column and a substantial influx of nutrients before weakening and probably contracting southward as arid conditions set in between c.2400 and 2100 cal yrs BP (Table 7.5). Following this, a shift back to wetter conditions occurs at approximately 2000 cal yrs BP, before the region experiences oscillating moisture availability, leading to fluctuating lake levels in response to an overall weakening in westerly influences and a return in strength of anticyclone circulation (Table 7.5). This shift between winter and summer circulation dominance culminates at ~1200 cal yrs BP, when south-easterly winds re-inforced by the South Atlantic Anticyclone is the principal climatic forcing governing the landscape and hydrology until ~920 cal yrs BP. From 900 cal yrs BP until the hiatus the region appears to be highly dynamic, with a shift toward a wetter climate and becoming progressively wetter from 600 cal yrs BP. This trend may be due to the intermittent influence of the westerlies during a period primarily dominated by anticyclonis flow, before the westerlies starts to enforce itself on the region and commanding climatic conditions until 445 cal yrs BP (Table 7.5). Post hiatus, the system appears to be recovering from the adverse conditions experienced during the hiatus. The relative lack of high resolution sites from nearby localities within the winter rainfall zone makes it difficult to determine the spatial continuity of the climatic expressions in the PV11.3 record with greater confidence. However, the available evidence suggests some coherence across the region with the PV11.3 record.

Table 7.5: Summary of environmental conditions at Princessvlei

Period (cal yrs BP)	Environmental Conditions
Root mat (~300 - ~200)	High nutrient loading, shallow waters, gradual recovery in lake levels, initially dry possibly related to conditions which created the hiatus but becomes wetter. Human activities may be affecting biological community
HIATUS	
700 – 445	Transitioning to eutrophic community in response to a wetter climate, winters are very wet, summer stable and calm. Increased interconnectivity between lakes and wetlands on the Cape Flats
@625	Became wet enough to continuously support macrophyte community
920 – 650	Increases in organic loading, Westerly winds weak but starts to intermittently influence hydrology, irregular moisture availability, submerged macrophyte community begins development but discontinuous temporally
1200 – 920	Increase in south-easterly winds probably through summer circulation dominance, drier interval, decrease in lake levels, groundwater more prevalent, high intensity/less frequent rain events, alternate state initiated. Vast amount of sediment deposition in a limited time
1400 – 1200	Weakening of the high wind exposure, lake levels begin to fluctuate, still more wet than dry, diminishment of wetland along the periphery of the lake, shift to oligotrophic system from a eutrophic system, initiation of SAA influence
2000 – 1530	Initially wet, then pulsed moisture availability, generally wet
2400 – 2100	Dry interval, introduction of oligotrophic taxa, increased influence of groundwater sustains water levels
2600 – 2400	Westerly Winds dominate, high nutrients, increased wind exposure, deep lake levels

Chapter 8. REGIONAL TO GLOBAL CLIMATE DYNAMICS

The complex interplay between atmospheric and oceanic forcings and geomorphology along the South African coast has created a diverse landscape. The southern Cape coastal plain is situated at the nexus of two competing climatic systems, namely the tropical easterlies and the polar westerlies, making it a pivotal area of importance in establishing the natural variability of the region. Through the comparison of the climatic and environmental reconstructions of the individual sites within this study it should be possible to determine where each record concurs and where they contradict and, in so doing, grasp the larger scale climatic fluctuations and their inevitable influences on the southern Cape coastal plain. This would aid in determining the effects of an extended and more pronounced winter rainfall zone during periods when the westerly belt migrates equatorward or alternatively, ascertain the broader environmental effects during intervals when the circumpolar vortex contracts poleward.

The Princessvlei and the Wilderness sites have been demonstrated to be sound repositories of evidence for environmental changes and their ecosystem responses during dynamic climatic conditions. The former showcases the winter rainfall zone, with the latter representing the year-round rainfall zone during the late Holocene. With respect to locality, Eilandvlei in the Touw River floodplain and Swartvlei in the neighbouring catchment should express the same climatic signals for portions of the record that overlap, i.e. the last 1400 years (see Chapter 6). It may follow that, at least in part, the Wilderness record experienced some of the same environmental expressions as that shown in the Princessvlei record, particularly during periods when polar westerlies dominate. However, where they differ it may be assumed that one of the driving mechanisms responsible is the predominance of tropical to sub-tropical climatic anomalies having precedence over the YRZ dynamics.

The three records from the Wilderness region consist of 202 individual diatom species, indicating the diversity of the system as well as the interaction of multiple source waters. On the other hand, the Princessvlei assemblage comprised of 94 individual diatom species. In total, 54 species occur in all four palaeo-records suggesting some similarity in environmental and climatic conditions experienced across the coastal plain (Fig. 8.1).

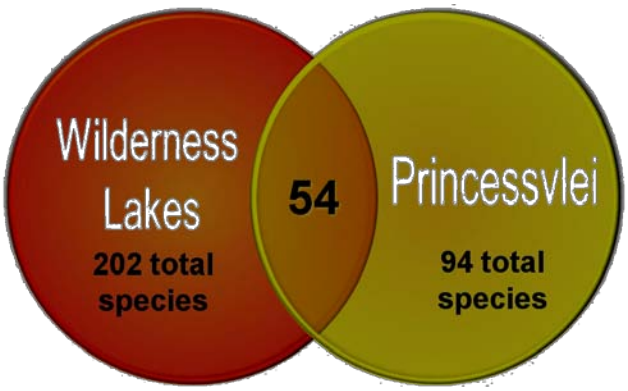

Figure 8.1: Summary of species numbers within and across sites, as well as displaying overlapping species occurrences between sites

The differences in deposition rates and sampling resolution between the Princessvlei and Wilderness records make direct comparisons rather limited and subjective. Notwithstanding, some indication of regional climatic forcing is evident between the records with similar demarcation of zones within records (Table 8.1). The discrepancy between the onset of zones may be as a result of the age-depth model utilised in each of the site's records, as the environmental transitions appear to be offset by a few decades. This issue may also be an artefact of spatial discontinuity, allowing for the onset or termination of environmental change to lag or dampen the signal, that is steep biogeographical gradients along the coastal axis may be an additional factor in determining the response time and effect of the environmental change subjected to the landscape. The following section outlines some of the possible regional climate signals identified in the records and relates it to published studies across the country before looking into the global comparability of the southern Cape sites in comparison to marine and terrestrial records.

Table 8.1: Comparison of assemblage zones from the three sites incorporated into this study

Princess (PV11.3)		**Eiland (EV11.1 and EV10.1)**		**Swart (SV10.1)**	
zone e	excluded	zone e	0 - -31	zone d	45 - -50
zone d	320 - 240	zone d	500 - 0	zone c	250 - 45
zone c	610 - 445	zone c	1200 - 500	zone b	730 - 250
zone b	1300 - 610	zone b	2050 - 1200	zone a	1400 - 730
zone a	2600 - 1300	zone a	4000 - 2050		

8.1. REGIONAL MOISTURE BUDGET

By comparing the moisture budget from the WRZ, YRZ and the SRZ it is hoped that this will aid in determining the changes in the overall moisture budget and the effects on the sites incorporated in this study (Fig. 8.2). Other than the PV11.3 and EV11.1 records, diatom records from Lake Sibaya and Verlorenvlei were utilised to provide a broader perspective. Lake Sibaya on the east coast of South Africa is situated in the summer rainfall zone and provided an 1800 year record of precipitation variability through diatom analysis (Stager et al., 2013). Stager et al. (2013) used the percentage representation of planktonic species in several cores from Lake Sibaya as a proxy for water depth after determining a strong contemporary correlation was evident between planktonic species and water depth. Verlorenvlei on the west coast of South Africa is representative of the winter rainfall zone. Sediment cores extracted from the lake basin provided a 1400 year diatom record representing hydrological fluctuations across the region (Stager et al., 2012). Changes in the percentage representation of dilute species in the Verlorenvlei record was linked to variability in rainfall, where increases in dilute-water species were interpreted as a shift toward wetter conditions (Stager et al., 2012).

Fluctuations in precipitation at Verlorenvlei would be in response to the migration of the westerly belt, whereas at Lake Sibaya responds to changes in the tropical easterlies and moisture availability over the southwestern Indian Ocean (Fig. 8.2) (Stager et al., 2012, 2013). For comparison, the records from this study include the percentage representation of brackish species from Eilandvlei (EV11.1), where a rise in brackish species is interpreted as an increase in moisture availability. This is based on the assumption that brackish species represent the *in-situ* community, which flourishes when sufficient freshwater mixes with marine waters. During drier periods, marine species dominate the system with a fair representation of fresh-brackish, aerophilic species. Eilandvlei represents the year-round rainfall zone and is expected to respond to changes in both the WRZ and SRZ moisture budget, based on both regimes influencing the YRZ. Presently, the YRZ receives rainfall from three main sources, *viz*. frontal depressions, ridging anticyclones and cut-off lows; the absence of any of these source waters would have a pronounced effect on the moisture budget of the YRZ. The Princessvlei record may represent the late Holocene WRZ through the fluctuations in the percentage representation of the diatom species, which favour nutrient-enriched environments. This is based on the premise that during wetter conditions nutrient availability is greater than during drier conditions where the only source of water to the lake system is oligotrophic groundwater. The combination of these records should give an indication

of the migration of source waters across South African during the late Holocene. The Stager et al. records only partially overlap the Eilandvlei and Princessvlei records, therefore comparisons can only be made for the last 2000 years.

Both the Eilandvlei and Princessvlei records indicate a drier phase prior to ~2100 cal yrs BP, after which humid conditions prevail until ~1660 cal yrs BP in the WRZ, whereas relatively moist conditions persists until at least 1200 cal yrs BP in the YRZ. A brief arid spell at Princessvlei circa 1600 cal yrs BP may have also affected the Wilderness region by briefly limiting a source of precipitation from the moisture budget. During the WRZ arid episode, the YRZ moisture budget is probably maintained by tropical rain-bearing systems, as higher water levels are experienced at Lake Sibaya and a rise in the P-E ratio indicates a wetter climate between 1710 and 1550 cal yrs BP (Stager et al., 2013). Even though wetter conditions return to the WRZ, the transitional state persists in the Wilderness region. This may be due either to the brief nature of the wet-event or that climatic fluctuations in the summer rainfall zone may be affecting the moisture budget in the YRZ. The former appears to be the most likely scenario. Although most SRZ palaeo-records indicate wetter conditions for most of the last 2000 years (see Scott et al., 2005; Brook et al. 2010; Neumann et al., 2010), finer temporal resolution records do reveal drier interludes. In particular, lower lake levels at Lake Sibaya are experienced between 1550 and 1160 cal yrs BP, with only a minor recovery from 1420 – 1350 yrs BP (Fig. 8.2). These patterns of fluctuating moisture availability between the SRZ and the WRZ may have been sufficient to maintain relatively humid conditions in the YRZ. During this period environmental conditions along the south coast appear to be dominated by westerly influence before tropical easterly influences begin to supplement moisture availability on the south coast. This would imply a strong representation of frontal depressions embedded in the southern westerlies after 2100 cal yrs BP until around 1700 cal yrs BP, before they are displaced poleward, mimicking sea ice presence (SIP) in the Southern Ocean (Nielsen et al., 2004). Fluctuations in sea ice presence in the East Atlantic Southern Ocean can be used as an indicator of the action of the westerly belt, where the persistence of sea ice would affect the positions of the Antarctic Polar Front and the Subtropical Polar Front, pushing frontal depressions toward the African continent and leading to pronounced moisture availability in the WRZ and YRZ (Reason et al., 2003). However, when sea ice presence is limited the exposure of the south and west coast of South Africa to frontal depressions is restricted, leading to a marked decline in precipitation in the WRZ.

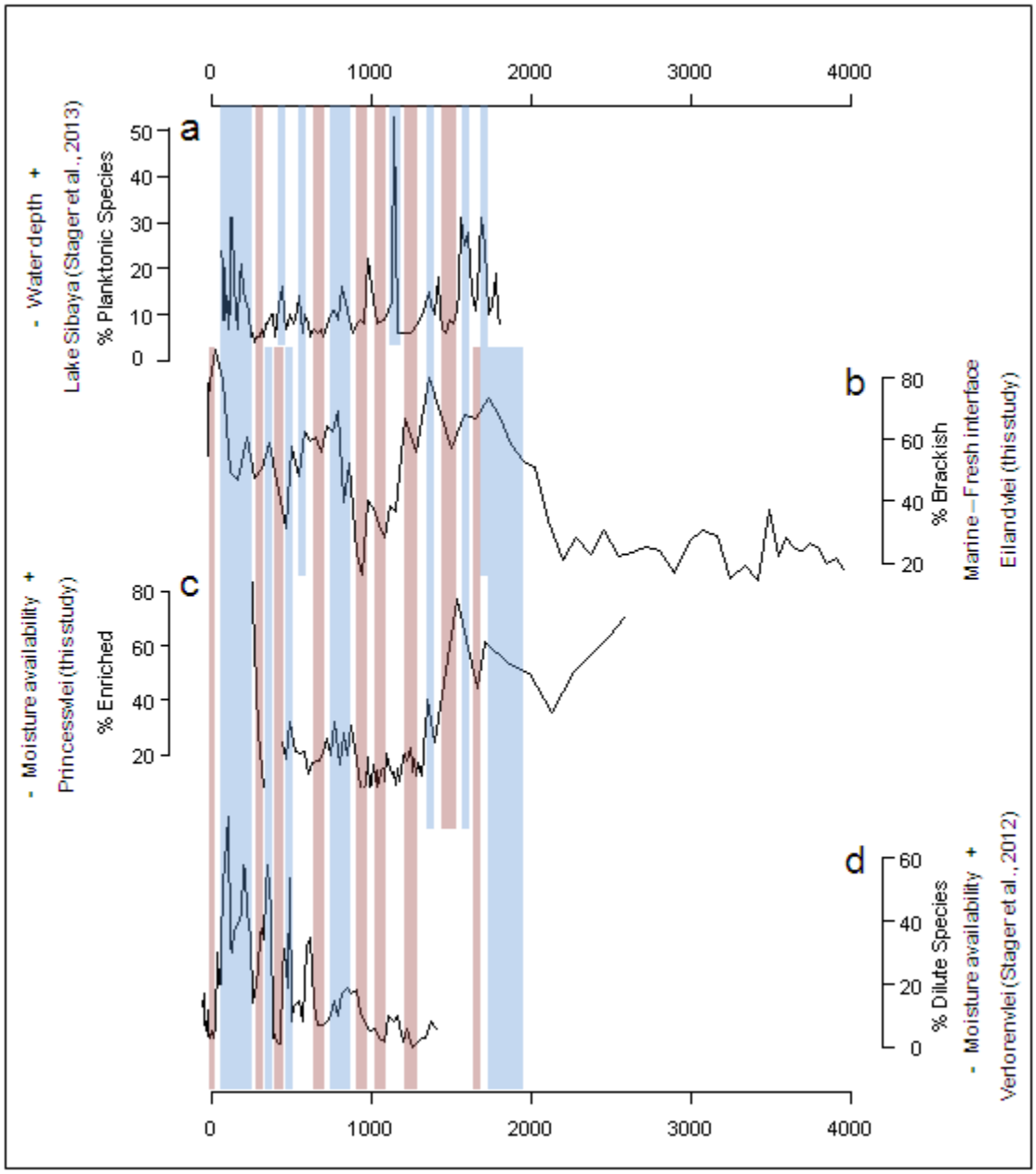

Figure 8.2: Variation of moisture availability along the coast of South Africa a) Planktonic diatom assemblage from Lake Sibaya, east coast (Stager et al., 2013) b) Percentage representation of diatom species which favour brackish environments from Eilandvlei, south coast (this study) c) Percentage representation of diatom species which favour nutrient-enriched environments from Princessvlei, south-west coast (this study) d) Percentage allocation of diatom species preferring dilute waters from Verlorenvlei, west coast (Stager et al., 2012). Blue-shaded boxes indicate generally wetter conditions while red-shaded boxes indicate generally drier conditions.

A decline in moisture availability occurs across all sites from ~1350 cal yrs BP, promoting a prolonged arid period from 1300 cal yrs BP for the western half of South Africa, which only culminates at ~960 cal yrs BP at Verlorenvlei, at ~945 cal yrs BP at Princessvlei and at ~930 cal yrs BP in the Wilderness. The different recovery times may relate to the passage of the cold fronts, influencing the west coast and

then, as the westerlies become more prominent, travelling further eastward along the south coast. However, the variability of the onset of greater moisture availability at each of the sites may also be explained by age uncertainties and the age-depth models employed by each respective site. The follow up to the diminishment in precipitation during the 400 year period forced Princessvlei into an alternate ecological state, resulting in a minor enriched-diatom component; however the fluctuations experienced during this alternate state are still interpreted as indicative of changes in precipitation (see subsection **7.3.2**). An additional proxy from Verlorenvlei, percentage representation of brackish-water diatoms, shows a slight increase in precipitation between around 1340 and 1190 cal yrs BP, although this was not sufficient to shift the lake system to freshwater conditions (Stager et al., 2012). Conversely, water levels at Lake Sibaya suggest the rapid onset of brief wet spells during this period in general. Lower lake levels at Lake Sibaya persist between c. 1360 and 1040 cal yrs BP, briefly interrupted at c. 1140 cal yrs BP by a sudden and marked rise in lake levels. This short-lived event is mirrored by a decline in enriched diatoms at Princessvlei, implying a predisposal to tropical easterly influence across the country with the possible southward migration of the tropical easterlies forcing a contraction in the westerly wind belt. Limited SIP between 1300 and 1100 cal yrs BP supports this notion (Nielsen et al., 2004).

Other than the short-lived wet episodes at Lake Sibaya most of the last 1000 years has been relatively stable and characterised by moderate moisture availability, with the period defined as the Medieval Climate Anomaly being generally wetter, particularly between c. 1000 – 975, c. 835 – 815 and c. 770 – 750 cal yrs BP. Although arid conditions continue until c. 850 cal yrs BP in the YRZ, a slow return to moist conditions begins from about 900 cal yrs BP. The shift to a slightly wetter climate in the WRZ is centered at about 920 yrs BP, where an increase in SIP is also evident after an extended period of absence in the Southern Ocean. Both SIP and the Princessvlei moisture budgets suggest a prolonged contraction of the westerly belt from ~1300 until before 920 cal yrs BP, with the decades preceding 920 cal yrs BP being some of the driest evident in all three rainfall regimes. The west coast appears to have experienced considerable fluctuations in moisture availability with increases occurring at c. 900 – 740, c. 640 – 590, c. 545 – 515, c. 485 – 440, c. 365 – 60 cal yrs BP. This trend is also evident at Princessvlei along the southwest coast, with the shift to moist conditions predating the west coast by approx. 50 years. Slightly less xeric conditions post-900 cal yrs BP allows for a slow ecosystem recovery at Princessvlei, suggestive of only intermittently higher moisture availability before a pronounced shift to a wetter climate occurs from 500 cal yrs BP. This would imply that the frequency of winter rainfall events appears to intermittently increase over the last 900 years, possibly related to a regular equatorward movement of the westerly belt before becoming more pronounced towards the present. Additionally, optimal

moisture availability in both the WRZ and SRZ benefits the YRZ moisture budget, allowing a rapid recovery post 850 cal yrs BP where relatively moist conditions are once again achieved by ~800 cal yrs BP. This development influences south coast dynamics, which have primarily been receiving summer rainfall, but with the additional source of intermittent winter precipitation from 900 cal yrs BP the region experiences a wet phase, which lasts until ~550 cal yrs BP. The wetter climate in the YRZ is maintained through the alternating moist conditions in the SRZ or the WRZ which supplements the south coast sufficiently to maintain a relatively wet and stable environment. However, it is at this point that the environmental signals of the YRZ and WRZ begin to diverge. When wet conditions prevail in the WRZ, the YRZ experiences a ~200 year dry phase from 500 – ~300 cal yrs BP. This implies a localisation of winter rain-bearing systems to the west and southwest coast with poor penetration along the south coast of South Africa.

High winter rainfall persists until a sudden yet brief decline at ~440 cal yrs BP, which caused riparian encroachment and a decrease in dilute diatom species at Verlorenvlei. At the same time a hiatus in the Princessvlei record, is observed possibly indicating that this arid spell may be the mechanism behind the lack in preservation in the PV11.3 record. Environmental evidence upon resumption of the PV11.3 record strongly suggests a recovery from an arid spell, shifting to progressively wetter conditions from ~300 cal yrs BP. On the other hand, Lake Sibaya becomes increasingly more fresh between c. 490 and 420 cal yrs BP, signifying a rise in precipitation along the east coast, which coincides with the relatively brackish conditions at Eilandvlei, but not before the lower precipitation from the WRZ negatively impacts the moisture budget of the YRZ. A recovery in lake levels at Verlorenvlei and the resumption of the Princessvlei record only occurs about a century later, circa 370 – 345 cal yrs BP, respectively. Both of the aforementioned records reveal a considerably wetter climate post-arid spell with only minor fluctuations in moisture availability, which directly impacted the south coast. Wetter conditions persist at Verlorenvlei until at least 70 cal yrs BP, before gradually declining and making some recovery in recent decades. The SRZ appears to remain relatively dry from ~400 to 230 cal yrs BP, after which increases in water level provide an environment for planktonic species to thrive in Lake Sibaya until the termination of the record at c. 60 cal yrs BP. The YRZ experiences a surplus in moisture availability in the later stages of the Eilandvlei record in response to wetter climates in both the WRZ and the SRZ.

The South African climate clearly has been affected by considerable fluctuations in its moisture budget over the later Holocene. It is evident that the YRZ is sensitive to any changes experienced in the neighbouring rainfall regimes, which are primarily affected by the position and strength of the westerly

belt and the tropical easterlies. When dry/wet episodes occur in both the WRZ and the SRZ, the YRZ is considerably impacted experiencing extensive arid/wet spells but appears to cope well when fluctuations between wet and dry episodes are sudden and short-lived.

8.2. ATMOSPHERIC VARIABILITY

Anticyclonic circulation over southern Africa plays a crucial role in moisture flux across the continent, as well as regulating oceanic circulation along the coast (see subsection **2.1.1**). Furthermore, the intensification of anticyclonic flow directly influences the nature of the Agulhas Current and its velocity flow, with changes in the latter influencing ring shedding into the Atlantic Ocean and the overall stability of the surface arm of the Atlantic Meridional Overturning Circulation (AMOC), thus having global impacts in ocean circulation and the formation of North Atlantic Deep Water (Caley et al., 2011; Backeberg et al., 2012). Ultimately, anticyclonic flow responds to solar insolation and changes in sea surface temperatures. Mason and Jury (1997, p. 38) surmised that during extended warmer and drier phases above-normal summer temperatures would be experienced; this is linked to the prevalence of anticyclonic flow, which they attributed to "adiabatic heating of descending air over the subcontinent and increases in solar radiation given less cloud cover". Hence, knowledge of variations in the position and the strength of the high pressure belt are of paramount importance as it has direct global consequences.

Easterly winds along the south coast dominate during the austral summer and autumn months as the South Atlantic Anticyclone ridges toward the continent. Increased easterly wind components can promote upwelling along the south coast, bringing cool, deep and nutrient-rich water to the surface and reducing water temperatures. Upwelling events were identified in the diatom fossil record at Eilandvlei and Swartvlei by the presence of *Paralia sulcata*, a known indicator species for vertical mixing of the water column (McQuoid and Nordberg, 2003; Abrantes et al., 2007). Peak occurrences of *P. sulcata* were shown to occur at c. 3950 – 3800, 3425 – 3250, 2900, 2550 and 2200 – 2100 cal yrs BP in the EV11.1 core (Fig. 8.3), before the isolation of the lake obscured the marine signal in the EV11.1 record. However, by incorporating the 1400 year record from Swartvlei the prevalence of *P. sulcata* can be extended. The cold water marine diatom shows increased proportions between c. 1150 and 830, at 615 cal yrs BP and recovers in the last century (Fig. 8.3). Although a relatively short temporal record and distinctly removed from direct marine water exchanges, the EV10.1 record shows notable trace proportions of *P. sulcata* at ~590 and at ~415 cal yrs BP. Additionally, marine taxa in the Princessvlei

core have been used as an indicator of the increased influence of south – southeasterly winds, which dominate during the austral summer months and are fuelled by the position and strength of the South Atlantic Anticyclone (see subsection **7.1.1**). Notable peaks in the PV11.3 record are centred at 1330 – 920, ~600 and at ~445 cal yrs BP, which corresponds well with the YRZ records (Fig. 8.3).

Intensification or prolonged poleward migration of the anticyclones during these periods may explain the increased representation of the marine diatoms during the stated intervals. The flow dynamics of the Agulhas Current and shelf environment are governed by the character of the anticyclones and tropical easterlies. The surge of *Paralia* implies greater easterly winds along the south coast, promoting upwelling and providing cooler waters on the Agulhas Bank. Along the southwestern coast, prolonged exposure to anticyclone circulation would lead to a drier climate, as well as displacing the rain-bearing systems embedded in the southern westerly belt polewards. In most cases, a drier climate is prevalent when peaks in SAA-indicator species occur at both regional sites; however confirmation of a warmer climate could not be ascertained with any significance. Hence, the SAA indicator species were compared to variations in climate profiles from South Africa during the late Holocene, particularly the grey scale from the Cold Air Cave speleothem (CAC), Makapansgat Valley and the inferred temperature profile from the Cango Caves (CC), near Oudtshoorn (Talma and Vogel, 1992; Lee-Thorp et al., 2001). The latter records are seen as representatives of the variability of the SRZ and YRZ climate over the last 4000 years, respectively (Fig. 8.3). Three events are singled out from the records, namely c. 3500 – 2900, c. 2200 – 2100 and 1300 – 900 cal yrs BP.

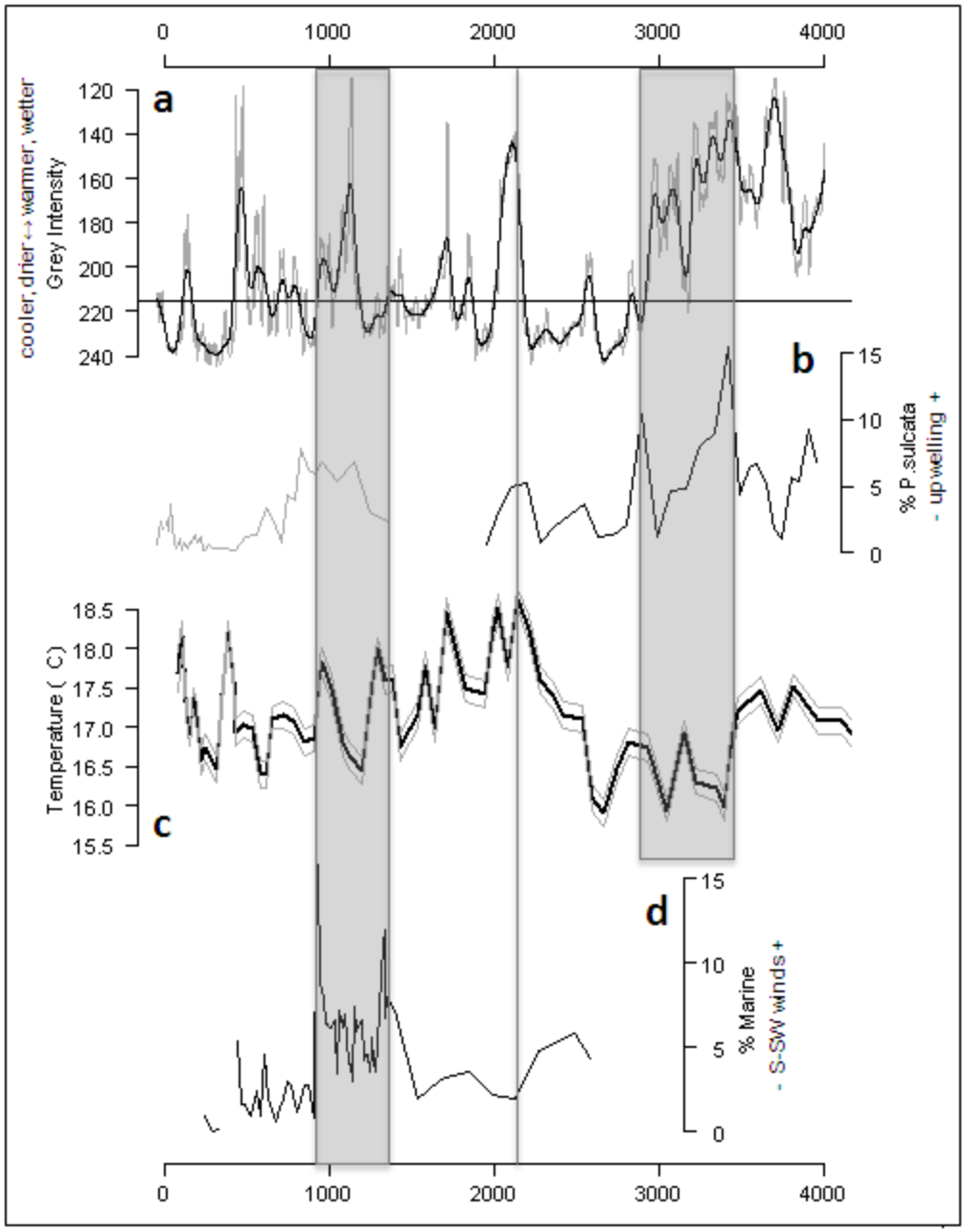

Figure 8.3: a) Cold Air Cave speleothem grey intensity plotted on an inverse y-axis with a 5-point smoothing spline (Holmgren et al., 1999; Lee-Thorp et al., 2001); b) Percentage representation of Paralia sulcata *from Eilandvlei, EV11.1 (black line) and Swartvlei, SV10.1 (grey line) (this study); c) Temperature profile with standard deviation derived from the Cango Cave $\delta^{18}O$ stalagmite sequence (Talma and Vogel, 1992); d) Percentage representation of marine taxa from Princessvlei (this study). The shaded boxes outline the three events discussed in the text.*

Event 1 is defined by two distinct peaks in *P. sulcata*, which occur at ~3450 and ~2900 cal yrs BP, with generally elevated proportional representation arising between ~3450 and ~3200 cal yrs BP. This would imply pronounced and prolonged exposure of the south coast to easterly winds fuelled by a ridging high pressure cell. The speleothem records indicate a transition toward a cooler climate at some point

between 3500 and 3200 yrs BP. The Cold Air Cave record reveals a shift from a variable moist/warm phase to a prolonged arid/cool period hinged at 3200 cal yrs BP. Evidence from the grey-scale index displays a transition from low intensity toward high intensity during *Event 1* but remaining within a warmer/wetter climate. Conversely, the Cango Caves recorded a shift toward a cooler climate with lower average temperatures between ~3500 and 2500 cal yrs BP, which corresponds with inferences of a global cooler climate (Mayewski et al., 2004). However, variability in average temperature from CC shows elevated temperatures in accordance with the timing of *Event 1*. During the transition, atmospheric instability may have played a significant role as the environment responded to shifting climatic conditions. Lamy et al. (2001) linked iron (Fe) content in marine sediments off the Chilean coast to the latitudinal shifts of the southern westerlies. Fluctuations in the Fe intensity indicated less humid conditions in southern Chile from ~3400 cal yrs BP, peaking at ~3230 cal yrs BP before rapidly transitioning to more humid conditions; implying a poleward migration of the westerlies, which would have been accompanied by the expansion of the mid-latitude high pressure belt across southern Africa (Lamy et al., 2001). Additionally, a multiproxy record from the Torres del Paine National Park, southern Chile shows a prominent warm, dry phase between 3200 and 2900 cal years BP (Moreno et al., 2009). Moreno et al. (2009) proposes that this warm phase represents one of the driest episodes of the 5000 years record and relates to a poleward contraction of the southern westerlies. This episode conforms well to the parameters of *Event 1*.

The relative absence of high-resolution marine records from the South African region makes it difficult to determine the regional cause-and-effect of changes in the character of the Agulhas Current during the late Holocene. However, the position of the Antarctic Polar Front (APF) would indirectly affect the point of retroflection of the Agulhas Current and ring shedding into the Atlantic (Read and Pollard, 1993), i.e. a contraction of the Antarctic Polar Front (APF) would displace both the STF and the westerly belt. Therefore, variations in sea ice presence (SIP) from the APF (at 50°S) could be used as an indicator of the migration of the front (Nielsen et al., 2004). SIP shows a marked decline at ~3430 and ~2890 cal yrs BP corresponding with peak *P. sulcata* distribution. The lack in persistence in sea ice at 50°S may imply a warmer climate and the contraction of circumpolar front leading to a southward displacement of southern hemisphere atmospheric disturbances, thereby substantiating the mechanisms driving *Event 1*. The overall view during this event suggests that a generally cooler environment prevailed punctuated by brief high intensity intrusions of the high pressure cells along the south coast of South Africa which coincided with increases in average temperatures leading to short-lived arid spells.

Event 2 lasts about a century between c. 2200 – 2100 cal yrs BP. Regionally, both Cold Air Cave and Cango Cave speleothem records show a shift to a much warmer environment, particularly after an extended period of cooler conditions, with the possibility of a wetter climate in the SRZ. The warmest temperature of the late Holocene at CC is registered at c. 2140 cal yrs BP, roughly coincident with a sudden decline in the CAC greyscale intensity starting at ~2165 cal yrs BP and lasting until c. 2025 cal yrs BP, with the lowest point occurring at ~2130 cal yrs BP. In addition, peak spread in C_4 grasses is shown to occur at CAC at 2100 cal yrs BP, indicating optimal conditions for the establishment of tropical grasses (Lee-Thorp et al., 2001). Further to the south, the Wilderness region experienced increased upwelling along the coast between c. 2200 and 2100 cal yrs BP, suggesting increased South Atlantic Anticyclonic activity. The event is barely evident in the Princessvlei marine species sequence, although the record does indicate a dry episode at c. 2120 cal yrs BP with a decline in proportional representation of nutrient-enriched species. Marine sediments off the Chilean coast register a transformation from peak humidity at ~2230 cal yrs BP to a rapid decline in relative humidity by 2100 cal yrs BP before recovering in a few decades to a moderately moist climate (Lamy et al., 2001). This trend details the swift yet abrupt character of the incident. A definitively warmer climate is experienced across South Africa accompanied by drier conditions particularly along the coast; evidence also suggests that the mechanism responsible for this event was the possible contraction of the westerly belt providing a prolonged exposure to anticyclonic and tropical easterly atmospheric disturbances.

The third and final event commences at ~1350 cal yrs BP before terminating at ~900 cal yrs BP. The timing and extent of the event is primarily based on the marine component in the PV11.3 sequence. The marine component combined with the elevated deposition of beach sands at the PV site was interpreted as the result of increased prevalence of south – south-easterly winds, fuelled by the poleward shift of the High Pressure Belt (see subsection **7.3.2**). Peak distribution of marine taxa occurs at c. 1330 – 1310 and c. 930 – 920 cal yrs BP but remains elevated throughout the intervening period. The latter peaks coincide with higher average temperatures at CC.

Well below-average SIP occurs in the East Atlantic Southern Ocean from c. 1300 – ~950 cal yrs BP, over and above a general decrease in sea surface temperatures in the Benguela Upwelling System (BUS) (Nielsen et al., 2004; Leduc et al., 2010). The previous records imply the strengthening of the Tropical Easterly winds, as well as the contraction of the circumpolar front and the displacement of frontal depressions to the south, resulting in a drier climate across the western half of South Africa. For instance, the southern margin of the Kalahari experienced a short-lived dry episode at ~1300 cal yrs BP

(Brook et al., 2010). A corresponding signal in the greyscale intensity at CAC is not evident, however, the grey scale progressively declines during this period before reaching intensities below 190 between ~1110 and 1085 cal yrs BP. Stager et al. (2013) mentions that the climatic interpretation of the CAC record lacks strong supportive evidence; this may be an explanation for the inconsistency of changes of the greyscale index relative to *Event 3*. Fluctuations in Fe content in the marine sediment core from the Chilean continental slope closely mirror the peaks and troughs in the marine content in the PV11.3 record (Lamy et al., 2001). However, the Fe content does not show a complete shift to less humid conditions, implying a constant but reduced supply of moisture from frontal systems embedded in the southern westerly belt along the Chilean coast. The combination of these signals suggests a warmer climate with an intensification and at times prolonged exposure to anticyclonic circulation coupled with sporadic aridity.

The inclusion of the SV10.1 *P. sulcata* sequence overlaps this third event but appears to lag behind the PV11.3 record, only beginning at c. 1150 and ending at around 750 cal yrs BP. This may be due to the site's location relative to WRZ site and possibly the buffering effect of two competing climatic systems from the polar and tropical regions offsetting the initial aridity which the WRZ experiences. Alternatively, the chronology of the SV10.1 core has not been fully resolved. The possibility of at least a partial marine reservoir effect can not be eliminated; the record could therefore be slightly older/younger than the age-depth model has predicted (see subsection **5.3.1**). Geochemical analysis of the SV10.1 core shows considerable marine derived elements in the lower half of the record before limited exchanges leads to a generally fresher lake (Franz, 2012). The nature of Swartvlei suggests varying degrees of marine deposition over the last 1400 years, hence a constant offset to the chronology could not be applied as would be possible in purely marine-derived sediments. The aforementioned attributes may be the cause of the slight discrepancy in the timing and duration of the third event between the SV10.1 and the other records apparently starting and ending later than in the other records mentioned. Without further investigations into the effects of the marine reservoir effect in transitional environments, such as estuaries and coastal lakes along the South African coast, only a limited interpolation between the records can be undertaken.

The temporal concurrence in the records provides evidence of the regional and global scale of the influence of increased anticyclone circulation. It is of interest to note that the onset of the three events generally occurs during environmental transitions in the CAC and CC records, suggesting that during atmospheric instability anticyclone activity may intensify. Conversely, low percentage representation of

P. sulcata is observed at ca. 3750, 2975, 2800 – 2275 and at ~2000 cal yrs BP in the EV11.1 record, as well as at 700 yrs BP and between 550 – 70 cal yrs BP in the SV10.1 record. The decline of *P. sulcata* at ~2000 cal yrs BP may be the combination of climatic factors but may also be as a result of the isolation of the lake after dune stabilisation, inhibiting marine water intrusions into the basin. In contrast, a weakening of the current as viewed through diminished upwelling may coincide with an equatorward shift of the high pressure belt, coupled with the expansion of the circumpolar vortex. This would lead to a decrease in the leakage into the Atlantic and affect global oceanic circulation. Notable events such as the global neoglacial advance between 3500 and 2500 yrs BP (see Mayewski et al., 2004), increased influence of Westerly winds along the south coast between 2800 and 2200 yrs BP (Carr et al., 2006b; Bateman et al., 2011) and the Little Ice Age event of the last 600 years correspond with some of the aforementioned *P. sulcata* low representation events. Although the events overlap considerably and may be related to an equatorward shift of the polar front leading to a greater influence of westerly winds, other attributes may be at play influencing south coast upwelling or indeed possibly obscuring the percentage representation of the marine diatom(s).

8.3. ENVIRONMENTAL SUMMARY

As outlined in the above and in previous chapters, the southern Cape coastal plain has experienced considerable climatic fluctuations during the past 4000 years, providing the region with periods of extended wet and dry spells. Figure 8.4 displays a simple generalised reconstruction based on the environmental interpretation of the diatom assemblages from the three sites. The trends observed in the simplified reconstructions appear to mirror each other, with only minor discrepancies in the onset of shifts between dry and wet states. In other words, the YRZ appears to mimic/respond to the WRZ, showing rapid transitions between wetter and drier phases, particularly in the last few centuries of the record before human activities in the catchment distorts the natural signal. It may appear that observed changes in the YRZ record are primarily a function of winter rainfall variability; however this study lacks a comparative 4000-year record from the SRZ, which would provide an additional dimension in interpreting the YRZ signal. The Lake Sibaya record does however provide some insights. Even so, from the available evidence it appears that the YRZ is sensitive to minor changes in the WRZ moisture budget. Nevertheless, by incorporating regional and global records a clearer understanding of the effects and a finer resolution to changes in the mechanisms responsible for climate variability can be ascertained.

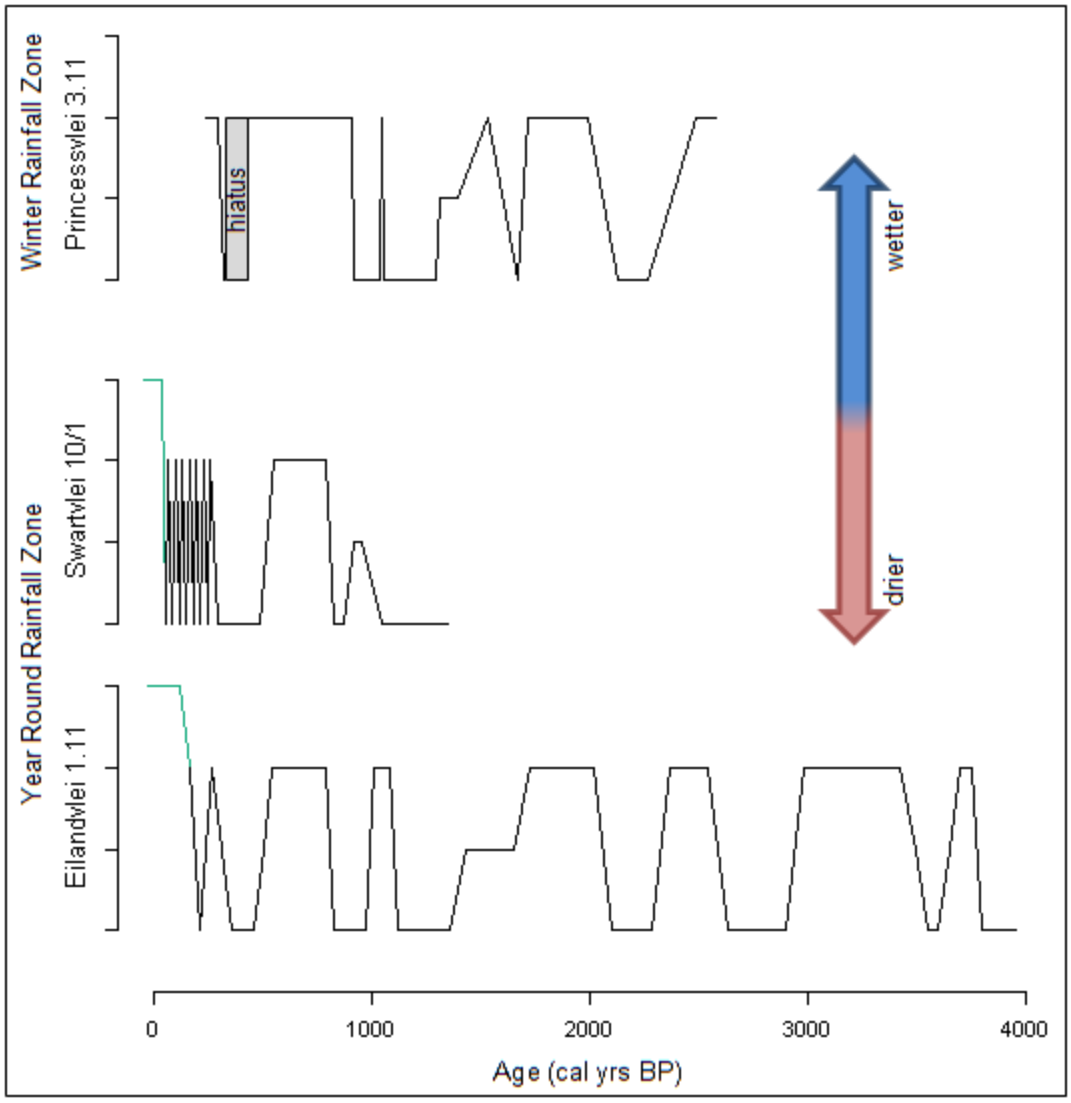

Figure 8.4: A simplified environmental reconstruction across the three sites incorporated into this study based on a numerical allocation against age (yrs BP) (scale: 0 – 3 where 0 = dry, 1 = transitional (where neither wet nor dry conditions are dominant but an intermediate state exists), 2 = wet and 3 = anthropogenic influence (green line))

8.4. CONCLUSION

Modification in the position and strength of atmospheric systems responsible for moisture distribution across the African continent has regional as well as global effects. Considerable similarities between winter rainfall sites and year-round rainfall sites across South Africa have shown that frontal depressions play a significant role in precipitation distribution along the west to south coast, but this should not downplay the importance of tropical easterly influenced rain-bearing systems to the overall moisture budget. From all accounts the variability of moisture as interpreted from the PV11.3 and EV11.1 sequences conform well with records in the vicinity and further afield, showcasing the regional response to the migration of the westerly belt in the high latitudes, the high pressure belt in the mid-latitudes and the tropical easterlies in the low latitudes.

Chapter 9. CONCLUDING REMARKS

The south coast of South Africa experiences both polar and tropical climatic anomalies along a west to east axis, giving rise to three rainfall regimes, namely the winter rainfall zone (WRZ), the year-round rainfall zone (YRZ) and the summer rainfall zone (SRZ), respectively. The purpose of this study was to determine the spatial and temporal variability of the WRZ and YRZ during the late Holocene based on the analysis of fossil diatoms preserved in sediments from appropriate lakes. The fundamental objective of this study was to supply, against a suitable chronology, an accurate account of the changes in natural processes over time by using the fossil diatom assemblage preserved in the lake sediments at several sites across an east-west axis along the southern Cape coast. Sites were chosen as representatives of their respective rainfall regimes and therefore an archive of environmental change within its boundaries. Hence, Princessvlei situated on the Cape Flats in the Greater Cape Town metropolitan area was expected to be an analogue of the winter rainfall regime, whereas lakes within the Wilderness Embayment were rendered an archetypal of the year-round rainfall regime. Lake sediments retrieved from the aforementioned lake systems provided continuous deposition for most of the late Holocene. The overall conclusion that can be extracted from this study is that moisture availability, wind direction and wind strength play a pivotal role in the way that ecosystems along the southern Cape coast function. However, recent developments linked to human activities have altered the natural functioning of these systems with conservation efforts being undertaken in an attempt to restore or maintain these sites.

9.1. CONSERVATION EFFORTS

In the past, conservation efforts have generally centred on the preservation of rare or threatened species in carefully selected areas with the eventual aim of designating the area as a nature reserve (Birks, 1996). In more recent decades conservation has evolved to include ecosystem enhancement with the potential to restore degraded landscapes (Birks, 1996). This shift has made it critical to determine the natural variability as well as the baseline value of a system earmarked for restoration. Historical information may offer some indication of community dynamics, but a palaeo-perspective can add a long term temporal evaluation. Both regions incorporated into this study are under either local or national conservation agency mandate, which actively attempts to maintain the current state of each respective system.

Most of the Wilderness Embayment falls under the directorate of the South African National Parks, who manages the way in which the systems function. At present, SANParks actively maintains the integrity of the system through the cutting of submerged aquatic plants in the interconnecting channels of the Wilderness Lakes, removal of alien invasives in selected areas and, of special interest to this project, the management of the estuary mouth of the Swart and Touw Rivers (Russell et al., 2012). SANParks allows water levels in Swartvlei to reach 2.0m AMSL, whereas water levels are allowed to reach 2.1 – 2.4m AMSL at Touw River Estuary before breaching of the sandbar is undertaken (Russell et al., 2012). Land modifications in the catchments have been considerable with ~30% of natural vegetation being lost to agriculture, plantation and urban sprawl between 1930 and 1991 (Russell et al., 2012).

The Indice de Polluosensibilité (IPS) is a measure of the sensitivity of the biological community to nutrient loading, whether the sources are from organic loading, salinity or anthropogenic inputs. In this capacity the diatom records can be utilised to determine the possible deviation from the natural state pre- and post-human influences. In the Wilderness region, European activities began ~200 years ago before most of the lake complex was designated a nature reserve in the 1950s. The IPS indicates that Eilandvlei and Swartvlei have remained relatively nutrient enriched, suggesting a biological community that is reasonably tolerant to the changes the system experiences. The sources of the fluctuations as expressed by the IPS are multiple and include the constant supply of marine waters, organic and nutrient loading from the catchment and charcoal deposition from the fire maintained fynbos ecosystem. In the last 200 years Eilandvlei has developed a diatom community that is increasingly more tolerant of these fluctuations than any previous assemblage over the 4000 year record, which may imply that activities in the catchment have escalated the introduction and deposition of various nutrient sources. This being said, it can be stated that the system was already in decline prior to the arrival of European settlers but was further impacted by the actions these settlers undertook. In contrast, the biological community in Swartvlei remained moderately tolerant to external forces throughout most of the record, before rapid fluctuations are observed during the last three centuries. In both lakes the last 60 years shows a return to a more moderately tolerant community, possibly suggesting that practices undertaken by the managing authorities is directly impacting the system.

On the other hand, the Princessvlei system falls under the management of Cape Nature, although the site is considerably degraded in so far as faunal and floral diversity has deteriorated and the lake itself experiences eutrophication (Kotzé, 2011). For these reasons, conservation efforts were deemed of low priority for the site, and a proposed development plan was given the go ahead if no objections were

brought forward by the local community and the developers adhered to conditions as outlined by the City of Cape Town (Kotzé, 2011). Currently, the future of Princessvlei is still being debated. The proposed development is seen as an opportunity to boost socio-economic opportunities to the surrounding areas (Kotzé, 2011). However, it has been noted that even in its degraded state the site plays a pivotal role in the larger ecological connectivity of the Cape Flats wetlands and lakes and has some of the last stands of Cape Flats Dune Strandveld and Cape Flats Sand Fynbos (Kotzé, 2011). The site is not only of ecological importance but also has historical and cultural significance (Kotzé, 2011).

The return of the IPS from this study can point out that Princessvlei naturally fluctuates between oligotrophic and eutrophic states dependent on climatic conditions. Hence, the current eutrophic state of the lake is not outside the natural boundaries of the system but rather has been enforced due to human activities and urban surface runoff within the catchment. The lack of a diatom record for the last 200 years for the PV11.3 core makes quantifying the human impacts on the system difficult, but post hiatus the system appears to be moving toward an oligotrophic state as is the case during drier periods. Therefore the current state of the system may be primarily a result of anthropogenic forcings in the catchment; however recent samples are required to confirm this. Additionally, the palaeo-record confirms the statement that the location of Princessvlei on the landscape plays a significant function in the ecological and hydrological processes of the Cape Flats. These two factors may assist in the decision-making process when the final judgement is made for the use of the land.

The managing authorities at Wilderness and Princessvlei have inherited sites that have been to various degrees impacted by prior human activities before conservation efforts where undertaken. The Wilderness region appears to still be within the systems natural boundaries, however, it has been noted that a freshening of the systems has occurred in the last few decades. This trend may be due to the stabilisation of the landscape, the building of the railway and coastline and/or the management of the estuary mouths. The systems do not appear to be negatively impacted by this trend, although the limitation of marine influx may affect lake levels during dry periods when marine waters previously supplemented the lakes. Conversely, Princessvlei needs more attention. The system appears to be an integral link to the ecological functioning of the Cape Flats wetlands but is considerably degraded to a degree that restoration may not be possible according to recent surveys (see Kotzé, 2012 for details).

9.2. FUTURE TRENDS AND OUTLOOK

An additional concern for these sites and any coastal regions is future sea level rise in response to a warmer climate. The coastal plain of South Africa has extensive regions of low elevation and is particularly susceptible to wave action and storm surge (Brundrit and Cartwright, 2012). Brundrit (1995) showed that over a 30 year period sea level rise along the west coast of South Africa was occurring at a rate of 0.12 ± 0.04 cm.year^{-1}, while the south coast experienced inconsistent sea level rise. Based on these projections, it is hypothesised that the rate of future sea level rise would double (Brundrit, 1995). Furthermore, the west and south-west coast are largely exposed to erosion, particularly the vast expanses of dunefields that characterise most of the coastline (Brundrit and Cartwright, 2012).

The palaeo-records from both regions have shown considerable marine interactions. The Wilderness region, being in closer proximity to marine influences, has at times been inundated during periods of marine transgressions. These transgressions have led to landscape modifications and hydrological adjustments in the back-barrier lakes; however the systems appear to be able to adjust to these marine incursions in due course. The more pressing concern may be the effects these incursions will have on the stability of the landscape as most of the urban sprawl will be affected, as most of the towns situated in the Wilderness Embayment are located either on the coast or in the low-lying valleys adjacent to the coastline. Preventative measures may need to be undertaken to avert property damage or erosional processes, either through the direct action of sea level rise or through indirect factors such as storm surge.

The Cape Flats also lies at a relatively low elevation. It is proposed that a warmer climate and higher sea levels may be accompanied by an increase in intensity and frequency of big storms, leading to erosion of the coast and undermining of rivers particularly along False Bay (Brundrit and Cartwright, 2012). Additionally, streamflow in the southwestern Cape is most responsive to changes in precipitation than to potential evapotranspiration as most rivers in the area are ephemeral in nature (New, 2002). These factors coupled with the knowledge gleaned from the PV11.3 palaeo-record suggest that erosion and aeolian activity may be the two main processes affecting the region during warmer and drier intervals. Preventative measures have already been suggested by Brundrit and Cartwright (2012).

9.3. CLOSING REMARKS:

Reconstructions of past climatic and environmental conditions for the Wilderness and Cape Flat regions have been suitably summarised in previous chapters (see Chapter 6 and 7.3), as well as cross correlated to determine regional-based climatic expressions (discussed in Chapter 8). It can be stated with some confidence that the sites are adequate representatives of their respective climate zones. At times these records have indicated dissimilar environmental trends, which may be related to several factors including variations in the influence of atmospheric circulation along the southern Cape coastal plain, differing catchment dynamics and/or marine reservoir effects affecting the age-depth models. The occurrences of age reversals in the Eilandvlei (EV10.1) and Swartvlei (SV10.1) records, as well as the possibility of a marine reservoir effect, may suggest that the chronology has a degree of uncertainty, however as outlined in Chapters 5.2.1, 5.3.1 and 7.2.1 a robust age-depth model has been formulated when lake level fluctuations are taken into account. Notwithstanding, the evidence provided has given a detailed account of the limnological development of each individual system and the region as a whole during the late Holocene. The use of diatoms as a proxy has revealed the natural variability in water quality in the lake systems and how this variability is in response to climatic drivers; this was achieved in both quantitative and qualitative approaches. These approaches included using modern indices (IPS) on the palaeo-record, conducting isotopic analysis on the silicate frustules and assigning autecological preferences to the diatom assemblage to reconstruct environmental conditions. The variety of approaches available through diatom analysis affords for a well-rounded and comparable reconstruction. Additionally, the potential of coastal lakes in recording lateral shifts in marine influences, as well as the effects and recovery on the lake ecosystem has been well documented particularly in the Wilderness records (see 6.1 and 6.3). The changes observed during this analysis appear to be the result of the interplay of natural processes within the watershed and the region during the Holocene and increased human influence over the last few centuries.

While this project has contributed knowledge of environmental conditions during the late Holocene and suitably resolved the aims and objectives as outlined in the introduction and addressed above, additional proxies may provide supplementary as well as complimentary information, which ultimately will afford a far more detailed account for each region, for instance pollen analysis will assist in verifying claims of wetland encroachment and therefore assist in the landscape reconstruction. Furthermore, knowledge of the modern distribution of both marine and lacustrine diatoms will assist in the validation of hypotheses presented in the above chapters and should be undertaken in the future. Nevertheless,

the Wilderness and Cape Flats sites have proven to be a vital source of information pertaining to the evolution of their respective regions and have demonstrated themselves as excellent receptors to changes in external environmental processes, documenting these variations in fossil rich sediments. This project has clearly demonstrated the viability of diatoms as a proxy for environmental change in South African records in both a qualitative and quantitative capacity. Future research in South Africa should attempt to include this proxy in not only a supplementary capacity to other biological proxies but as a stand-alone indicator that is far more sensitive to environmental fluctuations.

REFERENCES

Abdi, H., Williams, L.J., 2005. Principal component analysis. Wiley Interdisciplinary Reviews: Computational Statistics 2, 433–459.

Abrantes, F., Lopes, C., Mix, A., Pisias, N., 2007. Diatoms in Southeast Pacific surface sediments reflect environmental properties. Quaternary Science Reviews 26, 155–169.

Adams, J., Bate, G., 1994. The freshwater requirements of estuarine plants incorporating the development of an estuarine decision support system. WRC Report No 292/2/94. Water Research Commission. Pretoria

Aleem, A., 1950. Distribution and ecology of British marine littoral diatoms. Journal of ecology 38, 75–106.

Allanson, B., 2001. Some factors governing the water quality of microtidal estuaries in South Africa. Water SA 27, 373–386.

Allanson, B., Whitfield, A., 1983. The Limnology of the Touw River Floodplain, South African National scientific programmes report No. 79. South African National Scientific. Port Elizabeth.

Anderson, N., 1995. Using the past to predict the future: lake sediments and the modelling of limnological disturbance. Ecological Modelling 78, 149–172.

Anderson, P.M., O'Farrell, P.J., 2012. An Ecological View of the History of the City of Cape Town. Ecology and Society 17.

Avery, D., 1997. Micromammals and the Holocene environment of Rose Cottage cave. South African journal of science 93, 445–448.

Baars, J., 1979. Autecological investigations on marine diatoms. I. Experimental results in biogeographical studies. Hydrobiological Bulletin 13, 123–137.

Backeberg, B.C., Penven, P., Rouault, M., 2012. Impact of intensified Indian Ocean winds on mesoscale variability in the Agulhas system. Nature Climate Change 2, 608–612.

Bao, R., Alonso, A., Delgado, C., Pagés, J., 2007. Identification of the main driving mechanisms in the evolution of a small coastal wetland (Traba, Galicia, NW Spain) since its origin 5700 cal yr BP. Palaeogeography, Palaeoclimatology, Palaeoecology 247, 296–312.

Barker, S., Diz, P., Vautravers, M.J., Pike, J., Knorr, G., Hall, I.R., Broecker, W.S., 2009. Interhemispheric Atlantic seesaw response during the last deglaciation. Nature 457, 1097–102.

Barlow, R., Lamont, T., Kyewalyanga, M., Sessions, H., Morris, T., 2010. Phytoplankton production and physiological adaptation on the southeastern shelf of the Agulhas ecosystem. Continental Shelf Research 30, 1472–1486.

Bar-Matthews, M., Marean, C.W., Jacobs, Z., Karkanas, P., Fisher, E.C., Herries, A.I., Brown, K., Williams, H.M., Bernatchez, J., Ayalon, A., Nilssen, P.J., 2010. A high resolution and continuous isotopic speleothem record of paleoclimate and paleoenvironment from 90 to 53 ka from Pinnacle Point on the south coast of South Africa. Quaternary Science Reviews 29, 2131–2145.

Barron, J.A., Bukry, D., Bischoff, J.L., 2004. High resolution paleoceanography of the Guaymas Basin, Gulf of California, during the past 15 000 years. Marine Micropaleontology 50, 185–207.

Bate, G., Smailes, P., Adams, J., 2004. A water quality index for use with diatoms in the assessment of rivers. Water SA 30, 493–498.

Bateman, M.D., Carr, A.S., Dunajko, A.C., Holmes, P.J., Roberts, D.L., Mclaren, S.J., Bryant, R.G., Marker, M.E., Murray-Wallace, C. V, 2011. The evolution of coastal barrier systems: a case study of the Middle-Late Pleistocene Wilderness barriers, South Africa. Quaternary Science Reviews 30, 63–81.

Battarbee, R., 1999. The importance of palaeolimnology to lake restoration. Hydrobiologia 395/396, 149–159.

Battarbee, R.W., 1986. Diatom Analysis, in: Berglund, B. (Ed.), Handbook of Holocene Palaeoecology and Palaeohydrology. John Wiley & Sons Ltd., United States, pp. 527–570.

Battarbee, R.W., Charles, D.F., Bigler, C., Cumming, B.F., Renberg, I., 2010. Diatoms as indicators of surface-water acidity, in: Smol, J.P., Stoermer, E.F. (Eds.), The Diatoms: Applications for the Environmental and Earth Sciences. Cambridge University Press, New York, pp. 98–121.

Battegazzore, M., Morisi, A., Gallino, B., Fenoglio, S., 2004. Environmental Quality Evaluation of Alpine Springs in Nw Italy Using Benthic Diatoms. Diatom Research 19, 149–165.

Baxter, A., Meadows, M., 1999. Evidence for Holocene sea level change at verlorenvlei, western cape, South Africa. Quaternary International 56, 65–79.

Baxter, A.J., 1989. Pollen analysis of a Table Mountain cave deposit. Honours Thesis. University of Cape Town.

Baxter, A.J., 1997. Late quaternary palaeoenvironments of the Sandveld, Western Cape Province, South Africa. Doctoral Thesis. University of Cape Town.

Beal, L.M., De Ruijter, W.P.M., Biastoch, A., Zahn, R., 2011. On the role of the Agulhas system in ocean circulation and climate. Nature 472, 429–36.

Bennion, H., Sayer, C.D., Tibby, J., Carrick, H.J., 2010. Diatoms as indicators of environmental change in shallow lakes, in: Smol, J.P., Stoermer, E.F. (Eds.), The Diatoms: Applications for the Environmental and Earth Sciences. Cambridge University Press, New York, pp. 152–173.

Bere, T., Tundisi, J.G., 2010. The Effects of Substrate Type on Diatom-Based Multivariate Water Quality Assessment in a Tropical River (Monjolinho), São Carlos, SP, Brazil. Water, Air, & Soil Pollution 216, 391–409.

Biastoch, A., Böning, C., Schwarzkopf, F., Lutjeharms, J., 2009. Increase in Agulhas leakage due to poleward shift of Southern Hemisphere westerlies. Nature 462, 495–8.

Bickerton, I., 1982. Estuaries of the Cape: Part II synopses of available infomation on individual systems: Zeekoe (CSW 5). Report 414. Council of Scientific and Indistrial Research. Pretoria

Birch, G., Du Plessis, A., Willis, J., 1978. Offshore and onland geological and geophysical investigations in the Wilderness Lakes region. Transactions of the Geological Society of South Africa 81, 339–352.

Birks, H., 1996. Contributions of Quaternary palaeoecology to nature conservation. Journal of Vegetation Science 7, 89–98.

Blaauw, M., 2010. Methods and code for “classical” age-modelling of radiocarbon sequences. Quaternary Geochronology 5, 512–518.

Bond, G., Kromer, B., Beer, J., Muscheler, R., Evans, M., Showers, W., Hoffmann, S., Lotti-bond, R., Hajdas, I., Bonani, G., 2001. Persistent solar influence on North Atlantic climate during the Holocene. Science 294, 2130–2136.

Bradbury, J.P., 1999. Continental diatoms as indicators of long-term environmental change, in: Stoermer, E.F., Smol, J.P. (Eds.), The Diatoms: Applications for the Environmental and Earth Sciences. Cambridge University Press, Cambridge, UK, pp. 169–182.

Bradshaw, E.G., Rasmussen, P., Nielsen, H., Anderson, N.J., 2005. Mid- to late-Holocene land-use change and lake development at Dallund Sø, Denmark: trends in lake primary production as reflected by algal and macrophyte remains. The Holocene 15, 1130–1142.

Broecker, W.S., 2001. Was the Medieval Warm Period Global? Science 291, 1497–1499.

Brook, G., Scott, L., Railsback, L., Goddard, E., 2010. A 35ka pollen and isotope record of environmental change along the southern margin of the Kalahari from a stalagmite and animal dung deposits in Wonderwerk Cave, South Africa. Journal of Arid Environments 74, 870–884.

Brown, C., Magoba, R., 2009. Rivers and Wetlands of Cape Town: caring for our rich aquatic heritage. Report No TT 376/08. Water Research Commission. Pretoria

Brundrit, G., 1995. Trends of southern African sea level: statistical analysis and interpretation. South African Journal of Marine Science 16, 9–17.

Brundrit, G., Cartwright, A., 2012. Understanding the risks to Cape Town of inundation from the sea, in: Cartwright, A., Parnell, S., Oelofse, G., Ward, S. (Eds.), Climate Change at the City Scale: Impacts, Mitigation and Adaptation in Cape Town. Routledge, Cape Town, South Africa, pp. 21–37.

Butzer, K., Helgren, D., 1972. Late Cenozoic evolution of the Cape coast between Knysna and Cape St. Francis, South Africa. Quaternary Research 2, 143–169.

Caley, T., Kim, J.-H., Malaizé, B., Giraudeau, J., Laepple, T., Caillon, N., Charlier, K., Rebaubier, H., Rossignol, L., Castañeda, I.S., Schouten, S., Sinninghe Damsté, J., 2011. High-latitude obliquity as a dominant forcing in the Agulhas current system. Climate of the Past 7, 1285–1296.

Carr, A.S., Bateman, M.D., Roberts, D.L., Murray-Wallace, C. V., Jacobs, Z., Holmes, P.J., 2010. The last interglacial sea-level high stand on the southern Cape coastline of South Africa. Quaternary Research 73, 351–363.

Carr, A.S., Thomas, D.S., Bateman, M.D., 2006a. Climatic and sea level controls on Late Quaternary eolian activity on the Agulhas Plain, South Africa. Quaternary Research 65, 252–263.

Carr, A.S., Thomas, D.S., Bateman, M.D., Meadows, M.E., Chase, B., 2006b. Late Quaternary palaeoenvironments of the winter-rainfall zone of southern Africa: Palynological and sedimentological evidence from the Agulhas Plain. Palaeogeography, Palaeoclimatology, Palaeoecology 239, 147–165.

Cartwright, C., Parkington, J., 1997. The wood charcoal assemblages from Elands Bay Cave, south-western Cape – principles, procedures and preliminary interpretation. South African Archaeological Bulletin 52, 59–72.

Chase, B., 2005. Late Quaternary palaeoenvironment of the west coast of South Africa: the aeolian record. Doctoral Thesis. University of Oxford.

Chase, B., Meadows, M., Scott, L., Thomas, D., Marais, E., Sealy, J., Reimer, P., 2009. A record of rapid Holocene climate change preserved in hyrax middens from southwestern Africa. Geology 37, 703–706.

Chase, B., Meadows, M.E., 2007. Late Quaternary dynamics of southern Africa's winter rainfall zone. Earth-Science Reviews 84, 103–138.

Chase, B.M., Boom, A., Carr, A.S., Meadows, M.E., Reimer, P.J., 2013. Holocene climate change in southernmost South Africa: rock hyrax middens record shifts in the southern westerlies. Quaternary Science Reviews.

Chase, B.M., Meadows, M.E., Carr, A.S., Reimer, P.J., 2010. Evidence for progressive Holocene aridification in southern Africa recorded in Namibian hyrax middens: Implications for African Monsoon dynamics and the "'African Humid Period'". Quaternary Research 74, 36–45.

Chen, Y., Durbin, E.G., 1994. Effects of pH on the growth and carbon uptake of marine phytoplankton. Marine Ecology Progress Series 109, 83-94.

Clausnitzer, S., 2011. Bathymetrische und flachseismische Auswertung hydroakustischer Profile der Seen Eilandvlei, Rondevlei und Swartvlei im Garden Route National Park Wilderness Coastal Section, Südafrika. Bachelors Thesis. Friedrich-Schiller-Universität.

Cohen, A., Parkington, J., Brundrit, G.B., van der Merwe, N., 1992. A Holocene marine climate record in mollusc shells from the southwest African coast. Quaternary Research 38, 379–385.

Cohen, A., Tyson, P., 1995. Sea-surface temperature fluctuations during the Holocene off the south coast of Africa: implications for terrestrial climate and rainfall. The Holocene 5, 304–312.

Compton, J., 2001. Holocene sea-level fluctuations inferred from the evolution of depositional environments of the southern Langebaan Lagoon salt marsh, South Africa. The Holocene 11, 395–405.

Cooper, S., 1999. Estuarine paleoenvironmental reconstructions using diatoms, in: Stoermer, E.F., Smol, J.P. (Eds.), The Diatoms: Applications for the Environmental and Earth Sciences. Cambridge University Press, Cambridge, UK, pp. 352–373.

Cooper, S., Gaiser, E., Wachnicka, A., 2010. Estuarine paleoenvironmental reconstructions using diatoms, in: Smol, J.P., Stoermer, E.F. (Eds.), The Diatoms: Applications for the Environmental and Earth Sciences. Cambridge University Press, New York, pp. 324–345.

Cowling, R., 1983. Phytochorology and vegetation history in the south-eastern Cape, South Africa. Journal of Biogeography 10, 393–419.

Cowling, R., Cartwright, C., Parkington, J., Allsopp, J., 1999. Fossil wood charcoal assemblages from Elands Bay Cave, South Africa: implications for Late Quaternary vegetation and climates in the winter-rainfall fynbos biome. Journal of Biogeography 26, 367–378.

Cowling, R.M., Holmes, P.M., 1992. Endemism and speciation in a lowland flora from the Cape Floristic Region. Biological Journal of the Linnean Society 47, 367–383.

Cowling, R.M., Procheş, S., Partridge, T.C., 2009. Explaining the uniqueness of the Cape flora: incorporating geomorphic evolution as a factor for explaining its diversification. Molecular Phylogenetics and Evolution 51, 64–74.

Cremer, H., Wagner, B., 2003. The diatom flora in the ultra-oligotrophic Lake El'gygytgyn, Chukotka. Polar Biology 26, 105–114.

Croome, R., Tyler, P., 1973. Plankton populations of Lake Leake and Tooms Lake—oligotrophic Tasmanian lakes. British Phycological Journal 8, 239–247.

Damm, B., Hagedorn, J., 2010. Holocene floodplain formation in the southern Cape region, South Africa. Geomorphology 122, 213–222.

Das, S.K., Routh, J., Roychoudhury, A.N., 2008a. Biomarker evidence of macrophyte and plankton community changes in Zeekoevlei, a shallow lake in South Africa. Journal of Paleolimnology 41, 507–521.

Das, S.K., Routh, J., Roychoudhury, A.N., Klump, J.V., Ranjan, R.K., 2008b. Phosphorus dynamics in shallow eutrophic lakes: an example from Zeekoevlei, South Africa. Hydrobiologia 619, 55–66.

Dawson, S., 2007. Diatom biostratigraphy of tsunami deposits: Examples from the 1998 Papua New Guinea tsunami. Sedimentary Geology 200, 328–335.

De Vries, T., Schrader, H., 1981. Variation of upwelling/oceanic conditions during the latest Pleistocene through Holocene off the central Peruvian coast: A diatom record. Marine Micropaleontology 6, 157–167.

Deacon, H., 1995. Two late Pleistocene-Holocene archaeological depositories from the southern Cape, South Africa. The South African Archaeological Bulletin 50, 121–131.

Deacon, H., Geleijnse, V., 1988. The stratigraphy and sedimentology of the main site sequence, Klasies River, South Africa. The South African Archaeological Bulletin 43, 5–14.

Deacon, J., 1978. Changing patterns in the late Pleistocene/early Holocene prehistory of southern Africa as seen from the Nelson Bay Cave stone artifact sequence. Quaternary Research 10, 84–111.

Denys, L., de Wolf, H., 1999. Diatoms as indicators of coastal paleoenvironments and relative sea-level change, in: Stoermer, E.F., Smol, J.P. (Eds.), The Diatoms: Applications for the Environmental and Earth Sciences. Cambridge University Press, Cambridge, UK, pp. 277 – 297.

Dewar, G., Reimer, P., Sealy, J., Woodborne, S., 2012. Late-Holocene marine radiocarbon reservoir correction (ΔR) for the west coast of South Africa. The Holocene 22, 1481–1489.

Duller, G.A., Jacobs, Z., Wintle, A.G., Henshilwood, C.S., 2006. Extending the chronology of deposits at Blombos Cave, South Africa, back to 140 ka using optical dating of single and multiple grains of quartz. Journal of Human Evolution 51, 255–273.

Dunajko, A.C., Bateman, M.D., 2010. Sediment provenance of the Wilderness barrier dunes, southern Cape coast, South Africa. Terra Nova 22, 417–423.

Dunwiddie, P., LaMarche, V., 1980. A climatically responsive tree-ring record from Widdringtonia cedarbergensis, Cape Province, South Africa. Nature 286, 796–797.

Eddy, J.A., 1976. The Maunder Minimum. Science 192, 1189–202.

Eddy, J.A., 1983. The Maunder Minimum - A reappraisal. Solar Physics 89, 195–207.

Engelhart, S., Horton, B., Douglas, B., Peltier, W., Tornqvist, T., 2009. Spatial variability of late Holocene and 20th century sea-level rise along the Atlantic coast of the United States. Geology 37, 1115–1118.

Eshel, G., Levy, G., Mingelgrin, U., Singe, M., 2004. Critical evaluation of the use of laser diffraction for particle-size distribution analysis. Soil Science Society of America Journal 68, 736–743.

Espinosa, M., de Francesco, C., Isla, F., 2003. Paleoenvironmental reconstruction of Holocene coastal depositsfrom the Southeastern Buenos Aires Province, Argentina. Journal of Paleolimnology 29, 49–60.

Farmer, E.C., DeMenocal, P.B., Marchitto, T.M., 2005. Holocene and deglacial ocean temperature variability in the Benguela upwelling region: Implications for low-latitude atmospheric circulation. Paleoceanography 20, 1–16.

Finch, J., Hill, T., 2008. A late Quaternary pollen sequence from Mfabeni Peatland, South Africa: Reconstructing forest history in Maputaland. Quaternary Research 70, 442–450.

Findlay, D., Kling, H., Rönicke, H., Findlay, W., 1998. A paleolimnological study of eutrophied Lake Arendsee (Germany). Journal of Paleolimnology 19, 41–54.

Finkel, Z.V., Vaillancourt, C.J., Irwin, A.J., Reavie, E.D., Smol, J.P. 2009. Environmental control of diatom community size structure varies across aquatic ecosystems. Proceedings of the Royal Society B: Biological Sciences, 276(1662), 1627-1634.

Finkelstein, S. A., Davis, A.M., 2006. Paleoenvironmental records of water level and climatic changes from the middle to late Holocene at a Lake Erie coastal wetland, Ontario, Canada. Quaternary Research 65, 33–43.

Finne, M., Norström, E., Risberg, J., Scott, L., 2010. Siliceous microfossils as late-Quaternary paleo-environmental indicators at Braamhoek wetland, South Africa. The Holocene 20, 747–760.

Franceschini, G., Compton, J.S., Wigley, R.A., 2003. Sand transport along the Western Cape coast: gone with the wind? South African Journal Of Science 99, 317–318.

Franz, S., 2012. Geochemische und sedimentologische Untersuchungen von Seesedimenten des Swartvleis zur Rekonstruktion der spätholozänen Landschaftsentwicklung im Garden Route National Park, Südafrika. Master Thesis. Friedrich-Schiller-Universität Jena.

Fritz, S.C., Cumming, B.F., Gasse, F., Laird, K.R., 1999. Diatoms as indicators of hydrologic and climatic change in saline lakes, in: Stoermer, E.F., Smol, J.P. (Eds.), The Diatoms: Applications for the Environmental and Earth Sciences. Cambridge University Press, Cambridge, UK, pp. 41–72.

Fritz, S.C., Cumming, B.F., Gasse, F., Laird, K.R., 2010. Diatoms as indicators of hydrologic and climatic change in saline lakes, in: Smol, J.P., Stoermer, E.F. (Eds.), The Diatoms: Applications for the Environmental and Earth Sciences. Cambridge University Press, New York, pp. 186–208.

Gaiser, E., Ruhland, K., 2010. Diatoms as indicators of environmental change in wetlands and peatlands, in: Smol, J.P., Stoermer, E.F. (Eds.), The Diatoms: Applications for the Environmental and Earth Sciences. Cambridge University Press, New York, pp. 473–496.

Gasse, F., Juggins, S., Khelifa, L., 1995. Diatom-based transfer functions for inferring past hydrochemical characteristics of African lakes. Palaeogeography, Palaeoclimatology, Palaeoecology 117, 31–54.

Gee, G., Or, D., 2002. Particle-size analysis, in: Dane, J., Topp, C. (Eds.), Methods of Soil Analysis. Part 4: Physical Methods. Soil Science Society of America Book Series, Madison, Wisconsin, pp. 255–293.

Geldenhuys, C., 1993. Floristic composition of the southern Cape forests with an annotated checklist. South African Journal of Botany 59, 26–44.

Gell, P., Tibby, J., Little, F., Baldwin, D., Hancock, G., 2007. The impact of regulation and salinisation on floodplain lakes: the lower River Murray, Australia. Hydrobiologia 591, 135–146.

Gell, P.A., Sluiter, I.R., Fluin, J., 2002. Seasonal and interannual variations in diatom assemblages in Murray River connected wetlands in north-west Victoria, Australia. Marine and Freshwater Research 53, 981.

Georgiou, N., 2011. Reconstructing Late Quaternary Environments Using Sediment Analysis: Princess Vlei, Cape Town. Bachelor (Honours) Thesis. University of Cape Town.

Giffen, M., 1973. Diatoms of the marine littoral of Steenberg's Cove in St. Helena Bay, Cape Province, South Africa. Botanica marina 16, 32–48.

Gordon, N., García-Rodríguez, F., Adams, J., 2012. Paleolimnology of a coastal lake on the Southern Cape coast of South Africa: Sediment geochemistry and diatom distribution. Journal of African Earth Sciences 75, 14–24.

Gotelli, N., Colwell, R., 2001. Quantifying biodiversity: procedures and pitfalls in the measurement and comparison of species richness. Ecology letters 4, 379–391.

Grimm, E., 1997. TILIA: A Pollen Program for Analysis and Display, Book. Illinois State Museum, Springfield.

Grimm, E.C., 1987. CONISS: a FORTRAN 77 program for stratigraphically constrained cluster analysis by the method of incremental sum of squares. Computers & Geosciences 13, 13–35.

Grindley, J., Rogers, J., Pether, J., Woodborne, M., 1988. Holocene evolution of Rietvlei near Cape Town, deduced from the palaeoecology of some mid-Holocene estuarine Mollusca. Palaeoecology of Africa 19, 347–353.

Grine, F., Klein, R., Volman, T., 1991. Dating, archaeology and human fossils from the Middle Stone Age levels of Die Kelders, South Africa. Journal of Human Evolution 21, 363–395.

Grubb, P., 1977. The maintenance of Species-Richness in Plant Communities: the Importance of the Regeneration Niche. Biological Reviews 52, 107–145.

Hall, R., Smol, J., 1999. Diatoms as indicators of lake eutrophication, in: Stoermer, E.F., Smol, J.P. (Eds.), The Diatoms: Applications for the Environmental and Earth Sciences. Cambridge University Press, Cambridge, UK, pp. 128–168.

Hall, R.I., Smol, J.P., 2010. Diatoms as indicators of lake eutrophication, in: Smol, J.P., Stoermer, E.F. (Eds.), The Diatoms: Applications for the Environmental and Earth Sciences. Cambridge University Press, New York, pp. 122–151.

Harding, W., 1992. A contribution to the knowledge of South African coastal vleis: The limnology and phytoplankton periodicity of Princess Vlei, Cape Peninsula. Water SA 18, 121–130.

Harding, W., 1997. Phytoplankton primary production in a shallow, well-mixed, hypertrophic South African lake. Hydrobiologia 344, 87–102.

Harding, W., Taylor, J., 2011. The South African diatom index (SADI) – A preliminary index for indicating water quality in rivers and streams in Southern Africa. Working Paper.

Harding, W., Wright, S., 1999. Initial Findings Regarding changes in phyto- and zooplankton composition and abundance following the temporary draw down and refilling of a shallow, hypertrophic South African coastal lake. Lake and Reservoir Management 15, 47–53.

Harper, M., 1969. Movement and migration of diatoms on sand grains. British Phycological Journal 4, 97–103.

Harris, C., Burgers, C., Miller, J., Rawoot, F., 2010. O- and H-Isotope Record of Cape Town Rainfall From 1996 To 2008, and Its Application To Recharge Studies of Table Mountain Groundwater, South Africa. South African Journal of Geology 113, 33–56.

Harris, C., Oom, B., Diamond, R., 1999. A preliminary investigation of the oxygen and hydrogen isotope hydrology of the greater Cape Town area and an assessment of the potential for using stable. Water SA 25, 15–24.

Harrison, A., 1962. Hydrobiological studies on alkaline and acid still waters in the Western Cape Province. Transactions of the Royal Society of South Africa 36, 213–235.

Hart, R., 1995. South African coastal lakes, Book. Department of Environmental Affairs, Pretoria, South Africa.

Hassan, F., 1997. Holocene palaeoclimates of Africa. African Archaeological Review 14, 213–230.

Hassan, G.S., Espinosa, M. A., Isla, F.I., 2006. Modern Diatom Assemblages in Surface Sediments from Estuarine Systemsin the Southeastern Buenos Aires Province, Argentina. Journal of Paleolimnology 35, 39–53.

Haynes, D., Gell, P., Tibby, J., Hancock, G., Goonan, P., 2007. Against the tide: the freshening of naturally saline coastal lakes, southeastern South Australia. Hydrobiologia 591, 165–183.

Hellström, G., 1996. Preliminary investigations into recent changes of the Goukamma Nature Reserve frontal dune system, South Africa—With management implications. Landscape and Urban Planning 34, 225–235.

Hendrarto, I.B., Nitisuparjo, M., 2011. Biodiversity of benthic diatom and primary productivity of benthic micro-flora in mangrove forests on central Java. Journal of Coastal Development 14, 131–140.

Henshilwood, C., D'Errico, F., Marean, C., Milo, R.G., Yates, R., 2001. An early bone tool industry from the Middle Stone Age at Blombos Cave, South Africa: implications for the origins of modern human behaviour, symbolism and language. Journal of human evolution 41, 631–678.

Hodgson, D., Tyler, P., Vyverman, W., 1996. The palaeolimnology of Lake Fidler, a meromictic lake in south west Tasmania and the significance of recent human impact. Journal of Paleolimnology 18, 313–333.

Hogg, A.G., Hua, Q., Blackwell, P.G., Niu, M., Buck, C.E., Guilderson, T.P., Heaton, T.J., Palmer, J.G., Reimer, P.J., Reimer, R.W., Turney, C.S.M., Zimmerman, S.R.H., 2013. SHCal13 southern hemisphere calibration, 0–50,000 years cal BP. Radiocarbon 55, 1889–1903.

Holmes, P.M., Rebelo, A.G., Dorse, C., Wood, J., 2012. Can Cape Town's unique biodiversity be saved? Balancing conservation imperatives and development needs. Ecology and Society 17.

Holmgren, K., Karlen, W., Lauritzen, S., Lee-Thorp, J., Partridge, T., Piketh, S., Repinski, P., Stevenson, C., Svanered, O., Tyson, P., Karlén, W., 1999. A 3000-year high-resolution stalagmitebased record of palaeoclimate for northeastern South Africa. The Holocene 9, 295–309.

Horton, B., Corbett, R., Culver, S., Edwards, R., Hillier, C., 2006. Modern saltmarsh diatom distributions of the Outer Banks, North Carolina, and the development of a transfer function for high resolution reconstructions of sea level. Estuarine, Coastal and Shelf Science 69, 381–394.

Horton, B.P., Sawai, Y., 2010. Diatoms as indicators of former sea levels, earthquakes, tsunamis, and hurricanes, in: Smol, J.P., Stoermer, E.F. (Eds.), The Diatoms: Applications for the Environmental and Earth Sciences. Cambridge University Press, New York, pp. 357–372.

Howard-Williams, C., Liptrot, M.R., 1980. Submerged macrophyte communities in a brackish South African estuarine-lake system. Aquatic Botany 9, 101–116.

Huffman, T., 1996. Archaeological evidence for climatic change during the last 2000 years in southern Africa. Quaternary International 33, 55–60.

Hughes, M.K., Diaz, H.F., 1994. Was there a “Medieval Warm Period”, and if so, where and when? Climate Change 26, 109–142.

Huntley, B., 1996. Quaternary palaeoecology and ecology. Quaternary Science Reviews 15, 591–606.

Huston, M., 1979. A general hypothesis of species diversity. The American Naturalist 113, 81–101.

Illenberger, W., 1996. The geomorphologic evolution of the Wilderness dune cordons, South Africa. Quaternary International 33, 11–20.

Jacobs, R., Noten, T., 1980. The annual pattern of the diatoms in the epiphyton of eelgrass (Zostera marina L.) at Roscoff, France. Aquatic botany 8, 355–370.

James, N., Harrison, T., 2008. A preliminary survey of the estuaries on the south coast of South Africa, Cape St Blaize, Mossel Bay—Robberg Peninsula, Plettenberg Bay, with particular reference to. Transactions of the Royal Society of South Africa 63, 111–127.

Jerardino, A., 1993. Mid-Holocene to late-Holocene sea-level fluctuations-the archaeological evidence at Tortoise Cave, south-western Cape, South-Africa. South African Journal of Science 89, 481–488.

Jerardino, A., 1995. late Holocene Neoglacial episodes in southern South America and southern Africa: a comparison. The Holocene 5, 361–368.

Jerardino, A., 1997. Changes in shellfish species composition and mean shell size from a late-Holocene record of the west coast of southern Africa. Journal of Archaeological Science 24, 1031–1044.

Jiang, Y., Xu, Z., 1986. On the Spörer Minimum. Astrophysics and Space Science 118, 159–162.

Johansen, J.R., 2010. Diatoms of aerial habitats, in: Smol, J.P., Stoermer, E.F. (Eds.), The Diatoms: Applications for the Environmental and Earth Sciences. Cambridge University Press, New York, pp. 465–472.

Jolliffe, I., 2002. Principal Component Analysis, Book. Springer, New York, USA.

Jones, M., Tyson, P., Cooper, G., 1999. Modelling climatic change in South Africa from perturbed borehole temperature profiles. Quaternary International 57/58, 185–192.

Jordan, R.W., Stickley, C.E., 2010. Diatoms as indicators of paleoceanographic events, in: Smol, J.P., Stoermer, E.F. (Eds.), The Diatoms: Applications for the Environmental and Earth Sciences. Cambridge University Press, New York, pp. 424–453.

Julius, M.L., Theriot, E.C., 2010. The diatoms: a primer, in: Smol, J.P., Stoermer, E.F. (Eds.), The Diatoms: Applications for the Environmental and Earth Sciences. Cambridge University Press, New York, pp. 8–22.

Kain, H., Schultze, E., 1886. On a fossil marine diatomaceous deposit from Atlantic City, N. J.—II. Bulletin of the Torrey Botanical Club 13, 207–210.

Kelly, M., Bennion, H., Cox, E., Goldsmith, B., Jamieson, J., Juggins, S., Mann, D., Telford, R., 2005. Common freshwater diatoms of Britain and Ireland: an interactive key. Bristol. [URL: http://craticula.ncl.ac.uk/EADiatomKey/html/taxa.html]

Kingston, H., 1900. Notes on Some Caves in the Tzitzikama or Outeniqua District, Near Knysna, South Africa, and the Objects Found Therein. Journal of the Anthropological Institute of Great Britain and Ireland 30, 45–49.

Kirsten, K., 2008. Holocene Environmental Change at Groenvlei, Knysna, South Africa: Evidence from Diatoms. Master Thesis. University of Cape Town.

Klein, R., 1979. Paleoenvironmental and cultural implications of late Holocene archaeological faunas from the Orange Free State and north-central Cape Province, South Africa. The South African Archaeological Bulletin 34, 34–49.

Kotzé, P., 2011. Princessvlei – Tug of war over Cape Flats wetland continues. The Water Wheel 10, 18–21.

Kruger, A., 2002. Climate of South Africa: surface winds. WS43. South African Weather Service. Pretoria, South Africa.

Kruger, A., 2004a. Climate of South Africa: climate controls. WS45. South African Weather Service. Pretoria, South Africa.

Kruger, A., 2004b. Climate of South Africa: climate regions. WS45. South African Weather Service. Pretoria, South Africa.

Lamy, F., Hebbeln, D., Röhl, U., Wefer, G., 2001. Holocene rainfall variability in southern Chile: a marine record of latitudinal shifts of the Southern Westerlies. Earth and Planetary Science Letters 185, 369–382.

Lamy, F., Kilian, R., Arz, H.W., Francois, J.-P., Kaiser, J., Prange, M., Steinke, T., 2010. Holocene changes in the position and intensity of the southern westerly wind belt. Nature Geoscience 3, 695–699.

Lawrence, D., 1971. The nature and structure of paleoecology. Journal of Paleontology 45, 593–607.

Lawson, M., Thomas, D., 2002. Late Quaternary lunette dune sedimentation in the southwestern Kalahari desert, South Africa: luminescence based chronologies of aeolian activity. Quaternary Science Reviews 21, 825–836.

Leduc, G., Herbert, C.T., Blanz, T., Martinez, P., Schneider, R., 2010. Contrasting evolution of sea surface temperature in the Benguela upwelling system under natural and anthropogenic climate forcings. Geophysical Research Letters 37, 1–5.

Lee-Thorp, J., Holmgren, K., Lauritzen, S.-E., Linge, H., Moberg, A., Partridge, T., Stevenson, C., Tyson, P., 2001. Rapid climate shifts in the southern African interior throughout the Mid to late Holocene. Geophysical Research Letters 28, 4507–4510.

Leng, M.J., Barker, P. A., 2006. A review of the oxygen isotope composition of lacustrine diatom silica for palaeoclimate reconstruction. Earth-Science Reviews 75, 5–27.

Leng, M.J., Swann, G.E., 2010. Stable isotopes from diatom silica, in: Smol, J.P., Stoermer, E.F. (Eds.), The Diatoms: Applications for the Environmental and Earth Sciences. Cambridge University Press, New York, pp. 575–589.

Leventer, A., Crosta, X., Pike, J., 2010. Holocene marine diatom records of environmental change, in: Smol, J.P., Stoermer, E.F. (Eds.), The Diatoms: Applications for the Environmental and Earth Sciences. Cambridge University Press, New York, pp. 401–423.

Lewis, C., 2005. Late Glacial and Holocene palaeoclimatology of the Drakensberg of the Eastern Cape, South Africa. Quaternary International 129, 33–48.

Lewis, C.A., 2008. Late Quaternary climatic changes, and associated human responses, during the last ~45000 yr in the Eastern and adjoining Western Cape, South Africa. Earth-Science Reviews 88, 167–187.

Linder, H., Meadows, M., Cowling, R., 1992. History of the Cape Flora, in: Cowling, R. (Ed.), The Ecology of Fynbos: Nutrients, Fire and Diversity. Oxford University Press, Cape Town, South Africa, pp. 113–134.

Long, A.J., Woodroffe, S.A., Milne, G.A., Bryant, C.L., Wake, L.M., 2010. Relative sea level change in west Greenland during the last millennium. Quaternary Science Reviews 29, 367–383.

Lowag, J., van den Heuvel, M., 2000. Advanced Sub-bottom Profiler Equipment for Soil Investigation Campaigns During Dredging Projects. Port Technology International 1–4.

Lowe, J., Walker, M., 1984. Reconstructing quaternary environments, First. ed, Book. Longman Group Limited, London, UK.

Lutjeharms, J., Monteiro, P., Tyson, P., Obura, D., 2001. The oceans around southern Africa and regional effects of global change. South African Journal of Science 97, 119–130.

Magurran, A.E., 2004. Measuring biological diversity, Book. Blackwell Publishing Science Ltd., Oxford, UK.

Main, S., McIntire, C., 1974. The distribution of epiphytic diatoms in Yaquina Estuary, Oregon (USA). Botanica Marina XVII, 88–99.

Mann, M.E., 2007. Climate Over the Past Two Millennia. Annual Review of Earth and Planetary Sciences 35, 111–136.

Manning, M., Melhuish, W., 1994. δ14CO2 record from Wellington, in: Boden, T., Kaiser, D., Sepanski, R., Stoss, F. (Eds.), Trends 93 - A Compendium of Data on Global Change and Online Updates. Carbon Dioxide Information Analysis Center, Oak Ridge National Laboratory, Oak Ridge, TN, USA.

Marean, C., 1985. The faunal remains from Smitswinkelbaai Cave, Cape Peninsula. The South African Archaeological Bulletin 40, 100–102.

Marean, C., Abe, Y., Frey, C., Randall, R., 2000. Zooarchaeological and taphonomic analysis of the Die Kelders Cave 1 Layers 10 and 11 Middle Stone Age larger mammal fauna. Journal of Human Evolution 38, 197–233.

Marean, C.W., 2010. Pinnacle Point Cave 13B (Western Cape Province, South Africa) in context: The Cape Floral kingdom, shellfish, and modern human origins. Journal of human evolution 59, 425–43.

Marker, M., Holmes, P., 2002. The distribution and environmental implications of coversand deposits in the Southern Cape, South Africa. South African Journal of Geology 105, 135–146.

Marker, M., Miller, D., 1995. Further evidence of a Holocene high sea-level at Knysna. South African Journal Of Science 91, 392.

Marshall, H.G., Alden, R.W., 1990. A Comparison of Phytoplankton Assemblages and Environmental Relationships in Three Estuarine Rivers of the Lower Chesapeake Bay. Estuaries 13, 287–300.

Martin, A., 1956. The ecology and history of Groenvlei. South African Journal of Science 52, 187–192.

Martin, A., 1959. The stratigraphy and history of Groenvlei, a South African coastal fen. Australian Journal of Botany 7, 142–167.

Martin, A., 1960a. The Ecology of Groenvlei , A South African Fen: Part II. The Secondary Communities. The Journal of Ecology 48, 307–329.

Martin, A., 1960b. The Ecology of Groenvlei , a South African Fen: Part I. The Primary Communities. The Journal of Ecology 48, 55–71.

Martin, A., 1962. Evidence relating to the Quaternary History of the Wilderness lakes. Transactions of the Geological Society of South Africa 65, 19–42.

Martin, A., 1968. Pollen analysis of Groenvlei lake sediments, Knysna (South Africa). Review of Palaeobotany and Palynology 7, 107–144.

Mason, S., Jury, M., 1997. Climatic variability and change over southern Africa: a reflection on underlying processes. Progress in Physical Geography 21, 23–50.

Mayewski, P.A., Rohling, E.E., Stager, J.C., Karlen, W., Maasch, K., Meeker, L.D., Meyerson, E., Gasse, F., Kreveld, S. Van, Holmgren, K., Lee-Thorp, J., Rosqvist, G., Rack, F., Staubwasser, M., Schneider, R.R., Steig, E.J., 2004. Holocene climate variability. Quaternary Research 62, 243–255.

McGee, D., Laws, R., Cahoon, L., 2008. Live benthic diatoms from the upper continental slope: extending the limits of marine primary production. Marine Ecology Progress Series 356, 103–112.

McGlone, M.S., Nelson, C.S., Todd, A.J., 1984. Vegetation history and environmental significance of pre-peat and surficial peat deposits at Ohinewai, Lower Waikato lowland. Journal of the Royal Society of New Zealand 14, 233–244.

McLean, R., Corrigan, J., Webster, J., 1981. Heterotrophic nutrition in Melosira nummuloides, a possible role in affecting distribution in the Clyde estuary. British Phycological Journal 16, 95–106.

McQuoid, M., Nordberg, K., 2003. The diatom Paralia sulcata as an environmental indicator species in coastal sediments. Estuarine, Coastal and Shelf Science 56, 339–354.

Meadows, M., 1988. Late Quaternary peat accumulation in southern Africa. Catena 15, 459–472.

Meadows, M., Baxter, A., Parkington, J., 1996. late Holocene environments at Verlorenvlei, Western Cape Province, South Africa. Quaternary International 33, 81–95.

Meadows, M., Chase, B., Seliane, M., 2010. Holocene palaeoenvironments of the Cederberg and Swartruggens mountains, Western Cape, South Africa: pollen and stable isotope evidence from hyrax dung. Journal of Arid Environments 74, 786–793.

Meadows, M., Sugden, J., 1993. The late Quaternary palaeoecology of a floristic kingdom: the southwestern Cape South Africa. Palaeogeography, Palaeoclimatology, Palaeoecology 101, 271–281.

Meadows, M.E., Baxter, A.J., 1999. Late Quaternary Palaeoenvironments of the southwestern Cape, South Africa: a regional synthesis. Quaternary International 57/58, 193–206.

Meadows, M.E., Baxter, A.J., 2001. Holocene vegetation history and palaeoenvironments at Klaarfontein Springs, Western Cape, South Africa. The Holocene 11, 699–706.

Meischner, D., Rumohr, J., 1974. A light-weight, high-momentum gravity corer for subaqueous sediments. Senckenbergiana maritima 6, 105–117.

Menounos, B., 1997. The water content of lake sediments and its relationship to other physical parameters: an alpine case study. The Holocene 7, 207–212.

Mihaljević, M., Pfeiffer, T.Ž., 2012. Colonization of periphyton algae in a temperate floodplain lake under a fluctuating spring hydrological regime. Fundamental and Applied Limnology / Archiv für Hydrobiologie 180, 13–25.

Miller, D., Yates, R., Jerardino, A., Parkington, J., 1995. late Holocene coastal change in the southwestern Cape, South Africa. Quaternary International 29/30, 3–10.

Miller, D., Yates, R., Parkington, J., Vogel, J., 1993. Radiocarbon-dated evidence relating to a mid-Holocene relative high sea-level on the south-western Cape coast, South Africa. South African Journal Of Science 89, 35–44.

Mittelbach, G.G., Steiner, C.F., Scheiner, S.M., Gross, K.L., Reynolds, H.L., Waide, R.B., Willig, M.R., Dodson, S.I., Gough, L., 2001. What is the observed relationship between species richness and productivity? Ecology 82, 2381–2396.

Moreno, P., Francois, J., Villamartinez, R., Moy, C., 2009. Millennial-scale variability in Southern Hemisphere westerly wind activity over the last 5000 years in SW Patagonia. Quaternary Science Reviews 28, 25–38.

Mucina, L., Rutherford, M., 2006. The vegetation of South Africa, Lesotho and Swaziland, Book. South African National Biodiversity Institute, Pretoria.

Muylaert, K., van Nieuwerburgh, L., Sabbe, K., Vyverman, W., 2002. Microphytobenthos communities in the freshwater tidal to brackish reaches of the Schelde estuary (Belgium). Belgian Journal of Botany 135, 15–26.

Myers, N., Mittermeier, R.A., Mittermeier, C.G., Da Fonseca, G.A., Kent, J., 2000. Biodiversity hotspots for conservation priorities. Nature 403(6772), 853-858.

Navarro, J., 1982. A survey of the marine diatoms of Puerto Rico V. Suborder Raphidineae: families Achnanthaceae and Naviculaceae (excluding Navicula and Mastogloia). Botanica Marina XXV, 321–338.

Neumann, F., Scott, L., Bamford, M., 2011. Climate change and human disturbance of fynbos vegetation during the late Holocene at Princess Vlei, Western Cape, South Africa. The Holocene 21, 1137–1149.

Neumann, F.H., Scott, L., Bousman, C., van As, L., 2010. A Holocene sequence of vegetation change at Lake Eteza, coastal KwaZulu-Natal, South Africa. Review of Palaeobotany and Palynology 162, 39–53.

Neumann, F.H., Stager, J.C., Scott, L., Venter, H.J., Weyhenmeyer, C., 2008. Holocene vegetation and climate records from Lake sibaya, KwaZulu-Natal (South Africa). Review of Palaeobotany and Palynology 152, 113–128.

New, M., 2002. Climate change and water resources in the southwestern Cape, South Africa. South African Journal of Science 98, 369–376.

Nicholson, S.E., 2000. The nature of rainfall variability over Africa on time scales of decades to millenia. Global and Planetary Change 26, 137–158.

Nielsen, S.H., Koç, N., Crosta, X., 2004. Holocene climate in the Atlantic sector of the Southern Ocean: Controlled by insolation or oceanic circulation? Geology 32, 317.

Niyomsilpchai, T., Aryuthaka, C., Patarajinda, S., 2009. Epiphytic diatoms on the seagrass blades, Cymodocea rotundata and Thalassia hemprichii at Ban Pa Khlok, Phuket province, in: Proceedings of the 47th Kasetsart University Annual Conference. Kasetsart, pp. 579–587.

Norström, E., Scott, L., Partridge, T., Risberg, J., Holmgren, K., 2009. Reconstruction of environmental and climate changes at Braamhoek wetland, eastern escarpment South Africa, during the last 16,000 years with emphasis on the Pleistocene–Holocene transition. Palaeogeography, Palaeoclimatology, Palaeoecology 271, 240–258.

O'Driscoll, C., de Eyto, E., Rodgers, M., O'Connor, M., Asam, Z.-Z., Xiao, L., 2012. Diatom assemblages and their associated environmental factors in upland peat forest rivers. Ecological Indicators 18, 443–451.

Oksanen, J., Blanchet, F., Kindt, R., Legendre, P., Minchin, P.R., O'Hara, R., Simpson, G.L., Soly-Mos, P., Stevens, M.H.H., Wagner, H., 2012. Package "vegan". Community Ecology Package V2.0-5 258.

Parsons, R., Harding, B., 2002. The Role of Groundwater in Determining the Quantity and Quality of Inflows to a Hypertrophic Wetland System, in: Fourth International Ecohydraulics Symposium. Cape Town, South Africa, pp. 1–7.

Peet, R., 1974. The measurement of species diversity. Annual review of ecology and systematics 5, 285–307.

Petrov, A., Nevrova, E., 2007. Database on Black Sea benthic diatoms (Bacillariophyta): its use for a comparative study of diversity pecularities under technogenic pollution impacts, in: Berghe, E. Vanden, Appeltans, W., Costello, M.J., Pissierssens, P. (Eds.), Proceedings Ocean Biodiversity Informatics. Hamburg, Germany, pp. 153–165.

Plenković-Moraj, A., Kralj, K., Gligora, M., 2008. Effect of current velocity on diatom colonization on glass slides in unpolluted headwater creek. Periodicum biologorum 110, 291–295.

Punning, J.-M., Puusepp, L., 2007. Diatom assemblages in sediments of Lake Juusa, Southern Estonia with an assessment of their habitat. Hydrobiologia 586, 27–41.

Qian, S.S., King, R., Richardson, C.J., 2003. Two statistical methods for the detection of environmental thresholds. Ecological Modelling 166, 87–97.

Raal, P., Burns, M., 1996. Mapping and conservation importance rating of the South African coastal vegetation as an aid to development planning. Landscape and Urban Planning 34, 389–400.

Rajaram, S., Oono, Y., 2010. NeatMap--non-clustering heat map alternatives in R. BMC bioinformatics 11, 45.

Ramsay, P., 1995. 9000 years of sea-level change along the southern African coastline. Quaternary International 31, 71–75.

Ramsay, P., Cooper, J.A.G., 2002. Late Quaternary Sea-Level Change in South Africa. Quaternary Research 57, 82–90.

Randall, R., 1995. Ramsar: Wilderness Lakes, South Africa. List of Wetlands of International Importance. [URL http://www.ngo.grida.no/soesa/nsoer/resource/wetland/wilderness_ris.htm]

Raunio, J., Soininen, J., 2007. A practical and sensitive approach to large river periphyton monitoring: comparative performance of methods and taxonomic levels. Boreal environment research 12, 55–63.

Read, J., Pollard, R., 1993. Structure and transport of the Antarctic circumpolar current and Agulhas return current at 40°E. Journal of Geophysical Research 98, 12281–12295.

Reason, C., Jagadheesha, D., Tadross, M., 2003. A model investigation of inter-annual winter rainfall variability over southwestern South Africa and associated ocean-atmosphere interaction. South African Journal of Science 99, 75–80.

Reavie, E.D., Edlund, M.B., 2010. Diatoms as indicators of long-term environmental change in rivers, fluvial lakes, and impoundments, in: Smol, J.P., Stoermer, E.F. (Eds.), The Diatoms: Applications for the Environmental and Earth Sciences. Cambridge University Press, New York, pp. 86–97.

Reavie, E.D., Kingston, J.C., Kireta, A.R., Axler, R.P., Stoermer, E.F., Johansen, J.R., Sgro, G. V, 2004. 2004 Progress Report : Great Lakes Diatom and Water Quality Indicators, Natural Resources Research.

Rector, A.L., Verrelli, B.C., 2010. Glacial cycling, large mammal community composition, and trophic adaptations in the Western Cape, South Africa. Journal of human evolution 58, 90–102.

Reddering, J., 1988. Evidence for a middle Holocene transgression, Keurbooms, South Africa. Palaeoecology of Africa 19, 79–86.

Reid, M.A., Ogden, R.W., 2009. Factors affecting diatom distribution in floodplain lakes of the southeast Murray Basin, Australia and implications for palaeolimnological studies. Journal of Paleolimnology 41, 453–470.

Reimer, P.J., Bard, E., Bayliss, A., Beck, J.W., Blackwell, P.G., Bronk, C., Caitlin, R., Hai, E.B., Edwards, R.L., Friedrich, M., Grootes, P.M., Guilderson, T.P., Haflidason, H., Hajdas, I., Hatté, C., Heaton, T.J., Hoffmann, D.L., Hogg, A.G., Hughen, K.A., Kaiser, K.F., Kromer, B., Manning, S.W., Niu, M., Reimer, R.W., Richards, D.A., Scott, E.M., Southon, J.R., Staff, R.A., Turney, C.S., van der Plicht, J., 2013. IntCal13 and Marine13 radiocarbon age calibration curves 0 – 50,000 years cal BP. Radiocarbon 55, 1869–1887.

Reinwarth, B., 2012. The sedimentary record of Eilandvlei, Wilderness coast area, South Africa. Master Thesis. Friedrich-Schiller-Universität Jena.

Reinwarth, B., Franz, S., Baade, J., Haberzettl, T., Kasper, T., Daut, G., Helmschrot, J., Kirsten, K.L., Quick, L.J., Meadows, M.E., Mäusbacher, R., 2013. A 700-year record on the effects of climate and human impact on the southern Cape coast inferred from lake sediments of Eilandvlei, Wilderness Embayment, South Africa. Geografiska Annaler: Series A, Physical Geography 95(4), 345-360.

Rendall, D.A., Wilkinson, M., 1986. Environmental tolerance of the estuarine diatom Melosira nummuloides (Dillw.) Ag. Journal of Experimental Marine Biology and Ecology 102, 133–151.

Richardson, D., van Wilgen, B., 2004. Invasive alien plants in South Africa: how well do we understand the ecological impacts? South African Journal Of Science 100, 45–52.

Roberts, D., Bateman, M., Murray-Wallace, C., Carr, A., Holmes, P., 2009. West coast dune plumes: Climate driven contrasts in dunefield morphogenesis along the western and southern South African coasts. Palaeogeography, Palaeoclimatology, Palaeoecology 271, 24–38.

Romero, O., Boeckel, B., Donner, B., Lavik, G., Fischer, G., Wefer, G., 2002. Seasonal productivity dynamics in the pelagic central Benguela System inferred from the flux of carbonate and silicate organisms. Journal of Marine Systems 37, 259–278.

Romero, O., Mollenhauer, G., Schneider, R., Wefer, G., 2003. Oscillations of the siliceous imprint in the central Benguela Upwelling System from MIS 3 through to the early Holocene: the influence of the Southern Ocean. Journal of Quaternary Science 18, 733–743.

Romundset, A., Lohne, Ã.S., Mangerud, J., Svendsen, J.I., 2010. The first Holocene relative sea-level curve from the middle part of Hardangerfjorden, western Norway. Boreas 39, 87–104.

Rouault, M., 2011. Ocean atmosphere interactions in and around Southern Africa, in: Backeberg, B.C., Bernard, S., Johannessen, J., Shillington, F. (Eds.), Proceedings of the Joint Nansen-Tutu Centre Scientific Opening Symposium & Oceans Africa Meeting. Nansen-Tutu Centre of Marine Environmental Research, Cape Town, South Africa, p. 78.

Rouault, M., Johannessen, J., Collard, F., Bernard, S., 2009. Synthetic aperture radar products for the African marine environment. South African Journal Of Science 105, 85–86.

Russell, I., 1999. Changes in the water quality of the Wilderness and Swartvlei Lake systems, South Africa. Koedoe 42, 57–72.

Russell, I., 2013. Spatio-temporal variability of surface water quality parameters in a South African estuarine lake system. African Journal of Aquatic Science 38, 53–66.

Russell, I., Kraaij, T., 2008. Effects of cutting Phragmites australis along an inundation gradient, with implications for managing reed encroachment in a South African estuarine lake system. Wetlands Ecology and Management 16, 383–393.

Russell, I., Randall, R., Cole, N., Kraaij, T., Kruger, N., 2012. Garden Route National Park, Wilderness Coastal Section, State of Knowledge, Report. Sedgefield, South Africa.

Saunders, K.M., Mcminn, A., Roberts, D., Hodgson, D.A., Heijnis, H., 2007. Recent human-induced salinity changes in Ramsar-listed Orielton Lagoon, south-east Tasmania, Australia: a new approach for coastal lagoon conservation and management. Aquatic Conservation: Marine and Freshwater Ecosystems 17, 51–70.

Sawai, Y., Horton, B., Nagumo, T., 2004. The development of a diatom-based transfer function along the Pacific coast of eastern Hokkaido, northern Japan-an aid in paleoseismic studies of the Kuril subduction zone. Quaternary Science Reviews 23, 2467–2483.

Schalke, H., 1973. The Upper Quaternary of the Cape Flats area (Cape Province, South Africa). Scripta Geologica 15, 1–57.

Scheffer, M., Hosper, S., Meijer, M., Moss, B., Jeppesen, E., 1993. Alternative equilibria in shallow lakes. Trends in Ecology & Evolution 8, 275–9.

Schoeman, F., Archibald, R., 1976. The Diatom Flora of Southern Africa, CSIR Special Report WAT 50. Council for Scientific and Indutrial Research. Pretoria, South Africa.

Scholtz, A., 1986. Palynological and palaeobotanical studies in the southern Cape. Doctoral Thesis. University of Stellenbosch.

Schuette, G., Schrader, H., 1981. Diatom taphocoenoses in the coastal upwelling area off South West Africa. Marine Micropaleontology 6, 131–155.

Schumann, E., Cohen, A., Jury, M., 1995. Coastal sea surface temperature variability along the south coast of South Africa and the relationship to regional and global climate. Journal of Marine Research 53, 231–248.

Schumann, E., Perrins, L.-A., Hunter, I., 1982. Upwelling along the south coast of the Cape Province, South Africa. South African Journal Of Science 78, 238–242.

Schutte, K., Elsworth, J., 1954. The significance of large pH fluctuations observed in some South African vleis. Journal of Ecology 42, 148–150.

Scott, L., Bousman, C., Nyakale, M., 2005. Holocene pollen from swamp, cave and hyrax dung deposits at Blydefontein (Kikvorsberge), Karoo, South Africa. Quaternary International 129, 49–59.

Scott, L., Lee-Thorp, J.A., 2004. Holocene climatic trends and rhythms in southern Africa, in: Battarbee, R.W., Gasse, F., Stickley, C.E. (Eds.), Past Climate Variability through Europe and Africa. Springer Netherlands, Netherlands, pp. 69–91.

Scott, L, Woodborne, S., 2007. Vegetation history inferred from pollen in Late Quaternary faecal deposits (hyraceum) in the Cape winter-rain region and its bearing on past climates in South Africa. Quaternary Science Reviews 26, 941–953.

Scott, L, Woodborne, S., 2007. Pollen analysis and dating of Late Quaternary faecal deposits (hyraceum) in the Cederberg, Western Cape, South Africa. Review of Palaeobotany and Palynology 144, 123–134.

Sherrod, B.L., 2001. Evidence for earthquake-induced subsidence about 1100 yr ago in coastal marshes of southern Puget Sound, Washington. Geological Society of America Bulletin 113, 1299–1311.

Smol, J.P., Stoermer, E.F., 2010. Introduction, in: Smol, J.P., Stoermer, E.F. (Eds.), The Diatoms: Applications for the Environmental and Earth Sciences. Cambridge University Press, New York, pp. 3–7.

Snoeijs, P., 1999. Diatoms and environmental change in brackish waters, in: Stoermer, E.F., Smol, J.P. (Eds.), The Diatoms: Applications for the Environmental and Earth Sciences. Cambridge University Press, Cambridge, UK, pp. 298 – 333.

Snoeijs, P., Weckström, K., 2010. Diatoms and environmental change in large brackish-water ecosystems, in: Smol, J.P., Stoermer, E.F. (Eds.), The Diatoms: Applications for the Environmental and Earth Sciences. Cambridge University Press, New York, pp. 287–308.

Spaulding, S.A., Van de Vijver, B., Hodgson, D.A., Mcknight, D.M., Verleyen, E., Stanish, L., 2010. Diatoms as indicators of environmental change in Antarctic and subantarctic freshwaters, in: Smol, J.P., Stoermer, E.F. (Eds.), The Diatoms: Applications for the Environmental and Earth Sciences. Cambridge University Press, New York, pp. 267–283.

Spellerberg, I., Fedor, P., 2003. A tribute to Claude Shannon (1916–2001) and a plea for more rigorous use of species richness, species diversity and the “Shannon–Wiener” Index. Global Ecology and Biogeography 12, 177–179.

Stager, J., Mayewski, P., White, J., Chase, B., Neumann, F., Meadows, M., King, C., Dixon, D., 2012. Precipitation variability in the winter rainfall zone of South Africa during the last 1400 yr linked to the austral westerlies. Climate Of The Past 8, 877–887.

Stager, J.C., Ryves, D.B., King, C., Madson, J., Hazzard, M., Neumann, F.H., Maud, R., 2013. late Holocene precipitation variability in the summer rainfall region of South Africa Biomes. Quaternary Science Reviews 67, 105–120.

Stancheva, R., Mancheva, A., Ivanov, P., 2007. Taxonomic composition of the epilithic diatom flora from rivers Vit and Osum, Bulgaria. Phytologia Balcanica 13, 53–64.

Stoermer, E.F., Smol, J.P., 1999. Applications and uses of diatoms: prologue, in: Stoermer, E.F., Smol, J.P. (Eds.), The Diatoms: Applications for the Environmental and Earth Sciences. Cambridge University Press, Cambridge, UK, pp. 3–8.

Stuiver, M., 1980. Solar variability and climatic change during the current millennium. Nature 286, 868–871.

Stuiver, M., Quay, P.D., 1980. Changes in atmospheric carbon-14 attributed to a variable sun. Science 207, 11–19.

Stuut, J.-B.W., Crosta, X., van der Borg, K., Schneider, R., 2004. Relationship between Antarctic sea ice and southwest African climate during the late Quaternary. Geology 32, 909–912.

Stuut, J.-B.W., Prins, M.A., Schneider, R., Weltje, G.J., Jansen, J.F., Postma, G., 2002. A 300-kyr record of aridity and wind strength in southwestern Africa: inferences from grain-size distributions of sediments on Walvis Ridge, SE Atlantic. Marine Geology 180, 221–233.

Sullivan, M.J., 1999. Applied diatom studies in estuaries and shallow coastal environments, in: Stoermer, E.F., Smol, J.P. (Eds.), The Diatoms: Applications for the Environmental and Earth Sciences. Cambridge University Press, Cambridge, UK, pp. 334 – 351.

Sundbäck, K., Medlin, L.K., 1986. A light and electron microscopic study of the epipsammic diatom *Catenula adhaerens* Mereschkowsky. Diatom Research 1, 283–290.

Swann, G.E.A., Leng, M.J. 2009. A review of diatom $\delta^{18}O$ in palaeoceanography. Quaternary Science Reviews 28, 384-398

Tadross, M., Taylor, A., Johnston, P., 2012. Understanding Cape Town's climate, in: Cartwright, A., Parnel, S., Oelofse, G., Ward, S. (Eds.), Climate Change at the City Scale: Impacts, Mitigation and Adaptation in Cape Town. Routledge, Cape Town, South Africa, pp. 9–20.

Talma, A., Vogel, J., 1992. Late Quaternary paleotemperatures derived from a speleothem from Cango caves, Cape province, South Africa. Quaternary Research 37, 203–213.

Taylor, J., Harding, W., Archibald, C., 2007. An Illustrated Guide to Some Common Diatom Species from South Africa An Illustrated Guide to Some Common Diatom. Water Research Commission TT282/07. Water Research Commission. Pretoria

Thackeray, J., 1988. Molluscan fauna from Klasies River, South Africa. The South African Archaeological Bulletin 43, 27–32.

Thoms, M., Ogden, R., Reid, M., 1999. Establishing the condition of lowland floodplain rivers: a palaeo-ecological approach. Freshwater Biology 41, 407–423.

Trobajo, R., Sullivan, M.J., 2010. Applied diatom studies in estuaries and shallow coastal environments, in: Smol, J.P., Stoermer, E.F. (Eds.), The Diatoms: Applications for the Environmental and Earth Sciences. Cambridge University Press, New York, pp. 309–323.

Troeger, W., 1978. Epiphytic diatoms in farm ponds and experimental ponds in Bryan County, Oklahoma. Proceedings of the Oklahoma Academy of Science 58, 64–68.

Troels-Smith, J., 1955. Karakterisering af løse jordarter. Characterization of unconsolidated sediments. Danmarks Geologiske Undersøgelse 3.

Tyson, P., 1991. Climatic change in southern Africa: past and present conditions and possible future scenarios. Climatic Change 18, 241–258.

Tyson, P., 1999. Atmospheric circulation changes and palaeoclimates of southern Africa. South African Journal Of Science 95, 194–201.

Tyson, P., Lindesay, J., 1992. The climate of the last 2000 years in southern Africa. The Holocene 2,3, 271–278.

Underwood, G., 2002. Adaptations of tropical marine microphytobenthic assemblages along a gradient of light and nutrient availability in Suva Lagoon, Fiji. European Journal of Phycology 37, 449–462.

Underwood, G., Kromkamp, J., 1999. Primary production by phytoplankton and microphytobenthos in estuaries. Advances in ecological research 29, 93–153.

Vadeboncoeur, Y., Peterson, G., Vander Zanden, M.J., Kalff, J., 2008. Benthic algal production across lake size gradients: interactions among morphometry, nutrients, and light. Ecology 89, 2542–2552.

Valsecchi, V., Chase, B.M., Slingsby, J.A., Carr, A.S., Quick, L.J., Meadows, M.E., Cheddadi, R., Reimer, P.J., 2013. A high resolution 15,600-year pollen and microcharcoal record from the Cederberg Mountains, South Africa. Palaeogeography, Palaeoclimatology, Palaeoecology 387, 6–16.

Van de Vijver, B., Beyens, L., 1997. The epiphytic diatom flora of mosses from Strømness Bay area, South Georgia. Polar biology 17, 492–501.

Van der Putten, N., Hébrard, J.-P., Verbruggen, C., Van de Vijver, B., Disnar, J.-R., Spassov, S., de Beaulieu, J.-L., De Dapper, M., Keravis, D., Hus, J., Thouveny, N., Frenot, Y., 2008. An integrated palaeoenvironmental investigation of a 6200 year old peat sequence from Ile de la Possession, Iles Crozet, sub-Antarctica. Palaeogeography, Palaeoclimatology, Palaeoecology 270, 179–195.

Van Wilgen, B., Le Maitre, D., Cowling, R., 1998. Ecosystem services, efficiency, sustainability and equity: South Africa's Working for Water programme. TREE 13(9), 378

Vasudevan, M., Sivakholundu, K., Venkata, R.D., Kathiroli, S., 2007. Application of Parametric Acoustics for Shallow-Water Near-Surface Geophysical Investigations, in: OCEANS 2006-Asia Pacific. IEEE, pp. 1–4.

Vos, P.C., De Wolf, H., 1993. Diatoms as a tool for reconstructing sedimentary environments in coastal wetlands; methodological aspects. Hydrobiologia 269/270, 285–296.

Wachnicka, A., Gaiser, E., Boyer, J., 2011. Ecology and distribution of diatoms in Biscayne Bay, Florida (USA): Implications for bioassessment and paleoenvironmental studies. Ecological Indicators 11, 622–632.

Wagner, S., Zorita, E., 2005. The influence of volcanic, solar and CO2 forcing on the temperatures in the Dalton Minimum (1790–1830): a model study. Climate Dynamics 25, 205–218.

Walker, M., 2005. Quaternary Dating Methods, Book. John Wiley and Sons, Ltd, West Sussex, England.

Webley, L., 2007. Archaeological evidence for pastoralist land-use and settlement in Namaqualand over the last 2000 years. Journal of Arid Environments 70, 629–640.

Weilhoefer, C., Pan, Y., Eppard, S., 2008. The effects of river floodwaters on floodplain wetland water quality and diatom assemblages. Wetlands 28, 473–486.

Whitmore, T., 1989. Florida Diatom Assemblages as Indicators of Trophic State and pH. Limnology and Oceanography 34, 882–895.

Wilkinson, L., Friendly, M., 2009. The history of the cluster heat map. The American Statistician 63, 179–184.

Wojtal, A., Sobczyk, Ł., 2006. Composition and structure of epilithic diatom assemblages on stones of different size in a small calcareous stream (S Poland). Algological Studies 119, 105–124.

Wolin, J., 1996. late Holocene lake-level and lake development signals in Lower Herring Lake, Michigan. Journal of Paleolimnology 15, 19–45.

Wolin, J., Duthie, H., 1999. Diatoms as indicators of water level change in freshwater lakes, in: Stoermer, E.F., Smol, J.P. (Eds.), The Diatoms: Applications for the Environmental and Earth Sciences. Cambridge University Press, Cambridge, UK, pp. 182–202.

Wolin, J.A., Stoermer, E.F., 2005. Response of a Lake Michigan coastal lake to anthropogenic catchment disturbance. Journal of Paleolimnology 33, 73–94.

Wolin, J.A., Stone, J.R., 2010. Diatoms as indicators of water-level change in freshwater lakes, in: Smol, J.P., Stoermer, E.F. (Eds.), The Diatoms: Applications for the Environmental and Earth Sciences. Cambridge University Press, New York, pp. 174–185.

Wunderlich, J., Muller, S., 2003. High-resolution sub-bottom profiling using parametric acoustics. International Ocean Systems 7, 6–11.

Zalat, A.A., 2000. Distribution and Paleoecological Significance of Fossil Diatom Assemblages From the Holocene Sediments of Lake Manzala, Egypt. Diatom Research 15, 167–190.

Zong, Y., Horton, B.P., 1999. Diatom-based tidal-level transfer functions as an aid in reconstructing Quaternary history of sea-level movements in the UK. Journal of Quaternary Science 14, 153–167.

APPENDICES

APPENDIX ONE

Figure 1.1: Selected southern African palaeosites across the three rainfall regimes, from west – east: winter rainfall zone, year-round rainfall zone and summer rainfall zone also indicating the southern coast of South Africa (Source: Appendix One) (Pg. 3)

- ***Rainfall Data***: United Nations Environmental Programme - Global Resource Information Database. 2001. http://www.grid.unep.ch/
- ***Africa, South Africa data:*** Mucina, L., and Rutherford, M. C. 2006. The Vegetation of South Africa, Lesotho and Swaziland. South African National Biodiversity Institute, Pretoria
- ***GPS coordinates*** of palaeosites obtained from their respective published articles and referenced in the text

Figure 2.1: The major biomes of the south-western to southern coast of South Africa (Source: Appendix One) (Pg. 9)

- ***Digital Elevation Model***: Shuttle Radar Topography Mission 3. Version 4. http://www2.jpl.nasa.gov/srtm/world.htm
- ***Vegetation, Biomes, Africa, South Africa***: Mucina, L., and Rutherford, M. C. 2006. The Vegetation of South Africa, Lesotho and Swaziland. South African National Biodiversity Institute, Pretoria.

Figure 2.2: Generalised schematic of major atmospheric (white) and oceanic circulation (warm currents = red, cold currents = blue) across southern Africa. AnC = Angola Current, SEC = South Equatorial Current, MC = Mozambique Current, MCE = Mozambique Current Eddies, EMC = East Madagascar Current, AC = Agulhas Current, ARC = Agulhas Return Current, SIC = South Indian Ocean Current, STF = Subtropical Front, ACC = Antarctic Circumpolar Current, SAC = South Atlantic Current, BOC = Benguela Ocean Current, BCC = Benguela Coastal Current, SB = southern boundary, ABF = Angola-Benguela Front (source: see Appendix One) (Pg. Error! Bookmark not defined.**)**

- ***Ocean Bathymetry***: The National Oceanic and Atmospheric Administration. 2001. http://www.ngdc.noaa.gov/mgg/global/relief/ETOPO2/
- ***Atmospheric Circulation***: Chase et al, 2010
- ***Ocean Circulation***: Hutson, 1980; Zahn et al., 2009; Hutchings et al., 2009;

- Lutjeharms JRE and Bornman TG. 2010. The importance of the greater Agulhas Current is increasingly being recognised. *South African Journal of Science*. **160** (3/4): 1 – 4

Figure 2.4: Distribution of palaeo-sites across southern Africa discussed in text with respect to rainfall regimes, the demarcation of the rainfall zones are based on the percentage rainfall received over the course of the year. Winter rainfall = shades of pink, Year-round rainfall = yellow, Summer rainfall zone = shades of green (sources: see Appendix One) (Pg. 19)

- ***Rainfall Data***: United Nations Environmental Programme - Global Resource Information Database. 2001. http://www.grid.unep.ch/
- ***GPS coordinates*** of palaeosites obtained from their respective published articles and referenced in the text

Figure 4.6: Bathymetry of Eilandvlei (1m intervals, inset a) in the Wilderness Lake complex and Swartvlei (2m intervals, inset b) indicating the three core localities incorporated into this study in relation to the south coast of South Africa (inset c) (sources: Appendix One) (Pg. 53)

- ***Catchment, River, Land-use, coastline data***: Chief Directorate: Surveys and Mapping. Department of Land Affairs. http://csg.dla.gov.za/spatial.htm
- ***Vegetation, Biomes, waterbodies***: Mucina, L., and Rutherford, M. C. 2006. The Vegetation of South Africa, Lesotho and Swaziland. South African National Biodiversity Institute, Pretoria.
- ***Lake Bathymetry***: Clausnitzer 2011

Figure 4.7: The Cape Flats lakes situated on the Cape Peninsula (inset) showing PV11.3 core localty (red dot) at Princessvlei as well as groundwater contour lines and direction (source: Appendix) (Pg. 55)

- ***Catchment, River, Land-use, coastline data***: Chief Directorate: Surveys and Mapping. Department of Land Affairs. http://csg.dla.gov.za/spatial.htm
- ***Vegetation, Biomes, waterbodies***: Mucina, L., and Rutherford, M. C. 2006. The Vegetation of South Africa, Lesotho and Swaziland. South African National Biodiversity Institute, Pretoria.
- ***Groundwater contour lines and direction***: Parsons and Harding 2002

Figure 5.1: Geographical setting of the Wilderness Region showing underlying geology, rivers and water bodies (source: see Appendix One) (Pg. 66)

- ***Geology data***: AEON: Africa Earth Observatory Network
- ***Catchment, River data***: Chief Directorate: Surveys and Mapping. Department of Land Affairs. http://csg.dla.gov.za/spatial.htm

Figure 5.3: The lakes and rivers within the catchments (white lines) of the Wilderness Embayment, indicating the variability in electrical conductivity (in thousands mS) and pH of selected sites monitored by the Department of Water Affairs (source: see Appendix One) (Pg. 70)

- ***Digital Elevation Model***: Shuttle Radar Topography Mission 3. Version 4. http://www2.jpl.nasa.gov/srtm/world.htm
- ***Water Quality data***: Department of Water Affairs. http://www.dwa.gov.za/iwqs/wms/data/K_reg_WMS_nobor.htm
- ***Catchment, River data***: Chief Directorate: Surveys and Mapping. Department of Land Affairs. http://csg.dla.gov.za/spatial.htm

Figure 7.1: The geology of the Cape Flats (source: see Appendix One) (Pg. 133)

- ***Geology data***: AEON: Africa Earth Observatory Network
- ***Catchment, River, Places data***: Chief Directorate: Surveys and Mapping. Department of Land Affairs. http://csg.dla.gov.za/spatial.htm

Figure 7.3: The lakes and rivers within the catchments (white lines) of the Cape Flats Region, indicating the variability in electrical conductivity (in thousands mS) and pH of selected sites monitored by the Department of Water Affairs (source: see Appendix One) (Pg. 138)

- ***Digital Elevation Model***: Shuttle Radar Topography Mission 3. Version 4. http://www2.jpl.nasa.gov/srtm/world.htm
- ***Water Quality data***: Department of Water Affairs. http://www.dwa.gov.za/iwqs/wms/data/G_reg_WMS_nobor.htm
- ***Catchment, River data***: Chief Directorate: Surveys and Mapping. Department of Land Affairs. http://csg.dla.gov.za/spatial.htm

Diatom Analysis (after Battarbee, 1986) (Pg. 58)

1) The sediments were initially treated with hot 10% HCl to remove all carbonates from the sample. This was achieved by placing a small quantity of sediment into a beaker, covering it with 10% HCl and heating gently for 15 minutes while swirling the contents. This was repeated until all carbonates were dissolved.

2) Following this, the residue was diluted with distilled water and allowed to settle overnight, with excess supernatant liquid removed through pipetting the following morning.

3) The sample was then washed in 20ml of 30% H_2O_2 and heated gently in a water bath until all organic matter was removed, this was repeated several times to ensure complete removal of organic matter.

4) To remove coarse organic matter, e.g. roots; the residue was sieved through a 0.5mm screen.

5) The resultant residue was centrifuged and washed with distilled water at least three times.

6) Coarse mineral matter was removed by sieving through a mesh size not less than 0.5mm with deionised water.

7) The subsequent sample may have contained clays and finer mineral matter, by swilling the residue in a beaker, clays were removed by allowing the diatoms to sediment before decanting and discarding the suspended clay.

8) Following these steps, a final wash with deionised water was performed.

9) The prepared sample was checked by preparing wet mounts to ensure an adequate removal of diluent material and a proper separation of frustules into single valves.

10) Following these steps, 3 drops of the diatom solution was pipetted onto a clean cover slip (Battarbee, 1986) and diluted with a few drops of deionised water (Barnett, 1997); the solution was then been allowed to settle (Battarbee, 1986).

11) The water in the solution was left to evaporate on a hot plate at a low temperature (~40°C).

12) Lastly, after all the water had evaporated, the coverslip was mounted onto the microscope slide using a “resin of high refractive index” (Battarbee, 1986, p. 531) for this purpose Pleurax (R.I. = 1.73) was utilised.

Figure 11.1: Schematic of the inductive high temperature reduction device (iHTR) used to liberate oxygen molecules from the silicate frustule (source: Lücke et al., 2005, p. 1425) *(Pg. 60)*

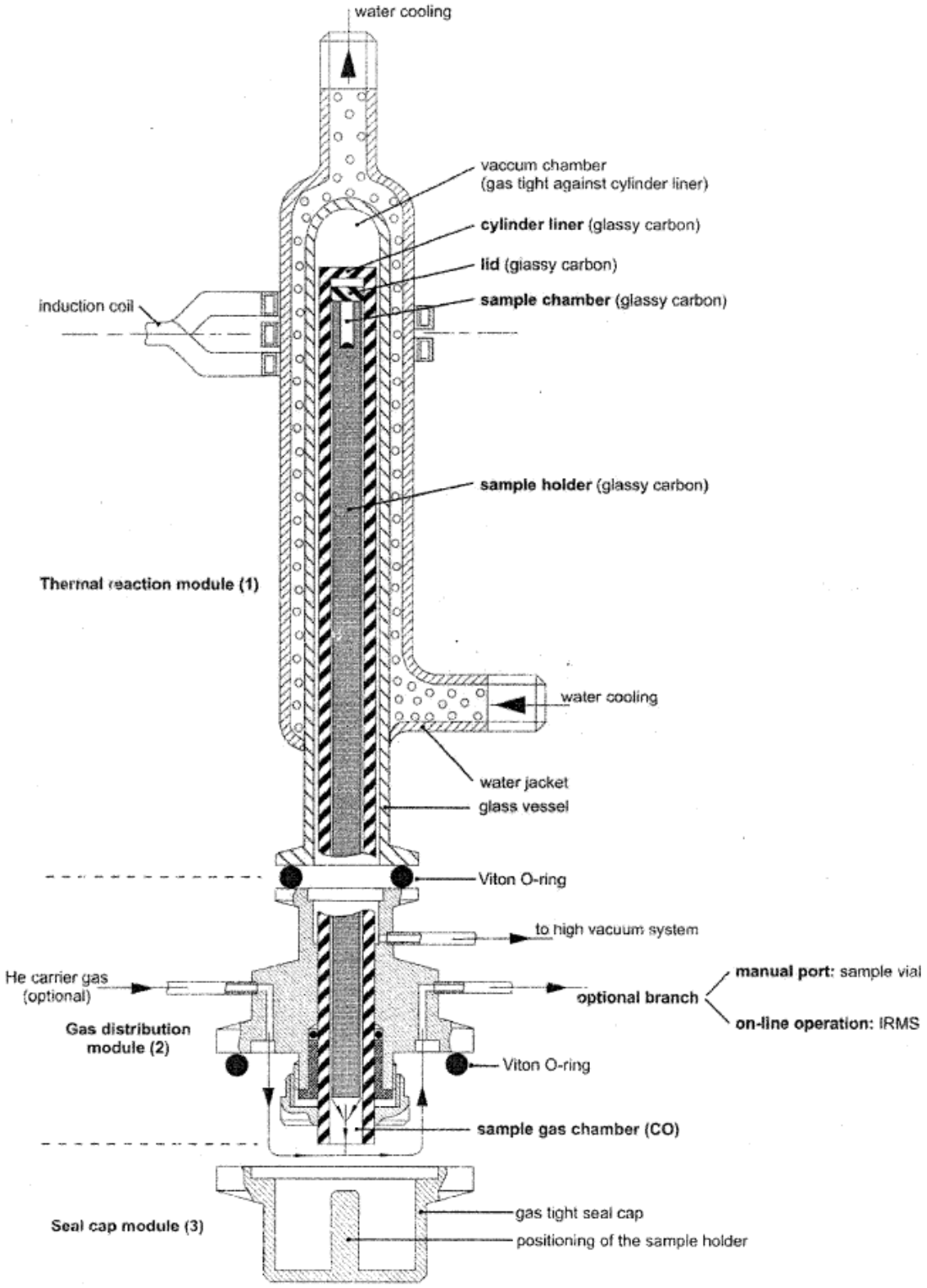

Figure 11.2: Schematic representation of sample preparation prior to iHTR (source: Leng and Barker, 2006) (Pg. 60)

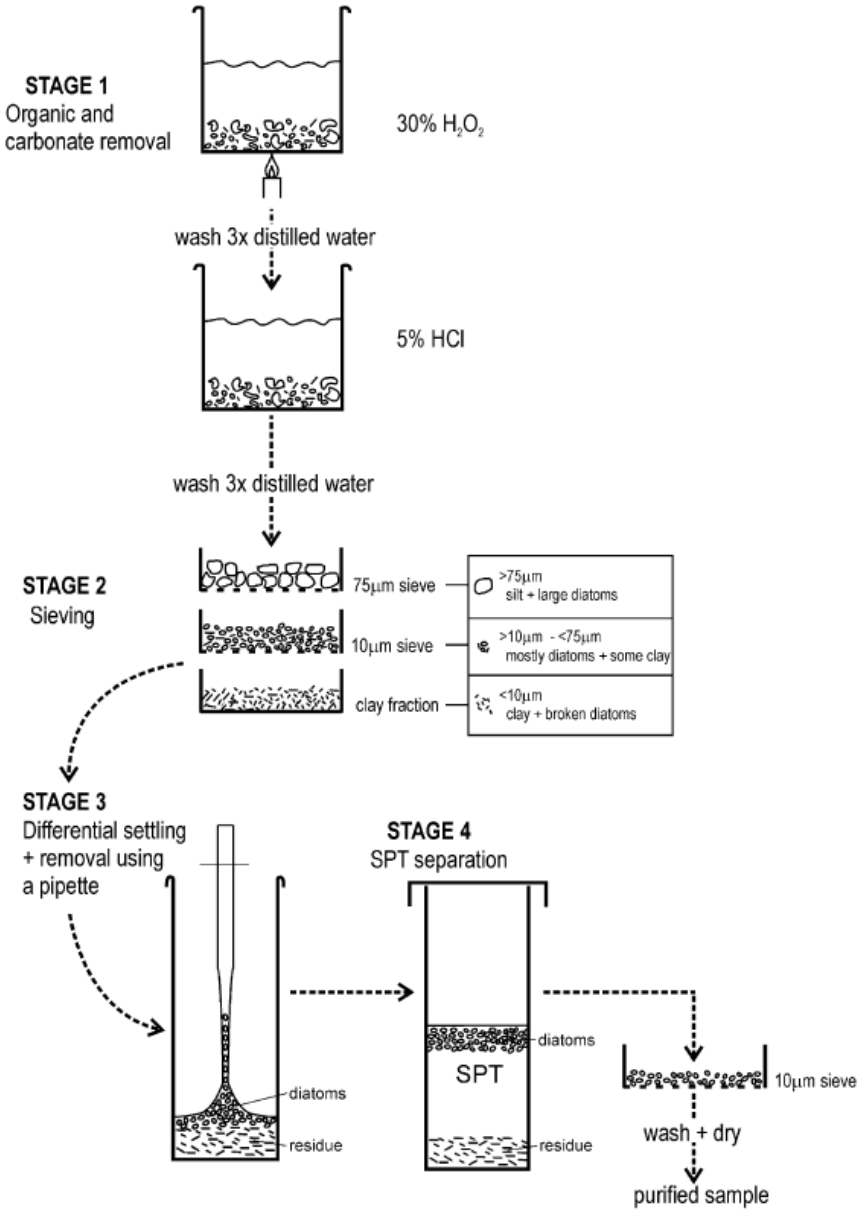

APPENDIX TWO

Table 11.1: Complete diatom species list with naming authority for all sites

Achnanthes brevipes Agardh var*. brevipes*
Achnanthes brockmannii Simonsen
Achnanthes inflata (Kützing) Grunow
Achnanthes javanica Grunow
Achnanthes oblongella Oestrup
Achnanthes subaffinis Cholnoky
Achnanthes swazi Cholnoky
Achnanthidium affine (Grun) Czarnecki
Achnanthidium crassum (Hustedt) Potapova & Ponader
Achnanthidium eutrophilum (Lange-Bertalot)Lange-Bertalot
Achnanthidium exiguum (Grunow) Czarnecki
Achnanthidium microcephalum Kütz.
Achnanthidium minutissimum (Kütz.) Czarnecki
Achnanthidium straubianum (Lange-Bertalot)Lange-Bertalot
Actinocyclus normanii (Greg.) Hust.
Actinocyclus sp.
Actinoptychus heliopelta Grunow in Van Heurck
Actinoptychus undulatus (Bailey)Ralfs
Actinoptychus vulgaris (Ehr.) Schuman
Amphipleura pellucida Kützing
Amphora acutiuscula Kützing
Amphora arcus Gregory
Amphora arenaria Donkin
Amphora coffeaeformis (Agardh) Kützing *var. coffeaeformis*
Amphora commutata Grunow
Amphora copulata (Kütz) Schoeman & Archibald

Amphora decussata Grunow
Amphora lunaris (A.Mann)
Amphora ostrearia Brébisson ex Kützing
Amphora ovalis (Kützing) Kützing
Amphora proteus Gregory
Amphora spectabilis Gregory
Amphora veneta Kützing
Aulacoseira ambigua (Grunow) Simonsen
Aulacoseira granulata (Ehr.) Simonsen
Aulacoseira granulata (Ehr.) Simonsen *var. angustissima* (O.M.)Simonsen
Aulacoseira muzzanensis (Meister) Krammer
Auliscus cf. sculptus (Wm.Smith) Ralfs in Pritchard
Bacillaria paradoxa Gmelin
Bacteriastrum sp.
Biddulphia capusina (Schmidt)
Biddulphia pulchella S.F. Gray
Brachysira brebissonii Ross in Hartley *ssp. brebissonii* Ross in Hartley
Brachysira vitrea (Grunow) Ross in Hartley
Caloneis aequatorialis Hustedt
Caloneis bacillum (Grunow) Cleve
Caloneis crassa (Gregory) Ross in Hartley
Caloneis sp.
Campylodiscus clypeus Ehrenberg
Catenula adhaerens Mereschkowsky
Chaetoceros sp.
Climacosphemia moniligera
Cocconeis costata Gregory *var. costata*
Cocconeis distans Gregory
Cocconeis engelbrechtii Cholnoky
Cocconeis pediculus Ehrenberg

Cocconeis placentula Ehrenberg *var. placentula*
Cocconeis pseudomarginata Gregory
Cocconeis scutellum Ehrenberg *var. scutellum*
Coscinodiscus radiatus Ehrenberg
Craspedodiscus elegans. Ehrenberg
Craspedostauros capensis E. J. Cox
Craticula accomoda (Hustedt) Mann
Craticula accomodiformis Lange-Bertalot
Craticula halophila (Grunow ex Van Heurck) Mann
Ctenophora pulchella (Ralfs ex Kütz.) Williams et Round
Cyclotella caspia Grunow
Cyclotella choctawhatcheeana Prasad
Cyclotella distinguenda A.K.S.K. Prasad *var. distinguenda* Hustedt
Cyclotella meneghiniana Kützing
Cylindrotheca closterium Reimann & Lewin
Cymbella affinis Kützing *var. affinis*
Cymbella turgidula Grunow in A.Schmidt & al. var*. turgidula*
Delphineis minutissima (Hustedt) Simonsen
Denticula subtilis Grunow
Diadesmis confervacea Kützing var*. confervacea*
Diatoma vulgaris Bory
Dimeregramma minor (Gregory)Ralfs
Diploneis chersonensis (Grunow) Cleve
Diploneis elliptica (Kützing) Cleve
Diploneis oblongella (Naegeli) Cleve-Euler
Diploneis smithii (Brebisson) Cleve var. *smithii*
Diploneis sp.
Discostella stelligera (Cleve et Grun.) Houk & Klee
Encyonema gracile Rabenhorst
Encyonema minutum (Hilse in Rabh.) D.G. Mann

Encyonema neogracile Krammer
Encyonema silesiacum (Bleisch in Rabh.) D.G. Mann
Encyonopsis cesatii (Rabenhorst) Krammer
Encyonopsis sp.
Encyonopsis subminuta Krammer & Reichardt
Entomoneis alata Ehrenberg
Entomoneis ornata (J.W.Bailey)Reimer
Entomoneis punctulata (Grunow) Osada & Kobayasi
Eolimna minima (Grunow) Lange-Bertalot
Eolimna subminuscula (Manguin) Moser Lange-Bertalot & Metzeltin
Epithemia adnata (Kützing) Brebisson
Epithemia sorex Kützing
Eunotia exigua (Brebisson ex Kützing) Rabenhorst var. *tenella* (Grunow) Nörpel et Alles
Eunotia flexuosa (Brebisson)Kützing
Eunotia formica Ehrenberg
Eunotia incisa Gregory var. *incisa*
Eunotia minor (Kützing) Grunow in Van Heurck
Eunotia pectinalis (Dyllwyn) Rabenhorst var. pectinalis
Eunotia zygodon Ehrenberg
Fallacia monoculata (Hustedt) D.G. Mann
Fallacia pygmaea (Kützing) Stickle & Mann ssp. *pygmaea* Lange-Bertalot
Fallacia sp.
Fallacia tenera (Hustedt) Mann in Round
Fistulifera saprophila (Lange-Bertalot & Bonik) Lange-Bertalot
Fragilaria biceps (Kützing) Lange-Bertalot
Fragilaria capucina Desmazieres var. *capucina*
Fragilaria exigua Grunow
Fragilaria tenera (W.Smith) Lange-Bertalot
Fragilariforma sp.
Frustulia rhomboides (Ehr.)De Toni

Frustulia rostrata Hustedt
Frustulia saxonica Rabenhorst
Frustulia vulgaris (Thwaites) De Toni
Gomphonema gracile Ehrenberg
Gomphonema parvulum (Kützing) Kützing var*. parvulum fo. parvulum*
Gomphonema venusta Passy. Kociolek & Lowe
Gyrosigma obscurum (W.Sm.) Griffith & Henfrey
Hantzschia amphioxys (Ehr.) Grunow in Cleve et Grunow 1880
Haslea sp.
Hippodonta capitata (Ehr.)Lange-Bert.Metzeltin & Witkowski
Hippodonta hungarica (Grunow) Lange-Bertalot Metzeltin & Witkowski
Isthmia enervis Ehrenberg
Kobayasiella sp.
Luticola goeppertiana (Bleisch in Rabenhorst) D.G. Mann
Lyrella lyra (Ehrenb.) Karayeva
Mastogloia braunii Grunow
Mastogloia crucicula (Grun.) Cleve var. *crucicula*
Mastogloia dansei (Thwaites) Wm.Smith
Mastogloia elliptica (C.A. Agardh) Cleve
Mastogloia fimbriata (Brightwell) Cleve
Mastogloia smithii Thwaites
Mastogloia sp.
Mastogloia vasta Hustedt
Mastogloia latecostata Hustedt
Mayamaea atomus (Kützing) Lange-Bertalot
Melosira nummuloides (Dillwyn) C.A. Agardh
Melosira varians Agardh
Navicula adamantiformis Archibald
Navicula angusta Grunow
Navicula cincta (Ehr.) Ralfs in Pritchard

Navicula cryptocephala Kützing
Navicula cryptotenella Lange-Bertalot
Navicula directa (W.M.Smith) Ralfs in Pritchard
Navicula erifuga Lange-Bertalot
Navicula oblonga Kützing
Navicula radiosa Kützing
Navicula tenelloides Hustedt
Navicula veneta Kützing
Navicymbula pusilla Krammer var. *pusilla*
Neidium affine (Ehrenberg)Pfitzer
Nitzschia amphibia Grunow fo. *amphibia*
Nitzschia brevissima Grunow
Nitzschia clausii Hantzsch
Nitzschia cocconeiformis Grunow in Cl.& Moller.
Nitzschia compressa (J.W.Bailey) Boyer
Nitzschia dissipata (Kützing)Grunow var. *dissipata*
Nitzschia laevis Hustedt
Nitzschia linearis (Agardh) W.M.Smith var. *subtilis* (Grunow) Hustedt
Nitzschia littorea Grunow in Van Heurck
Nitzschia nana Grunow in Van Heurck
Nitzschia palea (Kützing) W.Smith
Nitzschia pusilla (Kützing)Grunow
Nitzschia recta Hantzsch in Rabenhorst
Nitzschia sigma (Kützing)W.M.Smith
Nitzschia tryblionella Hantzsch in Rabh.
Opephora marina (Gregory) Petit
Paralia sulcata (Ehrenberg) Cleve
Petroneis humerosa (Brebisson ex Wm. Smith) Stickle & Mann
Pinnularia acrospheria W. Smith var. *acrospheria*
Pinnularia borealis Ehrenberg

Pinnularia divergens W.M.Smith var*. divergens*
Pinnularia gibba Ehrenberg
Pinnularia intermedia (Lagerstedt) Cleve
Pinnularia major (Kützing) Rabenhorst
Pinnularia sp. 1
Pinnularia sp. 2
Pinnularia subcapitata Gregory var. *subcapitata*
Pinnularia viridis (Nitzsch) Ehrenberg var. *viridis*
Placoneis clementis (Grun.) Cox
Placoneis placentula (Ehr.) Heinzerling
Plagiodiscus nervatus Grunow
Plagiotropis lepidoptera (Gregory) Kuntze
Planothidium biporomum (Hohn & Hellerman) Lange-Bertalot
Planothidium delicatulum (Kütz.) Round & Bukhtiyarova
Planothidium rostratum (Oestrup) Lange-Bertalot
Pleurosigma sp.
Pseudo-nitzschia sp.
Pseudostaurosira brevistriata (Grun.in Van Heurck) Williams & Round
Rhopalodia gibba (Ehr.) O.Muller var. gibba
Rhopalodia gibberula (Ehrenberg) O.Muller
Rhopalodia musculus (Kützing) O.Muller
Rossithidium linearis (W.Sm.) Round & Bukhtiyarova
Sellaphora bacillum (Ehrenberg) D.G.Mann
Sellaphora pupula (Kützing) Mereschkowksy
Sellaphora stroemii (Hustedt) Mann
Seminavis atlantica Garcia
Seminavis strigosa (Hustedt) Danieledis & Economou-Amilli
Stauroneis phoenicenteron (Nitzsch) Ehrenberg
Stauroneis sp.
Staurosira elliptica (Schumann) Williams & Round

Stephanodiscus agassizensis Hakansson & Kling
Stephanodiscus hantzschii Grunow in Cl. & Grunow
Surirella brebissonii Krammer & Lange-Bertalot var. *brebissonii*
Surirella fastuosa Ehrenberg
Surirella hybrida Grunow in Van Heurck
Surirella sp.
Synedra bacillaris (Grunow) Hustedt
Tabellaria fenestrata (Lyngbye)Kützing
Tabellaria flocculosa (Roth)Kützing
Tabularia fasciculata (Agardh)Williams et Round
Terpsinoe americana (Bailey) Ralfs
Thalassionema nitzschioides (Grunow)Mereschkowsky
Thalassiosira eccentrica (Ehrenberg) Cleve
Thalassiosira gravida Cleve
Thalassiosira weissflogii (Grunow) Fryxell & Hasle
Trachyneis aspera Ehr.
Triceratium reticulum Ehrenberg
Tryblionella apiculata Gregory
Tryblionella calida (grunow in Cl. & Grun.) D.G. Mann
Tryblionella coarctata (Grunow in Cl. & Grun.) D.G. Mann
Tryblionella hungarica (Grunow) D.G. Mann

Table 11.2: Eilandvlei (EV10.1) diatom species with ecological affinities; including salinity (f = fresh, fb = fresh-brackish, bf = brackish-fresh, b = brackish, mb = marine-brackish, m = marine, u = unknown), pH (a = acidophilic, c = circumneutral, k = alkaliphilic, b = alkalibiontic, u = unknown), Life form (a = aerophilic, b = benthic, p = planktonic, m = marine, u = unknown) and trophic state (uo = ultraoligotrophic, ot = oligotrophic, mt = mesotrophic, et = eutrophic, pt = polytrophic, ht = hypertrophic, mar = marine, u = unknown)

Species Name	Salinity	pH	Life Form	Trophic State
Achnanthes brevipes	fb	c	b	uo
Achnanthes oblongella	fb	c	b	uo
Achnanthidium exiguum	f	k	u	U
Achnanthidium straubianum	f	k	b	mt-et
Amphora acutiuscula	mb	k	b	U
Amphora coffeaeformis	b	k	b	Pt
Amphora copulata	fb	k	b	pt-ht
Amphora ostrearia	m	m	m	Mar
Amphora ovalis	fb	k	b	Pt
Amphora proteus	m	m	m	Mar
Campylodiscus clypeus	b	b	p	U
Catenula adhaerens	m	m	b	Mar
Chaetoceras sp	m	m	m	Mar
Cocconeis engelbrechtii	b	k	b	U
Cocconeis placentula	fb	k	b	Et
Cocconeis sp	u	u	u	U
Coscinodiscus radiatus	m	m	p	mar
Craticula cuspidata	fb	k	u	Et
Ctenophora pulchella	b	u	b	U
Cyclotella caspia	b	k	p	Et
Cyclotella distinguenda	b	k	p	Et
Cyclotella meneghiniana	f	k	p	Et
Cymbella lanceolata	fb	k	b	U
Delphineis minutissima	m	m	p	mar
Diploneis chersonensis	m	m	b	mar
Diploneis oblongella	fb	k	b	Uo
Diploneis smithii	b	c	b	U
Encyonema gracile	f	a	b	Ot
Encyonema minutum	f	c	u	mt-et
Entomoneis alata	m	b	u	U
Eunotia flexuosa	f	a	b	Ot
Eunotia formica	fb	a	u	Ot
Eunotia minor	fb	c	b	Et
Fallacia monoculata	fb	b	b	U

Species Name	Salinity	pH	Life Form	Trophic State
Fistulifera saprophila	b	c	u	Et
Fragilaria biceps	f	b	b	mt-et
Fragilaria tenera	f	a	b	mt-et
Frustulia saxonica	u	a	u	U
Gomphonema gracile	fb	c	b	ot-mt
Gomphonema venusta	u	c	u	U
Gyrosigma sp	u	u	u	U
Isthmia enervis	m	m	m	Mar
Luticola sp	u	u	u	U
Mastogloia smithii	b	k	u	mt-et
Melosira moniliformis	m	m	m	mar
Melosira nummuloides	b	k	b	E
Navicula cincta	fb	k	a	ot
Navicula cryptocephala	fb	c	b	pt
Navicula radiosa	fb	c	b	ot-et
Navicula veneta	bf	k	b	Pt
Navicymbula pusilla	fb	k	a-b	ot-et
Nitzschia clausii	b	k	b	pt-ht
Nitzschia cocconeiformis	m	m	m	mar
Nitzschia compressa	mb	k	b	U
Nitzschia dissipata	fb	k	b	u
Nitzschia palea	fb	c	b	pt
Nitzschia sigma	b	k	b	eu
Opephora marina	mb	k	b	m-e
Paralia sulcata	m	m	p	mar
Petroneis humerosa	m	m	b	mar
Pinnularia borealis	fb	c	a	m-e
Pinnularia borealis var. 1	fb	c	a	m-e
Pinnularia subbrevistriata	u	u	u	u
Pinnularia viridis	f	c	b	o-m
Planothidium delicatulum	b	b	u	u
Rhopalodia gibberula	bf	k	b	u
Rhopalodia musculus	b	b	u	u
Stauroneis phoenicenteron	fb	c	u	eu
Staurosira elliptica	fb	k	b	mt
Surirella brebissonii	b	k	b	eu
Synedra bacillaris	m	m	p	mar
Tabularia fasciculata	b	k	b	eu
Terpsinoë musica	m	k	b	u

Species Name	Salinity	pH	Life Form	Trophic State
Thalassirosira weissflogii	f	c	p	pt
Tryblionella apiculata	b	k	b	ht
Tryblionella calida	bf	c	b	eu
Tryblionella debilis	f	u	a-b	u
Tryblionella hungarica	bf	k	b	pt

Table 11.3: Eilandvlei (EV10.1) diatom species percentage representation against depth and age

Depth(cm)	**1**	**4**	**7**	**10**	**12**	**14**	**16**	**18**	**20**	**22**	**24**	**25**	**28**
Age (cal yrs BP)	**-47**	**-39**	**-30**	**-22**	**-16**	**-10**	**-4**	**35**	**87**	**138**	**189**	**215**	**243**
Achnanthes brevipes	0.6	0.6	0	0.4	0	0	0.2	0	0	0	0	0	0
Achnanthes oblongella	1.4	3.2	0.8	0.8	0.4	0	0.4	0.2	0	0.8	0.2	0	1.2
Achnanthidium exiguum	0	0	0	0	0	0	0	0	0	0	0	0	0
Achnanthidium straubianum	0	0.6	1	0	0.2	0.2	0	0.2	0.2	0	0.6	0.6	0.4
Amphora acutiuscula	0.6	0	0.2	0	0	0.2	0	0	0	0	0	0	0
Amphora coffeaeformis	0.4	0	0	0	0	0	0	0	0	0	0	0	0
Amphora copulata	0	0	0	0	0	0	0	0	0	0	0	0	0
Amphora ostrearia	0	0	0	0	0	0	0	0	0	0	0	0	0
Amphora ovalis	0.2	0	0	0	0	0	0	0	0	0	0	0	0
Amphora proteus	0	0	0.2	0.4	0	0.2	0	0	0	0	0.4	0	0
Campylodiscus clypeus	0	0	0	0	0	0.2	0	0	0.2	0.2	0	0	0
Catenula adhaerens	0.4	2	0.8	0.4	0.2	0	0.8	1	1.2	0.2	0.2	0	0.4
Chaetoceras sp	5	3	3.2	1.8	4.2	3.2	4	0.8	2.4	1.8	2.8	1.4	2.6
Cocconeis engelbrechtii	9.4	9	23.2	16	4.4	3.4	8.6	5.4	3.4	9.4	6	2.8	5.4
Cocconeis placentula	7	5.4	2.8	2.4	1.2	2	1.6	1.2	0.8	2.2	0.8	0.4	0.6
Cocconeis sp	0	0.2	0	0	0.2	0	0.6	0	0	0.2	0	0	0.2
Coscinodiscus radiatus	5.6	1.4	14.6	7.4	7.2	10	17.2	39.6	47.8	49	45.8	49.4	40.6
Craticula cuspidata	0	0.2	0	0	0	0	0	0	0.4	0.2	0	0	0
Ctenophora pulchella	0	0	0.2	0.2	0.2	0	0	0	0	0	0	0	0
Cyclotella caspia	15	15.2	6.6	19	30.8	2.2	5.2	0.2	2.2	5.2	5.8	0	0.2
Cyclotella distinguenda	2	6.8	3.4	10	17.6	2.2	1.4	0.6	1.4	4	1.6	1.2	1
Cyclotella meneghiniana	7	0.2	0.6	0.2	0.2	0	0	0	0	0	0	0	0
Cymbella lanceolata	0	0	0	0	0	0	0	0	0	0	0	0	0.2
Delphineis minutissima	0	0	0	0	0	0.2	0.4	0	0	0.2	0	0.2	0.2
Diploneis chersonensis	0	0	0	0	0	0	0	0	0	0	0	0	0.2
Diploneis oblongella	0	0	0	0	0	0	0	0	0	0	0.2	0	0
Diploneis smithii	0.6	0.8	0.6	0.4	0.6	0.4	0.6	0	0.4	0.4	0.8	0.2	0.8
Encyonema gracile	0	0	0	0	0	0	0	0	0	0	0.2	0	0
Encyonema minutum	0	0	0	0	0	0	0	0.2	0	0	0	0.2	0
Entomoneis alata	0.2	0.2	0	0	0	0	0.2	0	0	0	0.4	0	0
Eunotia flexuosa	0	0	0	0	0	0	0	0	0	0	0	0	0
Eunotia formica	0	0.2	0.2	0	0	0	0	0	0	0	0	0	0
Eunotia minor	0.8	0.6	0.2	0	0.4	0	0	0	0	0	0	0	0.2
Fallacia monoculata	3.2	1.6	0.8	0.8	0	0	0.4	0.2	0	0	0.2	0.2	0.4
Fistulifera saprophila	1.2	2	0.4	0	0	0	0	0	0	0	0	0	0.2
Fragilaria biceps	1	0.6	0.2	1	1.6	0	0.2	0	0	0.2	0	0.8	0.4

Depth(cm)	1	4	7	10	12	14	16	18	20	22	24	25	28
Age (cal yrs BP)	**-47**	**-39**	**-30**	**-22**	**-16**	**-10**	**-4**	**35**	**87**	**138**	**189**	**215**	**243**
Fragilaria tenera	0	0.4	1.2	0.6	0.4	0	0	0.4	0	0.2	0	0	0
Frustulia saxonica	0.2	0	0	0	0.2	0	0	0	0	0	0.2	0	0
Gomphonema gracile	0.4	0	0	0	0	0	0	0	0	0	0	0.2	0
Gomphonema venusta	0	0	0	0	0	0	0.2	0	0	0	0	0	0
Gyrosigma sp	0	0	0	0	0	0	0	0.2	0.2	0	0	0	0
Isthmia enervis	0	0	0	0	0	0	0	0	0	0.2	0	0	0
Luticola sp	0	0	0.2	0	0	0	0	0	0	0	0	0	0
Mastogloia smithii	0.8	0.2	0.4	0	0	0	0	0	0	0	0	0.2	0
Melosira moniliformis	0.8	0	0	0	0	0	0	0	0	0	0	0	0
Melosira nummuloides	17.2	10.2	19.8	18.4	16.4	65.2	45.8	41.4	34.8	17.6	14.8	15.6	34
Navicula cincta	0	0	0	0.2	0	0.2	0.2	0	0	0	0	0	0
Navicula cryptocephala	0	0	0	0	0	0	0	0.4	0	0	0	0	0.2
Navicula radiosa	0	0	0	0.2	0	0	0.2	0.2	0	0.2	0	0.2	0
Navicula veneta	0	0.2	0.2	0.2	0	0	0	0	0	0	0	0	0
Navicymbula pusilla	0	0	0	0	0	0	0	0	0	0	0.2	0.2	0
Nitzschia clausii	0	0.2	0	0	0	0	0	0	0	0.4	0.4	0	0
Nitzschia cocconeiformis	0.4	0	0	0.4	0.2	0.8	0	0	0	0	0	0	0
Nitzschia compressa	0.2	0.4	0.2	0.2	0	0.2	0.2	0	0	0	0	0.4	0
Nitzschia dissipata	0	0	0	0	0	0	0	0	0	0	0	0.2	0
Nitzschia palea	0	0.4	0	0	0	0	0	0	0.4	0	0	0	0
Nitzschia sigma	0	0	0.2	0	0	0	0.2	0	0	0.2	0	0	0
Opephora marina	0.8	0.4	0.2	0	0.2	0	0.6	0	0	0.2	0.2	0	0
Paralia sulcata	0	0	0	0	0	0	0.4	0	0	0	0	0	0
Petroneis humerosa	0	0	0	0	0	0	0	0	0	0.2	0	0	0
Pinnularia borealis	0	0.2	0	0	0	0	0	0	0	0	0	0	0
Pinnularia borealis var. 1	0.6	0	1.6	1	0.8	1.6	0	1	2	2.2	12.2	20.8	3
Pinnularia subbrevistriata	0	0	0	0	0	0	0	0	0	0	0	0	0
Pinnularia viridis	0	0	0	0	0	0	0	0	0	0	0	0	0
Planothidium delicatulum	0.4	0.8	0	0.2	0	0	0	0	0	0	0	0	0
Rhopalodia gibberula	0.2	0.2	0	0.4	0	0	0	0	0	0	0	0	0
Rhopalodia musculus	0	0	0	0	0	0	0	0	0	0	0	0	0
Stauroneis phoenicenteron	0	0	0	0	0	0	0	0	0	0	0	0	0
Staurosira elliptica	0	0	0	0	0	0	0	0	0	0	0	0	0
Surirella brebissonii	0	0	0.2	0	0.2	0	0.2	0	0	0	0	0	0.2
Synedra bacillaris	0	0	0	0	0	0	0	0	0	0	0	0	0
Tabularia fasciculata	9.2	6.2	9.2	9.8	3.8	4.8	2.4	2.6	0.4	0.8	1.4	0.4	2.2
Terpsinoë musica	0	0	0	0	0	0	0	0	0	0	0	0	0
Thalassirosira weissflogii	6	25.8	6.4	6.4	7.6	1.8	7.2	3	1.2	2.8	2.4	0.6	2.2

Depth(cm)	**1**	**4**	**7**	**10**	**12**	**14**	**16**	**18**	**20**	**22**	**24**	**25**	**28**
Age (cal yrs BP)	**-47**	**-39**	**-30**	**-22**	**-16**	**-10**	**-4**	**35**	**87**	**138**	**189**	**215**	**243**
Tryblionella apiculata	0.6	0	0.2	0.2	0.2	1	0.4	0.8	0.4	0.4	0.8	1.4	1.6
Tryblionella calida	0.2	0.2	0	0.6	0.6	0	0.2	0.4	0.2	0.6	1.4	2.4	1.4
Tryblionella debilis	0	0.4	0	0	0	0	0	0	0	0	0	0	0
Tryblionella hungarica	0.4	0	0	0	0	0	0	0	0	0	0	0	0

Depth(cm)	31	34	37	40	43	46	49	52	55	58	61	64
Age cal yrs BP	**271**	**299**	**327**	**356**	**384**	**412**	**524**	**541**	**558**	**575**	**592**	**610**
Achnanthes brevipes	0	0	0	0	0.2	0	0	0	0.2	0.4	0.2	0.2
Achnanthes oblongella	0.4	0	0.4	0.4	0.4	0	1.6	0.2	0.8	0.8	0.2	1.4
Achnanthidium exiguum	0	0	0	0.2	0	0	0	0	0	0	0	0
Achnanthidium straubianum	0	0	0	0	0	0.4	0.2	1	1.4	2.2	2.4	4.4
Amphora acutiuscula	0.4	0	0.2	0.2	0.2	0	0.4	0	0	0.4	0	0.2
Amphora coffeaeformis	0	0	0	0	0	0	0	0	0	0	0	0
Amphora copulata	0	0	0	0	0	0	0	0	0	0	0	0.2
Amphora ostrearia	0	0	0	0	0	0	0	0	0	0	0	0.4
Amphora ovalis	0	0	0	0	0	0	0	0	0	0	0	0
Amphora proteus	0	0	0	0	0	0.2	0.2	0	0.2	0.6	0.2	0.6
Campylodiscus clypeus	0	0	0	0.2	0	0	0	0	0	0	0.4	0
Catenula adhaerens	0.4	0.4	0	0	0.6	0	0.4	0	0	1	1.4	0.2
Chaetoceras sp	5.8	0.8	2.2	6.2	5.6	1.2	1.8	0.2	1	2.2	1.2	1.4
Cocconeis engelbrechtii	1.4	12.4	5.2	3.4	5	4	5.2	7	8.6	8.2	3.8	11.2
Cocconeis placentula	0.8	1.6	1	2	1.4	0.6	3.2	1.4	4.8	5.8	5	3.2
Cocconeis sp	0.4	0.2	0.2	0.4	0.6	0.2	0.8	0.6	0.8	1.2	0.6	1.8
Coscinodiscus radiatus	38.2	56.8	50.6	22.2	36.6	32.6	55.4	44.6	33.2	24.4	14.4	11.4
Craticula cuspidata	0	0	0	0	0	0	0	0	0	0	0	0
Ctenophora pulchella	0	0	0	0	0	0	0	0	0	0	0	0
Cyclotella caspia	0	0.2	0	8.2	0.6	0.6	1.2	1.6	3.6	7.2	2.6	2.8
Cyclotella distinguenda	0.2	1.8	2.4	3	2.8	1.4	3.4	9.4	14.2	7	9.2	18.8
Cyclotella meneghiniana	0	0	0	0	0	0.2	0.2	0.4	0.4	0	0	0.2
Cymbella lanceolata	0	0	0	0	0	0	0	0	0	0	0	0.2
Delphineis minutissima	0	0.2	0	0.2	0.4	0.2	0.4	1.6	2.6	1.6	3.2	3.6
Diploneis chersonensis	0	0	0	0	0	0	0	0	0	0	0	0.2
Diploneis oblongella	0	0	0	0	0	0	0	0	0	0	0.2	0.6
Diploneis smithii	0.2	0.6	0	1	0.6	1.2	0.4	0.2	0.4	1.2	1	2.2
Encyonema gracile	0	0	0	0	0	0	0	0	0	0	0	0
Encyonema minutum	0	0	0	0	0	0	0.4	0	0	0	0	0.2
Entomoneis alata	0	0	0	0.4	0.4	0.2	0	0.4	0.2	0.4	0.2	0
Eunotia flexuosa	0	0	0	0	0	0	0.2	0	0	0	0	0
Eunotia formica	0	0	0	0	0	0	0	0	0	0	0	0
Eunotia minor	0	0	0.2	0.2	0.2	0	0	0.2	0.2	0	0	1.2
Fallacia monoculata	0	0	0	0	0	0.6	1.2	1.4	1.2	1	1.8	4.2

Depth(cm)	31	34	37	40	43	46	49	52	55	58	61	64
Age cal yrs BP	**271**	**299**	**327**	**356**	**384**	**412**	**524**	**541**	**558**	**575**	**592**	**610**
Fistulifera saprophila	0	0	0	0	0	0	0	0	0	0	0.2	0.4
Fragilaria biceps	0	0.2	0.2	0.2	0.4	0	0	0	0.4	0.2	0.2	1.4
Fragilaria tenera	0	0.2	0.2	0.2	0	0	0.2	0	0	0.4	0.6	0.6
Frustulia saxonica	0	0	0	0	0	0	0	0.2	0	0	0.4	0.4
Gomphonema gracile	0	0	0	0	0	0	0	0	0	0	0	0
Gomphonema venusta	0	0	0	0	0	0	0	0	0	0	0	0.2
Gyrosigma sp	0	0	0	0	0	0	0	0	0	0	0	0
Isthmia enervis	0	0	0	0	0	0	0	0	0	0	0	0
Luticola sp	0	0	0	0	0	0	0	0	0	0	0	0
Mastogloia smithii	0.2	0.2	0	0.6	0.2	0	0.4	0.8	1.4	0.2	0	0.4
Melosira moniliformis	0	0	0	0	0	0	0	0	0	0	0	0
Melosira nummuloides	40.8	18.8	26.8	31	21.4	14.6	9.4	12.8	12.2	18.4	32.2	10
Navicula cincta	0	0	0.2	0.6	0	0	0.2	0	0.2	0.2	0	0
Navicula cryptocephala	0	0	0	0.2	0	0	0	0	0	0	0	0.6
Navicula radiosa	0.2	0.6	0.2	0	0	0	0	0.4	0.2	0.2	0.2	0
Navicula veneta	0	0	0	0	0	0	0	0	0	0	0	0
Navicymbula pusilla	0	0	0	0.2	0	0	0	0	0	0	0	0
Nitzschia clausii	0	0	0.2	0	0.2	0	0	0	0	0	0	0
Nitzschia cocconeiformis	0	0	0	0	0	0	0	0	0	0	0	0
Nitzschia compressa	0	0	0.6	0.8	2	0.4	0	0.4	0	0	0	0
Nitzschia dissipata	0	0.2	0	0.2	0	0.4	0	0.2	0	0	0	0
Nitzschia palea	0	0	0	0	0	0	0	0	0	0	0	0
Nitzschia sigma	0	0	0	0	0	0	0	0	0	0	0	0
Opephora marina	0	0	0	0	0	0	0	0	0	0	0	0.2
Paralia sulcata	0	0	0.2	0	0	0.6	0	0.4	0.2	0.4	0.8	0.2
Petroneis humerosa	0	0	0	0	0	0.2	0.2	0	0.6	0.4	0	0.2
Pinnularia borealis	0	0	0	0	0	0	0	0	0	0	0	0.2
Pinnularia borealis var. 1	3	0.8	5.4	10.8	12	33.8	7	7.6	5.6	6.2	7.4	8
Pinnularia subbrevistriata	0	0	0	0	0	0	0.2	0	0	0.2	0	0
Pinnularia viridis	0	0.2	0	0	0	0	0	0	0	0.2	0.2	0
Planothidium delicatulum	0	0	0	0	0.2	0	0	0	1	0.6	0.2	0
Rhopalodia gibberula	0	0.2	0.2	0	0.2	0	0	0	0	0	0	0.2
Rhopalodia musculus	0	0	0	0	0	0	0	0	0	0.2	0	0
Stauroneis phoenicenteron	0	0	0	0	0	0	0.2	0	0	0	0	0

Depth(cm)	**31**	**34**	**37**	**40**	**43**	**46**	**49**	**52**	**55**	**58**	**61**	**64**
Age cal yrs BP	**271**	**299**	**327**	**356**	**384**	**412**	**524**	**541**	**558**	**575**	**592**	**610**
Staurosira elliptica	0	0	0	0	0	0.4	0	0	0	0	0	0
Surirella brebissonii	0	0	0	0	0	0	0.6	0.2	0	0	0	0
Synedra bacillaris	0	0.2	0	0	0	0	0	0	0	0	0	0
Tabularia fasciculata	0.6	1.4	2	1.6	1.8	0.8	1.4	1.8	0.8	3.6	4.8	3.6
Terpsinoë musica	0	0	0	0	0	0	0	0	0.4	0	0.2	0
Thalassirosira weissflogii	1.8	0.8	0.2	1.8	1.8	0	2.8	2.2	2.4	2.6	3.8	1.6
Tryblionella apiculata	2.8	0.8	1	2	2.4	4	0.6	2	0.6	0.2	0.6	0.6
Tryblionella calida	2.4	0.4	0.2	1.6	1.8	1.2	0.2	0.8	0.2	0.2	0.2	0.4
Tryblionella debilis	0	0	0	0	0	0	0	0	0	0	0	0
Tryblionella hungarica	0	0	0	0	0	0	0	0	0	0	0	0

Table 11.4: Eilandvlei (EV11.1) diatom species with ecological affinities; including salinity (f = fresh, fb = fresh-brackish, bf = brackish-fresh, b = brackish, mb = marine-brackish, m = marine, u = unknown), pH (a = acidophilic, c = circumneutral, k = alkaliphilic, b = alkalibiontic, u = unknown), Life form (a = aerophilic, b = benthic, p = planktonic, m = marine, u = unknown) and trophic state (uo = ultraoligotrophic, ot = oligotrophic, mt = mesotrophic, et = eutrophic, pt = polytrophic, ht = hypertrophic, mar = marine, u = unknown)

Species Name	Salinity	pH	Life form	Trophic state
Achnanthes brevipes	fb	c	b	ut
Achnanthes brockmannii	m	m	m	mar
Achnanthes javanica	b	u	b	ot
Achnanthes oblongella	fb	c	b	ut
Achnanthes inflata	f	u	b	ot
Achnanthidium crassum	u	k	b	u
Achnanthidium minutissimum	f	c	b	o-e
Achnanthidium straubianum	f	k	b	m-e
Achnanthidium subaffinis	f	u	b	ot
Actinocyclus normanii	f	a	p	et
Actinocyclus sp.	u	u	u	u
Actinoptychus heliopelta	m	m	m	mar
Actinoptychus undulatus	m	m	m	mar
Actinoptychus vulgaris	m	m	m	mar
Amphora acutiuscula	b	k	b	u
Amphora arenaria	m	m	m	mar
Amphora coffeaeformis	b	k	b	pt
Amphora commutata	m	m	b	mar
Amphora copulata	fb	k	b	p-h
Amphora decussata	m	m	m	mar
Amphora lunaris	m	m	m	mar
Amphora ostrearia	m	m	m	mar
Amphora ovalis	fb	k	b	pt
Amphora proteus	m	m	m	mar
Amphora spectabilis	m	m	m	mar
Amphora veneta	bf	b	b	p-h
Aulacoseira ambigua	f	k	p	et
Auliscus cf. sculptus	m	m	m	mar
Bacillaria paradoxa	b	b	b	u
Biddulphia capusina	m	m	m	mar
Biddulphia pulchella	m	m	m	mar

Species Name	Salinity	pH	Life form	Trophic state
Brachysira brebissonii	f	a	b	ot
Caloneis aequatorialis	f	k	u	u
Caloneis crassa	m	m	m	mar
Campylodiscus clypeus	b	b	p	u
Catenula adhaerens	m	m	b	mar
Chaetoceros sp.	m	m	m	mar
Cocconeis costata	m	m	m	mar
Cocconeis distans	m	m	m	mar
Cocconeis engelbrechtii	b	k	b	u
Cocconeis pediculus	b	k	b	u
Cocconeis placentula	fb	k	b	et
Cocconeis pseudomarginata	m	m	m	mar
Cocconeis scuttellum	mb	k	b	et
Coscinodiscus radiatus	m	m	m	mar
Craspedodiscus elegans	m	m	p	mar
Craspedostauros capensis	m	m	m	mar
Craticula accomodiformis	u	u	b	et
Cyclotella caspia	b	k	p	et
Cyclotella choctawhatcheeana	m	m	m	mar
Cyclotella distinguenda	b	k	p	et
Cyclotella meneghiniana	f	k	p-b	et
Cylindrotheca closterium	m	m	m	mar
Cymbella affinis	f	k	b	ot
Delphineis minutissima	m	m	p	mar
Dimeregramma minor var. minor	m	m	m	mar
Diploneis crabro	m	m	p	mar
Diploneis oblongella	fb	k	b	ut
Diploneis smithii	b	c	b	u
Diploneis sp	u	u	u	u
Diploneis elliptica	fb	k	b	ot
Encyonema gracile	fb	i	b	ot
Encyonema silesiacum	f	c	b	o-e
Encyonopsis cesatii	fb	c	b	ot
Entomoneis ornata	fb	c	b	o-e
Entomoneis punctulata	b	u	b	u

Species Name	Salinity	pH	Life form	Trophic state
Epithemia adnata	fb	b	b	m-e
Epithemia sorex	fb	b	b	e-p
Eunotia flexuosa	f	a	b	ot
Eunotia incisa	u	a	b	ot
Eunotia minor	fb	c	b	et
Eunotia zygodon	f	a	b	u
Fallacia monoculata	fb	b	b	u
Fallacia pygmaea	bf	b	b	ht
Fallacia tenera	b	a	b	u
Fragilaria biceps	f	b	b	m-e
Fragilaria tenera	f	a	b	m-e
Frustulia rhomboides	u	c	u	u
Gomphonema gracile	fb	c	b	u
Gomphonema venusta	u	c	u	o-m
Gyrosigma obscurum	b	k	u	o-m
Hantzschia amphioxys	fb	c	a	p-h
Hippodonta hungarica	f	k	b	mt
Isthmia enervis	m	m	m	mar
Luticola goeppertiana	fb	k	b	p-h
Lyrella lyra	m	m	m	mar
Mastogloia braunii	b	c	b	u
Mastogloia crucicula	m	m	m	mar
Mastogloia danseii	bf	u	b	u
Mastogloia fimbriata	m	m	m	mar
Mastogloia latecostata	m	m	m	mar
Mastogloia smithii	b	k	b	m-e
Mastogloia sp	u	u	u	u
Mastogloia vasta	m	m	m	mar
Mayamaea atomus	fb	k	a	e-p
Melosira nummuloides	b	k	b	et
Melosira varians	bf	k	p-b	et
Navicula cincta	fb	k	a	ot
Navicula cryptocephala	fb	c	b	pt
Navicula directa	m	m	m	mar
Navicula erifuga	b	k	u	et

Species Name	Salinity	pH	Life form	Trophic state
Navicula oblonga	fb	k	u	e-p
Navicula radiosa	fb	c	b	o-e
Navicula tenelloides	fb	k	a	e-p
Navicula veneta	bf	k	b	pt
Navicymbula pusilla	fb	k	b	o-e
Navigiolum adamantiforme	u	k	u	et
Nitzschia amphibia	fb	k	b	pt
Nitzschia brevissima	b	c	b	u
Nitzschia clausii	b	k	b	p-h
Nitzschia cocconeiformis	m	m	m	mar
Nitzschia compressa	mb	k	b	u
Nitzschia dissipata	fb	k	b	u
Nitzschia laevis	m	m	m	mar
Nitzschia palea	fb	c	b	pt
Nitzschia pusilla	u	k	a	et
Nitzschia recta	u	k	b	et
Nitzschia sigma	b	k	b	et
Nitzschia tryblionella	b	k	u	u
Opephora marina	u	k	u	m-e
Paralia sulcata	m	m	p	mar
Petroneis humerosa	m	m	b	mar
Pinnularia acrosphaeria	u	c	b	u
Pinnularia borealis	fb	c	a	m-e
Pinnularia borealis var. 1	fb	c	a	m-e
Pinnularia intermedia	u	i	u	m-e
Pinnularia maior	f	i	u	ot
Pinnularia sp. 1	u	u	u	u
Pinnularia sp. 2	u	u	u	u
Pinnularia subcapitata	fb	i	b	ot
Pinnularia viridis	u	a	b	o-m
Plagiodiscus nervatus	m	m	m	mar
Plagiotropis lepidoptera	m	m	m	mar
Planothidium delicatulum	b	b	u	u
Pleurosigma sp	u	u	u	u
Pseudo-nitzschia	m	m	m	mar

Species Name	Salinity	pH	Life form	Trophic state
Rhopalodia gibba	fb	b	b	et
Rhopalodia gibberula	bf	k	b	u
Rhopalodia musculus	b	b	u	u
Rossithidium linearis	f	k	b	u
Sellaphora bacillum	f	k	b	et
Sellaphora pupula	u	c	b	p-h
Seminavis atlantica	m	m	m	mar
Seminavis strigosa	mb	k	b	u
Stauroneis phoenicenteron	fb	c	u	et
Stauroneis sp.	u	u	u	u
Staurosira elliptica	fb	k	b	mt
Stephanodiscus agassizensis	fb	k	p	et
Stephanodiscus hantzschii	fb	k	p	et
Surirella brebissonii	b	k	b	u
Surirella fastuosa	m	m	m	mar
Surirella hybrida	m	m	m	mar
Synedra bacillaris	m	m	p	mar
Tabellaria fenestrata	i	i	b	o-m
Tabellaria flocculosa	f	a	p-b	ot
Tabularia fasciculata	b	k	b	m-e
Thalassionema nitzschioides	m	m	m	mar
Thalassiosira eccentrica	m	m	m	mar
Thalassiosira gravida	m	m	m	mar
Thalassirosira weissflogii	f	c	p	pt
Trachyneis aspera	m	m	m	mar
Triceratium reticulum	m	m	b	mar
Tryblionella apiculata	b	k	b	ht
Tryblionella calida	bf	c	b	et
Tryblionella coarctata	b	k	b	u
Tryblionella hungarica	bf	k	b	pt

Table 11.5: Eilandvlei (EV11.1) diatom species percentage representation against depth and age

Depth (cm)	**11**	**13**	**15**	**17**	**19**	**21**	**23**	**25**	**27**	**29**	**31**	**33**	**35**	**37**
Age (cal yrs BP)	**-31**	**-26**	**-20**	**-15**	**-10**	**18**	**67**	**116**	**165**	**214**	**263**	**313**	**362**	**411**
Achnanthes brevipes	0.2	1	0.2	0.4	0.2	0.2	0	0	0	0	0	0	0	0
Achnanthes brockmannii	0	0	0	0	0	0	0	0	0	0	0	0	0	0
Achnanthes javanica	0	0	0	0	0	0	0	0	0	0	0	0	0	0
Achnanthes oblongella	0.6	0.6	1	1.6	1.2	0.6	0.2	0	1	0.4	1.2	0.6	2.4	0.4
Achnanthes inflata	0	0	0	0	0	0	0	0	0	0	0	0	0	0
Achnanthidium crassum	0	0	0.2	0.2	0	0	0	0	0	0	0	0	0	0
Achnanthidium minutissimum	0	0.4	0.2	0	0	0	0	0	0	0	0.6	0.2	0	0
Achnanthidium straubianum	1.4	0	0	0	0.2	0	0	0	0	0	0	0	0	0
Achnanthidium subaffinis	0	0	0	0	0	0	0	0	0	0	0	0	0	0
Actinocyclus normanii	0.8	0.6	0	0.2	0	0	0	0	0	0	0	0	0	0.2
Actinocyclus sp.	0	0	0	0	0	0	0	0	0	0.4	0	0	0	0
Actinoptychus heliopelta	0	0	0	0	0	0	0	0	0	0	0	0	0	0
Actinoptychus undulatus	0	0	0	0	0	0	0	0	0	0	0	0	0	0
Actinoptychus vulgaris	0	0	0	0	0	0	0	0	0	0	0	0	0	0
Amphora acutiuscula	0	0	0	0.2	0	0	0	0	0.2	0	0.4	0	0	0
Amphora arenaria	0	0	0	0	0	0	0	0	0	0	0	0	0	0
Amphora coffeaeformis	0.2	0.4	0.6	0.2	0.4	0	0.6	0	0	0.2	0.6	0	0	0
Amphora commutata	0	0	0	0	0	0	0	0	0	0	0	0	0	0
Amphora copulata	0	0	0	0	0	0	0	0	0	0	0	0	0	0
Amphora decussata	0	0	0	0	0	0	0	0	0	0	0	0	0	0
Amphora lunaris	0	0	0	0	0	0	0	0	0	0	0	0	0	0
Amphora ostrearia	0	0	0	0	0	0	0	0	0	0	0	0	0	0
Amphora ovalis	1	0.2	0.2	0.6	0	0	0.4	0	0.2	0.2	0.2	0.2	0.2	0.2
Amphora proteus	0	0	0	0	0	0	0	0	0	0	0	0	0	0
Amphora spectabilis	0	0	0	0	0	0	0	0	0	0	0	0	0	0
Amphora veneta	0	0	0	0	0	0	0	0	0	0	0	0	0	0
Aulacoseira ambigua	0	0	0.2	0	0	0	0	0	0	0	0	0	0	0
Auliscus cf. sculptus	0	0	0	0	0	0	0	0	0	0	0	0	0	0
Bacillaria paradoxa	0	0	0	0	0.2	0	0	0	0	0	0	0	0	0
Biddulphia capusina	0	0	0	0	0	0	0	0	0	0	0	0	0	0
Biddulphia pulchella	0	0	0	0	0	0	0	0	0	0	0	0	0	0
Brachysira brebissonii	0	0	0	0	0	0	0	0	0	0	0	0	0	0
Caloneis aequatorialis	0	0	0	0	0	0.2	0	0	0.2	0	0	0	0.2	0
Caloneis crassa	0	0	0	0	0	0	0	0	0	0	0	0	0	0
Campylodiscus clypeus	0	0	0	0	0	0	0.2	0	0	0	0	0	0.2	0
Catenula adhaerens	1.8	0.6	0.8	0.6	0.8	0.6	0.6	0.8	1	0.4	0.4	0.6	0.2	0.8

Depth (cm)	**11**	**13**	**15**	**17**	**19**	**21**	**23**	**25**	**27**	**29**	**31**	**33**	**35**	**37**
Age (cal yrs BP)	**-31**	**-26**	**-20**	**-15**	**-10**	**18**	**67**	**116**	**165**	**214**	**263**	**313**	**362**	**411**
Chaetoceros sp.	13.2	0.2	0.6	1.8	0.2	0.4	1.4	1.4	0.2	0.6	0.2	0.4	0.4	0.6
Cocconeis costata	0	0	0	0	0	0	0	0	0	0	0	0	0	0
Cocconeis distans	0	0.4	0	0.4	0	0	0.4	0	0	0.6	0.2	0.6	0.4	0.6
Cocconeis engelbrechtii	15.2	20	19.2	14.6	8	5.4	5.4	4.4	6.8	5.2	10.6	12	8.8	4
Cocconeis pediculus	0.2	0.2	0	0.2	0.4	0	0	0.4	0.6	0	0.2	0	0	0.4
Cocconeis placentula	8	7.4	4.8	6.4	8.4	3.6	1.4	0.8	2.6	1.8	4.6	1.4	6	3.6
Cocconeis pseudomarginata	0	0	0	0	0	0	0	0	0	0	0	0	0	0
Cocconeis scuttellum	0	0	0	0	0	0	0	0	0	0.2	0	0	0	0.4
Coscinodiscus radiatus	3.2	4.8	2.2	1.2	1.2	1.6	8.8	44.2	39	27.8	34	37.8	15.4	35
Craspedodiscus elegans	0	0	0	1.8	0	0	0	0.2	0	0	0	0	0	0
Craspedostauros capensis	0	0	0	0	0	0	0	0	0	0	0	0	0	0
Craticula accomodiformis	0	0	0	0	0	0	0	0	0	0	0	0	0	0
Cyclotella caspia	15.4	21	24.2	26	36.8	2.2	4.8	2	2.2	1	12.6	3.4	7.8	3.8
Cyclotella choctawhatcheeana	0	0	0	0	0	0	0	0	0	0	0	0	0	0
Cyclotella distinguenda	2.6	4.4	6	7	12.2	0.6	1	1	3.2	0.4	0.6	1.4	10.6	4.2
Cyclotella meneghiniana	0	0	0.6	0.2	0.4	0	0	0	0.2	0	0	0.2	0.4	0.4
Cylindrotheca closterium	0	0	0	0	0	0	0	0	0	0	0	0	0	0
Cymbella affinis	0	0	0	0.2	0	0	0	0	0	0	0	0	0	0
Delphineis minutissima	0.2	0	0.2	0	0	0	0.2	0	0.4	0	0	0.2	0.4	0
Dimeregramma minor var. minor	0	0	0	0	0	0	0	0	0	0	0	0	0	0
Diploneis crabro	0	0	0	0.2	0	0	0	0	0	0	0	0	0	0
Diploneis oblongella	0	0.2	0	0	0	0	0	0	0	0.2	0	0.2	0	0.2
Diploneis smithii	0.4	0.4	0.2	0.2	0.2	0.4	0	0.4	0.2	0.8	0	0.4	0.2	0.2
Diploneis sp	0	0	0	0	0	0	0	0	0	0	0	0	0	0
Diploneis elliptica	0	0	0	0	0	0	0.4	0	0.2	0.2	0.2	0	0.8	0.8
Encyonema gracile	0.2	0	0	0.2	0	0	0	0	0	0	0	0	0	0
Encyonema silesiacum	0	0	0.2	0	0	0	0	0	0	0	0.6	0	0	0
Encyonopsis cesatii	0	0.4	0.6	0	0	0	0	0	0	0	0	0	0	0
Entomoneis ornata	0	0	0	0	0	0	0	0	0	0	0	0	0	0
Entomoneis punctulata	0.6	1.4	4.6	3.6	1.6	0	0.2	0	0	0	0	0	0	0
Epithemia adnata	0	0	0	0	0	0	0	0	0	0	0	0	0	0
Epithemia sorex	0	0	0	0	0	0	0	0	0	0	0	0	0	0
Eunotia flexuosa	0.2	0	0	0	0	0	0	0	0	0	0.2	0	0	0
Eunotia incisa	0	0	0	0	0.2	0	0	0	0	0	0	0	0	0
Eunotia minor	0	0.2	0.4	0	0.2	0.2	0.2	0	0	0.4	0.4	0.4	0.4	0.2
Eunotia zygodon	0	0	0	0	0	0	0	0	0	0	0	0	0	0
Fallacia monoculata	4.6	0.8	1.2	1	0	0	0	0	0.4	0.2	0	0	0.8	3.4
Fallacia pygmaea	0	0	0	0	0	0	0	0	0	0	0	0	0	0

Depth (cm)	**11**	**13**	**15**	**17**	**19**	**21**	**23**	**25**	**27**	**29**	**31**	**33**	**35**	**37**
Age (cal yrs BP)	**-31**	**-26**	**-20**	**-15**	**-10**	**18**	**67**	**116**	**165**	**214**	**263**	**313**	**362**	**411**
Fallacia tenera	0	0	0.4	0	0	0	0	0	0	0	0	0.2	0	0
Fragilaria biceps	0	0	0	0	0	0	0.2	0.2	0	0	0	0	0	0
Fragilaria tenera	1	1.4	1.8	0.6	0.4	0	0	0	0	0	0	0.2	0	0
Frustulia rhomboides	0	0	0	0	0	0	0.2	0	0	0.2	0	0	0	0
Gomphonema gracile	0	0	0	0	0	0	0	0	0	0	0	0	0	0
Gomphonema venusta	0	0	0	0	0	0	0	0	0	0	0.2	0	0	0
Gyrosigma obscurum	0	0	0	0	0.2	0	0	0.4	0	0	0.2	0	0	0
Hantzschia amphioxys	0	0	0	0	0	0	0	0	0.2	0	0	0.4	0	0
Hippodonta hungarica	0	0	0	0	0	0	0	0	0.6	0	0	0	0	0
Isthmia enervis	0	0	0	0	0	0	0	0	0	0	0	0	0	0
Luticola goeppertiana	0	0	0	0	0	0	0	0	0	0.2	0.2	0	0	0
Lyrella lyra	0	0	0	0	0	0	0	0	0	0	0	0	0	0
Mastogloia braunii	0.6	0.2	0	0.2	0	0.4	0.2	0	0	0	0.4	0.2	0	0.2
Mastogloia crucicula	0	0	0	0	0	0	0	0	0	0	0	0	0	0
Mastogloia danseii	0	0	0	0	0	0	0	0	0	0	0	0	0	0
Mastogloia fimbriata	0	0	0	0	0	0	0	0	0	0	0	0	0	0
Mastogloia latecostata	0	0	0	0	0	0	0	0	0	0	0	0	0	0
Mastogloia smithii	1.4	0.4	0.4	0.6	0.6	0	0.4	0.6	0	0.2	0.8	0	0.4	0
Mastogloia sp	0	0	0	0	0	0	0	0	0	0	0	0	0	0
Mastogloia vasta	0	0	0	0	0	0	0	0	0	0	0	0	0	0
Mayamaea atomus	0.2	1	0.8	0.8	0	0	0.2	0.2	0	0	0	0	0.6	0
Melosira nummuloides	7.6	11.8	11.8	10.6	11.2	68.4	63.8	37.6	30.8	46.2	17	29.6	25.6	25.2
Melosira varians	0	0.2	0.4	0.4	0	0	0	0.8	0	0	0.2	0	0	0
Navicula cincta	0	0.4	0.6	0	0	0.2	0	0	0	0.2	0	0	0	0
Navicula cryptocephala	0.4	0	0.2	0.4	0.2	0	0	0	0	0	0.2	0	0	0
Navicula directa	0	0	0	0	0	0	0	0	0	0	0	0	0	0
Navicula erifuga	0	0	0	0	0	0	0	0	0	0	0	0	0	0
Navicula oblonga	0.6	0	0	0	0	0	0	0	0	0	0	0	0	0
Navicula radiosa	0.2	0	0	0	0.4	0	0	0	0	0.4	0.4	0.6	0.4	0
Navicula tenelloides	0.4	0.8	0.2	0.2	0.2	0	0.4	1	0.2	0	0.6	0	0	0
Navicula veneta	0.2	0.2	0.4	0	0	0	0	0	0	0	0	0	0.4	0
Navicymbula pusilla	0	0	0	0	0.2	0	0	0	0	0.2	0.2	0	0	0
Navigiolum adamantiforme	0	0	0	0	0	0	0	0	0	0.2	0	0	0	0
Nitzschia amphibia	0	0	0	0	0	0.2	0	0	0	0.4	0	0	0	0
Nitzschia brevissima	0	0	0	0	0	0	0	0	0	0	0	0	0	0
Nitzschia clausii	0	0	0	0	0	0	0	0	0	0.2	0.8	0	0.2	0
Nitzschia cocconeiformis	0	0	0.2	0	0.2	1.6	0	0	0	0	0	0	0	0
Nitzschia compressa	0	0	0	0	0.2	0	0	0	0	0	0	0.6	0.4	1

Depth (cm)	11	13	15	17	19	21	23	25	27	29	31	33	35	37
Age (cal yrs BP)	**-31**	**-26**	**-20**	**-15**	**-10**	**18**	**67**	**116**	**165**	**214**	**263**	**313**	**362**	**411**
Nitzschia dissipata	0	0	0	0	0	0	0	0	0	0	0	0	0	0
Nitzschia laevis	0	0	0	0	0	0	0	0	0	0	0	0	0	0
Nitzschia palea	0	0.6	0	0	0	0	0	0	0	0	0	0	0.2	0
Nitzschia pusilla	0	0	0	0	0	0	0	0	0	0	0	0	0	0
Nitzschia recta	0	0	0.2	0	0.2	0	0	0	0.6	0	0.4	0.2	0	0.4
Nitzschia sigma	0	0	0.2	0	0	0	0	0	0	0	0	0	0	0
Nitzschia tryblionella	0	0	0	0	0	0	0	0	0	0	0	0	0	0
Opephora marina	0.2	0.6	0.2	0.2	0.2	0	0.4	0	0	0	0	0.4	0	0
Paralia sulcata	0	0	0	0	0	0	0	0	0	0	0	0	0	0
Petroneis humerosa	0	0	0	0	0	0	0	0	0	0	0	0	0	0
Pinnularia acrosphaeria	0	0	0	0	0	0	0	0	0	0	0	0	0	0
Pinnularia borealis	0	0	0	0.2	0	0	0	0	0	0	0	0	0	0
Pinnularia borealis var. 1	0.2	0	0.2	0.2	0	0.2	0	1	1.8	2.2	0.6	1.2	4.4	8.2
Pinnularia intermedia	0	0	0	0	0	0	0	0	0	0	0	0	0	0
Pinnularia maior	0	0	0	0	0	0	0	0	0	0	0	0	0	0
Pinnularia sp.	0	0	0	0	0	0	0	0	0	0	0	0	0	0
Pinnularia sp. 2	0	0	0	0	0	0	0	0	0	0	0	0	0	0
Pinnularia subcapitata	0	0.2	0	0	0	0	0	0	0	0	0	0	0	0
Pinnularia viridis	0	0	0	0	0	0	0	0	0.2	0	0	0	0	0
Plagiodiscus nervatus	0	0	0	0	0	0	0	0	0	0	0	0	0	0
Plagiotropis lepidoptera	0	0	0	0	0	0	0	0	0	0	0	0	0.2	0
Planothidium delicatulum	1.6	0.4	0.2	0.4	0.2	0.6	0	0	0.2	0.4	0.2	0	0.4	0.2
Pleurosigma sp	0	0	0	0	0	0	0	0	0	0	0	0	0	0
Pseudo-nitzschia	0	0	0	0	0	0	0	0	0	0	0	0	0	0
Rhopalodia gibba	0	0	0	0	0	0	0	0	0	0	0	0	0	0
Rhopalodia gibberula	0	0.2	0	0.2	1	0	0	0	0	0.2	0	0	0	0.2
Rhopalodia musculus	0.2	0	0	0	0	0	0	0	0	0	0.2	0.2	0.2	0
Rossithidium linearis	0	0	0	0	0	0	0	0	0	0	0	0	0	0
Sellaphora bacillum	0	0	0	0	0	0	0	0	0	0	0	0	0	0
Sellaphora pupula	0	0	0	0	0	0	0	0	0	0	0	0	0	0
Seminavis atlantica	0	0	0.2	0	0	0	0	0	0	0	0	0	0	0
Seminavis strigosa	0	0.2	0	0	0	0	0	0	0	0	0	0	0	0
Stauroneis phoenicenteron	0	0	0	0	0	0	0	0	0	0	0.2	0	0	0
Stauroneis sp.	0	0	0	0	0	0	0	0	0	0	0	0	0	0
Staurosira elliptica	0.2	0.2	0.2	0.2	0	0	0	0	0	0	0	0.2	0	0.2
Stephanodiscus agassizensis	1.4	1.2	0.8	0.8	1.8	1.2	2.6	0.6	2.6	1.8	3.2	1.2	3.6	0.2
Stephanodiscus hantzschii	1.8	2.2	2	3.4	1.6	0	2.4	0.2	1.6	0.2	3.4	1.4	3	0
Surirella brebissonii	0.2	0	0.2	0.2	0	0	0	0.2	0	0	0	0.2	0.2	0

Depth (cm)	**11**	**13**	**15**	**17**	**19**	**21**	**23**	**25**	**27**	**29**	**31**	**33**	**35**	**37**
Age (cal yrs BP)	**-31**	**-26**	**-20**	**-15**	**-10**	**18**	**67**	**116**	**165**	**214**	**263**	**313**	**362**	**411**
Surirella fastuosa	0	0	0	0	0	0	0	0	0	0	0	0	0	0
Surirella hybrida	0	0	0	0	0	0	0	0	0	0	0	0	0	0
Synedra bacillaris	0	0	0	0	0	0	0	0	0	0	0	0	0	0
Tabellaria fenestrata	0	0	0	0	0	0	0	0	0	0	0	0	0	0
Tabellaria flocculosa	0	0	0	0.2	0	0	0	0	0	0	0	0	0	0
Tabularia fasciculata	8.4	11.6	9.6	10.4	5.4	8.2	2.2	0.6	1.8	1.6	1.8	1.8	3.2	1
Thalassionema nitzschioides	0	0	0	0	0	0	0	0	0	0	0	0	0	0
Thalassiosira eccentrica	0	0	0	0	0	0	0	0	0	0	0	0	0	0
Thalassiosira gravida	0	0	0	0	0	0	0	0	0	0	0	0	0	0
Thalassirosira weissflogii	3	0.2	0.4	0.2	2.8	0.4	0.2	0	0	0	0	0.6	0.4	0
Trachyneis aspera	0	0	0	0	0	0	0	0	0	0	0	0	0	0
Triceratium reticulum	0	0	0	0	0	0	0	0	0	0	0	0	0	0
Tryblionella apiculata	0	0.2	0	0.2	0.2	0.2	0.4	0.2	0	0.4	0.2	0	0.2	0.8
Tryblionella calida	0.2	0.2	0	0	0	1.8	0	0.4	0.4	1.2	0.4	0.4	0.2	1.2
Tryblionella coarctata	0	0	0	0	0	0	0	0	0	0	0	0	0	0
Tryblionella hungarica	0	0	0	0.4	0	0.6	0.2	0.4	0.4	2.6	0.4	0.4	0.2	1.8

EV11.1 continued

Depth (cm)	**39**	**41**	**43**	**45**	**47**	**49**	**51**	**53**	**55**	**57**	**59**	**61**	**63**	**65**
Age (cal yrs BP)	**460**	**503**	**539**	**575**	**611**	**647**	**683**	**719**	**755**	**791**	**827**	**864**	**900**	**936**
Achnanthes brevipes	0	0.6	0	0	0	0	0.2	0	0.2	0	0.2	0	0	0
Achnanthes brockmannii	0	0	0	0	0	0	0	0	0	0	0	0	0	0
Achnanthes javanica	0	0	0	0	0	0	0	0	0	0	0	0	0	0
Achnanthes oblongella	1	1.4	1.2	1	1	0.6	2.4	0.8	2	0.2	1.8	2.6	0.6	1.6
Achnanthes inflata	0	0	0	0	0	0	0	0	0.2	0	0	0	0	0
Achnanthidium crassum	0.2	0	0	0	0	0	0.2	0	0	0	0	0.2	0	0
Achnanthidium minutissimum	0	0	0.4	0.6	0.2	0	0	0	0	0	0.2	0	0.4	0
Achnanthidium straubianum	0.2	0	0	0.2	0	0.2	0.2	0	0.2	0	0	0	0	0.2
Achnanthidium subaffinis	0	0	0	0	0	0	0	0	0	0	0	0	0	0
Actinocyclus normanii	0.2	0	0	0	0	0	0	0	0	0	0	0	0	0
Actinocyclus sp.	0	0	0	0	0	0	0	0	0	0	0	0	0	0
Actinoptychus heliopelta	0	0	0	0	0	0	0	0	0	0	0	0	0	0
Actinoptychus undulatus	0	0	0	0	0	0	0	0	0	0	0	0	0	0
Actinoptychus vulgaris	0	0	0	0	0	0	0	0	0	0	0	0	0	0
Amphora acutiuscula	0	0	0	0	0	0.2	0	0	0	0.2	0.2	0	0	0
Amphora arenaria	0	0	0	0	0	0	0	0	0	0	0	0	0	0
Amphora coffeaeformis	0	0.2	0.4	0.6	1	0.4	0.8	0.2	0.2	0	0.4	0.2	0.6	0
Amphora commutata	0	0	0	0	0	0	0	0	0	0	0	0.2	0.2	0
Amphora copulata	0	0	0	0	0	0	0	0	0	0	0	0	0	0
Amphora decussata	0	0	0	0	0	0	0	0	0	0	0	0	0	0
Amphora lunaris	0	0	0	0	0	0	0	0	0	0	0	0	0	0
Amphora ostrearia	0	0	0	0	0	0	0	0	0	0	0	0	0	0
Amphora ovalis	0	0.2	0	0	0.2	0.2	0	0.2	1.6	0	0.8	0	0.6	0.4
Amphora proteus	0	0	0	0	0	0	0	0	0	0	0	0	0	0
Amphora spectabilis	0	0	0	0	0.2	0	0	0	0	0	0	0	0	0
Amphora veneta	0	0	0	0	0	0	0	0	0	0	0	0	0	0
Aulacoseira ambigua	0	0	0	0	0	0	0	0	0	0	0	0	0	0
Auliscus cf. sculptus	0	0	0	0	0	0	0	0	0	0	0	0	0	0
Bacillaria paradoxa	0	0	0	0	0	0	0	0	0	0	0	0	0	0
Biddulphia capusina	0	0	0	0	0	0	0	0	0	0	0	0	0	0
Biddulphia pulchella	0	0	0	0	0	0	0	0	0	0	0	0	0	0
Brachysira brebissonii	0	0	0	0	0.2	0	0	0	0	0	0.2	0	0	0
Caloneis aequatorialis	0	0	0	0	0	0	0	0	0	0	0	0	0	0
Caloneis crassa	0	0	0	0	0	0	0	0	0	0	0	0	0	0
Campylodiscus clypeus	0	0	0	0	0	0	0	0	0	0	0	0	0	0
Catenula adhaerens	1	0.4	0.4	0.6	0.4	1.2	1.4	0.4	1	0.2	0.8	1.2	0	1.8
Chaetoceros sp.	0	0.6	0.8	0.4	0.4	0.8	0.2	0.4	0.6	0.4	1.2	0.2	0.4	1.2

Depth (cm)	**39**	**41**	**43**	**45**	**47**	**49**	**51**	**53**	**55**	**57**	**59**	**61**	**63**	**65**
Age (cal yrs BP)	**460**	**503**	**539**	**575**	**611**	**647**	**683**	**719**	**755**	**791**	**827**	**864**	**900**	**936**
Cocconeis costata	0	0	0	0	0	0	0	0	0	0	0	0	0	0.6
Cocconeis distans	1.8	2.2	1.2	1	1.6	2	2	1.2	0.6	0.4	0	0.2	0	1
Cocconeis engelbrechtii	8.4	7.4	6.6	8.6	3.8	8.2	12.4	7.8	8	14.8	4	8.8	4.6	4
Cocconeis pediculus	1.2	0.8	2.8	0.6	1.2	2	0.6	0.4	0.6	2.2	0.8	1.8	1.2	0.2
Cocconeis placentula	9.2	7	7.4	8.2	10.8	8.4	9.8	7	8.6	5.8	9.8	11.2	6.4	5.2
Cocconeis pseudomarginata	0	0	0	0	0	0	0	0	0	0	0	0	0	0
Cocconeis scuttellum	0	0	0	0.2	0	0	0	0	0	0	0	0.2	0	1.2
Coscinodiscus radiatus	41.4	15	27	8.8	8.6	11.4	13	15	8	8.2	15.8	12.2	35.4	42
Craspedodiscus elegans	0	0.2	0	0	0	0	0	0	0	0	0	0	0	0
Craspedostauros capensis	0.2	0	0	0	0	0	0	0	0	0	0	0	0	0
Craticula accomodiformis	0.2	0	0	0	0	0	0	0	0.2	0	0	0	0	0
Cyclotella caspia	3	15	12.6	13.2	21.4	11.2	14.4	20	15.6	20.4	8.2	14	5.4	1.2
Cyclotella choctawhatcheeana	0	0	0	0	0	0	0	0	0	0	0	4	0	0
Cyclotella distinguenda	6.2	11.8	9	14.8	5	7.8	13.8	10	7.6	9.6	7	5.4	1.4	0.6
Cyclotella meneghiniana	0.2	0.8	0	0.8	0.6	0.2	0.2	0.4	1.2	1	0.2	0.2	0	0
Cylindrotheca closterium	0	0	0	0	0	0	0	0	0	0	0	0	0	0
Cymbella affinis	0	0	0	0	0	0	0	0	0	0	0	0	0	0
Delphineis minutissima	0	0	0	0.2	0	0	0	0	0.2	0.2	0.2	0	0.2	0.2
Dimeregramma minor var. minor	0	0	0	0	0	0	0	0	0	0	0	0	0	0
Diploneis crabro	0	0	0	0	0	0	0	0.2	0	0	0.2	0	0	0
Diploneis oblongella	0.4	0	0	0	0	0.4	0	0.2	0	0	0	0.8	0.2	0.6
Diploneis smithii	0.4	0.2	0	1.2	0.6	0.4	0.8	0.4	0.4	0.8	1	0.4	0.4	1
Diploneis sp	0	0	0	0	0	0	0	0	0	0	0	0	0	0
Diploneis elliptica	0	0.4	0.2	0	0.4	0.2	0.2	0.4	0.2	0	0	0.8	0	0
Encyonema gracile	0	0	0	0	0	0	0	0	0	0	0	0	0.2	0
Encyonema silesiacum	0	0	0	0.4	0	0	0	0	0	0	0	0	0	0
Encyonopsis cesatii	0	0	0	1	0	0	0	0	0	0	0.2	0	0.4	0
Entomoneis ornata	0	0.2	0	0	0	0	0	0.2	0	0.2	0	0	0	0
Entomoneis punctulata	0	0	0	0.2	0	0	0	0	0	0	0	0	0	0
Epithemia adnata	0	0	0.2	0	0	0.2	0	0	0	0	0	0	0	0
Epithemia sorex	0	0	0	0	0	0	0	0	0	0	0	0	0	0
Eunotia flexuosa	0.4	0.4	0	0	0	0	0	0	0	0	0	0	0	0
Eunotia incisa	0.4	0	0	0	0.2	0.2	0	0	0.4	0	0	0	0	0.2
Eunotia minor	0	0.2	0.4	0.6	0.4	0.4	0.2	0	0	0.8	0.6	0.2	0.4	0
Eunotia zygodon	0	0.2	0	0	0	0	0	0	0	0	0	0	0	0
Fallacia monoculata	3.4	2.4	4	2.4	4.2	5.4	2.8	2.2	2	3	2.2	4.6	3.8	2.8
Fallacia pygmaea	0	0	0.4	0	0	0	0	0	0	0	0	0	0	0.2
Fallacia tenera	0	0	0	0	0	0	0	0	0	0	0	0	0	0

Depth (cm)	39	41	43	45	47	49	51	53	55	57	59	61	63	65
Age (cal yrs BP)	**460**	**503**	**539**	**575**	**611**	**647**	**683**	**719**	**755**	**791**	**827**	**864**	**900**	**936**
Fragilaria biceps	0	0	0.4	0.2	0	0	0.2	0	0	0	0	0	0	0
Fragilaria tenera	0	0.4	0	0.2	0.6	0	0.4	0	0	0	0.2	0.2	0.2	0.2
Frustulia rhomboides	0	0	0	0	0	0	0	0	0.4	0.4	0	0	0	0
Gomphonema gracile	0	0	0	0.2	0.2	0	0.4	0	0.4	0	0	0	0.2	0
Gomphonema venusta	0	0.2	0	0.2	0	0	0	0	0	0.2	0	0	0	0
Gyrosigma obscurum	0	0	0.2	0	0	0.2	0.4	0.2	0.2	0	0	0	0.6	0
Hantzschia amphioxys	0.2	0	0	0	0	0	0	0	0	0	0	0	0	0
Hippodonta hungarica	0	0	0	0	0	0	0	0	0.2	0	0	0	0	0
Isthmia enervis	0	0	0	0	0	0	0	0	0	0	0	0	0	0
Luticola goeppertiana	0	0	0	0	0	0	0	0	0	0	0.2	0	0	0.2
Lyrella lyra	0	0	0	0	0	0	0	0	0	0	0	0	0	0
Mastogloia braunii	0.2	0	0.2	0	0	0	0	0	0	0	0	0	0	0
Mastogloia crucicula	0	0	0	0	0	0	0	0	0	0	0	0	0	0
Mastogloia danseii	0	0	0	0	0	0	0	0	0	0	0	0	0	0
Mastogloia fimbriata	0	0	0	0	0	0	0	0	0	0	0	0	0	0
Mastogloia latecostata	0	0	0	0	0	0	0	0	0	0	0	0	0	0
Mastogloia smithii	0.6	2	0.4	0.4	0.2	0.2	0.6	0	0	0.2	0	0	0.8	0.2
Mastogloia sp	0	0	0	0	0	0	0	0	0	0	0	0	0	0
Mastogloia vasta	0	0	0	0	0	0	0	0	0	0	0	0	0	0
Mayamaea atomus	0.6	0.4	0.2	1.8	0.8	1.4	0.6	0.6	0	0.2	0.8	1.6	0.6	0.4
Melosira nummuloides	7.4	16.2	10.8	19.2	22.8	24.8	7.6	18.2	22.2	12.2	11.2	16.2	3.6	3.2
Melosira varians	0	0	0.4	0	0	0.2	0	1.6	0	0.4	0.4	0.6	0	0
Navicula cincta	0	0	0	0	0.2	0	0	0.2	0	0.2	0	0	0	1.6
Navicula cryptocephala	2.8	1.4	0.2	0	0.4	0	0.2	0.4	1	0	0.2	0	0	0.4
Navicula directa	0	0	0	0	0	0	0	0	0	0	0	0	0	0
Navicula erifuga	0	0	0	0	0	0	0	0	0	0	0	0	0	0
Navicula oblonga	0.2	0	0	0	0	0.2	0.2	0	0.2	0.2	0	0	0	0
Navicula radiosa	0	0	0	0	0	0	0.4	0.4	0	0.2	0.4	0.8	0.8	0.4
Navicula tenelloides	0.2	0.4	0	0	0.4	0	0.4	0.2	0.4	0	0.4	0	0	0.8
Navicula veneta	0.2	0	0.2	0.2	0	0.2	0.4	0	0.2	0	0.2	0	0.4	0.4
Navicymbula pusilla	0	0	0	0.2	0	0.2	0.6	0	0	0	0	0	0.8	0.4
Navigiolum adamantiforme	0	0	0	0	0	0	0	0	0	0	0	0	0	0
Nitzschia amphibia	0	0	0	0	0.2	0	0	0	0.4	0	0	0	0	0
Nitzschia brevissima	0	0	0	0	0	0	0	0	0	0	0	0	0	0
Nitzschia clausii	0	0	0	0	0	0	0	0	0.2	0	0	0.2	0	0.6
Nitzschia cocconeiformis	0	0	0	0	0	0	0	0	0	0	0	0	0	0
Nitzschia compressa	0	0.2	0	0	0	0.2	0.2	0	0.2	0	0	0	0	0
Nitzschia dissipata	0	0	0	0	0	0	0	0	0	0	0	0	0	0

Depth (cm)	39	41	43	45	47	49	51	53	55	57	59	61	63	65
Age (cal yrs BP)	**460**	**503**	**539**	**575**	**611**	**647**	**683**	**719**	**755**	**791**	**827**	**864**	**900**	**936**
Nitzschia laevis	0	0	0	0	0	0	0	0	0	0	0	0	0	0
Nitzschia palea	0	0	0	0.6	0	0	0.2	0	0	0	0	0	0	0
Nitzschia pusilla	0	0	0	0	0	0	0	0	0	0	0	0	0	0
Nitzschia recta	0	0	0	0.2	0	0	0	0	0.2	0	0	0	1	0
Nitzschia sigma	0	0	0	0	0	0	0	0	0	0	0	0	0.2	0
Nitzschia tryblionella	0	0	0	0	0	0	0	0	0	0	0	0	0	0
Opephora marina	0	0.4	0	0	0.2	0.2	0.4	0	0	0.2	0.6	0.4	0.2	0.6
Paralia sulcata	0	0	0	0	0	0	0.2	0	0	0	0	0	0.2	0
Petroneis humerosa	0	0	0.2	0	0	0.2	0	0	0	0	0	0	0	0
Pinnularia acrosphaeria	0	0	0	0	0.2	0	0	0	0	0	0	0	0	0
Pinnularia borealis	0	0	0	0	0	0	0	0	0.2	0	0	0.2	0	0.4
Pinnularia borealis var. 1	2.6	2	3.2	1	1.8	2.4	2.4	2.8	3	3.6	19.4	2.2	21.6	19
Pinnularia intermedia	0	0	0	0	0	0	0	0	0	0	0	0	0	0
Pinnularia maior	0	0	0	0	0	0	0	0	0	0	0	0	0	0
Pinnularia sp.	0	0	0	0	0	0	0	0	0	0	0	0	0	0
Pinnularia sp. 2	0	0	0	0	0	0	0	0	0	0	0	0	0	0
Pinnularia subcapitata	0.4	0	0	0	0.2	0	0	0	0	0	0	0	0	0
Pinnularia viridis	0	0	0	0	0	0	0	0	0	0	0	0	0	0
Plagiodiscus nervatus	0	0	0	0	0	0	0	0	0	0	0	0	0	0
Plagiotropis lepidoptera	0	0	0	0	0	0	0	0	0	0	0	0	0	0
Planothidium delicatulum	0.4	0	0.4	0.2	0.4	0	0.8	0.4	0.4	0.4	0.2	0.4	0.2	0.4
Pleurosigma sp	0	0	0	0	0	0.2	0	0	0	0	0	0	0	0.2
Pseudo-nitzschia	0	0	0	0	0	0	0	0	0	0	0	0	0	0
Rhopalodia gibba	0	0	0	0	0.2	0	0	0	0	0	0	0	0.2	0
Rhopalodia gibberula	0	0.2	0	0	0	0.4	0.2	0.2	0	0.2	0.4	0	0.2	0.6
Rhopalodia musculus	0	0	0	0	0	0	0.4	0	0	0	0.2	0.4	0.2	0.2
Rossithidium linearis	0	0	0	0	0	0	0	0	0	0	0	0	0	0
Sellaphora bacillum	0	0	0	0	0	0	0	0	0	0	0	0	0	0
Sellaphora pupula	0	0	0	0	0	0	0	0	0	0	0	0	0	0
Seminavis atlantica	0	0	0	0	0	0.2	0	0	0	0	0	0	0	0
Seminavis strigosa	0	0.2	0	0	0	0	0	0	0	0	0	0	0	0
Stauroneis phoenicenteron	0	0	0	0	0	0	0	0	0	0	0	0	0	0
Stauroneis sp.	0	0	0	0.4	0	0.2	0	0	0	0	0	0	0	0
Staurosira elliptica	0	0	0.2	0	0	0	0	0	0	0	0	0.2	0.2	0
Stephanodiscus agassizensis	0.6	1	0.6	1.6	1.2	1.4	0.4	1.2	1.4	1.6	2.2	0.8	1	0
Stephanodiscus hantzschii	1.2	3.4	3.2	3.2	3.8	0.6	3.4	1.2	2.2	3.4	1.2	2.2	0.8	0.4
Surirella brebissonii	0.4	0	0.2	0.4	0.2	0	0.2	0.2	0.4	0	0.4	0.4	0.2	0.2
Surirella fastuosa	0	0	0	0	0	0	0	0	0	0	0	0.2	0	0

Depth (cm)	**39**	**41**	**43**	**45**	**47**	**49**	**51**	**53**	**55**	**57**	**59**	**61**	**63**	**65**
Age (cal yrs BP)	**460**	**503**	**539**	**575**	**611**	**647**	**683**	**719**	**755**	**791**	**827**	**864**	**900**	**936**
Surirella hybrida	0	0	0	0	0	0	0	0	0	0	0	0	0	0
Synedra bacillaris	0	0	0	0	0	0	0	0	0	0	0	0	0	0
Tabellaria fenestrata	0	0	0	0	0	0	0	0	0	0	0	0	0	0
Tabellaria flocculosa	0	0	0	0	0	0	0	0	0	0	0	0	0	0
Tabularia fasciculata	1.2	1.2	1.6	3	3	3	2.2	3.6	5.4	6.4	1.8	2.6	1	0.6
Thalassionema nitzschioides	0	0	0	0	0	0	0	0	0	0	0	0	0	0
Thalassiosira eccentrica	0	0	0	0	0	0	0	0	0	0	0	0	0	0
Thalassiosira gravida	0	0	0	0	0	0	0	0	0	0	0	0	0	0
Thalassirosira weissflogii	0	0.2	0.6	1	0.4	0	0.6	0	0.2	0.2	0.2	0	0	0
Trachyneis aspera	0	0	0	0	0	0	0	0	0	0	0	0	0	0
Triceratium reticulum	0	0	0	0	0	0	0	0	0	0	0	0	0	0
Tryblionella apiculata	0.6	0.6	0.2	0.2	0.2	1	0.2	0.6	0	0.8	2.2	0.6	1.4	1.4
Tryblionella calida	0.2	1.4	0.6	0	0	0.2	0	0.4	1	0.6	0.6	0.2	0.2	0.6
Tryblionella coarctata	0	0	0	0	0	0	0	0	0	0	0	0	0	0
Tryblionella hungarica	0.6	0.6	1	0	0	0.4	0.2	0.2	0	0	0.6	0.2	0.4	0.4

EV11.1 continued

Depth (cm)	67	69	71	73	75	77	79	81	83	85	87	89	91	93
Age (cal yrs BP)	**972**	**1008**	**1044**	**1080**	**1116**	**1152**	**1207**	**1281**	**1355**	**1429**	**1503**	**1577**	**1651**	**1725**
Achnanthes brevipes	0	0	0.4	0.2	0.8	0.4	0.2	0	0	0	0.2	0.2	0.2	0
Achnanthes brockmannii	0	0	0	0.2	0.2	0	0	0	0	0	0.2	0	0	0
Achnanthes javanica	0	0	0	0	0	0	0	0	0	0	0	0	0	0
Achnanthes oblongella	0.4	0.2	0.2	2.2	1.6	2	1	2	0.6	0.8	0.4	0.4	0	1
Achnanthes inflata	0.2	0	0.2	0	0	0.2	0	0.2	0	0	0	0.2	0	0
Achnanthidium crassum	0	0	0	0.8	0.2	0	0	0	0	0	0	0	0	0
Achnanthidium minutissimum	0.2	0.4	0.2	0.4	0.6	0.4	0	0	0.2	0.2	0.2	0.2	0	0.4
Achnanthidium straubianum	0	0.6	0	0	0.6	0.6	0	1.8	0	0	0	0	0	0.2
Achnanthidium subaffinis	0	0	0	0	0	0	0	0	0	0	0	0	0	0
Actinocyclus normanii	0	0	0.2	0	0	0	0	0	0	0.2	0	0	0	1.2
Actinocyclus sp.	0	0	0	0	0	0	0	0	0	0	0	0	0	0
Actinoptychus heliopelta	0	0	0	0	0	0	0	0	0	0	0	0	0	0
Actinoptychus undulatus	0	0	0	0	0	0	0	0	0	0	0	0	0	0
Actinoptychus vulgaris	0	0	0	0	0	0	0	0	0	0	0	0	0	0
Amphora acutiuscula	0.2	0.4	0	0	0	0	0	0	0	0	0	0	0	0
Amphora arenaria	0	0	0	0	0	0	0	0	0	0	0	0	0	0
Amphora coffeaeformis	0	0.2	0.4	1	1.4	0.2	0.6	0	0	0	0	0.4	0	0.2
Amphora commutata	0	0	0.4	1.2	1	0.2	0	0	0	0	0	0.2	0	0.2
Amphora copulata	0	0	0	0	0.4	0	0	0	0	0	0.2	0.2	0.2	0
Amphora decussata	0	0	0	0	0	0	0	0	0	0	0	0	0	0
Amphora lunaris	0	0	0	0	0	0	0	0	0	0	0	0	0	0
Amphora ostrearia	0	0	0	0	0	0	0	0	0	0	0	0	0	0
Amphora ovalis	0.4	0.4	0.4	0.2	2	1.8	0.2	0.2	0	0	0.2	0.2	0.2	0
Amphora proteus	0	0	0	0	0.2	0	0	0	0	0	0	0	0	0
Amphora spectabilis	0	0	0	0	0	0	0	0	0	0	0	0	0	0
Amphora veneta	0	0	0	0	0	0	0	0	0	0	0	0.2	0	0
Aulacoseira ambigua	0	0	0	0	0	0	0	0	0	0	0	0	0	0
Auliscus cf. sculptus	0	0	0	0	0	0	0	0	0	0	0	0	0	0
Bacillaria paradoxa	0	0	0	0.2	0	0	0	0	0	0	0	0	0	0
Biddulphia capusina	0	0	0	0	0	0	0	0	0	0	0	0	0	0
Biddulphia pulchella	0	0	0	0	0	0	0	0	0	0	0	0	0	0
Brachysira brebissonii	0	0	0	0	0	0.2	0	0	0	0	0	0.2	0	0
Caloneis aequatorialis	0	0	0	0	0	0	0	0	0	0	0	0	0	0
Caloneis crassa	0	0	0	0	0	0	0	0	0	0	0	0	0	0
Campylodiscus clypeus	0	0	0	0	0.2	0	0	0	0	0	0	0	0	0
Catenula adhaerens	0.2	2.2	0.8	1.2	1.6	1.4	0.2	1	0.2	1	0.8	0.2	0.4	0.4
Chaetoceros sp.	0.8	0	0.2	1.6	2.4	0.4	0.6	0.6	0.4	0.8	0.4	0.8	0.8	0.2

Depth (cm)	67	69	71	73	75	77	79	81	83	85	87	89	91	93
Age (cal yrs BP)	**972**	**1008**	**1044**	**1080**	**1116**	**1152**	**1207**	**1281**	**1355**	**1429**	**1503**	**1577**	**1651**	**1725**
Cocconeis costata	0	0	0	0.4	1.2	0.8	0	0.2	0	0	0	0	0	0
Cocconeis distans	0	1.2	0	0	1.8	0.2	1.2	3	0.8	1.8	2	0.8	0.6	1.6
Cocconeis engelbrechtii	6.2	6.2	2.6	6	2.6	4.8	7	5.4	6.8	9	7.6	6.6	3	9.4
Cocconeis pediculus	0.6	0	0.8	0.8	1.6	0.4	0.8	0.2	0.8	1.4	0.4	0.6	0	0
Cocconeis placentula	9.2	4.6	4.4	5.8	10	4.8	9.8	9.8	9	7.8	8.6	12.8	3.8	11.2
Cocconeis pseudomarginata	0	0	0	0	0	0	0	0	0	0	0	0	0	0
Cocconeis scuttellum	0	0	0	0	0	0	0	0	0	0	0.6	0	0.2	0
Coscinodiscus radiatus	20	31.8	34.2	21.8	2.6	18.6	4.4	4.4	1.4	13.4	17.2	0	15.2	0
Craspedodiscus elegans	0	0	0	0	0	0	0	0	0	0	0	0	0	0
Craspedostauros capensis	0	0	0	0	0	0	0	0	0	0	0	0.6	0	0
Craticula accomodiformis	0	0	0	0	0	0	0	0	0	0	0	0	0	0
Cyclotella caspia	9.8	2.2	4.6	6	6.6	8.2	20.2	19.2	14.8	8	8	7.6	6.8	8
Cyclotella choctawhatcheeana	0	0.2	1	3	1.4	3.6	2	9	0	1	0.4	0.6	0	0
Cyclotella distinguenda	4.4	0.8	2.6	2.6	1.2	2.4	5	7.4	6.8	6.8	3.4	4.4	8.6	7
Cyclotella meneghiniana	0.2	0.2	0.2	0.4	0	0.8	0.6	1.4	0.2	0.6	0	0.4	0.2	0
Cylindrotheca closterium	0	0	0	0	0	0	0	0	0	0	0	0	0	0
Cymbella affinis	0	0	0	0	0	0	0	0	0	0	0	0	0	0
Delphineis minutissima	0.4	0	0	0	0.4	0.6	0.4	0.6	0	0	0.6	2.8	3.8	0
Dimeregramma minor var. minor	0	0	0	0	0	0	0	0	0	0	0	0	0	0
Diploneis crabro	0	0	0	0	0.8	0.2	0	0	0	0	0	0	0	0
Diploneis oblongella	0.2	0.2	0.8	0.2	0.6	0.8	0	0.2	0	0	0.2	0	0	0
Diploneis smithii	0.4	1	0.8	0.4	0.2	0.4	0.6	0	0.8	0.6	0	0.4	0.2	0
Diploneis sp	0	0	0	0	0	0	0	0	0	0	0	0	0	0
Diploneis elliptica	0	0.2	0	2.2	2.2	0.8	0	0.2	0	0	0.4	0.4	0.2	0
Encyonema gracile	0	0	0.2	0	0	0	0	0	0	0	0	0	0	0
Encyonema silesiacum	0	0	0	0.2	0.2	0	0	0	0.2	0	0	0.4	0	0
Encyonopsis cesatii	0	0	0	0	0	0	0	0.2	0.2	0	0	0	0	0
Entomoneis ornata	0	0	0	0	0	0	0	0	0	0	0	0	0	0
Entomoneis punctulata	0	0	0	0	0	0	0	0	0	0	0	0	0	0
Epithemia adnata	0	0	0	0	0.2	0	0	0	0	0	0	0	0	0.4
Epithemia sorex	0	0	0	0	0	0	0	0	0	0	0	0	0	0
Eunotia flexuosa	0	0	0	0	0.2	0	0	0.2	0.2	0	0	0	0	0
Eunotia incisa	0	0	0	0	0	0	0.2	0	0	0.2	0	0.4	0	0
Eunotia minor	0.6	0.2	0	0.6	0.4	0.2	0.4	0	0.2	0.2	0.4	0	0.2	0.2
Eunotia zygodon	0	0	0	0	0	0	0.2	0	0	0	0	0	0	0
Fallacia monoculata	1.2	6.8	6	3.8	6	5	2	1	1.4	0.6	2.8	0.8	1	2.2
Fallacia pygmaea	0	1.2	0	0	0.8	0.8	0	1	0	0.2	0.2	0	0	0
Fallacia tenera	0	0	0.2	0	0.6	0	0	0	0	0	0.2	0	0	0

Depth (cm)	67	69	71	73	75	77	79	81	83	85	87	89	91	93
Age (cal yrs BP)	**972**	**1008**	**1044**	**1080**	**1116**	**1152**	**1207**	**1281**	**1355**	**1429**	**1503**	**1577**	**1651**	**1725**
Fragilaria biceps	0	0	0	0.8	0.4	0	0	0.2	0	0.2	0	0	0	0.2
Fragilaria tenera	0	0.4	0	0.2	0	0	0.2	1	0.2	0.2	0	1	0.2	0
Frustulia rhomboides	0	0	0	0	0.4	0	0	0	0	0	0	0	0	0
Gomphonema gracile	0	0	0	0	0	0	0.2	0	0.2	0	0	0	0	0
Gomphonema venusta	0	0	0	0	0.2	0	0	0	0	0	0	0	0	0
Gyrosigma obscurum	0.2	0	0.2	0	0.8	0.4	0.2	0	0	0	0	0	0	0
Hantzschia amphioxys	0	0	0	0	0.2	0	0	0	0	0	0	0	0	0
Hippodonta hungarica	0	0	0	0	0	0.2	0	0	0	0	0	0	0	0.2
Isthmia enervis	0	0	0	0	0	0	0	0	0	0	0	0	0	0
Luticola goeppertiana	0.2	0	0	0	0.2	0	0	0	0	0	0	0	0	0
Lyrella lyra	0	0	0	0	0	0	0.2	0	0	0	0	0	0	0
Mastogloia braunii	0.2	0	0.2	0	0.2	0	0	0.2	0	0	0	0	0	0.2
Mastogloia crucicula	0	0	0	0	0	0	0	0	0	0	0	0	0	0
Mastogloia danseii	0	0	0	0	0	0	0	0	0	0	0	0	0	0
Mastogloia fimbriata	0	0	0	0	0	0	0	0	0	0	0	0	0	0
Mastogloia latecostata	0	0	0	0	0	0.4	0	0	0	0	0	0	0	0
Mastogloia smithii	0	0.2	0.6	0.4	0.4	0.8	0.4	0.2	0	0.2	0.6	0.2	0.4	0
Mastogloia sp	0	0	0	0	0	0	0	0	0	0	0	0	0	0
Mastogloia vasta	0	0	0	0	0	0	0	0	0	0	0.2	0	0	0
Mayamaea atomus	0.2	0.8	0.8	1.8	1.2	1.8	0.6	0	0.4	0.8	1.6	1.6	0.4	0
Melosira nummuloides	14.4	19.6	15	5.6	9.2	9.8	20.4	16.6	44.8	37.8	30.8	45	43.2	45.2
Melosira varians	0	0.4	0	0.2	0	0	1	1.6	0	0	0.6	0	0.4	0.6
Navicula cincta	0.4	0.2	1	0.2	0.4	0.2	0.2	0.4	0	0	0.2	0.6	0	0
Navicula cryptocephala	0	0.4	1.2	0.6	1	0.8	0.4	0.2	0	0.2	0.4	0.4	0.2	0.4
Navicula directa	0	0	0	0	0	0	0	0	0	0	0	0	0	0
Navicula erifuga	0	0.2	0	0	0	0	0	0	0	0	0	0	0	0
Navicula oblonga	0	0	0	0	0	0	0	0	0	0	0	0	0	0
Navicula radiosa	0	0	1.2	0.4	0	0.8	2.6	0.2	0.6	0	0.8	0.2	0	0.4
Navicula tenelloides	0	0.2	1	1.6	0.8	1.4	0	0.4	0	0	0.2	0	0	0.2
Navicula veneta	0	0.2	0.2	0.2	0.2	0.2	0.2	0.2	0	0.2	0.4	0	0	0
Navicymbula pusilla	0.2	0.6	0	0	0.2	0.2	0	0	0	0	0	0.2	0.6	0
Navigiolum adamantiforme	0	0	0	0	0.2	0	0	0	0	0	0	0	0	0
Nitzschia amphibia	0	0	0	0	0.2	0	0	0	0	0	0	0	0	0.2
Nitzschia brevissima	0	0	0	0	0	0	0.4	0	0	0	0	0	0	0
Nitzschia clausii	0	0	0.6	0.2	0.2	0.2	0	0.4	0	0	0.2	0.2	0	0.2
Nitzschia cocconeiformis	0	0	0	0	0	0	0	0	0	0	0	0	0	0
Nitzschia compressa	0	0	0	0	0.4	0	0	0	0	0	0	0	0.2	0
Nitzschia dissipata	0	0	0	0	0	0	0	0	0	0	0	0	0	0

Depth (cm)	67	69	71	73	75	77	79	81	83	85	87	89	91	93
Age (cal yrs BP)	**972**	**1008**	**1044**	**1080**	**1116**	**1152**	**1207**	**1281**	**1355**	**1429**	**1503**	**1577**	**1651**	**1725**
Nitzschia laevis	0	0	0.4	0	0	0.2	0	0	0	0	0	0	0	0.2
Nitzschia palea	0	0	0.2	0	0.4	0.4	0.4	0	0	0.2	0	0	0.2	0.2
Nitzschia pusilla	0	0	0	0	0	0	0	0	0	0	0	0	0	0
Nitzschia recta	0	0	0	0	1	0	0.4	0	0.6	0.2	0	0.2	0	0
Nitzschia sigma	0	0	0.2	0.4	0.6	0	0	0	0	0	0	0	0	0
Nitzschia tryblionella	0	0	0	0	0	0	0	0	0	0	0	0	0	0
Opephora marina	0	0.6	0.4	0.6	1	1.4	0.4	0.4	0	0.2	0.2	0.2	0	0.2
Paralia sulcata	0	0	0	0	0	0	0	0	0	0.2	0	0	0	0
Petroneis humerosa	0	0.2	0	0	0.4	0.4	0	0.2	0	0	0.2	0	0	0
Pinnularia acrosphaeria	0	0	0	0	0	0	0	0	0	0	0	0	0	0
Pinnularia borealis	0	0	0	0	0	0	0	0	0.2	0	0	0	0	0
Pinnularia borealis var. 1	21.4	5.8	9.2	14.8	8.4	6.8	0.6	0	0.4	0	0	0	1	0
Pinnularia intermedia	0	0	0	0	0	0	0	0	0	0	0	0	0	0
Pinnularia maior	0	0	0	0.6	0.2	0	0	0	0	0	0	0	0	0
Pinnularia sp.	0	0	0	0	0	0	0	0	0	0	0	0	0	0
Pinnularia sp. 2	0	0	0	0	0	0	0	0	0	0	0	0	0	0
Pinnularia subcapitata	0	0	0.2	0.2	0	0	0	0	0	0.2	0	0.2	0	0
Pinnularia viridis	0	0	0	0	0	0	0	0	0	0	0	0	0	0
Plagiodiscus nervatus	0	0	0	0	0	0	0	0	0	0	0	0	0	0
Plagiotropis lepidoptera	0	0	0	0	0	0	0	0	0	0	0	0	0	0
Planothidium delicatulum	0.2	0.6	0.4	0.6	2.6	1.8	1	0.2	0	0	0.2	0.2	0.4	0.4
Pleurosigma sp	0	0	0	0	0	0	0	0	0	0	0	0	0	0
Pseudo-nitzschia	0	0	0.8	0	0	0	0	0	0	0	0	0	0	0
Rhopalodia gibba	0	0.2	0	0	0	0.2	0	0	0	0.2	0	0	0	0
Rhopalodia gibberula	0.2	0.6	0	0	0.6	0.2	0.2	0.4	0	0	0.8	0	0.2	0.2
Rhopalodia musculus	0	0.2	0	0.2	0.4	0.4	0.6	0	0	0.2	0	0	0	0
Rossithidium linearis	0	0.2	0	0	0	0	0	0.2	0	0	0	0	0	0
Sellaphora bacillum	0	0	0	0	0	0	0.2	0	0	0	0	0	0	0
Sellaphora pupula	0	0	0	0	0	0	0.2	0	0	0	0	0	0	0
Seminavis atlantica	0	0.2	0	0	0.2	0	0	0	0	0	0	0	0	0
Seminavis strigosa	0	0	0	0	0	0	0.2	0	0	0	0	0	0	0
Stauroneis phoenicenteron	0	0	0.2	0	0	0.2	0	0	0	0	0	0	0	0
Stauroneis sp.	0	0	0	0	0	0	0	0	0	0	0	0	0	0
Staurosira elliptica	0	0.4	0	0	1.4	0.6	0	0.6	0	0	0	0	0	0
Stephanodiscus agassizensis	1.4	1.2	0	1.2	0.6	0.4	0.8	0	0.4	0	1	1.6	1.6	1
Stephanodiscus hantzschii	1.4	0.8	0.8	1.6	2.2	3	2.4	2.8	2	0.2	2.4	2.6	1.4	2.6
Surirella brebissonii	0.4	0	0	0	0	0.2	0.4	0.2	0.4	0.2	0.2	0.2	0.4	0
Surirella fastuosa	0	0	0	0	0	0	0	0	0	0	0	0	0	0

Depth (cm)	**67**	**69**	**71**	**73**	**75**	**77**	**79**	**81**	**83**	**85**	**87**	**89**	**91**	**93**
Age (cal yrs BP)	**972**	**1008**	**1044**	**1080**	**1116**	**1152**	**1207**	**1281**	**1355**	**1429**	**1503**	**1577**	**1651**	**1725**
Surirella hybrida	0	0	0	0	0	0	0	0	0	0	0	0	0	0
Synedra bacillaris	0	0	0	0	0	0	0	0	0	0	0	0	0	0
Tabellaria fenestrata	0	0	0	0	0	0	0	0	0	0	0	0	0	0
Tabellaria flocculosa	0	0	0	0	0	0	0	0	0	0	0	0	0	0
Tabularia fasciculata	2.2	2.4	1.4	1.8	4.4	4.4	7.2	3	4.4	3	3	1.8	3.4	2.2
Thalassionema nitzschioides	0	0	0.2	0	0	0	0	0	0	0	0	0	0	0
Thalassiosira eccentrica	0	0	0	0	0.2	0	0	0	0	0	0	0	0	0
Thalassiosira gravida	0	0	0	0	0	0	0	0	0	0	0	0	0	0
Thalassirosira weissflogii	0.6	1	0	1	0.4	0	0	1.2	0	0.2	0	0.6	0.2	1.4
Trachyneis aspera	0	0	0	0	0	0	0	0	0	0	0	0	0	0
Triceratium reticulum	0	0	0	0	0	0	0	0	0	0	0	0	0	0
Tryblionella apiculata	0.4	1	1.6	1	2.6	0.8	0.2	0	0.4	0.8	0	0	0	0
Tryblionella calida	0	0.2	0.2	0	0.2	0	0.2	0	0	0	0	0	0	0
Tryblionella coarctata	0	0	0	0	0	0.2	0	0	0	0	0	0	0	0
Tryblionella hungarica	0.4	0	0	0.4	0.6	0	0	0	0	0	0.4	0	0	0

EV11.1 continued

Depth (cm)	**95**	**97**	**99**	**101**	**103**	**105**	**107**	**109**	**111**	**113**	**115**	**117**	**119**	**121**	**123**
Age (cal yrs BP)	**1799**	**1873**	**1947**	**2021**	**2102**	**2190**	**2278**	**2366**	**2454**	**2542**	**2630**	**2718**	**2806**	**2894**	**2982**
Achnanthes brevipes	0	0.2	0.2	0	0.6	1.2	1	1	0.4	1	1.6	1.2	1.2	0.2	0.4
Achnanthes brockmannii	0	0	0.4	0.4	0.2	0.4	0.6	0.4	1.2	0.6	0.4	0.2	0.8	0.8	1.6
Achnanthes javanica	0	0	0	0	0	0	0	0	0	0	0	0	0	0	0
Achnanthes oblongella	0.6	1.4	0.8	0.4	0.4	0	0	0	0.4	0	0	0.2	0	0	0.4
Achnanthes inflata	0	0	0	0	0	0	0	0	0	0	0	0	0	0	0
Achnanthidium crassum	0.2	0	0	1	0	0	0	0	2	0	0	0.2	0	0.6	0
Achnanthidium minutissimum	0	0.2	0	0.8	0.2	0.4	0.2	0	0	0	0.2	0.6	0.2	0.2	1
Achnanthidium straubianum	0	0.2	0.4	0	0	0	0	0	1.2	0	1.4	0.4	0	0	0.6
Achnanthidium subaffinis	0	0	0	0	0	0	0	0	0	0	0	0	0	0	0
Actinocyclus normanii	0	0	0.2	2	0	0	0	0.2	0.4	1	0.6	1	0.2	0.2	0
Actinocyclus sp.	0	0	0	0	0	0	0	0	0	0	0	0	0	0	0
Actinoptychus heliopelta	0	0	0	0.2	0	0.2	1.4	1.4	0.2	0.6	0.4	0.4	1	1	0.8
Actinoptychus undulatus	0	0	0	0	0	0	0	0.4	0	0	0	0	0	0	0
Actinoptychus vulgaris	0	0	0	0	0	0	0	0.4	0	0	0	0	0.4	0	0
Amphora acutiuscula	0.4	0.2	0	0	0.2	0.4	0	0	0.6	0.2	0	0.4	0	0.6	0
Amphora arenaria	0	0	0	0	0	0	0	0	0	0.6	0	0	0.2	0	0
Amphora coffeaeformis	0.8	0.2	1	0	0.6	0.2	0	0	1.4	0.6	0.6	0.4	0.4	1.4	1.4
Amphora commutata	0.2	0.2	0.2	1	1	1.4	1.8	1	1	1.2	0.8	1.2	0.6	0.8	1.2
Amphora copulata	0	0	0	0.2	0	0	0	0	0	0	0	0	0	0	0
Amphora decussata	0	0	0	0	0	0	0	0	0	0	0	0	0	0	0
Amphora lunaris	0	0	0	0	0	0	0	0	0.2	0.2	1.8	0.8	1	0.4	2
Amphora ostrearia	0	0	0	0	0	0.6	0	0.2	0	0	0.2	0.2	0.8	0.2	1.2
Amphora ovalis	0.2	1.2	0.4	0	1.2	1.2	4	1.6	1.2	2.6	3	2.8	2.8	7.6	3
Amphora proteus	0	0	0	0	0	0.8	0	0.2	0	0	0.8	0.6	0	0.4	0.4
Amphora spectabilis	0	0	0	0	0	0	0	0	0	0.2	0	0.6	0	0	0
Amphora veneta	0	0	0	0.4	0	0.4	0	1	0	0.2	0	1.6	0	0	0
Aulacoseira ambigua	0	0	0	0	0	0	0	0	0	0	0	0.4	0	0.2	0
Auliscus cf. sculptus	0	0	0	0	0	0	0	0	0	0	0	0	0	0	0
Bacillaria paradoxa	0	0	0	0.2	0.6	0.2	0.2	0.4	0	0.2	0.4	0	0.2	0.6	0.4
Biddulphia capusina	0	0	0	0	0	0	0	0	0	0	0	0	0.6	0.4	0.2
Biddulphia pulchella	0	0	0	0	0	0	0	0	0	0	0	0	0	0	0
Brachysira brebissonii	0	0	0	0	0	0	0	0	0	0	0	0	0	0	0
Caloneis aequatorialis	0	0	0	0	0	0	0	0	0	0	0	0	0	0	0
Caloneis crassa	0	0	0	0	0	0	0	0	0	0.4	0	0	0	0	0
Campylodiscus clypeus	0	0	0	0	0	0	0	0	0	0	0	0	0	0	0
Catenula adhaerens	0.4	0.4	0.4	1.6	1	0	0	0	0	0	0	0.2	0.2	0	0
Chaetoceros sp.	1	1.8	1.4	1.2	0.6	2.6	1.2	1.8	1.6	2	2.6	2.6	3	1.2	1.6

Depth (cm)	95	97	99	101	103	105	107	109	111	113	115	117	119	121	123
Age (cal yrs BP)	**1799**	**1873**	**1947**	**2021**	**2102**	**2190**	**2278**	**2366**	**2454**	**2542**	**2630**	**2718**	**2806**	**2894**	**2982**
Cocconeis costata	0	0	0	0	0	1.6	1.4	3.8	3	1	0.4	0.8	3.4	2.2	2.2
Cocconeis distans	1.2	0.6	0.8	0.4	0.4	0.2	0.2	0.4	2.4	0.4	0	0.4	0	0.8	1.4
Cocconeis engelbrechtii	10.2	10	7	11.4	0.4	0.4	0.2	0.2	1.4	5.2	0.4	0.4	0	0.2	0
Cocconeis pediculus	0.8	0	1.6	0	0	0	0	0	0	0	0.2	0	0	0	0
Cocconeis placentula	6.2	4.6	6	7.2	3.4	2.2	4.2	2.6	4.6	3.2	3.6	2.6	3	1	2.2
Cocconeis pseudomarginata	0.2	0.2	0	0	0	0	0.2	0	0	0	0	0.2	0	0.4	0
Cocconeis scuttellum	0.2	0.2	0.4	0.6	0.6	7	8	13.6	6.6	6.8	6.4	13.4	10.4	4.8	7.8
Coscinodiscus radiatus	2.4	10.4	16.6	5.2	0	0.2	0	0	0.4	0.2	1.8	0.2	2	0.6	0.6
Craspedodiscus elegans	0	1.2	0	0	0.6	0.4	1.2	0.2	0	0	0	0.2	0	0	0
Craspedostauros capensis	0	0	0	0	0	0	0	0	0	0	0	0	0	0	0
Craticula accomodiformis	0	0	0	0	0	0	0	0	0.4	0	0	0	0	0	0.4
Cyclotella caspia	18.4	10.2	4.6	3.6	7.2	1.8	16	8.6	8.4	3.2	10.4	8.6	8.6	5.8	6.8
Cyclotella choctawhatcheeana	1.6	0	0	0	0	0	0	0	0	0	0	0	0	0	0
Cyclotella distinguenda	11.2	5.4	4.8	3	3.6	9	3.2	2	2.4	3.4	3.6	0.8	3.4	1	4.4
Cyclotella meneghiniana	2.2	0	0.8	0	0	1.4	0.6	0	0	0.2	0.2	0.2	0.2	0.2	0.2
Cylindrotheca closterium	0	0	0	0	0	0	0	0	0.2	0	0	0	0	0.4	0
Cymbella affinis	0	0	0	0	0	0	0	0	0	0.8	0	0	0	0	0
Delphineis minutissima	1.4	0.6	0.6	1.2	0.2	0.8	0	0.4	0.2	0.2	0.2	0.2	0.2	0	0.4
Dimeregramma minor var. minor	0	0	0	0	0	0.2	0.4	0	0	0	0.2	0.2	0	1.4	0
Diploneis crabro	0	0.2	0.2	0.4	2.4	4.4	3.8	1.4	0.4	2.8	3.6	2.2	1.4	5	1.2
Diploneis oblongella	0.2	0	0	1.2	0.2	1	1.6	0.6	0.4	0.8	0.6	0.4	0.8	1.2	0.2
Diploneis smithii	0	0	0.2	0	0	0	0	0	0	0	0.2	0	0.6	0	0
Diploneis sp	0	0	0	0	0	0	0	0	0	0	0	0	0	0	0
Diploneis elliptica	0	0	0.2	1.4	0.6	12.4	8.4	5.6	2	3.8	7.2	4	4.6	7.6	0.6
Encyonema gracile	0	0	0	0.2	0	0.2	1.4	0.4	0.6	0.2	1.2	1.2	2.2	0	1.8
Encyonema silesiacum	0	0	0	0	0.6	0	0	0	0	0.2	0	0	0.2	0.2	0
Encyonopsis cesatii	0.4	0	0	0	0	0	0	1	0.2	0	0	0	0	0.2	0
Entomoneis ornata	0	0	0.2	0	0	0	0	0	0	0	0	0	0	0	0
Entomoneis punctulata	0	0	0	0	0	0	0	0	0	0	0	0	0	0	0
Epithemia adnata	0	0	0	0	0	0	0	0	0	0	0	0	0	0	0
Epithemia sorex	0	0	0	0	0	0	0	0	0	0	0	0	0.2	0	0
Eunotia flexuosa	0	0	0	0.2	0	0	0	0.2	0	0	0	0	0	0	0
Eunotia incisa	0	0.2	0.2	0	0	0	0	0	0	0	0.2	0	0	0	0
Eunotia minor	0	0.2	0.8	0.4	0	0.2	0.2	0.2	0.2	0	0	0	0	0	0
Eunotia zygodon	0	0	0	0	0	0	0	0	0	0	0	0	0	0	0
Fallacia monoculata	1.6	2	2.8	4	0.4	1.2	1.2	2.2	1.2	1	0	1.2	2.4	0.8	0.2
Fallacia pygmaea	0	0.2	0.2	0	0	0	0	0	0.2	0	0	0	0.2	0	0
Fallacia tenera	0	0	0.2	0	0	0	0.4	0	0.6	0	0.2	0	0.8	0	0.2

Depth (cm)	95	97	99	101	103	105	107	109	111	113	115	117	119	121	123
Age (cal yrs BP)	**1799**	**1873**	**1947**	**2021**	**2102**	**2190**	**2278**	**2366**	**2454**	**2542**	**2630**	**2718**	**2806**	**2894**	**2982**
Fragilaria biceps	0	0	0	1	0.4	0	0	0	0	0	0	0.2	0	0	0
Fragilaria tenera	0.2	0.4	0.4	0.4	0	0	0	0	0	0	0	0	0	0	0.4
Frustulia rhomboides	0	0.2	0	0	0	0.4	0	0	0	0	0	0	0	0	0
Gomphonema gracile	0	0	0	0	0	0	0	0	0	0	0	0	0	0	0
Gomphonema venusta	0	0	0	0	0.2	0.2	0	0	0	0	0	0	0.2	0	0
Gyrosigma obscurum	0.4	0	0.4	0	0	0	0	0	0.2	0	0.2	0	0.2	0	0.6
Hantzschia amphioxys	0	0	0	0	0	0	0	0	0	0	0	0	0	0	0
Hippodonta hungarica	0	0.2	0	0	0	0	0	0	0	0	0	0	0	0	0
Isthmia enervis	0	0	0	0	0	0	0	0	0	0	0	0	0	0	0
Luticola goeppertiana	0	0	0	0	0	0	0	0	0	0	0	0	0	0	0
Lyrella lyra	0	0	0	0	0	0	0.6	1.2	0.8	0.8	1.4	0.6	0.6	1.2	1.4
Mastogloia braunii	0.2	0	0	0	0.2	0	0.2	0	1.8	0.6	0.2	1	2	1.4	0.6
Mastogloia crucicula	0	0	0	0	0	0	0	0	0	0	0	0.2	0	0	0
Mastogloia danseii	0	0	0	0	0	0	0	0	0	0	0	0	0	0	0
Mastogloia fimbriata	0	0	0	0	0	0	0	0	0	0	0	0	0	0	0
Mastogloia latecostata	0	0	0	0	0.2	0.2	0	0	0	1.2	1.6	0	1.4	2.2	1
Mastogloia smithii	0.8	0.6	2	1	1.2	0.6	4	4.6	4	1.8	2.8	4.6	1.2	1.8	6.8
Mastogloia sp	0	0	0	0	0	0	0	0	0	0	0	0	0	0	0
Mastogloia vasta	0	0	0	0	0	0	1	0	0	0	1.2	0	0	0	0.8
Mayamaea atomus	1.2	0.2	1.4	0.2	0	0	0.4	0.4	1.8	0	0.8	0	0	1	0.6
Melosira nummuloides	17	25.8	27	25.4	9	4.4	1.6	2.2	1.6	2.6	1.2	3	1.4	0.8	1
Melosira varians	0.4	0	0	0	1.2	0.2	0.2	0.6	0	0.6	0	1	0.2	0.2	0.2
Navicula cincta	0	0.4	1	0.2	0.2	0.4	0.4	0.2	0.4	0.6	0.4	0.6	0.2	0.4	1.8
Navicula cryptocephala	0.4	1.2	0.8	1.2	0	0.2	0.6	0.2	3.8	0.4	0.6	0.4	0.4	0.8	0.6
Navicula directa	0	0	0	0	0	0	0	0.6	0	0	0.2	0.2	2	0.6	1
Navicula erifuga	0	0	0	0.2	0	0	0	0	0	0	0	0	0	0	0
Navicula oblonga	0	0	0	0	0	0.2	0	0	0	0	0	0	0	0	0
Navicula radiosa	0.8	0.2	0.2	0	0	0	0	0	1.2	0.2	0.4	0.4	0.2	0	0
Navicula tenelloides	0.4	0.2	0.2	0.8	0	0	0.8	0.2	1.6	0.2	0.8	0	0.2	0	1.4
Navicula veneta	0.6	0	0.4	0	0.4	0	0	0.2	0.8	0.2	0.2	0	0.2	0	0.2
Navicymbula pusilla	0.8	0	0	0.2	0	0	0.8	0.6	7	0.8	0.2	0.4	0.2	0	1.4
Navigiolum adamantiforme	0	1.2	0.6	0	0	0	0	0	0.2	0	0.2	0	0	0	0
Nitzschia amphibia	0.2	0	0	0	0	0	0	0	0	0	0.4	0	0	0	0
Nitzschia brevissima	0	0	0	0	0	0	0	0	0	0	0	0	0	0	0
Nitzschia clausii	0	0	0	0	0.6	0.2	0	0	0	0	0	0	0.2	0	0
Nitzschia cocconeiformis	0	0.2	0	0.2	0.6	0.2	0	0	0	0	0	0	0	0	0
Nitzschia compressa	0	0	0	0.6	5.4	0.8	0.4	0.6	0	0.6	0.4	0	1.4	0	0.2
Nitzschia dissipata	0	0	0	0	0.2	0	0	0	0	0	0	0	0	0	0

Depth (cm)	95	97	99	101	103	105	107	109	111	113	115	117	119	121	123
Age (cal yrs BP)	**1799**	**1873**	**1947**	**2021**	**2102**	**2190**	**2278**	**2366**	**2454**	**2542**	**2630**	**2718**	**2806**	**2894**	**2982**
Nitzschia laevis	0	0	0	0.2	0.2	1.8	0	0	0	0	0	0	0	0	0
Nitzschia palea	0	0	0	0	0.4	0.2	0	0.2	3.6	0	0.2	0.6	0.4	0.2	1
Nitzschia pusilla	0	0	0	0	0	0	0	0	0.2	0	0	0	0	0.2	0
Nitzschia recta	0	0	0.2	0	0.6	0.2	0.6	0.4	0	0.4	0	0	0.6	0.6	0.8
Nitzschia sigma	0	0	0	0	0.8	0	0	0	0	0	0	0	0	0	0
Nitzschia tryblionella	0	0	0	0	0	0	0	0	0	0	0	0	0	0	0
Opephora marina	0.4	0.6	1.6	0	0.4	0	0	0	1.4	0	0.2	0	0	0	0.4
Paralia sulcata	0	0	0.6	3	5	5.2	0.8	2	2.8	3.6	1.2	1.4	2	10.4	1.2
Petroneis humerosa	0	0.2	0	0	0.2	0.8	1.2	1	0	1.6	0.8	0.8	0.8	0.8	0.6
Pinnularia acrosphaeria	0	0	0	0	0	0	0	0	0	0	0	0	0	0	0
Pinnularia borealis	0	0	0	0	0.2	0	0	0	0	0	0.2	0	0	0	0
Pinnularia borealis var. 1	0	1.6	0.2	0.6	32.2	20.6	14.6	19.2	1.8	25	18.8	18.4	14.8	12.6	13.6
Pinnularia intermedia	0	0	0	0	0	0	0	0.6	0	0	0	0	0	0	0
Pinnularia maior	0	0	0	0	0.8	0.8	0.6	0.2	0	0	0	0	0.2	0.2	0
Pinnularia sp.	0	0	0	0.2	0	0	0.2	0.6	0	0.2	0.2	0	0.6	0	0.2
Pinnularia sp. 2	0	0	0	0	0	0	0	0	0	0	0	0	0	0	0.4
Pinnularia subcapitata	0	0	0	0	0	0	0	0	0	0	0	0	0	0	0
Pinnularia viridis	0	0	0	0	0	0	0	0	0	0	0	0	0	0	0
Plagiodiscus nervatus	0	0	0	0	0	0	0	0	0	0	0	0	0	0	0
Plagiotropis lepidoptera	0	0	0	0	0	0	0	0	0	0	0	0	0.4	0.4	0
Planothidium delicatulum	0.4	0.2	0.6	0.8	0	0.2	0.2	0	0.4	0	0	0	0.2	0.4	0.2
Pleurosigma sp	0	0	0	0.2	0.2	0	0	0	0	0	0	0.2	0	0	0
Pseudo-nitzschia	0	0	0	0	0	0	0	0	0	0	0	0	0	0	0
Rhopalodia gibba	0	0	0	0	0	0	0	0	0	0	0	0	0	0	0
Rhopalodia gibberula	0.6	0.8	0	0.4	0	0	0	0.4	0.6	0.2	0	0.2	0.8	1.4	0.2
Rhopalodia musculus	0	0	0	0.2	0	0.2	0.4	0.4	1.2	0.6	0.4	0.6	0	0.6	1.2
Rossithidium linearis	0	0.2	0	1.6	0.4	0.6	0.2	1	1.8	1.8	0.8	0.6	0.6	0.2	3.8
Sellaphora bacillum	0	0	0	0	0	0	0	0	0.4	0.2	0.2	0	0	0	0.4
Sellaphora pupula	0	0	0	0	0	0	0	0	0	0	0	0	0	0	0
Seminavis atlantica	0	0.2	0	0.2	0	0.2	0.4	0.6	0	0.8	1.2	1.4	0.6	0.2	0.2
Seminavis strigosa	0	0	0	0	0	0	0	0	0	0.8	0	1.6	0	1.8	0
Stauroneis phoenicenteron	0	0	0.2	0	0	0	0	0.2	0.4	1.2	0	0	0.4	0.2	1.6
Stauroneis sp.	0	0	0	0	0	0	0	0	0	0	0	0	0	0	0
Staurosira elliptica	0.2	0.4	0	0.2	0	0	1.2	0.2	1.4	0	0.2	0.6	0.2	0.6	1.4
Stephanodiscus agassizensis	1	3.4	0.6	2.2	0.6	1	0.8	1.2	0.8	1.8	1.6	1	0	0.8	0.6
Stephanodiscus hantzschii	5.4	3.2	4.4	2.6	2.8	1.8	1.8	2.4	2.8	0.8	1.2	3	2	1.6	0.6
Surirella brebissonii	0.2	0.2	0.8	0	0.8	0.6	0	1.2	2.4	1	1.6	1.2	2.4	0.2	1.6
Surirella fastuosa	0	0	0	0	0.2	0.2	0	0.2	0	0.2	0	0	0.2	0.8	0

Depth (cm)	**95**	**97**	**99**	**101**	**103**	**105**	**107**	**109**	**111**	**113**	**115**	**117**	**119**	**121**	**123**
Age (cal yrs BP)	**1799**	**1873**	**1947**	**2021**	**2102**	**2190**	**2278**	**2366**	**2454**	**2542**	**2630**	**2718**	**2806**	**2894**	**2982**
Surirella hybrida	0	0	0	0	0	0	0	0	0	0	0	0	0	0	0
Synedra bacillaris	0	0	0	0	0	0.2	0.4	0.2	0	0.2	0.4	0.2	0	0	0
Tabellaria fenestrata	0	0	0	0.4	0	0	0	0	0.2	0.2	0	0.2	0	0.4	0
Tabellaria flocculosa	0	0	0	0	0	0	0	0	0	0	0	0	0	0	0
Tabularia fasciculata	4.8	3.6	2.2	2.6	2.8	0.8	0.4	0.2	1.6	0.2	0	0.2	0	0	0.6
Thalassionema nitzschioides	0	0	0	0	0	0	0.2	0	0	0.2	0	0	0.2	0.2	0.2
Thalassiosira eccentrica	0	0	0	0.6	0	0	0	0	0.8	0	0.4	0	0	0	0.4
Thalassiosira gravida	0	0	0	0	0	0	0	0	0	0	0	0	0	0	0.2
Thalassirosira weissflogii	1.2	1.6	0.4	1	0.4	0.6	0.6	2	1.4	2	0.4	0.6	0.6	3	0.8
Trachyneis aspera	0	0	0	0	0.2	0.2	0.2	0	0	0.2	0.4	0	0.4	0.8	0.2
Triceratium reticulum	0	0	0	0	0	0	0	0	0	0	0	0	0	0	0
Tryblionella apiculata	0.4	0	0	1.4	0.8	0.6	0.2	0.2	0.4	0.4	0.8	0.4	0.2	0.2	0
Tryblionella calida	0	0.8	0.2	0.4	0.6	0	0	0	0	0	0	0	0	0	0
Tryblionella coarctata	0	0	0	0	1.6	0.6	1	0.4	0.8	0.8	0.2	1	1	0.2	0.8
Tryblionella hungarica	0	0	0	0	0.8	0	0	0	0	0	0	0	0	0	0

EV11.1 continued

Depth (cm)	125	127	129	131	133	135	137	139	141	143	145	147	149	151	153
Age (cal yrs BP)	**3070**	**3158**	**3246**	**3334**	**3422**	**3492**	**3543**	**3594**	**3645**	**3696**	**3747**	**3799**	**3850**	**3901**	**3952**
Achnanthes brevipes	0.6	1.4	0.4	1	0.8	0.8	1.2	0.8	1.2	0.4	1	1	1.6	1.4	0.4
Achnanthes brockmannii	1.2	0.8	0.2	0.4	0.4	1	0.6	2	1.2	1.2	1.8	0.6	0.8	1.4	0
Achnanthes javanica	0	0	0	0	0	0	0	0	0	0	0	0	0	0	0.2
Achnanthes oblongella	0.4	0	0	0.4	0	0.2	0	0	0.4	0	0.4	0	0	0.2	0
Achnanthes inflata	0	0	0	0	0	0	0	0	0	0	0	0	0	0.2	0
Achnanthidium crassum	1	0.2	0	1.4	0	0.8	0.8	0	0.4	0	0.2	1	0.8	1	0.8
Achnanthidium minutissimum	0	0.4	1.2	0	0.2	0.6	0.2	0	1	0.6	1.6	0.4	0	0	0
Achnanthidium straubianum	0	0.4	0	0	0	0	0	1	1.4	1.2	1.4	0.4	0	0.2	0
Achnanthidium subaffinis	0.2	0	0	0	0	0	0	0	0.2	0.2	1	0	0.2	0	0.4
Actinocyclus normanii	1	1.4	0.4	0	0.4	0	1.2	0.4	0.4	0	1.8	0.4	0.2	0.2	1.2
Actinocyclus sp.	0	0	0	0	0	0	0	0	0	0	0	0	0	0	0
Actinoptychus heliopelta	0.2	1.4	0.8	1	1.8	0.4	0.4	0.2	0.4	0.2	0.4	1.4	2	2.4	2.2
Actinoptychus undulatus	0	0	0	0	0	0	0	0	0	0	0	0	0	0.2	0
Actinoptychus vulgaris	0	0	0	0	0	0	0.2	0	0	0	0	0	0	0	0
Amphora acutiuscula	0.2	0	0	0	0	0.2	0	0	0	0	0	0	0	0	0
Amphora arenaria	0	0.2	0.2	0	0	0	0	0.2	0	0.2	0	0.4	0	0	0
Amphora coffeaeformis	1.8	0.8	0	1	0.2	1	1.2	0.8	2.2	1.4	2.4	0.4	2.2	1	1.6
Amphora commutata	0	0.6	1	0.4	0.6	0.2	0.4	0.2	0	1.4	0	0.2	0	0.6	0
Amphora copulata	0	0	0	0	0	0	0	0	0	0.2	0	0	0.2	0	0
Amphora decussata	0	0	0	0	0	0	0	0	0	1	0	0	0	0	0
Amphora lunaris	0	0.2	1	1.2	3.4	0	0.2	0	0	0	0	0.4	0	0.6	0
Amphora ostrearia	0	0.4	0.4	0.8	0.2	0.6	1	0.4	0.8	1	0	1.4	0.6	0.4	0.2
Amphora ovalis	4.4	4.4	9	5	4	2	3.2	2.2	3	3.6	1.4	1.8	1.2	1.4	2
Amphora proteus	0.8	0.2	1.2	0	0.6	0.8	0	0.8	0.4	0	0.6	0	1.6	0	2.4
Amphora spectabilis	0.2	0	0	0	0	0	0.6	0	0	0	0.2	0	0	0	0
Amphora veneta	0.4	0	0.2	0	0.4	0	0.4	0	1	0	0.8	0	0.6	0	0.4
Aulacoseira ambigua	0.6	0	0	0	0.4	0	0	0	0	0	0	0	0	0	0
Auliscus cf. sculptus	0.2	0	0	0.4	0.2	0	0.2	0.6	0	0	0	0	0	0	0
Bacillaria paradoxa	1.4	1.4	3	0.4	0.8	0	0.2	1	0	0.2	0	0.4	0	0.2	0
Biddulphia capusina	0	0.4	0.2	0.4	1.8	0	1	0.2	1	0	0.2	0.4	0	0.4	0
Biddulphia pulchella	0	0	0	0	1.2	0	0	0	0	0	0	0	0	0	0
Brachysira brebissonii	0	0	0	0	0	0	0	0	0	0	0	0	0	0	0
Caloneis aequatorialis	0	0	0	0	0	0	0	0	0	0	0	0	0	0	0.6
Caloneis crassa	0	0	0	0	0	0	0	0	0	0	0	0	0	0	0
Campylodiscus clypeus	0	0	0	0	0	0	0	0	0	0	0	0	0	0	0
Catenula adhaerens	0.6	0	0	0	0.4	0.2	0	0.2	0.4	0	0	0	0.6	0	0.4
Chaetoceros sp.	1.8	1.8	2.4	0.8	2.4	1.6	1	1	1.4	2.6	2.4	1	0.8	1.4	1.6

Depth (cm)	125	127	129	131	133	135	137	139	141	143	145	147	149	151	153
Age (cal yrs BP)	**3070**	**3158**	**3246**	**3334**	**3422**	**3492**	**3543**	**3594**	**3645**	**3696**	**3747**	**3799**	**3850**	**3901**	**3952**
Cocconeis costata	2.6	2	0.6	1	1.2	4.8	3.4	3.2	3	6.6	7.2	7	7	5.4	9.6
Cocconeis distans	0.6	0.2	1.4	0.4	1	0.6	0.4	1	1	1.6	0.4	1.8	0.4	1	1.4
Cocconeis engelbrechtii	1.8	0.4	0	0	0.4	0	0	0.6	0.4	0	0.8	0	0	0	0
Cocconeis pediculus	0	0	0	0	0	0.4	0	0	0	0	0	0	0	0	0
Cocconeis placentula	5.6	7.2	1.4	4.6	1.2	4	3.8	3.4	2.6	4.6	3.2	3.4	4.8	3	2
Cocconeis pseudomarginata	0	0	0.2	0.8	2.2	0.2	1.6	0.6	0.8	0.2	0.2	0	0.4	1	0.2
Cocconeis scuttellum	6.2	8.4	4	11.6	4.4	8	6.4	8.2	9.8	8.4	3.2	7	6.4	9	7.2
Coscinodiscus radiatus	0.4	0.4	0.4	0.4	0	0.2	1	0.4	0.4	0.8	0	0.4	0.6	0.2	1.2
Craspedodiscus elegans	0	0	0.2	0	0	0	0	0	0	0.2	0	0	0	0	0
Craspedostauros capensis	0	0	0	0	0	0	0	0	0	0	0	0	0	0	0
Craticula accomodiformis	0	0	0	0	0	0	0	0.2	0	0	0	0.2	0	0	0.2
Cyclotella caspia	7.2	12.4	1.4	2.8	1	7.6	7.4	4.6	7.6	9.2	8	9.2	5.8	6.4	4.4
Cyclotella choctawhatcheeana	0	0	0	0	0	0	0	0	0	0	0	0	0	0	0
Cyclotella distinguenda	0.4	1.8	0	3	1.6	2	0.8	2.6	1.2	0.8	0	2	0.2	1.2	0.4
Cyclotella meneghiniana	0.4	0	0	0	0.4	0	0	0.2	0.2	0.4	0.2	0	0	0	0
Cylindrotheca closterium	0	0	0.2	0	0	0	0	0	0	0	0	0	0	0	0
Cymbella affinis	0	0	0	0	0	0	0	0	0	0	0	0	0	0	0
Delphineis minutissima	0.2	0	0	0.2	0.4	0.4	0.4	1	0.2	1.2	0	1.2	0.8	1.2	1
Dimeregramma minor var. minor	0.4	1	1	1.4	0.6	0.2	0.6	0.6	0.8	0.6	0.4	1	0.2	1	0.4
Diploneis crabro	1	3.2	3.4	2.4	2.8	0.2	3.8	2.2	3	1	2.8	1.4	1.8	3.6	3
Diploneis oblongella	0.6	0.6	1.4	0.4	1	1.6	0.6	1.4	0.4	0.4	2	0.6	0.8	1	0.4
Diploneis smithii	0	0	0	0	0	0	0	0	0	0	0	0	0	0	0
Diploneis sp	0	0	0.2	0	0	0	0	0	0	0	0	0	0	0	0
Diploneis elliptica	1.2	2.6	19.4	7	8	0.6	4.2	1.4	2.2	2	2	0	1	1.6	1.4
Encyonema gracile	0	1.4	0.6	3.4	0.4	1	0.8	1.6	0.4	1.8	1	1.8	1.4	1.4	1.6
Encyonema silesiacum	0.2	0	0	0	0	0	0	0	0.2	0	0	0	0.6	0	0.4
Encyonopsis cesatii	0	0.2	0.2	0.2	0	0.4	0.4	0	0	1.6	0.6	0.4	1.2	0.4	0
Entomoneis ornata	0	0	0	0	0	0	0	0	0	0	0	0	0	0	0
Entomoneis punctulata	0	0	0	0	0	0	0	0	0	0	0	0	0	0	0
Epithemia adnata	0	0.4	0	0	0	0	0	0	0	0	0	0	0	0	0
Epithemia sorex	0	0	0	0	0	0	0	0.2	0	0	0	0	0	0	0
Eunotia flexuosa	0	0	0	0.2	0	0	0	0	0	0	0	0	0	0	0
Eunotia incisa	0	0.2	0	0	0	0	0	0	0	0.4	0.2	0	0	0	0.2
Eunotia minor	0.2	0.2	0	0.4	0.2	0.2	0	0	0	0.2	0.2	0	0.2	0.2	0.4
Eunotia zygodon	0	0	0.2	0.2	0	0	0	0	0	0	0.2	0	0.2	0.2	0.2
Fallacia monoculata	4	2	0.8	1.2	1	2.4	1.8	2.4	2.8	3.4	3.2	2.4	3.4	1.2	2
Fallacia pygmaea	0	0.6	1.4	0	0	0	0	0.2	0	0.4	0	0	0	0	0
Fallacia tenera	0	1.6	0	0	0	8.6	0	0	0	0.8	0	1.4	0	0.2	0

Depth (cm)	125	127	129	131	133	135	137	139	141	143	145	147	149	151	153
Age (cal yrs BP)	**3070**	**3158**	**3246**	**3334**	**3422**	**3492**	**3543**	**3594**	**3645**	**3696**	**3747**	**3799**	**3850**	**3901**	**3952**
Fragilaria biceps	0.2	0	0	0.4	0	0.2	0	0	0.2	0.2	0	0	0	0	0
Fragilaria tenera	0	0	0.4	0.6	0.4	1	0.6	0.4	0.2	0.4	0.2	0.4	0.4	0	1
Frustulia rhomboides	0	0	0.2	0.2	0	0	0	0	0	0.4	0	0	0	0.2	0
Gomphonema gracile	0	0	0	0	0	0	0	0	0	0	0	0	0	0	0
Gomphonema venusta	0.2	0	0.2	0	0.4	0	0.2	0	0	0	0.2	0	0.2	0	0.2
Gyrosigma obscurum	0	0	0.6	0.2	3	0	0	0.2	0	0.2	0	0.6	0	0.6	0
Hantzschia amphioxys	0	0	0	0	0	0	0	0.2	0	0	0	0	0	0	0
Hippodonta hungarica	0	0	0	0	0	0	0	0	0	0	0	0	0	0	0
Isthmia enervis	0	0	0	0	0	0	0	0	0	0	0	0	0	0.4	0
Luticola goeppertiana	0	0	0	0	0	0	0	0	0	0	0	0	0	0	0
Lyrella lyra	1	0.2	0.4	0.2	0.6	0.8	0.4	0.6	0.2	0.4	0.4	1.6	1.2	2.6	2.2
Mastogloia braunii	1.6	0	1.4	2.4	0.8	1.4	2.2	2	2	1	2.6	0.4	1.2	2.8	1
Mastogloia crucicula	0.4	0	0.2	0	0.4	1	0.4	0.2	0.2	0	0.8	0	0	0	1
Mastogloia danseii	0	0	0	0	0	0	0	0	0.6	0.2	0.2	0	0	0	0
Mastogloia fimbriata	0	0	0	0	0	0	0.2	0	0	0	0	0	0	0	0
Mastogloia latecostata	0.6	0.8	1.4	1.8	0.6	0.6	0.8	1.6	0.8	0.8	0	1	2	1.6	0.8
Mastogloia smithii	10.6	2.6	1	3.2	1.8	8.4	3.8	8.4	2.8	3.6	4.2	3.8	4	3.6	3
Mastogloia sp	0	0	0.4	0	0.4	0	0	0	0	0	0	0	0	0	0
Mastogloia vasta	0	1.6	0.4	0	0	0	0	0	0	0	0	2.8	0	2.8	0
Mayamaea atomus	1	1	0.8	0.2	1	1.6	0.4	1.6	1	1.8	1.2	1.8	0.8	0.4	1
Melosira nummuloides	1.2	1.2	1.6	2.4	0.6	0.6	1.8	1.2	2.4	1.2	2.2	0.6	0.8	0.6	0.6
Melosira varians	0.6	0	0	0.2	0	1.2	0.4	0	0.4	0.2	0	0.2	0	0	1.4
Navicula cincta	1.2	2	0.2	0	0.2	0.2	0.4	0.8	0.2	0.2	0.8	1.2	0.2	0.6	0.4
Navicula cryptocephala	0.2	0.6	0	0.2	0	0.6	0.4	1.4	0.6	1	0	3.8	0.2	1	0.6
Navicula directa	0	0.4	0.2	0.6	0.4	0.6	0.8	0.6	0	0.4	0	0.4	0	0.2	0
Navicula erifuga	0	0	0	0	0	0	0	0	0	0	0	0	0	0	0
Navicula oblonga	0	0.2	0	0	0	0	0	0	0	0	0	0	0.4	0	0
Navicula radiosa	0.2	0.6	0	0.4	0.2	0	0	0.2	0	0	0.6	0.2	0	0.8	1
Navicula tenelloides	0.2	0.8	0	0.2	0	0.8	0.2	1.8	0.4	1	0.4	1.4	0	0.2	0
Navicula veneta	0	0.2	0	0	0.2	0.2	0	0.6	0	0.2	0	0	0.4	0	0.6
Navicymbula pusilla	0.8	0.6	0	0.6	0.4	2.4	0	2.4	0	1.2	1	2.2	0.6	1.4	0.6
Navigiolum adamantiforme	0	0	0	0	0	0	0	0	0	0.2	0	0	0	0	0
Nitzschia amphibia	0	0	0	0	0	0.2	0	0	0	0.2	0	0	0	0.2	0
Nitzschia brevissima	0	0.2	0	0	0	0	0	0	0	0	0	0	0	0	0.2
Nitzschia clausii	0.2	0	0	0	0.2	0	0	0	0	0	0	0	0	0	0.4
Nitzschia cocconeiformis	0	0	0.2	0	0	0	0	0	0	0	0.2	0.2	0.6	0	0
Nitzschia compressa	0.2	0.4	0	0.4	0.2	0.4	1	0.6	0.6	0.6	0.4	0.2	0.6	0.4	0.2
Nitzschia dissipata	0	0	0	0	0.2	0	0	0	0	0.2	0	0	0	0	0

Depth (cm)	125	127	129	131	133	135	137	139	141	143	145	147	149	151	153
Age (cal yrs BP)	**3070**	**3158**	**3246**	**3334**	**3422**	**3492**	**3543**	**3594**	**3645**	**3696**	**3747**	**3799**	**3850**	**3901**	**3952**
Nitzschia laevis	0	0	0.8	0	0.6	0.2	0	0.2	0	0	0.2	0.2	0	0	0.8
Nitzschia palea	1	0.2	0.2	0	0	0.6	0.2	0.4	0.6	0.2	0.4	0.2	1	0.2	0
Nitzschia pusilla	0.6	0	0	0	0	0	0	0.6	0	0	0	0	0	0	0
Nitzschia recta	0	0.4	2.2	0.6	1.8	0.2	0.6	0.2	0.6	0.2	0	1	0.6	0.4	0.6
Nitzschia sigma	0	0.2	1.6	0	1.4	0	0	0.4	0	0	0	0.4	0	0.2	0
Nitzschia tryblionella	0	0	0	0	0	0	0	0	0	0	0	0.2	0	0.2	0
Opephora marina	0	0.2	0	0.2	0	1.4	0	0	0	0	0	0.4	0	0	0
Paralia sulcata	4.6	4.8	8	9	15.4	4.4	6.4	6.6	5.2	1.8	1	5.6	5.4	9.2	6.8
Petroneis humerosa	0.2	0.6	0	0.2	0.4	0	2	1	1.2	0.4	0.8	0.6	1.4	1.2	0.6
Pinnularia acrosphaeria	0	0	0	0	0	0	0	0	0	0.2	0	0	0	0	0
Pinnularia borealis	0	0	0	0	0	0	0	0	0.2	0.2	0.2	0	0	0	0
Pinnularia borealis var. 1	3.2	5.4	9.8	7.8	10	1.6	11.6	4.2	4.2	2.8	1.8	3.6	9.8	4.6	6.2
Pinnularia intermedia	0	0	0	0	0.4	0	0	0	0.2	0	0	0	0	0.8	0.2
Pinnularia maior	0	0	0	0	0	0	0.2	0.2	0	0.2	0.2	0.2	0	0	0
Pinnularia sp.	0	0.6	0	0	0.2	0	0.2	0.2	0	0	0	0.2	0	0.4	0
Pinnularia sp. 2	0	0	0	0	0	0	0	0	0	0	0	0	0	0	0
Pinnularia subcapitata	0	0	0	0	0	0	0	0	0	0	0	0	0	0	0
Pinnularia viridis	0	0	0	0	0	0	0	0	0	0	0	0	0.2	0	0
Plagiodiscus nervatus	0	0.2	0	0	0	0.2	0	0	0	0	0	0	0	0	0
Plagiotropis lepidoptera	0.6	0	0	0.2	0	0	0	0.4	0.2	0	0	0	0	0.4	0
Planothidium delicatulum	0	0.4	0	0	0.2	0.2	0.8	0.4	0.6	0	1.6	0.4	0.4	0.2	1.4
Pleurosigma sp	0	0	0	0	0.8	0	0.4	0	0	0	0	0.4	0.2	0	0
Pseudo-nitzschia	0	0	0	0	0	0	0	0	0	0	0	0	0	0	0
Rhopalodia gibba	0	0	0	0	0	0	0	0	0.2	0	0	0	0	0	0
Rhopalodia gibberula	0.2	0.4	0.2	1	0.4	0.2	1	0.6	0.6	0.2	0.2	1.2	0	0.2	0.4
Rhopalodia musculus	1.2	1	0.2	0.6	0.4	1	0.8	2	0.2	0.6	1	0.8	1.8	0.2	0.4
Rossithidium linearis	0.6	1	0.4	0.6	0.4	0.8	0.6	0.6	0.4	2.2	2.4	0.6	3	1	0.2
Sellaphora bacillum	0	0	0	0	0	0.2	0	0	0	0	0	0.6	0	0	0
Sellaphora pupula	0	0	0	0	0	0	0	0	0	0.4	0	0	0.4	0	0.4
Seminavis atlantica	1.2	0.8	0.4	0.6	0	0.2	0.4	0	1.2	0.4	0.2	0.2	1	0.4	0
Seminavis strigosa	0.4	0	0.4	0	0.2	0	0.6	0.4	0.2	0	0	0	0	0	0
Stauroneis phoenicenteron	0.2	0	0.2	0	0	0.2	0.4	0.2	0	0.4	0.4	0.2	0.2	0	0
Stauroneis sp.	0	0	0	0	0	0	0	0	0	0	0	0	0	0	0
Staurosira elliptica	1	0.4	0.2	1.8	0.8	4.8	0.2	1.6	1.6	1.8	0.2	0.8	0.8	0.2	1.8
Stephanodiscus agassizensis	2.8	1.2	0.2	0.4	0.2	0.8	0.6	0.4	0.6	1.4	1.2	0.4	0.6	0.4	2.2
Stephanodiscus hantzschii	3.4	0.4	0.6	1	1	1.8	1.8	1.2	2.4	3	4.6	1.8	3.4	0.2	2.8
Surirella brebissonii	1.4	1.8	1	0.6	0.6	2.8	0.6	2	1.6	2.8	0.8	0.6	1	2.4	1.4
Surirella fastuosa	0	0	0.4	0.2	1.6	0	0	0.2	0.2	0	0	0	0	0	0

Depth (cm)	125	127	129	131	133	135	137	139	141	143	145	147	149	151	153
Age (cal yrs BP)	**3070**	**3158**	**3246**	**3334**	**3422**	**3492**	**3543**	**3594**	**3645**	**3696**	**3747**	**3799**	**3850**	**3901**	**3952**
Surirella hybrida	0	0	0.2	0	0.2	0	0	0	0	0	0	0	0	0	0
Synedra bacillaris	0	0	0.4	0	0	0.4	0.4	0.4	0.8	0	0	0.4	0.4	0	0.2
Tabellaria fenestrata	0.4	0.2	0.2	0.6	0	0	0.4	0.4	1.4	0	0	0.2	0.6	0.6	2
Tabellaria flocculosa	0	0	0	0	0	0	0	0	0	0	0	0	0	0	0
Tabularia fasciculata	0	0.4	0	0.4	0	1.2	0	0.2	0.8	0.4	1.2	1	1	0.2	0
Thalassionema nitzschioides	0	0.2	0.8	1.8	0	0	0	0.2	0	0.2	0	0	0	0.2	0
Thalassiosira eccentrica	0	0.2	0	0.2	0.4	0	0.6	0	0	1.2	0	0.4	0	0	0
Thalassiosira gravida	0	0	0	0	0	0	0	0.2	0	0	0	0.4	0	0.4	0
Thalassirosira weissflogii	6	0.6	0.2	0.2	1.8	0.4	2.4	0.4	7.6	0.6	12.6	0.6	2.4	0.2	2.6
Trachyneis aspera	0	0.4	0.2	0.6	0.4	0	0.8	0.8	0.4	0	0	0	0	0.6	0.4
Triceratium reticulum	0	0	0.2	0.2	0	0	0	0	0	0	0	0	0	1	0
Tryblionella apiculata	0.4	0	1	0.2	0.4	0	0.2	0.2	0.2	0.6	0	0.2	0.2	0.6	0.4
Tryblionella calida	0	0.2	0	0	0	0	0	0	0	0	0	0	0	0	0
Tryblionella coarctata	0.2	1.2	0.4	0.6	0	0.4	0.4	0.4	0.2	0.2	0.2	0.6	0	0.6	0
Tryblionella hungarica	0	0	0	0	0	0	0	0	0	0	0	0	0	0	0

Table 11.6: Swartvlei (SV10.1) diatom species with ecological affinities; including salinity (f = fresh, fb = fresh-brackish, bf = brackish-fresh, b = brackish, mb = marine-brackish, m = marine, u = unknown), pH (a = acidophilic, c = circumneutral, k = alkaliphilic, b = alkalibiontic, u = unknown), Life form (a = aerophilic, b = benthic, p = planktonic, m = marine, u = unknown) and trophic state (uo = ultraoligotrophic, ot = oligotrophic, mt = mesotrophic, et = eutrophic, pt = polytrophic, ht = hypertrophic, mar = marine, u = unknown)

Species Name	Salinity	pH	Life form	Trophic state
Achnanthes brevipes	fb	c	b	ut
Achnanthes oblongella	fb	c	b	ut
Achnanthidium affine	un	un	un	un
Achnanthidium crassum	f	k	b	un
Achnanthidium straubianum	f	k	b	m-e
Actinoptychus heliopelta	m	m	m	mar
Amphora acutiuscula	bm	k	b	un
Amphora arcus	m	m	m	mar
Amphora coffeaeformis	b	k	b	pt
Amphora commutata	m	m	b	mar
Amphora ostrearia	m	m	m	mar
Amphora ovalis	fb	k	b	pt
Amphora proteus	m	m	m	mar
Amphora veneta	bf	b	b	p-h
Bacillaria paradoxa	b	b	b	un
Bacteriastrum sp.	un	un	m	un
Brachysira brebissonii	f	a	b	ot
Campylodiscus clypeus	b	b	p	un
Catenula adhaerens	m	m	b	mar
Chaetoceros sp.	m	m	m	mar
Climacosphemia moniligera	m	m	m	mar
Cocconeis engelbrechtii	b	k	b	un
Cocconeis pediculus	b	k	b	un
Cocconeis placentula	fb	k	b	et
Cocconeis scutellum	mb	k	b	et
Coscinodiscus radiatus	m	m	m	mar
Craspedodiscus elegans	m	m	p	mar
Craticula accomoda	fb	k	b	un
Craticula halophila	b	k	b	un
Ctenophora pulchella	b	un	b	un
Cyclotella caspia	b	k	p	et
Cyclotella distinguenda	b	k	p	et
Cyclotella meneghiniana	f	k	p	et
Delphineis minutissima	m	m	p	mar

Species Name	Salinity	pH	Life form	Trophic state
Denticula subtilis	b	un	b	un
Diadesmis confervacea	bf	c	a	un
Diatoma vulgaris	fb	k	b	un
Diploneis chersonensis	m	m	p	mar
Diploneis oblongella	fb	k	b	ut
Diploneis smithii	b	c	b	un
Encyonema gracile	fb	a	b	ot
Encyonema minutum	f	c	un	m-e
Entomoneis alata	m	m	m	mar
Eolimna minima	fb	k	un	et
Epithemia adnata	fb	b	b	m-e
Epithemia sorex	fb	b	b	et
Eunotia exigua var. tenella	un	a	un	un
Eunotia formica	fb	a	un	un
Eunotia minor	fb	c	b	un
Eunotia pectinalis var. undulata	un	c	un	un
Fallacia monoculata	fb	b	b	un
Fallacia pygmaea	bf	b	b	ht
Fragilaria biceps	f	b	b	m-e
Fragilaria tenera	f	a	b	m-e
Fragilariforma	un	un	un	un
Frustulia rostrata	un	un	un	un
Frustulia saxonica	un	a	un	un
Gomphonema gracile	fb	c	b	un
Gomphonema parvulum	un	i	b	un
Gomphonema venusta	un	c	un	o-m
Gyrosigma obscurum	b	k	b	o-m
Haslea sp	un	un	un	un
Mastogloia elliptica	b	k	b	un
Mastogloia smithii	b	k	b	m-e
Melosira nummuloides	b	k	b	et
Navicula cincta	fb	k	a	ot
Navicula cryptocephala	fb	c	b	pt
Navicula radiosa	fb	c	b	o-e
Navicula veneta	bf	k	b	pt
Navicymbula pusilla	fb	k	b	o-e
Navigiolum adamantiforme	un	k	un	et
Nitzschia amphibia	fb	k	a-b	pt
Nitzschia cocconeiformis	m	m	m	mar

Species Name	Salinity	pH	Life form	Trophic state
Nitzschia compressa	mb	k	b	un
Nitzschia dissipata	fb	k	b	un
Nitzschia linearis var. subtilis	un	c	b	un
Nitzschia littorea	b	un	un	un
Nitzschia nana	b	c	un	un
Nitzschia palea	fb	c	b	pt
Opephora marina	mb	k	b	m-e
Paralia sulcata	m	m	p	mar
Petroneis humerosa	m	m	b	mar
Pinnularia borealis	fb	c	a	m-e
Pinnularia borealis var. 1	fb	c	a	m-e
Pinnularia gibba	un	c	un	un
Pinnularia maior	f	i	b	ot
Pinnularia subcapitata	fb	i	b	ot
Pinnularia viridis	un	a	b	o-m
Planothidium delicatulum	b	b	b	un
Rhopalodia gibberula	bf	k	b	un
Rhopalodia musculus	b	b	un	un
Staurosira elliptica	fb	k	b	mt
Surirella brebissonii	b	k	un	et
Synedra bacillaris	m	m	p	mar
Tabellaria flocculosa	f	a	b-p	ot
Tabularia fasciculata	b	k	b	et
Terpsinoë americana	un	un	un	un
Thalassirosira weissflogii	f	c	p	pt
Tryblionella apiculata	b	k	b	ht
Tryblionella calida	bf	c	b	et

Table 11.7: Swartvlei (SV10.1) diatom species percentage representation against depth and age

Depth (cm)	**1**	**2**	**3**	**4**	**5**	**6**	**7**	**8**	**9**	**10**	**11**	**12**	**13**
Age (yrs BP)	**-44**	**-28**	**-12**	**4**	**20**	**37**	**53**	**69**	**85**	**101**	**117**	**133**	**149**
Achnanthes brevipes	1.6	1.4	0.8	4	1.8	2.6	0	1.6	0	0.8	0	0.2	0
Achnanthes oblongella	1.2	2.4	2	2.4	0.6	0.6	1	1.2	0	0.6	0.8	0.4	0.2
Achnanthidium affine	0.4	0	1.4	0	0.6	0	0.2	0	0.2	0	0	0	0.8
Achnanthidium crassum	0.2	0	0	0	0	0	0	0	0	0	0	0	0
Achnanthidium straubianum	4.2	0.4	1	0.6	0.8	0	0.4	1.4	0.6	1	0	0.4	0.4
Actinoptychus heliopelta	0	0	0	0	0	0	0	0	0	0	0	0	0
Amphora acutiuscula	0.4	0	0.2	1.2	0.6	3.2	0.2	0.2	0	0.2	0.2	0	0
Amphora arcus	0.6	0	0	0	0	0	0	0	0	0	0	0	0
Amphora coffeaeformis	1.4	0.6	0.4	1.2	0.6	1.6	0.6	0	0.2	0.2	0.4	0	0.4
Amphora commutata	0	0	0	0.6	0.8	0	0.2	1.4	0.2	0.2	0	0.4	0
Amphora ostrearia	0.2	0	0	0.2	0.2	1.4	0.2	0.4	0	0.2	0	0	0
Amphora ovalis	0.8	0.8	1	1	0.6	2.2	0	0.6	0.4	0.2	0.2	0.4	0
Amphora proteus	1.4	1.2	2.2	6.8	2.4	5.4	1.2	4.8	2	6	0.2	1.8	0.4
Amphora veneta	0.6	0	0	0	0.2	0	0	0	0	0	0	0	0
Bacillaria paradoxa	1.4	0.2	0.4	0	0.2	0	0	0.2	0	0.2	0	0	0
Bacteriastrum sp.	0	0	0	0	0	1.4	0	0	0	0	0	0	0
Brachysira brebissonii	0	0	0	0	0.2	0	0	0	0	0	0	0	0
Campylodiscus clypeus	0.4	0	0	0.2	0	0	0	0.4	0	0	0	0.2	0
Catenula adhaerens	3.4	5.8	1.6	4.4	0.8	2.6	3.2	7.6	1.6	13	1.4	10.8	1
Chaetoceros sp.	5	3.2	3.8	5.2	9.8	1.8	3	3	6.8	3.6	4	1	2.4
Climacosphemia moniligera	0	0.4	0	0	0.2	0	0.2	0	0	0	0	0	0
Cocconeis engelbrechtii	13.2	27.8	28.4	17.8	18.2	25.2	12.8	16.6	12.8	13.6	24.4	20	18.2
Cocconeis pediculus	1.6	0	0.8	1	0.4	0.6	1.6	1.4	1.2	0	0	1.8	0
Cocconeis placentula	9.8	6.4	12.6	6.8	5.8	2.6	7.2	5.8	4.4	6.4	4.4	7.2	3.6
Cocconeis scutellum	0	0.4	0	0	0.2	0	0	0	0	0	0	0	0
Coscinodiscus radiatus	0.2	0	0	0	0.8	5	21.6	5	39	6.4	42.8	13.2	54.4
Craspedodiscus elegans	0.2	0	0	0.6	0.4	4.4	1.2	1.4	0	3	0.4	1.6	0.2
Craticula accomoda	0	0.4	0	0.2	0.6	0	0.4	0.2	0	0	0	0.2	0
Craticula halophila	0.6	0.8	0.8	0.8	1.6	0.2	0.8	0.6	0.2	0.4	0	0	0.2
Ctenophora pulchella	0.4	0.4	0	0	0.2	0.2	0	0	0	0	0	0	0
Cyclotella caspia	4.2	0.6	4.2	1.6	3.2	0.4	4.2	2.4	4.4	2.2	3	1.8	0.6
Cyclotella distinguenda	2	4	2	3.8	6	4.2	9.8	9.4	5	9.8	2	12.6	1.2
Cyclotella meneghiniana	7.6	1.4	5.2	1.6	3.2	0.2	1.8	1.6	2.6	3	2.6	3.8	1
Delphineis minutissima	0.4	0	0	0.8	0	0	0	1.4	0.2	0	0	0.4	0
Denticula subtilis	0	0	0	0	0.2	0	0	0	0	0	0	0	0
Diadesmis confervacea	0	0	0	0	0	0	0	0	0	0	0	0	0

Depth (cm)	1	2	3	4	5	6	7	8	9	10	11	12	13
Age (yrs BP)	**-44**	**-28**	**-12**	**4**	**20**	**37**	**53**	**69**	**85**	**101**	**117**	**133**	**149**
Diatoma vulgaris	0	0	0	0	0	0	0	0	0	0	0	0	0
Diploneis chersonensis	0.8	1.4	0	0.8	1.6	2	1.6	4	0.6	2.4	0	0.4	0
Diploneis oblongella	0.4	0	0.6	0	0.2	0.8	0	0	0	0	0	0	0.2
Diploneis smithii	0.8	0.6	0.8	2	0.8	1.4	1.4	2	0.6	2.2	0.8	1.4	0.6
Encyonema gracile	0.6	0	0.4	0.4	0.4	0	0	0	0.2	0	0	0.2	0
Encyonema minutum	0.6	0.4	0.2	0	0.2	0.4	0.2	0	0	0	0	0	0
Entomoneis alata	0	0	0	0	0.2	0	0	0	0	0	0	0	0
Eolimna minima	0.4	0	0	0	0	0	0	0	0	0	0	0	0
Epithemia adnata	0	0	0	0	0	0	0	0	0	0	0	0	0
Epithemia sorex	0	0	0	0	0	0	0	0	0	0	0	0	0
Eunotia exigua var. tenella	0	0.4	0	0	0	0	0	0	0	0	0	0	0
Eunotia formica	0.2	0.4	0.4	0.8	0.4	1	0.6	0.2	0.4	0	0.2	0.2	1
Eunotia minor	0	0	0.4	0	0	0	0.2	0	0	0	0	0.2	0
Eunotia pectinalis var. undulata	0	0.2	0	0	0.2	0	0	0	0	0	0.2	0	0
Fallacia monoculata	4.8	6	1.8	2.8	1.2	2.2	0.4	3	0.4	2	0.2	0.8	0.2
Fallacia pygmaea	0	0	0	0	0	0	0	0	0	0	0	0	0
Fragilaria biceps	0.8	1.6	0.4	0.8	1	0.2	0.8	0.4	0.2	0.6	0.2	0.4	0.4
Fragilaria tenera	1.4	0.6	0.6	0.4	1.4	0	0.2	0.6	0.2	0	0.4	0.2	0.8
Fragilariforma	0	0.4	0.2	0	0	0	0	0	0	0	0	0	0
Frustulia rostrata	0.8	0	0	0	0	0	0	0	0	0	0	0	0
Frustulia saxonica	0.4	0	0.4	0	0.4	0	0.2	0	0	0	0	0	0
Gomphonema gracile	1.2	0	0	0	0.2	0	0	0	0	0	0	0	0
Gomphonema parvulum	0.2	0	0.2	0	0	0	0	0	0	0	0	0	0
Gomphonema venusta	0	0.2	0.2	0	0	0.4	0	0	0	0.2	0	0	0
Gyrosigma obscurum	0.6	0.2	0	0.2	0.2	0.2	0.2	0	0	0.2	0	0	0
Haslea sp	0.4	0	0	0	0	0	0	0	0	0	0	0	0
Mastogloia elliptica	0.4	0	1.2	0	0.4	0	1	0	0.4	0	0.2	0	0.2
Mastogloia smithii	0.6	0.2	0.2	0.2	0.2	0.2	0.6	0	0	0	0	0	0
Melosira nummuloides	5.2	11	5.4	9	8.8	5.2	7.8	3	6	4.2	1.8	2.8	6.8
Navicula cincta	1.4	0.8	1	0	0.2	0.8	0.6	0.4	0.8	0.6	0.4	0.2	0.4
Navicula cryptocephala	0.4	0.6	0.6	0	0.6	0	0.2	0.2	0.4	0.2	0	0.4	0
Navicula radiosa	0.2	0.6	0.6	0	1.2	0.6	0	0	0	0	0	0	0
Navicula veneta	0.6	0	1	0	1.4	0	0	0	0	0	0	0	0
Navicymbula pusilla	0.2	0.6	0.4	0	0	0.6	0.8	0	0	0	0	0.2	0
Navigiolum adamantiforme	0	0	0	0.4	0	0	0.2	0.2	0	0.2	0	0	0
Nitzschia amphibia	0	0	0.2	0	0	0	0	0	0	0	0	0	0
Nitzschia cocconeiformis	0	0.4	0	0	0.2	0.2	0	0	0	0	0	0	0
Nitzschia compressa	0.2	1	0.2	1.8	0	2	0.4	0.6	0	1.6	0.2	1.6	0

Depth (cm)	**1**	**2**	**3**	**4**	**5**	**6**	**7**	**8**	**9**	**10**	**11**	**12**	**13**
Age (yrs BP)	**-44**	**-28**	**-12**	**4**	**20**	**37**	**53**	**69**	**85**	**101**	**117**	**133**	**149**
Nitzschia dissipata	2.8	0	0	0	0	0	0	0	0	0	0	0	0
Nitzschia linearis var. subtilis	0	0	1.2	0.6	0.6	0.2	0.2	0.2	0.2	0.2	0.2	0	0.4
Nitzschia littorea	0.4	0	0	0	0	0	0	0	0	0	0	0	0
Nitzschia nana	0	0	0	0	0	0	0.2	0	0	0	0	0	0
Nitzschia palea	0.2	0.2	0.6	0.4	0.2	0	0	0	0	0.2	0	0	0.2
Opephora marina	2.6	2.4	0.4	0	0.6	0	0	0	0	0.2	0	0	0
Paralia sulcata	0.6	2.4	1.8	2.4	1.6	3.6	0.8	0.4	1	0.2	0.8	0.4	0.8
Petroneis humerosa	0	0	0	1	0	3.2	0.4	1.2	0.2	0.8	0	0.4	0.2
Pinnularia borealis	0.2	0	0.4	0.2	0	0	0.2	0	0	0	0.4	0.2	0
Pinnularia borealis var. 1	0	0.6	0	0.8	0.2	2.8	0.6	1.8	0	0.8	0.4	1	0
Pinnularia gibba	0	0	0.4	0	0	0	0	0	0	0	0	0	0
Pinnularia maior	1	1.4	1	0.8	1	1.2	1.4	5.6	0	1.8	0	0.6	0
Pinnularia subcapitata	0	0	0.2	0.2	0.4	0	0	0	0	0	0	0	0
Pinnularia viridis	0	0	0	0	0	0	0	0	0	0.2	0	0	0
Planothidium delicatulum	0.4	1.2	0.2	0.2	0	0	0	1	0	0.2	0	0.4	0
Rhopalodia gibberula	0.2	0	0	0	0.4	0	0.6	0.2	0	0	0	0.2	0
Rhopalodia musculus	0.4	0.4	0.6	0.2	0.4	0	0.6	0	0	0	0	0	0
Staurosira elliptica	0	0	0	0	0	0	0	0	0	0	0	0	0
Surirella brebissonii	0	0	0.2	0	0	0	0	0	0	0	0	0	0
Synedra bacillaris	0.8	2.8	0.2	0	0.2	3.2	0	1.2	0.8	0.8	0	0	0
Tabellaria flocculosa	0.2	0	0.2	0.2	1.2	0.4	0	0.2	0	0	0	0	0.8
Tabularia fasciculata	0.4	1.8	2.2	4	5	1	0.2	0.4	0.6	2.4	1.2	2.6	0.2
Terpsinoë americana	0	0	0.2	0	0	0	0	0.2	0	0	0	0.2	0
Thalassirosira weissflogii	2.2	0	4	5.8	5.2	0	5.6	4	5.2	6.6	5.4	6.6	1.6
Tryblionella apiculata	0.6	0.6	0	0.2	0.2	0.4	0	0.4	0	0	0	0.2	0
Tryblionella calida	0	0	0	0.6	0.2	0	0	0	0	0.2	0.2	0	0.2

SV10.1 continued

Depth (cm)	**14**	**15**	**16**	**17**	**18**	**19**	**20**	**22**	**26**	**30**	**34**	**38**	**42**
Age (yrs BP)	**165**	**181**	**197**	**213**	**229**	**246**	**262**	**294**	**358**	**422**	**487**	**551**	**615**
Achnanthes brevipes	0.6	0	1.2	0.2	0.8	1	0.8	1.4	1.6	0.8	0.8	3.8	3.6
Achnanthes oblongella	1.8	1.4	1	1.2	0.2	0.2	1	0	0.4	0.2	0	0.6	0
Achnanthidium affine	0	0	0	0	0	0	0	0	0	0	0	0	0
Achnanthidium crassum	0	0	0	0	0	0	0	0	0	0	0	0	0
Achnanthidium straubianum	0	0	0	0.6	0	0	0	0	0	0	0	0	0
Actinoptychus heliopelta	0	0	0	0	0	0	0	0	0	0	0	0.2	0
Amphora acutiuscula	0	0	0.2	0	0.2	0	0.2	0	0	0.2	0.2	0	0.4
Amphora arcus	0	0	0	0	0	0	0	0	0	0	0	0	0
Amphora coffeaeformis	0.6	0.8	0.2	0	1.4	0	0.4	1.8	2	1.4	1.2	1.6	1.2
Amphora commutata	0.8	0	1	0	2	0.4	1	0.8	0.4	0.4	0.8	1.4	1.8
Amphora ostrearia	1.6	0	2	0.4	4	0.4	6.2	7	1	2.6	6	2.8	2.6
Amphora ovalis	0	0	0.4	0	0.2	0	1	0.2	0.6	0.8	1	2	1.8
Amphora proteus	3	0.8	2	0.6	2.8	0.8	1.6	0.8	2.2	1.6	1	3	1.4
Amphora veneta	0	0	0	0	0	0	0	0	0	0	0	0	0
Bacillaria paradoxa	0	0	0	0	0	0	0	0	0	0	0	0	0
Bacteriastrum sp.	0	0	0	0	0	0	0	0	0	0	0	0	0
Brachysira brebissonii	0	0	0	0	0	0	0	0	0	0	0	0	0
Campylodiscus clypeus	0	0	0.6	0.2	0	0	0.6	0	0.2	0	0	0	0
Catenula adhaerens	6.2	1.2	3.8	1.8	6.8	1.2	4	4.2	7.2	7	5.2	5	4.8
Chaetoceros sp.	2.4	5	0.4	1.2	1.2	0.8	1.6	1	1.2	1.4	1.8	0.4	3.6
Climacosphemia moniligera	0	0	0	0	0	0	0	0	0	0	0	0	0
Cocconeis engelbrechtii	15.4	20.2	7.8	16	6.2	13.2	2.6	2	0.8	1.4	2.2	2	3
Cocconeis pediculus	2.2	0.6	2.4	0.4	1	0.2	1.2	0.2	1.8	0.6	1.4	0.4	0.8
Cocconeis placentula	5.2	3.2	5.4	3	6	4.8	9.2	9.6	13.8	11.8	12.4	9.2	12
Cocconeis scutellum	0	0	0	0	0	0	0.2	0.2	0	0	0	0	0.2
Coscinodiscus radiatus	11.2	24.2	3.8	18.4	2.6	20.8	1.6	0.2	1	0.8	0.8	0.6	0.2
Craspedodiscus elegans	3.8	0.4	7.2	2.4	5.6	5	9.8	3.2	2.4	0.4	4.2	8.8	3
Craticula accomoda	0.2	0	0	0	0	0	0	0.2	0.4	0.6	0.4	0	0
Craticula halophila	0.4	0.2	0.4	0	0	0	0.4	0	0	0	0	0	0
Ctenophora pulchella	0	0	0	0	0	0	0	0	0	0	0	0	0
Cyclotella caspia	1.2	2	0.8	1	0.6	2.6	0	0	0.2	0.2	0.4	1.4	1.6
Cyclotella distinguenda	7.4	4	11.2	3.6	7.4	1.8	3.2	1.4	1.2	0.8	2.6	1.6	3.6
Cyclotella meneghiniana	0.8	3.2	2.6	6.4	2.8	6.6	0.4	0	0.2	0.2	0.8	1.4	1.6
Delphineis minutissima	0.6	0.4	1.8	0.4	1.8	0.8	1.6	1	1.6	3.2	1.6	1.2	2.6
Denticula subtilis	0	0	0	0	0	0	0	0	0	0	0	0	0
Diadesmis confervacea	0	0	0	0	0	0	0	0	0	0	0	0	0
Diatoma vulgaris	0.4	0	0	0	0	0	0	0	0.2	0	0	0	0

Depth (cm)	14	15	16	17	18	19	20	22	26	30	34	38	42
Age (yrs BP)	**165**	**181**	**197**	**213**	**229**	**246**	**262**	**294**	**358**	**422**	**487**	**551**	**615**
Diploneis chersonensis	1.2	0.6	7.2	2.8	12.2	3	8.6	8.2	6.2	2.6	10.8	11.2	7.8
Diploneis oblongella	0	0	0	0	0	0	0	0	0	0	1.2	0	0.4
Diploneis smithii	3.8	0.6	2.6	0.4	4	1.2	1.8	3.8	1.8	4.8	3.2	3.2	3
Encyonema gracile	0	0	0	0	0	0	0	0	0	0	0.6	0.2	0
Encyonema minutum	0.2	0.8	0	0	0	0	0	1.2	0.4	0.4	0.6	0.4	0
Entomoneis alata	0	0	0.4	0	0	0	0	0	0.2	0.2	0.4	1	0.2
Eolimna minima	0	0	0	0	0	0	0	0	0	0	0	0	0
Epithemia adnata	0	0	0.2	0.2	0	0	0.2	0	0	0	0	0	0
Epithemia sorex	0	0	0	0	0	0	0	0	0	0	0	0.2	0
Eunotia exigua var. tenella	0	0	0	0	0	0	0	0	0	0	0	0	0
Eunotia formica	1	0.6	1.2	0.6	0	0.2	0	0.2	0.2	0.2	0.2	0.4	0.2
Eunotia minor	1	0	0.4	0	0.6	0.4	1.2	2.2	2.6	0.2	1	1.4	0.6
Eunotia pectinalis var. undulata	0	0	0	0	0	0	0	0	0	0	0	0	0
Fallacia monoculata	0.8	0.2	1.6	1.6	1.4	0.4	1	2.4	2.8	3.4	3.8	4.2	4
Fallacia pygmaea	0	0	0	0	0	0	0	0	0	0	0	0.2	0
Fragilaria biceps	0.4	0.2	0.8	0.2	0.2	0	0.6	0.2	0.2	0.2	0.2	0.8	0.4
Fragilaria tenera	0	1.2	0.6	0.2	0	0.4	0	0	0	0	0	0	0
Fragilariforma	0	0	0	0	0	0	0	0	0	0	0	0	0.6
Frustulia rostrata	0	0	0	0	0	0	0	0	0	0	0	0	0
Frustulia saxonica	0	0	0	0	0	0	0	0	0	0	0	0	0
Gomphonema gracile	0	0	0	0	0	0	0	0	0	0	0	0	0
Gomphonema parvulum	0	0	0	0	0	0	0	0	0	0	0	0	0
Gomphonema venusta	0	0.4	0.2	0	0	0	0	0	0	0	0	0	0
Gyrosigma obscurum	0	0	0	0	0	0	0	0	0	0	0	0	0
Haslea sp	0	0	0	0	0	0	0	0	0	0	0	0	0
Mastogloia elliptica	0	0	0	0	0	0	0	0	0	0	0	0.2	0.2
Mastogloia smithii	0.6	0	0	0.2	0.2	0.2	0	0.4	0	0	0	0.2	0.8
Melosira nummuloides	7.4	15.8	7.6	19.6	7.6	18.4	7	3.4	4.2	5	5.4	8.4	4.6
Navicula cincta	0	0.4	0.2	0	0.2	0	1	0.4	1.6	1.6	0.6	1.4	0.6
Navicula cryptocephala	0	0.4	0	0	0	0	0	0	0.2	0	0	0	0
Navicula radiosa	0	0	0	0	0	0	0	0	0	0	0	0	0
Navicula veneta	0	0	0	0	0	0	0	0	0	0	0	0	0
Navicymbula pusilla	0.2	0	0	0	0	0	0	0.6	0	0.4	0	0.2	0.4
Navigiolum adamantiforme	0	0	0.2	0.2	1.2	0.4	1.2	0.4	1	1	0.6	0.8	1.2
Nitzschia amphibia	0	0	0	0	0	0	0	0	0	0	0	0	0
Nitzschia cocconeiformis	0	0	0.2	0.2	1	0.2	1.6	0.4	0.4	0.2	0.8	0.6	0.2
Nitzschia compressa	2.2	0	1.2	0.8	2	1	7.4	10.2	7	2.6	3.4	2.4	2.8
Nitzschia dissipata	0	0	0	0	0	0	0	0	0	0	0	0	0

Depth (cm)	14	15	16	17	18	19	20	22	26	30	34	38	42
Age (yrs BP)	**165**	**181**	**197**	**213**	**229**	**246**	**262**	**294**	**358**	**422**	**487**	**551**	**615**
Nitzschia linearis var. subtilis	0	0	0.2	0	0.2	0	0.4	0.4	0.4	0.8	0	0	0
Nitzschia littorea	0	0	0	0	0	0	0	0	0	0	0	0	0
Nitzschia nana	0	0	0	0.2	0	0	0	0	0	0	0	0	0
Nitzschia palea	0	0.8	0	0	0	0	0	0	0	0	0	0	0
Opephora marina	0.2	0	0.2	0	0	0	0	0	0	0	0	0	0
Paralia sulcata	0.8	1.4	0.8	1.2	0.2	0.2	0.6	0.4	0.4	0.2	1.2	1.4	3.4
Petroneis humerosa	0.6	0	1	0.4	2.2	0	1	0	0.6	0.6	2.2	4.2	1.8
Pinnularia borealis	0.2	0	0.2	0	0	0	0	0	0.4	0	0	0	0
Pinnularia borealis var. 1	1	0	2.8	1.2	3.2	1	9.6	24.2	22.8	33.4	10.4	2.6	4.4
Pinnularia gibba	0	0	0	0	0	0	0	0	0	0	0	0	0
Pinnularia maior	1.4	0.8	3	1.2	4.4	0.8	3.8	3.8	3.4	3.6	5.4	3.2	6.6
Pinnularia subcapitata	0	0.2	0	0	0.2	0	0	0	0	0	0	0	0
Pinnularia viridis	0	0	0	0	0.2	0	0	0	0	0	0	0	0
Planothidium delicatulum	0.6	0	0	0.2	0.2	0.4	0	0	0	0.2	0.2	0	0
Rhopalodia gibberula	0.2	0	0	0.2	0	0	0.2	0	0	0	0	0.2	0
Rhopalodia musculus	0.2	0	0	0	0	0	0	0.2	0	0	0	0	0
Staurosira elliptica	0	0	0	0	0	0	0	0	0	0	0	0	0
Surirella brebissonii	0	0	0	0.4	0	0	0	0.2	0	0	0	0	0
Synedra bacillaris	0	0	0	0	0	0.2	0	0	0	0	0	0	0
Tabellaria flocculosa	0	0.8	0.4	0.4	0	0	0	0	0	0	0	0	0
Tabularia fasciculata	4.4	2.2	4.6	0.8	1.2	1.2	0.8	1	0.6	0.4	1.2	1.8	2.4
Terpsinoë americana	0	0	0.6	0.2	0.2	0.4	0.6	0	0	0	0	0	0
Thalassirosira weissflogii	5	4.8	5.2	8.8	3.2	9	2	0.2	1.4	0.6	1.6	1	2.4
Tryblionella apiculata	0.6	0.2	0	0	0.2	0	0.4	0	0	0.6	0	0.8	0.6
Tryblionella calida	0.2	0	0.2	0	0.2	0.4	0.4	0.4	0.8	0.4	0.2	0	0.6

SV10.1 continued

Depth (cm)	**46**	**50**	**54**	**58**	**62**	**66**	**70**	**74**	**78**	**82**	**86**	**90**
Age (yrs BP)	**660**	**702**	**744**	**786**	**829**	**871**	**913**	**955**	**1047**	**1146**	**1245**	**1343**
Achnanthes brevipes	2.4	2.6	4	1	1.2	4	2.8	2.6	4.2	2.6	2.4	5.4
Achnanthes oblongella	0	0.2	0.2	0	0.4	0	0	0.4	1	0.2	0.4	0.6
Achnanthidium affine	0	0	0	0	0	0	0	0	0	0	0	0
Achnanthidium crassum	0	0	0	0	0	0	0	0	0	0	0	0
Achnanthidium straubianum	0	0	0	0	0	0	0	0	0	0	0	0
Actinoptychus heliopelta	0	0	0	0	0.4	0	0	0	0	0.4	0	0
Amphora acutiuscula	0	0.2	0	0	0	0.4	0.2	0.2	0.4	0	0.6	1.4
Amphora arcus	0	0	0	0	0	0	0	0	0	0	0	0
Amphora coffeaeformis	0.8	0.2	0.4	1.2	0.4	1	0.6	0	0	0.2	1.8	0.8
Amphora commutata	0.2	0.6	0.8	1	1.8	1.8	1.4	0.8	2.4	2.6	0.4	1.6
Amphora ostrearia	1.8	0.2	3.2	1.8	2.2	0.8	1.2	0.4	0.4	1.4	2.6	4
Amphora ovalis	0.4	1.6	3.2	0.8	0	2	1.2	0.8	0.4	0.8	1.4	1.8
Amphora proteus	1.6	2.8	3.4	2.8	3.4	3	3.6	3.2	2.4	1.2	2.4	6
Amphora veneta	0	0.4	0	0	0	0	0	0	0	0	0	0
Bacillaria paradoxa	0	0	0	0	0	0	0	0	0	0	0	0
Bacteriastrum sp.	0	0.4	0.8	1	1.6	1.8	3.4	2.6	3.6	1.8	1	1.8
Brachysira brebissonii	0	0	0	0	0	0	0	0	0	0	0	0
Campylodiscus clypeus	0.2	0	0	0	0	0	0	0	0	0	0	0
Catenula adhaerens	6	5	3.8	5.8	3.4	1.8	2.8	2.2	6.4	7.2	10.8	5.8
Chaetoceros sp.	1.6	1.8	3.2	3.2	8	3.4	2.4	5.2	10	5.2	6.2	8
Climacosphemia moniligera	0	0	0	0	0	0	0	0	0	0	0	0
Cocconeis engelbrechtii	3.8	13.8	3.2	3	2.2	3.4	2.6	13.6	9.2	3.6	2	6.8
Cocconeis pediculus	0.4	2	0	0	0	0	0.2	0.2	0	0.2	0.8	3.8
Cocconeis placentula	15	13.4	5.2	8	4.4	3.4	5	4.6	5.8	4.8	6.6	6.4
Cocconeis scutellum	0	0.2	0	0	0	0.2	0	0	0	0	0	0
Coscinodiscus radiatus	0.2	3	0	0.4	0	1	0.8	1	0.4	0.6	0	0
Craspedodiscus elegans	7	2.2	7.6	9.6	13.6	11.8	4.4	1.2	3.4	6.8	3	1
Craticula accomoda	0	0	0	0	0	0	0	0	0	0	0	0
Craticula halophila	0	0	0	0	0	0	0	0	0	0	0	0
Ctenophora pulchella	0	0	0	0	0	0	0	0	0	0	0	0
Cyclotella caspia	2.8	2.8	2	3	2.6	2	4.2	4.4	2.2	2.2	1.4	0.4
Cyclotella distinguenda	4.4	7.4	10.4	6.6	8	10	26	17.8	8.4	6.4	3	1
Cyclotella meneghiniana	1.8	4.6	2.4	1.8	3.4	2.4	2	0.2	0	0	0	0.2
Delphineis minutissima	1.2	1.6	2.2	5.2	2	1.6	0	1.2	0.6	3.4	1.2	2
Denticula subtilis	0	0.2	0	0	0	0	0	0	0	0	0	0
Diadesmis confervacea	0	0	0	0	0	0	0.4	0	0	1.2	0	0
Diatoma vulgaris	0	0	0	0	0	0	0	0.4	0	0	0	0

Depth (cm)	**46**	**50**	**54**	**58**	**62**	**66**	**70**	**74**	**78**	**82**	**86**	**90**
Age (yrs BP)	**660**	**702**	**744**	**786**	**829**	**871**	**913**	**955**	**1047**	**1146**	**1245**	**1343**
Diploneis chersonensis	9	4.2	10.6	7.6	6.4	7.4	3.4	3	5	6.2	6	10.8
Diploneis oblongella	0.4	0	0.2	0.2	0.4	0	0.8	0	0	0	0.4	2.2
Diploneis smithii	2.8	2.6	5.2	4.4	4.6	2	2	3.4	4.4	3.2	3.4	3
Encyonema gracile	0.6	0	0	0	0	0	0	0	0	0	0	0
Encyonema minutum	0.2	0	0	0	0	0	0	0.4	0.2	0	0.2	0.4
Entomoneis alata	0.8	0	0	0	0	0.2	0	0	0	0	0	0
Eolimna minima	0	0	0	0	0	0	0	0	0	0	0	0
Epithemia adnata	0	0	0	0	0	0	0	0	0	0	0	0
Epithemia sorex	0	0	0	0	0	0	0	0	0	0	0	0
Eunotia exigua var. tenella	0	0	0	0	0	0	0	0	0	0	0	0
Eunotia formica	0.4	1	0.2	0	0	0	0	0	0.8	0	0.4	0
Eunotia minor	1	0	0	0	0	0	0	0	0	0	0	0
Eunotia pectinalis var. undulata	0	0	0	0	0	0	0	0.2	0	0	0	0
Fallacia monoculata	7.8	4	3	5	4.2	2.6	3.2	3.4	4.6	5.8	6.4	3.6
Fallacia pygmaea	0	0	0	0	0	0	0	0	0	0	0	0
Fragilaria biceps	0	0.4	0.8	0.2	0.2	0	0.2	1	0.6	0.2	0	0.2
Fragilaria tenera	0	0	0	0	0	0	0	0	0	0	0	0.2
Fragilariforma	0	0.6	0	0	0	0	0	0	0	0.6	0	0
Frustulia rostrata	0	0	0	0	0	0	0	0	0	0	0	0
Frustulia saxonica	0	0	0	0	0	0	0	0	0	0	0	0
Gomphonema gracile	0	0	0	0	0	0	0	0	0	0	0	0
Gomphonema parvulum	0	0	0	0	0	0	0	0	0	0	0	0
Gomphonema venusta	0	0.4	0	0	0	0.2	0	0	0	0	0	0
Gyrosigma obscurum	0	0	0	0	0	0	0	0	0	0	0	0
Haslea sp	0	0	0	0	0	0	0	0	0	0	0	0
Mastogloia elliptica	0	0.2	0	0	0	0	0	0	0	0	0	0
Mastogloia smithii	0.2	0	0.4	0	0	0.6	0.2	0.2	0.6	0	0.2	0.2
Melosira nummuloides	6.8	4.4	0.6	4.4	2	2	3.4	1.8	1.8	3	2.4	1.8
Navicula cincta	0.4	0	0.8	0.4	0.4	0.8	0	1	1	0	1.2	0
Navicula cryptocephala	0	0	0	0	0	0	0	0	0	0	0	0
Navicula radiosa	0	0	0	0	0	0	0	0.4	0	0	0	0
Navicula veneta	0	0	0	0	0	0	0	0	0	0	0	0
Navicymbula pusilla	0.4	0.6	0	0.4	0	0	0	0	0	0	0.2	0
Navigiolum adamantiforme	0.8	0.8	0.8	1	0.6	0	0	0	0	0	0	0
Nitzschia amphibia	0	0	0	0	0	0	0	0	0	0	0	0
Nitzschia cocconeiformis	0.8	0	0.4	0	0.4	0.6	0	0.6	0.2	0.2	0	0.6
Nitzschia compressa	2.8	0.8	2.4	1.6	1.8	2.8	1.4	1	1.4	2.2	2.6	3
Nitzschia dissipata	0	0	0	0	0	0	0	0	0	0	0	0

Depth (cm)	**46**	**50**	**54**	**58**	**62**	**66**	**70**	**74**	**78**	**82**	**86**	**90**
Age (yrs BP)	**660**	**702**	**744**	**786**	**829**	**871**	**913**	**955**	**1047**	**1146**	**1245**	**1343**
Nitzschia linearis var. subtilis	0	0.4	0	0	0	0	0	0	0	0	0	0
Nitzschia littorea	0	0	0	0	0	0	0	0	0	0	0	0
Nitzschia nana	0	0	0	0	0	0	0	0	0	0	0	0
Nitzschia palea	0	0	0	0	0	0	0	0	0	0	0	0.2
Opephora marina	0.2	0	0	0	0.2	0	0	0	0	0	0	0.4
Paralia sulcata	2.4	0.8	4.4	4	7.8	6.2	6	6.8	5.4	6.8	3	2.4
Petroneis humerosa	1.2	1.2	2.2	1.6	1.2	2	1.4	1	2.6	1.2	1.2	0.6
Pinnularia borealis	0	0	0	0.4	0	0	0	0	0	0	0	0
Pinnularia borealis var. 1	2.2	0.6	0.8	0.8	2.4	7	1.8	0.6	0.6	7.4	13.6	6
Pinnularia gibba	0	0	0	0	0	0	0	0	0	0	0	0
Pinnularia maior	3	2.6	7.4	5.8	4.4	4.6	2.6	1	2.2	1.2	4.4	1.6
Pinnularia subcapitata	0.2	0	0.4	0	0	0	0	0	0	0	0	0
Pinnularia viridis	0	0	0	0	0	0	0	0.6	0	0	0	0
Planothidium delicatulum	0	0.8	0	1	0.6	0.2	0.4	1	1.2	1.8	1	0.2
Rhopalodia gibberula	0	0	0	0	0.2	1.2	0.4	0.8	1	0	0.4	0
Rhopalodia musculus	0	0	0	0	0	0	0	0	0	0	0	0
Staurosira elliptica	0	0	0	0	0	0	0	0	0	0	0	0
Surirella brebissonii	0.2	0	0	0	0.8	0.8	0	0.4	1	1.4	3	1
Synedra bacillaris	0	0	0	0	0	0	0.2	0	0	0	0	0
Tabellaria flocculosa	0	0	0	0	0	0	0	0	0	0	0	0
Tabularia fasciculata	0.8	3	1.6	1.2	0.6	2	1.8	3.8	1	1	0.6	0.4
Terpsinoë americana	0	0	0	0	0	0	0	0	0	0	0	0.4
Thalassirosira weissflogii	2	2.4	1	3.6	1.6	1	5.6	4.2	2.4	4.4	1.4	2
Tryblionella apiculata	0.8	0.2	0.8	0.2	0.2	0	0	0.4	0.6	0.6	0	0
Tryblionella calida	0.2	0.8	0	0	0	0	0	0	0.2	0	0	0

Table 11.8: Princessvlei (PV11.3) diatom species with ecological affinities; including salinity (f = fresh, fb = fresh-brackish, bf = brackish-fresh, b = brackish, mb = marine-brackish, m = marine, u = unknown), pH (a = acidophilic, c = circumneutral, k = alkaliphilic, b = alkalibiontic, u = unknown), Life form (a = aerophilic, b = benthic, p = planktonic, m = marine, u = unknown) and trophic state (uo = ultraoligotrophic, ot = oligotrophic, mt = mesotrophic, et = eutrophic, pt = polytrophic, ht = hypertrophic, mar = marine, u = unknown)

Species name	Salinity	pH	Life form	Trophic state
Achnanthes brevipes	fb	c	b	ot
Achnanthes oblongella	fb	c	b	uo
Achnanthes subaffinis	f	c	b	ot
Achnanthes swazi	f	un	b	ot
Achnanthidium crassum	f	k	b	un
Achnanthidium eutrophilum	un	un	b	et
Achnanthidium exiguum	f	k	un	o-e
Achnanthidium microcephalum	f	un	b	o-m
Achnanthidium minutissimum	f	c	b	o-e
Achnanthidium straubianum	f	k	b	m-e
Amphipleura pellucida	fb	k	b	m-e
Amphora coffeaeformis	b	k	b	et
Amphora copulata	fb	k	b	pht
Amphora proteus	m	m	m	mar
Amphora veneta	bf	b	b	pht
Aulacoseira ambigua	f	k	p	et
Aulacoseira granulata	fb	k	p	et
Aulacoseira granulata var angustissima	f	k	p	et
Aulacoseira muzzanensis	f	b	p	et
Brachysira vitrea	un	c	un	o-m
Caloneis bacillum	fb	k	b	et
Caloneis sp	un	un	un	un
Cocconeis distans	m	m	m	mar
Cocconeis placentula	fb	k	b	m-e
Craspedostauros capensis	m	m	m	mar
Cyclotella meneghiniana	f	k	p	et
Cymbella turgidula	un	k	un	o-m
Diploneis oblongella	fb	k	b	uo
Diploneis smithii	b	c	b	un
Discotella stelligera	f	c	p	ot
Encyonema neogracile	f	i	b	ot
Encyonema silesiacum	f	c	b	o-e
Encyonema subminuta	un	un	un	ot
Encyonopsis cesatii	fb	c	b	ot

Species name	Salinity	pH	Life form	Trophic state
Encyonopsis sp	un	k	un	un
Eolimna minima	fb	k	b	e-p
Eolimna subminuscula	fb	k	b	pht
Epithemia adnata	fb	b	b	m-e
Epithemia sorex	fb	b	b	e-p
Eunotia formica	fb	a	un	dot
Eunotia minor	fb	c	b	un
Fallacia sp	un	un	un	un
Fistulifera saprophila	fb	c	b	et
Fragilaria biceps	f	b	b	m-e
Fragilaria capucina	fb	c	p	o-e
Fragilaria exigua	un	un	un	un
Fragilaria tenera	f	a	b	uo
Frustulia vulgaris	fb	k	b	o-e
Gomphonema gracile	fb	c	b	un
Gomphonema parvulum	fb	c	b	pht
Hippodonta capitata	fb	k	un	et
Hippodonta hungarica	f	k	b	mt
Kobayasiella sp	un	un	un	un
Mastogloia braunii	un	c	b	un
Mastogloia elliptica	b	k	b	et
Melosira nummuloides	b	k	p	et
Navicula angusta	f	a	b	ot
Navicula cincta	fb	k	b	pt
Navicula cryptocephala	fb	c	b	o-e
Navicula cryptotenella	fb	k	b	o-e
Navicula radiosa	fb	c	b	o-e
Navicula veneta	bf	k	b	et
Navicymbula pusilla	fb	k	b	o-e
Neidium affine	un	un	un	un
Nitzschia amphibia	fb	k	b	pht
Nitzschia clausii	b	k	b	pht
Nitzschia palea	fb	c	b	e-p
Nitzschia recta	fb	k	b	e-p
Opephora marina	b	k	b	e-p
Petroneis humerosa	m	m	m	mar
Pinnularia borealis	fb	c	a	m-e
Pinnularia divergens	un	a	un	ot
Pinnularia intermedia	un	i	un	m-e

Species name	Salinity	pH	Life form	Trophic state
Pinnularia subcapitata	fb	i	b	ot
Pinnularia viridis	un	c	b	o-m
Placoneis clemetis	bf	k	un	et
Placoneis placentula	un	un	un	et
Planothidium biporomum	fb	k	b	ot
Planothidium delicatulum	b	b	un	et
Planothidium rostratum	fb	k	b	et
Pseudostaurosira brevistriata	fb	k	b	o-e
Rhopalodia gibba	fb	b	b	e-p
Rhopalodia gibberula	bf	k	b	un
Sellaphora pupula	fb	c	b	pht
Sellaphora stroemii	un	un	un	pht
Staurosira elliptica	fb	k	b	m-e
Stephanodiscus agassizensis	fb	k	p	et
Stephanodiscus hantzschii	fb	k	p	et
Surirella sp	un	un	un	un
Thalassiosira eccentrica	m	m	m	mar
Thalassiosira lentiginosa	m	m	m	mar
Thalassirosira weissflogii	f	c	p	pt
Tryblionella calida	bf	c	b	et
Tryblionella hungarica	bf	k	b	pht

Table 11.9: Princessvlei (PV11.3) diatom species percentage representation against depth and age (H = hiatus)

Age (cal yrs BP)	**240**	**293**	**320**	**H**	**445**	**468**	**491**	**519**	**554**	**576**	**599**	**622**	**668**	**690**	**713**	**747**
Depth (cm)	**3**	**7**	**9**	**H**	**13**	**15**	**17**	**20**	**23**	**25**	**27.5**	**29.5**	**33**	**35**	**37**	**40**
Achnanthes brevipes	0	0	0		0	0	0	0	0	0	0.2	0	0	0	0	0
Achnanthes oblongella	0.4	0.8	4.2		2.2	0.8	1.6	1	2.6	1.4	0.4	2	0.8	0.6	0	1
Achnanthes subaffinis	0	1.8	2.2		3.8	13.4	8	7.2	18	14.2	30.6	42	41.6	41	20.8	34.4
Achnanthes swazi	0	0	0		0	0.4	1.6	0.8	1.6	3.8	4	1.2	1.8	1.4	2.4	1.6
Achnanthidium crassum	0	0	0.2		2.2	0.4	0.8	1.2	0	0.2	1.2	0	0	0.2	0	0.8
Achnanthidium eutrophilum	0.4	0	0.4		0.6	0.4	0	0.2	0	0.4	0	0	0	0	0	0
Achnanthidium exiguum	0	0.6	1.6		0	0	0	0	0	0	0	0.2	0.2	0	0	0
Achnanthidium microcephalum	0	0.8	0		4	2.6	3.2	2	10.6	4.8	2.8	1.8	6.2	2.4	1.6	2.8
Achnanthidium minutissimum	0	1.8	0		1.2	2.4	0.6	2.4	2.8	4.2	2.6	1.2	0.2	2	0.8	1.4
Achnanthidium straubianum	0	0.8	0.8		4.2	0.8	1.6	1.2	3.8	0.8	2.2	0.6	0.2	3.8	1	0.6
Amphipleura pellucida	0	0	0		0	0	0.4	0.8	0	0	0	0	0	0	0	0
Amphora coffeaeformis	0.2	0	0		0	0	0	0	0	0	0.2	0	0	0	0	0
Amphora copulata	0	0	0		0	0	0.4	0	0	0.4	0	0.4	0.2	0.2	0.2	0
Amphora proteus	0	0	0		0	0	0	0	0	0	0	0	0	0	0	0
Amphora veneta	0.2	0	0		0	0	0	0	0	0	0	0	0	0	0	0
Aulacoseira ambigua	60.6	0	0		0.8	3.4	4	4	0	0.6	0.2	0	0.2	1	0.4	0.2
Aulacoseira granulata	7	9.2	0		0	0	0	0	0	0	0	0	0	0	0	0
Brachysira vitrea	0	0	0		0.2	0	0.2	0	0.2	0	0	0	0	0	0	0
Caloneis sp	0	0	0		0.2	0	0	0	0	0	0	0	0	0	0	0
Cocconeis distans	0.2	0	0.2		3.8	1	0.4	0.6	0.4	0.4	4.2	1.8	0.6	1.4	2	3
Cocconeis placentula	1	3.2	2.8		18	19.4	12.2	26.2	13.6	12.6	5.2	0	0.2	0.2	0	0
Craspedostauros capensis	0	0	0		1.4	0.6	0.6	0.2	1.2	0.4	0.4	0.2	0	0	0	0
Cymbella turgidula	0	0	0		0	0.6	0.2	0	0	0	0	0	0	0	0	0
Diploneis oblongella	0	0	0		0	0.2	0	0.2	0.2	0	0	0	0	0	0	0
Diploneis smithii	0	0.2	0		0.6	0.4	0.2	0.8	1.2	1	0.8	0.2	0	0	0	0
Discotella stelligera	0.2	0	0.8		14.2	19.4	10.2	10.4	3	4	1.6	0.8	0	0.6	0.4	0
Encyonema gracile	0	0	0		0	0.2	0.8	0	1	0.2	0.4	0	0	0	0	0
Encyonema silesiacum	0	0	0		0	0	0	0	0.2	0.2	0.2	0	0	0	0	0
Encyonema subminuta	0	0	0		0	0.2	0.2	1	0	0.6	0.2	0	0.2	0	0	0
Encyonopsis cesatii	0	0	0		0	0	0	0	0	0	0	0	0	0	0	0
Encyonopsis sp	0	0	0		0.2	0	0	0	0	0	0	0	0	0	0	0
Eolimna minima	0.2	2	0		0	3	0.6	2.2	0	0	0	0	0	0	0	0
Eolimna subminuscula	0	57.4	59.4		1	0	0.2	0	0	1.4	1.2	0.2	0	0.2	0	0.4
Epithemia adnata	0	0	0		0	0	0.4	0	0	0	0	0	0	0	0	0
Epithemia sorex	0.4	0	0		0	0	0	0	0	0	0	0	0	0	0	0
Eunotia formica	0	0	0		0	0	0	0	0	0	0	0	0	0	0	0

Age (cal yrs BP)	240	293	320	H	445	468	491	519	554	576	599	622	668	690	713	747
Depth (cm)	**3**	**7**	**9**	**H**	**13**	**15**	**17**	**20**	**23**	**25**	**27.5**	**29.5**	**33**	**35**	**37**	**40**
Eunotia minor	0	0	0		0.6	0	0	0	0.8	0.4	0	0	0	0	0	0
Fallacia sp	0.4	0	0.2		0.2	0	0.2	0	0	0.8	0	0	0	0	0	0
Fragilaria biceps	0	0	0		0	0	0.4	0	0	0	0	0	0	0	0	0
Fragilaria capucina	0	0.2	0		2	5	2.2	1.8	0.6	0.8	0	0.6	0.2	0	0.2	0
Fragilaria exigua	0	0	0		0	0	0.2	0	0	0	0	0	0	0	0	0
Fragilaria tenera	0	0.2	0		0	0.2	0	0	0	0.2	0	0	0	0	0	0
Frustulia vulgaris	0	0	0		0	0	0	0	0	0.2	0	0	0	0	0	0
Gomphonema gracile	0	0	0		0.8	0	0.2	0.2	1.2	1.4	1	0	0.2	0	0	0.2
Gomphonema parvulum	0	0.8	0		0	0	0	0.4	0	0	0	0	0	0	0	0
Hippodonta hungarica	0	0	0		0	0.4	0.2	0.2	1	0.8	0	2.6	0.4	0.6	1.8	0.8
Kobayasiella sp	0	0	0		0	0	0	0	0	0	0	0	0	0	0	0
Mastogloia braunii	0	0	0		0.2	0	0	0.4	0.2	0	1	0.2	0	0.4	0	1.8
Melosira nummuloides	1.8	0	1.4		12.4	1.4	11	5.4	11	7.4	5	7.4	1.6	2.4	1	1
Navicula angusta	0	0	0		0	0.2	0.4	0	0	0	0	0	0	0	0	0
Navicula cincta	0	0.4	0.4		2.6	4.4	2.4	2.4	2.6	9.4	4.6	2.4	0.8	0.6	1.2	2.2
Navicula cryptocephala	0	0	0		0	0.8	4.2	4.4	0.2	0.4	0.4	0	0	0	0	0.2
Navicula cryptotenella	0.4	0	0		3	0	1.4	0.2	3.6	1.4	0.6	0.2	0.2	0	0	0
Navicula radiosa	0	0	0		1.2	1.4	1.6	3	2	1.4	1.4	0	0	0.2	0	0
Navicula veneta	0.4	0	0		0.2	0	0.6	0.2	0	1	0	0.6	0	0.2	0.2	0
Navicymbula pusilla	0	0	0		0	0	0	0	0	0	0	0	0	0	0	0
Neidium affine	0	0	0		0	0	0	0	0	0	0	0.2	0	0	0	0
Nitzschia amphibia	0.4	0.8	0		0	0	0	0	0	0	0	0	0	0	0	0
Nitzschia clausii	0	0	0		0	0.2	0	0	0	0	0	0	0	0	0	0
Nitzschia palea	0	0.4	0		0	0.2	0	0	0	0	0	0	0	0	0	0
Nitzschia recta	0	0.2	0.2		0	0.6	2.2	1.2	1.4	0.6	0.8	0	0	0	0	0.2
Opephora marina	0	0.2	0		1.4	1	2.8	2	3.2	3.6	1.2	1.4	1	1	0.8	0.4
Petroneis humerosa	0	0	0		0	0	0	0	0	0	0	0	0	0	0	0
Pinnularia borealis	0	0	0		0.2	0	0	0	0	0	0.2	0	0	0	0	0
Pinnularia divergens	0	0	0		0	0.4	0.8	0.8	1	0	0.2	0	0.2	0	0	0
Pinnularia intermedia	0	0	0		1.2	0	0.4	0	0	0	0	0	0	0	0	0
Pinnularia subcapitata	0	0	0		0	0	0	0	0	0	0	0	0	0	0	0
Pinnularia viridis	0	0	0.2		0	0.2	0	0	0	0	0	0	0	0	0	0
Placoneis clemetis	0	0	0		0	0	0	0	0.2	0	0	0	0	0	0	0
Placoneis placentula	0	0	0		0.6	0.2	0	0	0.2	0	0	0	0.2	0	0	0
Planothidium biporomum	0	0	0		0	0	0	0	0.2	0.6	13	19	23.2	16.8	33.8	23.8
Planothidium delicatulum	0.8	2	2		0.4	0	0	0	0	0.8	0	0.2	0	0	0	0
Planothidium rostratum	0	0	0		0	0	0	0	0.2	0.8	4.2	6.8	14	14.4	22.2	16.4
Pseudostaurosira brevistriata	1.2	0.2	3.2		2.6	1.2	2.6	0.6	1.8	3.8	2.4	3.2	2.6	3.8	6.4	3.4

Age (cal yrs BP)	**240**	**293**	**320**	**H**	**445**	**468**	**491**	**519**	**554**	**576**	**599**	**622**	**668**	**690**	**713**	**747**
Depth (cm)	**3**	**7**	**9**	**H**	**13**	**15**	**17**	**20**	**23**	**25**	**27.5**	**29.5**	**33**	**35**	**37**	**40**
Rhopalodia gibba	0	0	0		0	0	0	0	0	0.2	0	0	0	0	0	0.2
Rhopalodia gibberula	0.2	0	0		0	0	0	0	0	0	0	0	0	0	0	0
Sellaphora pupula	0	0	0		0.2	0	0.8	1.4	1	1.2	0.2	0	0.2	0	0	0
Sellaphora stroemii	0	0	0		0	0	0	0	0	0.2	0	0	0	0	0	0
Staurosira elliptica	1.4	1	15.8		3.4	3.8	4.6	6.8	2.4	4.8	3.2	1.8	2.4	3.2	1.2	1.6
Stephanodiscus agassizensis	1.2	0.6	1		0.2	0	0.2	0	0	0	0.4	0.2	0	0	0	0
Stephanodiscus hantzschii	1.2	8.2	0		0.2	0.8	0.2	1	0	0	0	0	0	0	0	0
Surirella sp	0	0	0		0	0	0.2	0	0	0	0	0	0	0	0	0
Thalassiosira eccentrica	0.8	0	0		0	0	0	0	0.2	0	0	0	0	0	0	0
Thalassiosira lentiginosa	0	0	0		0.2	0	0.6	0.2	0.6	0.2	0	0	0	0	0	0
Thalassirosira weissflogii	2	0.6	0.2		0	0.6	0.6	0	0	0.2	0.4	0	0	0	0	0
Tryblionella calida	0	0	0		0	0	0	0	0	0	0	0	0	0	0	0
Tryblionella hungarica	0	0	0		0	0	0	0	0	0	0	0	0	0	0	0

PV11.3 continued

Age (cal yrs BP)	770	804	827	850	873	909	919	930	945	960	971	981	997	1012	1027
Depth (cm)	**42**	**45**	**47**	**49.5**	**51**	**55**	**57**	**59.5**	**62**	**65**	**67**	**69.5**	**72**	**75**	**78**
Achnanthes brevipes	0	0	0	0	0	0	0	0	0	0	0	0	0	0	0
Achnanthes oblongella	0.4	0.4	0.8	1	1	1.2	6	6.4	4.4	5.8	1.6	4.8	5.4	2.6	4
Achnanthes subaffinis	31.4	30	21.6	35.2	35.8	43	34.6	38.4	43	38.4	36	36.4	27.6	37	39.6
Achnanthes swazi	2.2	5	3	4.4	1.6	8.6	2.4	1.2	0.8	1.2	2.2	1.8	1.8	2.2	2.6
Achnanthidium crassum	0	0	0.2	0	0	0.4	0	0	0	0	0	0	0	0	0
Achnanthidium eutrophilum	1	0.2	0	0.2	0.4	0.2	0	0	0	0	0	0	0	0	0
Achnanthidium exiguum	0	0	0	0.4	0	0	0	0	0.2	0	0	0.2	0	0.2	0.2
Achnanthidium microcephalum	4.8	2.8	2.4	2.4	9	3.2	1	0.2	1.2	1.2	1	1.2	3.6	1.8	1
Achnanthidium minutissimum	2.8	4.6	1.6	2	0	2.6	1.4	0.2	0.4	1	0.6	0	0.6	0.8	1
Achnanthidium straubianum	0.6	0	5	0.4	0	2	0	3.4	4.4	0.4	2.2	0	1.6	1.8	0
Amphipleura pellucida	0	0	0	0	0	0	0	0	0	0	0	0	0	0	0
Amphora coffeaeformis	0	0	0	0	0	0	0	0	0	0	0	0	0	0	0
Amphora copulata	0.4	0	0.2	0	0.2	0	0	0	0	0	0	0	0	0	0
Amphora proteus	0	0	0	0	0	0	0	0	0	0	0	0	0	0	0
Amphora veneta	0	0	0	0	0	0	0	0	0	0	0	0	0	0	0
Aulacoseira ambigua	0	0.4	0	0	7	1.6	0	0	0	0	0	0	0	0	0
Aulacoseira granulata	0	0	0	0	0	0	0	0	0	0	0	0	0	0	0
Brachysira vitrea	0.4	0	0	0	0	0	0	0	0	0	0.2	0	0	0.2	0
Caloneis sp	0	0	0	0	0	0	0	0	0	0	0	0	0	0	0
Cocconeis distans	2.6	1.2	1.8	2.8	2.4	0.8	13.4	15.8	8.8	8	6.4	6.4	6.2	6.2	6.6
Cocconeis placentula	0	0	0.4	0	0	0.2	0.6	1.2	0	0	0	0	0.8	0.4	0.2
Craspedostauros capensis	0	0	0	0	0.4	0	0	0	0	0	0	0	0	0	0
Cymbella turgidula	0.2	0.2	0	0	0.4	0	0	0	0.2	0	0	0	0	0	0
Diploneis oblongella	0	0	0	0	0.2	0	0	0	0	0	0	0	0	0	0
Diploneis smithii	0	0	0	0	0.4	0	0	0	0	0	0	0	0	0.2	0
Discotella stelligera	0.2	1	0.4	0.2	1.2	1	0.8	0	0.2	0	0	0.2	0.2	0.2	0.2
Encyonema gracile	0	0	0	0	0	0	0.2	0	0	0	0	0	0	0	0
Encyonema silesiacum	0	0	0	0	0	0	0.4	0	0	0	0	0	0	0	0
Encyonema subminuta	0	0	0.2	0	0	0.2	0	0.6	0	0	0	0	0	0	0.2
Encyonopsis cesatii	0	0	0	0	0	0	0	0	0	0	0	0	0	0	0
Encyonopsis sp	0	0	0	0	0	0	0	0	0	0	0	0	0	0	0
Eolimna minima	0	0	0	0	0	0	0	0	0	0	0.2	0	0	0	0
Eolimna subminuscula	0.2	0.2	0.2	0	0.2	1	2	3	0	0	0	3.4	6	2	1.8
Epithemia adnata	0.2	0	0	0	0	0	0	0	0.2	0	0	0	0	0	0
Epithemia sorex	0.2	0	0	0	0	0	0.2	0	0	0	0	0	0	0	0
Eunotia formica	0	0	0	0	0	0	0	0	0	0	0	0	0	0	0
Eunotia minor	0	0.2	0	0	0.2	0	0	0	0	0	0	0	0	0	0

Age (cal yrs BP)	**770**	**804**	**827**	**850**	**873**	**909**	**919**	**930**	**945**	**960**	**971**	**981**	**997**	**1012**	**1027**
Depth (cm)	**42**	**45**	**47**	**49.5**	**51**	**55**	**57**	**59.5**	**62**	**65**	**67**	**69.5**	**72**	**75**	**78**
Fallacia sp	0	0	0	0	0	0	0	0	0	0	0	0	0	0	0
Fragilaria biceps	0	0	0	0	0	0	0	0	0	0	0	0	0	0	0
Fragilaria capucina	0.2	0.2	0	0.4	0.6	0.4	0.8	1.2	0.8	0.4	1.2	0.4	0.4	1.2	0.8
Fragilaria exigua	0	0	0	0	0	0	0	0	0	0	0	0	0	0	0
Fragilaria tenera	0	0	0	0	0	0.2	0	0	0	0	0	0	0	0	0
Frustulia vulgaris	0	0	0	0	0.6	0	0	0	0	0	0	0	0	0	0
Gomphonema gracile	0.6	0.2	0	0.2	0.4	0	0	0	0	0	0	0	0	0	0
Gomphonema parvulum	0	0	0	0	0	0	0	0	0	0	0	0	0	0	0
Hippodonta hungarica	1.2	1	0	0	1.6	0.6	1.2	0	0	0	0.2	0.2	0	0.4	0.2
Kobayasiella sp	0	0	0	0	0	0	0	0	0	0	0	0	0	0	0
Mastogloia braunii	0.6	1	0.4	1.8	0.2	0.2	0.6	0	0.6	0.2	0	0.2	0	0.2	0
Melosira nummuloides	8.8	1.6	0	0.2	14.4	0.8	4.6	0	0.4	0	0.4	0	0	0	0.2
Navicula angusta	0	0	0	0	0	0	0	0	0	0	0	0	0	0	0
Navicula cincta	1	3.2	0.8	1.8	2	1.8	2	0.8	0	0.2	1.2	1	1.4	0.4	0.6
Navicula cryptocephala	0	0	0	0.2	0	0.2	2	0	0	0	0	0	0	0	0
Navicula cryptotenella	0.2	0.4	0	0	0.4	0	1	0	0	0	0	0.2	0	0.2	0.2
Navicula radiosa	0.2	0	0	0	0.2	0	1.2	0	0	0	0	0	0	0	0.2
Navicula veneta	1	0.2	0	0	0	0	0	0.2	0.2	0	0	0.2	0	0	0
Navicymbula pusilla	0.8	0	0	0	0	0	0	0	0.2	0	0	0.4	0.2	0	0
Neidium affine	0	0	0	0	0	0	0	0	0	0	0	0	0	0	0
Nitzschia amphibia	0	0	0	0	0	0	0	0	0	0	0	0	0	0	0
Nitzschia clausii	0	0	0	0	0	0	0	0	0	0	0	0	0	0	0
Nitzschia palea	0	0	0	0	0.2	0.2	0	0	0	0	0	0	0.2	0	0
Nitzschia recta	0.4	0	0	0.2	0.6	0.4	0.6	0	0	0	0	0	0	0	0
Opephora marina	0.8	1	0.4	0.6	4	1	1.4	1.4	0.6	0.4	0.6	1.2	1	1.2	0
Petroneis humerosa	0	0	0	0	0	0	0	0	0	0	0	0	0	0	0
Pinnularia borealis	0	0	0	0	0	0	0	0	0	0	0	0	0	0	0
Pinnularia divergens	0	0	0	0	0.4	0	0	0	0	0	0	0	0	0	0
Pinnularia intermedia	0	0	0	0	0	0	0	0	0	0	0	0	0	0	0
Pinnularia subcapitata	0	0	0	0	0	0	0	0	0	0	0	0	0	0	0
Pinnularia viridis	0	0	0	0	0.2	0	0	0	0	0	0	0	0	0	0
Placoneis clemetis	0	0	0	0	0	0	0	0	0	0	0	0	0	0	0
Placoneis placentula	0	0	0	0	0.8	0	0.2	0.4	0.2	0	0	0	0	0	0.2
Planothidium biporomum	13.4	27.8	31	23.6	5.2	8.8	10.8	14.8	23.4	30.4	26.6	33	31.6	23.2	30
Planothidium delicatulum	0.4	0	0	0	0	0	0	0	0	0	0	0	0	0	0
Planothidium rostratum	17.6	12	27.6	18	2.4	13.4	3.6	6.6	5.6	8.2	17.4	5.4	9	14	7.4
Pseudostaurosira brevistriata	1.2	2.4	1.6	2.2	2.8	3.2	2.4	2.2	1.6	2.4	0.6	2	1	0.4	1.4
Rhopalodia gibba	0	0	0	0	0	0	0	0	0	0	0	0	0	0	0

Age (cal yrs BP)	**770**	**804**	**827**	**850**	**873**	**909**	**919**	**930**	**945**	**960**	**971**	**981**	**997**	**1012**	**1027**
Depth (cm)	**42**	**45**	**47**	**49.5**	**51**	**55**	**57**	**59.5**	**62**	**65**	**67**	**69.5**	**72**	**75**	**78**
Rhopalodia gibberula	0	0	0	0	0	0	0	0	0	0	0	0	0	0	0
Sellaphora pupula	0.2	0	0	0	0.8	0	0.4	0	0	0	0	0	0	0	0
Sellaphora stroemii	0	0	0	0	0	0	0	0	0	0	0	0	0	0	0
Staurosira elliptica	1.6	1.8	0.4	1	0.8	2	1.6	1.6	2.4	1.4	1	1.4	1.2	2	1.2
Stephanodiscus agassizensis	0	0	0	0	0	0	0	0.4	0	0	0	0	0	0	0
Stephanodiscus hantzschii	0	0	0	0	0	0	0	0	0	0	0	0	0	0	0
Surirella sp	0	0	0	0	0	0	0	0	0	0	0	0	0	0	0
Thalassiosira eccentrica	0	0	0	0	0	0	0	0	0	0	0	0	0	0	0
Thalassiosira lentiginosa	0.2	0	0	0	0	0	0	0	0	0	0	0	0	0	0
Thalassirosira weissflogii	0	0	0	0	0	0	0.4	0	0	0	0.2	0	0	0	0
Tryblionella calida	0	0	0	0	0	0	0	0	0	0	0	0	0	0	0
Tryblionella hungarica	0	0	0	0	0	0	0	0	0	0	0	0	0	0	0

PV11.3 continued

Age (cal yrs BP)	**1033**	**1048**	**1058**	**1074**	**1084**	**1094**	**1115**	**1125**	**1141**	**1151**	**1166**	**1177**	**1192**	**1202**	**1213**
Depth (cm)	**79.5**	**82**	**84**	**87**	**89**	**91**	**95**	**97**	**100**	**102**	**105**	**107**	**110**	**112**	**114**
Achnanthes brevipes	0	0	0	0	0	0	0	0	0	0	0	0	0	0	0
Achnanthes oblongella	3	2.4	4.4	0.6	3.2	0.8	1.4	4	1.4	3.8	3.2	2.8	4.4	1	2
Achnanthes subaffinis	36.4	45.4	31	30.2	33.2	33.2	27	31.8	37.6	34.2	25.8	29.4	22.4	23.4	21
Achnanthes swazi	2	0.6	2.6	2.2	2.8	0	2	2.6	2.2	2.2	2.4	3	1.2	0	1.6
Achnanthidium crassum	0.6	0	0	0	0.2	0	0.2	0	0	0	0	0	0.4	0	0
Achnanthidium eutrophilum	0	0	0	0	0	0.4	0.2	0	0	0	0	0	0	0	0
Achnanthidium exiguum	0	0	0	0	0.4	0	0	0.2	0	0.2	0	0.4	0	0	0
Achnanthidium microcephalum	0.8	1.8	1.2	1.4	0.6	2.4	1.2	1	1.6	2.2	0.8	0.6	0.8	1	1.8
Achnanthidium minutissimum	1.6	0.2	2	1.8	0.6	1.2	1.2	1.4	1	0.2	1.6	2	1.6	4.2	1.8
Achnanthidium straubianum	1.6	0.8	0	0.6	0.6	1	1.2	0	1	1.4	0.4	1	0.2	0.6	1.8
Amphipleura pellucida	0	0	0	0	0	0	0	0	0	0	0	0	0	0	0
Amphora coffeaeformis	0	0	0	0	0	0	0	0	0	0	0	0	0	0	0
Amphora copulata	0	0	0	0	0	0	0	0.2	0	0	0	0	0	0.2	0
Amphora proteus	0	0	0	0	0	0	0	0	0	0	0	0	0.2	0	0
Amphora veneta	0	0	0	0	0	0	0	0	0	0	0	0	0	0	0
Aulacoseira ambigua	0	0	0	0	0	0	0	0	0	0	0	0	0	0	0.4
Aulacoseira granulata	0	0	0	0	0	0	0	0	0	0	0	0	0	0	0
Brachysira vitrea	0	0	0	0	0	0	0.2	0	0	0	0	0	0	0	0.2
Caloneis sp	0	0	0	0	0	0	0	0	0	0	0	0	0	0	0
Cocconeis distans	5.8	3.4	7.2	6.2	6.4	7	4	4	3	7.4	6	6.2	6.4	4.2	4.6
Cocconeis placentula	0	0	0	0	0	0	0	0	0.8	0	0.2	1	0.2	0.2	0
Craspedostauros capensis	0	0	0	0	0	0	0	0	0	0	0	0	0	0	0
Cymbella turgidula	0	0.2	0	0.4	0	0	0	0	0	0	0	0	0	0	0.2
Diploneis oblongella	0	0	0	0	0	0	0	0	0	0	0	0.2	0	0	0
Diploneis smithii	0	0	0	0	0	0	0	0.2	0	0	0	0	0.2	0	0
Discotella stelligera	0.2	0	0.2	0	0.2	0	0	0	0	0.2	0.2	0	0	0	0
Encyonema gracile	0	0	0	0	0	0	0	0	0	0.2	0	0	0	0	0.2
Encyonema silesiacum	0	0.2	0	0	0	0	0	0	0	0	0	0	0	0	0.2
Encyonema subminuta	0.2	0	0	0	0	0	0.4	0	0	0	0.2	0	0.4	0	0
Encyonopsis cesatii	0	0	0	0	0	0	0	0	0	0	0	0	0	0	0
Encyonopsis sp	0	0	0	0	0	0	0	0	0	0	0	0	0	0	0
Eolimna minima	0	0	0	2.2	0	0	0	0	0	0	0	0	0	0	0.2
Eolimna subminuscula	2	1.2	0.6	0	1	0.2	2.8	0	0	0	1.6	2.2	0.6	1	0.8
Epithemia adnata	0	0	0	0	0	0	0	0	0	0	0	0	0	0.2	0
Epithemia sorex	0	0	0	0	0	0	0	0	0	0	0	0	0	0	0
Eunotia formica	0	0	0	0	0	0	0	0	0	0	0	0	0	0	0.2

Age (cal yrs BP)	1033	1048	1058	1074	1084	1094	1115	1125	1141	1151	1166	1177	1192	1202	1213
Depth (cm)	**79.5**	**82**	**84**	**87**	**89**	**91**	**95**	**97**	**100**	**102**	**105**	**107**	**110**	**112**	**114**
Eunotia minor	0	0	0.2	0	0	0	0	0	0	0	0	0	0	0	0
Fallacia sp	0	0	0	0	0.2	0	0	0	0	0	0	0	0	0	0
Fragilaria biceps	0	0	0	0	0	0	0	0	0	0	0	0	0	0	0
Fragilaria capucina	1.4	0.4	1.6	1.4	0.4	1.2	1.4	1.4	0.6	0.6	0.6	0.8	1.4	0.2	0.6
Fragilaria exigua	0	0	0	0	0.2	0	0	0	0	0	0	0	0	0	0
Fragilaria tenera	0	0	0	0	0.2	0	0	0	0	0	0	0	0	0	0
Frustulia vulgaris	0	0	0	0	0	0	0	0	0	0	0	0	0	0	0
Gomphonema gracile	0	0	0	0	0	0	0.2	0	0	0	0	0	0	0	0
Gomphonema parvulum	0	0	0	0	0	0	0	0	0	0	0	0	0	0	0
Hippodonta hungarica	0	0.4	0.4	0	0.4	0.4	0.2	0	0	0.2	0	0.2	0.2	0.4	0.2
Kobayasiella sp	0	0	0	0	0	0	0	0	0	0	0	0	0	0	0
Mastogloia braunii	0.2	0	0.2	0	0.4	0.2	0.2	0.2	0	0	0.8	0.6	0	2	1.8
Melosira nummuloides	0.4	0.2	0	0.8	0	0.2	1	0	0	0	0.4	0	0.2	1	0.8
Navicula angusta	0	0	0	0	0	0	0	0	0	0	0	0	0	0	0
Navicula cincta	0.6	0.2	0.6	1.2	1.4	1.2	1.2	0.8	0.8	1.2	1.2	1.8	2.4	0.2	0.4
Navicula cryptocephala	0	0	0.2	0	0	0	0	0	0.2	0	0	0	0.2	0	0
Navicula cryptotenella	0	0	0	0	0	0	0	0.4	0.2	0.2	0	0	0	0	0
Navicula radiosa	0	0	0	0	0	0	0	0	0	0.2	0	0	0	0	0
Navicula veneta	0.2	0	0	0	0.2	0	0	0	0	0	0	0.2	0.2	0	0.4
Navicymbula pusilla	0	0	0	0	0	0	0	0	0	0	0	0	0	0	0
Neidium affine	0	0	0	0	0	0	0	0	0	0	0	0	0	0	0
Nitzschia amphibia	0	0	0	0	0	0	0	0	0	0	0	0	0	0	0
Nitzschia clausii	0	0	0	0	0	0	0	0	0	0	0	0	0	0	0
Nitzschia palea	0	0	0	0.2	0	0	0	0.2	0	0	0	0	0	0.2	0
Nitzschia recta	0	0	0	0	0	0	0.2	0	0.2	0	0	0	0.4	0	0.6
Opephora marina	0.2	1	0.6	0.6	0.4	0.8	0.8	0.4	0.2	1.6	0.6	0.4	0.6	0.6	2
Petroneis humerosa	0	0	0	0	0	0	0	0	0	0	0	0	0	0	0
Pinnularia borealis	0	0	0	0	0	0	0	0	0	0	0	0	0	0	0
Pinnularia divergens	0	0	0	0	0	0	0	0	0	0	0	0	0	0	0
Pinnularia intermedia	0	0	0	0	0	0	0	0	0	0	0	0	0	0	0
Pinnularia subcapitata	0	0	0	0	0	0	0	0	0	0	0	0	0	0	0
Pinnularia viridis	0	0	0	0	0	0	0	0	0	0	0	0	0	0	0
Placoneis clemetis	0	0	0	0	0	0	0	0	0	0	0	0	0	0	0
Placoneis placentula	0	0.2	0	0	0	0	0.2	0.6	0	0	0	0	0.2	0	0
Planothidium biporomum	25.2	30.6	28.8	35	33.6	27.8	35.6	35.6	33.4	32.8	33.6	32	34.2	38.2	36.8
Planothidium delicatulum	0	0	0	0	0	0.2	0	0	0	0	0	0	0	0	0
Planothidium rostratum	12.2	8	14	11	9.4	17.6	11.8	10.8	13.2	6.8	12.8	8.8	11	18.4	13.4
Pseudostaurosira brevistriata	1.2	1	2.8	2.8	2.4	1.4	2.4	0.8	1.2	1.4	3.2	1.2	1.6	2.2	4

Age (cal yrs BP)	**1033**	**1048**	**1058**	**1074**	**1084**	**1094**	**1115**	**1125**	**1141**	**1151**	**1166**	**1177**	**1192**	**1202**	**1213**
Depth (cm)	**79.5**	**82**	**84**	**87**	**89**	**91**	**95**	**97**	**100**	**102**	**105**	**107**	**110**	**112**	**114**
Rhopalodia gibba	0	0	0	0	0	0	0	0	0	0	0	0	0	0	0
Rhopalodia gibberula	0	0	0	0	0	0	0	0	0	0	0	0	0	0	0
Sellaphora pupula	0	0	0.2	0	0	0	0	0.4	0	0.2	0.2	0.2	0.2	0.2	0
Sellaphora stroemii	0	0	0	0	0	0	0	0	0	0	0	0	0	0	0
Staurosira elliptica	3.2	1.4	1.2	1.4	1.4	1.8	2.4	1.8	1.2	2.4	2.8	4	1.8	0.4	1.6
Stephanodiscus agassizensis	0	0	0	0	0	0	0	0	0	0	0.2	0.4	0	0	0
Stephanodiscus hantzschii	0	0	0	0	0	0	0	0	0	0	0	0	0	0	0
Surirella sp	0	0	0	0	0	0	0	0	0	0	0	0	0	0	0.2
Thalassiosira eccentrica	0	0	0	0	0	0	0	0	0	0	0	0	0	0	0
Thalassiosira lentiginosa	0	0	0	0	0	0	0	0	0	0	0	0	0	0	0
Thalassirosira weissflogii	0	0	0	0	0	0	0	0	0	0	0	0	0	0	0
Tryblionella calida	0	0	0	0	0	0	0	0	0	0	0	0	6.4	0	0
Tryblionella hungarica	0	0	0	0	0	0	0	0	0	0	0	0	0	0	0

PV11.3 continued

Age (cal yrs BP)	**1228**	**1239**	**1249**	**1259**	**1269**	**1280**	**1290**	**1311**	**1321**	**1331**	**1336**	**1352**	**1393**
Depth (cm)	**117**	**119**	**121**	**123**	**125**	**127.5**	**129.5**	**133**	**135**	**137**	**138**	**141**	**145**
Achnanthes brevipes	0	0	0	0	0	0	0	0	0	0	0	0	0
Achnanthes oblongella	1.4	3.8	6.2	2.4	0.8	3	1	2	6.2	2.6	2.2	1.6	2
Achnanthes subaffinis	23.4	13.6	12.6	17.6	14.2	20.2	16.6	30	24.4	27	20.2	13.2	20
Achnanthes swazi	1	1	0.8	0.4	0.6	0.4	0.8	0.8	1.2	1	1	0.2	2
Achnanthidium crassum	0	0.2	0.4	0	0.4	0.2	0	0	0	0	0.6	0	0
Achnanthidium eutrophilum	0	0.2	0	0	0.6	0	0.4	0.6	1.2	0	0.2	0.2	0
Achnanthidium exiguum	0	0.4	0.2	0	0.4	0	0	0	0.2	0.2	0	0	0.2
Achnanthidium microcephalum	1	1	0.4	2.2	0.6	0.4	0.8	3.4	1.2	0.4	0.8	1.6	0.6
Achnanthidium minutissimum	1.2	2	1.4	0.8	2	2.6	4.4	2.8	3.8	1.4	5	1.4	2.8
Achnanthidium straubianum	0.8	0	0.6	0.4	1.2	0.4	0	1.2	1.4	0.2	2.6	0.4	0.6
Amphipleura pellucida	0	0	0	0	0	0	0.4	0	0	0	0	0.6	0
Amphora coffeaeformis	0	0	0	0	0	0	0	0	0	0.4	0	0	0
Amphora copulata	0	0	0	0	0.2	0	0	0	0.4	0	0.2	0.4	0.4
Amphora proteus	0	0	0	0	0	0	0	0	0	0	0	0	0
Amphora veneta	0	0	0	0	0	0	0	0	0	0	0	0	0.2
Aulacoseira ambigua	0	0	0	0	0.4	0	1.6	0	1	2.8	3.2	4	4.4
Aulacoseira granulata	0	0	0	0	0	0	0	0	0	0	0	0	0.6
Brachysira vitrea	0	0.2	0.2	0	0.4	0	0.4	0	0	0.2	0	0	0
Caloneis sp	0	0	0	0	0	0	0	0	0	0	0	0	0
Cocconeis distans	4.6	3.6	4.8	5.4	4.2	3.2	5	8.6	10.6	10	6.6	7.4	6.6
Cocconeis placentula	0	0	0	0	0.4	0.4	0	0.2	0	0.2	0.6	0	0.4
Craspedostauros capensis	0	0	0	0	0	0.4	0.2	0.4	0	0	0	0	0.4
Cymbella turgidula	0	0	0.2	0.2	0	0	0	0	0	0.8	0.4	0.4	1
Diploneis oblongella	0	0	0	0	0	0	0	0.2	0	0	0.4	0	0.2
Diploneis smithii	0.2	0.2	0	0.4	0.4	0	0.2	1.2	0.4	1.4	1	1.4	2
Discotella stelligera	0	0.4	0	0	0.4	0	0.8	1.2	0	0.8	1.2	0.6	3.6
Encyonema gracile	0	0	0.2	0	0	0.6	0.2	0.4	0.2	0.2	0.4	0.2	0.2
Encyonema silesiacum	0	0.4	0	0	0.4	0	0.4	0.4	0.2	0	0.4	0.4	0.2
Encyonema subminuta	0	0.2	0	1.2	0.4	0.6	1	0.4	0	0.2	0.4	0.8	0
Encyonopsis cesatii	0	0	0	0	0	0	0	0	0	0.2	0	0	0
Encyonopsis sp	0	0	0	0	0	0	0	0	0	0	0	0	0
Eolimna minima	0	0	0	0	0	0	2	0	0	0	0	0	0
Eolimna subminuscula	1.6	1	2.4	1.4	2.2	1.8	0	1.8	1.8	0	2.6	0	1.2
Epithemia adnata	0	0	0	0	0	0	0	0	0	0	0	0	0
Epithemia sorex	0	0	0	0	0	0	0	0	0	0	0	0	0
Eunotia formica	0	0	0	0	0	0.2	0	0	0.2	0	0	0	0
Eunotia minor	0	0	0	0	0	0	0	0.2	0	0.2	0	0	0.4

Age (cal yrs BP)	1228	1239	1249	1259	1269	1280	1290	1311	1321	1331	1336	1352	1393
Depth (cm)	**117**	**119**	**121**	**123**	**125**	**127.5**	**129.5**	**133**	**135**	**137**	**138**	**141**	**145**
Fallacia sp	0	0	0	0	0	0	0	0	0	0	0	0	0
Fragilaria biceps	0	0	0	0	0	0	0	0	0	0	0	0.2	0
Fragilaria capucina	0.4	1	0.4	0	0.4	1.6	1.6	1.4	1	0.8	1.6	0.2	0.8
Fragilaria exigua	0	0	0	0	0.2	0	0	0	0	0	0	0.2	0.2
Fragilaria tenera	0	0.2	0	0	0.4	0.2	0.4	0	0	0	0.2	0	0.2
Frustulia vulgaris	0	0	0	0	0	0	0	0	0	0.2	0	0.2	0
Gomphonema gracile	0.2	0	0.2	0.2	0.2	0.4	0.2	0.2	0.2	0.2	0	0	0
Gomphonema parvulum	0	0	0	0	0	0	0.2	0	0	0	0	0	0
Hippodonta hungarica	0.8	0.2	0.4	1.2	1	1.2	2.2	2.6	2.2	1	2.8	3.6	1
Kobayasiella sp	0	0	0	0	0	0	0	0	0	0	0	0	0.2
Mastogloia braunii	2.8	2	1.2	4.6	4.2	1.2	4.2	1.6	2	1.8	1.6	3.4	0.8
Melosira nummuloides	1	1.6	0.8	1.8	3.4	1.4	3.2	5	8	17	9.8	27.2	9.2
Navicula angusta	0	0	0	0	0	0	0	0	0.2	0	0	0.6	0
Navicula cincta	1.8	0.6	1.4	1.2	3.6	3.6	5.4	4.4	2.2	2.8	4.8	2.4	8.2
Navicula cryptocephala	0	0.6	0	0	0.8	0.2	2.4	0	0	0.2	0.4	0.6	0.8
Navicula cryptotenella	0.2	0	0.2	1	1	0.2	0.8	2	1.2	1.2	0	1.4	1.8
Navicula radiosa	0	0.6	0	0.4	0.8	0.8	0.4	0.8	1.2	0.4	1.2	5.8	1.4
Navicula veneta	0	0.4	0.4	0	0.4	0	0.2	0	0	0	0	0	0
Navicymbula pusilla	0	0	0	0	0	0.2	0	0.4	0.2	0	0	0	0
Neidium affine	0	0	0	0	0	0	0	0	0	0	0.2	0	0
Nitzschia amphibia	0	0	0	0	0	0	0	0	0	0	0	0	0
Nitzschia clausii	0	0	0	0	0	0	0	0	0	0	0	0	0
Nitzschia palea	0	0	0	0.2	0	0	0.6	0	0	0	0.2	0	0.4
Nitzschia recta	0.6	0.2	0.2	0.2	0.6	0.4	1.4	1.8	0.8	0.6	2	1.4	0.6
Opephora marina	1	2.6	2.6	1.6	1.4	2	1.8	1.6	0.8	3	1.6	4	4.2
Petroneis humerosa	0	0	0	0	0	0	0	0	0	0	0	0	0
Pinnularia borealis	0	0	0	0	0	0	0	0	0	0	0	0	0
Pinnularia divergens	0	0	0	0	0	0	0	0	0	0.6	0.4	0.4	0.2
Pinnularia intermedia	0	0	0	0	0	0	0.2	0	0	0	0	0.2	0
Pinnularia subcapitata	0	0	0	0	0	0	0	0	0	0	0.2	0	0
Pinnularia viridis	0	0	0	0	0.2	0	0	0	0	0.2	0	0.2	0
Placoneis clemetis	0	0	0	0	0	0	0	0	0	0	0	0	0
Placoneis placentula	0.4	0.2	0	0	0	0.4	0.4	0.4	0.2	0	0.4	0	0
Planothidium biporomum	34.2	36.2	41.8	40.4	34	39.8	27.4	13.2	11.2	4.8	4.4	2.6	5.8
Planothidium delicatulum	0	0	0	0	0	0	0	0	0	0	0	0	0
Planothidium rostratum	15.6	16.2	12.6	9.2	10.6	6.8	5.2	1.6	6.6	5.2	6	0.6	1.8
Pseudostaurosira brevistriata	2.2	4	3.4	3.2	2.4	1.6	3.4	3.2	3.8	2.4	3.2	4.4	3.4
Rhopalodia gibba	0	0.2	0	0	0.2	0	0	0	0	0.2	0	0	0

Age (cal yrs BP)	**1228**	**1239**	**1249**	**1259**	**1269**	**1280**	**1290**	**1311**	**1321**	**1331**	**1336**	**1352**	**1393**
Depth (cm)	**117**	**119**	**121**	**123**	**125**	**127.5**	**129.5**	**133**	**135**	**137**	**138**	**141**	**145**
Rhopalodia gibberula	0	0	0	0	0	0	0	0	0	0	0	0	0
Sellaphora pupula	0	0.8	0.2	0	0.2	0.6	0.2	0.2	0	0.2	0.4	0.4	0.2
Sellaphora stroemii	0	0	0	0	0	0	0	0	0	0	0	0	0
Staurosira elliptica	2.6	3.2	3.4	1.6	3	1.8	1.8	2.4	2.4	1.8	4.2	2	3
Stephanodiscus agassizensis	0	0	0	0	0.2	0.2	0	0	0	0	0	0	0.2
Stephanodiscus hantzschii	0	0	0	0	0	0.2	0	0	0	0	0	0	0
Surirella sp	0	0	0	0	0	0	0	0	0	0	0	0	0
Thalassiosira eccentrica	0	0	0	0	0	0	0	0	0	0	0	0	0
Thalassiosira lentiginosa	0	0	0	0.2	0	0	0	0.2	0.6	2	0.2	0.6	0.2
Thalassirosira weissflogii	0	0	0.4	0	0	0	0.2	0	0	0.6	0.4	0	2.2
Tryblionella calida	0	0	0	0	0	0	0	0	0	0	0	0	0
Tryblionella hungarica	0	0	0	0	0	0	0	0	0	0	0	0	0

PV11.3 continued

Age (cal yrs BP)	**1530**	**1666**	**1712**	**1849**	**1986**	**2123**	**2260**	**2488**	**2579**
Depth (cm)	**148**	**151**	**152**	**155**	**158**	**161**	**164**	**169**	**171**
Achnanthes brevipes	0	0	0	0	0	0.2	0	0	0
Achnanthes oblongella	0.4	0.6	0.4	0.8	0.4	0.8	0.8	0.8	0.2
Achnanthes subaffinis	3.4	14.6	9	10.8	11.8	17.4	11.2	2.4	1.4
Achnanthes swazi	1	1.6	0.8	0.8	1.8	7.6	4.2	0.6	0.2
Achnanthidium crassum	0	0.2	0	0.2	0.2	0.4	0	0	0
Achnanthidium eutrophilum	0	0	0.2	0	0.2	0	0	0	0
Achnanthidium exiguum	0	0	0	0.2	0	0	0.2	0	0
Achnanthidium microcephalum	0.6	1.2	1.4	0.4	0.6	2	0.2	1	0.6
Achnanthidium minutissimum	0.8	1	0.4	0.8	0.4	3.2	2.2	0.6	0
Achnanthidium straubianum	1.2	0.2	0.8	0	1.2	0.8	0.6	2.4	0
Amphipleura pellucida	0.2	0.2	0	0	0.2	0.4	0	0	0
Amphora coffeaeformis	0	0	0	0	0.2	0	0.2	0	0
Amphora copulata	0	0	0.2	0	0	0	0	0	0.2
Amphora proteus	0	0	0	0	0	0	0	0	0
Amphora veneta	0	0	0	0	0	0	0	0	0
Aulacoseira ambigua	44.2	20.2	16.2	12	9	3	3	23	14.4
Aulacoseira granulata	0.4	0.8	0	0.4	0.2	0.2	0.2	2.6	0
Brachysira vitrea	0	0.2	0	0.2	0.2	0.6	0.4	0.2	0.4
Caloneis sp	0	0	0	0	0	0	0	0	0
Cocconeis distans	0.6	2.8	1.8	3	1.6	1	1.8	2	0.6
Cocconeis placentula	0	0	0	0.2	0	0	0	0	0
Craspedostauros capensis	0	0.2	0	0	0.2	0.8	0.6	0.4	1
Cymbella turgidula	0.6	0.2	0	0	0.2	0.2	0	0.6	1
Diploneis oblongella	0	0	0.2	0	0.4	0	0	0	0
Diploneis smithii	0.6	1.4	2	2.6	0.8	0.8	2	3.4	2.4
Discotella stelligera	1.2	1.2	1.8	3.2	2	1	1.2	1	0
Encyonema gracile	0.2	0.6	0	0.2	0.2	1.2	0.4	0.4	0.4
Encyonema silesiacum	0	0.2	0.4	0.2	0.4	0	0.4	0	0
Encyonema subminuta	0.8	0.2	0.4	0	0.4	0.4	0.4	0.4	0.4
Encyonopsis cesatii	0	0	0	0	0	0	0	0	0.2
Encyonopsis sp	0	0	0	0	0	0	0	0	0
Eolimna minima	0	0	0	0	0	0	0	0	0
Eolimna subminuscula	0.2	0	0.2	0.2	0.4	0.4	0	0	0
Epithemia adnata	0	0	0.4	0	0.4	0	0.2	0.2	0.6
Epithemia sorex	0	0	0	0	0	0	0.4	0.2	0
Eunotia formica	0	0	0.2	0	0	0.6	0	0.2	0
Eunotia minor	0.2	0.6	0	0.2	0	0	0	0.2	0

Age (cal yrs BP)	**1530**	**1666**	**1712**	**1849**	**1986**	**2123**	**2260**	**2488**	**2579**
Depth (cm)	**148**	**151**	**152**	**155**	**158**	**161**	**164**	**169**	**171**
Fallacia sp	0	0	0	0	0	0	0	0	0
Fragilaria biceps	0	0	0	0	0	0.4	0	0	0
Fragilaria capucina	0.4	0.8	0.2	0.6	0.6	0.4	0	0	0
Fragilaria exigua	0	0.2	0.2	0	0	0.2	0	0.2	0.6
Fragilaria tenera	0	0	0	0	0	0.2	0	0	0
Frustulia vulgaris	0.2	0	0	0	0	0	0	0.4	0
Gomphonema gracile	0.2	0.2	0	0.2	0.4	0.6	0.2	0	0
Gomphonema parvulum	0	0	0	0	0	0	0	0	0
Hippodonta hungarica	1.2	1	0.6	0.8	0.8	1.2	0.8	1	1.8
Kobayasiella sp	0	0	0	0	0.6	0	0	0	0
Mastogloia braunii	0.4	1	1.2	1.2	0.8	1.2	0.8	0.8	1.2
Melosira nummuloides	28	13.4	41	34.6	32.4	24.4	38	18.6	46
Navicula angusta	0	0	0	0	0	0.6	1	0.8	0
Navicula cincta	1.4	5.2	1.4	2	3.6	3.8	1.6	0.8	0
Navicula cryptocephala	0	0	0	0	1.2	0.6	1.6	0.2	0
Navicula cryptotenella	0	0.8	0.8	2.4	0.8	2.4	1.2	0.2	2
Navicula radiosa	1	1.2	1	1.4	1.4	2.4	2	3.4	2.8
Navicula veneta	0	0.2	0	0	0.2	0	0	0	0
Navicymbula pusilla	0	0.4	0	0	0	0	0	0	0
Neidium affine	0	0	0	0	0	0	0	0	0
Nitzschia amphibia	0	0	0	0	0	0	0	0	0
Nitzschia clausii	0	0.2	0	0	0	0	0	0	0
Nitzschia palea	0	0	0	0	0	0.6	0	0	0
Nitzschia recta	0.6	1.2	0.4	0.6	1	0.6	0.2	0	0
Opephora marina	0	1.2	0.4	1.8	1.2	1.2	0.6	1.4	1.8
Petroneis humerosa	0	0	0	0.2	0	0	0	0	0
Pinnularia borealis	0	0	0	0	0	0	0	0	0
Pinnularia divergens	0.2	0	0	0	0.2	0	0	0.4	0.8
Pinnularia intermedia	0.2	0	0	0	0	0	0.8	0.4	0
Pinnularia subcapitata	0	0	0	0	0	0	0	0	0
Pinnularia viridis	0	0	0	0.2	0.2	0.2	0	0.6	0
Placoneis clemetis	0	0	0	0	0	0	0	0	0
Placoneis placentula	0	0	0	0	0	0	0	0	0
Planothidium biporomum	1	10.4	7	5.8	8.8	3.4	0.6	0.2	0
Planothidium delicatulum	0	0	0	0.2	0	0	0.2	0	0
Planothidium rostratum	1.2	2.4	0.6	0.4	1.2	0.2	0	0	0
Pseudostaurosira brevistriata	1.8	4.2	1.8	2.8	2.4	0.8	5.6	3.6	5
Rhopalodia gibba	0	0.2	0	0	0.6	0.4	0.4	0	0

Age (cal yrs BP)	**1530**	**1666**	**1712**	**1849**	**1986**	**2123**	**2260**	**2488**	**2579**
Depth (cm)	**148**	**151**	**152**	**155**	**158**	**161**	**164**	**169**	**171**
Rhopalodia gibberula	0	0	0	0	0	0	0	0	0
Sellaphora pupula	0	0	0	0.2	0.2	0.2	0.2	0	0.2
Sellaphora stroemii	0	0	0	0	0	0	0	0.2	0
Staurosira elliptica	1	2.6	2.2	3.8	3.4	5.6	4.2	2.8	2.8
Stephanodiscus agassizensis	0.2	0.4	0	0.8	0	0.2	0.2	0	0
Stephanodiscus hantzschii	0.6	0.6	0	0	0.2	0.4	0.4	8.2	0
Surirella sp	0	0	0	0	0	0	0	0	0
Thalassiosira eccentrica	0	0	0	0	0	0	0	0	0
Thalassiosira lentiginosa	1.4	0	1.4	0.4	0.4	0.2	2.4	3.4	2.8
Thalassirosira weissflogii	0.2	0	0.2	0	0.4	0.4	0	0	0
Tryblionella calida	0	0	0	0	0	0	0.2	0.6	0
Tryblionella hungarica	0	0	0	0	0	0.2	0	0	0

APPENDIX THREE

Figure 11.3 Palaeo-environmental summary of key sites across southern Africa sorted by rainfall regime, as mentioned in the text

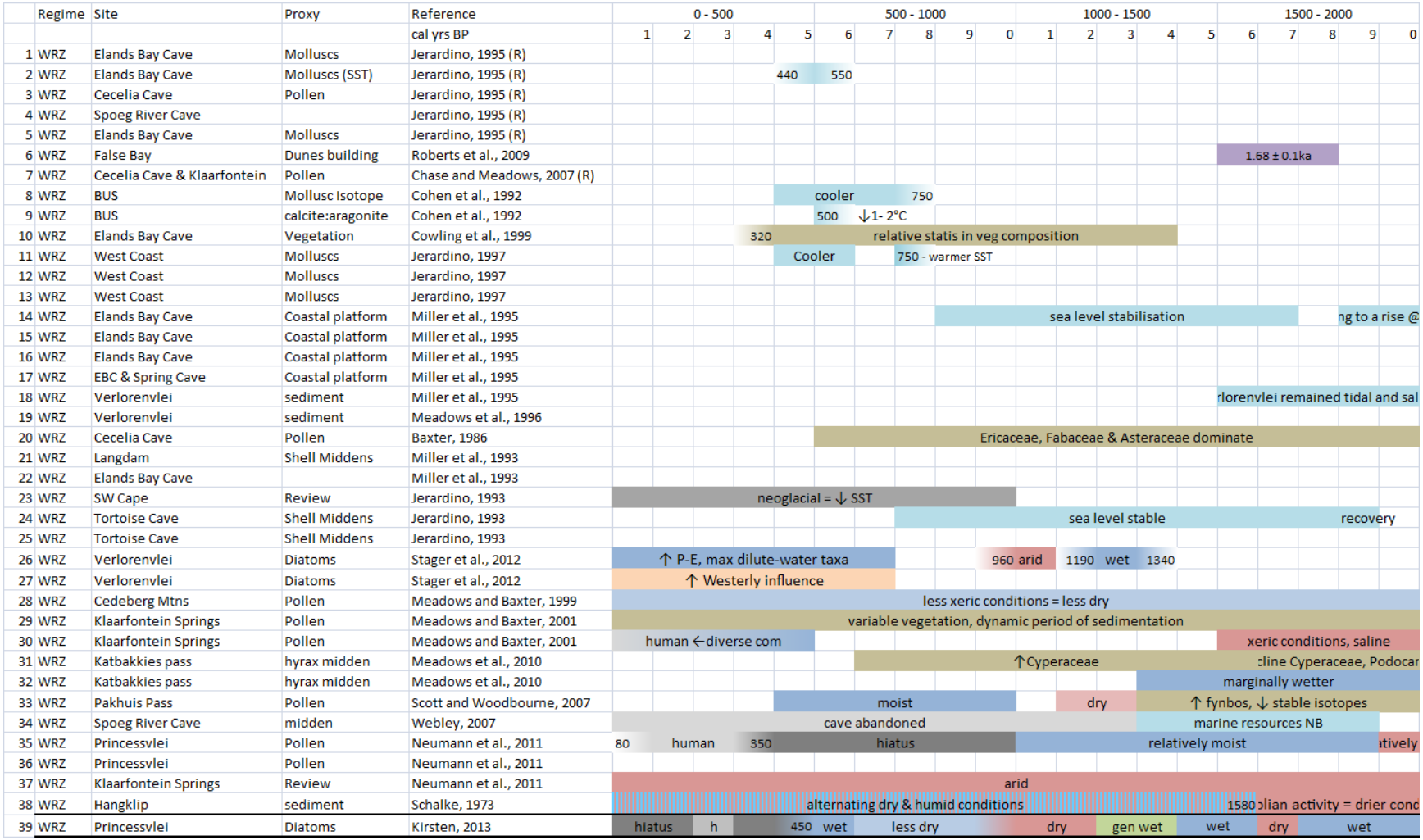

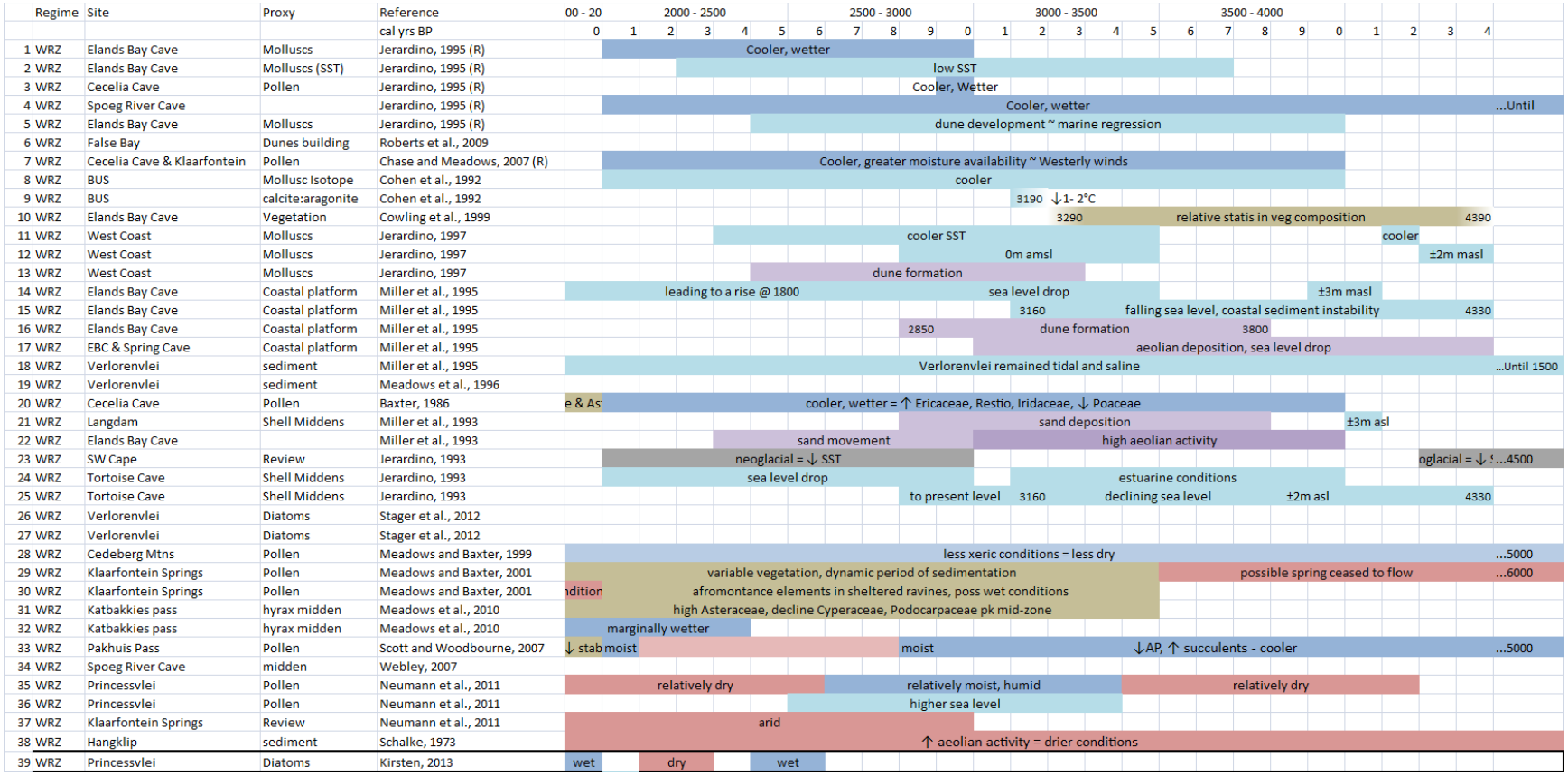
Regime
Site
Proxy
Reference
cal yrs BP
00 - 20
2000 - 2500
2500 - 3000
3000 - 3500
3500 - 4000
0 1 2 3 4 5 6 7 8 9 0 1 2 3 4 5 6 7 8 9 0 1 2 3 4
1 WRZ Elands Bay Cave Molluscs Jerardino, 1995 (R) Cooler, wetter
2 WRZ Elands Bay Cave Molluscs (SST) Jerardino, 1995 (R) low SST
3 WRZ Cecelia Cave Pollen Jerardino, 1995 (R) Cooler, Wetter
4 WRZ Spoeg River Cave Jerardino, 1995 (R) Cooler, wetter ...Until
5 WRZ Elands Bay Cave Molluscs Jerardino, 1995 (R) dune development ~ marine regression
6 WRZ False Bay Dunes building Roberts et al., 2009
7 WRZ Cecelia Cave & Klaarfontein Pollen Chase and Meadows, 2007 (R) Cooler, greater moisture availability ~ Westerly winds
8 WRZ BUS Mollusc Isotope Cohen et al., 1992 cooler
9 WRZ BUS calcite:aragonite Cohen et al., 1992 3190 ↓1- 2°C
10 WRZ Elands Bay Cave Vegetation Cowling et al., 1999 3290 relative statis in veg composition 4390
11 WRZ West Coast Molluscs Jerardino, 1997 cooler SST cooler
12 WRZ West Coast Molluscs Jerardino, 1997 0m amsl ±2m masl
13 WRZ West Coast Molluscs Jerardino, 1997 dune formation
14 WRZ Elands Bay Cave Coastal platform Miller et al., 1995 leading to a rise @ 1800 sea level drop ±3m masl
15 WRZ Elands Bay Cave Coastal platform Miller et al., 1995 3160 falling sea level, coastal sediment instability 4330
16 WRZ Elands Bay Cave Coastal platform Miller et al., 1995 2850 dune formation 3800
17 WRZ EBC & Spring Cave Coastal platform Miller et al., 1995 aeolian deposition, sea level drop
18 WRZ Verlorenvlei sediment Miller et al., 1995 Verlorenvlei remained tidal and saline ...Until 1500
19 WRZ Verlorenvlei sediment Meadows et al., 1996
20 WRZ Cecelia Cave Pollen Baxter, 1986 e & As cooler, wetter = ↑ Ericaceae, Restio, Iridaceae, ↓ Poaceae
21 WRZ Langdam Shell Middens Miller et al., 1993 sand deposition ±3m asl
22 WRZ Elands Bay Cave Miller et al., 1993 sand movement high aeolian activity
23 WRZ SW Cape Review Jerardino, 1993 neoglacial = ↓ SST oglacial = ↓ ...4500
24 WRZ Tortoise Cave Shell Middens Jerardino, 1993 sea level drop estuarine conditions
25 WRZ Tortoise Cave Shell Middens Jerardino, 1993 to present level 3160 declining sea level ±2m asl 4330
26 WRZ Verlorenvlei Diatoms Stager et al., 2012
27 WRZ Verlorenvlei Diatoms Stager et al., 2012
28 WRZ Cedeberg Mtns Pollen Meadows and Baxter, 1999 less xeric conditions = less dry ...5000
29 WRZ Klaarfontein Springs Pollen Meadows and Baxter, 2001 variable vegetation, dynamic period of sedimentation possible spring ceased to flow ...6000
30 WRZ Klaarfontein Springs Pollen Meadows and Baxter, 2001 ndition afromontance elements in sheltered ravines, poss wet conditions
31 WRZ Katbakkies pass hyrax midden Meadows et al., 2010 high Asteraceae, decline Cyperaceae, Podocarpaceae pk mid-zone
32 WRZ Katbakkies pass hyrax midden Meadows et al., 2010 marginally wetter
33 WRZ Pakhuis Pass Pollen Scott and Woodbourne, 2007 ↓ stab moist moist ↓AP, ↑ succulents - cooler ...5000
34 WRZ Spoeg River Cave midden Webley, 2007
35 WRZ Princessvlei Pollen Neumann et al., 2011 relatively dry relatively moist, humid relatively dry
36 WRZ Princessvlei Pollen Neumann et al., 2011 higher sea level
37 WRZ Klaarfontein Springs Review Neumann et al., 2011 arid
38 WRZ Hangklip sediment Schalke, 1973 ↑ aeolian activity = drier conditions
39 WRZ Princessvlei Diatoms Kirsten, 2013 wet dry wet

	Regime	Site	Proxy	Reference	0 - 500					500 - 1000					1000 - 1500					1500 - 2000				
				cal yrs BP	1	2	3	4	5	6	7	8	9	0	1	2	3	4	5	6	7	8	9	0
40	YRZ	Nelson Bay cave	Molluscs	Cohen and Tyson, 1992																				
41	YRZ	Wilderness	Dunes building	Bateman et al., 2010							Westerly Wind activity													
42	YRZ	Groenvlei	Lake sediments	Martin, 1968	Human					sand ↓/climate → immigration & spread of wet & dry forest type														
43	YRZ	Groenvlei	Lake sediments	Martin, 1968						Marine influence wanes, *Podocarpus* ↑														
44	YRZ	Cango Caves	Speleothem	Jerardino, 1995 (R)		Cooler										Cooler								
45	YRZ	Cango Caves	Speleothem	Jerardino, 1995 (R)																				
46	YRZ	Algoa Dunes	Dunes building	Jerardino, 1995 (R)																				
47	YRZ	Nelson Bay cave		Cohen and Tyson, 1992							650													
48	YRZ	Cango Caves	Speleothem	Tyson, 1991					450	cooling														
49	YRZ	Cape Agulhas	Lunettes	Carr et al., 2006a					450		Drier					1250								water ero
50	YRZ	Cape Agulhas	Lunettes	Carr et al., 2006b																				
51	YRZ	Cape Agulhas	Lunettes	Carr et al., 2006a + b					Wly		Wly					Wly								
52	YRZ	Norga	Peat	Carr et al., 2006b																	Drier			
53	YRZ	Uitenhage + Stampriet	Aquifer	Chase and Meadows, 2007 (R)																				
54	YRZ	VVV, GV, Norga	Pollen	Chase and Meadows, 2007 (R)														Arid episode						
55	YRZ	VVV, GV, Norga	Pollen	Chase and Meadows, 2007 (R)														Forest spread						
56	YRZ	South Coast Plain	Alluvial sediment	Damm and Hadedorn, 2010	Arid								875	flood/cooler										
57	YRZ	Boomplaas Cave	δ13C	Deacon, 1995						herders														
58	YRZ	Cango Caves	Speleothem	Talma and Vogel, 1992			cooler		450															
59	YRZ	Groenvlei	Diatoms	Martin, 1959	freshwater, eutrophic...discontinuity in record																			
60	YRZ	Algoa Dunes		Jerardino, 1993																				
61	YRZ	Soetendalsvlei	Diatoms	Gordon et al., 2012	freshwater, eutrophic conditions																			
62	YRZ	Norga	Peat	Scholtz, 1986	warmer, more mesic													. winter winds → ↓forest; drier, poss c						
63	YRZ	Norga	Peat	Scholtz, 1986	peat formation = reliable all-season rainfall, moisture surplus throughout the year																			
64	YRZ	Eilandvlei (EV1.11)	Diatoms	Kirsten, 2013	human			dry		wet			dry		wet	dry			cool/~dry				wet	
65	YRZ	Eilandvlei (EV10/1	Diatoms	Kirsten, 2013	human			dry		wet														
66	YRZ	Swartvlei (SV10/1)	Diatoms	Kirsten, 2013				dry		wet						dry								

	Regime	Site	Proxy	Reference	00 - 20	2000 - 2500					2500 - 3000					3000 - 3500					3500 - 4000									
				cal yrs BP	0	1	2	3	4	5	6	7	8	9	0	1	2	3	4	5	6	7	8	9	0	1	2	3	4	
40	YRZ	Nelson Bay cave	Molluscs	Cohen and Tyson, 1992		max summer temperatures lower, winter either warmer or not sig different																							
41	YRZ	Wilderness	Dunes building	Bateman et al., 2010							Westerly Wind activity																		
42	YRZ	Groenvlei	Lake sediments	Martin, 1968		Higher water table, marine influence, dune activity																							...~7800
43	YRZ	Groenvlei	Lake sediments	Martin, 1968	: wane ↑ scru	? sand ↓/climate																							
44	YRZ	Cango Caves	Speleothem	Jerardino, 1995 (R)							Cooler																		
45	YRZ	Cango Caves	Speleothem	Jerardino, 1995 (R)		Winter rainfall seasonality																							...5000
46	YRZ	Algoa Dunes	Dunes building	Jerardino, 1995 (R)							Sea Level drop														rise		drop		
47	YRZ	Nelson Bay cave		Cohen and Tyson, 1992		lower max temperature in Agulhas Current																							
48	YRZ	Cango Caves	Speleothem	Tyson, 1991		Neoglacial advance															warmer								
49	YRZ	Cape Agulhas	Lunettes	Carr et al., 2006a	er erosion						Drier																		
50	YRZ	Cape Agulhas	Lunettes	Carr et al., 2006b																							Dune dvlpment		...4700
51	YRZ	Cape Agulhas	Lunettes	Carr et al., 2006a + b							Wly winds																		
52	YRZ	Norga	Peat	Carr et al., 2006b		Drier																							
53	YRZ	Uitenhage + Stampriet	Aquifer	Chase and Meadows, 2007 (R)							Cooling																		
54	YRZ	VVV, GV, Norga	Pollen	Chase and Meadows, 2007 (R)		Arid episode																							
55	YRZ	VVV, GV, Norga	Pollen	Chase and Meadows, 2007 (R)							Forest spread																		...4500
56	YRZ	South Coast Plain	Alluvial sediment	Damm and Hadedorn, 2010		Khoisan																							
57	YRZ	Boomplaas Cave	δ13C	Deacon, 1995		Higher summer temperatures/↑ SRZ																							
58	YRZ	Cango Caves	Speleothem	Talma and Vogel, 1992		warmer					cooler										warmer								
59	YRZ	Groenvlei	Diatoms	Martin, 1959	ic...dis	↓ lagoon, less saline, ↓ productivity																			brackish lagoon, marine sp↓				...5000
60	YRZ	Algoa Dunes		Jerardino, 1993		±2m bsl (regression)																					regression		...4500
61	YRZ	Soetendalsvlei	Diatoms	Gordon et al., 2012	utroph	marine derived organic matter																							...7500
62	YRZ	Norga	Peat	Scholtz, 1986	old, winter winds → ↓forest; drier, poss cool	optimal forest spread																							
63	YRZ	Norga	Peat	Scholtz, 1986		peat formation = reliable all-season rainfall, moisture surplus throughout the year																							
64	YRZ	Eilandvlei (EV1.11)	Diatoms	Kirsten, 2013	wet	dry			wet		dry					wet				dry		wet		dry					
65	YRZ	Eilandvlei (EV10/1	Diatoms	Kirsten, 2013																									
66	YRZ	Swartvlei (SV10/1)	Diatoms	Kirsten, 2013																									

	Regime	Site	Proxy	Reference	0 - 500					500 - 1000					1000 - 1500					1500 - 2000				
				cal yrs BP	1	2	3	4	5	6	7	8	9	0	1	2	3	4	5	6	7	8	9	0
67	SRZ	Kalahari		Jerardino, 1995 (R)					Humid															
68	SRZ	Cold Air Cave	Speleothem	Holmgren et al., 1999				370	425													wet, warmer		
69	SRZ	Transvaal	agriculture	Hoffman, 1996					drier			wetter, warmer						wetter, warmer						
70	SRZ	Interior	Review	Klein, 1999		drier												relatively moist						
71	SRZ	Sn En Cape Drakensberg		Lewis, 2011	moist conditions sufficient for human occupation																			
72	SRZ	Kalahari	Lunettes	Lawson and Thomas, 2002																				
73	SRZ	Cold Air Cave	Speleothem	Lee-Thorp et al., 2001	lower humates = grasses ↑																			
74	SRZ	Cold Air Cave	Speleothem	Lee-Thorp et al., 2001			250	drier / cooler (↓ 1°C)... ↓ C4 grasses																
75	SRZ	En Cape Drakensberg		Lewis, 2008	drier but comparatively moist															wet				
76	SRZ	Barkly East	charcoal	Lewis, 2008	*Cliffortia* utilised = relatively moist																			tilised = dry
77	SRZ	Tiffendell		Lewis, 2008																				
78	SRZ	Lake Eteza	Pollen	Neumann et al., 2010	20	drier, less swampy					savani				moist coastal element = moist environ									
79	SRZ	Lake Sibaya	Pollen	Neumann et al., 2010	↓ forest, neophytes intro										↓ trees, ↑ Poaceae									
80	SRZ	Lake Sibaya	Diatoms	Stager et al., 2013																				
81	SRZ	Mfabeni Peatland	Pollen	Finch & Hill, 2008																				
82	SRZ	Braamhoek Wetland	Pollen, isotopes	Norström et al., 2009	relatively wet, &/or less evaporative condns															?relatively humid				
83	SRZ	East Coast	Beachrock	Ramsay, 1995	0m asl										falling to present level					rising, ±1.5m asl by 1610				
84	SRZ	Blydefontein Basin	Pollen	Scott et al., 2005	drying				subhumid						dry		subhumid, grassy							
85	SRZ	Austerlitz	hyrax midden	Chase et al., 2010														progressive aridification						
86	SRZ	Wonderwerk Cave	Speleothem	Brook et al., 2010											wetter	dry	wetter							
87	SRZ	Klein Spitzkoppe	hyrax midden	Chase et al., 2009	wetter			marked aridity																
88	SRZ	Klein Spitzkoppe	hyrax midden	Chase et al., 2009								750	wetter		1150									
89	SRZ	Braamhoek Wetland	siliceous fossils	Finne et al., 2010	high degree of local moisture, benthics dominant																			
90	Gen	Geo1023-5	Marine Record	Shi et al., 2000	*Podocarpus* gradually declines = Climate + Human																			
91	Gen	Geo1023-5	Marine Record	Shi et al., 2001	↑ Charcoal → ↑ burning = Human																			
92	Gen	MD96-2094	Marine Record	Stuut et al., 2004	Low trade wind intensity, low winter rainfall																			
93	Gen	Review	Various	Tyson and Lindsey, 1992	150		325	450				gen warmer			gen cooler					1750	cooler			
94	Gen	Review	Various	Tyson and Lindsey, 1992		↑ Westerlies & ↓ Elies						↑ Easterly												
95	Gen	Review	Various	Hassan, 1997																				
96	Gen	OPD 1084B	forams	Farmer et al., 2005	modern			↑ Upwelling, cooler SST																
97	Gen	GEOB3313-1	Fe intensity	Stager et al., 2012		LIA = ↑ P-E						↓P-E												
98	Gen	Kuiseb River	Review: YRZ - WRZ	Scott and Vogel, 2000	?dry, ↑ karroid							↑δ13C			↓δ13C, lowest @ 1000 = less rainfall									
99	Gen	Review	Review	Scott and Lee-Thorp, 2004																				
100	Gen	Review	Review	Scott and Lee-Thorp, 2004																				

	Regime	Site	Proxy	Reference	00 - 20	2000 - 2500					2500 - 3000					3000 - 3500					3500 - 4000									
				cal yrs BP	0	1	2	3	4	5	6	7	8	9	0	1	2	3	4	5	6	7	8	9	0	1	2	3	4	
67	SRZ	Kalahari		Jerardino, 1995 (R)		humid events																							
68	SRZ	Cold Air Cave	Speleothem	Holmgren et al., 1999	t, warr	cooler							cooler																
69	SRZ	Transvaal	agriculture	Hoffman, 1996																									
70	SRZ	Interior	Review	Klein, 1999	relatively moist																								...4600
71	SRZ	Sn En Cape Drakensberg		Lewis, 2011	moist conditions sufficient for human occupation																								...~6300
72	SRZ	Kalahari	Lunettes	Lawson and Thomas, 2002		2.17±0.29			2.35±0.22																				
73	SRZ	Cold Air Cave	Speleothem	Lee-Thorp et al., 2001	lower humates = grasses ↑															higher humates									...6500
74	SRZ	Cold Air Cave	Speleothem	Lee-Thorp et al., 2001		C4 pk					pk	↑ aridity/cooler			pk					variable warm/moist period									
75	SRZ	En Cape Drakensberg		Lewis, 2008	wet	less wet					relatively wet									semi-arid									
76	SRZ	Barkly East	charcoal	Lewis, 2008	*Europys* utilised = dry conditions																								...7183
77	SRZ	Tiffendell		Lewis, 2008							gully erosion = moist conditions																		
78	SRZ	Lake Eteza	Pollen	Neumann et al., 2010	ement	dry, grassy environment															↑ precip, ↑ sea level								...6500
79	SRZ	Lake Sibaya	Pollen	Neumann et al., 2010																									
80	SRZ	Lake Sibaya	Diatoms	Stager et al., 2013																									
81	SRZ	Mfabeni Peatland	Pollen	Finch & Hill, 2008	drier, cooler																								
82	SRZ	Braamhoek Wetland	Pollen, isotopes	Norström et al., 2009		?relatively humid					warm, relatively dry																		...7500
83	SRZ	East Coast	Beachrock	Ramsay, 1995		rising, ±1.5m asl by 1610					±2m bsl					highstand (±3m asl, pk 3880 & 3360)													...5080
84	SRZ	Blydefontein Basin	Pollen	Scott et al., 2005	umid, g	dry		subhumid								relatively cool, dry climate													
85	SRZ	Austerlitz	hyrax midden	Chase et al., 2010		progressive aridification															ure av								...4825
86	SRZ	Wonderwerk Cave	Speleothem	Brook et al., 2010		wetter										wet but dry								warm and wet					...5000
87	SRZ	Klein Spitzkoppe	hyrax midden	Chase et al., 2009		marked aridity															↑ humidity, wetter								
88	SRZ	Klein Spitzkoppe	hyrax midden	Chase et al., 2009									aridity α solar activity																4800
89	SRZ	Braamhoek Wetland	siliceous fossils	Finne et al., 2010	hoistu	dry																							
90	Gen	Geo1023-5	Marine Record	Shi et al., 2000	declir	Dry forest expansion > High humidity esp @ beginning														Afromontane + Miombo woodland pk									...4800
91	Gen	Geo1023-5	Marine Record	Shi et al., 2001		*Brigantedinium* ssp minima = ↓ Upwelling (BUS)																							
92	Gen	MD96-2094	Marine Record	Stuut et al., 2004		Low trade wind intensity, low winter rainfall																							...12000
93	Gen	Review	Various	Tyson and Lindsey, 1992		Neoglacial advance																							
94	Gen	Review	Various	Tyson and Lindsey, 1992																									
95	Gen	Review	Various	Hassan, 1997	↓ rainfall																								
96	Gen	OPD 1084B	forams	Farmer et al., 2005		↑ Upwelling, cooler SST															warmer SST								...5800
97	Gen	GEOB3313-1	Fe intensity	Stager et al., 2012																									
98	Gen	Kuiseb River	Review: YRZ - WRZ	Scott and Vogel, 2000	@ 100	↑δ13C grassy environment, more rainfall																							...before
99	Gen	Review	Review	Scott and Lee-Thorp, 2004		arid					Cango Caves = cooler, poss drier									EBC = arid (ostrich shells)									...4700
100	Gen	Review	Review	Scott and Lee-Thorp, 2004		rising summer rainfall seasonality																							...5000